Conference:

Agricultural Engineering

2017

VDI-MEG

LAND.TECHNIK AgEng 2017

The Forum for Agricultural Engineering Innovations

Mit
USB-Stick

CONFERENCE

Agricultural Engineering

Conference:

Agricultural Engineering

Hannover 10. und 11. November 2017

2017

VDI-MEG

LAND.TECHNIK AgEng 2017

The Forum for Agricultural Engineering Innovations

Bibliographische Information der Deutschen Bibliothek
Die Deutsche Bibliothek verzeichnet diese Publikation in der Deutschen Nationalbibliographie; detaillierte bibliographische Daten sind im Internet unter http://dnb.ddb.de abrufbar.

Bibliographic information published by the Deutsche Bibliothek
(German National Library)
The Deutsche Bibliothek lists this publication in the Deutsche Nationalbibliographie (German National Bibliography); detailed bibliographic data is available via Internet at http://dnb.ddb.de.

Der VDI-Bericht, der die Vorträge der Tagung enthält, erscheint als nichtredigierter Manuskriptdruck. Die einzelnen Beiträge geben die auf persönlichen Erkenntnissen beruhenden Ansichten und Erfahrungen der jeweiligen Vortragenden bzw. Autoren wieder.

Printed in Germany.

ISSN 0083-5560

ISBN 978-3-18-092300-0

VDI-Berichte 2300

Foreword

This book summarises the proceedings of the 75th conference “LAND.TECHNIK – AgEng 2017”, which took place in Hannover on November 10th and 11th following the tradition of odd years. Therefore it is a well established prelude to AGRITECHNICA, the world’s most important fair for agricultural machinery, which started on November 12th with the preview days.

The conference was successfully organized in cooperation with the “Max Eyth Society for Agricultural Engineering” (VDI-MEG), a technical division of the Association of German Engineers (Verein Deutscher Ingenieure, VDI) and the European Society of Agricultural Engineers (EurAgEng). This collaboration has been accepted both by academia and industry at national and international levels. During recent years the number of participants has increased to about 1000 from more than 15 nations.

The conference offered 75 presentations about the latest innovations, machine developments, and technical concepts and methods as a foretaste of the firework of impressions at the AGRITECHNICA.

LAND.TECHNIK – AgEng is one of the most important events for the international community of agricultural engineers to discuss the possibilities of addressing future global challenges together. We hope that this book will stimulate the productive international dialog among decision-makers, developers, researchers and students to meet current and future challenges.

Prof. Dr.-Ing. Henning J. Meyer
Chairman of the Program Committee of the
Conference LAND.TECHNIK – AgEng 2017

Claus Grøn Sørensen
President of European Society of
Agricultural Engineers (EurAgEng)

Prof. Dr.-Ing. Peter Pickel
President of VDI Max Eyth Society
for Agricultural Engineering
(VDI-MEG)

Content

75 Conferences on Agricultural Engineering – a great Period of Innovations

Highlights of a Success Story

Univ.-Prof. Dr.-Ing. Dr. h.c. **K.Th. Renius**, Technical University of Munich

Abstract

The first periodic German conference on agricultural engineering took place 1934 in Berlin, directed by *Prof. W. Kloth*. Basic data of all 75 conferences are listed in two tables. The war forced an interruption with a renewal at FAL Braunschweig by *Kloth* 1951. VDI Branch of Agricultural Engineering became engaged from 1962 including MEG from 1983. In 1990, the 48. conference was organized in Berlin commonly with EurAgEng testing a new European format. A change of the location in the uneven years to Hannover (ahead of Agritechnica) and the merger with AgEng conferences in 2007 completed a remarkable success story.

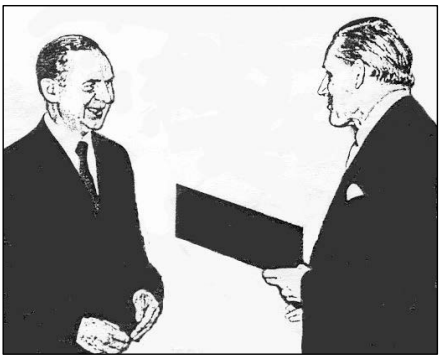

Fig. 1 (left): *Willi Kloth* 65 (1956), congratulated by *Theodor Stroppel* [3]

1. Conference foundation and its first phase under Kloth and Stroppel

Highlights of the conference prehistory are, for example, outlined in reviews of *A. Stroppel* [1] and *H. J. Matthies* [2].

The first periodic German conference on agricultural engineering took place in Berlin, Jan. 30 - Febr. 1, 1934.

The driving force was *Dr.-Ing. Willi Kloth* (1891-1967), supported by his *Chief Engineer Theodor Stroppel* (1901-1981).

Kloth was at that time Founder and Head

Table 1: The first 22 conferences, most chaired by W. Kloth [4], supported by Th. Stroppel [5, 6]

No. / Year	Location	Chairman	Organizer	Chair VDI Section
1 - 8*) 1934-1941	Berlin	Kloth	Inst. of Agric. Machinery Techn. Hochschule Berlin	-
9-17/1951-59 18-22/1960-64	Braun- schweig	Kloth Batel	Inst. of Agric. Engineering Fundamentals at FAL	1958-59: Kloth 1960-61: Friedrich 1962-64: Segler

*) paper documented for No. 1-5 by RKTL brochures No. 56, 61, 71, 88 and 91

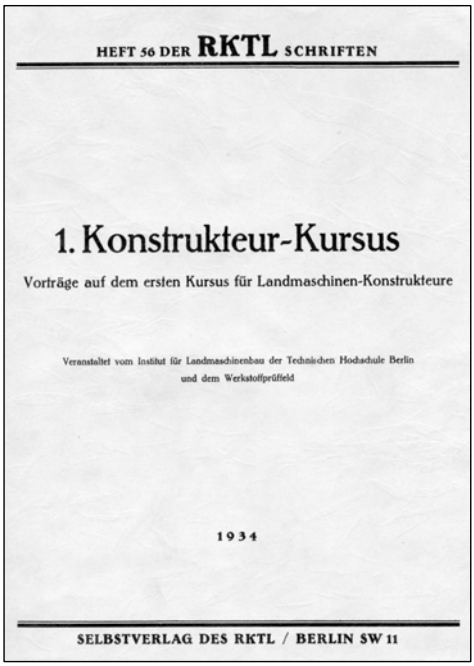
HEFT 56 DER RKTL SCHRIFTEN

1. Konstrukteur-Kursus

Vorträge auf dem ersten Kursus für Landmaschinen-Konstrukteure

Veranstaltet vom Institut für Landmaschinenbau der Technischen Hochschule Berlin und dem Werkstoffprüffeld

1934

SELBSTVERLAG DES RKTL / BERLIN SW 11

Fig. 2: Documentationa of the first conference

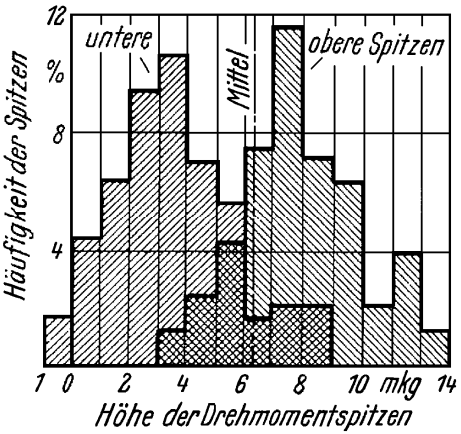

Fig. 3: First load spectrum in engineering [9], histogram of PTO torque load peaks of a binder

of the Institute of Agricultural Machinery at Technical University Berlin [4] with affiliated RKTL Material Test Institute. His basic idea was to create a new link between research institutions and manufacturers of agricultural machinery for an efficient use of research results, for improved co-operations and critical discussions as well.

Several companies expressed initially their concerns fearing loss in advanced knowledge but this did not happen as stated in a review of *Kloth* in 1952 [7].

The content of the first five conferences was published by RKTL [8], **Fig. 2**.

The importance may be recognized by three papers, a first from *Kloth,* addressing the historical publication of the wordwide first load spectra, **Fig. 3**, by *Kloth* and *Stroppel* [9]. They had measured torque loads in the PTO drive line from the tractor to a binder at 550 rpm, processing them statistically to load spectra.

Kloth was recognizing the potential of light weight design pointing out so early the need of statistic load analysis for fatigue modelling, wear forecast and safety clutch settings. We can call him one of the world wide first pioneers of this discipline [4].

Dr. Kloth (Prof. from 1940 [4]) directed not only the first phase of the conferences 1934-1941 in Berlin but also a relaunch 1951-1959 in Braunschweig.

The Federal Research Institute of Agriculture (FAL) was founded in 1948 at Braunschweig-Völkenrode and appointed him as Full Professor and Head of Institute of Agricultural Engineering Fundamentals (1948-1958).

Table 2 is listing the subjects and the authors of the meeting 1951.

Kloth received an honorary PhD from HU Berlin 1956 and many other outstanding awards. *Prof. Batel* as his successor took over the chairmanship for the conferences from 1960 until 1964.

Table 2: The first conference after the war 1951

Subject	Speaker/author
Design in Germany and USA	W. Kloth
Tractor and implement in USA	H. Meyer
Forces at a plow body	G. Getzlaff
Tractor-implement forces	H. Skalweit
Implement lift kinematics	K. Hain
Hydraulic three point lift design	A. Seifert
Stiffness of frames	W. Bergmann
Design of spoke wheels	H. Müller
Design of soft crosspoints	W. Bergmann
Model use for design	W.G. Brenner
Static similarity fundamentals	W. Bergmann
Fundamentals of soil mechanics	W. Söhne
Aerodynamics for agric. machinery	U. Blenk
Pneumatic conveying design	G. Segler
Review on disc plows	W. Söhne

Papers were documented in GRUNDLAGEN DER LANDTECHNIK (1951-90), perfectly reviewed by its first chief editor *Theodor Stroppel*. As a second example I would like to show an extract of a publication on the design of frames, **Fig. 4**, [10]. The often underestimated increase of torsion stiffness by replacing open cross profiles by closed ones was demonstrated *by W. Bergmann* **,** the stiffness increased in this case 30 times !. I could use these fundamentals well for my lectures and for several consultationsl.

A third impressive example of a basic publication was a paper of *Walter Söhne*, first-time presenting his famous pressure bulbs under tires. He demonstrated already in 1951 the

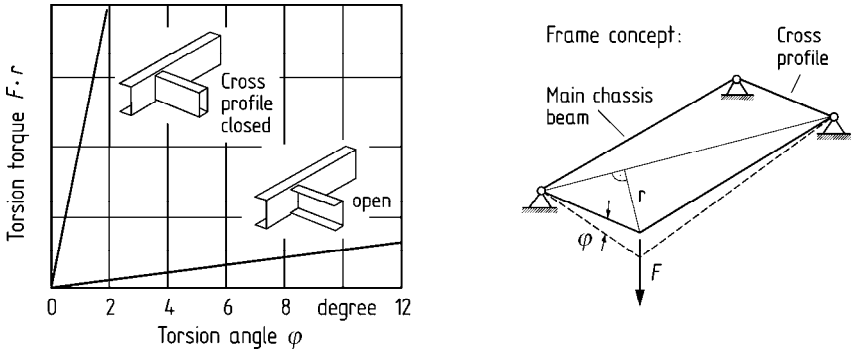

Fig. 4: Influence of cross profiles on frame stiffness. Closed cross profiles instead of open ones increase torsion stiffness dramatically, diagram reproduced from [10]

important influence of tire loads on the soil pressures in the deeper layers, **Fig. 5.**

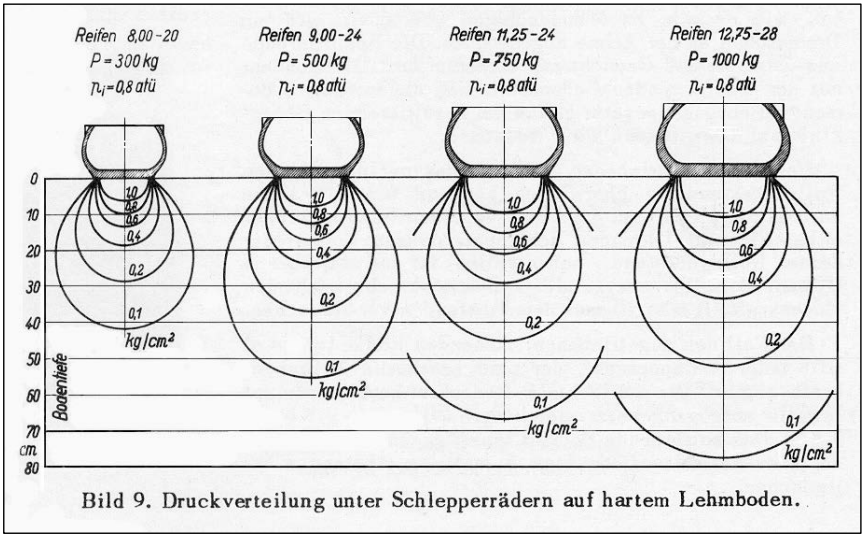

Fig. 5: First (original) diagram of *W. Söhne's* "pressure bulbs": Lines of constant vertical soil pressure under tires of unique inflation and contact pressures for a firm soil [11]

These three examples and many other excellent papers were typically for the outstanding level of the 1951 conference and the following meetings. Many contributions are documented in the GRUNDLAGEN DER LANDTECHNIK, over five decades, being a source of basic fundamentals until today.

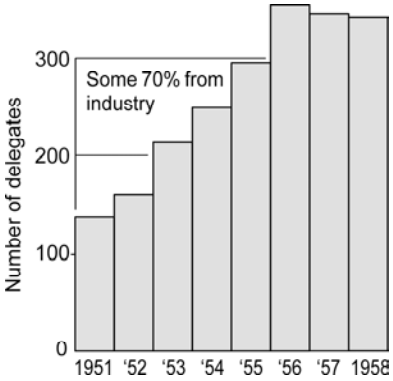

The result of the outstanding quality of the conferences was a permanent improved level of the German agricultural engineering and, consequently, also a permanent increase of the number of conference delegates, **Fig. 6**.

It may be respected, that also the outstanding high percentage of delegates from industry, in the first years some 70%, was indicating the value of the conference and its influence on agricultural innovations.

Fig. 6: Number of delegates of the first conferences 1951-1958. Diagram based on [8].

The development of this conference entered a new phase when the VDI Branch of Agricultural Engineering (VDI-L) was founded, which was taking place in 1958, **Table 3** [12].

Table 3: Development of the German societies of agricultural engineering after World War II

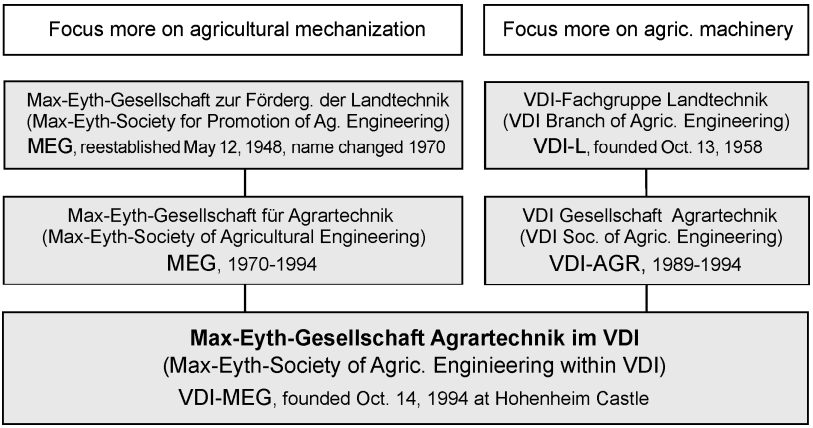

2. Conference organization moving towards VDI and MEG

The “VDI Fachgruppe Landtechnik” (VDI Branch of Agricultural Engineering) was becoming engaged in the conference organization from 1962, **Table 4.**

Prof. Georg Segler (1906-1978) was the driving wheel of grading up the conference importance by engaging both, the VDI and the MEG.

He was supported by *Kloth*, whose annual meetings ended in 1964 after an overlapping in 1962, 1963 and 1964, Table 1 and 4, but *Kloth's* successful philosophy of focusing on engineering fundamentals was integrated in the new format.

In 1983, *Prof. H.J. Matthies* (1921-2016) took over the chair of the VDI-L (Table 4). In this year, the Conference Landtechnik was for the first time organized commonly by VDI and MEG under the chairmanship of *Prof. Alfred Stroppel* (a son of *Theodor Stroppel*) and with support of *Prof. H. Eichhorn*, at that time President of MEG. *Matthies* presented in his conference welcome the vision, that MEG and VDI-L should put together all efforts to make a further step of co-operation by merging the two societies.

Some years later, this vision was accompanied by a memorable meeting of German professors, organized by *A. Stroppel* (Ulm Oct. 9, 1990), welcoming colleagues from universities of East Germany (the former DDR) along with the German unification.

Table 4: The German conferences 1962-2017 - data courtesy *Dr. A. Herrmann*, VDI-MEG

No.	Year	Location	Conf. Chairman	Organizer	Society Chairman
20	1962	Köln	-	VDI Agric. Eng. Dep.	Prof. Segler
21	1963	Heidelberg	-	VDI Agric. Eng. Dep.	Prof. Segler
22	1964	Münster	-	VDI Agric. Eng. Dep.	Prof. Segler
23	1965	Braunschweig	-	VDI Agric. Eng. Dep.	Prof. Segler
24	1966	Stuttgart	-	VDI Agric. Eng. Dep.	Prof. Segler
25	1967	Braunschweig	-	VDI Agric. Eng. Dep.	Prof. Segler
26	1968	München	-	VDI Agric. Eng. Dep.	Prof. Segler
27	1969	Braunschweig	-	VDI Agric. Eng. Dep.	Prof. Segler
28	1970	Ulm	-	VDI Agric. Eng. Dep.	Dr. Eggenmüller
29	1971	Braunschweig	-	VDI Agric. Eng. Dep.	Dr. Eggenmüller
30	1972	München	-	VDI Agric. Eng. Dep.	Dr. Eggenmüller
31	1973	Braunschweig	-	VDI Agric. Eng. Dep.	Dr. Eggenmüller
32	1974	Stuttgart	-	VDI Agric. Eng. Dep.	Prof. Schilling
33	1975	Braunschweig	-	VDI Agric. Eng. Dep.	Prof. Schilling
34	1976	München	-	VDI Agric. Eng. Dep.	Prof. Schilling
35	1977	Braunschweig	-	VDI Agric. Eng. Dep.	Prof. Schilling
36	1978	Nürnberg	-	VDI Agric. Eng. Dep.	Prof. Schilling
37	1979	Braunschweig	-	VDI Agric. Eng. Dep.	Prof. Schilling
38	1980	Neu-Ulm	-	VDI Agric. Eng. Dep.	Dipl.-Ing. Logos
39	1981	Braunschweig	Prof. Stroppel	VDI Agric. Eng. Dep.	Dipl.-Ing. Logos
40	1982	Neu-Ulm	Prof. Stroppel	VDI Agric. Eng. Dep.	Dipl.-Ing. Logos
41	1983	Braunschweig	Prof. Stroppel	VDI Agric. Eng. Dep.+ MEG	Prof. Matthies
42	1984	Neu-Ulm	Prof. Renius	VDI Agric. Eng. Dep.+ MEG	Prof. Matthies
43	1985	Braunschweig	Prof. Renius	VDI Agric. Eng. Dep.+ MEG	Prof. Matthies
44	1986	Neu-Ulm	Prof. Renius	VDI Agric. Eng. Dep.+ MEG	Prof. Matthies
45	1987	Braunschweig	Prof. Renius	VDI Agric. Eng. Dep.+ MEG	Prof. Matthies
46	1988	Neu-Ulm	Prof. Renius	VDI Agric. Eng. Dep.+ MEG	Prof. Matthies
47	1989	Köln	Prof. Renius	VDI Agric. Eng. Soc.+ MEG	Prof. Göhlich
48	1990	Berlin	Prof. Göhlich	VDI Agric. Eng. Soc.+MEG+AgEng	Prof. Göhlich
49	1991	Braunschweig	Prof. Renius	VDI Agric. Eng. Soc.+ MEG	Prof. Göhlich
50	1992	Freising-Weih.	Prof. Renius	VDI Agric. Eng. Soc.+ MEG	Dr. Welschof
51	1993	Braunschweig	Prof. Harms	VDI Agric. Eng. Soc.+ MEG	Dr. Welschof
52	1994	Hohenheim	Prof. Harms	VDI Agric. Eng. Soc.+ MEG	Dr. Welschof
53	1995	Braunschweig	Prof. Harms	VDI-MEG (Merger)	Prof. Renius
54	1996	Berlin	Prof. Hahn	VDI-MEG	Prof. Renius
55	1997	Braunschweig	Prof. Hahn	VDI-MEG	Prof. Renius
56	1998	München	Prof. Auernhammer	VDI-MEG	Dr. Ratschow
57	1999	Braunschweig	Prof. Auernhammer	VDI-MEG	Dr. Ratschow
58	2000	Münster	Prof. Auernhammer	VDI-MEG	Dr. Ratschow
59	2001	Hannover	Prof. Auernhammer	VDI-MEG, Coop. with EurAgEng	Dr. Ratschow
60	2002	Halle	Prof. Auernhammer	VDI-MEG	Dr. Ratschow
61	2003	Hannover	Prof. Auernhammer	VDI-MEG, Coop. with EurAgEng	Dr. Ratschow
62	2004	Dresden	Dr. Ehlert	VDI Wissensforum + VDI-MEG	Prof. Frerichs
63	2005	Hannover	Dr. Ehlert	VDI Wissensforum + VDI-MEG	Prof. Frerichs
64	2006	Bonn	Dr. Ehlert	VDI-MEG + EurAgEng + CIGR	Prof. Frerichs
65	2007	Hannover	Dr. Ehlert	VDI Wiss.+VDI-MEG+EurAgEng	Prof. Frerichs
66	2008	Hohenheim	Dr. Ehlert	VDI Wissensforum + VDI-MEG	Prof. Frerichs
67	2009	Hannover	Prof. Lang	VDI Wiss.+VDI-MEG+EurAgEng	Prof. Böttinger
68	2010	Braunschweig	Prof. Lang	VDI Wissensforum + VDI-MEG	Prof. Böttinger
69	2011	Hannover	Prof. Lang	VDI Wiss.+VDI-MEG+EurAgEng	Prof. Böttinger
70	2012	Karlruhe	Prof. Lang	VDI Wissensforum + VDI-MEG	Prof. Böttinger
71	2013	Hannover	Prof. Lang	VDI Wiss.+VDI-MEG+EurAgEng	Prof. Böttinger
72	2014	Berlin	Prof. Meyer	VDI Wissensforum + VDI-MEG	Prof. Böttinger
73	2015	Hannover	Prof. Meyer	VDI Wiss.+VDI-MEG+EurAgEng	Prof. Pickel
74	2016	Köln	Prof. Meyer	VDI Wissensforum + VDI-MEG	Prof. Pickel
75	2017	Hannover	Prof. Meyer	VDI Wiss.+VDI-MEG+EurAgEng	Prof. Pickel

The idea of *Prof. Hans Jürgen Matthies,* to merge MEG and VDI-AGR, was not only supported by the conferences but also by several special meetings of leading German personalities such as *Prof. H. Eichhorn, Prof. H. Göhlich, Prof. A. Gego, Dr. G. Welschof; Dr. F. Meier, Prof. H. Schön* and *Prof. K.-Th. Renius* [12] – usually chaired by *Matthies.*

The merger could finally take place in Oct. 14, 1994 at the beautiful Hohenheim Castle directed by *Prof. Matthies*, Table 3 [1, 12]. *Prof. Renius* was elected as its first President [13].

3. Facing Europe by again widened circles

An important step versus "more Europe" was the famous Conference AgEng'84 in Cambridge, UK, chaired by *Prof. John Matthews*, supported by *Prof. Francis Sevilla*, France and from Germany by *Prof. Horst Göhlich*. The huge success motivated to continue with this conference: AgEng'86 in Noordwijkerhout, the Netherlands (*A. Hagting*), AgEng'88 in Paris, France (*F. Sevilla*), AgEng'90 in Berlin, Germany (*H. Göhlich*). The Berlin meeting was the first combination with our annual German conference and a successful step towards a European Society replacing the "AgEng Working Party" (which had prepared the first four AgEng Conferences). The European Society of Agricultural Engineers, the EurAgEng, was ready in 1961, officially established January 1, 1992. *Professor Francis Sevilla* (1949-2010), an outstanding promoter, was elected as its first President.

EurAgEng celebrates 2017 its 25^{th} anniversary – our congratulation and very best wishes!

The mentioned unification of the two German societies in 1994 became a powerful platform for further improvements. *Prof. H. Auernhammer* being the chairman of the German conferences 1998-2003 (Table 4) could achieve a co-operation with DLG (German Society of Agriculture) and ICC (Hannover Fair) to run the annual conference "Landtechnik" 2001 for the first time ahead of AGRITECHNICA. The increased participation of 469 delegates (63% from industry) confirmed the new concept. *Auernhammer* proposed in the EurAgEng Board Meeting April 12, 2003 in Rome, to make a further step 2003 in Hannover by a parallel English session "Young Engineers for Europe". This was realized, but in the meantime there was an important meeting of the EurAgEng Council June 6, 2003 in Leuven/Belgium in which *Prof. Auernhammer* (and the German delegates *Prof. Renius* and *Prof. Zaske*) now proposed a complete merger of the German VDI-MEG Conference "Landtechnik" with the "AgEng Conference" in the uneven years, ahead of Agritechnica. After critical discussions, the Council decided realizing this from 2007, supported by *Prof. Josse de Baerdemaeker* (Belgium, EurAgEng President 1996/98). This was a wise decision for both parties as the number of delegates increased to 659, later on even to about 1000. Our acknowledgement may address all engaged colleagues for contributing to this outstanding success story.

References

[1] Stroppel, A.: Vorgeschichte und Entstehung der VDI-Fachgruppe Landtechnik (Foundation of the VDI Branch of Agric. Engng.). In: Renius, K.Th. (ed.): 25 Jahre VDI-Fachgruppe Landtechnik, 1-15. Düsseldorf: VDI Fachgruppe Landtechnik 1983.

[2] Matthies, H.J.: Die strukturelle Entwicklung der deutschen Landtechnik im 20. Jahrhundert (Structure development of the German agricultural engineering during the 20th century). Plenary pesentation at Landtechnik Conference Braunschweig Oct. 10, 1995. Revised version in: Supplement of Landtechnik 51 (1996) No. 1, 2-9.

[3] Söhne, W.: 100 Jahre Willi Kloth (Willi Kloth born 100 years ago). Plenary presentation at the 49. Internationale Tagung Landtechnik, Braunschweig 1991.

[4] Söhne, W.: Professor Willi Kloth zum Gedenken (Commemorating Professor Willi Kloth). Grundl. Landtechnik 18 (1968) No. 1, 11-13.

[5] Söhne, W.: Theodor Stroppel zum 75. Geburtstag (Congratulating Theodor Stroppel on his 75. birthday). Grundl. Landtechnik 26 (1976) No. 4, 150.

[6] Söhne, W.: Theodor Stroppel †. Grundl. Landtechnik 31 (1981) No. 4, 142-143.

[7] Kloth, W.: Entwicklungsmöglichkeiten der Landtechnik von der Grundlagenforschung her gesehen (Development of agricultural engineering from the view of basic research). Grundl. Landtechnik 3 (1952), 5-11.

[8] Stroppel, Th.: Die Tagungen der Landmaschinen-Konstrukteure 1934 -1958. (Conferences of agric. engineering 1934-1958). Grundl. Landtechnik 10 (1958), 1-3.

[9] Kloth, W. and Th. Stroppel: Der Energiefluß im Zapfwellenbinder (Energy flow within the PTO driven binder), Teil I-III (Part I-III). Technik in der Landwirtschaft 13 (1932), No. 2, 49-50, No. 3, 66-69 and No. 4, 88-91 (see also Z. VDI 78 (1934) No. 21, 629-632 and Z. VDI 80 (1936) No. 4, 85-92).

[10] Bergmann, W.: Steifigkeit sperriger Bauteile (Stiffness of bulky design elements). Grundl. Landtechnik 1 (1951), 61-67.

[11] Söhne, W.: Das mechanische Verhalten des Ackerbodens bei Belastungen unter rollenden Rädern sowie bei der Bodenbearbeitung (Soil mechanics under loaded rolling tires and soil tillage mechanics). Grundl. Landtechnik 1 (1951), 87-94

[12] Matthies, H.J. et al.: Geschichte der Max-Eyth-Gesellschaft Agrartechnik im VDI (History of the Max-Eyth-Society of Agricultural Engineering, section of VDI). Düsseldorf: VDI-MEG 2006.

[13] Renius, K.Th.: 50 Jahre Agrartechnik im VDI – ein Stück Landtechnikgeschichte. (50 years of agric. engineering within VDI – a piece of agricultural engineering history). Der Goldene Pflug, 28 (2008), 4-12. Hohenheim: Soc. German Museum of Agriculture.

Electrified Utility Tractor

Wolfgang Breu, **Benno Pichlmaier**,
AGCO GmbH, Marktoberdorf

Abstract

Although the diesel engine will most probably remain the dominating power source for large scale tractors in the years to come, battery electric systems are showing a high potential for emission reduction and energy efficiency improvements in smaller utility tractors. There is an opportunity for new ideas and fresh thinking in agriculture following the progress of electric drive systems and battery technology.
Yet another aspect comes into play creating a supporting environment for electric machinery in agriculture: Many farmers - especially in Germany - have installed large scale solar power and biogas plants providing a perfect infrastructure for own on farm green energy use, especially as feeding electricity into the grid becomes less and less attractive.

The Fendt e100 battery electric utility tractor is the next step in a journey to create sustainable and professional farm machinery. Its heart is a 100 kWh high performance battery and a 50 kW rated power electric motor. New approaches for energy and temperature management go side by side with practical charging solutions and electric implement interfaces based on Isobus communication and the AEF standards.

Challenges

Since 2001 AGCO has been working on a broad range of electrification projects to build knowledge and prepare technology in this discipline. The starting point was a diesel-electric power drive project (“MELA”), followed by the E-RoGator diesel-electric drive sprayer in 2010, the Fendt X Concept tractor in 2013 and lately the electric driven rake Fendt Former 12555X in 2015. Electrical drivetrain components are available and meanwhile have become state of the art. The same applies to the electric high voltage safety systems, power electronics, brake choppers and other components.
The challenge for a fully electric tractor is the energy storage - in this case a battery - which has to be compact and light enough to run a smaller tractor up to five working hours with one charge under its typical load spectrum. It also has to deliver reliability for about up to 10.000

working hours within ten years as expected primary use life cycle estimation. The invest and overall operating costs have to be attractive for markets to reach significant volume and yield the benefits related to lower emissions and energy consumption in agriculture and also municipal use.

Tractor Concept

In the initial project phases various concepts were evaluated and some general decisions were made as follows:

- The rated power of the machine should be below 60 kW, expanding the actual Fendt product range.
- Customers should be able to use their existing conventional implements as well as electrified ones where beneficial and available.
- The charging technology needs to be practical like e.g. supporting a CEE (Commission on the Rules for the Approval of the Electrical Equipment) standard power outlet.
- The system voltage should be within the agreed AEF standard of 700 V DC +/- 10 %.

Some modules of the battery tractor share a common platform with the Fendt 200 P series (e.g. cab, hydraulics, transmission) perfectly supporting typical target applications: on a farm as a multipurpose machine and in cities as the flexible utility tractor for municipal use. By using a Fendt Vario gearbox for the driveline all components of the PTO, the hydraulics and other auxiliary drives can remain unchanged. Instead of a diesel engine, a 50 kW electric motor delivers superior torque and dynamic response with low noise and zero emission.
Battery, charging device, power electronics with integrated brake chopper and the high voltage coupling modules were all designed and packaged to fit under the hood with no compromise in visibility and styling.

Most cooling components are installed in front of the battery. An innovative heat pump system delivers all required fluid temperatures. The power distribution unit (PDU), which interlinks the high voltage components, is fixed next to the CCS Type 2 (Combined Charging System) connector on the left vehicle side. A DC/DC converter powers the 12 V circuit and charges a small 12 V battery used to buffer this low voltage circuit and support the startup process of all electronic systems. Two high voltage connectors and Isobus interfaces are installed on the tractor: one at the front and one at the rear.

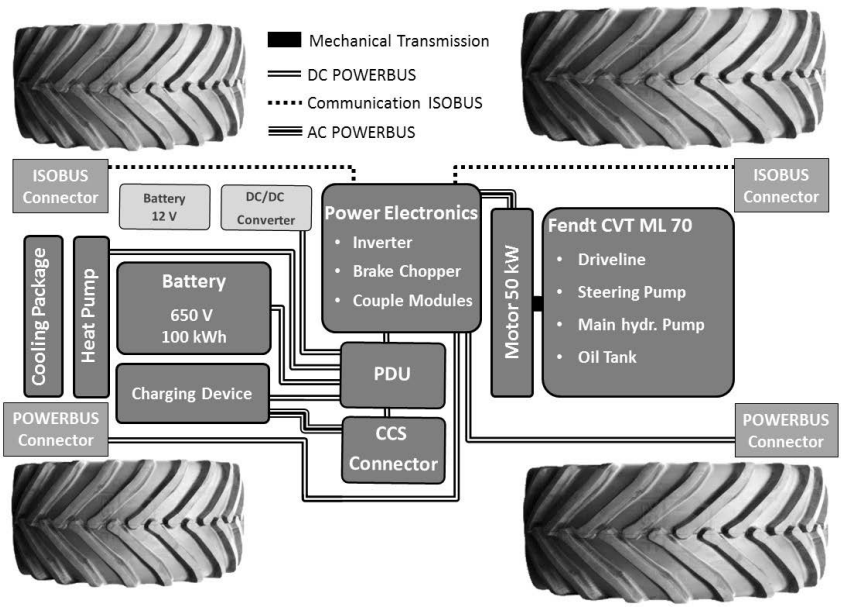

Fig. 1: Fendt e100 Vario system overview

Battery

Developing a battery, which meets the tough requirements of a mobile working machine as a main power source, was obviously one of the biggest challenges of the project. The vehicle specifications require a small and light battery, fast charging times, standard connectors, voltage level according to AEF Standard, an energy capacity of min 90 kWh and a high number of reliable charging cycles. On top of that, it has to deliver high electrical current in all relevant ambient temperature conditions.

As result a battery has been developed, which works at a voltage of 650 V, storing 100 kWh of electrical energy at a volume of 320 l and a weight of 590 kg. It is built out of Li-Ion 18650 cells. These are connected in a 180 (serial) times 46 (parallel) package. With this concept and the cell type, the costs could be brought down to an acceptable level while delivering the required performance values. The accumulator includes a battery management system (BMS), a safety concept and sophisticated temperature controls.

Thermo Management

A typical Li-Ion cell ideally needs to operate in a temperature range between 15 and 25 °C to guarantee a long battery lifetime and reach high numbers of charging cycles.

An innovative thermo management has been developed to actively cool and heat the system. The switchable heat pump efficiently supplies the tractor with cold or warm fluids as needed. It is also designed to recuperate energy from the installed heat exchangers to further improve energy efficiency.

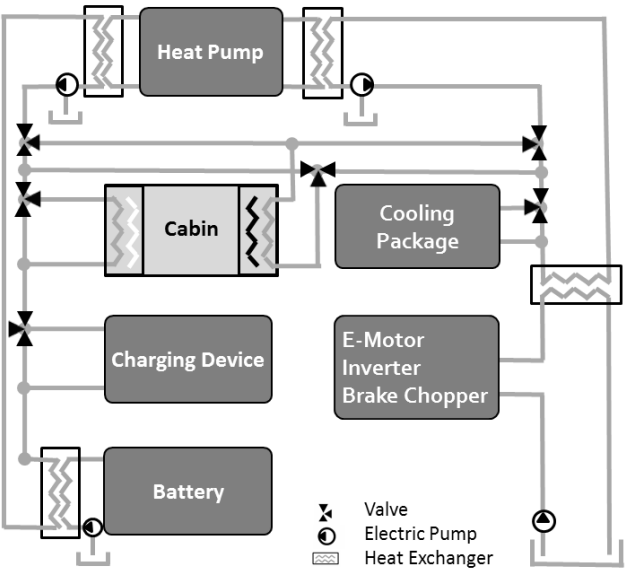

Fig. 2: Thermomanagement

Energy Management

A smart energy management supports the driver while working. The system permanently monitors energy flow, state of charge and remaining operating time for the current consumption level. With the aid of a specially developed smart device application, the operator is able to plan his working day and needed energy resources in a very simple way.

Charging

Perfectly charging a Li-Ion battery is a complex topic. Wrong charging can destroy a battery within a few cycles. Charging at too low or too high temperatures will cause a loss of battery lifetime. Furthermore the right charging current for the specific needs of each customer and operating schedule have to be identified. This clearly shows the importance of an elaborate charging management. The Fendt e100 offers various charging modes and powers:

- One phase power AC socket: 16 A @ 230 V (3.6 kW charging)
- Three phase AC socket: 32 A @ 400 V (22 kW charging)
- DC Power: 200 A @ 700 V (140 kW charging)

A suitable charging hardware and software is installed to handle these charging modes. The Fendt e100 uses the CCS Type 2 standard connector. The battery can be charged within 40 minutes at 200 A @ 700 V DC (quick charging station required) or within 5 hours at 32 A @ 400 V plugged into the CEE standard connector, available on nearly any farm.

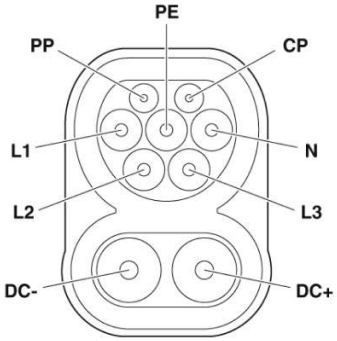

PP:	Proximity Pilot
CP:	Control Pilot
L1, L2, L3:	Three-Phase AC
PE:	Protect Earth
N:	Neutral
DC (-):	DC negative
DC (+):	DC positive

Fig. 3: Pinout CCS Type 2 Connector [1]

Benefits

The Fendt e100 is a fully electric utility tractor and has been designed to suit farming and forestry applications as well as municipal operations. A dedicated 100 kWh high performance battery pack was developed as well as an energy efficient thermo-management using a heat pump system.

The concept offers the following major benefits:

- Zero local emissions and less noise, perfect for municipal or on-farm operations.
- Reduced energy costs. Ready to use and store energy produced on the farm.
- Less maintenance and fluids, no exhaust after treatment systems.
- Less CO_2 emissions, down to zero when using renewable sources.
- Highly efficient driveline with energy recuperation.
- Superior driving dynamics and strong torque from zero rpm.
- Full compatibility to conventional implements while also providing electric interfaces.

---

[1] Phoenix Contact, www.phoenixcontact.com

Battery electric autonomous agricultural machine – Simulation of all operations on a Swedish farm

Jonas Engström, **Oscar Lagnelöf**,
RISE – Research Institute of Sweden,
Agrifood and Bioscience, Uppsala, Sweden

1. Abstract

In the project "Concept study battery-powered autonomous agricultural machine", an electric autonomous agricultural machine system has been compared with a conventional diesel tractor by simulating all machine activities in a field on an organic dairy farm of 200 hectares during one year (1). Combine Harvesting was not included.

The results show that it is possible to replace a conventional tractor (160 kW) with two autonomous battery powered machines (36 kW engine, 113 kWh battery) with 15% lower costs. Even better, energy consumption would be reduced by 58% and greenhouse gas emissions by 92% compared to diesel when energy consumption and greenhouse gas emissions from battery manufacturing were included. Furthermore, as an effect of a battery electric drivetrain, local emissions were avoided and the sound pollution greatly reduced. The high reduction in both energy usage and GWP emissions can be explained by the higher efficiency of electric power drivelines and by the very low greenhouse gas emissions and environmental impact in the Swedish electricity mix.

We also see that the weight of the conventional diesel tractor is more than four times the weight of the autonomous battery-powered, and that's only the tractor without any implements or payload. In the sensitivity calculations, changes in the cost of implements or driver / operator costs have the greatest impact on the total cost. It is also important for the total cost not to have a charger with too low power. The battery price, however, does not have such a big impact on the total cost.

Continued research is needed to verify the theoretical simulation by building a test platform where knowledge can be gathered about the problems and opportunities in practical work - both in the field of battery-electric operation and autonomous driving for agricultural machines.

2. Motivation

For a conventional agricultural tractor the main environmental effects originates from the usage phase, more specifically from the diesel exhausts. Emissions from machinery in Sweden have increased by about one third compared since 1990, according to the Swedish Environmental Protection Agency.

Today battery prices are sinking fast and the capacity is getting better and better. There are more and more battery cars on the streets. This study investigates the feasibility of a battery electric and autonomous tractor. By combining battery power with autonomous control the machine can work 24/7 and go to the charging station whenever needed, and then go back to work, and thus have high capacity despite the low energy capacity in a battery compared to a diesel tank.

3. Method

This study investigates the feasibility of a battery electric and autonomous tractor through simulation. The simulated farm is an organic dairy farm of 200 ha with 5 crops in the crop rotation cycle and traditional plough among the used implements. Only in-field machine operations are included in the simulations, except for transportation of inputs (manure, fertilizer, seeds etc.) and outputs (grain, silage bales etc.) to and from the farm.

The simulation model was built in MS Excel with each component on a separate sheet. Each activity on each crop is represented by a row in the model. In total, the model consists of 10 sheets that are linked to each other:

- **Battery**. The battery is modelled with charge cycles, service life, capacity, costs, as well as energy consumption and carbon dioxide emissions for the manufacture of the battery. Swedish electricity mix is used as a basis for the carbon dioxide emissions calculations (2) (3). For the battery a cell price of 360 Euro/kWh is used based on list prices, then costs for depreciation, interest, BMS and storage structure are added and a total price of 0,24 Euro/kWh and charge cycle is calculated in the model.
- **Charger**. Modelling of charger and electricity consumption with power, greenhouse gases and costs. Swedish electricity mix is used as a basis for the carbon dioxide emissions calculations. The cost for the charger is based on list prices and ends up in a cost of 0,04 Euro/kWh. In the simulation no other users than the machines on the

farm are using the charger, so the cost could be significantly lower if the cost is split with other users. (4)

- **Tractor**. Modelling of driver and operator, tractor costs, control system, electric driveline, weight and transport distance. Costs are based on list prices for tractors in Sweden with costs deducted for cabin and diesel engine and added for electric driveline and autonomous control system. (5) (6)
- **Field implements**. Modelling of implements pulled or powered by the tractor. Maximum power requirements, energy use, harvesting, maximum width, capacity and costs are calculated. Costs are based on list prices for implements in Sweden. (7)
- **Transportation**. Here wagons are modelled for transport and their collection, loading, unloading and distribution of goods. Max power requirements, energy use, load capacity and costs are calculated. Costs are based on list prices for implements in Sweden. (8)
- **Conditions**. The crop rotation, all the operations and the data needed to model these are collected here. For example, data is entered for all crops that need ploughing, so data from field implements is inserted and further calculated here. (9)
- **Capacity**. Modelling of how wide or large the implements can be given a certain power on the tractor and then in turn their capacity, cargo capacity, costs and energy consumption they have. Finally, costs and time requirements are calculated.
- **Timeliness**. The fictional timeliness costs are calculated that occur when the machines have too low capacity and an operation is being done too late. For example, if the sowing becomes delayed, a fictional cost for harvest loss occurs. In this sheet also modelling of dependencies between different operations is made, for example, that harrowing must be performed before sowing and if an earlier operation takes too long or starts too late, the start date for the next operation will be moved forward. (10)
- **Costs**. Compilation of costs and key figures for all operations.
- **Optimization and results**. Here are key ratios for the results of a modelled scenario presented. The optimization is done by using MS Excel and Evolutionary Solver.

4. Results

The simulation resulted in a distribution of energy usage between the different machine operations as shown in Fig. 1. The operation with the largest energy usage was ploughing and after that the transportation and spreading of slurry.

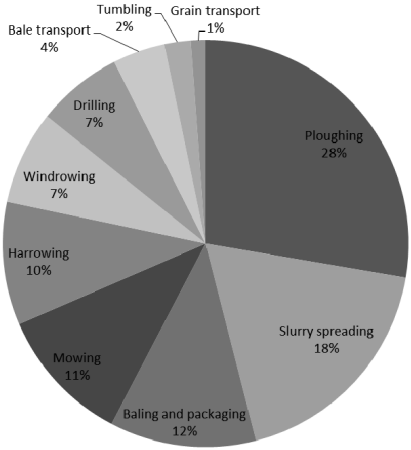

Fig. 1: Distribution of energy consumption during one year of machinery usage on the simulated farm. The combine harvester is excluded from the simulation due to the high specialisation.

When a conventional diesel powered tractor with a driver was modelled the economic optimum was one tractor of 160 kW. The optimum setup for an autonomous battery powered machine was two machines, each at 36 kW motor power and a battery capacity of 113 kWh, as shown in Table 1. The costs were estimated to be 15% lower for the two autonomous battery powered machines.

Table 1: Comparison of specifications between two autonomous controlled and battery powered machines and one diesel powered and driver controlled machine managing the farms all task during one year.

Alternative	Number of machines	Power per machine (kW)	Machine hours per machine (hours/ year)	Energy reservoir (kWh)	Work hours per day (h)	Total cost (SEK / year)
Diesel powered with driver	1	160	545	2 940	10	655 800
Autonomous battery powered	2	36	995	113	24	559 900

The different costs for the modelled machines had a distribution as shown in Fig. 2. The single largest cost for the diesel machine was the implements, followed by the operator and the tractor itself. For the autonomous battery powered machines the single largest cost was also the implements followed by the machine and the battery costs.

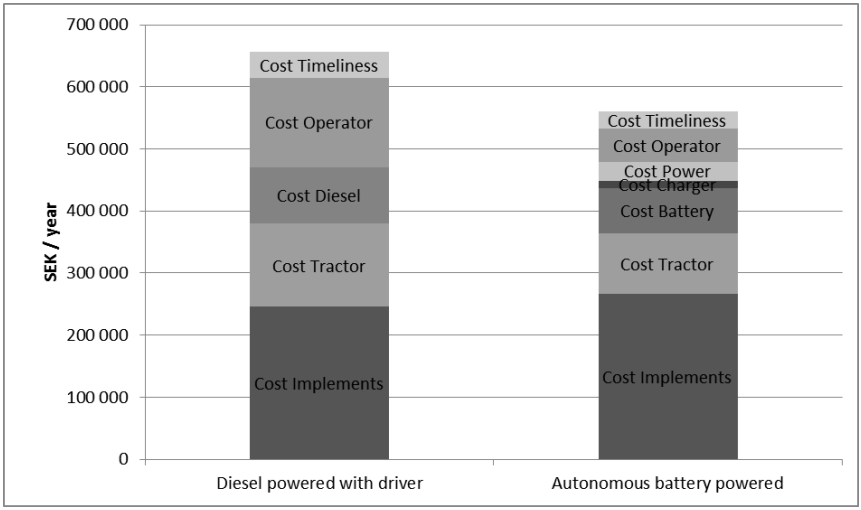

Fig. 2: Comparison of costs between two autonomous controlled and battery powered machines and one diesel powered and driver controlled machine managing the farms all task during one year.

When comparing the energy usage for the different set ups the diesel powered machine needed almost 90 MWh of energy for one year, while the autonomous battery powered machines ended up with a usage of 37 MWh (when adding the energy needed for the battery production). That is a reduction of 58% in energy usage.

One big driver for changing to a battery electric driveline is the big potential in reducing the carbon dioxide footprint of using the machine. In this simulation the reduction of GWP was 92%, even when adding the emissions when producing the battery. The electricity needed for the production of the battery and for charging the machines is assumed to be Swedish electricity mix. If the battery production is powered with average European electricity mix, then the reduction in GWP is 82%.

Table 2: Energy usage and GWP for diesel powered and driver controlled compared to autonomous controlled and battery powered.

Alternatives	Energy usage (kWh / year)	Relative diff. energy usage	GWP (100y, kg / year)	Relative diff. GWP
Diesel powered and driver controlled	89 230	0%	23 650	0%
Autonomous battery powered excl. battery manufacturing	33 860	62%	440	98%
Autonomous battery powered incl. battery manufacturing (European electricity mix)	37 330	58%	4 310	82%
Autonomous battery powered incl. battery manufacturing (Swedish electricity mix)	37 330	58%	1 986	92%

Sensitivity analysis

Several scenarios were simulated where different input figures were changed.

- **Battery price**. A cell price of 50% of the baseline price of 492 USD/ kWh results in a total cost decrease of 4%. A 100% higher cell price than the baseline results in a total cost increase of 12%.
- **Implement cost**. An implement cost at 50% of the baseline price results in a total cost decrease of 25 %. An implement cost at 100% higher than the baseline results in a total cost increase of 48 %.
- **Distance charge station to field**. In the baseline simulation the distance between the field and charger was 4 km and the cost reduction when using the autonomous system was 15%. If the distance was decreased to 2 km the relative cost would increase to 16%, and if the distance would increase to 6 km the relative cost would decrease to 12%.
- **Charger power**. If the charger power is lowered to 25 kW, than the total cost would increase by 30%, compared to the baseline charger power of 100 kW. If the charger power would increase to 300kW than the cost would roughly be the same.
- **If the battery powered tractor would not be autonomous** and instead have a driver then the cost would increase 61% compared to autonomously controlled ma-

chines. The optimum power would also increase to 94 kW and the battery capacity to 234 kWh.

- **If the diesel powered tractor would not have a driver** and instead be autonomous then the optimum power would be 92 kW and end up in a reduction of 22% compared to the driver controlled diesel powered tractor.

5. Conclusions

The results show that it is possible to replace a conventional tractor (160 kW) with two autonomous battery powered machines (36 kW engine, 113 kWh battery) with 15% lower costs. Even better, energy consumption would be reduced by 58% and greenhouse gas emissions by 92% compared to diesel when energy consumption and greenhouse gas emissions from battery manufacturing were included.

Furthermore local emissions would be avoided and the sound pollution greatly reduced. The high reduction in both energy usage and GWP emissions can be explained by the higher efficiency of electric power drivelines and by the very low greenhouse gas emissions and environmental impact in the Swedish electricity mix.

6. References

(1) Engström och Lagnelöf, 2017. Batteridriven autonom jordbruksmaskin – Simulering av maskinaktiviteter på en svensk gård. SP Rapport 2017:27, RISE Jordbruk och Livsmedel, ISSN 0284-5172, Uppsala 2017

(2) Gode. J, Martinsson. F, Hagberg. L, Öman. A, Höglund. J, Palm. D, 2011. Miljöfaktaboken 2011- Uppskattade emissionsfaktorer för bränslen, el, värme och transporter; Värmeforsk ISSN 1653-1248.

(3) Romare, M. Dahllöf, L., 2017. The Life Cycle Energy Consumption and Greenhouse Gas Emissions from Lithium-Ion Batteries, IVL Swedish Environmental Research Institute , Report C 243, ISBN 978-91-88319-60-9

(4) Siemens, 2016b. DC Plug-in Chargers – Solutions for fast charging of EVs; Siemens, S.A. Mobility Division – Urban Transport

(5) Maskinkalkylgruppen, 2017. Maskinkostnader 2017. HIR Skåne och LRF Konsult m fl, Linköping

(6) DLG, 2017. DLG Test Center Technology and Farm Inputs, DLG (Deutsche Landwirtschafts-Gesellschaft – German Agricultural Society. Groß-Umstadt, Tyskland

(7) Lindgren et al, 2002. Jordbruks- och anläggningsmaskiners motorbelastning och avgasemissioner. Rapport Lantbruk och industri nr 308, Jordbrukstekniska institutet, Uppsala

(8) Engström et al, 2015. Energieffektivisering av jordbrukets logistik – pilotprojekt för att undersöka potentialer, Rapport 441, Lantbruk & Industri. JTI – Institutet för jordbruks- och miljöteknik, Uppsala

(9) Bovin, 1999. Växtföljd i ekologiskt lantbruk. Råd i praktiken. Jordbruksinformation 1999:16. Jordbruksverket (SJV), Jönköping

(10) Gunnarsson et al, 2002. Optimisation of field machinery for an arable farm converting to organic farming. Agricultural systems 80 (2004) 85-103

Electric traction drive on a plough

More power for the driveline

Dipl.-Ing.(FH) **Rainer Bumberger**,
PÖTTINGER Landtechnik, Grieskirchen;
Dipl.-Ing.(FH) **Wolfgang Klinger**, ZF Friedrichshafen AG, Passau;
Dipl.-Ing. **Decho Botev**, John Deere, Mannheim;

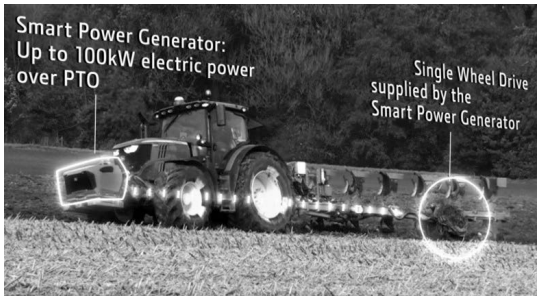

Abstract

Pulling force is one of the main criteria to match a plough with a tractor. To find the right combination, the following points have to be considered:

Tractor: weight, right ballasting, wheel width, engine power, lifting force capability

Plough: number of furrows, working width/depth, weight

The farmer tries to optimize the system by combining his tractor with a highly efficient plough, and ballasting the tractor correctly, always having the tractor slip in mind, in order to optimize working quality and efficiency.

Providing the opportunity to drive an additional (fifth) wheel on the plough to help with traction, offers new possibilities:

- Capability to pull up to two more furrows with the same tractor, keeping the same low slippage, but increasing efficiency up to 33%
- Capability to utilize Engine-Power-Boost for traction already at typical ploughing speed
- Reduced soil compaction due to decreased ballast need on the tractor

- Energy saving:
  - using Power-Boost, the engine can be run at lower speed
  - reduced number of field crossing

Solution approach

The PTO driven John Deere “Smart Power Generator Module” can be mounted to the front of the tractor. The Module does not only provide electric power to the system. It also provides inverters to control the plough drive according to the ISOBUS commands from the job controller on the plough.

For the traction management on the plough, ZF Friedrichshafen AG developed an electrical single-wheel drive named GPE50. A two stage planetary gear box ensures a high power density to fulfill the traction requirements. The 400Vrms induction motor is integrated in the wheel hub unit to save space.

Robust and proven design thanks to a new combination of well-known components ensure improved traction, increased driving comfort and reduced soil compaction.

Customer benefits

Efficient pulling force and traction are the most important criteria for a tractor-plough combination.

For this purpose, the tractor must be chosen in such a way that on the one hand enough power is available, but on the other hand the tire width and ballasting are correspondingly matched, so that the plough can be optimally used.

The goal is a very good working quality at the lowest possible cost.

Trying to optimize the system, the following points have to be considered:

- Tractor: weight, optimal ballasting, wheel width, engine power, pulling force capability
- Plough: number of furrows, working width/depth, weight

Only the consideration of all parameters brings the farmer to the optimal combination and a higher efficiency.

The slip reduction, effected by the improved traction, results in an increased productivity. The increase consists on the optimized working quality and / or the possibility of using up to two additional plough shares. The result is a higher area performance, reduced personnel costs and less fuel consumption.

Fuel saving and thus reduction of CO2 emissions:

In a 10-hectare field with a length of 500m and a width of 200m, the use of a two shares larger plough can save 9.3km driving distance in the field. Calculating the savings to an average total life of a plough with 8.000ha would mean a cost saving of 14.074 EUR.

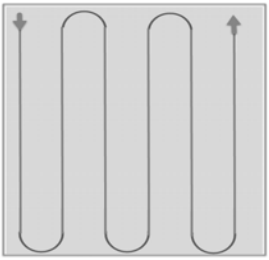

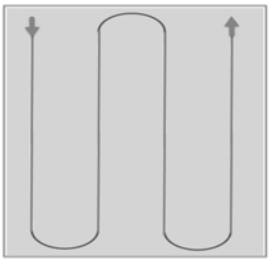

Field A		Field B	
500	m length	500	m length
200	m width	200	m width
10	ha	10	ha
45	cm furrow width	45	cm furrow width
6	Furrows	8	Furrows
2,7	m working width	3,6	m working width
74,1	Field turns	55,6	Field turns
37,0	km distance traveled in the field	27,8	km distance traveled in the field

	distance traveled in the field A-B	9,3	km

over lifetime

29630	km distance traveled	22222	km distance traveled

	reduced distance traveled A-B	7407	km

Running tractor without plough	7407	km
Diesel consumption only tractor without plough	1,9	Liter/km (1 EUR/Liter)
Cost saving over lifetime	14.074	€

Reduced personnel costs:

Due to the higher area performance, less manpower is required for the activity of ploughing. Calculated to approximately 4.500 hours of total lifetime of an 8-furrow plough with medium heavy soil, this results in a time saving of around 25% with a simultaneous area increase of about 33%. At an assumed rate of 15 EUR / h, the savings of 16.875 EUR would be for personnel costs over the entire lifetime of the plough.

Increasing performance		
before	6	Furrows
after	8	Furrows
increased area performance	33,3	%
increased time saving	25,0	%

Reduced personal costs		
Personal costs	15	EUR/h
Lifetime (4500h * 25%)	1125	h
	16.875 €	

Total savings

Reduced personal costs at 25€/h	16.875 €
Reduced Diesel consumption	14.074 €
	30.949 €

The electrical transmission of the power to the fifth driving wheel is not an additional load to the tractor transmission and an increased motor boost in the plough mode is possible. The traction support provides additional driving stability and performance, which is clearly noticeable in particular uphill.

Additional benefit:

Ploughing where others can't work anymore. In addition to permanent support and optimization, this concept also offers the possibility of ploughing in situations where a conventional plough is limited. E.g. a moist area in the field or strongly changing soil conditions.

John Deere Smart Power Generator:

The Smart Power Generator is a PTO-driven device, mounted to the tractor front hitch. It converts the mechanical PTO power to electrical power and can provide up to 100kW continuously. An oil cooled three-phase permanent magnet synchronous machine is used as generator. The e-machine speed is matched to the PTO shaft speed over a mechanical gearbox.

The Smart Power Generator is cooled by a standalone air-to-water and air-to-oil cooling package. There is no need for connection to the tractor cooling circuit or to the tractor hydraulic system.

The module is equipped with four water cooled inverters. One of them controls the generator and ensures stable DC voltage in the common DC link. The other three inverters can control implement-mounted e-machines, eliminating the need for inverters on the implement. Therefore the module can drive up to three motors. In the plough application only one e-drive is used.

Standardized hybrid AEF[1] connectors and cables are used to connect implement e-machines to the Smart Power Generator. The AEF connector has a power sockets for the three-phase e-drive and a signal interface for real-time high-speed communication. The high speed bus is used for e-machine control. In addition the Smart Power Generator has an ISOBUS interface. This enables the plough job controller to control its traction e-drive via ISOBUS, while the operation strategy of the Smart Power Generator is seamlessly integrated into the tractor drive strategy.

[1] (AEF stays for Agricultural Industry Electronics Foundation).

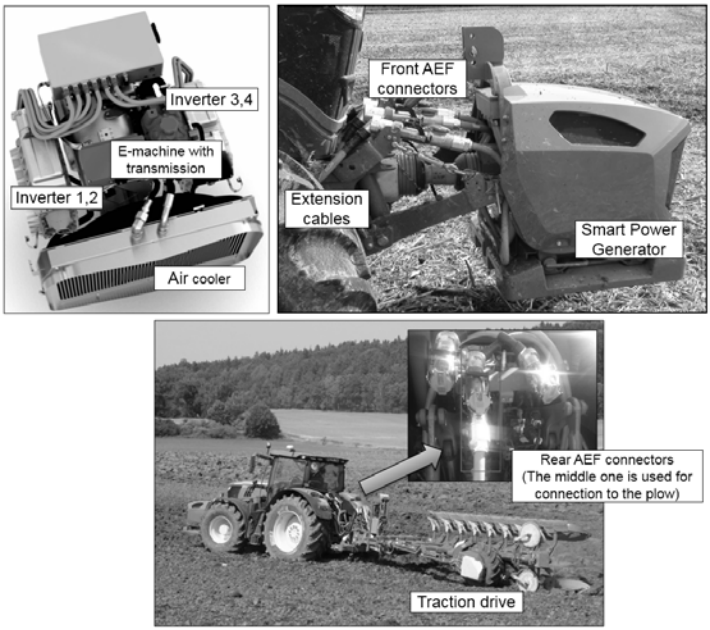

John Deere Smart Power Generator - Component Overview

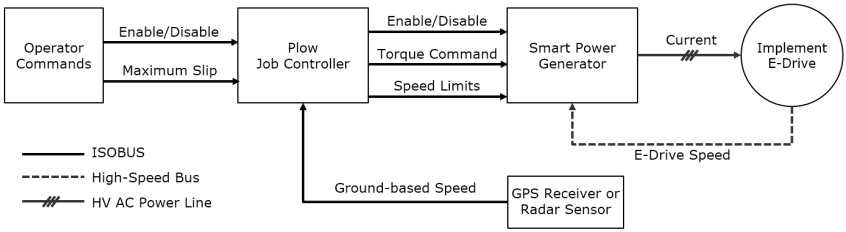

John Deere Smart Power Generator and Electric Traction Drive on a Plough - Signal Flow Diagram

The GPE50 eTrac drive from ZF:

The above shown increase of performance and productivity will promote a more widespread use of electric systems and requires a significant traction force at the plough attachment. To provide a large traction torque during field operation a high gearbox ratio has been selected.
Further key challenges in agricultural applications are keeping the initial investment reasonably low and the availability high. This has been achieved by using fully industrialized and proven components with the right volumes.

The electric motor itself is a high-speed asynchronous motor with a high power density. The motor comes with an internal air circulation cooling. Additionally an optional fluid cooling system is available to enlarge the performance even more, wherever necessary. Furthermore the motor is already proved under road service conditions and provides secure connection under vibration stress and excellent tightness against environmental influences.

To transfer the traction torque safely to the wheel an existing construction machinery drive hub is used with an integrated multidisc brake set and gear stage. This subcomponent assembly is already applied in comparable environment and operation conditions over a long time and in huge numbers. Therefore gained product experience can be transferred directly to the new plough application.
A second high speed transmission stage is added to achieve the required high ratio. This transmission stage is designed for durable, quiet running at high-speed use.

Consequently the use of existing industrialized components has given the opportunity to provide a completely new electric single drive which can withstand harsh agricultural application requirements. Furthermore time to market can be put to the smallest possible limit, due to existing production capabilities.

Technical data	GPE50
Output torque max. [Nm]	16.500
Continuous motor power [kW]	50
Gearbox ratio [-]	36
Wheel speed max. [rpm]	280
Wheel load max. [kg]	5.000

Electrified Front-Wheel Drive Concepts for Tractors Designed for Improved Traction Functions

Dipl.-Ing. **Raphael Himmelsbach**, Dr.-Ing. **Bastian Volpert**,
ZF Friedrichshafen AG, Friedrichshafen;
Dr.-Ing. **Karl Grad**, ZF Friedrichshafen AG, Passau

Abstract

State-of-the-art four-wheel drives (4WD) for tractors with an 4WD clutch but no differential between front and rear axle have good traction capability at a reasonable cost, but disadvantages regarding e.g. tire wear, driving behavior and tension in the driveline. With improved front-wheel drive concepts and the good controllability provided by electric drives, these disadvantages can be eliminated. Alternatively, a more precise, intelligent 4WD clutch actuation or a longitudinal differential could produce an improvement, but both options have clear limitations. Our solution, presented here, is an adjustable front-wheel drive. This article explains the advantages of this compared to a standard driveline and to a tractor with the abovementioned alternative enhancements. We present two implementation options, each integrated into the vehicle driveline architecture in a different way and with different requirements in terms of the electrical supply system.

Introduction and state of the art

Over time, 4WD has become an established feature in tractor drivelines. Both in Europe and other regions, today's mid- to high-performance tractors are almost exclusively supplied and distributed with 4WD. Historically, the four-wheel driveline consists of a rigid coupling between the front and rear axle along with an four-wheel clutch and the respective transverse locking differentials. This rigid coupling provides good traction performance, as it distributes the transmission input torque to the axles based on external boundary conditions. However, it also leads to tension in the driveline and has drawbacks in terms of tire wear, soil protection and vehicle handling [1]. The rigid coupling is cheap to produce and also makes it possible to add a four-wheel braking system at a reasonable cost.

When the four-wheel clutch is engaged, current tractor models generally have a front wheel lead of 2–5%. The lead built into the design takes account of the fact that over vehicle service life, the accelerated wear on the smaller front wheels produces a lag in the speed ratio. The lead is calculated using the ratio of the wheel speeds, and usually the SRI (speed radius

index) of the tires. The actual, effective lead is a factor of tire tolerance, wear and deflection as well as cornering. Depending on the manufacturer and the tires, aside from the customary production tolerances, the rolling circumference differs to a varying extent from a theoretical one calculated using the SRI. In short, under operating conditions there can be a sustained lead variation of up to ±10% for straight-on driving [2]. In addition, it should be possible to increase the lead, at least briefly, by around another 27% for tension-free four-wheel cornering. This value, depending on vehicle geometry and steering angle, is for a 200 hp class reference tractor and is within accepted limits.

To make operation more convenient, the shift system for the four-wheel clutch was automated. Automatic four-wheel shifting based on steering angle and speed, as well as automatic activation on braking, is now standard. Activation based on slip and load condition has also been introduced [3]. However, continuously improved automatic shifting in combination with an “on or off” four-wheel clutch can only shift between rigid four-wheel coupling and straightforward rear-axle drive. Tension-free 4WD on firm subsoil, for example when transporting loads or when steering, is unachievable with an automatic clutch.

It improves the tractor’s maneuverability by making the shift system dependent on the steering angle, but doesn’t provide 4WD on tight turns. It is possible to resolve this with additional gears on the front axle. The most well-known of these systems is the Kubota Bi-Speed, which has two gear ratios for the front axle. In Japan especially, where fields are often small, this is very common as it can improve maneuverability in comparison with 4WD with a disengaged four-wheel clutch. However, this does not counter the other drawbacks of a rigid axle coupling.

Another option for preventing driveline tension is an interaxle differential. With highly variable axle loads and a constant torque ratio in the differential, this often means that the differential is locked for longer, which has an adverse effect on its cost-benefit ratio.

Potential solutions for variable torque distribution between front and rear axle

Variable torque distribution between the front and rear axle can solve the abovementioned problems. Possible technical solutions are shown in Figure 1.

A mechanical interaxle differential always comes with the drawback of a fixed torque ratio, which means that a solution such as a superposition gear is required to produce the variability. This type of superimposed axle drive can also be electric, consisting of a motor and generator. Changing axle loads require more power to be constantly redirected between the two axles. Another option for controlling torque distribution in conjunction with a mechanical differential is power dissipation, e.g. by brake actuation which converts drive power to heat.

However, as this reduces maximum output power, it is not practical for sustained equalization on tractors.

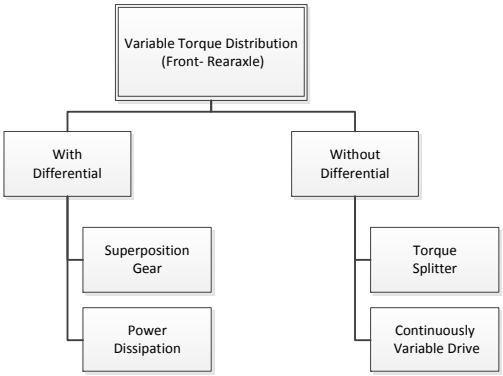

Fig. 1: Options for variable torque distribution between front and rear axle

There are other variable torque distribution concepts which can be incorporated in the torque splitter assembly. Using individual clutches on each axle is one option. Another is the LT3 concept [4], consisting of four controllable hydraulic final drives on the wheel. A controlled four-wheel clutch can also influence torque distribution. This is often used in AWD passenger car drivelines (e.g. Haldex clutch) and more recently, in a few cases, in tractors [5]. However, this can only vary torque distribution to a certain extent, as it is not possible to increase the speed of the front wheels. Generally speaking, torque splitter concepts use the clutch or a hydraulic throttle in the final drive to handle equalization of wheel circumferential speed differences. Consequently, continuous adjustment is disadvantageous because it reduces driveline efficiency.

ZF solutions

Our solution to this issue is a continuously variable front axle drive which can be implemented with or without power splitting [2]. A progression on this is individually controlled front wheels [6], but the advantages do not justify the additional cost. The variability required on the front axle can be achieved with a hydraulic or electric drive. Electric drives are well-suited to driveline traction operations based on their advantages in terms of efficiency and controllability as well as very easy integration in today's system architectures. Moreover, the power electronics on electric drives does an excellent job when it comes to automatic torque sens-

ing. Whether or not the drive is better with power splitting depends on a number of factors. The electric power requirement is a key differentiator between the two concepts.

Image 2 shows the electric power as a factor of the lead required. On a power-split system, this characteristic curve is dependent on the design of the lockup point, in this case during synchronous circumferential speeds. Based on this definition, the power required is a factor of spreading, i.e. the speeds required, not design [7]. Using this in motor and generator operation can reduce continuous power to around 10% compared with an all-electric front axle. For cornering, a maximum of 27% is required for brief periods.

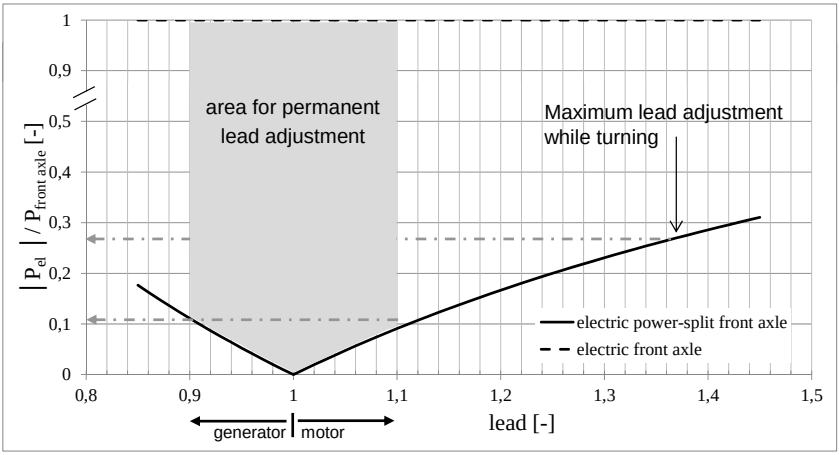

Fig. 2: Electric power of a power-split front-wheel drive as a factor of required lead

An all-electric front-wheel drive has to provide all the power, including short-term torque peaks, which means there is no choice but to equip the tractor with a correspondingly powerful high voltage electrical system. An additional option is a rigid four-wheel coupling to the rear axle, which is beneficial in terms of four-wheel braking (image 3, left). Consequently, the traction motor can be smaller, since a variable setting provides little benefit in situations with higher tractive effort in the field combined with relatively high slip values.

As shown in image 4, we developed a slimline electric motor for this purpose. This type of drive delivers additional functionality. It can provide additional drive boost power without loading the transmission. This assumes that the generator is fitted in front of the transmission input and therefore the power does not flow through the transmission. Furthermore, a battery enables hybrid functions such as regenerative braking, thus reducing the load on the service

brake. This type of architecture can also help reduce the number of transmission construction kit variants.

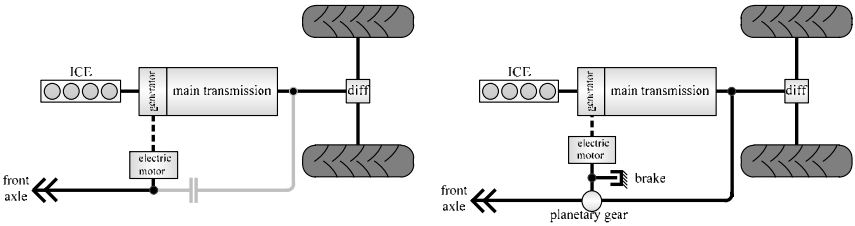

Fig. 3: Continuously variable front-wheel drive – left: without power splitting; right: with power splitting

An electromechanical power-split system (image 3, right) only has to provide enough output to equalize differing wheel circumferential speeds rather than powering the whole axle. This power level, being lower, can be covered by an inexpensive 48 volt system which will still have enough output to feed other 48 V consumers on the tractor or implements. The power-split implementation requires a planetary gear, which is usually good to integrate in place of the four-wheel clutch in the tractor transmission.

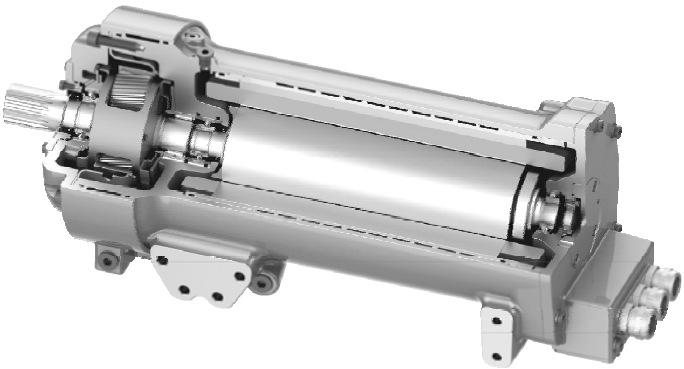

Fig. 4: Electric central drive for front axle with reduction gear stage

Image 5 shows the integration in a ZF continuously variable transmission. We also succeeded in integrating an additional brake for a four-wheel braking system into the existing installation space. The oil-cooled electric motor integrated in the transmission is connected to the planetary gear with a pair of spur gears featuring an extra ratio. This reduces torque demand

on the electric motor. We also installed oil separators to reduce churning losses and to take account of the electric motor's complex cooling circuit.

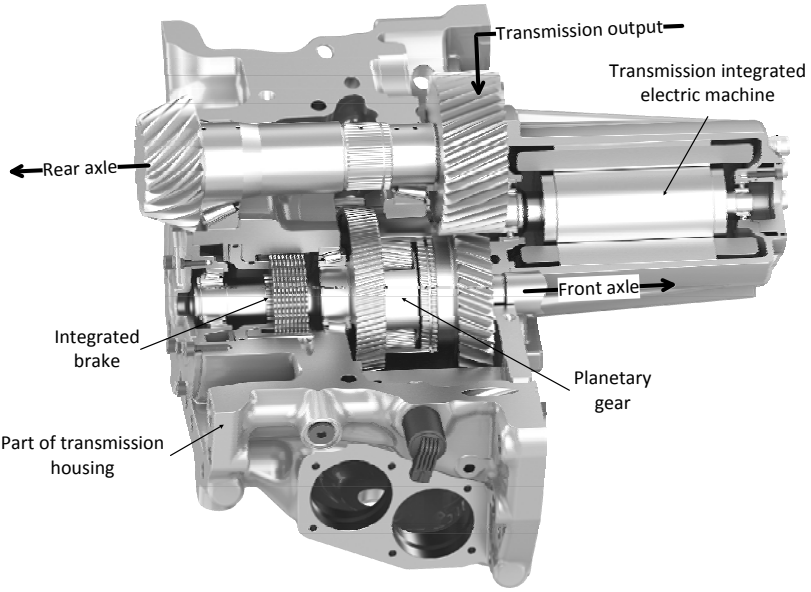

Fig. 5: Power-split front-wheel drive integrated in a ZF transmission

Advantages for the customer

The benefits of these solutions counter the abovementioned issues around a rigid four-wheel coupling. The resulting advantages are:

- Comfortable, permanent 4WD
- Reduced tire wear
- Improved soil protection
- Increased driving safety
- Smaller turning circle
- Reduced fuel consumption

In terms of steering, the speed of the front axle can be increased and the turning radius thus be reduced. Controlling the front axle can also provide full-time 4WD, because for example, the drive suffers no tension even when pulling trailers on the road. Certain situations are too great a challenge for today's automatic 4WD systems and therefore, in practice, require a manual shift. Generally speaking, continuously controlled 4WD reduces driver strain. It can also reduce tire wear as well as improving soil protection and driving safety.

Traction efficiency accounts for a large proportion of losses, from the internal combustion engine to tractive force on the rear of the tractor [8]. This is especially poor if tension occurs in the driveline, which can be the case if slip values are low, i.e. on firm subsoil or with low tractive forces. Equal wheel circumferential speeds always deliver near-optimum traction efficiency under various boundary conditions, preventing tension and thus also reactive power in the driveline at all times [1]. The two solutions for full-time front axle control described in this article can automatically reduce fuel consumption and improve drawbar power throughout the vehicle lifecycle.

Bibliography

[1] Brenninger, M.: Stufenlos geregelter Allradantrieb für Traktoren, TU Munich, Dissertation, 2003.

[2] Grad, K.: Zur Steuerung und Regelung des Allradantriebs bei Traktoren, TU Munich, Dissertation, 1997.

[3] Knechtges, H.; Renius, K. Th.: Gesamtentwicklung Traktoren. In: Frerichs, L. (Ed.): Yearbook Agicultural Engineering 2015. Braunschweig: Institute of Mobile Machines and Commercial Vehicles, 2016.

[4] Engelmann, D.; Müller, W.; Geimer, M.: Project “Line Traction 3” - Mechanical driveline with active wheel hubs, 4th International VDI Conference - Transmission in mobile machines, Friedrichshafen, 2016. In: VDI-Berichte 2276. Düsseldorf: VDI Publishing, 2016.

[5] Geimer, M.; Renius, K. Th.; Stirnimann, R.: Motoren und Getriebe bei Traktoren. In: Frerichs, L. (Ed.): Yearbook Agricultural Engineering 2015. Braunschweig: Institute of Mobile Machines and Commercial Vehicles, 2016.

[6] Woopen, T.: Adaptive Mild Hybrid Powertrain for Four-wheel Driven Tractors, ATZoffhighway, 02/2017

[7] Reick, B. et al.: Analyse eines beispielhaften elektrisch leistungsverzweigten Stufenlosgetriebes (ECVT). 74th International Conference Land.Technik, Cologne, 2016. In: VDI-Berichte 2273. Düsseldorf: VDI Publishing, 2016.

[8] Pichelmaier, B.: Traktionsmanagement für Traktoren, TU Munich, Dissertation, 2012

Automatic plant disease diagnosis using mobile capture devices

Alexander Johannes, **Maximilian Seitz**,
BASF SE, Limburgerhof

Abstract

Disease diagnosis of early symptoms is a vital ingredient in integrated pest management strategies. Early phytosanitary treatment minimizes yield losses and increases the efficacy and efficiency of the treatments. If solutions can be optimized to achieve early detection, any potential yield losses could be minimized. In addition, the need for an early disease treatment is becoming more relevant with increasing appearances of resistance pathogen strains, such as rusts, in Europe. Furthermore, unexpected annual weather variations and the effects of climate change tend to add uncertainty to the decision making in disease management, also inducing high incidences and severe outbreaks of new endemic diseases (Coackley et al., 19999; Garrett et al. 2007). Hence, it is important for research and crop protection advisories to expand their portfolio of tools to help farmers detect plant diseases as early as possible, avoiding any further losses.

Past research has tried to address automated plant disease identification by computerized visual diagnostic methods appropriate for the identification and evaluation of the spread of a disease over a certain region. These fail, however, when trying to detect early symptoms, as they rely on airborne imagery of the disease in its later stage for detection.

The use of automated identification systems based in images can facilitate the early detection of diseases for farmers and technicians. Unfortunately, such systems perform poorly under real field conditions when run on mobile devices. This project provides insight into a trainable system to identify plant diseases by image processing based the previously established techniques in combination with statistical inference methods. The resulting algorithm has been validated for three different kinds of European endemic wheat diseases (Puccinia recondita f.sp. tritici, Puccinia striiformis, Septoria tritici, Pyrenphora tritici-repentis). It has been deployed on a real smartphone application under real field conditions in a pilot study located in Spain and Germany over more than 36 plant varieties. Results from real field tests received AuCs (Area under the Receiver Operating Characteristic –ROC– Curve (Fawcett T. 2006)) of higher than 0.8 when global color constancy on the image were applied by means

of the developed algorithm, succeeding to provide real time conditions and making it possible to cope with a number of different diseases at once. The AuC decreased to 0.7 when a no color constancy algorithm was applied on the processing workflow. However, using a shades of gray color constancy algorithm, AuC values of higher than 0.8 could be assured. We also validated the algorithms performance when dealing with early diseases. Although a small decrease in performance could be observed when dealing with early diseases, the algorithm could demonstrate very similar performances for early and late diseases.

The preliminary hot-spot detection and its ulterior description by color and textural descriptors allow for real time performance, since only suspicious regions are trained and described by the higher-level classifiers and descriptors.

The presented image processing technology opens up new possibilities for the detection of weeds and diseases in their early stages. In a next step, 300 agronomists and farmers are going to test the technology under practical conditions. Based on the analysis of an In-App tracking and an online survey, any necessary adjustments for future versions can be easily collected. Furthermore, this will help to extend treatment strategies based on the system's generated detection result. By following a multi-disciplinary approach, a technology for the agricultural practice is established that could help to minimize yield losses and therefore guarantee food security in the upcoming years.

1. Introduction

The identification of early symptoms for diseases is one of the major milestones for the crop protection industry but also for two social and environmental challenges: increasing the yield or minimizing yield losses to ensure food security for 9 billion people in 2050 and increasing the efficacy of the phytosanitary treatments to reduce their use.

Agrios (2006) divides the measurement of plant diseases into three parts: Measuring of the incidence, severity and yield loss. Incidence is described as the proportion of the plant which is diseased. The severity is specified as proportion of area which is infected. And the yield loss is the share of the harvest which is destroyed or which has an effect to the quality of the produce. Even though severity and yield loss are of a much bigger importance for the grower, the incidence of a disease is much more difficult to measure and in some cases not possible until it is too late due to incipient incidence that is not detected by the farmers. It is necessary to take into account that the detection of early symptoms is a usual threshold considered for integrated pest management strategies of diseases in cereals. Consequently, research needs to focus on activities that can identify diseases in an early stage, so that targeted activities can be triggered, symptoms can be treated and even epidemics can be prevented. If

solutions can be advanced to achieve this, the corresponding yield losses could be minimized. The annual yield loss of 20 – 40% of agricultural productivity is therefore due to impacts of pathogens, animal and plant weeds (Oerke, 2006). Studies have shown that yield losses per year accumulate up to $ 5 billion in the US (Savary et al., 2012). Another example for leaf rust epidemics and their respective impact on losses during 2001 – 2003 in Mexico equated $ 32 million in durum wheat (Herrera-Foessel et al., 2006). Therefore, the use of resistant varieties or crop protection applications can minimize the loss risk significantly as it is shown by a survey of Chai et al. (2015) where a decrease of yield losses could be verified between 1985 and 1999 due to the usage of resistant varieties and fungicides. Nevertheless, an increase on the yield loss can be observed since 2000 due to new rust races. In Europe new multi-virulent rust strains appeared in 2011. Several wheat varieties became affected and the new strains seems to be very aggressive based on field observations. These recently appeared races named as Warrior and Warrior (-) (data from Global Rust Reference Center, 2017) have changed European situation and urged research to elaborate on tools to help farmers detect the early presence of rust in the field avoiding to increase losses. Unexpected annual weather variation and the effects of climate change for diseases management tend to add uncertainty to decision making and inducing high incidence and severe outbreaks of endemic diseases unknown before (Coakley et al., 1999; Garrett et al., 2007).

As new pathotypes are emerging, it is essential to detect upcoming diseases in an early stage to prevent or minimize yield losses. Especially an early detection is almost impossible and requires very specific knowledge, as symptoms are not yet well developed. There is a need to provide image processing based plant disease identification, to diagnose diseases in their early development stages to be able to react in time with crop protection applications. At the same time, it is necessary to increase the reliability of disease identification and validate it on real environment. Other sensor devices for direct or indirect color variation detection could provide useful information as severity and spreading in the plant or crop but they do not produce enough information to diagnose a specific damage in the plant, including biotic (disease, pest and weeds) and abiotic hazards.

This paper gives an insight into a trainable system to identify plant diseases which has been validated in three European endemic wheat diseases by image processing based techniques in combination with statistical inference methods to solve the above mentioned technical problem. Plant disease identification as used herein includes the determination of a probability that a particular disease is present. Typically, plant diseases cause characteristic damage

on the surface of plant elements (e.g. leaf, root, blossom, fruit, flower, stem, etc.). Therefore, characteristic symptoms become visible on some elements of an infected plant.

2. Related Work

Different research has addressed automated plant disease identification by computerized visual diagnostic methods. Satellite or Airborne remote sensing have been proposed for disease identification. Huang et al . (2007) performed a comparative study of in-situ and airborne hyperspectral images in order to evaluate tailored spectral indexes to detect yellow rust in wheat. Mahlein et al (2013) developed spectral disease indexes to detect the presence of sugar beet diseases by selecting the two most discriminant wavelengths per disease whereas Moshou et al. (2005) extracted suitable spectral indices by an unsupervised approach. Although these methods are appropriate to evaluate and identify the extension of a disease over a region, they fail on the detection of early symptoms as they require the presence of the disease on its later stage to be easily recognizable by airborne imagery. Other authors (Sankaran et al. 2010) make an exhaustive review on advanced techniques for plant disease diagnosis analyzing the volatiles produced by a diseased plant in order to develop specific electronic sensors.

In order to identify the diseases based on early symptoms, automatic picture analysis has been proposed by different authors. Sanakki et al. (2011) introduced an approach to automatically grade diseases on plant leaves. The proposed system uses image processing techniques to analyze color specific information in an image of the infected plant. A k-means clustering method is performed for every pixel in the image to extract clusters with infected spots. The segmented image is saved and the total leaf area is calculated. Finally, the disease spreading on plant leaves is graded by employing Fuzzy Logic to determine a particular disease. A high computational effort is required for such an image processing based method although some initiatives have reduced the computational cost (Xie et al., 2016). Other authors (Siricharoen et al., 2016) satisfactorily used an approach combining texture, color and shape features to detect the presence of a disease. However, they focus on leafs containing one disease at the same time and not focusing on early symptoms.

Other initiatives such as PlantVillage (Hughes and Salathé, 2015) have released more than 50,000 expertly curated images of healthy and infected leaves of different 14 different crops (apple, blueberry, corn, grape…) 12 of them having also healthy leaves and a total number of 26 different diseases. The use of deep convolutional neural networks have been already proposed (Mohanty et al., 2016; Sladojevic et al., 2016), obtaining accuracies greater than 99% when the testing images belong to the same dataset. However, when the model is tested against images collected from online trusted sources (Sladojevic et al., 2016), the

accuracy is degraded down to 31.4%. The fact that the database is taken under controlled conditions and the presence of only late stage diseases on the database precludes its use as a real digital farming application. Besides this, the existing databases (Mohanty et al., 2016) does not consider the case where more than one disease are present in the same plant; therefore, models trained and tested on it will only be able to detect the most visible disease, which is not necessarily the one of most importance for the crop.

3. Materials & Methods

In order to develop an algorithm capable of distinguishing diseases at early stages, an extensive image database has been created for wheat crop. Although wheat crop is used for validation purposes, the algorithm has been designed to be used on different crops and diseases and can be applied to other crops such as barley or corn. An acquisition campaign took place during the years 2014, 2015 and 2016 in Germany and Spain coincident with the crop season. Images were acquired at field conditions on the field with seven different devices: iPad, iPhone4, Dell-tablet, Samsung Galaxy Note, Windows Phone, Samsung S3, iPhone5. The acquisition campaign was designed to last the whole crop season, so that pictures of the disease at different phenological growth stages could be acquired. In order to assure variability, the pictures were taken in at least 36 different wheat varieties searching for the symptoms in the most common or recently commercialized ones with different resistance disease level and different life cycle. Examples of pictures acquired during these campaigns can be seen in the Figure 1.

Fig. 1: Examples of pictures of infected images in the dataset

The three diseases considered in this work were septoria, rust and tan spot (Clark et al., 2010) . Besides them pictures containing other diseases such as powdery mildew or abiotic damages were included to assure the algorithm is able to generalize the absence of disease appropriately.

The early symptoms of septoria are characterized by water-soaked (chlorotic or yellowed)

patches which quickly turn to ashen grey-brown oval lesions surrounded by a chlorotic halo, randomly distributed on leaves. Later in the season, the disease severity increased, these lesions frequently coalesce to produce large areas of brown-dry tissue and can appear in the whole plant, from the lower to upper leaves. Depending on the climate and the fungus implied, the patches contain the visible black pycnidia (small black points) which are the most characteristic sign of septoria in mature lesions.

Symptoms of brown-red and yellow rust at early stages seen as individual pustules yellow to orange-brown in color and about 0,5-1,0 mm. A Chlorotic halo surrounded the pustules is quite common which appear even before de pustule formation but not always appears. Later in the season, the brown pustules (brown-red rust) tend to be scattered at random compared with the more striped symptoms of yellow rust.

The first foliar symptoms caused by tan spot appear as small (1 to 2 mm), light brown blotches that develop into oval-shaped, light brown, necrotic lesions, sometimes bordered with a thin yellow halo. Later in the season, these lesions coalesce to produce large areas of brown tissue, similar to septoria symptoms in late stages.

A total number of 3637 images of wheat diseases have been taken under natural conditions during 2014 and 2015 on both pilot sites and they have been used as a training and development database. The details of these dataset are summarized in Table 1:

Table 1: Generated database for training purposes

Database name (acquisition time)	Rust	Septoria	Tan spot
Wheat 2014 (W-2014)	471	700	183
Wheat 2015 (W-2015)	516	1805	457

Taking into account the symptoms and signals for the above mentioned diseases, the pictures were taken from an expanded leaf, form the upper leaf surface, avoiding pictures of symptoms or signals located in the margins or in the tip of the leaves. The image for these databases should be representative of the disease symptoms which appear in a cluster of plants or in a field. The picture showed damaged and not damaged tissue and were performed avoiding direct light.

In order to design and validate an algorithm capable of identify crop diseases at their early stages, all dataset images were accurately segmented by expert technicians. All the spots presenting each disease as well as the image region comprising the leaf were segmented. A specific segmentation was done for each disease (see Figure 2).

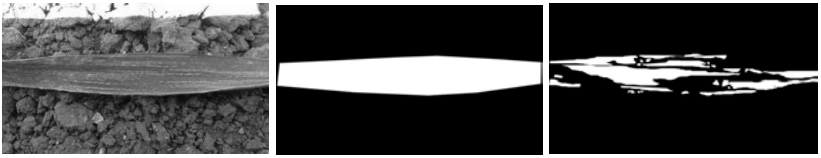

Fig. 2: Manual segmentation process left) original image, center) leaf region, right) segmented rust hot-spots

To validate the classification results under real conditions, a group of 20 farmers and technicians belonging to Neiker-Tecnalia performed a pilot validation test with wheat crop in Germany and Spain. A smartphone application was given to them and they acquired images containing healthy leaves, rust, septoria, tan spot, other common diseases as Powdery mildew (*Blumeria graminis* f. sp. *tritici*) and abiotic diseases on the field under natural conditions. A gray cardboard was given to the farmers in order to optionally help them taking the picture under windy conditions. However, no information from the cardboard was used by the developed algorithm. The taken images were diagnosed online by the application and the results were stored to calculate performance of the system at real conditions. These images were validated by a technician at Neiker and this groundtruth was checked against previous algorithm results already stored on the database.

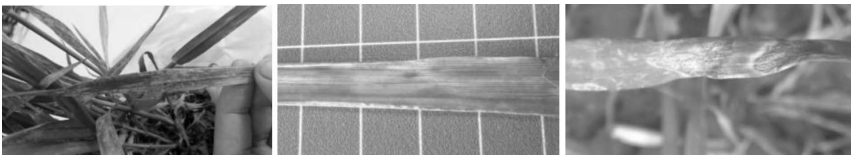

Fig. 3: Validation dataset images left) image taken in a green-house, center) image taken in the field using the accessory gray-board, right) image taken in the field

During the validation of the system, a total of 179 images were taken (examples of these images can be seen in the Figure 3). From those images, 96 presented at least rust, 88 septoria and 18 contained tan spot (Table 2).

Table 2: Distribution of diseases for the pilot validation database

Database name (acquisition time)	Rust	Septoria	Tan spot	Healthy or other diseases	Total images
Pilot database (P-2016)	96	88	18	27	179

A screenshot of the application is shown at Figure 4.

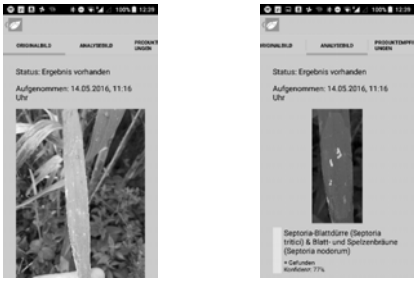

Fig. 4: Left image, the leaf photo taken by the farmer is shown; Right image, the output result from the algorithms is visualized

4. Disease identification algorithm

Although several algorithms have been proposed on the literature for disease identification, they have not demonstrated their capabilities under natural conditions as a step decrease on their accuracy was seen when the images are taken in real field conditions. To overcome this inconvenience, an algorithm pipeline that is able to work under image acquisition variable conditions is proposed. These variabilities can be caused, among others, by differences on the acquisition sensor, image scale, illumination, background and picture orientation. We propose a generic algorithm being able to be trained for different crops and diseases. To validate this versatility, the algorithm has been tested with three wheat diseases that present different visual characteristics. The proposed algorithm minimizes the accuracy loss under these variability conditions while coping with both early and late stage diseases.
In order to achieve this, a hierarchical approach based on the following stages is proposed:

a) Image preprocessing: The acquired image is processed by means of color constancy algorithms to minimize the natural illumination variability effects. After that, leaf is segmented and isolated from the rest of the image. Different approaches have been

taken depending on the nature of the image (natural image, existing draft mask from the user input…).

b) Disease identification algorithm that comprises the following steps:
    a. Extraction of disease candidate regions: The segmented leaf isolated image is corrected to achieve color constancy, normalized and candidate sub-regions susceptible of containing diseases, called Hot-Spots, are extracted.
    b. Each extracted Hot-Spot region is analyzed in detail by local descriptors that extract and categorize each region in terms of its visual characteristics. Next, each Hot-Spot is checked against different disease detection inference models.
    c. All this information is gathered and processed by a high-level classifier, called meta-classifier, that is able to extract the complementarities of the different inherent features that are embedded within an image.

This global layout of the algorithm is described in the Figure 5. Each stage is detailed in the following sub-sections.

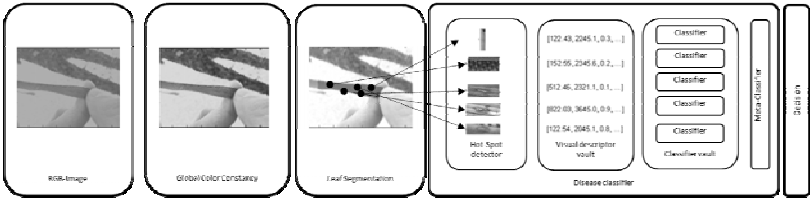

Fig. 5: Global algorithm layout

4.1. Image preprocessing module.

This module performs color constancy normalization on the acquired images to reduce the effects for natural image variability. After that, the portion of the image that contains the leaf is segmented and isolated to obtain a color normalized leaf image. In order to achieve this normalization several steps are involved (Figure 6) and described in the following paragraphs.

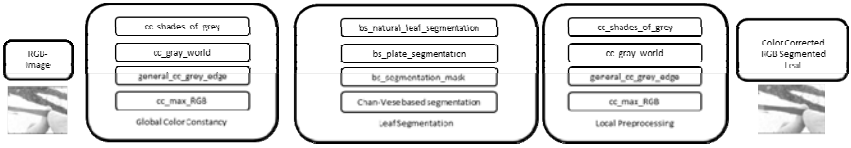

Fig. 6: Diagram for color constancy and image leaf segmentation

4.1.1. Global Color Constancy

The differences in color appearance of the images in the database are due to various factors, such as changes in the physical lighting conditions (caused by weather, location, date and time of capture, orientation, etc.), differences in terms of color response and reproducible gamut among the diverse capture device models and individual units, or variability in the in-device image preprocessing and compression pipeline on a per-device and per-image basis. Such lack of control in the image acquisition workflow implies that a full color normalization process is not feasible, unless a relatively large set of color patches (printed under a color-managed workflow and measured with a colorimeter) are included with each and every capture and used to compute and apply a per-image color normalizing transformation (Finlayson et al., 2015). The cost and non-convenience of deploying such a solution at scale makes this approach inadvisable.

However, a color constancy transformation that aims at reducing the variance of the images in terms of white balance (while leaving out the color-gamut diversity) can be computed and applied per image in a feasible manner. Therefore, as a first preprocessing step, a global color constancy method is proposed in order to try to make the system more robust to changing illumination conditions during the recording of the images, and thus reach better classification results. The proposed method uses image statistics information to model the lighting conditions that were present while the image was captured, estimates such illuminant's color, and applies an inverse transform that maps the recorded colors to a common white point, yielding a white-balanced image. Shades of gray (Finlayson and Trezzi, 2004), Gray world (Buchsbaum, 1980), Gray edge (van de Weijer et al., 2007) and Max-RGB (Land and McCann, 1977) color constancy algorithms have been proposed and evaluated to this respect.

4.1.2. Leaf segmentation

Leaf segmentation is a module to extract one or more portions from the prior color-constant image. Plant element extraction is set up in such a way that the portions extracted from the color-normalized image correspond to a leaf. Therefore, the extractor performs image processing operations which segment the portions of the image associated with plant elements

from other portions in the image which do not provide any information on the disease (e.g. image background).
Two different alternatives for leaf extraction were considered:

4.1.2.1. Automated natural image leaf segmentation

The automated natural image leaf segmentation algorithm computes a binary leaf mask without any user intervention. The segmentation pipeline in this step relies on the Simple Linear Iterative Clustering (SLIC) (
Achanta et al., 2012) superpixel extraction algorithm, although other approaches such as Quickshift (Vedaldi and Soatto, 2008) or Felsenszwalb's efficient graph-based image segmentation (Felzenszwalb and Huttenlocher, 2004) could be also used. SLIC adapts a k-means clustering-based approach in the CIELAB color space while keeping a configurable spatial coherence as to enforce compactness. Next is the analysis of each of the generated superpixels (segments) to distinguish between leaf and non-leaf segments, by means of the extraction of different visual features. Each of such features maps a value to each superpixel, representing a weighting factor. The used features are the following: (1) mean, maximum or variance of a Gaussian weighting function, (2) mean, maximum or variance of the magnitude of the Local Binary Patterns (LBP) Ojala et al., 2002 flatness of the superpixel (3) maximum of the average of the b color channel and average of the inverted a color channel or (4) intra-superpixel perceptual color variance.
In a third step, all the probabilities available for each superpixel are combined either by means of the product or the sum of the individual probabilities. This yields a unique real value in the range [0, 1] for each superpixel, representing its probability of being part of the leaf. In the last step, a threshold value is selected and the image is binarized so that all the pixels pertaining to a superpixel with combined probability greater or equal such threshold are considered as being part of the leaf. The result can be seen in Figure 7.

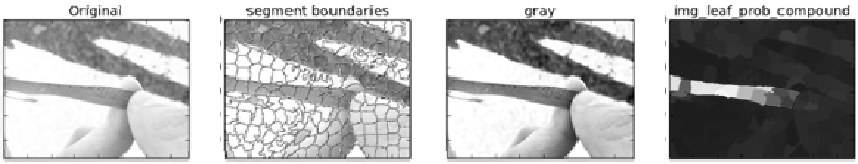

Fig. 7: Natural image segmentation algorithm

4.1.2.2. User input mask refinement method

Under real use cases it can happen that the taken image can be quite blurred or with strong artifacts or that the user wants to check a specific region of the leaf. In this case, a manually generated mask can be used to delimitate the region of interest (Figure 8 – center image). However, this input mask generated by the user is not systematically generated and it is just a rough estimation of the region where the identification algorithm should focus. Because of this, an additional step of user input mask refinement is required.

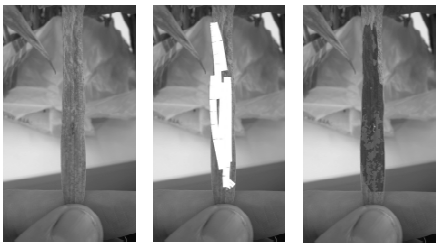

Fig. 8: Leaf mask refinement algorithm left) original image, center) input mask given by a user through the smartphone app right) in blue, the refined mask (blue) with the detected diseases (other colors)

In order to perform the leaf mask refinement, an initial segmentation is defined with its starting point as the user's given input mask. After that, Chan-Vese (2001) segmentation algorithm over the saturation(s) image channel is performed. The use of active contours without edges allows us to divide the image on two differentiated regions that minimize their internal variability. In practical terms, each interaction of the active contour minimization flows into a more homogeneous and accurate leaf mask estimation.

4.2. Disease identification classifier

The disease identification classifier performs the identification of one or several diseases over the previously segmented leaf (Figure 9). First, a primary segmentation is done in order to detect and select any suspicious sub-region on the leaf as a disease candidate (Hot-Spots). Each disease candidate is then analyzed by the extraction of specific visual features of the candidate region and the use of a specific statistical inference model for the specific disease. It is noteworthy to indicate that this sub-segmenting approach smartly increases the accuracy of the system when working with early diseases. The hypothesis is

that this training mechanism helps to deal with early stage diseases, as the classifiers are trained to distinguish among the candidate detected hot-spots the segmented candidate regions are trained for disease/not disease characterization, allowing a better training of the discriminative features. Once each Hot-Spot is properly identified, a meta-classifier module weights all individual decision to make a global assessment.

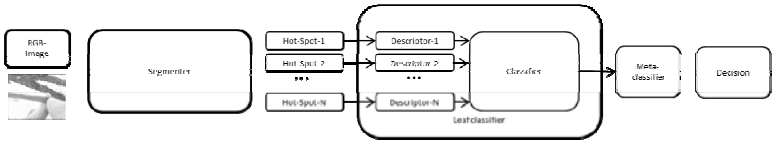

Fig. 9: Diagram of the disease identification classifier

4.2.1. Primary segmentation module

The developed primary segmentation algorithm consists of a Naïve Bayes classifier (Lewis, 1998) that robustly models the color features that are always present on an infected image. This initial segmentation is performed over selected color channels including Lab and HSL. Based on these features, the image is segmented into different feature clusters (Computer Vision – A Modern Approach) where a cluster represents a group of pixels having similar visual feature values (e.g., color values or textural values). Each image blob feeds a Naïve Bayesian segmentation model. The Bayesian model acceptance threshold is selected to assure that every blob in the image feasible for presenting the desired disease is classified as a candidate.

In view of the full image content the identified candidate regions typically cover only a relatively small number of pixels when compared to the number of pixels of the entire image. Consequently, the amount of data that is used as the basis for the next stages of image processing is significantly reduced by the Naïve-Bayes filter mechanism and thus, the computational cost of the algorithm reduced. The visual feature statistics of each identified cluster is then confronted with this Naïve-Bayes classification model. Each identified image cluster is analyzed and its disease likelihood probability is calculated and is segmented by using the Bayes segmentation model. This model is biased according to the predefined threshold to ensure a low percentage (e.g. 1% - 5%) of discarded positives while maintaining a low rate of false positives. That is, after the application of the Bayesian filter to the clusters only such clusters above the predefined threshold are kept as candidate region for further analysis. In other words, the predefined threshold ensures that every candidate region in the image will be segmented for further analysis. Those candidate regions can then

again be processed in the cluster function to receive more precise results as the infected area can be further isolated. Detected candidate hot-spot regions are depicted in Figure 10.

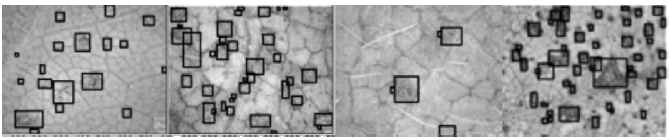

Fig. 10: Primary segmentation based on Lab clustering and Bayes classifier showing the detected candidate hotspots

One of the biggest advantages of this approach is that it makes a first segmentation that eliminates the regions in the images that have useless visual information.

4.2.2. Hot-Spot identification module

Each obtained Hot-Spot region is described by means of two visual descriptors. A first descriptor designed to sample the color of the disease contains information about the mean and standard deviation of the Lab channels over each segmented Hot-Spot blob. In order to also capture the color of the healthy plant as reference, the descriptor concatenates the mean and variance of the Lab channels on the pixels from the Hot-Spot blob bounding boxes that do not belong to the Hot-Spot region. A second descriptor, designed to map the Hot-Spot texture is also calculated for each blob. Concretely, a Uniform LBP descriptor over the RGB channels is used in order to describe blob texture assuring rotation invariance.

For each disease and descriptor, a Random-Forest based classifier is trained with the extracted descriptors that allow tagging each Hot-Spot blob with a disease feasibility value. In a second step a meta-classifier is used, to compute a confidence score for the particular disease by evaluating all determined probabilities of the candidate regions. A classification decision for one or more diseases is processed based on the entire picture. Information considered within the meta-classifier are for example, the probability given by the different descriptors, location, size or shape of the candidate regions, weighting of each classifier and the confidence necessary for an assessment to be taken into account.

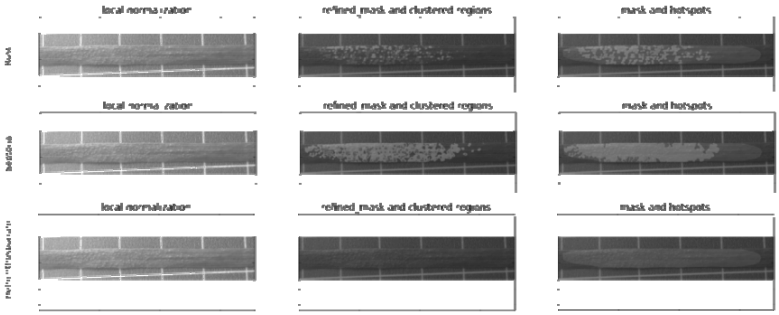

Fig. 11: Left) RGB image after local color constancy; Center) Located rust Hot-Spots candidates for each disease extracted by the primary segmentation; Right) green: HotSpots identified as the disease, red: candidate hot-spots refused by the hotspot identification module.

This process can be seen in Figure 11 that shows a leaf that presents only rust disease. Each row depicts an attempt of the algorithm of detecting one specific disease. The primary segmentation algorithm performs a first attempt to detect candidate spots. In the case of this leaf, candidate spots are found for septoria and rust and none for tan spot as it is depicted on the central column. The candidate spots for septoria and rust were further analyzed and only rust spots were detected as real spots (depicted in green on the right column) whereas the candidate hot-spots for septoria were detected as not real septoria and depicted in red. This is caused by the ability of the hot-spot classifier to combine the textural information from the LBP descriptor that is able to distinguish between the high frequency textures of rust and the lower level frequencies of septoria.

5. Results

The presented algorithm was developed on Python programming language and deployed as a service on a Linux based processing server. The deployed service was connected to a middleware server that managed the connections from Android and Windows-phone applications. Average processing time of the algorithm was 5.2 seconds with a standard deviation of 2.6 seconds depending on the number suspicious hot-spots found.

In order to validate the results of the proposed method, a database was created using the images acquired in 2014 and 2015 (named W-2014 and W-2015) with 987 images containing rust, 2505 containing septoria and 657 containing tan spot on a total of 3637 images.

This training database was divided into training and validation sets. In order to avoid overfitting and biasing, the dataset was divided into ten folds where the picture acquisition date was used as set divider. This means that, at each fold, the pictures belonging to the acquisition dates selected for training will be selected for the training set whereas the rest were selected for validation. At each fold, 90% of the acquisition dates were set as train and the remaining 10% were set as validation.

The Area under the Receiver Operating Characteristic (ROC) Curve (AuC Bradley, 1997; Fawcett, 2006) was selected as the most suitable algorithm performance metric, in order to account for the class imbalance present in the dataset (in such cases, the use of accuracy is discouraged). The AuC for a binary classification problem is constructed by first sorting all the samples by the disease presence probability predicted by the model for each of them. The classification threshold value is then moved all the way from 0 to 1, and the result at each threshold value is mapped into the plot representing False Positive (x-axis) vs. True Positive rates (y-axis), and measuring the resulting area (in the $[0, 1]$ range, higher is better) under such curve. AuC values over 0.85 were obtained for all diseases on the k-fold validation sets. It is important to remark that even diseases at very early stages were identified. An additional test was performed in order to quantify the effects of color constancy normalization on the identification metrics. It can be seen in Table 4, the use of color constancy normalization increases the overall accuracy from 0.75 up to 0.81.

Table 3: Classification AuC metrics for color normalized images and images without normalization

Preprocessing color algorithm	Rust	Septoria	Tan spot
Gray world [22]	0.83	0.87	0.82
Max-RGB [24]	0.81	0.85	0.83
Shades of gray [32]	0.85	0.90	0.89
Gray edge [34]	0.83	0.81	0.75
Without color constancy algorithm	0.77	0.73	0.72

Detailed metrics for each disease are depicted in Table 5:

Table 4: Identification results on the K-fold validation dataset

Disease	AuC		Sensitivity	Specificity
Rust	0.85	0.82	0.7	0.95
Septoria	0.90	0.85	0.91	0.79
Tan spot	0.89	0.73	0.69	0.78

In order to validate the results under real conditions, a pilot study was set in Germany and Spain in 2016. The pilot users employed a specific developed identification smartphone application as described in section 3. The results of the pilot validation can be seen in the Table 6. Captures leaves were divided into early stage diseased plants and medium-late stage diseased plants to validate early disease detection. Figure 13 shows an example of early diseases leaves included on the early set database.

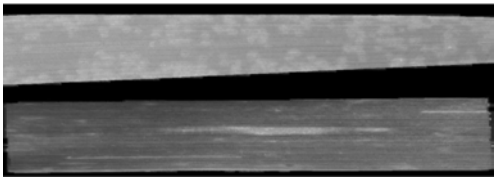

Fig. 12: Example of images with early diseases from the validation set

Table 5: Identification results on the May-2016 pilot

Disease	AuC	Accuracy	Sensitivity	Specificity
Rust (Early)	0,81	0,78	0,80	0,76
Septoria (Early)	0,81	0,76	0,75	0,77
Tan spot (Early)	0,83	0,73	0,76	0,70
Rust (medium-late)	0,83	0,81	0,80	0,82
Septoria (medium-late)	0,82	0,79	0,80	0,78
Tan spot (medium-late)	0,81	0,82	0,96	0,69

We observed a small decrease on the AuC from an average 0.88 to 0.81 when moving into real field conditions. Compared with other results that fail when moving into real conditions (Sladojevic et al. 2016), the developed algorithm can cope better with the variability of real light illumination, different acquisition devices and multi-located users under real use conditions. Besides this, performance is not degraded too much when dealing with early diseases. Detailed numbers are depicted in Table 6 and in Figure 12.

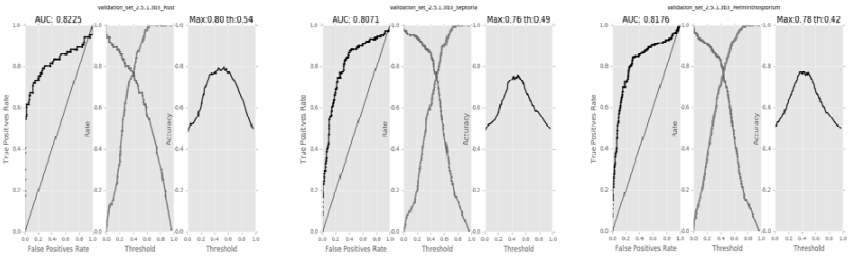

Fig. 13: Average AuC, accuracy and FAR/FRR curves for rust, septoria and tan spot diseases obtained at real pilot conditions

Detailed algorithm results are shown on the next pictures (Figure 14):

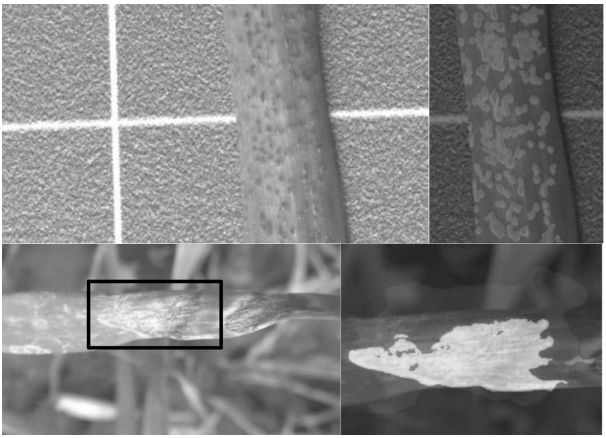

Fig. 14: Algorithm results under pilot conditions
(cyan: detected septoria, purple: detected rust)

6. Conclusion

In this proposal a general use multi-disease identification algorithm has been presented. The algorithm was validated over three different kinds of diseases (rust, septoria and tan spot) on wheat images. The algorithm has been deployed on a real smartphone application and validated under real field conditions in a pilot study located in Spain and Germany over more than 36 wheat varieties. The results on real field tests obtained AuCs (Area under the Receiver Operating Characteristic –ROC– Curve) higher than 0.8 when assuring global color constancy on the image by means of the developed algorithm succeeding on real time conditions and being able to cope with different diseases simultaneously. The AuC decreased to 0.7 when no color constancy algorithm is applied on the processing workflow. However, the use of shades of gray color constancy algorithm assures AuC values higher than 0.8. We have also validated algorithm performance when dealing with early diseases. Although there is a small degradation on the performance of the algorithm when dealing with early diseases, the algorithm can obtain almost the similar performance on early and late diseases.

The preliminary hot-spot detection and its ulterior description by color and textural descriptors allow real time performance as only the suspicious regions are trained and described by the higher level classifiers and descriptors.

The presented image processing technology provides new possibilities for the detection of weeds and diseases in earlier stages. Next steps will be focused on measuring how this early stage detection can help the user to react in time and plan for some preventive activities, e.g. crop protection application. Being able to react in an early stage could minimize the yield losses and therefore guarantee the food security in the upcoming years.

References

Achanta, R., Shaji, A., Smith, K., Lucchi, A., Fua, P., Süsstrunk, S., 2012. SLIC superpixels compared to state-of-the-art superpixel methods. IEEE Trans. Pattern Anal. Mach. Intell. 34 (11), 2274–2282.

Agrios, G.N., 2006. Plant Pathology, fifth ed. Academic Press, p. 952. ISBN: 9780120445653.

Bradley, A.P., 1997. The use of the area under the ROC curve in the evaluation of machine learning algorithms. Pattern Recogn. 30 (7), 1145–1159.

Buchsbaum, G., 1980. A spatial processor model for object colour perception. J. Franklin Inst. 310 (1), 1–2.

Chai, Y., Pardey, P., Beddow, J., Hurley, T., Kriticos, D., Joachim-Braun, H., 2015. The global occurrence and economic consequences of stripe rust in wheat. In: Advancing Pest and Disease Modeling Workshop. University of Minnesota, CSIRO, and CIMMYT. <http://www.globalrust.org/sites/default/files/2014% 20BGRI%20Pardey.pdf> (accessed 14th October 2016).

Chan, T.F., Vese, L.A., 2001. Active contours without edges. IEEE Trans. Image Process. 10 (2), 266–277.

Clark, B., Bryson, R., Tonguc, L., Kelly, C., Jellis, G., 2010. The encyclopaedia of cereal diseases. HGCA and BASF plc, Crop Protection.

Coakley, S.M., Scherm, H., Chakraborti, S., 1999. Climate change and plant disease management. Annu. Rev. Phytopathol. 37, 399–426.

‘‘Computer Vision - A Modern Approach”, by Forsyth, Ponce, Pearson Education ISBN 0-13-085198-1, pp. 301–307.

Fawcett, T., 2006. An introduction to ROC analysis. Pattern Recogn. Lett. 27 (8), 861– 874.

Felzenszwalb, P.F., Huttenlocher, D.P., 2004. Efficient graph-based image segmentation. Int. J. Comput. Vision 59, 167. http://dx.doi.org/10.1023/B: VISI.0000022288.19776.77.

Finlayson, G.D., Trezzi, E., 2004. Shades of gray and colour constancy. In: Color and Imaging Conference Jan (1), pp. 37–41.

Finlayson, G.D., Mackiewicz, M., Hurlbert, A., 2015. Color correction using rootpolynomial regression. IEEE Trans. Image Process. 24 (5), 1460–1470.

Garrett, K.A., Dendy, S.P., Frank, E.E., Rouse, M.N., Travers, S.E., 2007. Climate change effects on plant disease: genomes to ecosystems. Annu. Rev. Phytopathol. 44, 489–509.

Herrera-Foessel, S.A., Singh, R.P., Huerta-Espino, J., Crossa, J., Yuen, J., Djurle, A., 2006. Effect of leaf rust on grain yield and yield traits of durum wheats with race-specific and slow-rusting resistance to leaf rust. Plant Dis. 90 (8), 1065– 1072.

Huang, W., Lamb, D.W., Niu, Z., Zhang, Y., Liu, L., Wang, J., 2007. Identification of yellow rust in wheat using in situ spectral reflectance measurements and airborne hyperspectral imaging. Precision Agric. 8 (4–5), 187–197.

Hughes, D.P., Salathé, M., 2015. An open access repository of images on plant health to enable the development of mobile disease diagnostics. Computers and Society. In Computer Science. Cornell University Library. arXiv:1511.08060v2 [cs.CY].

Land, E.H., McCann, J.J., 1977. Lightness and retinex theory. JOSA 61 (1), 1–11.

Lewis, D.D., 1998. Naive (Bayes) at forty: the independence assumption in information retrieval. In: European Conference on Machine Learning. Springer, Berlin Heidelberg, pp. 4–15. April.

Mahlein, A.K., Rumpf, T., Welke, P., Dehne, H.W., Plümer, L., Steiner, U., Oerke, E.C., 2013. Development of spectral indices for detecting and identifying plant diseases. Remote Sens. Environ. 128, 21–30.

Mohanty, S.P., Hughes, D.P., Salathé, M., 2016. Using deep learning for image-based plant disease detection. Front. Plant Sci. 7.

Moshou, D., Bravo, C., Oberti, R., West, J., Bodria, L., McCartney, A., Ramón, H., 2005. Plant disease detection based on data fusion of hyper-spectral and multispectral fluorescence imaging using Kohonen maps. Real Time Imaging 11 (2), 75–83.

Oerke, E.C., 2006. Crop losses to pests. J. Agric. Sci. 144, 31–43.

Ojala, T., Pietikainen, M., Maenpaa, T., 2002. Multiresolution gray-scale and rotation invariant texture classification with local binary patterns. IEEE Trans. Pattern Anal. Mach. Intell. 24 (7), 971–987.

Sankaran, S., Mishra, A., Ehsani, R., Davis, C., 2010. A review of advanced techniques for detecting plant diseases. Comput. Electr. Agric. 72 (1), 1–13.

Sannakki, Sanjeev S., Rajpurohit, Vijay S., Nargund, V.B., Kumar, Arun, Yallur, Prema S., 2011. Leaf disease grading by machine vision and fuzzy logic. Int. J. Comput. Technol. Appl. 2 (5), 1709–1716.

Savary, S., Ficke, A., Aubertot, J.N., Hollier, C., 2012. Crop losses due to diseases and their implications for global food production losses and food security. Food Secur. http://dx.doi.org/10.1007/s12571-012-0200-5.

Siricharoen, P., Scotney, B., Morrow, P., Parr, G., 2016. A lightweight mobile system for crop disease diagnosis. In: Campilho, A., Karray, F. (Eds.), Image Analysis and Recognition. ICIAR 2016. Lecture Notes in Computer Science, vol. 9730. Springer, Cham.

Sladojevic, S., Arsenovic, M., Anderla, A., Culibrk, D., Stefanovic, D., 2016. Deep neural networks based recognition of plant diseases by leaf image classification. Comput. Intelligence Neurosci. http://dx.doi.org/10.1155/2016/328980.

van de Weijer, J., Gevers, T., Gijsenij, A., 2007. Edge-based color constancy. IEEE Trans. Image Process. 16 (9), 2207–2214.

Vedaldi, A., Soatto, S., 2008. Quick shift and kernel methods for mode seeking. In: European Conference on Computer Vision, Marseille, France.

Xie, X., Zhang, X., He, B., Liang, D., Zhang, D., Huang, L., 2016. A system for diagnosis of wheat leaf diseases based on Android smartphone. Opt. Measur. Technol. Instr. http://dx.doi.org/10.1117/12.2246919.

Fully automated decision support for fungicide applications

Dr. **Marek Schikora**, **Matthias Tempel**,
Bayer AG, Langenfeld

Abstract

Modern agriculture is facing serious challenges in the forthcoming years: By 2050 two billion additional people will have to be fed. Today, large amounts of food are already lost on the field due to different crop stresses like diseases. Crop protection is one the key elements for sustainable agriculture and food safety. Especially larger fields have significant biomass and leaf area variations that benefit from different amounts of active ingredients to control and prevent diseases. Therefore, a variable application rate is preferable in contrast to flat rate applications. It enables farmers to save crop protection volumes, which is beneficial for their profit, the environment and the crops are less stressed. In this article we present FIELD MANAGER, an automated decision support tool to advice farmers on timing and dosing fungicide decisions for winter wheat. The system analyses a variety of data sources, like multi-spectral satellite imagery, field specific weather, farm management information, variety and product characteristics. This data is the basis for a fully automated decision support system.

1. Introduction

Crop protection is one the key elements for sustainable agriculture and food safety. Its effectiveness depends on using the right product with the right dosage at the right time. Knowing the exact cause of stresses; i.e. which specific disease; and the right time to perform spray applications can prevent damage and thus save the harvest. In addition it has to be considered that a field is not homogeneous. Especially larger fields have significant biomass and leaf area variations that benefit from different amounts of active ingredients to control and prevent diseases. Therefore, a variable application rate is preferable in contrast to flat rate applications. It enables farmers to save crop protection volumes, which is beneficial for their profit, the environment and the crops are less stressed. In this article we present FIELD MANAGER, an automated decision support tool to advice farmers on the right fungicide decisions for winter wheat. The system analyses a variety of data sources, like multi-spectral

satellite imagery, field specific weather, farm management information, variety and product characteristics.

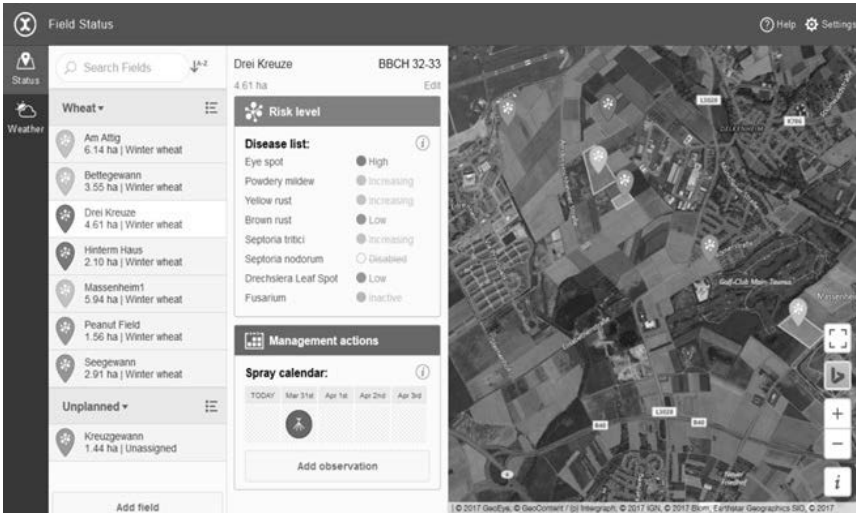

Fig. 1: Screenshot of the FIELD MANAGER

The first component consists of sophisticated disease models that calculate the risk for eight of the most critical winter wheat diseases. These models predict for each day the current risk level for all diseases individually and aggregate them into a spraying recommendation in order to prevent diseases before they cause irreversible crop damage. The models are trained and calibrated with multi-year field trials and field observations by the users.

The second component uses remote sensing analytics to cluster a field's variability in up to 5 zones with a grid size of 3x3 meters. The application rates for the zones are based on the field's variability and the risk models from the first component. In task planning the system will try to find the optimal solution for all selected fields to make the tank recipe compatible.; i.e. one tank recipe for several fields. It generates maps that can be uploaded to sprayers for automatic variable rate applications in the field.

The third component is a recommendation module that automatically suggests the best time to perform a fungicide application. The system can be used to group fields that require pro-

tection into tasks and in addition it suggests spraying date, products and dose rates for each field zone.

A spray parameter file is generated and made available via thumb drive towards the sprayer's controller. Standardized telematic system interfaces will be added soon – fueling agmachineries mechatronic systems with agronomic expertise to create measureable value.

2. System Architecture

The FIELD MANAGER is completely located in the cloud. The user can reach the system via a normal web browser. His personal farm and fields are stored on secured servers, so that he can reach the system from any computer using usual username and password combination.

The application itself is based on micro-services which handle the incoming requests of the users. Each micro-service is designed to perform a particular task, e.g. download and manage weather information for a field or calculate the growth stage of the crop planted on the field. This software architecture allows flexible scaling of components on the need of users and enables highest availability times.

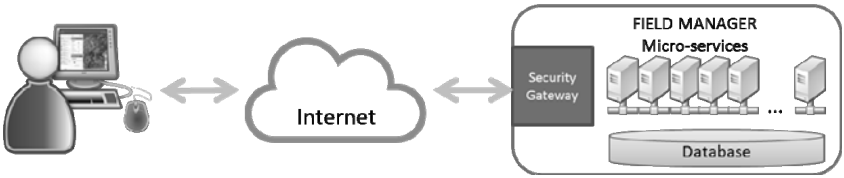

Fig. 2: FIELD MANAGER system architecture

3. The field status

In the field status section is the central element to operate the system. Here the user can add fields to his farm either drawing them on map imagery background (using Google Maps or Bing) or upload digital field boundaries, like shapefiles, into the system. Having the fields created, the next step is to assign which variety was seeded on the individual fields. With that information our agronomic decision engine can tell him if an action is necessary.

a. Weather

One of the core data source for the FIELD MANAGER is field specific weather. For each field in the system we are providing weather data with an hourly resolution for the past (last 30 years), current and future conditions. This data gets automatically updated each day. For the

user we are evaluating the conditions for the next 24 hours and give advice about the spray conditions. The system is differentiating for each hour between three stages: Favorable, less favorable and unfavorable weather conditions, to perform a spray application.

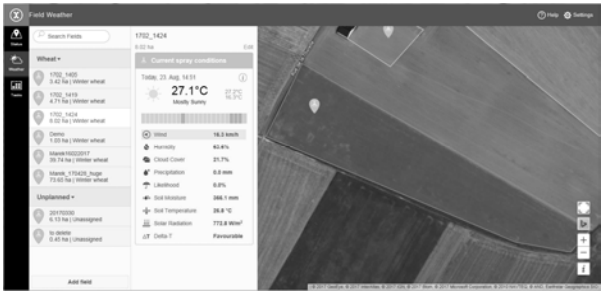

Fig. 3: The spray weather conditions for a field. Highlighted are the factors that cause the less favorable spray conditions. Here the winds speed.

b. Growth stage estimation

Another feature of the FIELD MANAGER is the automatic estimation of the growth stage for the current day. Hereby, we have used observation data we have gathered for a couple of years for various varieties, various locations and various times to create a model that is able to predict the growth stage of crop for a particular day. The user is able to modify this estimate with an observation on his own field with the observation feature, see Section 3.d.

c. Disease risk estimation & application recommendation

One of the key features of FIELD MANAGER is the ability of the system to evaluate the field specific disease risk. For winter wheat we are currently supporting the eight major diseases: eye spot, powdery mildew, yellow rust, brown rust, septoria tritici, septoria nodorum, drechslera leaf spot and fusarium. For each disease the developed decision engine calculates the risk level for an infection on a particular day. To do so we are using the growth stage model, weather data, variety characteristics and information about the actions performed on that field in its recent history. The model itself was developed using expert knowledge and field trial data from the last 20 years and is improved and modified season by season to deliver the most reliable results. FIELD MANAGER is able to aggregate the individual risk to one risk icon for that field, so that the user has a quick overview for his farm. In addition to the risk level the system calculates a spray window in which a fungicide application would have the most benefit to prevent infections.

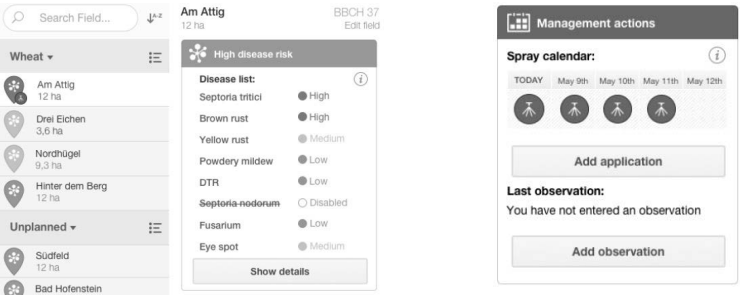

Fig. 4: Risk status: Aggregated disease risk per field on the left side. For the field "Am Attig" detailed information for each disease is presented. On the right the spray recommendations for the next days are shown.

d. Observations

To have a better performance of the system the user is able to give feedback on the estimations regarding growth stage and disease activity in his field. With this additional knowledge the models are recalibrated and become so more user and field specific. This enables even more precise estimates.

Fig. 5: Observation section. Here, the user can add his observations for growth stage and disease activity for each field individually.

4. Zone specific fungicide application

Having the right time to perform a fungicide application the FIELD MANAGER supports the farmer with a variable rate application map. This map is based on the biomass diversity that is present in the field. The system processes automatically remote sensing data provided by satellites to compute these measurements. To do so we have developed a fully automated

satellite toolchain that is able to download, correct and analyse satellite images, so that they can form the starting point for a spray application map. But a biomass map is not enough to perform an efficient and accurate fungicide application. The FIELD MANAGER assigns application rates to the individual zones. This process uses expert knowledge and manufacturer-agnostic product characteristics, which have been transformed to a dosage algorithm for variable rate application (VRA). Examples of this can are visualized in Figure 6.

Dosing	Average	Total
Water	215.3 l/ha	1251.6 l
Aviator Xpro	1.0 l/ha	5.8 l
Zones	**Area (ha)**	**Percent (%)**
Zone 1	1.2 ha	20.6
Zone 2	2.9 ha	50.5
Zone 3	1.2 ha	20.8
Zone 4	0.4 ha	6.4
Zone 5	0.1 ha	1.8

Fig. 6: Left: VRA spray application map with 5 zones based on biomass diversity. Right: Tank recipe generated for the user with a listing of the amount of product used for each zone.

This application map can be downloaded as shapefile or ISOXML file, so that it can easily be uploaded to a sprayer terminal.

5. Summary

In this article we have presented the FIELD MANAGER a fully automated cloud based decision support system for fungicide applications. The system is able to predict a field specific infection risk and inform the user a about the best time to perform a fungicide application. To optimize the spray application satellite imagery is used to compute the biomass diversity which is the basis for a variable rate application. The generate application maps can be downloaded and injected into spray terminals. The system has been piloted in the 2015/2016 season with 36 farmers. The current version has been used by more than 400 farmers (~34.000 ha) in the season 2016/2017 in Germany and France.

Real-time Smart Farming Services

Yield optimization of potato harvesting

Prof. **Wolfgang Maaß**, Deutsches Forschungszentrum für Künstliche Intelligenz, Saarbrücken (DFKI);
Iaroslav Shcherbatyi, Deutsches Forschungszentrum für Künstliche Intelligenz (DFKI), Saarbrücken;
Sven Marquardt, Grimme Landmaschinenfabrik GmbH & Co KG, Damme;
Arndt Kritzner, Logic Way GmbH, Schwerin;
Benedikt Moser, FIR e.V. an der RWTH Aachen, Aachen

Abstract

Agriculture resembles general production processes in many respects by being “production on the field”. Therefore, it is straightforward to apply concepts known by Industrie 4.0 to agricultural environments. In contrast to, for instance, automotive production, agricultural machines are constantly moving while products are rather static during growth phases. Harvesting and logistic processes increase the complexity by moving machines and moving crop. In this highly dynamic environment, sensor data is increasingly collected for any kind of signal, such as machine data (e.g., oil pressure, speed of rotation) and supervision data (e.g., video signals). Data flows in as packages or streams via communication protocols as defined by ISOBUS. Using this increasing amount of data for making decisions in real-time is currently a challenging task.

In this paper, we introduce a framework for processing agricultural data by leveraging on-board computational devices in combination with cloud infrastructures. The concept of smart services is introduced as a means for processing data and providing services to various stakeholders. Special emphasis is given to real-time decision-making. The framework is derived from the more general acatech reference model for the *Smart Services Welt* initiative. Smart service environments are based on generic and domain-specific software-based services. This gives rise to a software market to which incumbents and new entrants will provide software-based services. Of particular interest are data analytical services based on various Artificial Intelligence methods.

The proposed *RESFAST* framework is exemplified by a potato harvesting process. We introduce the concept of a *nPotato* that senses physical impacts during the harvesting process. This data is analyzed locally on a harvesting machine in real-time. Impacts are categorized and accumulated over time. Farmers are informed about the current accumulated impact so that he/she can act accordingly and adjust machine configurations and driving speed. Furthermore economic forecasting services are used for making market price predictions that, in turn, are combined with impact analyses. Together, farmers receive information about the current status and the predicted return-on-investment. It is shown how data and results are used by cloud services for analyzing across different dimensions, such as geographical areas, time, and crop types.

Collection and analysis of sensor data from an artificial potato

Today's agriculture already uses digital technologies in many areas to optimize the yield from fields, but also in barns. Digital technologies are currently used mainly for machine control and for administrative processes. However, technologies of the Internet of Things and Robotics are increasingly moving into agriculture and enable both the networking of machines and the automated control of agricultural activities in real time. In order to generate a benefit for the farmer, collected data are compacted and offered to the farmer via smart, analytical services [2] in the right situation at the right time.

The example of potato cultivation is investigated by a consortium of research and industrial partners within the framework of the research project Smart Farming World (https://www.smart-farming-welt.de) funded by the German Federal Ministry of Economic Affairs and Energy, as data on physical effects (e.g., beatings), temperature and humidity can be used over the life cycle of a field crop during sowing, harvesting, transport and storage in order to achieve an economically optimal yield. For example, potatoes suffer from high speeds of the harvesters and harvesting belts, which subsequently lead to losses in the crop during storage by putrefaction.

The intelligent "pain-sensitive" potato (nPotato) is a plastic object of the weight and the size of a real potato, which is equipped with sensors for impacts and rotations. Data is locally analyzed on the farm machine by using machine learning methods and provides insights to the farmer in real time. This includes classifying impacts and continuously calculating damage distributions for the crop for the field. Results are linked to a second statistical method, which uses historical potato prices over the past few years to forecast monthly average prices for the next three individual months. The results of both services are integrated into a projected financial return. This allows the farmer to always access the

predicted yield value of the current crop for the next three months. If the forecast is below the target yield, the farmer can make direct contact with the driver of the machine in order, for example, to chance the set up of the harvesting machine or remove obstacles.

Realt-time Harvesting Analysis

The nPotato detects acceleration and rotation events in real-time in order to convert these into the potato according to the type of potato, which in turn are classified. The classification is carried out by means of a deep learning model, which was trained in advance via fall experiments. In this experiment, potatoes of a certain type are dropped from different heights onto a smooth metal surface. The potatoes are then peeled, deep-fried, and checked by experts at the pits. The results are incorporated into the learning process of the deep learning model. The parameters of the model are transferred to the computational units of the potato harvester and thus are available as a classification mechanism (see Fig. 1).

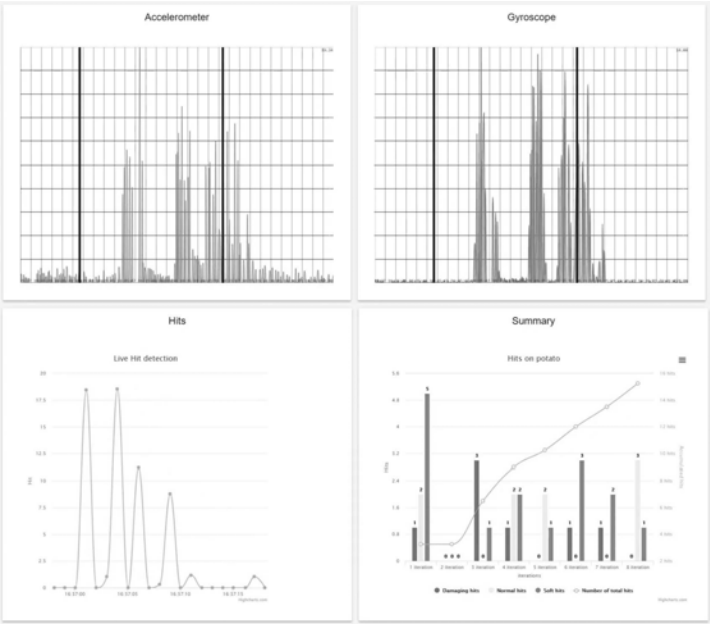

Fig. 1: Upper part: raw data on accelerations (left) and rotations (right) of the nPotato; lower part: diagramm with classified impacts (left) and development over time by several iterations in the harvester (right).

Incoming data streams are classified by a deep learning model over a time window of five seconds [4]. Thus the farmer recognizes the collected number of light, medium and strong impacts on the nPotato. Since the nPotato is automatically withdrawn from the harvesting process at the end, this process can be carried out continuously (see Figure 2, top right). Several rounds are integrated via a statistical distribution so that average values can be displayed to the farmer.

Economic Forecasting Model

Based on historical potato price data, another deep learning model was trained. Since the potato market price is subject to daily volatility, which are difficult to predict, we use a long-term prediction of monthly averages relative to the day of the harvest, i.e., the monthly average prices of the next month, the second month and the third month after harvest. Together with the proportion of undamaged potatoes, it is also possible to predict what the total profit can be achieved. By linking to a farm management system, the production costs and thus the pre-tax (EBT) result can be determined for a particular field (see Figure 3) [5]. This gives farmers the opportunity to act more autonomously, which strengthens their market position.

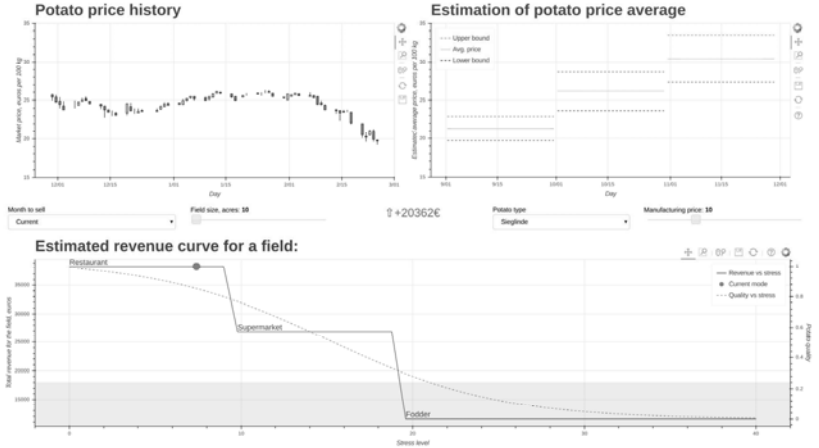

Fig. 2: Yield service for different sales classes (quality grade I, II and III)

The graduation is carried out using quality grades. Quality class I are products of good quality with slight defects, quality class II are marketable with permissible errors, whereas

quality grade III potatoes are only used as animal feed and consequently yield a lower yield. Too many strong impacts on potatoes cause the product to slip into quality class III. In the example in Fig. 2, this is equivalent to an economic loss for the considered building field.

RESFAST Platform and Technical Architecture

The analysis of the potato movements during the harvesting process, the transport and storage, the prediction of medium market prices and the integration of the two analyzes are respectively smart services, which analytically consolidate captured data in real time and offer it in the form of digital services. These smart services are part of the "Realtime Smart Farming Services" platform (RESFAST) (see Figure 4). The goal of RESFAST is the rapid development of new smart-farming services, which work on different data streams. RESFAST couples local analysis on the agricultural machine with central cloud services.

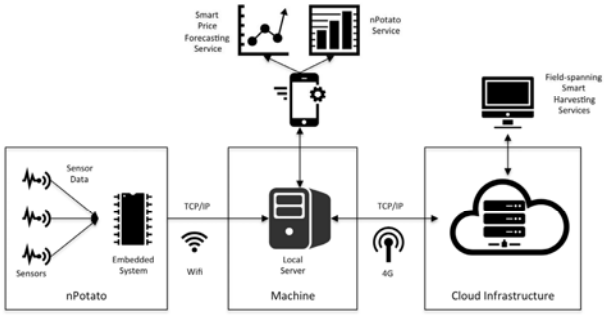

Fig. 3: RESFAST architecture

The nPotato forecast service determines damages directly on the basis of sensory data. With the combination of decentralized smart services and cloud services, the modern farmer can always see the state of the harvest. Because the RESFAST architecture is vendor-independent, the platform can be used across different machines. Thus, the farmer can increasingly make operational decisions in real time to reduce his entrepreneurial risk.

On the RESFAST platform, third-party generic and specific smart services can be installed and linked together. Smart services support the business processes and take account of the organizational structure of role concepts via a web-based authorization process (supported by OAuth 2.0). Thus, RESFAST provides a smart service platform on which data-driven smart agriculture can be efficiently implemented.

Summary and outlook

Farming companies are increasingly generating more data through intelligent machines and other sensor units, which can be evaluated by smart farming services and made available to the modern farmer as knowledge and decision-making aids in real time. As a result of the increasing automation, entire production processes can be optimized over time by adapting networked smart services to the processes and decisions of the farmer and optimizing the overall system. This, in turn, is the basis for the use of agricultural robots, resulting in a further strengthening of the automation of agriculture in the long term. Such an agricultural robot could, for example, an autonomous harvesting machine for potatoes, which takes decisions on the basis of the information obtained from the nPotato independently and makes settings. However, the use of nPotato as a sensor node and smart service does not have to be confined to the harvesting phase of potatoes. Technological advances that lead to a significantly lower energy consumption can ensure that the nPotato is already integrated into the field during the sowing of the regular potatoes and thus runs through the entire life cycle. The nPotato thus becomes the digital shadow or product memory of a potato. On the one hand, the entire value chain of potato production can be optimized and on the other hand the transparency for the end user can be drastically increased. In the future, however, not only the potato will have a digital shadow. Also conceivable are digital twins of other field crops such as corn or lettuce. The use of smart services in agriculture is just beginning and holds great potential for the future.

[1] Hu, Y. C.; Patel, M.; Sabella, D.; Sprecher, N.; Young, V. (2015): Mobile edge computing. A key technology towards 5G. ETSI White Paper, 11 (11) (2015), S. 1-16.

[2] Kagermann, H.; Riemensperger, F.; Hoke, D.; Helbig, J.; Stocksmeier, D.; Wahlster, W.; Schweer, D. (2014): Smart Service World: Recommendations for the Strategic Initiative Web-based Services for Businesses. Berlin: Acatech-National Academy of Science and Engineering.

[3] Quigley, M; Conley, K.; Gerkey, B.; Faust, J.; Foote, T.; Leibs, J.; Wheeler, R.; Andrew, Y. Ng. (2009): ROS: an open-source Robot Operating System. In: ICRA workshop on open source software, (3) 2009, S. 5.

[4] Schmidhuber, J. (2015): Deep learning in neural networks: An overview. Neural networks 61 (2015), S. 85-117.

[5] Sørensen, C. G.; Fountas, S.; Nash, E.; Pesonen, L.; Bochtis, D.; Pedersen, S. M.; Basso, B.; Blackmore, S. B. (2010): Conceptual model of a future farm management information system. In: Computers and Electronics in Agriculture 72 (01) (2010), S. 37-47.

The Technical Concept of a Manufacturer-Independent Web-Based Data Exchange Platform for the Agricultural Sector

Dr. **Johannes Sonnen**, Dr. **Jens Möller**,
DKE-Data GmbH & Co. KG, Osnabrück

Abstract

This paper describes the concept for a new, web-based data-exchange platform for farmers and agricultural contractors. The platform can be used to link machinery and agricultural software by different manufacturers in order to simplify operational processes. The user has exclusive control over who exchanges what data with whom and for how long. The data-exchange platform only transports data; no data is stored. This unique and non-discriminatory method of data transportation that can be combined and configured individually for each user effectively solves a key issue in the digitalisation of agriculture.

Starting Situation

The optimisation of agricultural production processes and the availability of a high-quality information and communication technology will be essential over the coming years. The increasing complexity of agricultural processes and the growing volume of data and information are leading to increased demand for new data-management concepts, with new features being requested such as manufacturer-independent data transfers, data evaluations, documentation of processes and support in decision making. There are also calls for machinery data to be collected automatically, and transferred to the system used by the farmer or contractor. Users expect the systems to be easy to operate. It is important that the agricultural management software sector, as well as the agricultural manufacturers themselves, all respond to these trends and proceed accordingly. In light of the increasing demand from customers for the networking of the different participants involved in agricultural production processes, the connections that need to be established are becoming all the more complex.

Customer Requirements:

As of yet, there is still no approach that allows farmers to link up the products they use (machinery and software) in a customised manner and to have individual control of the desired data exchange. In addition to the established manufacturers of agricultural software,

new software products for particular applications are also being offered by other companies, including a number of start-ups. Many of these applications require manufacturer-independent access to machinery data in order to support farmers with their aim of production process optimisation. As existing manufacturer-specific solutions do not provide any central access to this data, multiple individual interfaces to the manufacturers need to be set up and managed, which can be time-consuming and complex. From a farmer's perspective, the valuable expertise of these providers is therefore unusable.

A New, Manufacturer-Independent Approach

With the new, manufacturer-independent and web-based data-exchange platform "agrirouter", practically all software applications and machinery can be linked via an open interface. This is performed via a communication unit on the machines. Software applications such as Farm Management Information Systems (FMIS) or apps by third-parts providers can also be linked on a farmer's agrirouter platform. This open approach makes it possible for additional market operators (e.g. manufacturers of input materials, agricultural trading sector etc.) to provide their digital products on the platform. Within the data-exchange platform itself, there is an integrated marketplace with a list of all certified apps and communication units divided into various categories, giving the end user a quick and central overview of the products on offer.

In the future, end users will be able to create free, personalised accounts at my-agrirouter.com. As well as creating an account, end users will also be able to link up their machinery by entering a unique TAN number into the communication unit. This number (or multiple numbers) can be generated in advance within the user's agrirouter account. Following the initial connection with the communication unit, the unit will be assigned a token from agrirouter, which will need to be saved for the subsequent registration processes. If the communication unit offers the option to save multiple tokens and to manage these by selecting different profiles, this means that the communication unit can also be used by several farms. In the future, farmers and/or contractors will increasingly be equipping their tractors with an ISOBUS communication unit, as the connected devices may vary from agrirouters point of view. agrirouter will only check the communication unit certificate assigned via the certification procedure. All DKE-Data company members and third-party hardware providers can present their communication units for certification. Thanks to this approach, mobile communication units on the farm can also be used across different machines, and do not need to spend too long on self-propelled vehicles that are only used for short periods of time, for example.

Once the machinery has been connected, the end user will select his or her preferred apps from the marketplace, thereby completing the individual configuration of his or her agrirouter account (see Fig. 1).

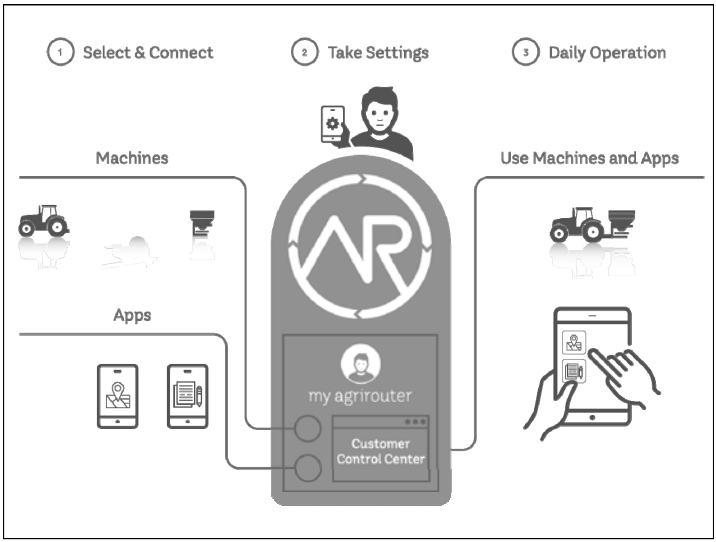

Fig. 1: Working with the “agrirouter” data-exchange platform

App instances are connected via the communication unit, by entering a pre-generated TAN number. The app instance also receives a token from agrirouter, which will need to be saved for all subsequent authentication processes. Once the communication units (machines) and apps have been connected, the end user will need to use a responsive agrirouter web interface to define rules regarding which data (and to what extent) can be exchanged with which connected end points, and for what period of time (see Fig. 1). It is important to note that each software developer can offer an agrirouter-ready application. There are no other technical requirements that need to be met here, such as a specific operating system or interface design. The apps simply need to undergo a certification process similar to that for the communication units. Prior to the certification process, the app developer will receive the necessary interface documents (Integration Guide) as well as access to an agrirouter test environment in which they can test their app in relation to correct login and data exchange functionality. Once an app has successfully passed a certification process, the certified version will be included in the marketplace in the categories selected by the app provider.

The app developer must ensure that content such as descriptions and screenshots of the app is written in the languages in which the app is to be provided to end consumers. When an app is submitted for certification, the app developer must check the available message formats that can be transported on agrirouter, and specify the ones that it is able to send and receive. The app developer is free to view the different message formats for the agronomic data. The resulting abilities of an app to send or receive message formats is used by agrirouter to prevent end users from setting incorrect rules. For example, the end user will not be able to set any rules that include the sending of messages with format M1 to a communication unit if the communication unit is not able to receive this format. In addition to the message formats for agronomic data, other message formats can also be easily incorporated. DKE-Data company members also have the option of having manufacturer-specific message formats created for non-agronomic data. This makes it possible for the DKE-Data company members to offer their machines with intelligent additional functions in order to stand out from the competition.

Once the user has defined his or her individual rules at a message-format level, he or she will then use the connected machines and apps with agrirouter simultaneously working in the background (see Fig. 1). The user will not need to log into his or her account again until he or she wishes to connect a new communication unit or software application or to make changes to the rules. App developers are given the option to incorporate a "Go to my agrirouter account" button to make the login process easier for the end user. This makes it possible for the user to configure "his" or "her" router individually, and to have complete control of his or her data.

agrirouter Data-Exchange Platform: Technical Details

The end points (machines and apps) connected by the user to his or her agrirouter identify themselves via their assigned certificates and tokens in order to retrieve messages from their OUT-boxes.

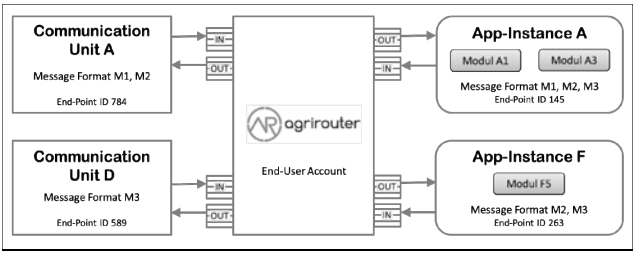

Fig. 2: Agrirouter detailed overview

The agrirouter works passively here, i.e. it places the messages into the OUT-boxes in accordance with the rules defined by the user. The connected app instances, which nowadays often have functions with a modular design, can take a look at the contents of the OUT-box before retrieving the dedicated messages (see **Fig. 2**). Each message is kept in an IN-box or OUT-box for a maximum of 4 weeks if it is not opened during this time. After 3 weeks, the user will receive a notification explaining that the message will be deleted in 1 week. Communication units installed on machines, and app instances that send messages, all place their collected or generated data into the IN-box of the assigned agrirouter account. The defined rules then apply, and the messages are placed into the correct OUT-boxes accordingly. Unlike with normal Post-System, agrirouter can duplicate messages if multiple OUT-boxes are to receive the same information. An example of defined rules is shown in **Fig. 3**. In this example, the user has specified that the message format M2 from end point ID 784 and the message format M3 from end point ID 589 should be transferred to the OUT-box of connected end point ID 263. It can also be seen in **Fig. 3** that the message formats can have different transmission cycles.

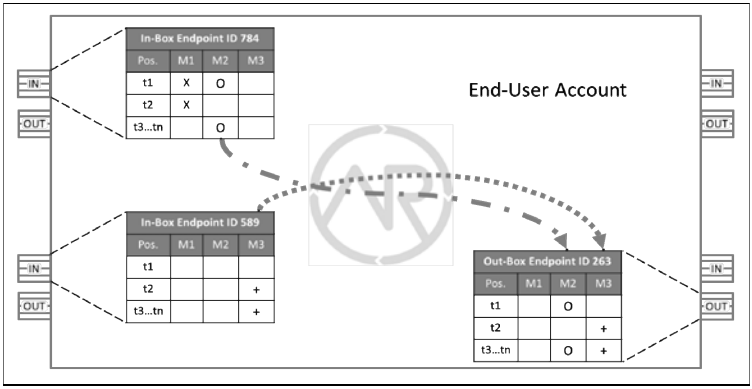

Fig. 3: Example of rules defined by a user

In addition to the direct delivery of messages to individual dedicated end points (see example in **Fig. 3**), the user can also set up his or her agrirouter in a way that is comparable to a truck driving around with the incoming data and each connected app instance taking what it needs. If a farmer or contractor wishes to deny an app instance access to the data, he or she can deactivate individual end points or delete them altogether. If a farmer is working together with a contractor, both parties can exchange data with one another once the two agrirouter

accounts have been linked. This enables the contractor to virtually share with the farmer only the local yield and humidity values for its forage harvester, for example: The farmer can then in turn set appropriate rules for this data, so that the data generated by the contractor is incorporated in the farmer's documentation application for example.
Both users and app providers can see transparent information as to the amount of transported data for their accounts, and in the case of the app providers, the amount of each individual app instance.

Guaranteeing Fail-Safe Operation

When developing the technical design of the overall system, a conscious effort was made to create an extremely high level of reliability in order to increase the security of the transported data to a maximum. For example, **Fig. 4** shows that the Configuration Module which enables the user to adjust the settings via a browser is separate from the actual Messaging Module.

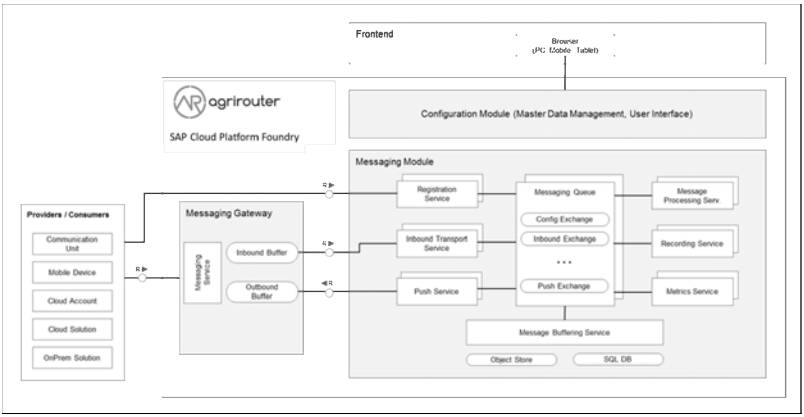

Fig. 4: Agrirouter technical structure

All of the settings adjusted by the user are replicated in the Messaging Module in order to ensure that the transportation of data is maintained if the Configuration Module fails. If the core element of the Messaging Module fails, incoming messages will continue to be stored in the IN-boxes. Delivery of these messages will then be delayed until the Messaging Module is back in operation. This is designed to keep data losses to an absolute minimum. In order to meet agricultural peak times, each component being used can be scaled to the application. level independently from the other components.

Developing a User Interface for Controlling Swarm Technology

Prof. **Jens Krzywinski**, TU Dresden, Dresden

Abstract

Agricultural technology faces radical changes: growing world population, productivity limitation by reaching physical limits of working width, processing speed and payloads and digitalization. A substantial increase of productivity could only reached by improving the human-machine-cooperation [1]. One possible approach could be a collaborative concept named Feldschwarm©. The Feldschwarm© works as a swarm of self-sufficient diesel-electric power machines sharing a tractor as swarm leader followed by a number self-powered implements. Major Challenges for controlling a swarm are (1) the vast increase of accessible information, (2) the separation of operator and machine and (3) the varying number of connected machines. We face these challenges by using a user-centred design approach incorporating user experience design and multimodal interaction for designing the human-machine-interface.

Challenges in Agricultural Technology

Agricultural technology faces radical changes: growing world population, productivity limitations by reaching physical limits of machine dimensions and digitalization.

The growth of world population and the associated increasing demand for food is a major challenge for agricultural production [2], [3]. The increase in yield can be achieved mainly by accessing new land or increasing production efficiency. In the past, agricultural machines increase their productivity by mechatronic solutions of single working tasks and by raising the working width, processing speed and payloads. Now, limits of machines are reached because of e. g. soil compaction, complexity of the overall system and physical dimensions for traffic transport.

The electrification of single working tasks provided a lot of information, processed and managed by the operator. By digitalization, the next technological revolution, the amount of information will increase even further. Until there are no fully automatic agricultural machines, which will take approximately 10 to 20 years, these information have still be processed by the machine operator.

Facing the Challenges: User-Centred Design, User Experience Design and new interaction technologies for Agricultural Equipment

Facing the challenges in agricultural technology, a substantial increase of productivity could reached by improving the human-machine-cooperation [4]. In that sense, the human-machine-interface becomes one of the major topics. User-Centred Design (UCD) puts the operator in the focus of product development. UCD is a point of view for decisions of product development, which includes anthropometric, cognitive, emotional and social aspects of product use by the operator. We applied a user experience design approach to incorporate all of these aspects of human-machine-interaction.

The human-machine-cooperation of highly automated machines is characterized by an equivalent division of working tasks and flexible also situational function reallocation [4]. In human-machine-systems, four main tasks may be distinguished: (1) planning, (2) communication, (3) management and (4) navigation [5]. The operator is the manager of the system: he or she takes the decisions e. g. order sequence. The machine supports the operator by providing recommendations. Hence, the main issues for enabling an optimal decision are communicating all relevant information and show possible solutions. We use an experience-integrated design approach for accessing all of the human aspects (social, emotional, cognitive and anthropometric), which are involved in decision making.

In recent years, there are new interaction technologies for display, selection and navigation information which could be used for facing the challenges of human-machine-interfaces of agricultural machines (figure 1). Heading straight forward from touchscreens, there are head-up displays, head-mounted displays or virtual reality googles (e. g. Oculus Rift, HTC Vive). Eye-tracking, gesture control and tangible interface are new technical possibilities for input devices.

Fig. 1: New interaction technologies and their estimated market maturity

The Feldschwarm© as a Collaborative Machine Concept

Digitalization will enable fully automatic agricultural machines in the future. Yet, it is technically and economically not possible now. In that sense, we propose a future-oriented collaborative machine concept named Feldschwarm©. [6] The Feldschwarm© works as a swarm of self-sufficient diesel-electric powered machines. It consists of several drones and one leading vehicle, which are linked by master-slave-system.

The Feldschwarm© incorporate the operator as an important part of the system and use his or her characteristics for improve the productivity. The operating tasks of a swarm change in a significant way from driving and working with one physically coupled implement to controlling a variety of self-propelled machines and their parameters. Major changes are the separation of operator and machine, the varying number of connected machines and the vast increase in accessible information. The question, how future working environments enable machine operators to supervise and control a network of electrified machines in a reliable, safe and healthy way may be answered by intelligent mobile operating devices.

We propose three concepts of controlling a swarm (figure 2): (1) swarm leader concept, (2) the mobile HMI concept and (3) a mobile control room-concept [7].

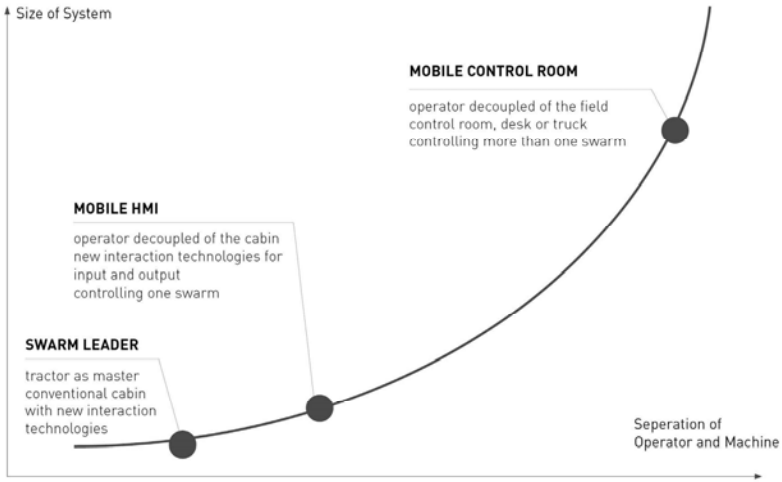

Fig. 2: Concepts for controlling a swarm, ordered by separation of operator and machine and the size of system

The concept *Swarm Leader* consists of a tractor followed by several drones. The tractor is the master of the system. The tractor cabin is a conventional cabin that include new interaction technologies for controlling the following drones (e. g. touchscreens, head-up displays). The concept *Mobile HMI* decoupled the operator from the cabin by using mobile input- (see figure 3) and mobile output devices (AR Googles).

Fig. 3: Prototype of an input device for the concept *Mobile HMI*

The concept *Mobile Control Room* is characterized by a swarm of machines (working on the field) and a control room which is fully detached of the field. The control room could be a desk in a control room, at home or a truck and uses gesture controls, tangibles and Virtual Reality. All concepts are characterized by an adaptive, situation adjusted interaction enabled by the new interaction technologies. They differ in some parameters e.g. the degree of automation.

Literature

[1] Geisberger, Eva; Broy, Manfred (Hg.) (2015): Living in a networked world. Integrated research agenda Cyber-Physical Systems (agendaCPS). München: Utz, Herbert (acatech STUDIE).

[2] Federal Institute for Population Research. (2014). Development of the World Population by Continents, 1500-2150.

[3] Amrhein-Bläser, C. (2013). Wandel in der Landwirtschaft: Wie sieht die Ernährungswirtschaft im Jahr 2050 aus? Technologie-Informationen - Wissen und Innovationen aus niedersächsischen Hochschulen, 2/2013 (Analysen, Strategien und Handlungsempfehlungen).

[4] Grote, Gundula; Ryser, Cornelia; Wäfler, Toni; Windischer, Anna; Weik, Steffen (2000): KOMPASS. A method for complementary function allocation in automated work systems. In: *International Journal on Human-Computer Studies* (52), S. 267-287, zuletzt geprüft am 11.09.2017.

[5] Timpe, Klaus-Peter; Baggen, Robert (2002): Mensch-Maschine-Systemtechnik. Konzepte, Modellierung, Gestaltung, Evaluation. 2. Aufl., Stand: Februar 2002. Düsseldorf: Symposion.

[6] https://www.ivi.fraunhofer.de/ Forschungsvorhaben Feldschwarm© gestartet

[7] Krzywinski, Jens; Lorenz, Sebastian; Apitz, Frank: Agricultural HMI Visions 2020-30. Different concepts for new harvesting systems and user oriented operating solutions. In: 73rd International Conference on Agricultural Engineering LAND.TECHNIK AgEng 2015 - Innovations in Agricultural Engineering for Efficient Farming.

Autonomous Agricultural Machines

The Next Evolution in Farming

Chris Foster, **John Posselius**, CNH Industrial, New Holland, PA, USA;
Brad Lukac, CNH Industrial, Burr Ridge, IL, USA

Abstract

Many organisations are performing research in the development of autonomous agricultural machines. Removing the operator from the vehicle provides many challenges, but also allows for many new possible opportunities. The operator present on today's agricultural machines perform a wide variety of abstract tasks, and there are significant challenges in getting electronic and software systems to effectively replicate all of these tasks. In August 2016 CNH Industrial presented their Autonomous Concept Vehicles at the Farm Progress Show in Boone, IA. 4 main sub-systems were added to the vehicles to enable autonomous operations in the field, and allow operation without an operator on-board: Machine Automation Kit, Communication Network, Command & Control System, and a Sensing & Perception System. While there are significant technical challenges in the development of autonomous agricultural machines, there are also social considerations that need to be accounted for. As the on-road industries are learning, there are many socially or culturally accepted exceptions/rules that need to be taken into consideration, if an autonomous product is to be successful in the market.

System Architecture

As shown in Fig. 01 four main subsystems that enable autonomous agricultural machines are envisioned:

1. Machine Automation Kit: additional hardware required for autonomous operation
2. Command & Control System: data management and user interface to control vehicles
3. Sensing & Perception: Sensing systems used to perceive and interact with surrounding environment
4. Communications & Networking: Network that allows for remote interaction with the vehicles

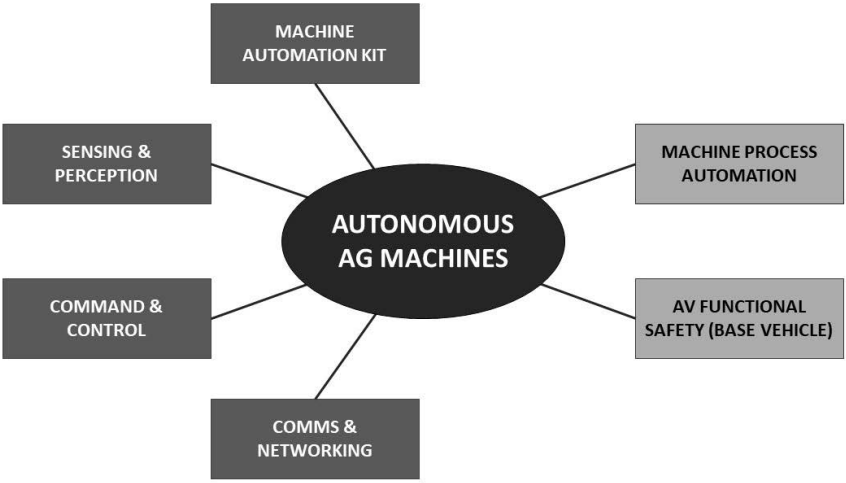

Fig. 1: Autonomous Machine System Architecture

These autonomous vehicle subsystems are built on top of an autonomous ready base vehicle that has the following vehicles systems built into it:

1. Machine Process Automation: automation of internal processes within the machine
2. AV Functional Safety: base vehicle systems redesigned with possibility of no onboard operator

Machine Process Automation involves the design and implementation of control systems internal to each specific machine, and that are pertinent to the operation of that particular piece of equipment. For example, in a combine harvester some of the internal processes that need to be automated consist of the threshing, cleaning and residue management systems. The automation of these sub-systems enables autonomy but can also be sold independent of autonomous agricultural machines as operator/user assist features that provide improved productivity, efficiency and operator comfort.

Functional Safety is an important design process that all manufacturers work through in the design of their equipment. Most of the functional safety analysis that has been performed on agricultural equipment to date has been performed under the consideration that there is nearly always and operator present in the cab of the machine system (e.g. tractor with baler). In autonomous agricultural machines, there will most often not be an operator present in at

least one or more of the machines being operated. The assumption of an agricultural machine operating with no operator on-board will require a significant amount of rework on the functional safety analysis for these machines, and will lead to the redesign of many base vehicle systems, such as steering & braking for example.

Machine Automation Kit

The machine automation kit consists of any additional hardware and software components that are required to enable autonomous machine operations. The processing requirements for autonomous machine operations is significantly greater than the embedded processing power that is presently on-board agricultural machines today. Some electronic hardware companies have foreseen this and will soon be making available embedded hardware that addresses this requirement for increased processing power.

The integration of these components into the base vehicle is no-trivial task. Interfaces into the base vehicle systems such as steering, braking, transmission, engine, etc. are required. This is complicated further by the fact that a machine system can consist of multiple pieces of equipment (e.g. tractor with planter, combine harvester with header, etc.), that may come from different manufacturers. Implement/attachment control systems are becoming more and more complex, and the interface of these autonomous agricultural machine systems needs to be considered as well. This is no small challenge, and through the collaboration of design teams at all levels of machine design solutions will need to be thought through and implemented.

Command & Control System

The Command & Control systems primarily consist of hardware and software systems that allow users, both remote and on-board, to interact with and control one or more autonomous agricultural machines. This system accesses and utilises all data pertinent in the planning and control of the autonomous agricultural machines (e.g. maps, equipment geometry, crop types, system process maps, etc.). System elements encompassed by Command and Control are mission planning & optimisation, mission implementation and monitoring, alerts and warnings to local and remote operators and data manipulations. These are are primarily accessed and managed through a set of software systems, which can be relatively complex.

In the CNH Industrial Autonomous Concept Vehicle that was launched at the Farm Progress Show in Boone, Iowa, USA in August 2016 two command and control interface concepts

were shown. One of the Command & Control concepts shown was a remote base station located in a farm office, as shown in Fig 02. The other was a local operator user interface that could be used on-board or within line of sight of a piece of equipment, as shown in Fig 03. These Command & Control interfaces had screens including interactive maps, gauge panels, and live video feeds from equipment working in the field.

Fig. 2: Remote command and control base station concept shown as part of CNH Industrial Autonomous Concept Vehicle launch at Farm Progress Show in Boone, IA, USA in August 2016.

Fig. 3: On-board command and control system concept shown as part of CNH Industrial Autonomous Concept Vehicle launch at Farm Progress Show in Boone, IA, USA in August 2016.

Communications & Networking

The Communications and Networking system is used to remotely relay information/data to autonomous vehicles from remote command & control interfaces. Large areas of agricultural land globally have poor communications coverage. This will need to be addressed to enable large scale deployment of autonomous agricultural machines. There a variety of technologies and approaches that can be used to address this. While there is a lot of well understood science in the design of radio systems, the implementation of radio systems in practice has some art to it as well.

Sensing & Perception

The Sensing & Perception system is responsible for allowing the vehicle to perceive and interact with the surrounding environment. The agricultural environment is diverse and there are many features of interest that the vehicle will need to detect and plan how to react. The design of these systems is probably one of the biggest challenges facing the robotics industry at present. When you look at everything a human operator does while operating a piece of equipment they are collecting information:

- about the machine performance
- about the surrounding environment within which the machine is operating

They are then processing this information to:

- determine if adjustments to the machine operation are needed,
- if adjustments to the machine operation are needed, what to adjust and how
- determine if there are any hazardous situations in the vicinity of the machine that may need to be reacted to,
- if a reaction is required, how to react to the particular situation, and what actions to take

It is very challenging to get machines to perform these same tasks. Machines are presently very good at precise and repetitive actions (e.g. pick and place), while humans are very good at more abstract tasks (e.g. collecting information about a new situation that has not been seen before and determining how to react). Many researchers are working on improving the performance of machines in the more abstract tasks of sensing and perception for autonomous vehicles.

The environment in which machines/vehicles operate is very complex and the interactions between features in the surrounding environment is not straight forward. For example if someone wants the machine operator to stop so they can talk with them, they could perform one or more of the following actions:

- make eye contact with the machine operator
- use body language to show an intention to walk towards the machine (e.g. put a foot forward in preparation for motion towards the vehicle)
- wave at the machine operator with an arm to get the machine operators attention

This type of interaction is not the same every time, and how it is performed may depend on the social and cultural practices of that region. Because of the variations and complexity of this interaction it is presently difficult to get a machine to accurately replicate and react like a human to this situation. There are many different sensing technologies that are available and under development. At present, it appears unlikely that one single sensing technology can perform to the required levels in all operating conditions, but a combination of sensing technologies that provide redundancy may provide a sufficient level of performance. Obscurants such at dust and various forms of precipitation present particular challenges for

some sensing technologies. Some of the sensing technologies that the robotics industry is presently looking at for use on autonomous vehicles are:

- LiDAR
- 3D TOF Cameras
- Radar
- Ultrasonic sensors
- Stereo-Cameras
- IR Cameras
- Monocular Mono-chrome or RGB cameras

Conclusions

While the development of autonomous agricultural machines has been on-going for some time, and significant progress has been made, there are many challenges that are yet to be overcome. But with the advances and greater social acceptance of autonomous passenger cars, the farming industry is showing a greater and greater interest in autonomous ag machines. Farmers are looking at autonomous agricultural machines to address problems such as skilled labour shortages, greater productivity from each machine, and to provide greater accuracy of field operations. The future is coming, whether we're ready for it or not.

Fig. 4: CNH Industrial Autonomous Concept Vehicle shown at Farm Progress Show in Boone, IA, USA in August 2016

High Voltage OnBoard Networks

The AEF Power Interface is ready to become an ISO standard

Dipl.-Ing.(FH) **Harald Dietel**, Sensor-Technik Wiedemann Kaufbeuren

Abstract

Electric drives are becoming increasingly important in agricultural technology, as they have a number of significant advantages over hydraulic drives or the PTO. They are more precise, efficient and offer more possibilities for automation, and will thus pave the way for a new generation of agricultural equipment.

The AEF created a separate Project Team “High Voltage OnBoard Networks” to address the premise that electric motors of implements should be compatible with every tractor model, and that the output of the tractor should be the only limitation of power.

What has long been missing was a standardized interface for both direct and alternating current capable of providing enough power for large electric motors. The AEF has been working on a solution since 2010 and expects the interface to be ready for launch this year.

The undisputed decision that high-voltage on-board networks should be based on ISOBUS was a fundamental one, i.e. ISOBUS is necessary for the power supply of the implement.

The new interface delivers 700 V direct current, or three-phase 480 V alternating current providing up to 150 kW power.

The High Voltage project team consists of four subgroups working on definitions for mechanical and functional compatibility as well as on safe and reliable operation. One of the most important milestones was the specification of the face and pins of the interface to ensuring that the two parts fits together even if they are supplied by different manufacturers.

First steps to the change of technology on implements

In the year 2009 most of the implement manufacturers thought it was time for a new generation of implements powered by electrical energy. The other solutions PTO and hydraulic equipment seemed to be at their limits. Electric drives have specific advantages, for example high dynamic, more precise, much more efficient and better equipped for automation. Therefore the agricultural world wanted to use the motion control equipment of the stationary industry like robots, tooling and packaging machines for this new application.

A small number of agriculture companies started developing an electrical power interface between tractor and implements. After the initial developments, the AEF created a dedicated project team to continue the investigation. The scope was clearly defined:

Power Interface for 700 VDC or 480 VAC / 150kW, controlled by the ISOBUS

- AEF proposal as input for standardization to an ISO/IEC standard
- Technical specification needed for interoperability / cross compatibility
- Proposal of a physical interface for reliable and safe operation

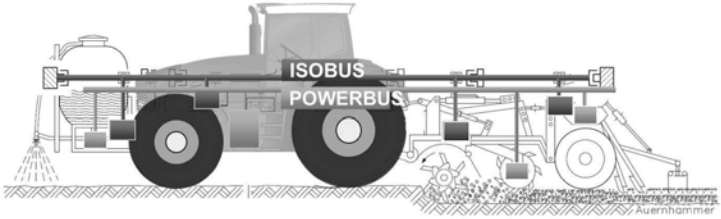

Fig. 1: Electric Power is controlled by ISOBUS

The scope indicates the requirements of such an interface are not easy to fulfil because of the harsh environmental conditions, combined with the need for easy handling, as well as safe and reliable operation. Furthermore cross compatibility demanded that the two sides of a connector must fit each other even when produced by different manufacturers. In addition there must be one interface for both, DC and AC power including a feedback for AC motors and an Interlock.

Within the AEF the importance of ISOBUS technologies today and in the future is undisputed and so the decision that high-voltage on-board networks should be based on ISOBUS was a fundamental one, i.e. ISOBUS is necessary for the power supply of the implement.

AEF Project Team 7 “High Voltage”

Within a very short time, all the important agricultural companies, universities, institutes and experts of connectors, motors, generators and inverters were part of the project team. Divided into four sub groups, nearly 100 persons from 51 companies started working on the interface and the definitions of how to run it, as well as the safety aspects.

Fig. 2: 51 Companies are part of project team “High Voltage”

Sub Group 1 “Physical Interface” developed the requirements of the interface. Up to 10 specialized connector manufacturers worked on a common solution. Most importantly the individual designs of the different manufacturers had to be cross compatible. The solutions were tested in the field as well as laboratories.

Sub Group 2 “Safety” did advanced risk analysis under the lead of TÜV Rheinland. The outcome was the specification of safety aspects required by the other Sub Groups.

Sub Group 3 “Implement manufacturer” as the important stake holder this group produced the requirements specification for the “High Voltage” team work and is still testing the outcome in the field. Their feedback was necessary for the work of all the other Sub Groups.

In Sub Group 4 “Physical and Logical Interface” all definitions for a safe usage of the electric power interface were identified and specified.

Final solution of the interface

One of the main demands of the interface is interoperability and cross compatibility. Most important is that each manufacturer can offer an individual solution as long as both sides of the connector fits those of other manufacturers.

The most important points of the interface specifications are:

- As small as possible (easy to handle)
- Pins sized for 700 VDC (direct current) or 3 phase 480 VAC (alternating current)
- Interlock for detecting the status of the connector being properly mated
- Control pins for feedback signals from implement 360° shielded
- Isolation according IEC 60664-1 (rated impulse 6kV / pollution degree 3)
- Rated current 200 V
- Contacts shall accept up to 70mm^2 cable
- Phase contacts shall be finger proofed according IPXXB/IP2X of IEC 60529
- Protection IP6k9k and IP67 in mated condition
- 3000 mating cycles

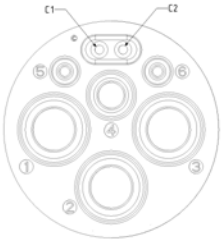

Tractor Side (Front View)

Implement Side (Front View)

Pin	Signal DC	Signal AC
1	DC +	Phase L1
2	Not used	Phase L2
3	DC -	Phase L3
4	EPBC	
5	Interlock	
6	Interlock	
C1	Not used	Feedback
C2	Not used	Feedback

Fig. 3: Layout of the face of the power connector

Current status of guidelines as basis of standardization

There are four AEF guidelines which have been released or are in final approval status to describe the power interface and its function:

AEF 030 DIG 0_2 High Voltage - Electric Power Interface

Description of the physical interface including the specification of contacts, pinning, isolation, protection and dimensions including drawings and step files (Status on 21st of August. To be released (RIG status) in November)

AEF 031 RIG 1_0 High Voltage - Safety Requirements

Description of all safety aspects of the connection, but no functional safety aspects which are the responsibility of the tractor and implement manufacturers

AEF 032 RIG 1_0 High Voltage - DC Logical and Operational Interface

Description of how to run the interface with DC current and all aspects of usage, limitations and the quality of electric power.

AEF 0xx WDIG 0_1 High Voltage - AC Logical and Operational Interface

Description of how to run the interface with AC current and all aspects of usage, limitations and the quality of electric power.
(Status on 21st of August. To be released (RIG status) in June 2018)

Next steps

The standardization process in becoming an ISO Standard has already started. The proposal is that the guidelines will be used by a new ISO Group in TC23 (Agriculture and Forest) and

SC19 Electronic. This working group with the proposed name WG9 “HV” should work on the following 5 subjects: Common, Physical, Safety, DC current and AC current.
In addition the new prototypes will be tested in the field meanwhile the first applications can be seen at Agritechnica 2017.

Fig. 4: First prototypes of the power interface from TE and Harting which have been tested successfully for cross compatibility

Automatic Adjustments of Combine Harvesters

Dipl.-Math. **H. Vöcking**, Dipl.-Ing. **C. Heitmann**, Dipl.-Ing. **A. Wilken**,
CLAAS Selbstfahrende Erntemaschinen GmbH, Harsewinkel

Abstract

In this paper a combination of systems for modern combine harvesters is presented, which adjusts all settings from the threshing system up to the cleaning automatically, so that an optimal operation is always ensured.

After describing the motivation in detail the used mathematical methods are illustrated. The realization of the system brings up some technical issues, especially the need for appropriate sensors, which are depicted in the next section. Another challenge is the definition of what the operator states as optimal, as his goals may vary in different harvesting situations. Therefore a user interface was designed that lets the operator set his demands in a comprehensible way.

Motivation

Modern combine harvesters feature a lot of electronic assistance systems to help their operators in order to keep up the high performance of the machine at any time. Starting from automatic guidance and steering systems over situation based speed control up to the automatic adjustment of the separation and cleaning aggregates with CEMOS[1] AUTOMATIC [1],[2] the driver can specify his requirements and the systems react and adjust the machine's settings accordingly. However, so far the adjustment of the tangential threshing process itself is not automated, though the optimal performance of the combine harvester depends directly on well-adjusted settings of the threshing drum and the concave. Therefore the systems have to be extended to automatically adjust the speed of the threshing drum and the concave clearance. With all these settings done in an optimal way, the advantages of a tangential threshing system in combination with a rotary separation can be fully exploited as the threshing system and the separation are adjusted independently from each other. Also for walker machines the correct adjustment of the threshing unit is very important as its settings are the only way to affect the separation losses.

The mathematical methods for calculating optimal settings for a given process are well-known and have been enhanced and adapted to the process within combine harvesters dur-

[1] CEMOS: CLAAS elektronisches Maschinen-Optimierungs-System

ing the development of the automatic separation and automatic cleaning systems. So the extension to an automated threshing unit is the next logical step towards the optimal adjustment of the overall process within the combine harvester.

The aim of the system is keeping the performance of the combine as high as possible throughout the harvest while considering multiple objectives resulting from the harvesting process. Without an automation solution the operator has to adjust the aggregates of the combine frequently to handle varying situations and to meet his different demands regarding the machine's throughput, the grain quality, the straw quality etc. With the system presented here the operator is relieved because the optimal settings are calculated and adjusted continuously based on the current situation.

Mathematical Methods

In order to get the best suiting settings for the combine a numerical optimization with multiple objectives is used. The optimization needs a mathematical representation of the relevant parts of the process within the machine. Figure 1 shows the main influences and actuators.

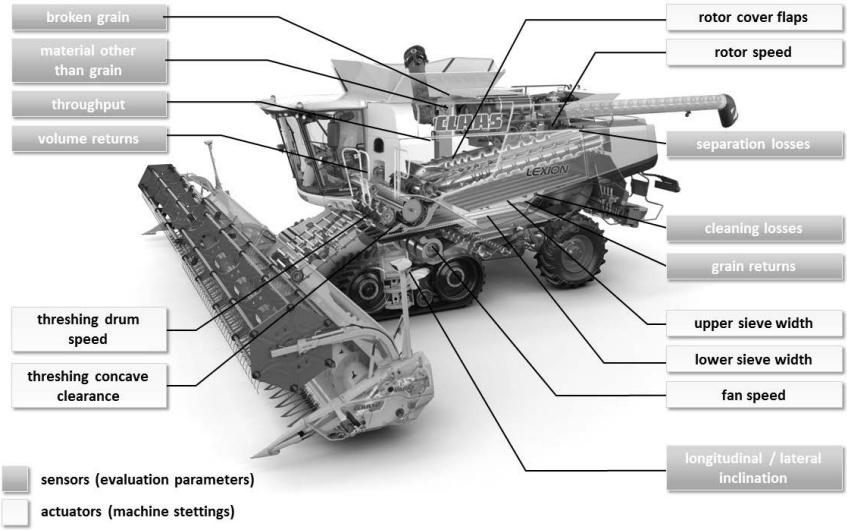

Fig. 1: Main settings and measurement values for the harvesting process

Based on the sensor values and the current settings of the aggregates multiple models of the process are calculated while harvesting. These models provide the mathematical relationship

between the aggregate's settings, the values, which cannot be influenced, like the longitudinal or lateral inclination, and the resulting objectives, like the losses or the cleanliness of the material that reaches the grain tank. All these values are measured and stored continuously to adapt the models accordingly.

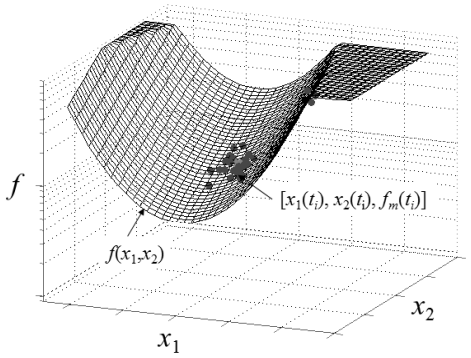

Fig. 2: Schematic of building a process model form measured values

Figure 2 shows in principle how the adaption of the modelled process works. During harvesting the objectives f_m in view are measured with the corresponding settings and influences x_j. With these data a linear regression can be done to obtain a model $f(x_1,x_2)$ that fits the measurement data and thereby the actual conditions on the field.

Each automatic system builds its own regression models of those parts of the process that can be affected by the respective aggregates. For the threshing system, e.g., the following models are relevant:

Broken grain: $BG = f_{BG,thresh}(tp, n_{td}, w_{con})$

Unthreshed ears: $TH = f_{TH,thresh}(tp, n_{td}, w_{con})$

Load: $LD_{thresh} = f_{LD,thresh}(tp, n_{td}, w_{con})$

with throughput tp, threshing drum speed n_{td} and concave clearance w_{con}. The automatic systems for adjusting the separation and cleaning build their own models of the respective processes.

The overall aim to minimize the separation losses L_{sep} and cleaning losses L_{clean} combines all these models. Within each automatic system these models are used for a numerical optimization. Its aim is finding settings for the aggregates so that every objective changes to a value beneath given limits while achieving the maximum possible throughput. However, in many

situations these objectives may conflict with each other. This multi-objective optimization problem is solved by using a weighted sum of the single objectives, for example for the threshing system:

$$f_{thresh}(tp, n_{td}, w_{con}, \alpha, \beta) = w_{sep}\, L_{sep} + w_{clean} L_{clean} + w_{BG}\, BG + w_{TH} TH + w_{LD}\, LD_{thresh}$$

For a given throughput tp and inclination values α and β the weights w_{sep}, w_{clean}, w_{BG}, w_{TH} and w_{LD} are adjusted so that a minimization of f_{thresh} yields the necessary settings for n_{td} and w_{con} to fulfill the boundary conditions. This is done for increasing levels of throughput until no solution can be found. In that way the highest possible throughput is determined and there are also optimal settings calculated for lower levels of throughput.

In most cases there is more than one solution that satisfies all the conditions. It depends on the selection of the weights which of the possible solutions is used. So there are still degrees of freedom for the operator to define his demands like getting very clean grain in contrast to getting the highest possible throughput. This corresponds to real life. Experienced drivers also adjust the settings of the combine in order to obtain satisfactory results for their current requirements.

All automatic systems in combination are in this way able to calculate optimal settings for the combine that continuously adapt to the current situation and meet the operator's requests.

Sensors

In the previous section the online adaption of the process models is described. To gather the necessary measurement values appropriate sensors are needed. For most of the objectives like losses or the amount of material in the returns the sensors are well-established on combine harvesters. Extending CEMOS AUTOMATIC to the threshing system requires the detection of the breakage level, because the aim of the threshing system is to be aggressive enough so that no kernels remain in the ears while not being too aggressive to produce broken kernels. To detect the amount of broken kernels in the grain tank the CLAAS GRAIN QUALITY CAMERA [3] was developed. It is located at the top of the grain elevator and evaluates pictures from the grain flow that is transported to the grain tank (see figure 3).

This position of the camera enables a reasonable measurement though not the complete material is captured on the pictures. The fast processing and evaluation of the pictures gives a statistically accurate result that can be used for building up a process model of the threshing process.

Besides the amount of broken kernels the camera is also able to detect the cleanliness of the grain by identifying the amount of material other than grain within the crop flow. This is an

important value for the cleaning process and is used for the model in the automatic cleaning system.

Fig. 3: Position of the GRAIN QUALITY CAMERA and an evaluated picture

With the GRAIN QUALITY CAMERA sensors for the relevant objectives including those of the threshing process are available.

User Interface

The goal of CEMOS AUTOMATIC is to automatically set the aggregates of the combine to the operator's demands. Not every driver is so experienced that he knows which setting of the machine has to be changed to achieve the required result. It also helps experienced drivers as they do not have to adjust the settings of the combine continually to varying conditions throughout a harvest day on their own. However, as stated before there is still the possibility for the operator adjust his requirements as the machine's settings, which are calculated by the automatic systems, are always a compromise between all the competing objectives. In some situations it may be more important to get very clean grain whereas in other situations the maximization of the throughput is the most important objective to finish the harvest as soon as possible, e.g., because of weather conditions.

With the assistance systems on the combine getting more and more complex, a simple HMI is necessary to let the driver define his demands. Figure 4 shows the interface for adjusting CEMOS AUTOMATIC. It combines the settings for all automatic systems at a central point in the CEMOS terminal.

The definition of the requirements in natural language instead of adjusting the settings of the aggregates directly makes the adjustment of the combine much easier. The settings made in this interface are translated to internal objectives for the automatic systems and finally influence the weights for the optimization. So the result of the numerical optimization can be controlled by the operator in an easy and comprehensible way.

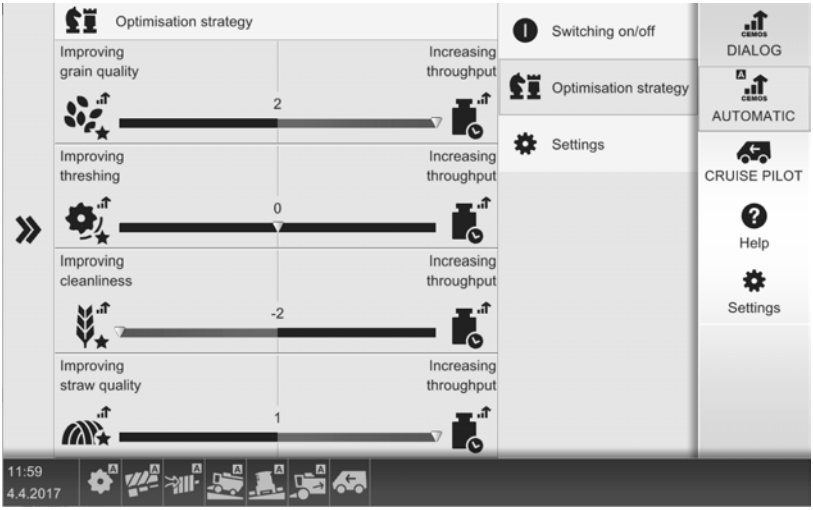

Fig. 4: Adjustment for CEMOS AUTOMATIC

Conclusion

The shown extension of CEMOS AUTOMATIC provides the possibility to control the complete process in a combine form the tangential threshing system over the separation up to the cleaning. The use of an additional camera-based sensor enables the adaption of internal process models to fit the current field conditions so that optimal settings for the machine's aggregates can be determined. Depending on the current situation the driver can define his requirements to adjust the behavior of the automatic systems. To ease this complex task a simple user interface was developed. In this way the combine harvester can always operate at its optimal performance level.

[1] S. Neu, H. Vöcking, A. Wilken: Online Modellbildung verfahrenstechnischer Prozesse. VDI- Berichte 2173, 417-424, VDI Verlag, Düsseldorf, 2012

[2] S. Terörde, S. Neu: Online modelling of harvesting processes. 4th International Conference on Machine Control & Guidance, March 19-20, Braunschweig, 2014

[3] M. Escher, T. Krause: Grain Quality Camera. 4th International Conference on Machine Control & Guidance, March 19-20, Braunschweig, 2014

Optimized material flow and cleaning capacity with new return pan system in a combine harvester

B.Sc **Morten L. Bilde**, B.Sc **Thomas T. Revsbeck**,
AGCO, Randers, Denmark;

Abstract:

This paper addresses the development process and final design of a new return pan system for combine harvesters. The objective of the research and development program presented has been to increase the cleaning shoe capacity within the limited machine envelope of modern combine harvesters, while at the same time make the overall combine performance insensitive to uncontrollable input variables like crop conditions and field terrain. This research has led to the development of a new return pan system consisting of two individual pans with a contoured surface design.

Background

Over the years, the capacity and efficiency of combine harvesters have been incrementally enhanced by ongoing scaling of parameters like threshing cylinder dimensions, number of straw walkers and sieve areas. As combine harvesters of today have reached the limit for both weight and overall size, the industry has been challenged to increase the crop processing capacity without increasing the vehicle envelope. This challenge, has led to the continued development of highly efficient axial rotary threshing and separation processors. As axial processors have increased the overall efficiency of today's high-capacity combine harvesters, the cleaning system has become the capacity limiting process.

Opportunities for increasing the overall capacity of a cleaning system without increasing the system envelope can thus be found in how the grain and MOG mixture is delivered to the cleaning system. First of all, the more evenly the material is distributed across the width of the cleaning system, the more even the fluidization of the material layer that can be achieved. Secondly, the more the material is stratified into grain and MOG components, the higher the segregation efficiency that can be expected along the length of the sieve area is.

State of the art

The threshing and separation processes in a combine are carried out using a variety of different technologies across combine brands and models. Fig 1 illustrates a cross section of an axial combine layout. Regardless of technology and design, the processor generally consists of a threshing section (1) and a downstream separation section (2). From the processor,

the separated grain and MOG mixture is conveyed to the cleaning shoe (5) by means of two oscillating pans. The first pan, which this paper refers to as the stratification pan (3), collects the separated material from the threshing section and conveys this to the cleaning shoe. This material mixture will normally consist of 80 % grain and 20% MOG for wheat. The second pan, which this paper refers to as the return pan (4) collects the material from the separation section and conveys this to the rear section of the stratification pan. This material composition consists typically of 20% grain and 80% MOG for wheat.

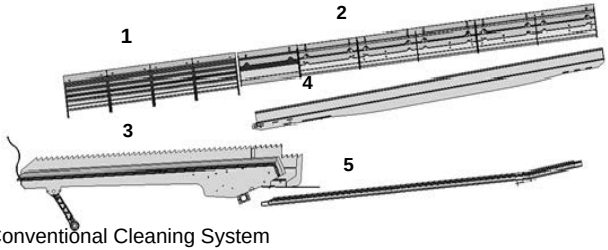

Fig. 1: Conventional Cleaning System

Different characteristics of the described layout for material conveyance influence the performance of the downstream cleaning system.

First and foremost, the stratification of the grain and MOG on the stratification pan has a direct influence on the efficiency of the downstream cleaning process of the cleaning shoe. The stratification efficiency can furthermore be correlated to the traveled distance of the material along the length of a stratification pan with a given design and kinematic motion. As the separated grain and MOG from the threshing section drops directly down on the stratification pan, the separation profile of the threshing section correlates directly to the feeding profile of the stratification pan. As the separation profile changes with changes in crop conditions, due to throughput and processor settings, these variables have a direct influence on the stratification efficiency and thereby the overall cleaning shoe performance. Secondly, the efficiency of the cleaning shoe is highly dependent on how evenly the grain and MOG mixture is being distributed across the width of the system. Though the return pan ensures that all the material from the separation section is collected and delivered with the same traveling distance to the cleaning system, the material distribution across the width of the stratification pan and cleaning shoe will ultimately correlate to the separation profile across the width of the separation section. The material distribution across the width of the system is therefore influenced by the variances in the separation profile across the width of both the threshing section and the separation section of the processor.

Method

With the objective of optimizing the design of the return pan layout, a research program has been carried out with focus on the two most important parameters influenced by the return pan described above.

The test results presented in the following sections are all gathered on a full-scale cleaning shoe test stand and in a controlled and repeatable lab test environment. A 70/30% grain/MOG mixture has been used for all tests.

Optimization of the stratification process

In order to optimize the performance and sensitivity of the stratification process, different return pan designs have been tested.

By way of example, the following three return pan concepts illustrated in Fig. 2 were tested.

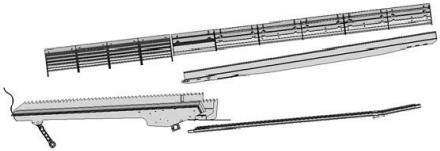

(A) Baseline- conventional return pan

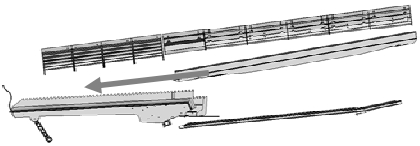

(B) Conventional return pan extended 800 mm

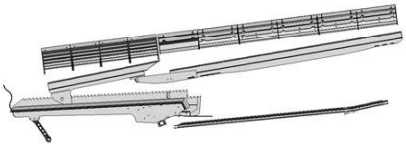

(C) Dual return pan concept

Fig. 2: Return Pan Concepts used for Test Iterations

In Fig 3, the test results are presented as cleaning shoe loss in proportion to total separated MOG from both the threshing section and the separation section of the processor.

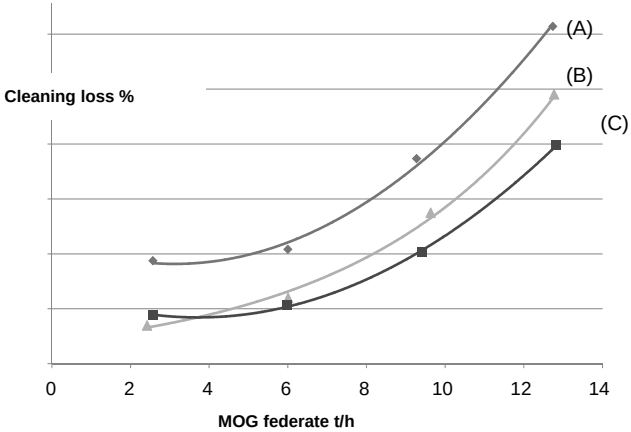

Fig. 3: Results – Return Pan Design Concepts

As seen on Fig. 3, the extended return pan (B) lead to a higher cleaning shoe capacity as all material is being delivered to the front portion of the stratification pan with increased stratification of the grain and MOG mixture as a result. The dual return pan (C) reveals a further capacity increase, even though not all material is being delivered to the front of the stratification pan. This is due to the fact that the grain-rich material from the threshing section is being kept segregated from the MOG-rich material from the separation section.
The dual return pan concept was therefore selected as the preferred concept for all subsequent design iterations.

Optimization of material distribution

By the nature of axial rotary threshing and separation processes, the distribution profile of the separated grain and MOG is uneven across the width of the system and will furthermore fluctuate with changes in conditions and combine settings. With the dual return pan concept as the basis, contoured surfaces of both pans were designed with the objective of developing a return pan system capable of providing the cleaning shoe with an even material distribution in all conditions, without active control systems. From numerus design iterations, Fig. 4 illustrates the preferred and final design of the new return pan system supporting a twin-axial threshing and separation processor.

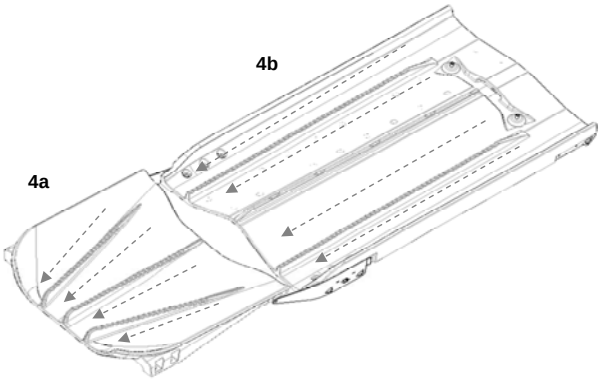

Fig. 4: Contoured Dual Return Pan System (D)

The front return pan (4a) collects the grain and MOG separated from the threshing section, and delivers it to the center section of the stratification pan. The rear return pan (4b) collects the grain and MOG separated from the separation section and delivers it to the outer sections of the stratification pan. The sum of these three material streams result in evenly distributed material being delivered to the cleaning shoe. Said distribution is consistent and independent of the separation profile delivered from the twin-axial processor. Furthermore, the contoured surfaces of the return pan system increase the insensitivity of the system to side-hill conditions, without any active controlled compensation system. Fig. 5 presents the results of a test series, comparing the contoured dual return pan (D) with the dual return pan (C) at 9 degree side-hill.

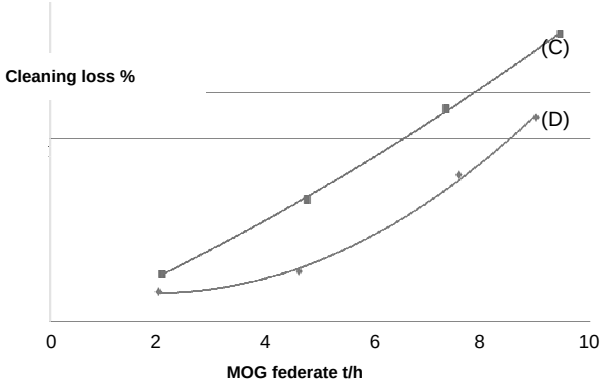

Fig.5: Results - Return Pan Hillside Testing

Industrialization of Design

In order to manufacture the complex geometry of the new return pan system in a weight and cost efficient manner, it was necessary to look at different manufacturing technologies. Based on recommendations, it was decided to make the curved double return pans using a plastic roto-mold process. The design consists of a self-supporting, light weight structure, made from a polyethylene plastic shell, filled with foam. The shell material includes an additive that prevents static electricity build up during operation. The shell material is both wear resistant and tough at low temperatures. The shell is filled with polyurethane closed cell foam to provide additional stability to the structure.

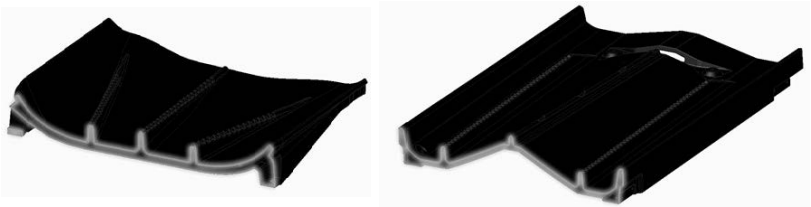

Fig. 6 Foam Filled Shell structure

Conclusion

The research program treated in this paper has proven the distribution and pre-processing of the grain and MOG mixture before delivered to the separation area of the cleaning shoe to have a high influence on overall cleaning shoe capacity. Increasing the pre-stratification of the grain and MOG mixture by increasing the time and distance for the mixture to travel on the stratification pan has a positive influence on the cleaning shoe capacity. Furthermore, keeping the grain rich material from the threshing section separate from the MOG-rich material from the separation section of the processor has a positive influence on the pre-stratification and therefore on the overall cleaning shoe capacity.

In addition, it has been proven that a contoured profile of the return pans contributes to an even material distribution across the width of the cleaning shoe unaffected by processor separation profile and furthermore makes the cleaning shoe less sensitive to side-hill conditions compared to conventional return pan systems.

It has also been proven that it is possible to manufacture the contoured return pans as a single low-weight self-supporting component using composite plastic technologies.

Combine Harvester Concave Adjustment System

Independent adjustment of the concave inlet and outlet clearance

B.Sc. **B. Broholm**, B.Sc. **A. Morrison**,
AGCO Research & Advanced Engineering Global Harvest, Randers

Abstract

This paper explains the development of a dual sided Concave Adjustment System (CAS) for a combine harvester. The design evolution ranges from a single side, clam shell type CAS, to a fixed ratio dual side CAS, ending with an independently operated dual sided CAS.

The choice of actuator for the CAS has changed throughout the design of the CAS. This paper will also explain the added benefits of using a hydraulic actuator compared to an electric actuator for this type of system.

1. Introduction

The overall principal of the combine harvester is to separate the grain from the remainder of the crop. This is done by the threshing of the crop between the keystock of the concave and the rotating rasp bar threshing element of the rotor/threshing cylinder. To obtain the most effective threshing, it is important to regulate and maintain the correct clearance between the concave and threshing element.

While developing a new axial threshing system for a combine harvester it has been necessary to also develop a new concave adjustment system to fit the threshing system.

The design criteria for the newly developed threshing system were as follows:

- Higher throughput of crop
- Higher grain quality
- Higher straw quality
- Lower power consumption
- Less complicated

Through the project, several iterations of the threshing system have been investigated, which has led to the axial threshing/processor system with the independent dual sided concave adjustment.

Section 2 will present the design steps for the CAS, section 3 will explain the chosen actuator for the movement and adjustment of the CAS and section 4 & 5 will present the resulting design and conclusion.

2. CAS – Development & Design

For clarification purpose, the different types of concave adjustment systems are described below in Figure. 1 – Different CASs.

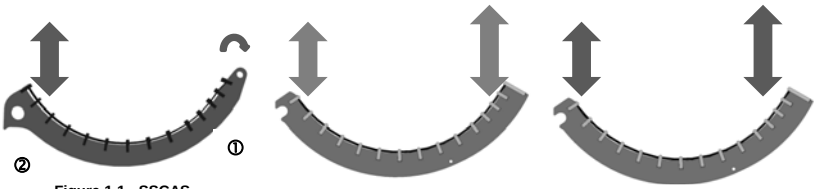

Figure 1.1 - SSCAS

Figure 1.2 - DSCAS

Figure 1.3 - ICCAS

Figure 1 – Different CASs

Concave inlet at right ①, outlet at left ②.

Clockwise rotor rotation for all the figures.

Figure 1.1: Single Sided CAS, vertical movement of outlet side of the concave, inlet side pivots.

Figure 1.2: Dual Sided CAS – fixed ratio; vertical movement with a mechanically fixed ratio between the movement of the inlet and outlet side of the concave.

Figure 1.3: Dual Sided CAS – independently controlled, vertical movement of inlet side of the concave independent from the movement of the outlet side of the concave.

2.1 Single sided concave adjustment

During the initial phases of the development project, the space constraints for the CAS did not allow for a complex structure. The Single Sided CAS (SSCAS) was developed from the well-known principal of the concave adjustment system from a traditional transverse threshing cylinder [1][2]. The clam shell type single sided CAS works by the inlet side of the

concave being hinged with no vertical movement and the outlet side of the concave moving up and down as shown on Figure. 1. Figure 2 shows the design at its initial stage.

Figure 2 - Model of single sided CAS

Lab and field studies showed a lack of threshing capabilities with this simpler CAS design. Comparison charts for the different CASs will be shown in section 4 - Results.

2.2 Dual sided concave adjustment – fixed ratio

The dual sided CAS with a fixed ratio of the movement between the inlet and outlet of the concave was developed as a way to obtain a more thorough yet gentle threshing of the crop. The CAS now allowed a vertical movement of the outlet of the concave, as was the case for the single sided CAS, as well as the inlet side of the concave. The improved design had the inlet side of the concave mechanically connected to the outlet side which allowed a uniform movement and a more ideal concave clearance to be obtained. Figure 3 shows one of the initial designs of the dual sided CAS.

Figure 3 - Model of early design of the dual sided CAS

During the testing of this design of the CAS, the forces on the vertical hangers were investigated. The findings suggested limitations to the current design and it was evident that a completely new design had to be developed

2.3 Dual sided concave adjustment – independently controlled

Based on the data from the previous design, the CAS was redesigned to its current form. Figure 4 shows a model of the current design of the Independently Controlled Concave Adjustment System (ICCAS).

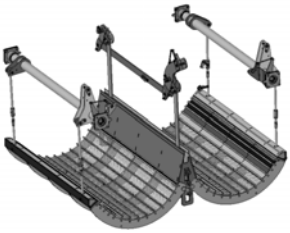

Figure 4 - Model of final design of the ICCAS

The dual sided concept has been kept the same based on the results and experiences from previous testing and due to design constraints defined by the overall project. The main advantage for this design, is the ability to independently adjust the inlet and outlet sides of the concave. It can in certain conditions be of added benefit to the threshing capabilities of the system, to adjust the ratio of concave clearance between the inlet and outlet of the concave.

Whilst continuously developing on the CAS, focus have also been on the before mentioned overall design criteria. Our lab testing equipment allows for monitoring and logging all key data and using this collected data has been essential to reaching the high level of performance on all parameters as seen with the ICCAS.

3. Actuator for the CAS

During the design of the CAS, the feasibility of using an electric to control the concave clearance was investigated. With the added stiffness in the system of the ICCAS, compared to the earlier designs, the electrical actuator proved to be insufficient for the application. Instead a hydraulic system was developed to withstand the increased magnitude of the loading pattern and also allowing the incorporation of a hydraulic release function into the ICCAS design.

3.1 Overload protection

In the previous designs of the CAS a shear pin has been used as an overload protection for the CAS. Due to the characteristics of the loading pattern a shear pin was found to be too unreliable and a new solution had to be incorporated into the redesign of the CAS.

With the hydraulic system being developed to control the ICCAS it was possible to incorporate a release function which engages in the event a large lump of material or a foreign object is introduced into the ICCAS. In the event of an overload of the system, a series of hydraulic pressure relief vales will be activated and will enable the ICCAS to increase the concave clearance to allow the obstacle to clear the system. This feature ensures a longer life of the components of the ICCAS but also a smoother operating experience for the operator of the machine.

4. Results

4.1 Independently Controlled Concave Adjustment System

During the entire development project, extensive testing has been done both on previous designs as well as on the newly developed ICCAS. Figure 5 – CAS comparison, below shows the three previously described CAS test results for losses at comparable through-puts along with the similar data for a transverse hybrid threshing unit.

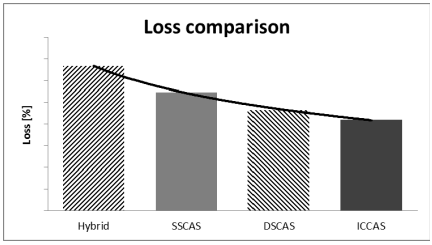

Figure 5 - CAS comparison

Data for the chart are for comparable through-puts and are for the threshing and separation systems only

The charts show significant development over the course of the project along with improvements relating to the project design criteria. The remaining design criteria which are

not shown in the charts are very hard to quantify the results for, as it comes down to perception and opinions more than measurable data.
As the chart in Figure 5 shows, there has been a continued development through the project to minimize the loss of the machine. It has been a challenge to improve the design to meet the strict criteria for the loss, but through the extensive testing and iterative designs it has been possible to meet the loss threshold.

4.2 Release Function

The development of the release function for the ICCAS has until now showed its functionality and eligibility for the system by reducing the strain on the ICCAS along with minimizing the plugging events of the system. The data collected up to this point in time is not released to be published, but lab test results imply that the release function significantly prolong the life of the components of the ICCAS.

5. Conclusion

The nature of a development project is that information and knowledge are gathered all through-out the project. With that in mind it is important to realize that some decisions through the project might have been based on limited data or knowledge. This has led to the multiple design iterations in order to gather the needed data and knowledge to proceed forward with the development.
The testing and validation are done in a few selected conditions and the results are indicating that the ability to adjust the inlet and outlet clearance of the concave independently can increase the threshing ability of the system in different conditions other than the ones tested.
The ICCAS can also be an added benefit for adaptive adjustment of the combine, where the combine can be set for the specific crop condition. The ICCAS can provide the range of settings needed to allow the optimal threshing for that condition.
The current design of the ICCAS is to date the final design, but additional knowledge and information about the system allows the designers to continue to improve and optimize on the design, which will continue into the foreseeable future.

Literature

[1] Miu, P.: Combine harvesters. Theory, Modeling and Design, Boca Raton Florida USA: CRC Press 2016.
[2] MF Centora & Delta combines, Brochure, AGCO, Denmark 2013

Concept for Weed Seed Separation in Combine Harvesters

Dipl.-Ing. **S. Pantke**, Dipl.-Ing. **Ch. Korn**,
Prof. Dr.-Ing. habil **Th. Herlitzius**, TU Dresden, Dresden;
Th. Leonhardt, Saat-Gut Services Czwalinna GmbH, Nauen;
R. Zürn, Zürn Harvesting GmbH & Co. KG, Schöntal-Westernhausen

Abstract

In modern high-performance agriculture, the focus on clean fields increases. Due to herbicide resistant weeds, political pressure and public interest alternative, non-chemical procedures are gaining a new relevance in weed control. One possible approach is the separation of weed seeds in combine harvesters in order to prevent the distribution of weed seeds back to the fields. Objective is to develop a weed seed separation device in cooperation with industry partners as a retrofit or OEM kit for combine harvesters and plot combines.Two methods to separate weed seeds in combine harvesters are tested. On the one hand, a vibro-fluidization system is evaluated, and on the other hand a system that uses the deflecting properties of particles is investigated. The tests are carried out with different parameters to find the optimal settings for the separation process. Under lab conditions, up to 65 % of the weed seeds could be separated by using the deflecting properties and up to 95 % by vibro-fluidization.

Keywords: combine, weed seed control, separation, vibro-fluidization, deflecting properties,

Why Weed Seed Separation?

Weed control is getting more and more important for modern agriculture all over the globe. As a consequence of the increasing number of herbicide resistant weeds (Fig. 1) and public interests, new methods are requested to minimize the impact of weeds to field hygiene and yield. As a result the application of glyphosat and other chemicals can be reduced.

The main benefits of weed seed separation during the harvest are:

- Less effort for weed control
- Less manpower
- Reduction of herbicide usage and subsequent tillage
- Using weed seeds as secondary crops (flowering mixture for bees and other pollinators, bio material)

A very promissing way to minimize weed pressure is to reduce spreading of weed seeds with the combine residue. For instance, the seeds of those weeds, which are growing at the field boundary are spread inside the field by the chaff spreaders supporting further distribution by the harvester. Thus, the main objective of research described in this paper is the development of a functional unit to avoid the discharge of germinable weed seeds once they have entered the machine. In addition to the weed seeds already gathered in the grain bin it is the task to separate the remaining seeds in the residue stream from the MOG (material other than grain).

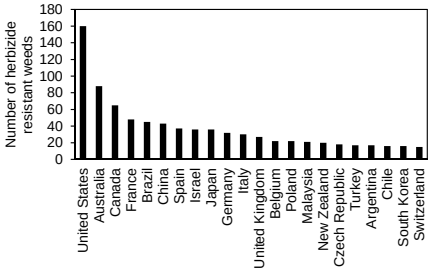

Fig. 1: Number of Resistant Weeds [1]

State of the Art

At present there is a an increasing effort spent on researching solutions for the weed control issue. A few promising technologies are already available at the market or are still under development. One way is to collect the entire residue and take it off the field or burn it on the fields after the harvest. Thus the weed seeds are taken off the fields and germination and spread are prevented. Examples are the *Chaff Carts* and the *Bale-Direct-System*, which are towed behind solutions for combine harvesters (see Fig. 2). The *Chaff Carts* is used to collect the chaff and weed seeds and remove them from the field. With the *Bale-Direct-System* the chaff with the weed seeds is compressed into a bale utilizing a towed behind baler. Another way of weed control is using a high voltage device, called *Electroherb* which destroys the weed plants and roots by electrical current [2]. The latest version of *Harrington Seed Destructor* (HSD), the *Integrated Harrington Seed Destructor (iHSD)* is a device, which is attached to the combine like the chaff spreader. It processes the residues including the weed seeds by grinding them in a cage mill, which reduces germination cabability to a large extent [3]. The research program „Sweedhart“ is also investigating methods to use weed seeds, neutralize them e.g by heat treatment or separate the fractions off-site the field [4]. Another approach called *“Kompakternte”* (see Fig. 3) is to harvest the field and directly collecting grain and chaff in the bin instead the standard cleaning process performed by the combine cleaning shoe. The separation of grain and chaff is done in a downstream stationary process, which avoids redistribution of weed seeds into the field as well [5].



Fig. 2: Left: Chaff Cart towed behind the combine [6] (e.g. Grain King); middle: Bale Direct System [7] (e.g. GLENVAR); right: Electroherb (Zassa GmbH) [8]



Fig. 3: Left: Integrated Harrington Seed Destructor (de Bruin Engineering) [9]; right: “Kompakternte” [5]

Objectives, approach and method

The new approach is to develop a weed seed separation device as a retrofit kit or OEM kit for combine harvesters and plot combines. It has to separate the weed seeds during the harvest with minimal impact on the harvesting process and a maximum weed seed separation effect. Therefore it is necessary to find a technique of separating weed seeds from MOG (material other than grain) in the harvester with high efficiency, high separation precision, low energy demand and a low process sensitivity to interfering influences.

Based on preliminary investigation it was found that the preferred place in a combine harvester to separate the weed seeds is the area behind the cleaning system. At this point in the combine material flow, grain is already separated and the long straw is processed as another material stream by the straw walkers or separation rotors. Installation of retrofit kits behind the cleaning shoe seems doable for most of the common machines due to the available space. Furthermore, this position is possible for all machine types, e.g. walker machine, a rotor machine or an hybrid machine.

For the separation process the properties of the weed seeds and in particular, their differences to the other processed material (grain and MOG) in the combine are important. The most important weeds and their main properties as growth height, seed loss before harvest, seed kernel width and length and TKW (thousand kernel weight) are summarized based on literature reseach as shown in Fig. 4 through Fig. 7 [10] [11] [12] [13] [14].

For better comparsion properties of wheat fractions, grain, chaff and chopped straw are additionally given for the thousand kernel weight and the dimenensions in Fig. 5 and Fig. 6.

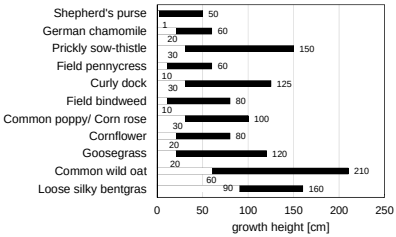

Fig. 4: Growth height of weeds

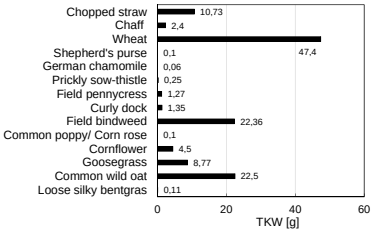

Fig. 5: Thousand kernel weight (TKW) of weed seeds and wheat fractions

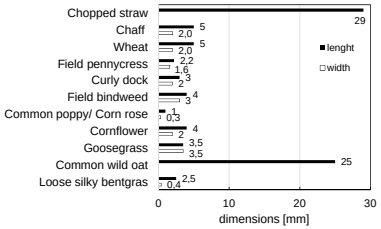

Fig. 6: Dimensions of the weed seeds and wheat fractions

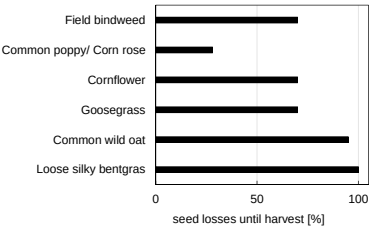

Fig. 7: Seed losses until harvesting

A sufficient growth height of weed plants is a prerequisite for the separation process. A usual cutting height of the cutter bar is about 10 cm. Fig. 4 shows that almost all weed plants are growing higher than 10 cm, which makes a pickup and separation process possible. Only the growth height of shepherd´s purse is less than 10 cm, which exludes it from processing, since the plant remains uncut in the field. Another fact to take into account is that weed plants are adapted to spread their seeds as soon as possible in the season (see Fig. 7). In contrast, the cereal plants are especially bred for strong embrace between the

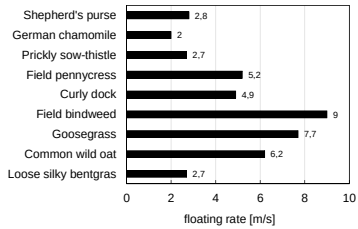

Fig. 8: Floating rate of a selction of particles

e head. Hence, a certain amount of not fed into the combine due to the

fall out before harvest. Weight of weed seeds and geometric dimensions are further important properties for the separation of the material fractions (see Fig. 5 and Fig. 6). These are relevant for processes which are based on size comparison (sieving processes) or the aerodynamic characteristics. The floating rate (see Fig. 8) (air classifier) and the seed size (sieve classifier) are also relevant. Further key factors are the deflecting properties of the particles. Caused by the different elastic deformation characteristics, particles are deflected at different angles after a contact. This feature can also be used for separating materials, such as weed seeds.

Above described characteristics indicate two possible separation solutions which were examined. The first investigated method is the separation of a mixture of weed seeds and MOG on an oscillating sieve with air stream which can be designated as vibro-fluidization, similar to the separation process in the cleaning system of a combine. This methode is described in the following chapter, the corresponding test rig is shown in Fig. 10. The second approach for the separation is based on deflecting properties of the several particles in the mixture, the utilized test rig is illustrated in Fig. 14.

The material for the test procedure is shown in Fig. 9. The mixture of weed seeds contains more than 15 different types such as cornflower, goosegras and wild oat for example.Wheat chaff or respectively chopped wheat straw is used to simulate the MOG of the cleaning system.

Fig. 9: a) Weed Seeds; b) Chaff; c) Chopped straw; d) Wheat grain

Test procedure and results of vibro-fluidization tests

For the vibro-fluidization tests a test rig at the laboratory of the chair of agricultural systems technology (AST) is used as shown in Fig. 10. The test rig exists of a blower (a) which provides the air stream for the sieves, an oscillating sieve (p) and the scale (m) under the sieve and some additional equipment. For the tests the material is put onto the sieve in

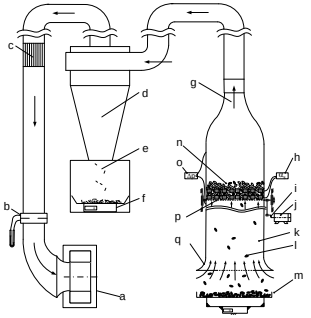

Fig. 10:Test rig for vibro-fluidization

layers (n). After setting up the test parameters (Table 1) such as fluid velocity, sieve amplitude and frequency and sieve hole width, the test is started and the material mass which is falling through the sieve during the separation process is measured temporally resolved. Based on the captured data of the separated mass, the separation time t_{80} is determined, which represents the time until 80% of the inittially included mass of weed seeds is separated. Next to that, the purity of the sieve throughput is calculated, which represents the percentage of weed seeds to the total separated mass. By the variation of parameters listed in Table 1, the setting for the optimal separation is found. For the tests standard sieves with round or square holes are used (see Table 1).

Table 1: Parameters for vibro-fluidization tests

	Parameter	Value
1	Sieve frequency, amplitude, test duration	f= 5 Hz, a= 20 mm amplitude, t= 10s
2	Sieve parameter	4 mm round hole sieve
		5 mm round hole sieve
		8 mm square hole sieve
3	Fluid velocity	v= 0 m/s; 0,5 m/s; 0,75 m/s; 1 m/s; 1,25 m/s
4	Ratio MOG/Weed Seed	75:25 …99:1
5	MOG feed rate	up to 3,25 t/h

Fig. 11 and Fig. 12 show the test results. The separation time and thus the quality of the separation process depends on the fluid velocity and the sieve selection. With increasing the hole size of the sieves the t_{80}- time is getting shorter and also the fluid velocity has an influence. Fluid velocity is limited otherwise particles are fluidized too much and are carried out instead of getting separated.

The optimal fluid velocity is between 0,7 m/s and 1,1 m/s, depending on the sieve hole size. The best result was reached with the 8 mm square hole sieve at a fluid velocity of 0,86 m/s and t_{80}=3,2 s.

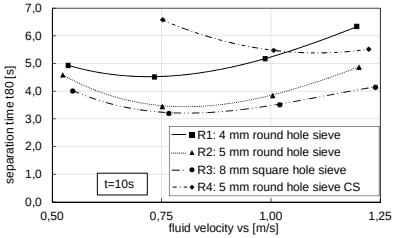

Fig. 11: Separation time t_{80}

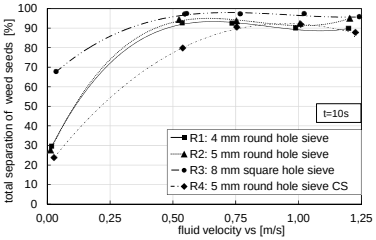

Fig. 12: Total separation of weed seeds

The test R4 with other MOG (chopped straw= CS) has different characteristic and the optimal fluid velocity is higher than in the other test settings. The total separation of weed seeds is as well affected by the fluid velocity and the sieve configuration. As shown in Fig. 12 total separation increases higher air velocities. Thus, it is possible to separate up to 95% of the weed seeds during the test time of 10 seconds. Also important for a reliable process is the purity of the separated weed seeds. It is not possible to clean out the weed seeds only without compromising efficiency. A certain amount of chaff/MOG will be always separated as well. The purity is highly effected by the sieve hole size and the fluid velocity (see Fig. 13).

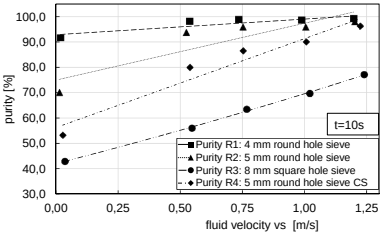

Fig. 13: Purity of the separated weed seeds

The best purity is reached, as expected, with the smallest sieve holes and highest fluid velocity. But for the best separation parameters the purity drops down to ca. 43 % at a MOG:weed seed ratio of 75:25. For a machine use case it will need additonal lab and field tests to find preferred adjustments to get a reliable quality of operating.

Impact Plate Tests

The operating principle of the impact plate (see Fig. 14) is pretty elementary. The material mixture is accelerated in a test channel by an air stream, which is produced by a blower. The tested mixture consists of MOG and weed seeds. These components are injected into the channel by a conveyor belt and an auger injector as a defined material flow. The accelerated particles hit the impact plate and are getting deflected depending on their specific properties. The idea is, that straw and the other material is not as much deflected as the weed seeds, wich does not allow the weed seeds to follow the air stream and makes them fall into the

storage containers (see Fig. 14). Effects of weed seed separation by the impact plate for the test parameters MOG-feed rate, fan speed and impact plate angle at three angles were investigated (see Table 2).

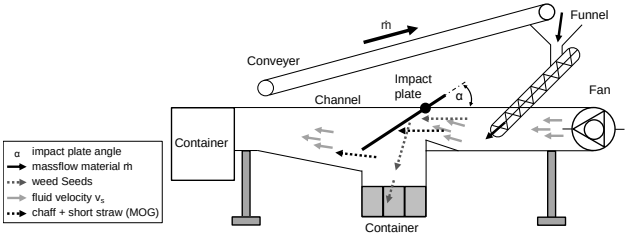

Fig. 14: Impact plate test rig

Table 2: Parameters for impact plate tests

	Parameter	Low	Middle	High
1	MOG feed rate [g/s] (referring to a combine through-put)	50 (1,08 t/h)	100 (2,16 t/h)	150 (3,24 t/h)
2	Fan speed n [min^{-1}] (Fluid velocity)	925 (10,7 m/s)	1000 (11,4 m/s)	1075 (12,1 m/s)
3	Impact plate tilt angle α [°]	35	37,5	40

Fig. 15 and Fig. 16 show the test results of the separation tests. The total weed seed separation is depending on the impact plate angle and the MOG feed rate. The separation is better with a higher impact plate angle and small MOG feed rate. In particular the MOG feed rate has an effect, because with more material in the channel the particles have to penetrate a thicker material layer which causes more particle contacts and more particle deflections. It was shown that a thin material layer is necessary for a successful separation. This can be achieved by high flow velocities in the channel. The best result of 65 % separated weed seeds in the tests is achieved at a plate angle of 40° and 50 g/s MOG feed rate (see Fig. 15). Another important parameter in the separation process is also the purity of the separated material. It describes the portion of MOG, which gets into the weed seed container. Some MOG particles have similar deflecting properties (e.g. straw knots) as weed seeds and are separated as well. The separated MOG portion is shown in Fig. 16 and it is evident, that the plate angel has an effect, more than the MOG feed rate. The target should be to separate as much as possible weed seeds, while separating a small amount of chaff. For a functional and

trustworthy weed seed separation device a combination of the two tested methods is possible. The final prototype has to be approved in lab tests before starting field trials.

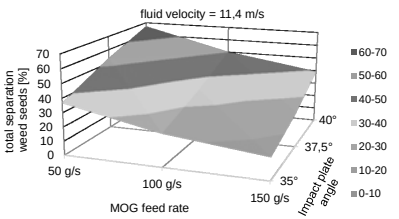

Fig. 15:Total separation of weed seeds

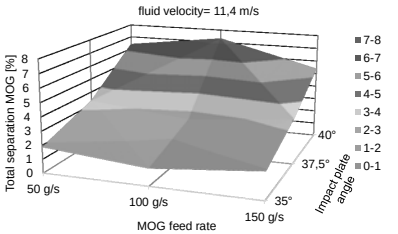

Fig. 16: Total separation of MOG

Summary

For weed control actions it is possible to use alternative ways, other than chemical weed eradicators. Two methods of selecting weed seeds in a combine harvester are tested at a laboratory scale. The one method uses an oscillating air floated sieve for separating the weed seeds from the MOG. The other way is to use the different deflecting properties of the material to separate the fractions. Both systems are able to separate weed seeds (vibro-fluidization: up to 95 % of weed seed separation, impact plate: up to 65 %). However the methods do have limitations in material throughput and are just tested under laboratory conditions yet. Small material throughput means better separation results in general. Optimal parameters for the methods are found in the researches and still have to be proven in field tests. The project is subsidized by VDI/VDE Innovation + Technik GmbH.

References

[1] “weedsience,” [Online].
Available: www.weedscience.org. [Accessed 14 07 2017].

[2] “zasso.eu,” [Online].
Available: http://zasso.eu/. [Accessed 16 08 2017].

[3] “http://www.ihsd.com/,” [Online].
Available: http://www.ihsd.com/. [Accessed 23 08 2017].

[4] “https://sweedhart.eu/,” [Online].
Available: https://sweedhart.eu/. [Accessed 23 08 2017].

[5] “http://www.kompakternte.de/,” [Online].
Available: http://www.kompakternte.de/. [Accessed 23 08 2017].

[6] “http://grainking.com,” [Online].
Available: http://grainking.com.au/chaff-carts/. [Accessed 23 08 2017].

[7] “http://www.glenvarbaledirect.com.au/,” [Online].
Available: http://www.glenvarbaledirect.com.au/. [Accessed 01 02 2017].

[8] “AgriExpo,” [Online].
Available: http://trends.agriexpo.online/project-62620.html. [Accessed 24 07 2017].

[9] “http://oconnorscaseih.com.au,” [Online].
Available: http://oconnorscaseih.com.au/our-products/new-products/case-ih-combine-harvesters/ihsd-integrated-harrington-seed-destructor/. [Accessed 23 08 2017].

[10] H. Klaaßen and J. Freitag, Ackerunkräuter und Ackerungräser rechtzeitig erkennen, Limburgerhof: Landwirtschaftsverlag, 2004.

[11] K. Gehring and S. Thyssen, “Integrierter Pflanzenschutz-Leitunkräuter in Getreide,” Freising-Weihenstephan, 2011.

[12] J. Kahrs, “Untersuchungen zur pneumatischen Aufnahme von Unkrautsamen,” Universität Hohenheim, 1998.

[13] W. Roder, “Zur Schadwirkung der Unkräuter im Getreidebau,” Institut für Landwirtschaftliche Informationen und Dokumentation, Berlin, 1989.

[14] P. Wacker, “Bekämpfung von Unkräutern bei der Getreideernte,” *Landtechnik,* no. 6/89, pp. 215-219, 1989.

The CLAAS AXION 900 TERRA TRAC Product Range

Benefits of the CLAAS Axion 900 halftrack tractor concept equipped with CLAAS Big Driver Terra Trac

M.-Eng. **François Haussmann**, CLAAS Tractor;
Dipl.-Ing. **Robert Obermeier-Hartmann**,
CLAAS Industrietechnik, Paderborn

1. Abstract

With the Axion 900 Terra Trac, CLAAS combines its expertise in tractors and tracks development to create an innovative and unique machine. This document shows how the Axion 900 Terra Trac offers the benefits of a track machine in terms of pulling capacity, efficiency and soil protection with a dynamic behavior similar to the one of a wheel tractor. It also shows that thanks to an optimized version of the Terra Trac Gen III, the Axion 900 becomes an all axle suspended tractor, offering the highest level of comfort to its driver and takes advantage of its architecture to offer a very high autonomy.

2. Market situation: wheels vs tracks

Where the standard tractor ends and the track tractor does begin? Right from the beginning of the last century, tractor's concept with tracks have been opposed to wheel machines. The last two decades have seen a tremendous increase of the installed power on tractors and have led to the surge of full track tractors above 350hp. However, a grey area remains in the 350hp – 500hp range and leaves many customers having to cope with the advantages and disadvantages of each architecture.

The two main arguments for tractors equipped with tracks are an improved traction efficiency and a lower ground pressure due to a larger foot print. Figure 1 shows how the traction efficiency varies in relation to the Pull/Weight ratio of the tractor and the type of drivetrain used to bring the power to the ground (single, duals, triples tires or tracks). A tractor equipped with duals can reach a similar power delivery efficiency than a track tractor but at a much lower Pull/Weight ratio, which means that the track tractor can either pull more for the same weight or be lighter for the same pulling force. Figure 1 also shows that the power delivery efficiency of a track tractor surpasses the one of a tractor with duals whenever the Pull/Weight ratio rises above 0.45.

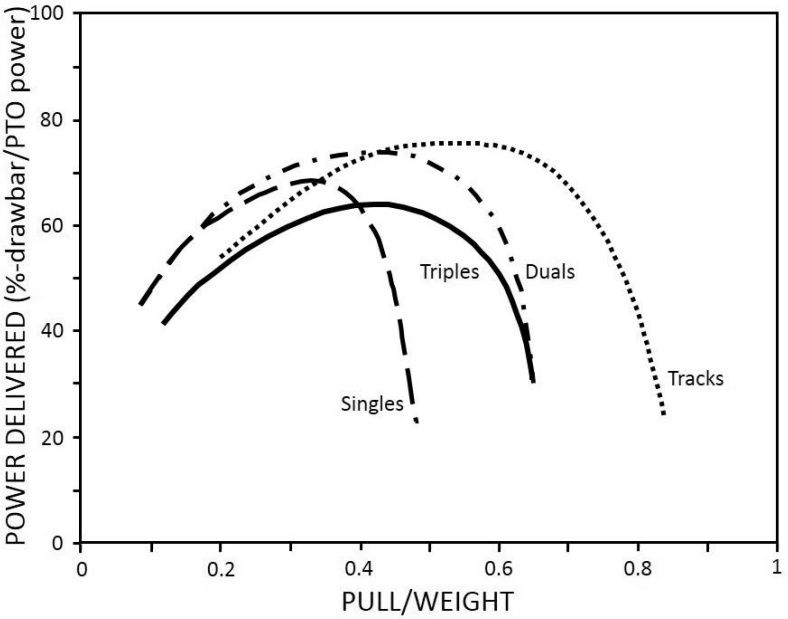

Fig. 1: Power Delivery Efficiency vs. Pull to Weight at 16400 kg total tractor weight [1]

However, the main drawbacks of having tracks are a degradation of drivability, versatility and comfort. Not only have full track tractors the tendency of tipping over when going over bumps but also have poor steerability, especially on wet surfaces, and tend to sweep earth aside as they turn (berming). Four tracks drivetrains reduce some of those disadvantages but come at a higher cost.

Comes then the idea of the halftrack tractor with delta tracks mounted on the rear axle in place of the wheels. This concept can be seen as a good alternative versus duals. Indeed it offers a reduction of the ground pressure on the rear axle and better traction performances while giving the opportunity to drive legally on the road without having to go through the trouble of disassembling the duals. However, current halftrack tractors perform significantly worse in terms of comfort than their wheel counterparts. On top of that, the additional tracks weight and the drag on the ground while turning lead to a pronounced understeering behaviour (see figure 2). This can be reduced by adding ballast weight to the front axle, meanwhile defeating partially the benefits in regards to soil compaction.

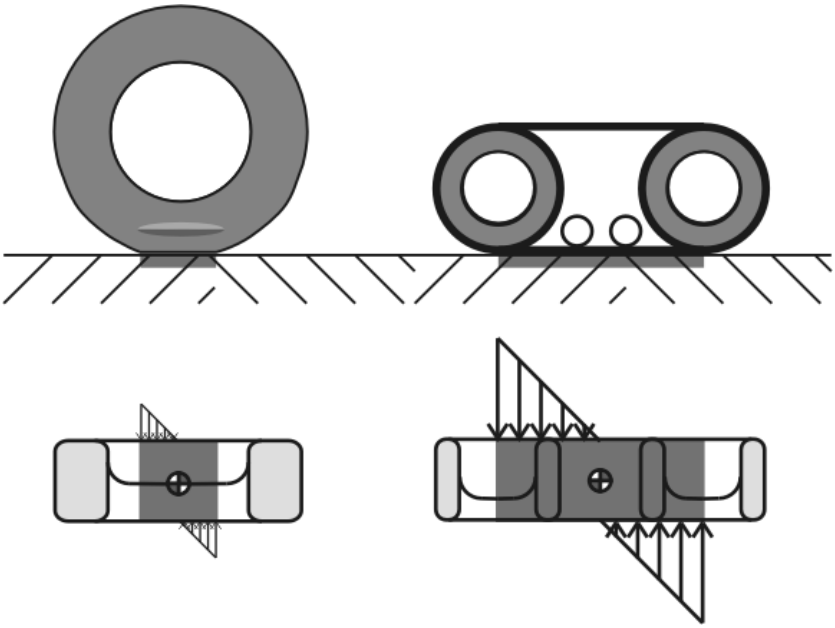

Fig. 2: Schematisation of the wheel and track turning resistance

The following table synthesises the above described subjective evaluation of each concept.

Table 1: Subjective comparison of different tractor concepts in the 350 – 500 HP range

	Wheels		Current Half Track	Tracks	
	Single	Duals		Two Tracks	Four Tracks
Steerability	++	+	-	--	-
Versatility	++	-	+	--	--
Driving on road	++	--	+	-	-
Mobility in the wet	--	-	+	++	++
Comfort	+	+	-	--	-
Traction Efficiency	--	-	+	++	++
Ground Pressure	--	+	+	++	++
Costs	++	++	+	-	--

3. Improving the Half Track concept: the Axion 900 Terra Trac

Fig. 3: The Axion 900 Terra Trac

The target of CLAAS Tractor with the Axion 900 Terra Trac was to develop a tractor in the 350hp – 500hp range which would solve the weaknesses of the halftrack concept as it exists on the market today.

The final design is the combination of the Axion 900 with an adaptation of the Terra Trac Gen III, two well-known, reliable and performant products of the CLAAS group. Taking advantage of its unique architecture and with help of additional specific technical developments, the Axion 900 Terra Trac offers, among others, the following features:

- Power: up to 445hp.
- Maximum permissible weight: 22T.
- Comfort: fully suspended axles & fully suspended cabin.
- Steerability: comparable to a wheel tractor with reduced influence of front ballast.
- Autonomy: 860 litres tank capacity / 12h to 14h of autonomy.
- Mobility: Swivelling tracks up to +/-15°.
- Ground pressure reduction: Tracks on the rear & CTIS on the front wheels.
- Efficiency: 1500rpm @ 40kph & Traction efficiency of the tracks.
- Speed: top speed of 40kph legally on the road.

The steerability of the Axion 900 TT is comparable to a wheel tractor and could be obtained thanks to a steering assistance system adjusting in real time the speed of the tracks in order to steer in near accordance to the Ackermann diagram, as shown in figure 4.
This system is able to achieve a near perfect geometrical turn with minimal influence of the amount of front ballast used, and is particularly useful at low speeds and when the traction of the front axle is limited.

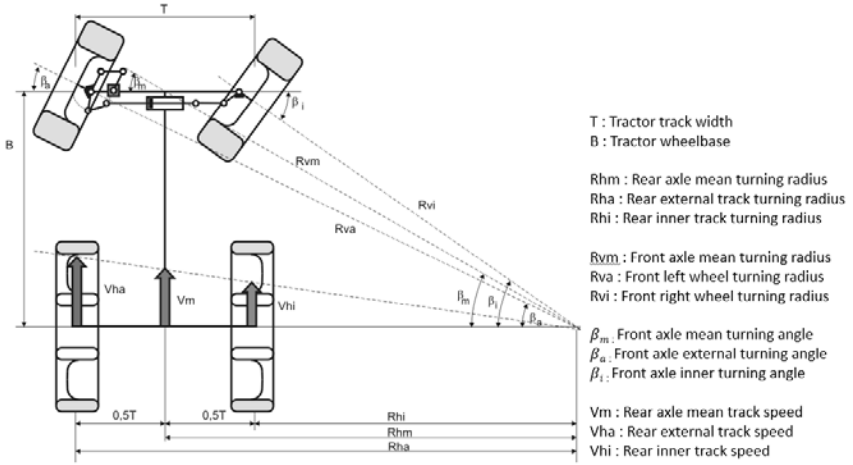

Fig. 4: Schematisation of the speed adjustment to the tracks while turning

4. The Terra Trac Big Driver

Starting the study on an existing tractor, it was essential to fulfil our development targets with as few modifications as possible to the wheel machine, meanwhile respecting regulations constraints (eg. maximum width) and durability targets of mechanical components such as the cardan shafts. Indeed, modifications to the tractor beam was to be minimised and its rear axle original output to be kept to its original position. On the other hand, it was also essential to benefit from years of experience of development and production of the Terra Trac as well as the efficiency of the friction drive concept and the comfort of its suspension system. Taking all these requirements and constraints into account, we developed the Terra Trac Big Driver, dimensioned for the toughest tractor pulling conditions, while keeping its unique kinematics and suspension abilities. Figure 5 shows a section view of the Terra Trac Big Driver. Depending on the targeted application, the Terra Trac Big Driver concept can be derived for belt width from 18’ to 35’.

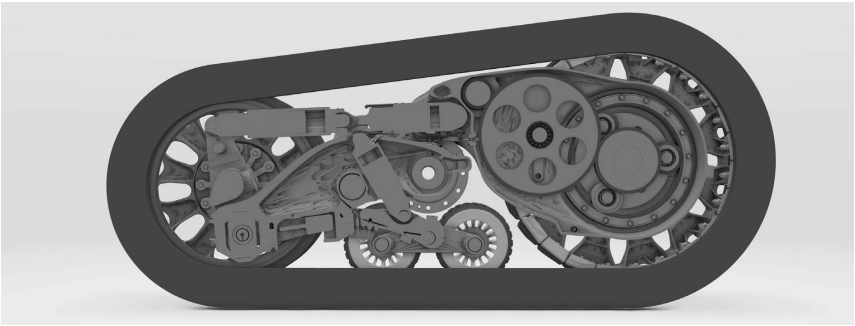

Fig. 5: The new Terra Trac Big Driver section cut

One further modification consists of the use of a clever assembly on the driver of external pads, separated from one another, and assembled onto the wheel hub as show in Figure 6. This design allows for maximum scraping of dirt on the inner side of the belt. Moreover, this design facilitates maintenance and reduces repair costs.

Fig. 6: The new “Big” driver

As shown on Figure 7, the structural connection is ensured by housings on each side of the rear axle, around which the Terra Trac Big Driver can swivel up to an angle of +/- 15°, thus providing maximum mobility to the Axion 900 Terra Trac.

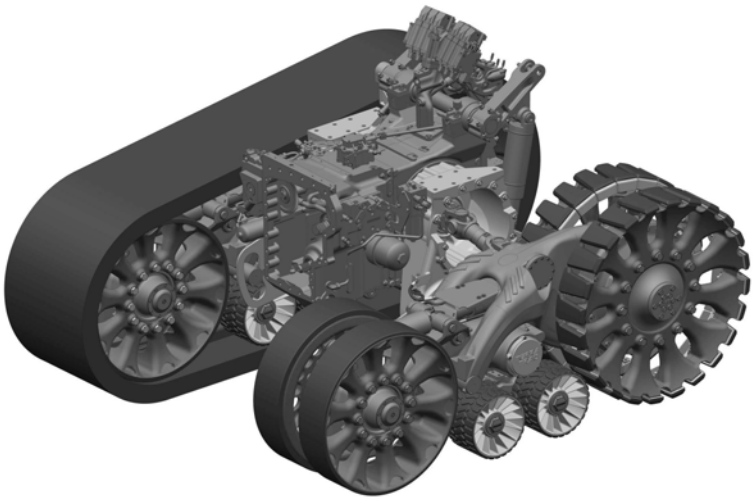

Fig. 7: The Terra Trac Big Driver Rear axle system

5. Summary

The combination and adaptation of two well established CLAAS products in one tractor redefines the halftrack tractor concept in the 350 – 500hp range while performing beyond the standard wheel tractor and full track tractor concepts in many regards. Not only does the Axion 900 Terra Trac provides high efficiency under high pulling conditions, it also provides outstanding driving comfort and behaviour as well as a great autonomy. This will translate for farmers into undisturbed and efficient working days with the possibility to operate in wet conditions while offering a great versatility of usage.

6. References in this document

[1] Reed J. Turner: SINGLE, DUAL AND TRIPLE TIRES AND RUBBER BELT TRACKS IN PRAIRIE SOIL CONDITIONS, Alberta Farm Machinery Research Centre, 1993

The Potential of CVTs in Tracked Tractors around 400 hp

Dipl.-Ing. **Sven Krieger**, Dipl.-Ing. **Eduard Schnur**,
Dr.-Ing. **Martin M. Brenninger**, AGCO GmbH, Marktoberdorf

Abstract

The market segment of around 400 hp has a significant demand for tracked tractors with continuous variable transmission (CVT). Five concepts of how to put tracks on a tractor are pointed out. A high-level evaluation is done.

Introduction

Even though the power level of agricultural tractors is constantly increasing, the range around 400 hp is still a very relevant one. The discussion on how to address soil compaction, traction and row crop abilities is on-going in this market segment. Central tyre inflation systems have been investigated [1]. More and more systems – like VarioGrip made by FENDT – become available. Apart from tyres, putting tracks on agricultural tractors has become more popular in the recent years. Several concepts have shown up or have been further developed. Tracks have become even more important for big harvesting machinery. Pros and cons are discussed in [2]. Geischeder [3] compares the ground pressure of a modern track system with several tyre setups. The duty-cycle of a tractor with tracks has been investigated by Mariutti [4].

On the other hand, the discussion around CVT versus power-shift is a lasting one. Fig. 1 shows the clear trend of an increased number of Vario-CVT that has been produced by AGCO GmbH between 1996 and 2016. In [5] the next step, from CVT to CVDT, has been pointed out.

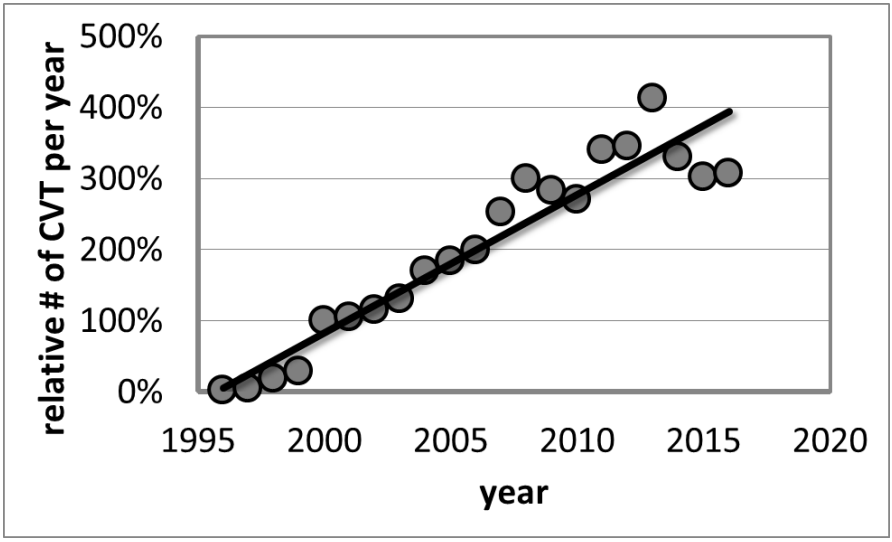

Fig. 1: Relative number of CVT produced by AGCO GmbH

AGCO has not only strongly influenced the market of tractors with CVT. AGCO also has quite a legacy in track-type tractors. AGCO has been taking over the design of the Challenger tractors from Caterpillar in 2002. These tractors had been introduced in 1986 with the model 65. Caterpillars experience on tracks goes back to the days before the merging of Best and Holt in 1925. For all of this, the AGCO Challenger tractors inherit knowledge of rubber-belt tracks and tracks in total of many decades in the field.

Around 400 hp, the market is demanding versatile machines. Roading capabilities, row-crop and heavy pull are all typical applications in this segment. Thus, it feels like a natural demand to merge CVTs into track-type agricultural tractors. The question on which concept to go for arises.

Concepts of tracked tractors

Five different vehicle concepts shall be taken into consideration. Fig. 2 provides an overview.

The easiest way is to take a standard tractor and put tracks on without changing the core of the machine. Like people do in the aftermarket. Usually, not even the axles are changed. The track-system can be mounted onto those. The setup can be reversed into a machine with wheels. With some higher degree of integration, the standard tractor axles are redesigned to

adapt them to the needs of the tracks. The drive for adjusting the output speed of the axle to the need of the belt might be fully integrated into the axle in this case. Such a tractor is not meant to be reverted into a wheeled one.

Three of the concepts in Fig. 2 allow for both degrees of integration: Aftermarket type tracks or specialized axles.

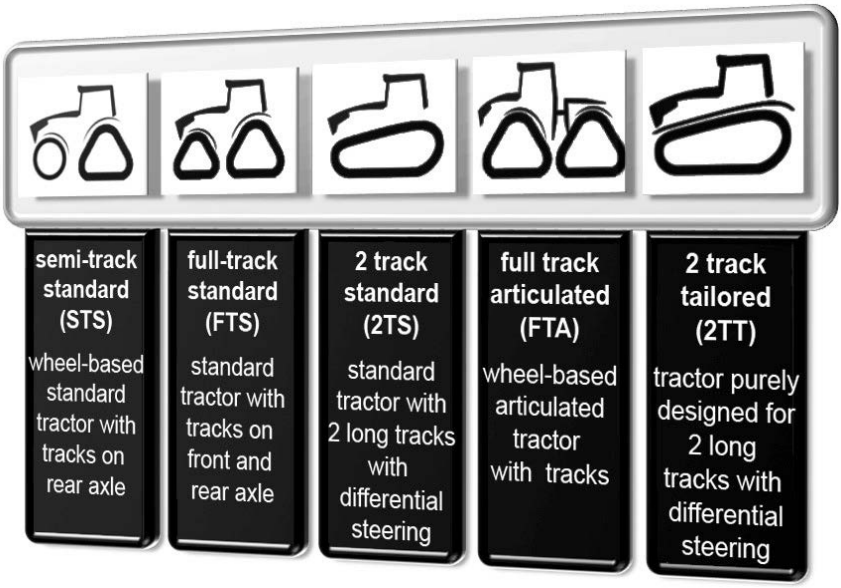

Fig. 2: Concepts of agricultural tractors with tracks to be regarded for the range around 400 hp.

‘Semi-track standard’ (STS) describes the possibility to use a standard tractor – with CVT, in our case – and put tracks on the rear axle only. Standard tractors usually have more weight on the rear-axle than on the front axle, even more when pulling. And people do not really care a lot for front ballast in some countries. Coming from this aspect, it might seem obvious to have the track system on the rear axle only. The front axle can be left untouched. The aftermarket type of solution (STS-A) is possible here. When a more integrated solution is desired (STS-I), only the rear axle needs to be changed. The steering is done with the standard steering system of the front axle.

The concept ‘full-track standard’ (FTS) offers four tracks on a standard tractor. This is what is done every now and then in the aftermarket (FTS-A). With more effort, one might think of a more integrated solution (FTS-I).

In case of the solution ‘2 track standard’ (2TS), an aftermarket solution does not really make sense. A standard tractor provides the base for this design which has two tracks only. Both are relatively long. There needs to be an additional steering system. The tractor is forced to turn by different speeds of the two tracks (differential steering). Driving one track faster than the other generates a yaw rate. The goal is to keep as many elements of the original wheeled standard tractor as possible. Some compromises are taken in order to reach a very high level of commonality among wheeled and tracked version.

Articulated tractors can be also equipped with tracks, ‘full-track articulated’ (FTA). Several levels to tailor the tractor to the needs of the tracks are possible. It is most obvious to either take a wheeled articulated and put aftermarket type tracks on (FTA-A) or have a more integrated solution by re-designing the axles (FTA-I).

When designing a tractor with two tracks and a differential steering system (2TS), a lot of things have to be changed on the original standard tractor anyway. Some undesired compromises might be needed. ‘Two track tailored’ (2TT) avoids these compromises. The machine is designed to fully serve the needs of a tracked tractor.

Evaluation of the concepts

The goal is to get a product with tracks and CVT. Table 1 shows a condensed approach to evaluate the concepts that have been shown. Any of these evaluations is perfect. Personal opinion, the background of when the evaluation is done and by whom play a huge role. One simple example might point out how important the product line-up of a tractor manufacturer is. Putting an aftermarket track on an articulated tractor might be easy. But if you do not have an articulated tractor in the range around 400 hp, designing a new tractor might destroy your setup of platforms. Your effort to get to a tractor rises. In such a manner, this table is meant to be a start of a discussion rather than representing the very truth.

Table 1: Evaluation of the different concepts taken into regard – condensed version. (From advantage to disadvantage: ++, +, 0, -, --)

criteria	STS-A	STS-I	FTS-A	FTS-I	2TS	FTA-A	FTA-I	2TT
Efficiency	--	--	-	0	-	-	0	+
Effectiveness	--	--	-	-	-	-	0	+
Modularity	++	+	++	0	0	++/-	0/--	-
Versatility	0	0	0	+	0	-	0	+
Comfort	0	0	0	0	+	0	0	+
Development effort	++	+	++	+	0	++/--	+/--	-
Soil interaction	-	-	+	+	0	0	0	0

Many more or different criteria could be taken into account. Some of the items shown include others. When talking about efficiency, all of the various systems of a tractor plus the tractor reacting with its environment, esp. with the soil, need to be taken into regard. Some criteria are left out, for example durability. Some might discuss whether tracks that are bought or tracks made in house do have the same durability. The durability of the tracks is regarded to be a goal here.

Instead of discussing each and every evaluation in this table, a focus on some remarkable topics may make more sense here.

One might wonder why the 2TT gets the best rating in efficiency. Even though the system might have some drawbacks when cornering, there is the lowest number of elements involved in the powertrain and the efficiency of these elements including tracks is regarded to be very high. In addition, the concept provides a route to a machine that might be relatively light-weight if desired. Therefore, the rolling resistance becomes relatively low in some applications. And the machine is tailored to being a tracked tractor. Balancing for example can be taken into account right away from scratch. The weight distribution front to rear is very important for the efficiency and the effectiveness of tracks, especially if they are long. 2TT can come with low weight in case of applications with little demand for pulling force and can be ballasted for heavy duty applications and always with the perfect weight distribution.

The '-A' solutions are regarded to have a negative effect on efficiency compared to integrated solutions that offer more degrees of freedom to optimize. The STS versions are evaluated to be less good in efficiency as the FTS concepts as you need to find a compromise in the slip between the wheeled front axle and the tracked rear axle. The FTA has some drawbacks in the number of elements, the high weight in low pull applications etc.. The 2TS is rated

worse than a 2TT for the compromises that need to be taken: More elements, worse in balance. The more you pay attention to avoid these compromises a 2TS-machine becomes a 2TT tractor.

In total, the 2TT gets the best rating here. Please remember that this discussion is about the segment of around 400 hp. And it is all about the market demands you would like to serve, which is a versatile one in this case.

All of the solutions that simply put tracks on a wheeled standard tractor have a clear advantage when talking about modularity. You can offer a tracked tractor easily. The other criteria or further demands like providing enough life-time of the tracks might become the more important items for decision.

And if you do not have an articulated tractor for around 400 hp, the effort to create a tracked one is relatively high and the product is far away from the rest of a tractor manufacturer's product line-up.

The 2TT is regarded to be the most versatile concept. The possibility to use the short tractor in light-weight and heavy-duty applications is enhanced by a tight cornering down to steering on the spot. The CVT supports this feature. A Vario-driven 2TT machine can turn on the spot while providing drawbar pull. Again, the judgment over versatility might differ with the product a manufacturer is heading for: Either a versatile track-type tractor or a tracked machine that can be reverted in a wheeled one with all of the advantages of wheels.

Concerning comfort, the 2TT concept offers enough space to provide a relatively sophisticated suspension system for the tracks. Other concepts need to cope with unsuspended tracks, the suspension becomes expensive, or it has to deal with some other negative aspects.

The drawbacks of the 2TT in modularity and development effort can be faced by an intensified modularity on the component level. Investigations have shown that a transaxle for a 2TT can be done with only 12% new parts coming from having drivetrains for standard tractors only.

Compared to the FTS, the FTA gets some worse evaluation in soil-interaction as it is a heavy concept not really fitting best for row crop etc.. The STS has the problem to have high slip on the front axle and low slip on the rear axle. And the 2Tx get some reduction because of the shearing the long tracks do when cornering.

When a quick and dirty solution is desired to get to a vehicle with tracks and the focus is put on modularity and product line-up, the FTS concepts seem to be very attractive for the range around 400 hp. The machines are versatile, the development effort is relatively low.

But the more and more integration work and adaptation to tracks you want to do, the more a specialized track-type tractor with two tracks and a differential steering concept becomes

obvious. Especially if a manufacturer can build on decades of experience in MTS (Mobile Track System), rubber belt tracks, differential steering axles and the 2TT concept.
In addition, a hydrostatic power-split transmission with all of the hydraulics it has, it matches very well with a hydrostatic differential steering concept.
Manufacturers with a different background might find other solutions to be suitable for their line-up.

Integration of a CVT

The different concepts are to be evaluated differently when a CVT shall be put on. The volumes of track-type tractors in this market segment might be regarded to be not enough for justifying the development of a dedicated CVT. The integration of an existing CVT becomes relevant.
The STS and the FTS concepts are very easy to handle. If a CVT tractor becomes the base of the development you are almost done since some speed adaptations might be nescessary. And in case of a more integrated version, there could be the desire to have a drop (or a rise) in the drivetrain that is different to the standard machine. Most of the work is in the merging of the tracks into the vehicle. Structural stiffness and robustness might become an issue. If the drivetrain of the standard tractor is not prepared for the loads of a tracked vehicle, the rework of the housings etc. becomes significant.
In case of FTA, there needs to be a CVT for an articulated tractor, with all of the drops etc. that are needed there. In case of a CVT that is designed to comprise a power-pack to be the core of the CVT, this power-pack might be reused. But the rest will have to be redesigned to match the articulated tractor. Assuming that the manufacturer already has an articulated machine with CVT in the product line-up, the effort is very low. Transmission and axles are usually separated in these machines. Just the axles or may be some transmission ratio have to be adjusted.
If work to the structure is needed anyway – because the current product does not take into account the loads of a track-type tractor – the road to go to a 2TT is not too far. The work is more to the integration of CVT and differential steering axle.
The choice of concept is not really bound to the CVT. On the other hand, a CVT can offer additional customer benefit to a track-type tractor. Geared neutral for example offers – like mentioned – the possibility of geared turns on the spot to a 2Tx concept. The avoidance of shifts is an even bigger advantage on a track-type tractor than it is on a wheeled one. The stiff track system runs much smoother if there are no peaks in the drawbar pull that come from shifting. And modern CVTs allow for low engine revolutions at maximum speed. This

does not only help to reduce fuel consumption but also limits the noise level. Such a tractor is well prepared for roading.

Summary

When a well-managed modularity is achieved on a component level, the road blocks to a CVT tractor dedicated to tracks become only small hurdles. A transaxle with CVT and differential steering functionality can be derived from a product for standard tractors with only 12% of new parts. The integration of CVT and tracks can lead to a tailored product that comprises the advantages of both. A versatile machine can be achieved that is very usable in both, row-crop and heavy-pull applications. Especially when built on the legacy of many decades.

[1] Rempfer, Martin: Grundlagen der automatischen Reifenluftdruckverstellung bei Traktoren. Band Fortschrittberichte VDI : Reihe 14, Nr. 111. VDI-Verl., 2003

[2] Paar, Johannes: Raupenlaufwerke oder Räder?, Landwirt, 2016, Ausgabe 20

[3] Geischeder, Rupert: Bodenbelastung und Bodenbeanspruchung unterschiedlicher Fahrwerkskonfigurationen. Dissertation am Lehrstuhl für Agrarsystemtechnik der Technischen Universität München, 2011.

[4] Mariutti, Hubert: Lastkollektive für die Fahrantriebe von Traktoren mit Bandlaufwerken. Fortschr.-Ber. VDI: Reihe 12, Nr. 530. Düsseldorf: VDI Verlag 2003

[5] Graf, Michael: CVDT, The Next Level in Tractor Transmission Technology. LAND.TECHNIK AgEng 2015

Development of an Intelligent Stretch Brake System

Dipl.-Wirtsch.-Ing (BA) & MBA **Christian Ehlert**,
Dipl.-Ing. **Lars Erger**, CLAAS Tractor, Paderborn

Abstract

Introduced 100 years ago to replace horses pulling implements, wheeled tractors became multifunctional mobile working machines throughout the course of agricultural history. Amongst others, transport applications have become a widespread usage profile. Within this application, speeds and loads have increased over the years. Today, tractors run 50 kph (sometimes even 60kph) and tow masses up to a convoy weight of 40t (in some countries even 50t). Jackknifing on agricultural convoys has become a frequently seen accident. Occurrence has increased in the recent years with the introduction of CVT transmissions, as it is common to decelerate the tractor by changing transmission ratio. However, the phenomenon of jackknifing is likely to become more common on power shift transmissions with automatic drive controllers, too. In 2010, 90% of accidents in Germany with agricultural tractors happened on public roads [1]. Figure 1 illustrates the sequence of events leading to jack knifing on tractor-trailer combinations.

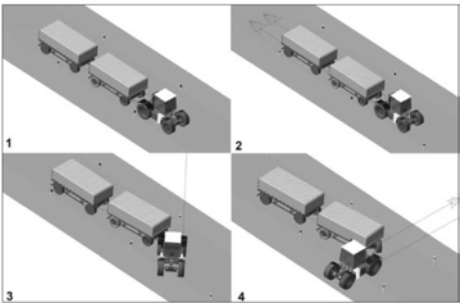

Fig. 1: Jackknifing Example, Tractor with 2 Trailers [2]

Other industries, such as on highway trucks, have introduced ABS and ESP on trailers or automated brake actuation based on coupling forces to overcome this problem. What the automatic systems have in common is that they keep the convoy stretched to avoid jack knif-

ing. Unlike with trucks, tractors nowadays only use manually actuated systems to avoid jack knifing, e.g. brake actuation of the service brake with parallel actuation of the drive pedal.
In order to prevent jackknifing, CLAAS has developed a system to detect critical driving situations based on existing sensors, and to act fully automatic on the trailer brakes without actuating the tractor service brakes.

1. The Jack Knife Phenomenon

Jack knifing can occur in different driving situations. In general, a convoy faces the risk of jack knifing when the generated brake force (tractor) is bigger than the tractive capacity in the tire ground contact (braked axle(s)), and when the braking system of the tractor is not engaged (which otherwise would lead to engagement of the trailer braking system [3]). In 2004, Wiegandt explained this mechanism including the risks during the engagement process of the convoy braking system [3].
When the service brakes of the tractor are not engaged, the brake power of the tractor equals the sum of all losses in the system. Whilst in pull mode the losses in the system should be as low as possible, the industry has developed various systems and strategies to increase losses in push mode in order to maintain a working speed / driving speed in downhill conditions without using the service break. Below is an incomplete list of strategies / systems, which have become frequently seen on standard tractors:
Engine brake (especially seen on tractors with CVT transmissions)
Exhaust flap
Visco fan controls
Engine retarder
VTG charger control
With these systems, more than 100kW of brake power can be generated in addition to the service brakes [4]. This brake force is transferred to the underground via the tires. Whilst the maximum transferable force ($F_{X,Y}$) is determined by the vehicle vertical force acting on the tire ($F_{Z,W}$) and the traction coefficient (μ_{max}), the resulting force (F_{Res}) is split into the longitudinal force ($F_{X,W}$) and lateral force ($F_{Y,W}$). The maximal transferable force is represented by the radius of the circle in Figure 2, and calculated with equation 1:

$$F_{X,Y} = \mu_{max} * F_{Z,W} \quad (1)$$

If the vector of the resulting force F_{Res} exceeds the maximum radius of the circle (hence the maximal transferable force $F_{X,Y}$), the driving stability is no longer given. It is obvious that in this context driving situations with no lateral forces and engaged all-wheel drive are less risky than cornering with lateral and longitudinal forces without engaged all-wheel drive. Further-

more, trailers with transfer of vertical forces to the rear axle are preferable when compared to trailers without transfer of vertical forces, as the vertical force increases the rear axle load, and therefore the maximum transferable force within the tire soil contact (see equation 1). The push from an un-braked trailer in a curve will increase the risk for accidents as the maximum permissible longitudinal force ($Fmax_{X,W}$) will be reduced consequently to the increasing lateral force ($F_{Y,W}$).

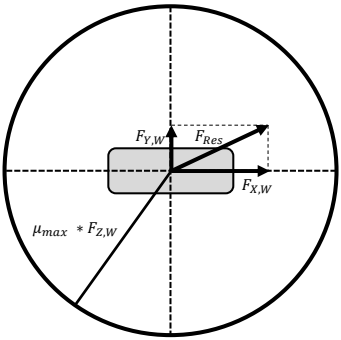

Fig. 2: Kamm´s Circle, [5, 6]

The unknown and most volatile variable in this calculation is the traction coefficient μ. Söhne published reference data for different undergrounds in 1964 (see Figure 3), which serves as a basis for further calculations. Although agricultural tires have evolved a lot in the recent years, the basic findings Söhne published are still valid.

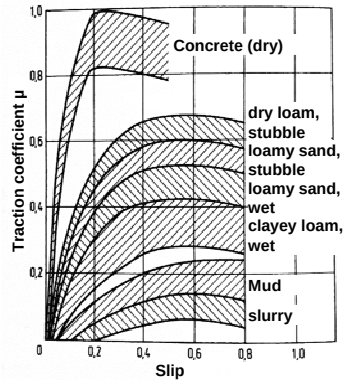

Fig. 3: Traction Coefficient μ over Slip – Curves for Different Undergrounds [7]

Internal calculations show that even tractors driving solo and without systems to generate additional brake force can enter unstable driving situations only by using the inner losses of the drivetrain at high engine RPM. Figure 4 shows that at low vehicle speeds and with high engine RPM the tire capacity is insufficient to transfer the braking forces to the ground, the tractor risks blocking tires or jack knifing.

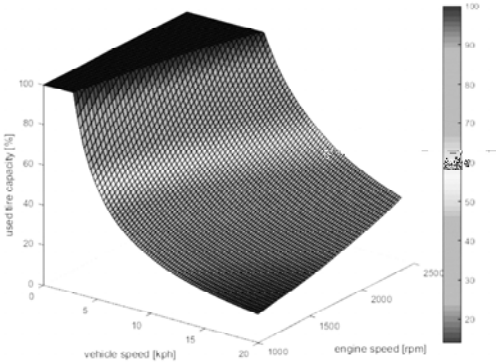

Tractor Mass:	8,5t
Rear Axle Load:	4,7t
Engine:	4,5l
Friction Coefficient:	0,6
Fan Speed:	1500
4WD:	not engaged
Rear Axle Losses	3kW
Gearbox torque losses	70Nm

Fig. 4: Use of Tire Capacity over Speed and Engine RPM [4]

Based on these fundamentals and the increasing population of CVT transmissions in the market, the wider use of systems to generate brake forces in tractors and the evolving usage profile of agricultural tractors with higher weights and increasing share of transport application the need for assisting systems to increase driving safety is obvious.

2. Use Cases for Automated Stretch Brake

In the beginning of the development phase, the relevant use cases for the application of the automated stretch brake have been defined.

As soon as the tractor gets into push mode the system shall engage the brakes of the trailer in order to stretch the convoy.

If a constant speed is requested (eg. cruise control) and the tractor is accelerating by slope, the system shall engage the brakes of the trailer in order to stretch the convoy.

With a speed command of 0 kph without engaged tractor service brakes, the system shall engage the brakes of the trailer during the deceleration shortly before standstill in order to stretch the convoy.

3. Technical Concept of the System

The target of the automated stretch brake is to keep the tractor trailer combination stable in critical driving situations. Following Wiegandt [8], critical driving situations are only occurring in push mode and can be sensed by the actual wheel slip, and in particular, the change rate of the wheel slip. Sensors which are necessary to calculate wheel slip and wheel slip change rate are not standard equipment on tractors. In addition, internal tests show that the reaction time from detection of wheel slip until engaged trailer brakes is too long to secure driving stability. The automated stretch brake therefore bases its first actuation on the detection of a push state of the tractor and then controls the estimated coupling forces. As an alternative the coupling force could be sensed in the coupling point to the tractor. Coupling systems for agricultural tractors exist in many different variants (clevis hitch, ball type hitch, three point hitch). Therefore the integration of a sensing system to measure coupling forces has been avoided in order to keep the system simple and free of mechanical constraints. Instead of measuring the coupling force the actual tractor state (push or pull) and the coupling force are derived from internal signals (see Figure 5).

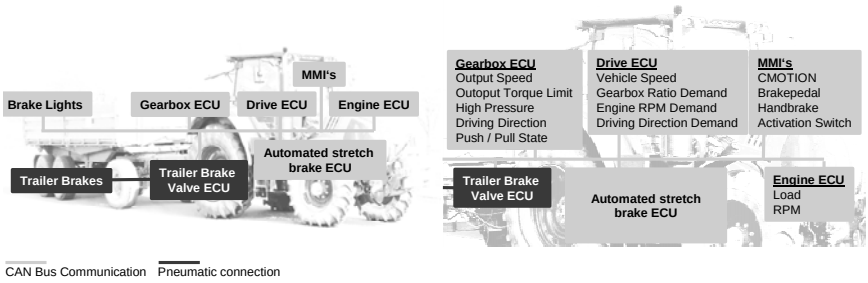

Fig. 5: System Sketch of the Automated Stretch Brake

The automated stretch brake system is a close loop controller which is acting on the trailer brake valve to control the coupling forces. The coupling forces at the coupling point remain positive (tractor pulls). In order to avoid inadequate and too frequent use of the system, it can be disabled via a switch in the cabin.

4. Findings during the Development Phases

Forces and losses within the tractor are mostly known or can be calculated, or at least estimated. In addition, this accounts for most of the relevant external forces as well. A critical factor which remains unknown and cannot be learned easily during operation is the brake performance of the trailer implement in relation to the demanded brake pressure. Modern

tractors provide adjustment possibilities of the trailer brake lead, which reduce this effect, but the proper application cannot be guaranteed. Thus, the validation effort to cover trailer brakes with different performances has been increased. In the future it would be beneficial to identify the mounted trailer / implement in the tractor terminal. Storing the ideal brake lead for each trailer / implement in an implement data base would cure this/these problem/s. The technical necessities are already provided in modern tractors today, eg. electronically controlled brake valves provide solutions to adjust brake lead based on CAN messages. A second improvement can be expected by systems which will support the driver to couple trailers in the right order to the tractor. The trailer which reacts the earliest to the brake signals from the tractors has to be at the end of the convoy..

5. Summary and Conclusion

Based on the given trends in the agricultural industry and the technical evolution of the machines the need for assisting systems to increase driving safety is obvious. With the focus on transport application (road and field) CLAAS has developed a fully automatic assistance system based on existing sensor technology. The system controls the coupling forces between tractor and trailer via the brakes of the trailer without any active intervention of the driver. This does relieve the driver during driving and increase the safety of the operations. Future evolutions can be expected in systems which will help the driver to define the right order of braked trailers in longer convoys and to adjust the trailer brake lead fully or semi-automatic.

References

[1] N.N.; Gesamtverband der deutschen Versicherungswirtschaft e.V: Personenschadenunfälle mit landwirtschaftlichen Zugmaschinen. Tagung. Berlin: 15.07.2010

[2] Wiegandt, M.; Harms, H.-H. – Automated Deceleration of Agricultural Tractors. 58 Landtechnik 4 / 2013, pp. 248 – 249

[3] Wiegandt, M.; Grundlagen eines Traktorbremsmanagements (2004), pp. 116 - 122

[4] CLAAS internal calculations

[5] Isermann, R. (Publisher), - Fahrdynamik-Regelung (2006), pp. 37 – 40.

[6] Heißing, B.; Ersoy, M. (Publisher), Fahrwerkhandbuch (2007), pp. 59 – 65.

[7] Söhne, W.; Allrad oder Hinterachsantrieb bei Ackerschleppern hoher Leistung. Grundlagen der Landtechnik H. 20 (1964), pp.44-52.3

[8] Wiegandt, M.; Grundlagen eines Traktorbremsmanagements (2004), pp. 93 - 101

Real-time View and Documentation of Manufacturer Independent Machine Data

Julian Schroeter, Dr. **Wolfgang Angermair**, Dr. **Sebastian Pauli**,
FarmFacts GmbH, Pfarrkirchen

Abstract:

This paper describes the main composition of a general Farm Management Information System (FMIS) supplemented with Machine Management functions. The system is capable of receiving, processing and managing agricultural machinery data regardless of the data origin from agricultural machines or data sent by a mobile application, data structure and, last but not least, manufacturer brands.

Introduction and Aim:

Due to the ongoing challenge of growing world population and subsequent rising demand for foodstuff all over the world, the improvement of crop yield and quality of agricultural land is one of the most important challenges of our time [1]. In addition, farmers are constantly facing new demands in the form of additions and changes in regulations, as well as more stringent reporting and documentation requirements [2]. As part of the development of agricultural production and the rising pressure of continuous documentation, farmers seek easy to use documentation, process controlling, precision farming systems (prescription maps based on earth observation) and decision support with high machine compatibility [3].

Approach

In recent years, there has been an immense development of information systems specialized in the specific needs of agriculture. In Germany, already more than half of all farms use digital applications and additional 30% are discussing or planning to implement a system [4]. The focus of most systems lies on the assistance with managerial tasks. The software is used to advise farm managers in their core business, in helping to observe guidelines and regulations, and in simplifying documentation requirements [5]. Firstly, the FMIS market consists of several producers, including general IT companies and agricultural based IT businesses.

On the other hand, machine manufacturers also develop and offer software specialized for their own brand of agricultural machinery. The situation has positive as well as negative aspects: support and compatibility within one manufacturer is simplified, but many farmers are tied to one specific manufacturer. The status-quo is represented by farmers generally having machines from several manufacturers. Considering that they are currently not compatible, this slows down digitalization, connectivity and efficiency in agriculture.

As of today, there is a challenge of merging data from different data streams. Data from one source is usually taken for generating one task documentation. Additionally, there are only a few systems that can receive, process and present agricultural data streams in a genuine real-time view.

Material and Methods:

The paper demonstrates a comprehensive concept of Machine Management function inside a FMIS. The concept and the core functions of the Machine Management were established by conducting several expert rounds with six renowned agricultural machinery companies, which included AGCO, Krone, Kuhn, Pöttinger, Lemken and Rauch. The software concept has a broad variation of functionality, which will be

- Timekeeping and documentation
- Light version of warehouse management module
- Field & task management
- Disposition of work groups
- Native app including daily to do list
- Monitoring / Map overview
- Semi-automatic data postprocessing
- Semi-automatic report generation
- Cross Compliance documentation (partly)
- Production controlling and optimization

FMIS upgrade through Machine Management functionalities

Farmers have plenty of requirements for data management which are all met by the NEXT Farming Machine Management software. First, automation is key: nowadays, the process of data collection is automated, the collection starts automatically when machines start working and will also be automatically transferred to the systems which will process the data.

The software package will meet those tasks by using the data management solution AGRI-router, which will handle the automatic and seamlessly easy transfer of machine data towards the management system.

Second of all, farmers demand an easy access to their data and a fast and efficient way of evaluating their data. Farmers have to evaluate enormous amounts of data to make economical and environmentally-sound decisions [5]. Management software can, in some cases, be very complex and complicated to use due to the sheer amount of functionality. The software package therefore has a thoughtful designed concept to overcome that complexity. It has an easy to use approach, where the user is carried through the software by well thought outline with easy to understand buttons. The platform deliberately does not offer the whole functionality that one would expect from an FMIS, but is broken down to the core functions that a farmer really needs. Yet in addition to that, the platform offers a straight forward API based on ODATA which makes it possible for third party providers to supply even more functionality for a specific customer. The platform will also run as a web-based Java application which will be available all other the world in different languages via a web browser, there is no need to save your data on a hard drive or on a stationary computer, the application will have all the data at hand everywhere, at every time.

Data Security is one of the biggest concerns a farmer has regarding farm management systems which is why the data will be stored under the highest data security standards. The software will be hosted on a German Server Farm and the data of the farmers is truly private, it will not be used for further use. For very sensitive data like e.g. payment details, the software concept counts on a strong partnership with third party provider who are specialized and haven even higher security standards.

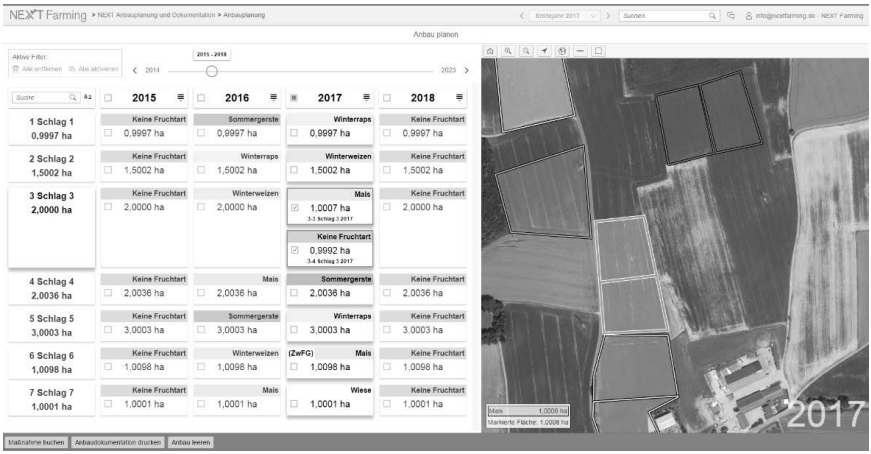

Fig. 1: Example for an easy to use design – use case: crop planning

Another crucial requirement for the modern farmer is that the recorded and received data information must be processed and evaluated in a fast, easy and semi-automatic way. Therefore, the software will offer a data processing solution, that assists the farmer to keep complete record of his tasks and to create a Cross Compliance documentation in a few short steps.

Of course, the documentation will be based on the received information of the machine data. An example of the processing can be seen in Fig. 2, which shows the semiautomatic process of recording used resource by field, with automatic recognition of field boundaries.

The process tool will not only be filled by machine data alone, there will also be a mobile application included in the package which allows farms not just to add some additional information to the task, but also to records tracks specific to the field boundary. This enables the farmer to use the advantages of digital farming even though his fleet might not meet every precondition for the usage of modern software technology.

The software subsequently will be able to merge different streams of information into one solely task. Therefore, the farmer will strongly benefit from reducing the time of manual input. The data processing tool will result in a much more precise and efficient analysis of every business process on a farm. Additionally, end users will be able to export reports in various

formats, including PDF and Excel sheets. They include for instance crop documentation, plant protection documentation and field history documentation.

Fig. 2: Example Data Post Processing

Conclusion:

From paper to machine management towards Farm Management Information System: the platform enables farmers to get an easy and comfortable way to start with digital farming and to accelerate their businesses. The well-thought concept benefits from three pools of expertise: by bringing together experts from software development, agricultural machine manufacturing experts and business oriented farmers, the software has all important core functions the modern farmer desperately needs. The machine management functionalities are perfectly integrated into the FMIS, therefore farmers will benefit from state of the art farm applications.

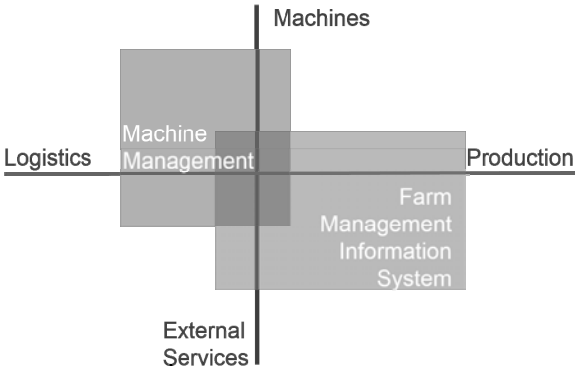

Fig. 3: Machine management integration matrix (source: DKE, Dr. Jens Möller)

The concept of a fully integrated Machine Management system shows that it is vital to join the competencies of industry experts and use specific knowledge, working as a collective. This implies many advantages to the end customer, the farmer. Farmers will only have to use one complete AG data management tool which will be accepted by a consortium of agricultural manufacturers. There is no need for application hopping, only one place to store, manage, process and evaluate data. Due to the open structure of the software platform, machine manufacturers will offer machine specific apps, that will be available via an integrated app shop. The end customer decides whether to make use of the additional software provided by manufacturers.

[1] FAO. (2009). How to feed the World in 2050. *Food and Agricultural Organization of the United Nations*.

[2] Bernhardt, H., & Kaiser, B. (2007). Arbeitszeitaufwand für die Dokumentation im Ackerbau. *Arbeitswirtschaft - Landtechnik*, S. 180-181.

[3] Pauli, Sebastian, Wolfgang Angermair, Georg Tüller, and Heinz Bernhardt. “Evaluation of Documentation Data from Electronic Recording Systems in Biomass Harvest Logic.” *VDI-MEG (Hrsg.): Land.Technik 2012. Mit Erfahrung und Innovationskraft zu mehr Effizienz, November 2012: 205-210.*

[4] Rohleder, B., & Krüsken, B. (2016). *Digitalisierung in der Landwirtschaft.* Berlin: bitkom.

[5] Sørensen, C.G., et al. “Conceptual model of a future farm management information system.” *Computers and Electronics in Agriculture, Volume 72, Issue 1, June 2010: 37-47.*

A multilevel simulation framework for highly automated harvest processes enabled by environmental sensor systems

Jannik Redenius, M.Sc., **Matthias Dingwerth**, M.Sc.,
Prof. Dr. **Arno Ruckelshausen**, Faculty of Engineering and Computer Science, Osnabrück University of Applied Sciences;
Prof. Dr. **Joachim Hertzberg**,
Institute of Computer Science, Osnabrück University;
Dipl.-Ing. **Thilo Krause**, Dr.-Ing. **Boris Kettelhoit**,
CLAAS Selbstfahrende Erntemaschinen GmbH, Harsewinkel

Abstract

This article proposes the concept of a simulation framework for environmental sensors with multilevel abstraction in agricultural scenarios. The implementation case study is a simulation of a grain-harvesting scenario enabled by LiDAR sensors. Environmental sensor models as well as kinematics and dynamic behavior of machines are based on the robotics simulator Gazebo. Models for powertrain, machine process aggregates and peripheral simulation components are implemented with the help of MATLAB/ Simulink and with the robotics middleware Robot Operating System (ROS). This article deals with the general concept of a multilevel simulation framework and in particular with sensor and environmental modeling.

1. Introduction

Extensive field tests are necessary to represent the diversity of possible constellations in environment-based functions and cooperative processes in agriculture. Due to harvesting periods, such tests are only possible to a limited extent and there are rarely ideal conditions for testing function thresholds. Measurements depend on a variety of environmental disturbances and in particularly harvesting tests cannot be reproduced. Environmental models can support the development process of machine control functions that are based on environmental sensing [1]. The development process of advanced driver assistance systems (ADAS) in automotive uses frameworks for simultaneous vehicle dynamics, drive train and environmental sensor simulation for reducing the number of time- and cost-intensive vehicle tests [2]. However, agricultural harvest scenarios require more complex machine and environmental models, since the steering and longitudinal guidance as well as machine coopera-

tion rely on the harvesting process prior to navigation. An appropriate mapping of plants and soil, yield parameters, possible further process participants and obstacles is necessary. As ADAS development tools are optimized for vehicle, sensor, and environmental models for cars, they need substantial modification for being suitable for agricultural off-road scenarios. This article proposes the concept of a multilevel simulation framework that is suitable for agricultural harvest scenarios, thereby including control functions, sensor integration up to machine cooperation.

2. Materials and Methods

2.1 Multilevel Simulation

Since environmental automation functions are often interdependent with other functions or process participants, the simulation has to serve several function levels (fig. 1). Through the requirements of model-, software- or hardware-in-the-loop test scenarios and with regard to limited resources, simplified models for partial functions that do not require supervision can be chosen. On the other hand, it is also possible to isolate individual simulation components.

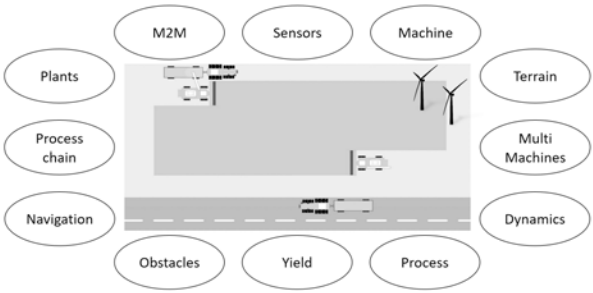

Fig. 1: Levels for multilevel simulation environmental automation functions

2.2 Simulation Framework

In order to provide the greatest possible flexibility in environmental modeling and implementation of own sensor concepts, the open source robotics simulator Gazebo [3] is chosen in this work. It offers a wide range of available and fully exposed sensor models and an Open World scenario simulation which is generally suitable for agricultural scenarios [4].

Another main component of the simulation framework is MATLAB/ Simulink [5], which serves as an interface to the previous development process and allows the use of many already existing model components, including models for powertrain, suspension and process simulation of a harvesting machine. Message transport between Gazebo Simulation and

MATLAB/ Simulink uses the middleware ROS [6], based on a publisher-subscriber or service based interaction model. An implementation example is the well-known LiDAR-sensor-based steering control by crop edge detection in harvest (fig. 2).

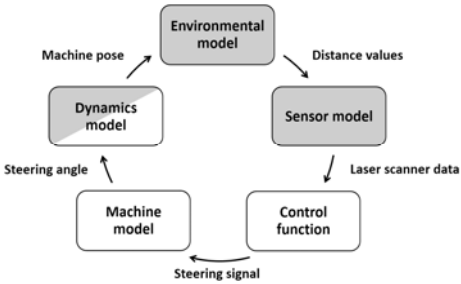

Fig. 2: Flow chart for a LiDAR-sensor-based steering control simulation with model parts in Gazebo Simulator (grey area boxes) and MATLAB/ Simulink (white area boxes)

2.3 Environmental Model

The environmental model holds an environmental representation on which field-related sensor data can be generated. These include soil, crop, stationary objects, and vehicles.
The environment has to be represented in a way so that it is suitable for multiple environmental sensor systems. These include environmental sensors such as LiDAR, camera, and radar sensors, as well as GPS, IMU and odometry sensor systems. Access to stored map related data of the surroundings as an additional virtual sensor is also possible. All components are represented by a 3D contour such as the soil topography or the 3D machine representation. The terrain topography can be described by means of measured values from previous measurements (or mathematically), texturing for vision sensors or speed-dependent crop mass flow are possible.

2.4 Environmental Sensor Systems

The environmental sensor models relate to the respective machine position and form the interface between environmental simulation and vehicle function. The modeling is carried out by experiments based on measured values. The possibility to implement new machine and function concepts as well as sensor systems and other plant species will be discussed in the further course of the project. For the LiDAR sensor simulation, three different model approaches for the generation of sensor data output were implemented in the sense of scalability (fig. 3). For real-time capability there is no physics simulation of laser pulses, beam deflection or time-of-flight but a phenomenological behavior simulation based on the

preexisting GPU accelerated ray casting plugin of Gazebo. The first approach is a position-dependent reproduction of measured data instead of route models. Real sensor data from field tests are first transformed to a plant height and located in a grid. It is possible to replay a real measurement but with the possibility of slightly different trajectory and variable speed to represent an active control for function stability consideration. This approach can also be extended by the use of primitive bodies to reflect the effects of shading at crop edges.

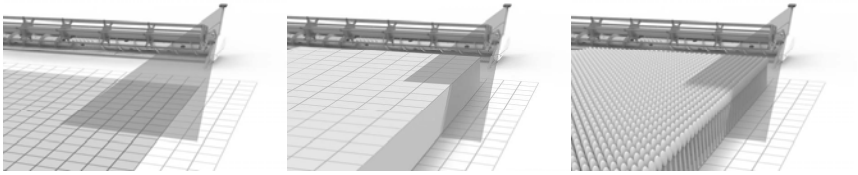

Fig. 3: Sensor model concepts

The second approach is to use primitive bodies together with empirically determined sensor parameters. The height and number of plants influences a laser distance measurement. Sensor properties, such as the spot size, have a strong influence on the measured height [7]. This sensor-specific behavior can be described by parameters such as the standard deviation of the distance measurement in known crop conditions and modeled as a function of the height and the number of plants. The third approach is based on full generic sensor data by a 3D-surface plant model of individual plant contours without prior measurement. The realization of multiple types of plant stocks is possible. For this purpose, a simplified plant contour model and a matching sensor model was developed. For a more realistic sensor behavior, a plurality of individual distances according to the ray casting principle are combined to form a measurement as a function of the desired measurement spot size. According to the desired sensor behavior, both the smallest distance values, but also any percentiles of the measured distance values, can be selected for determining the output distance value. The choice of the sensor representation depends on detail and performance requirements of the application. The generation of measurement data can be deterministic or stochastic. In addition generic sensor data extracted by this 3D-surface plant model can provide input for one of the other model approaches in order to gain a performance profit.

3. Application Example

An exemplary implementation and validation is based on LiDAR-based edge detection as an established environment-based function in grain harvesting. This example is intended to test the basic concept and the interplay of the individual software components on the basis of an

existing concept. To generate sensor data for model parametrization and validation real field models have been built with different crop densities (fig. 4) as a first step. Those models have been measured using two high resolution laser scanners with different beam sizes.

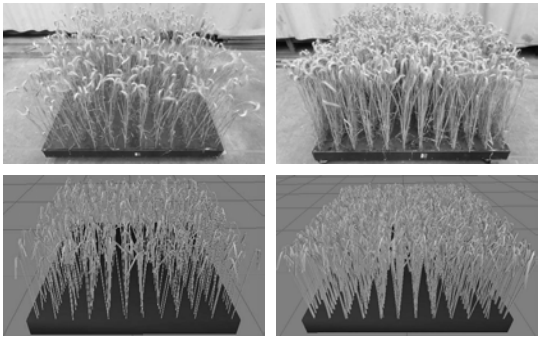

Fig. 4: Real model (top) and 3D-surface model (bottom) of 200 (left) and 600 (right) crop plants per square meter

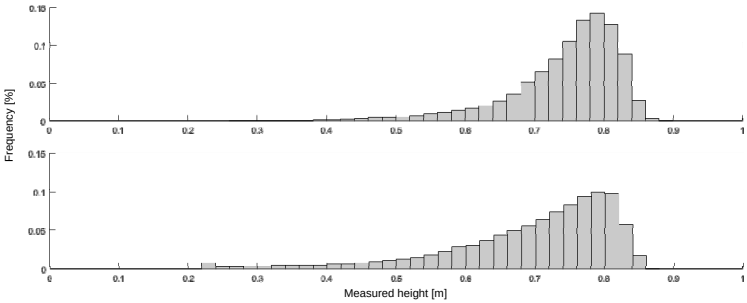

Fig. 5: Normalized histogram of measured field height in real model (top) and 3D-surface model (bottom) of crop plants with a real and simulated laser scanner

Fig. 6: LiDAR-sensor-based edge detection with 3D-surface model of crop plants

A scenario for LiDAR crop edge detection and steering control was built in simulation (fig. 5 & 6). It uses the same algorithm and control architecture as the CLAAS Laser Pilot. Machine dynamics can be simulated by multi-bodies in Gazebo or by a single-track model in MATLAB/ Simulink. Based on the environmental and sensor model concepts challenging cases such as broken edges, tight turning curves or low crop density can be investigated.

4. Conclusion

A concept of a simulation framework for environmental sensors with multilevel abstraction in agricultural scenarios was proposed and successfully implemented. An example of the LiDAR-based steering control by crop edge detection demonstrates the potential of the environment for optimizing and creating new processes, in particular control systems algorithms and sensor integration. Used in an early stage of development it can support recognizing implementation errors. By systematic and reproducible function tests of software components optimization of algorithms is possible prior to field tests and may reduce the complexity of real experiments. Future work will focus on further simulation function levels.

5. Acknowledgements

The project is supported by funds of the “it's OWL” innovation project "Electronic Environmental Sensing for Harvesting Machines" (2014 - 2017).

References

[1] Linz., A. et al.: Modelling environment for an electrical driven selective sprayer robot in orchards. Proc. 11th European Conference on Precision Agriculture, 2017, pp. 848–853

[2] Stay safe on the Roads: Euro NCAP tests with virtual test drives. dSpace Magazine, 2014, no. 2, pp. 44-47

[3] Koenig, N. & Howard, A.: Design and Use Paradigms for Gazebo, An Open-Source Multi-Robot Simulator. Proc. IEEE/RSJ Int. Conf. IROS, 2004, pp. 2149-2154

[4] Harms, H. et al.: Robotic Tools for advanced agriculture Automation. Proc. VDI-MEG Conf. Agricultural Engineering (AgEng), 2015, pp. 119 –125

[5] MatLab & Simulink: Simulink Reference R2016b, The MathWorks, Inc., http://www.mathworks.com/help/releases/R2016b/pdf_doc/simulink/slref.pdf, 2016

[6] Quigley, M. et al.: ROS: an open-source Robot Operating System. Proc. ICRA Workshop on Open Source Software, 2009

[7] Saeys, W. et al.: Estimation of the crop density of small grains using LiDAR sensors. Biosystems Engineering, 2009, 102, no. 1, pp. 22-30

Reference Data and Collaborative Identifier Sharing in Agricultural Field Operations

B. E. Craker, AGCO, Duluth, GA, USA;
R. A. Ferreyra, S. T. Rhea, Ag Connections, Murray, KY, USA;
C. Graumans, Ag Gateway Europe, Amsterdam, Netherlands;
U. Kaempf, **M. Nachtmann**, BASF, Limburgerhof;
F. Schuster, Agrobase-Logigram, Archamps, France;
J. A. Wilson, AgGateway Global Network, Raleigh, NC, USA

Abstract

Contemporary agriculture requires the continuous exchange of information between farmers and partners such as agronomists, input suppliers, custom applicators, and customers. A critical component of this interoperability is identification, where a name or code (the "identifier") is used to reference a kind of object (e.g., a specific crop protection product) or a particular instance of an object (e.g., one of a farmer's fields).

There are multiple motivations for uniquely identifying resources in production agriculture data exchange. Examples include unambiguously specifying the resources being allocated to a particular field operation (e.g., products, fields, people, equipment); and enabling an audit trail (the aspiration of having farm-to-fork traceability) and regulatory compliance for all the processes of interest.

A special case in identification is Reference Data, a set of shared controlled vocabularies that allow all participants in a data exchange process to unambiguously identify concepts of interest. A noteworthy example is identifiers for crop inputs, such as seeds, crop protection products, and fertilizers. Reference data is increasingly being sourced through application programming interfaces (APIs) accessible by FMIS over the Internet. This presents an interoperability problem, however, because there is currently no product reference data standard format.

AgGateway's collaborative identification model provides a solution to the aforementioned problems (need for identifiers; distributed identifier sourcing; and a lack of standard formats for identifiers or product reference data). It uses a concept called the CompoundIdentifier to enable associating multiple unique identifiers (conceivably in multiple formats) to each data object, and provides a standardized API design to enable sourcing product reference data identifiers.

This paper describes AgGateway-Europe's Identity Project. It is focused on enabling principled decision-making in agricultural field operations. In particular, it focuses on the step of a farmer's process where, given a set of observations and measurements, an actor with expertise (e.g., a consultant or agronomist) recommends a field operation such as the application of one or more crop protection products, and communicates that recommendation back to the farmer. Important aspects of the system include a flexible identification scheme that can accommodate the myriad types of identifiers currently in use in FMIS; a distributed system for finding and accessing pertinent product reference data; and semantics to inform the data transfer process.

Keywords: information systems; compliance; identification; record linkage; standards

Introduction

Electronic data exchange has become critically important for business operations throughout the world. Over time, various industries have defined standard transactions to implement their respective electronic data interchange (EDI) initiatives. Without *controlled vocabularies* (i.e., common standard codes), their efforts are very expensive and challenging to implement. If common product codes were not in use, how would a customer order? If trading partner data were not standardized, would the delivery be made to the right place? Without standard identifiers for consumers, could we know who our end customer really is? If locations were not standardized, could we implement traceability in the agriculture industry?

In North America, AgGateway, a consortium of companies, laid some important groundwork for industry-wide identification in the agriculture supply chain. The resulting system is the Ag Industry Identification System (AGIIS) [1], infrastructure to house common, standard identifiers for trading partners, locations, products, and consumers.

Having AGIIS in place for supply chain, AgGateway moved on to standardizing data exchange in field operations (harvesting, irrigation, etc.) with its Standardized Precision Ag Data Exchange (SPADE) [2] and Precision Ag Irrigation Language (PAIL) [3] projects, seeking to implement, and maintain compatibility with, existing standards such as ISO 11783 [4] and ISO 19156 [5] whenever possible.

The SPADE project motivated the development of a flexible framework, the Agricultural Data Application Programming Toolkit (ADAPT) [6], to interconvert between the myriad proprietary formats of farm management information systems (FMIS), machinery, advisory systems and data stores. ADAPT consists of an open-source common data / object model and a system of open-source and proprietary format conversion plugins.

AgGateway's collaborative model for standards implementation in e-agriculture drew attention outside its original North American scope. This led to the creation of AgGateway Europe, the renaming of the original organization to AgGateway North America, and the creation of a coordinating umbrella organization, the AgGateway Global Network. As of this writing, initiatives are underway in Latin America and Japan for the creation of additional regional AgGateway organizations.

This paper is focused on AgGateway Europe; specifically, on a newly-chartered project called the *Identity: Keys for Agriculture Data Exchange* Project (henceforth, "Identity Project"). Its purpose is to evaluate the need in Europe for an identification system similar to that used by North American companies; and, if such a need exists, to implement such a system for the benefit of European agriculture, using / adapting, to the degree possible, existing work such as ADAPT.

The Core Document Model

Growers use multiple *documents* to exchange field operations data as part of their business processes. Work has been done on standardizing farm processes [7], but until recently the documents and many terms used within them had yet to be unambiguously defined. The Core Documents (Table 1) emerged from AgGateway's SPADE and PAIL projects [2] [3]: they define the data exchanged during the planning and execution of a field operation. The definitions are quite flexible, in view of the myriad ways in which different growers implement their record-keeping in response to regionally-specific regulatory requirements, particular characteristics of their markets or farming operations, and personal preference. [6]

Table 1: Core documents. Adapted from [6].

Document	**Actor**	**Description / Meaning**
Plan	Farmer together with advisor(s)	"This is how we're going to grow a particular crop on some particular land during a particular time interval"
Observations	Crop scout, sensors	"This is what's happening in the field "
Recommendation	Someone with *expertise*; e.g., an advisor, a retailer, an input supplier.	"This is the course of action I recommend"
Work Order	Someone with *authority*; e.g., the farmer, or an agent thereof.	"This is what (the course of action) we are going to do."
Work Record	The operator of the field operation, or a task controller on the machine.	"This is what actually happened."

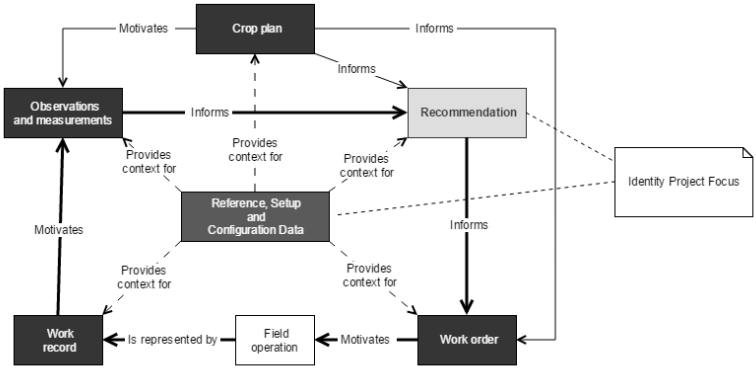

Fig. 1: AgGateway's Core Documents Model, showing relationships among the documents.

Reference Data

Figure 1 shows the Core Documents being afforded context by Reference, Setup, and Configuration Data, defined in Table 2. Reference Data and the Recommendation Document are of particular interest in this paper. As an example, imagine a scenario where a crop advisor is making a crop protection product recommendation for a grower, given observations of a pest in the field. In addition to agronomic criteria, it is necessary to consider regulatory compliance implications, an aspect of particular concern in Europe [8]. Examples:

- How much of each of this product's active ingredients has already been applied in the field this year? How many times? Product labels typically mandate strict limits.
- How soon does the grower intend to harvest? Spraying cannot happen too close to harvest because the label will likely mandate a crop-specific pre-harvest interval.
- Were other crop protection products applied recently? When? There are label-mandated, product-specific limits to how soon workers can re-enter a field following an application.

There are multiple such criteria to consider when deciding whether to apply a product, and multiple scenarios (e.g., export, customer-specific production contracts, etc.) the grower works in. In order for this decision-making process to happen in a scaleable and sustainable way (i.e., where the grower and advisor can afford to do it ongoing), the reference data must be machine-readable, and easily usable in the context of the grower's FMIS. Moreover, this needs to happen in a way that *both* the advisor and the grower (who may have different FMIS) can understand exactly what the products, ingredients, and constraints mean.

Table 2: Reference, Setup, and Configuration data. Adapted from [3].

Category	Description / Meaning
Reference Data	Data that a manufacturer makes available to support the purchase, setup and/or use of their products. It pertains to **all instances** of a manufacturer's product; i.e., reference data is not grower-specific or specific to an individual sale or single instance of a thing. For example, the product name, registration number and dates, and active ingredients are reference data for a crop protection product, but a batch or lot number is not.
Setup Data	Setup data provides information needed to set up data exchange between the grower and machinery or other actors (e.g., crop advisors). It refers to specific instances of grower-specific pertaining to the grower, farms, fields, and actors. This may include farm names, field boundaries, the specific products the grower has a permit to use, etc. It does not include information regarding their state.
Configuration Data	Specifies the particular state of specific instances of things such as farm equipment and instruments (e.g. soil sensors, irrigation pivots, combines, etc.) This may include their location, what they are connected to, who installed them, etc.

The Identity Project

Goals

The overall objective of the Identity Project is to build infrastructure to improve interoperability among different systems (FMIS, databases, applications) that are used to support field operations planning, execution and recording. This includes leveraging existing work done by the North American SPADE / PAIL / ADAPT projects [6] and adapting it to European conditions. Attention is also being paid to the work done by the Agricultural Industry Electronics Foundation (AEF, http://aef-online.org) on ISO 11783 [4] implementation.

An important aspect of the project is enabling the grower to set permissions for sharing subsets of their data. Special attention is also being paid to comparing the value of independent data exchange platforms and peer-to-peer systems for grower-partner communication. This is particularly important given the recent emergence of numerous independent data-exchange platforms in the marketplace.

The Identity Project will also provide insights about the applicability of the ADAPT toolkit [6] to support data exchange in crop protection and make clear how this relates to the ISOXML standard for similar types of data exchange. A proof-of-concept Phase 1 of the project is underway, using ADAPT to exchange Reference Data and Recommendations in a crop protection context. Long-term, the Identity Project will contribute to:

- Enable more accurate, effective, and efficient use of crop inputs (e.g., crop protection, seed and fertilizer products) according to their label and good agricultural practices.

- Improve distribution of Reference Data for fertilizer, seed and crop protection products: identifiers, composition of products, application instructions, etc.
- Lower costs and increase yields for farmers, and ease their record-keeping burden.
- Contribute to sustainable agriculture.
- Enable the secure, permissioned, sharing of field operations data among multiple organisations, using a common data model.

Scope

The project's ultimate scope is to enable machine-readable Core Document exchange (initially, Recommendations) with special interest in enabling digital Reference Data access; for example:

1. A farmer sets up permissions enabling other organisations to access subsets of his/her data. All subsequent data exchange happens as per the permissions in place.
2. The farmer shares a crop Plan with other stakeholders of interest (e.g., crop advisor).
3. The farmer shares in-field Observations and Measurements with the crop advisor.
4. The advisor creates a crop/field-specific recommendation / application prescription map for crop inputs, using the farmer-provided documents, and Reference Data. The recommendation is checked against regulatory constraints, and sent to the grower.
5. The farmer performs the field operation based on the Recommendation received, and creates a Work Record which can then be shared with others.

Identity Project Workflow and Progress

Figure 2 shows the workflow of Phase 1 of the Identity Project as a vertical Business Process Modeling & Notation (BPMN) diagram. There are 3 different swimlanes on this diagram, representing activities performed by three distinct groups within the project:

- AgGateway-Europe project participants. This team is responsible for gap-checking existing AgGateway models, and working with the AGNA team to make changes as needed.
- AgGateway-North America Teams ("AGNA"), from the SPADE3 and ADAPT projects. Their role is to support the Identity Project by extending existing models, API designs and other infrastructure to accommodate European needs.
- Reference Data Providers, who will ensure the data model meets European needs, and provide Reference Data (specifically, crop protection product identifiers, associated data).

Two parallel proof-of-concept (POC) implementations of a Product Reference Data API (RDAPI) are planned: One by the AGNA team, and the other by participating Reference Data Providers. The design of these APIs is meant to be the same, albeit providing product information from different sources; the underlying intent is to demonstrate the distributed

nature of this RDAPI architecture, whereby multiple providers can, each with their own business model, provide reference data to support field operations data exchange.

Tasks 1.1, 1.2, and 1.3 (Figure 2) in the Phase 1 POC are already in progress. Work will continue on the remaining tasks over the course of early 2018.

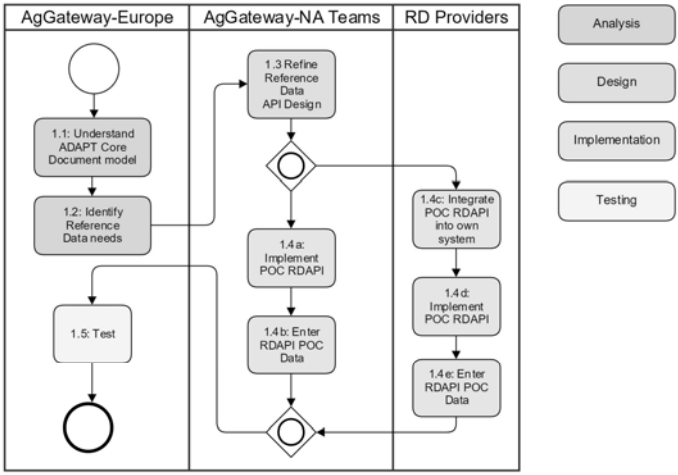

Fig. 2: Workflow for the development process of Phase 1 of the Identity Project.

Discussion

The Value of Controlled Vocabularies

Using shared controlled vocabularies in data collection enables “apples-to-apples” comparisons. The value of this approach can be shown with an example from one of the authors’ own experience:

A vegetable processor buys from several dozen growers. For multiple reasons (food safety, production management, etc.) the processor needs detailed information about each grower’s application of crop protection products to the crop. The growers all used the same Reference Data (in this case, they were using the same FMIS), so it was easy to make reports for the processor that compared or aggregated usage of the products, because they had the same identifier for each product. Had the growers been using different sets of Reference Data (a typical case in today’s industry), a complex and labor-intensive process of record linkage [9] would have been necessary in order to interoperate.

The CompoundIdentifier enables progress without “picking winners”

The variety of FMIS providers in the industry currently spans multiple generations of identification technology (integers, strings, UUIDs, URIs, etc.) A standards-making effort that seeks to promote participation in the industry necessarily has to accommodate this reality.

For this reason the underlying identification technology used by ADAPT, called the “Compound Identifier”, is in effect a “basket” of identifiers that can accommodate (and associate) multiple identification options, while enabling the future emergence of a dominant, emergent mechanism (e.g., IRIs) [10]. This enables not only dealing with different *sources* of identifiers (via record linkage, as previously mentioned), but with different *formats* as well.

Difficulties

Several challenges exist for use of product reference data in Europe:

- Stakeholders need product regulatory information that is machine-readable and easily transferable among different systems and countries. This is only partially available today.
- Regulatory data is country-specific, often available in text form only, and often needing further interpretation (e.g., due to a lack of controlled vocabularies) to be usable.
- Product Reference Data (especially its regulatory aspects) changes often (and thus requires frequent updates), and those changes may include country-specific data model changes, and multi-language support. This requires a great amount of work, which is currently economically viable only in large countries.
- Regulatory data is not yet well linked with different standard code systems that could be used at an international level; only product packaging notation is standardized [11].

Conclusions

Agriculture is a global industry that increasingly requires decision-making based on scientific principles and accurate data exchange among stakeholders. This requires a global language to describe the resources used in field operations; i.e., Reference Data. The work described herein sets the stage for adoption of Reference Data for product identification in Europe, looking to make existing sources of data findable, accessible, interoperable, and reusable (as opposed to creating new sources). Work is ongoing to address the difficulties that lie ahead. A multi-stakeholder, collaborative, industry-based effort such as AgGateway-Europe provides a powerful framework for achieving this end.

References

[1] AgGateway (2015). The Ag Industry Identification System (AGIIS): A Critical Building Block to Facilitate eBusiness. http://s3.amazonaws.com/aggateway_public/AgGatewayWeb/About%20Us/AgGatewayAGIISFlyer_V_3_10815.pdf (1 June 2017).

[2] AgGateway (2015). *The Spade Project*, PDF, http://s3.amazonaws.com/aggateway_public/AgGatewayWeb/About%20Us/CommunicationsKit/AgGatewaySPADE3_11415.pdf (1 June 2017).

[3] D. Adhikari, D.T. Berne, R.A. Ferreyra, C.C. Hillyer, S. Melvin, B.K. Nef (2016). *Data Exchange Standard for Precision Irrigation*. ASABE Paper No. 2458371. St. Joseph, MI.: ASABE

[4] International Organization for Standardization (2015). *ISO 11783-10:2015 Tractors and machinery for agriculture and forestry -- Serial control and communications data network -- Part 10: Task controller and management information system data interchange*. International Organization for Standardization, Geneva, Switzerland.

[5] ISO (2011). ISO 19156:2011 *Geographic information -- Observations and measurements*. International Organization for Standardization, Geneva, Switzerland.

[6] D.B. Applegate, A.W. Berger, D.T. Berne, R. Bullock, B.E. Craker, D.G. Daggett, R.A. Ferreyra, A. Gowler, S.C. Haringx, C. Hillyer, T. Howatt, B.K. Nef, S.T. Nieman, L.T. Reddy, S.T. Rhea, J.M. Russo, P. Sanders, E.D. Schultz, T.W. Shearouse, M.W. Stelford, J.W. Tevis, J.W. Wilson, J.A. Wilson (2016). *Toward geopolitical-context-enabled interoperability in precision agriculture: AgGateway's SPADE, PAIL, WAVE, CART and ADAPT*. Proceedings of the 13th International Conference on Precision Agriculture, July 31 – August 4, 2016, St. Louis, Missouri, USA.

[7] ISO (2009). ISO 22006 Quality management systems – Guidelines for the application of ISO 9001:2008 to crop production. International Organization for Standardization, Geneva.

[8] European Parliament and of the Council of 21 (2009). Directive 2009/128/EC, establishing a framework for Community action to achieve the sustainable use of pesticides (Text with EEA relevance) ELI: http://data.europa.eu/eli/dir/2009/128/2009-11-25

[9] I.P Fellegi, and A.B. Sunter (1969). *A Theory for Record Linkage*, Journal of the American Statistical Association, 64, 1183-1210.

[10] D.T. Berne, B.E. Craker, R.A. Ferreyra, C.C. Hillyer, S.T. Rhea, J.W. Tevis, J.A. Wilson, J.W. Wilson (2017). *A rising tide lifts all the boats: AgGateway's Collaborative Model for Identification in Field Operations*. ASABE Paper No. 1701020. ASABE, St. Joseph, MI.

[11] UN/CEFACT (1992). Recommendation 21 / Rev 2: Codes for Passengers, Types of Cargo, Packages and Packaging Materials (with complementary codes for package names). Geneva.

Efficiency Optimisation of a Forestry Crane by Implement Hydraulics with Energy Recovery

M. Sc. **Chris Geiger**, Prof. Dr.-Ing. **Marcus Geimer**,
Karlsruhe Institute of Technology, Institute of Mobile Machines,
Karlsruhe

1. Abstract

Forwarders are an essential part in fully mechanised timber harvesting chains. Due to a suboptimal energy usage at the implement hydraulics, caused by unused energy recovery, there is a great potential for an optimisation of the machines to increase its sustainability and environmental compatibility. Hence, innovative solutions for this challenge are designed within the project 'Forwarder2020' at the Karlsruhe Institute of Technology (KIT), embedded in and sponsored by the European program 'Horizon 2020', managed by the project leader HSM Hohenloher Spezial-Maschinenbau GmbH & Co. KG.

The focus in this treatise is on the energy efficiency of a forestry crane, for example mounted on a forwarder. On current machines there is no built-in system to recover energy. An energy recuperation and regeneration system is therefore developed for forestry cranes.

To compare the efficiency of different machines or system architectures and to evaluate the energy recovery potential of loading processes, reference loading cycles have been established based on field measurements of real logging processes. These standardized reference cycles represent recurrent loading cycles in a working environment.

2. Motivation

In a fully mechanised harvesting process like cut-to-length (CTL) logging system, a harvester fells the trees and crosscuts them into specific lengths. This pre-processing includes a separation of the logs into different assortments with characteristic lengths. In the next process step forwarders are loading the logs and move them from the felling site to forestry roads. There, the forwarder unloads the logs and piles them to specific assortments, whereby a further transportation via forestry trucks is easily achievable. [1][2]

In Nordic countries like Sweden or Finland, up to 100% of the harvest is achieved by the CTL-system, whereas in Germany it is used about 35 %. As forwarders are used for the logging process in motor manual systems too, they are an essential part in mechanised timber harvesting chains. [3]

The main task of a forwarder is loading and unloading of logs, which sums up to 80 – 85 % of total working hours, by what means 15 – 20 % of the time forwarders are driving [4]. Regarding to this, loading processes are an important starting point for an energy efficiency improvement. During these loading cycles, there are common situations like lowering the crane or a practically horizontal movement of the grapple where the potential energy of the system due to active loads can be reused.

Hence, in the first part of this paper, loading cycles of forwarders used in CTL systems are examined to derive characteristic patterns for further evaluations and to estimate the energy recovery potential of forestry cranes based on this reference cycles.

As there are no built-in systems for energy recovery on in-market machines, the second part of this paper describes an innovative system for energy recuperation and regeneration in crane systems of forwarders. The efficiency improvement potential will exemplary be shown on the defined loading cycles. With these reference cycles, different machines and systems can be compared in relation to energy efficiency.

3. Loading cycles of forwarders used in cut-to-length systems

To achieve a sufficient database for the evaluation of loading cycles, measurements in the forest under real conditions in a CTL thinning process took place. Therefore, an in-market machine with a crane as shown in figure 1 was used. The crane consists of a crane pillar, inner boom, outer boom and telescope including the related cylinders. The forwarder was equipped with sensors for cylinder positions and chamber pressures for all consumers. The pressure and flow supplied by the hydraulic pump were also measured. Furthermore, the control signals from the crane joysticks were recorded as well as significant engine variables like engine speed or fuel consumption. With these data, the energy consumption of the machine or individual consumers can be determined, as well as characteristic movement patterns for loading processes, resulting in reference loading cycles.

Figure 2 shows exemplarily for a forest alley the determined distribution of the collected logs, whereas the centre of the crane pillar is located at x = y = 0 m. The distribution shows clearly the machine operators' preferred position of the forwarder for the loading process, which is rectangular towards the log at the height of the crane pillar. At this position, the view over the machine, logs to be picked up and environment enables the machine operator to execute an optimal loading process. This results corresponds to similar experiments carried out in [5].

Based on observations of forwarders working in forest alleys, a loading cycle of a forwarder includes the following phases:

I. Motion of the grapple from the load bunk to the log
II. Gripping of the log
III. Retraction motion of the grapple including the log towards the load bunk
IV. Positioning and dropping of the log

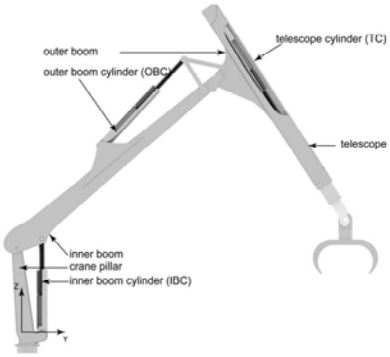

Fig. 1: Schematic sketch of a forestry crane

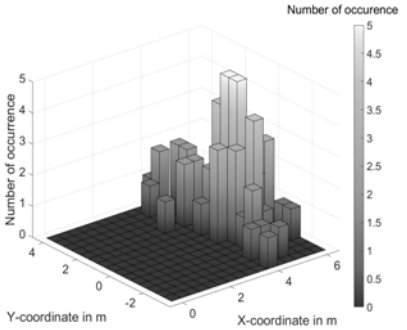

Fig. 2:Spatial distribution of collected logs

For a first evaluation of the loading cycles, the position of the inner boom cylinder (IBC), cf. figure 1, is compared for different loading cycles measured in the forest. Figure 3 shows the normalized position of the IBC for randomly chosen loading processes measured in a forest alley. Hereafter, all cylinders are fully extracted at position 1. For a comparison of loading cycles the IBC is more suitable as loading cycles start and end with a movement of the IBC than one of the other cylinders, cf. figure 3. Remarkable is that the characteristic profile of each loading process seams similar, although the starting position and loading time differs.

The difference in the starting position is caused by an increasing loading height due to more logs in the load bank. The time difference, resulting in more dispersed lines starting at t = 10 s, occurs because of varying positions of the logs, the difficulty of gripping logs lying on the ground or different retracting movements towards the load bank due to manoeuvring around not chopped trees. The exact movement pattern is explained in chapter 3.

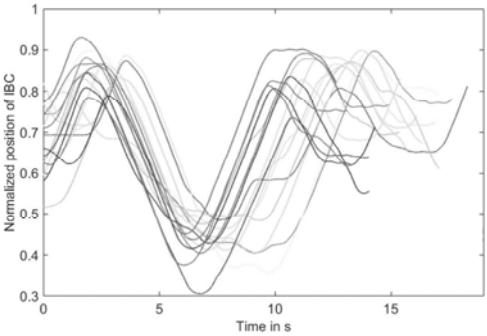

Fig. 3: Normalized position of inner boom cylinder for different loading cycles

Combining the results shown in figure 2 and figure 3, machine operators prefer a specific relative position of a forwarder towards the logs and following a characteristic movement pattern to load the log. These conclusions are in accordance with results achieved in [1] and [5]. To map these findings onto reproducible reference cycles, a laboratory test setup as shown below was developed and installed following [6]. Thus, deviations in the cylinder position at the beginning of the cycle or varying loading times can be prevented. With this reference cycles efficiency of different machines or system architectures can be compared.

4. Definition of normalized loading cycles

The laboratory test setup is shown in figure 4. Corresponding to the achieved results, a log (length 4 m, weight 320 kg) is placed at a log centre distance of 4.6 m and 8.5 m next to the machine to cover significant, realistic log positions. 8.5 m are considered because in the future field of application, the number of forest alleys should be decreased to reduce the impact of forestry machines on the soil, whereby environmental sustainability is enhanced. By following the findings displayed in figure 2, the position in y-direction of the log is chosen between crane pillar and first tyre of the front wagon. The load bunk of the forwarder is empty.
Several operators repeated the loading process for each distance at least 15 times. The measurement for each loading cycle starts with the crane tip placed centred over the empty load bunk and stops when the same position is achieved after putting the log in the load bunk. During the loading cycle, the movement follows the steps as described in chapter 2.

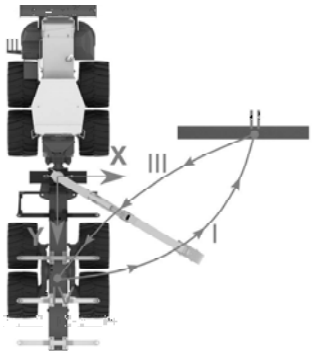

Fig. 4: Laboratory test setup

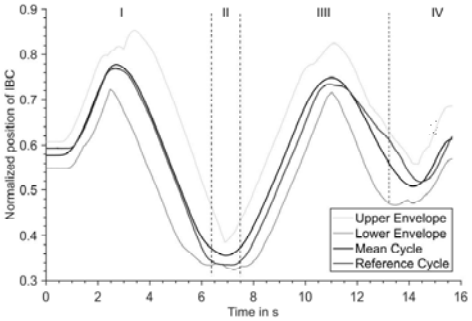

Fig. 5. Normalized position of inner boom cylinder

Exemplarily for middle-distance ranges, the total loading cycle times differ about 7 % around a mean value of 15.2 s. To compare the different cycles and filter out reference cycles which fits best a mean cycle, the time series of the loading cycles are scaled to an equal length. This principle is widely used and known as Uniform Scaling (US) and described in different treatises [6][7]. After using the principle of US, a mean loading cycle for middle-distance ranges is achieved by taking the arithmetic mean of all cycles.

The black graph in figure 5 shows exemplarily the mean position of the IBC over time. The green respectively red graph represents the upper respectively lower envelope of the measured loading cycles. The loading process is divided into four phases as characterised in chapter 2. Striking is the small deviation of the amplitude and loading time of the considered cycles, which confirms that the operators are highly skilled and experienced.

By calculating the normalized root mean square error (NRMSE), the alignment quality between a tested cycle and the mean cycle can be compared. The reference loading cycle is equivalent to the cycle with the lowest NRSME. This reference cycle for middle-distance ranges (log centre distance of 4.6 m) is shown in figure 5 via the blue graph. Same proceeding is done with the data series of the other consumers, e.g. the OBC, leading to the same loading cycle as reference cycle.

By using US and NRSME, an independent reference cycle can be evaluated. This procedure can be repeated for the significant log positions, which concludes in a reference cycle for both middle-distance and long-distance ranges.

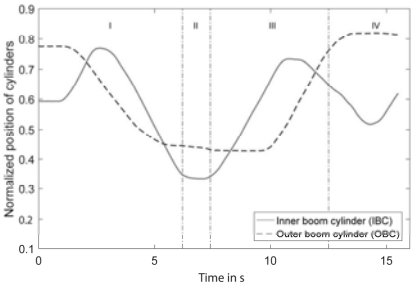

Fig. 6: Reference cycle for middle-distance ranges

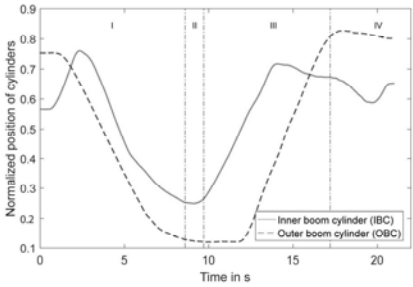

Fig. 7: Reference cycle for long-distance ranges

The course of both IBC and OBC of the reference cycle for middle-distance ranges is displayed in figure 7, for long-distance ranges in figure 8. Although they show different cycle times, the characteristic movement pattern is similar. At the beginning, the crane tip has to be lifted over the load bunk poles, resulting in an extension of the IBC. Simultaneously, the OBC is retracted and therefore the crane tip moving lateral from the crane pillar. After passing the poles, the grapple is moved directly towards the log by lowering the inner boom and lifting the outer boom, whereby the telescope can be extracted (not illustrated). At the lowest position of IBC and OBC, the log is picked up. Afterwards it is retracted towards the forwarder while at the same time lifted over the poles (IBC and OBC extending) and finally lowered down into the empty load bunk (IBC retracting). The inner boom upward movement at the very end of the cycle results from positioning the crane tip at the starting point.
With these achieved reference cycles for both middle-distance and long-distance ranges, a reproducible evaluation of energy efficiency of different machines and system architectures is possible. Furthermore, the theoretical potential for energy recuperation can be estimated.

5. Energy recovery potential of forestry cranes of forwarders

As seen in figures 6 and 7, there are frequent situations where the inner boom cylinder (IBC) and outer boom cylinder (OBC) are acting simultaneously. As a result, exemplary for a lateral movement of the crane tip, the inner boom is lowered while the outer boom has to be lifted at the same time. Therefore, theoretically all of the potential energy from lowering the inner boom could be transferred to the outer boom, which would make the motion way more energy efficient. Energetically this means an idealized horizontal, lateral movement of the crane tip neglecting friction and further losses does not require any energy.

Figure 8 respectively figure 9 shows the position of IBC (red graph) and OBC (blue dashed graph) over cycle time and the theoretical usable power due to lowering inner or outer boom for middle-distance ranges respectively long-distance ranges. This power is calculated for time ranges when IBC is retracting and OBC extending, as only there energy reuse is possible, by equation 1:

$$P = \Delta p \cdot Q \qquad (1)$$

with P: Power in W

Δp: Pressure difference between cylinder and environment in Pa

Q: Volume flow in m^3/s

Most potential for energy reuse is in the IBC taking into account that the total mass of the crane is lowered. As the mass of the outer boom is significant lower, also the usable power is less than for the inner boom while lowering down. Furthermore, the time proportion is less than for the IBC.

There are significant periods where both IBC and OBC are extending or retracting. Here, an energy regeneration is possible by transferring the usable power between the different cylinders. For example, taking the reference cycle as shown in figure 8, from 2.5 s on the IBC is retracting while the OBC is expanding.

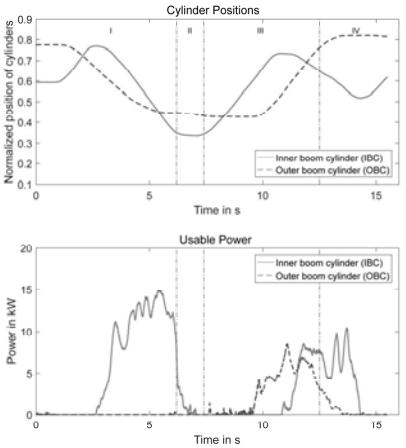

Fig. 8: Middle-distance reference cycle

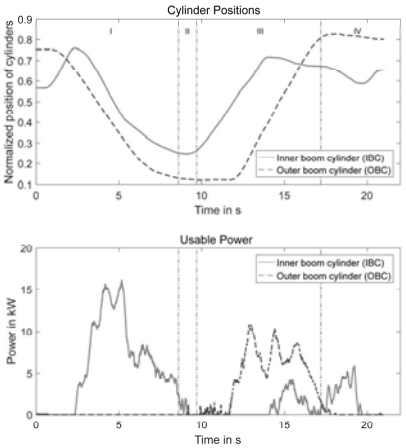

Fig. 9: Long-distance reference cycle

The released power from the IBC can be transferred to the OBC and be used for the process of lifting the outer boom. Same proceeding can be used inversely from 10 s on to support the

lifting of the inner boom. Another possibility is to recuperate the released energy, e.g. by using a hydraulic accumulator. In this case, the energy released during lowering processes is stored temporarily and reused e.g. for lifting processes.

In comparison, the reference cycle pictured in figure 9 for long-distance ranges shows a similar pattern. Here the periods where energy regeneration is possible are longer compared to the cycle shown in figure 8. As the log is arranged further away from the machine, the inner boom has to be lowered more than in middle distances, simultaneously the outer boom has to be lifted more during extending, cf. the time period up to 9 s in figure 9.

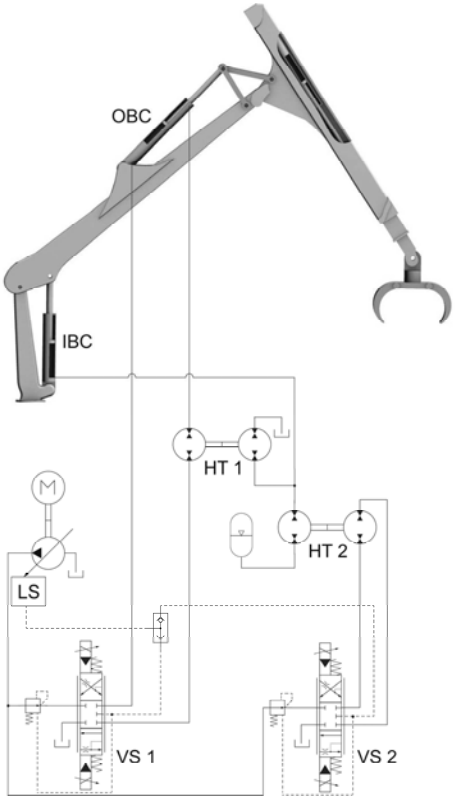

Fig. 10: Circuit diagram of new hydraulic system [8]

6. Concept of energy-saving crane system

The concept of an energy-saving crane system is shown in figure 10 [8]. With this hydraulic system, both energy recuperation and regeneration are possible. This system can be used independently from specific crane designs as the interfaces are between the crane and the valve block mounted on the forwarder. The system connects the IBC and OBC by a hydraulic transformer. The hydraulic transformer converts the usable power P by adjusting the pressure difference and volume flow, cf. equation 1, for the different cylinders.

For a further explanation of the innovative system, an extending, lateral and horizontal movement serves as a simplified example. This motion implies lowering the inner boom while simultaneously lifting the outer boom. For this, valve section (VS) VS 1 is actuated while VS 2 remains in normal position, so that there is no volume flow over the hydraulic trans-

former HT 2. Therefore, oil flows from the bottom chamber of IBC towards the hydraulic transformer HT 1, resulting in a movement of the HT 1 as VS 1 is additionally actuated. This leads to a volume flow from the left side of HT 1 towards OBC, while simultaneously the emitted power from the right side is transferred via a mechanical connection to the left side. Due to this, the hydraulic pump needs to supply the same volume flow, but with a significant lesser oil pressure compared to a state-of-the-art system. In this modus energy regeneration takes place.

If additionally the crane tip has to be lowered down, either valve section VS 2 has to be switched or the hydraulic transformer has to be manipulated in a way that the left and right side are mechanically decoupled. By that, oil flows through the hydraulic transformer HT 2 into the accumulator and is recuperated. By switching VS 2 into the opposite position, the accumulated oil flows towards the IBC resulting in lifting the inner boom. Especially considering several loading processes, the stored energy of lowering the grapple including logs towards the load bunk (cf. phase four) can be used to lift the crane over the load bunk poles for the next loading process, cf. figures 8 and 9.

7. Conclusion and Perspectives

Reference loading cycles for middle- and long-distances ranges for forestry cranes used in CTL-processes are determined via measurements under real working conditions. Based on these reference cycles, the energy recovery potentials of cranes mounted on a forwarder are evaluated. Furthermore, an innovative hydraulic system for energy regeneration and recuperation including hydraulic transformers is presented, which will reduce the fuel consumption of forwarders significantly as the motor load decreases.

In further steps, a simulation model of a forestry crane, which combines a multi-body and a hydraulic simulation, integrated in a holistic model of a forwarder, can be parameterized and validated. The energy efficiency of the innovative hydraulic concept can be determined by modifying the validated simulation model, including a parameter study for an optimal configuration of the integrated system. The reference cycles will be used to compare the energy efficiency of the energy-saving crane system to current state of art. Afterwards, a demonstrator including the new hydraulic system will be set up and measured.

8. Acknowledgements

This project has received funding from the European Union's Horizon 2020 research and innovation programme under grant agreement No 727883.

9. References

[1] Morales, D.: Increasing the Level of Automation in the Forestry Logging Process with Crane Trajectory Planning and Control. Journal of Field Robotics 31(3), p. 343–363, 2014

[2] Manner, J.: Automatic and Experimental Methods to Studying Forwarding Work. PhD thesis, Swedish University of Agricultural Sciences, 2015

[3] Cacot, E.: Developing full-mechanized harvesting systems for broadleaved trees: a challenge to face the reduction of the manual workforce and to sustain the supply of hardwood industries. 2006 Council on Forest Engineering (COFE) Conference Proceedings: "Working Globally – Sharing Forest Engineering Challenges and Technologies Around the World" Coeur d'Alene, July 22-Aug 2,2006

[4] Manner, J.: Load level forwarding work element analysis based on automatic follow-up data. Silva Fennica vol. 50 no. 3, 2016

[5] Morales, D.: Path-Constrained Motion Analysis: An Algorithm to Understand Human Performance on Hydraulic Manipulators. IEEE TRANSACTIONS ON HUMAN-MACHINE SYSTEMS, VOL. 45, NO. 2, 2015

[6] Deiters, H.: Standardisierung von Lastzyklen zur Beurteilung der Effizienz mobiler Arbeitsmaschinen. PhD thesis, Technische Universität Braunschweig, 2009

[7] Yankov, D.: Detecting Time Series Motifs Under Uniform Scaling. Proceedings of the 13th ACM SIGKDD international conference on Knowledge discovery and data mining, San Jose, California, USA, 2007

[8] Hohenloher Spezial-Maschinenbau GmbH & Co. KG. Gebrauchsmusterschrift DE 20 2014 006 861 U1, 2015

Holistic Tractor Setup and Optimization System

CLAAS Electronic Machine Optimization for the Tractor

M. Sc. **Lennart Meyer**,
CLAAS Selbstfahrende Erntemaschinen, Harsewinkel;
M. Sc. **Pierre Noyer**,
Claas Tractor, Vélizy-Villacoublay, France

1. Abstract

The usage profile of tractors has evolved from pure pulling machines to multifunctional mobile working machines in the course of agricultural engineering history. Tractors are working in combination with various types of implements in various applications. Working efficiently in the different tasks requires manual adjustment of several tractor and implement settings.

The introduction of electronic systems on tractors (GPS, headland management, electronically controlled engines, automatic transmissions, electro-hydraulic valves, tire inflation systems…) drastically increased the quantity of possible settings. Today setting up the tractor requires sophisticated knowledge about the specific tractor (including its architecture and its subsystems), the implement, the terra mechanics and the agricultural process. However, even for experienced users it is hard to handle this complexity and to use the full potential of the tractor implement combination in terms of performance, efficiency, soil protection and working quality.

CLAAS Tractor has developed a new system to support the user in handling the complexity of modern tractors. Unlike known support systems, which are covering only single aspects (e.g. ballasting apps…), CLAAS takes an holistic approach, taking into account all common tractor applications (tillage, seeding, crop care, …). Furthermore, the system helps to reduce the necessary user knowledge. Users are relieved from technical aspects, which enables them to concentrate on agricultural aspects of the working process. The presentation will provide an insight into the functioning of the system and the way it has been developed.

2. Introduction

The context of farming has been changing over the past decades, leading to a steady increase in size of farming operations and a change in organizational structure from a family based to an employee based workforce [1]. Along with these changes came the introduction of ever growing machine size and installed power, to boost productivity, in the production

process. Besides the increase of machine dimensions and installed power the last two decades have brought the introduction of new technologies. By use of sensor technologies and data management a change of crop production processes, shifting from an experience based to a knowledge focused approach was possible. The target has changed from producing a maximum quantity to producing at the economical optimum.

Closely linked to this evolution stands the focus on increased sustainability by making more efficient use of inputs, such as crop care chemicals, fertilizers and seeds. Not only are the input factors, but also the natural resources such as soil a major focus for the farm manager who has to respect legal regulation as well as to secure his assets for the future. To support these trends machinery manufacturers and specialized equipment suppliers have been working on a number of systems, which shall support the user in mastering these challenges. These new systems support the operators by automatically adjusting and controlling the tractor or implement, partially relieving him from his duties. This also allows less trained personnel to work at high productivity and increases the quality of the work. However, not all parts of the settings process are covered by assistance of automated systems and thus the level of experience of the user remains a great impact on the working performance.

3. Problem Statement

Support for optimization of the machine is offered to the user by many equipment and machine manufactures in various shapes and forms. Solutions are ranging from simple operating advices through specialized tools to direct assistance by trained experts. In many cases this support is limited to a single optimization target within the full working process and a link to an overall optimization goal is thus missing. Considering possible interactions between targeted operation strategies and the individual subsystem settings remains in the responsibility of the operator. Only by integration of all individual phases of the agricultural task into a holistic optimization approach this issue can be solved.

Today no system supports the user in finding the optimum settings for his tractor implement combination throughout the different phases of the working process. As the interaction between settings are only partly known to the operator a clear guideline for adjusting the machine settings from the most basic to the most advanced setting is needed. As many steps are required for setting the machine it is possible to proceed with countless orders to set up a machine, which will lead to a more or less well adapted result. Some important steps during the setup process may be forgotten and other may not even be known to the operator. Furthermore, with current systems the user is asked to make a technical setting, by e.g. adjusting engine speed based on RPM. This requires that the he has deeper knowledge of the

technical system tractor and implement and that he is aware about which of the technical parameters needs to be adjusted to achieve his goal in the best way.
This leads to the requirement for a system, which is able to support users lacking the above mentioned knowledge or experience in finding the best setting through all phases of the working process.

4. Methodology of Tractor Optimization State of the Art

Machine optimization has always been a focus of the professional user and over time different methodologies have been established to find the correct settings of the machine, reaching from experience based observations to more advanced knowledge based systems. For agricultural tractors, manufacturers provide the users of their products with recommendations for correct setting of machine ballast. Solutions including dedicated sections in operating manuals, preformatted calculation tables [2] or web applications are widely availed. Tire pressure recommendations have been made through tire tables, which correlate driving speed and tire load to minimal allowed tire pressures. Nowadays these are being replaced by more simple to use consumer device applications. Furthermore not only the optimization of basic settings is covered, but onboard systems have been made available to improve optimized operation.
During the last few years a strong development of vehicle automation technology in agricultural environment took place. The strongest driver for the innovation was the introduction of electronics on agricultural machinery. Especially the introduction of communication standards like ISOBUS, offer a wide range of opportunities, to reduce complexity for the machine operator. The communication allows to consider the tractor and the implement as a common system much like on self-propelled machines. This brings the benefit for the operator of not having to manually control the process continuously. Through sensors, actuators and interlinking control loops, many implements are able to partially or fully control their process autonomously. Furthermore implemented automation routines include sequences or status definitions for different working states. The role of the driver is now focused on process surveillance and enabling the execution of automated actions.
The next step of this development allows implements to actively send messages to the tractor to control the parameters of the tractor itself [3]. This allows the implement to achieve an optimum working point for the targeted task and selected strategy. Multiple tractor and implement manufacturers are working on this field of technology, pushing for the development of virtual self-propelled machines with functions such as TECU Class III, also known as Tractor Implement Management TIM. A challenge of this development is the necessity to add

electronic control units and process knowledge, with a control strategy on an implement, to give the right commands to the tractor. Two levels of complexity are working against the full automation of tractor implement management solutions. First of all, a multitude of tractor implement combinations are available and control strategies may differ according to the given environmental conditions, (crop type, type of tillage, etc.) or user preferences (performance vs. quality, vs. fuel efficiency). All these different factors need to be considered in an optimization strategy which leads to great complexity for implementation of all potential combinations that may occur in practical use. Secondly, this technology requires sensor technology, and computing on the implement side. While for more complex implements this technology is state of the art, simpler implements such as those used in tillage operations are often not integrating this pre-requisite.

When focusing on self-propelled machines a number of optimization systems exist, which support the user in finding correct settings, optimizing according to different overall targets [4]. CLAAS for example offers an array of CEMOS functionalities for their combine harvesters. In conjunction with other automation systems such as the CRUISEPILOT, these systems will insure that working quality of the combine harvester is kept at a steady and high level, while operating the machine efficiently and with high throughput. Expert knowledge on which settings will best fit a given situation, are the base for stored optimization routines. This means knowledge for an experienced user is actively transferred to a technical system, which will provide it in form of advices or automated settings adaptation, if needed. By regular checks the situation is reevaluated and in case of changed environmental conditions a readjusting is done. Furthermore, the system can help the user to solve issues when they occur by predefined solution trees.

A number of support system in form of consumer device based APPs are available [5]. Here the requirement of interaction by the user is given to transfer the recommendation of the assistance system to the machine.

A holistic approach that considers the set-up, the work preparation and the working phase of an agricultural tractor-implement task could not be identified yet with any of the optimization support systems. The following chapters will show, how a holistic optimization approach for tractor-implement combinations will support the user in tractor implement optimization.

5. Analysis and Requirement Identification

To define the highest necessities for improving, tractor setup and setting workshops were made. In these workshop the experts identified the biggest potentials to raise the efficiency. These potentials were approved by theoretical calculations. To get additional opinions from

actual machine users customer workshops were made. These customers were asked to choose the ballasting and the tire inflation pressures for a given tractor implement combination for a tillage application. The results were compared to the theoretical optimal values and the potential efficiency gain was calculated. The reasons for non-optimal set up, especially in real world conditions, were seen in unawareness of the loss of efficiency, uncertainty about the right settings and in the complexity of looking up data to calculate optimal settings. It became obvious that users need support. Three phases in the operation of the tractor were identified, in which an optimization system can assist the user in operating the tractor in an optimal way. These phases are:

- The **setup phase** takes place on the farm, when hooking the implement to the tractor. In this phase, the user will be led by a step by step wizard to have a good basic setup for the tractor implement combination, especially in terms of ballasting and tire inflation pressures.
- The **work preparation phase** takes place on the field, right before working. The user is led to set up assistance systems like for example the headland management, but also mechanical adjustments of tractor implement settings.
- During the **working phase**, the user is assisted to optimize the tractor implement combination regarding working quality, performance or efficiency by a dialog based expert system. This expert system generates optimization proposals depending on operating conditions, user inputs, implement type, sensor data etc.

The next step in requirement identification was gathering of the most common tractor implement applications. The applications were grouped into arable farming, forage production, material handling, transport, municipal operations and other tasks. For example for arable farming the applications tillage, sowing, crop care, slurry/dung techniques and harvesting could be found. For every application the information for generic implements were introduced. In the tillage example, there are the implements plough, disc harrow, chisel plough etc. For this generic implements the optimizations are specified in requirements for every phase of work.

6. The System

The implementation of CEMOS for tractor consists of four main parts: The user interface, the calculation module, the databases and the expert system. In the following, these four parts are described in detail.

User Interface

The main goal of the user interface is to make the handling of the tractor as intuitive as possible. To accomplish this, the whole interface is natural speaking. All settings are focused on the working process and technical settings are avoided. Where several steps are needed, the user is guided by a step by step wizard. In this wizard the user gets an overview of the next steps and an estimation is given how many steps are needed to be done. The user interface is designed to help the user in all three previous mentioned phases of operation.

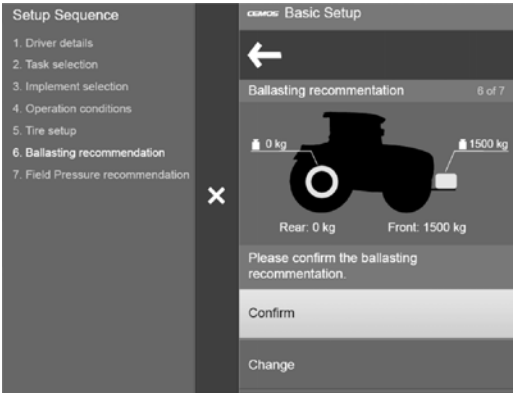

Fig. 1: Basic setup up wizard

In the **set up phase** the implement is connected to the tractor. The user is guided by a step by step wizard through the process of basic setup to help him doing all the settings for his implement. This wizard dialog is shown in **Fehler! Verweisquelle konnte nicht gefunden werden.**.

Other settings like loading headland management sequences or function key assignments are also done within this wizard. The user can enter the wizard in any step. If the user, for example, just wants to change the implement but not the task he is currently working on, the wizard is started with the implement selection. As more information is depending on the changed entry, the user is again guided by the wizard through the steps until all necessary information is entered.

Model-in-the-Loop Tuning of Hitch Control Systems of Agricultural Tractors

Dr. **Thomas H. Langer**, Danfoss Power Solutions, Nordborg, Denmark

Abstract

The farming industry worldwide is facing challenges in order to be more productivity, efficient and leave a smaller footprint on the environment. The success relies on the efficient operation of the agricultural machinery including the agricultural tractor.

One of the major and even one of the most energy consuming operations for an agricultural tractor is soil preparation, especially ploughing. To be efficient, the tractor should be able to transform the highest possible amount of the engine power into a pulling force on the implements, i.e. the plough. From theory of tire mechanics, it is known, that slip is necessary in order to transmit force. Slip, which is relative speed between the pulling wheel and the ground, is also an expression of loss. Hence, it is crucial to have just enough slip to pull the implement without wasting to much energy.

The well-known electro-hydraulic hitch control system for agricultural tractors facilitates a control scheme, that based on sensors can relax the hitch by lifting the implement, reducing the pulling load and limits the slip without compromising working depth too much. Even though this technology is mature, the tuning of the control parameters poses a major challenge, partly because the set of parameters must fit both very hard dry soils as well as wet soil – and these conditions are difficult to obtain within a short time period. In other words, identification and tuning of the parameters can be challenging in terms of time, conditions and repeatability resulting in semi-optimum set of parameters.

In this paper a model-in-the-loop tuning approach is proposed and demonstrated. By harvesting experimental data, this can be used as foundation for standardized test field in order to conduct repeatable tests. These experimental data can be utilized in a simulation model, that represents the mechanical properties for the plough, tractor and tire-soil interaction. The output of the simulation serves as signal to stimulate the controller on the tractor. By this approach the hitch control parameters can be tuned and improved any time a year without available fields. With the possibility to conduct repeatable tests with no variation on the boundary conditions, the loop time for each iteration can as well be reduced significantly.

Introduction

A modern agricultural tractor that conducts soil preparation facilitates at least a three-point rear hitch system, that can raise and lower an implement in such a way that it can be positioned in a transport mode or working mode. In work mode, precise control of the working depth by adjusting the rear hitch is an integrated part of soil preparation. Therefore, modern tractors with electro-hydraulic controlled hitch includes a control scheme, that makes the operation easier for the operator [1], Fig. 1.

Force/draft control continuously measure the draught force by help of load cells. The purpose of the force control is to avoid stalling the diesel engine if the resistance of the soil increased due to field variation [2]. A modern force control system calculates the average resistance force itself and uses that as a reference [3].

Slip control continuously compare the wheel speed with the ground speed, measured by a radar. If the slip exceeds a reasonable threshold, the controller lifts the implement proportional to the calculated slip. The purpose is to keep the tractor driving forward, if the net traction coefficient of the ground drops [3].

Both force and slip control compromises the working depth, but is necessary assistance to avoid stalling of the engine and to have a fuel-efficient operation, since any wheel slip is equal to loss.

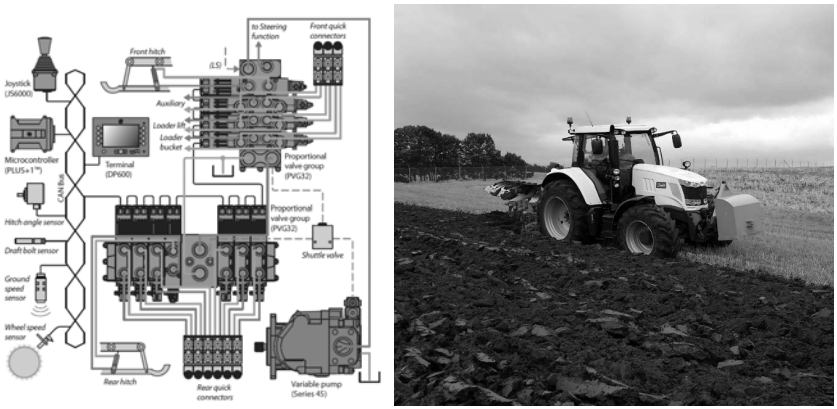

Fig. 1: Hitch control system and ploughing

A modern hitch control system also facilitates other features, such as active damping of the implement to avoid pitching when driving [4,5].

Challenges in Parameter Tuning and Optimization

A wide spread of soil conditions, both net traction coefficient and resistance of the soil, poses a major challenge when the optimum set of control parameters shall be identified. State-of-the-art is to conduct full scale tests in fields at various locations in various weather conditions different times a year. A set of control parameters that might be good for one set of field conditions, might not be working well in other fields – and even at in same field, each set of parameters must be evaluated a relative long distance to overcome statistical deviations of the field. Hereby, tuning and optimization of control parameters (or test of new better adaptive algorithms) may be very time consuming and costly.

This paper proposed instead a model-in-the-loop setup, as shown in Fig. 2. By having a plant model representing the fields and the tractor-plough-interaction with that field, adjusting parameters can be done in a couple of hours, since all conditions can be tested in shorter reproducible loops since the model eliminates the real-world deviation. This even allows the engineers to utilize optimization routines.

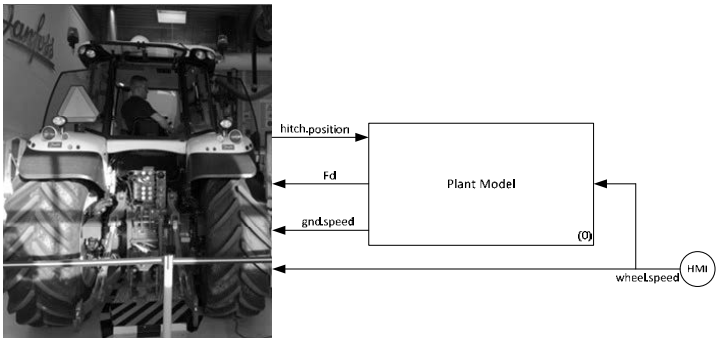

Fig. 2: Model-in-the-loop testing of hitch control system

Tractor-Plough-Soil Model

The content of the Plant Model (0) is shown in Fig. 3. It consists of six blocks (1)-(6) that contains empirical data and mathematical models. For the given problem, it is assumed that the behavior of the system can be approximated to steady-state. This assumption is based on the fact that the sum of forces on the driving direction will only vary slightly around zero, and hence the delay due to inertia will have negligible influence on the results.

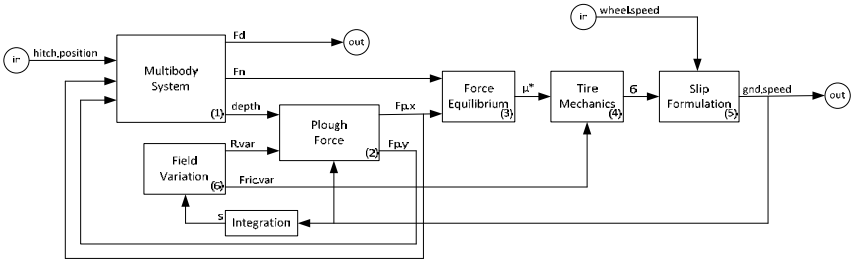

Fig. 3: Tractor-plough-soil simulation model

Multibody System (1)

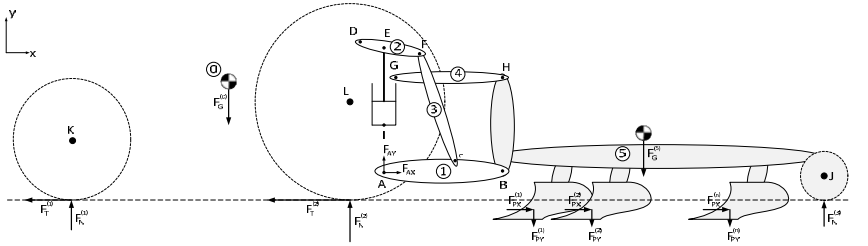

Fig. 4: Multibody system representation of tractor with plough.

The mechanical system of constrained bodies in Fig. 4 must satisfy the set of independent constraint equations:

$$\Phi_{(q)} = 0$$

, where q is the vector containing the global coordinates of the six bodies [6].

Since the system can freely rotate and move vertically with respect to the ground, two additional equations are needed, to determine the complete set of global coordinates:

$$\begin{bmatrix} \sum F_y \\ \sum M \end{bmatrix} = 0$$

It is assumed, that all horizontal forces are attacking in the same vertical coordinate, hence, their contribution to the total torque M is equal to zero.

By solving the above equation, the individual depth of each mouldboard is hereby determined for use in block (2).

The normal forces on the three tires are both needed in above equations, as well as input to block (3). The normal forces are also the vertical tire forces and can be estimated as simple as a spring based on empirical data, or described per the established tire models [7] or the even more advantage studies, such as [8], that takes soft soil and ground deformation into account.

From the multibody model, Fig. 4, it is possible to extract the draught force signal F_{AX} which is sent to the hitch controller for stimulating. The reaction force vector for the multibody model can be determined by:

$$g^c = \Phi_q^T \lambda$$

Φ_q^T is the Jacobian matrix (the time derivative of the constraint equations $\Phi_{(q)}$, and λ is a vector containing the Lagrangian multipliers:

$$\lambda = \left(\Phi_q^T\right)^{-1} g^{ext}$$

g^{ext} is vector will all external forces. After determined λ, the draught force can be calculated by

$$F_{AX} = \Phi_q^T(1{:}2,1{:}2)\,\lambda(1{:}2)$$

Plough Force (2)

The forces acting in a mouldboard, Fig. 5, can be described by fully of semi-empirical models and data. [9] have shown that both horizontal (x) and vertical (y) force components are acting on mouldboards. [10] have shown, that the draught force is dependent on the geometric properties of tools, such as harrows and ploughs. [11] has developed a detailed force prediction models for mouldboards. All these studies show, that the plough force is highly dependent on ploughing speed and ploughing depth. The faster and deeper, the higher forces.

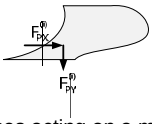

Fig. 5: Forces acting on a mouldboard.

[11] also shows, that the plough forces depend on the soil condition characterized by five parameters 1) bulk unit weight, 2) cohesion, 3) angle of shearing resistance, 4) soil–metal friction angle and 5) adhesion.

Force Equilibrium (3)

Knowing the plough forces and the normal forces on the tires, equilibrium for the x-direction is defined as:

$$\sum F_x = 0 = F_{draught} - F_{traction} = \sum_{i=1}^{n} F_{p.x}^{(i)} - \mu \sum_{j=1}^{2} F_N^{(j)}$$

The friction coefficient μ is an empirical value, but is here treated as an artificial friction coefficient, denoted μ^*. In other words, the necessary friction coefficient for pulling the plough is derived:

$$\mu^* = \frac{\sum_{i=1}^{n} F_{p.x}^{(i)}}{\sum_{j=1}^{2} F_N^{(j)}}$$

The horizontal force equilibrium can be further expanded to include rolling resistance as well, which will give an even more realistic value of the artificial friction coefficient. Values of rolling resistance coefficients can be found in [12].

Tire Mechanics (4)

In tire mechanics, the friction coefficient μ, also called the net traction coefficient, can be determined as a function of the wheel slip σ based on empirical data [12]. Fig. 6 shows the net traction coefficient for different ground types. Hence, the net traction coefficient for a tractor working in the field will vary somewhere between the curves for mud and dry loam respectively.

In this paper, oppositely, the wheel slip is determined as a function of the artificial friction coefficient μ^*. Hence, the necessary slip σ for pulling the plough is determined.

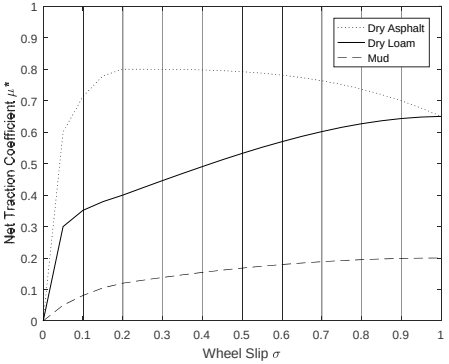

Fig. 6: Net traction coefficient [12]

Slip Formulation (5)

Based on the identified slip σ, the prescribed wheel speed ω and the radius r of either the front or the rear tire, the ground speed $\dot{s}$ can be determined [13]:

$$\sigma = \frac{\omega \cdot r - \dot{s}}{\omega \cdot r}$$
$$\downarrow$$
$$\dot{s} = (1 - \sigma) \cdot \omega \cdot r$$

Field Variation (6)

Field variation represents empirical or user-defined data as a function of the travelled distance, that describes the variation of the net traction coefficient curve, Fig 6, and one or more of the five soil parameters by [12] – at least the bulk unit weight.

Bibliography

[1] Hesse, Horst, and W. Schrader. 1984. “Hitch System Comparison — Mechanical, Hydraulic, Electronic.” SAE Paper No. 841130.

[2] Cordesses, L., J. P. Poirier, and C. Véron. 2002. “Performance Analysis of a Three Point Hitch Controller.” In Proceedings of the 2002 IEEE/RSJ. Lausanne, Switzerland.

[3] “System Description - Hitch Control.” 2008. Danfoss Power Solutions. http://files.danfoss.com/documents/11036124.pdf.

[4] Langer, Thomas H., Kaspar Holm-Petersen, and Dirk Metker. 2016. “Comfort Evaluation Criteria for Pitching Vibration Damping of Agricultural Tractors.” In 74th Internationale Tagung Landtechnik (Agricultural Engineering), VDI Berichte Nr. 2273:437–44. Cologne, Germany: VDI Wissensforum.

[5] Andersen, Torben O., Michael R. Hansen, and Finn Conrad. 2003. “Robust Control of Occillations in Agricultural Tractors.” In Proceedings of IMECE 2003. Washington, USA.

[6] Nikravesh, Parviz E. 1988. Computer-Aided Analysis of Mechanical Systems. Englewood Cliffs, New Jersey: Prentice Hall.

[7] Pacejka, Hans B. 2006. Tyre and Vehicle Dynamics. 2nd ed. Butterworth-Heinemann.

[8] Senatore, C., and C. Sandu. 2011. “Off-Road Tire Modeling and the Multi-Pass Effect for Vehicle Dynamics Simulation.” Journal of Terramechanics 48 (4): 265–76.

[9] Godwin, R. J. 1975. “An Extended Octagonal Ring Transducer for Use in Tillage Studies.” Journal of Agricultural Engineering Research 20 (4): 347–52.

[10] Bögel, Tim, Andre Grosa, and Thomas Herlitzius. 2016. “Identification of parameters for influencing work result and draft force consumption of passive pulled wedge shaped tools.” In 74th Internationale Tagung Landtechnik (Agricultural Engineering), VDI Berichte Nr. 2273:437–44. Cologne, Germany: VDI Wissensforum.

[11] Godwin, R. J., M. J. O’Dogherty, C. Saunders, and A. T. Balafoutis. 2007. “A Force Prediction Model for Mouldboard Ploughs Incorporating the Effects of Soil Characteristic Properties, Plough Geometric Factors and Ploughing Speed.” Biosystems Engineering, no. 97: 117–29.

[12] Goering, Carroll E., Marvin L. Stone, David W. Smith, and Paul K. Turnquist. 2003. Off-Road Vehicle Engineering Principles. American Society of Agricultural.

[13] Kiencke, U., and L. Nielsen. 2005. Automotive Control Systems: For Engine, Driveline and Vehicle. Springer-Verlag, Berlin.

Coupled CFD-DEM simulation of separation process in combine harvester cleaning devices

Dipl. -Ing. **Chr. Korn**, Prof. Dr.-Ing. **Th. Herlitzius**,
Chair of Agricultural Systems and Technology, Institute of Natural Materials Technology, Technical University of Dresden

Abstract

The present paper contributes to the application of the coupled CFD-DEM approach (CFD – Computational Fluid Dynamics; DEM – Discrete Element Method) for the simulation of the separation process of grain and material other than grain (MOG) in the cleaning device of a combine harvester. The large number of influencing factors, their interactions, the wide range of scatter of properties, which are typical for biogenic particles, and the resulting complexity of the separation process require a strategic approach for the creation of a valid simulation model. The study presented in this paper investigates the separation process therefore at two levels, which differ by the degree of process abstraction. The numerical results prove the applicability of the numerical method by the comparison to corresponding experiments in general. However, deviations can also be identified which emphasize the need for further research to improve parameterization and modeling.

Introduction and state of the art

The load on the cleaning device of combine harvesters has steadily increased in recent years due to overall growth of throughput and the intensified production of short straw by the use of separation rotors instead of straw walkers, e.g. [1]-[3]. Today, functional development or optimization is predominantly performed empirically on `trial and error` base, which is not efficient. Those tests are time-consuming, expensive, hard to reproduce and rarely enable process insight view. The separation process is subject to the impact of a huge variety of influences and multi-layered dependencies of them, e.g. [4], and is still not fully understood today.

In recent decades numerical methods for the simulation of dispersed multiphase flows have been developed to very powerful tools e.g. [5] and [6]. There is a variety of methods which were established in different fields of applications due to their characteristics, numerical effort and gain of information. Biogenic particles like grains or legumes, as processed in the combine cleaning device, are subject to complex physical properties and a large variability of

these, depending on the origin of the material and the particular harvesting conditions. In most cases, these particles are non-spherical. A biogenic particle can further be composed of different materials at different locations at the particle volume, which hampers a uniform modeling and parameterization of e.g. a contact model. Another special feature of biogenic particles is the possibility of absorbing water, which leads to a change of physical properties and of contact behavior. It is well known from literature e.g. [7] and practical experience that mean particle moisture and particle surface moisture significantly influence the separation process. Therefore it is necessary to consider the effect of moisture within the simulation.

Present multiphase simulation methods cannot account for the above mentioned biogenic characteristics and hence are not able to provide reliable results immediately. Most of the models for particle contact or interaction with the surrounding fluid, which are available in commercial codes, have emerged from the fields of process engineering and chemical engineering. Their application to biogenic particles and the necessary approximation of particle shape cause uncertainties regarding accuracy and reliability of the results.

Numerical methods have been applied to several functional processes in grain harvesting technology and in particular to separation. Schwarz et al. use the DEM code PASIMODO to compute particle motion on the stratification pan of a combine harvester [8]. The separation process of grain and long straw on the straw walkers of a conventional combine is in the focus of the numerical investigations of Lenaerts, et al. [9]. Pförtner and Böttinger [10] publish numerical and experimental results of separation of grain and short straw in a vertical oscillating box using composite sphere particles in a pure DEM environment. In a later publication, Pförtner, Böttinger, et al. [11] imprint a constant flow field, which is computed by CFD to the domain. Ma, Li and Xu [12] simulate rice-grain and straw particles in a variable-amplitude screen box in the EDEM software environment under different frequency and turning angle conditions. Li, Li and Gao [13] utilize a coupled CFD-DEM approach (EDEM by DEM-Solutions and FLUENT by ANSYS) to simulate the screening process of rice grain and straw particles in a simplified cleaning device of a rice combine harvester. Other authors focus on the parameterization of DEM particles, e.g. Prüfer, et al. [14]. The goal is to provide a valid database for users, derived from standardized or enhanced experiments, e.g. rotating drums, for a variety of agricultural materials. Moisture, scattering particle properties and other specific characteristics of biogenic particles have not been modeled and tested in literature of numerical investigations so far.

Objectives

The Institute of Agricultural Systems and Technology (AST) of the Technical University of Dresden (TUD) has been working on the simulation of material transport, processing and separation in the functional elements of harvesting machinery for several years.The overall objective of the research is the development of valid and efficient numerical models for their application in CAE environment. Within this paper, the focus is set to the separation process in the combine cleaning device; the subordinate objectives can be specified as follows:

- Identification of significant parameters and their sensitivity to numerical results.
- Consideration and evaluation of biogenic particle characteristics e.g. scatter of properties, to numerical simulation.
- Incorporation of the moisture as an influencing factor on separation efficiency.
- Determination of driving factors for computational effort and opportunities to reduce.
- Estimation of the accuracy of the simulation model by comparison with experimental results.
- Exploration of sources of uncertainties and deviations and based on this, definition of further research needs.

This paper gives a brief extract of the results obtained so far within the scope of the above mentioned objectives of the research.

Numerical tool

In an earlier publication, the methodology to select a provisionally suitable simulation tool is described, see [15]. With regard to necessary two-way-coupling, the available computational resources and the demand for the tracking of individual particles to determine grain loss and purity, only the coupled CFD-DEM approach is able to fulfill all of these requirements. *Star-CCM+v9.06* is used for the numerical investigations described here.

Limitation of parameter range

The block diagram in Fig. 1 summarizes the results of the investigations of various authors regarding parameter influences on the separation process, among those e.g. [4], [7], [16] and [17]. The diagram illustrates the complexity of the separation process and the multi-layered dependencies between target values and parameters. The relationships between parameters are indicated by arrows. In the block diagram, the limited parameter range of the simulation

is shown embedded in the entire range of parameters of the real separation process. A distinction is made between input parameters for the simulation, which are directly set by the user, and those parameters, which are gained by specific models or are a superposition of different basic material and particle properties (derived properties).

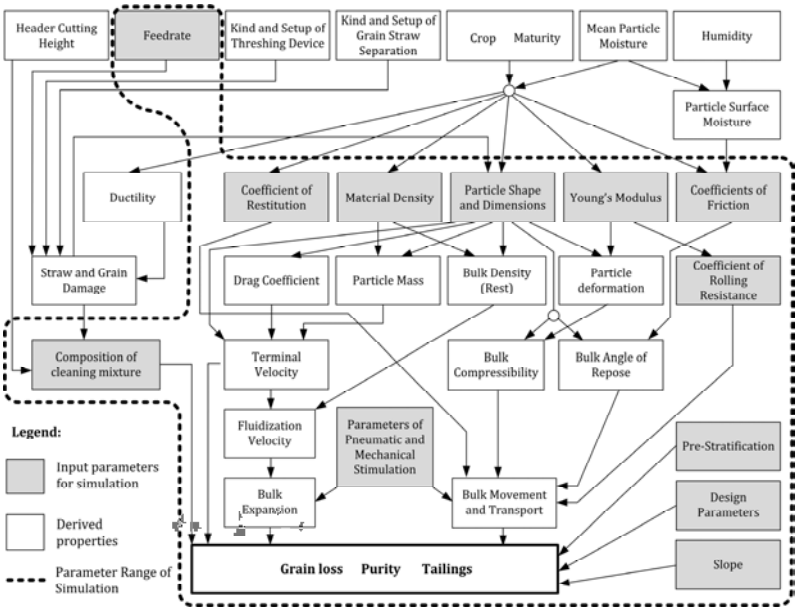

Fig. 1: Parameters and interactions to grain loss, purity and tailings developed on the base of literature review. Identification of input parameters for the simulation.

Problem solving procedure

In a **1st step** the separation process is simplified in the simulation and in the experiment on a high level. This corresponds on the one hand to the size of the domain, which represents a 200 x 200 mm section of the chaffer of the cleaning device. By this, the quantity of particles is reduced, which allows a higher number of computations. On the other hand, the separation is carried out as a batch system, not as a continuous process. The mechanical oscillation and pneumatic stimulation by air flow are pure vertical, which enables to suppress the transportation process and emphasize the working mechanisms of the separation. DEM particles are designed and parameterized based on mean, or respectively, selected values of the lit-

erature analysis. This initial configuration contains particles for grain, chaff and short straw which are composites of spheres. This downsized domain is used to perform a comprehensive numerical parameter sensitivity study of the basic material, particle and interphase properties. A similar experiment is designed for comparison to numerical results. This comparison is based on macroscopic values like separation time and purity. Both, simulation and experiment identified the particle size of grain and straw particles as the most sensitive parameter to separation.

Hence, in the **2nd step**, a sample of chopped straw, which is primarily used in separation tests instead of chaff, is classified into length classes by a screening machine. Subsequently, a sample of each of the length-classes is separated manually into the components: straight stalks, bended stalks, heads and leaves. After that, a sample of straight stalks and bended stalks is taken and length and width of the particles is measured using digital image processing with Matlab®. Finally, the mass of the individual particles is determined and the mean particle mass and the distribution are calculated.

The distribution of the particle dimensions and related properties (e.g. mass) are implemented in *Star-CCM+v9.06* by normal distribution functions in the **3rd step.**

According to literature, e.g. [4], moisture cannot be related directly to separation process; it rather influences separation via material properties. This is valid in a range of mean particle moisture, which is below a level where cohesive forces become dominant due to high surface moisture. Mean particle moisture affects next to other properties, the particle dimensions, the particle solid density coefficients of static and dynamic friction, as well as the coefficient of restitution. The listed properties are subsequently implemented in the **4th step** in the simulation as a user defined function (UDF). The UDF expresses the properties as a quadratic model with respect to the mean particle moisture.

In the **5th step,** the size of the domain is increased. Numerical and experimental tests of separation of grain and MOG in a 200 mm wide segment of a cleaning device are carried out. The preferred particle design, parameterization and models from the 1st … 4th step are taken over. Previously used DEM particles for chaff and short straw are replaced by straight and bended straw particles with normally distributed size (length and diameter), which reproduce chopped straw. A mechanical and pneumatic stimulation is imprinted to the system similar to the real cleaning device, which forces separation and transportation along the sieves. A second parameter study is performed, taking mainly process parameters like MOG feedrate, MOG composition, intensity of mechanical and pneumatic stimulation etc. into account. A lab test rig is designed similar to the numerical model to perform experimental tests for comparison. Fig. 2 summarizes the applied problem solving procedure.

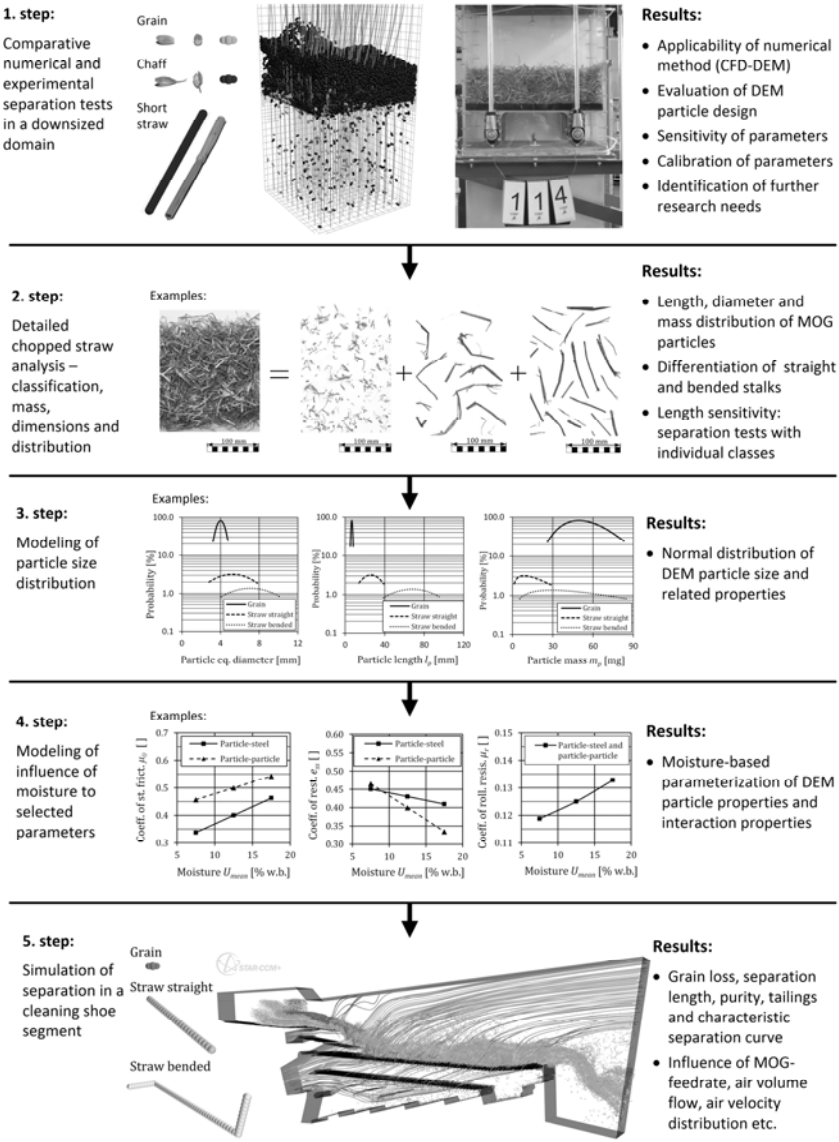

Fig. 2: Problem solving procedure

Results and discussion

A three-dimensional model is designed based on the geometry of a given combine cleaning device, see Fig. 2. The cleaning device segment has a reduced width of 200 mm, whereas the length (≈4390 mm) and all other dimensions meet the original dimensions. The air flow is applied to the main channel and the secondary channel based on a distribution. As shown in Fig. 2, straight and bended straw particles are injected into the cleaning device segment in two alternating layers above stratification pan. Grain is fed on top of the developed straw layer with a temporal delay. The simulation is transient and runs up to 12 s of physical time, whereas the last two seconds are taken as stationary period for data evaluation.

Based on the chopped straw analysis of the *2nd and 3rd step* from above, the particles are injected using a normally distributed diameter, which influences the length of the DEM particles in the same way. Within the test program, the standard deviation of straight and bended straw particles size is multiplied by a factor of 0; 0.25; 0.5 and 0.75. A factor of 1 represents the nominal standard deviation based on the results of *2nd step*. The standard deviation of grain injector diameter is constant at 1. As demonstrated by Fig. 3, for zero distribution (all particles of a class have the same size) the grain loss is almost zero. For rising values of standard deviation, the grain loss increases over-proportional.

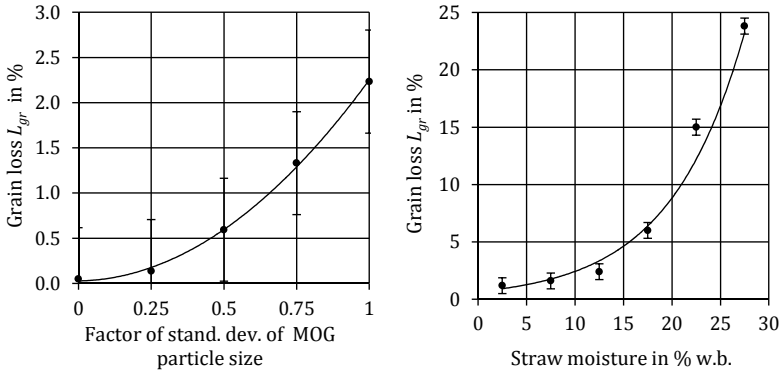

Fig. 3: Results of simulation. Left: Grain loss as affected by factor of standard deviation of MOG particle size. Right: Grain loss as affected by straw moisture. MOG feedrate q_{MOG}=1.79 kg/(s m) ; Factor of fluid velocity at main inlet 1

This indicates that, if only large MOG particles are present in the system, the separation proceeds comparatively easy. If, on the other hand, smaller MOG particles are added, the gaps

between the large particles are filled and the migration of grain through the straw layer is hampered. In order to study the effect of the straw moisture model to grain loss also in the functional outer limits, the range of moisture investigated here exceeds the practical range of harvesting conditions. Values between 2.5 …27.5 % are tested. As shown in Fig. 3, the influence of straw moisture can be well described with an exponential function. Without a base for experimental comparison, it can just be concluded that the influence of straw moisture is plausible and reflects the practical experience generally.

Corresponding experimental tests are carried out to evaluate and validate the numerical results. In contrast to the simulations, the test rig has a width of 700 mm to keep the wall effects of the sidewalls low. Fig. 4 shows a comparative snapshot of the simulation and a similar experiment for a relative MOG feedrate of 2.38 kg/(s m), which is equal to a MOG feedrate of 12 t/h for full system width.

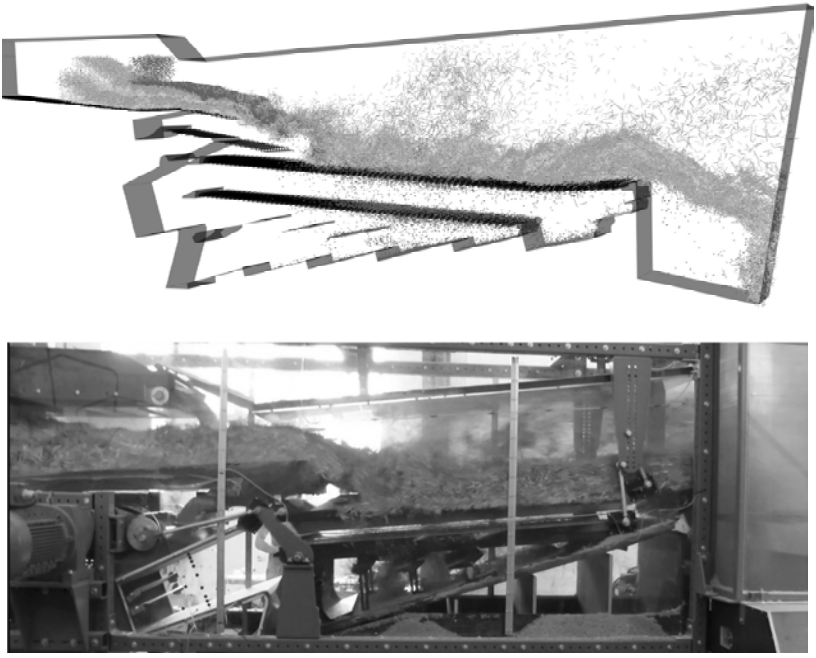

Fig. 4: Snapshots of numerical separation (upper picture) and experimental separation (lower picture) in a combine cleaning device segment at stationary period for rel. MOG feedrate of 2.38 kg/(s m).

The interaction between relative MOG feedrate and the factor of fluid velocity at main inlet in terms of grain loss are shown in Fig. 5 for experimental and numerical results. The characteristic curves show commonly a shift of the optimum to higher fluid velocities for increasing MOG feedrate, indicated by the dashed line. In general, the simulation matches the experiment very well for low and moderate MOG feedrate. However, major deviations occur for high MOG feedrate, e.g. 2.38 kg / (s m). Here, the simulation is much more sensitive to fluid velocity which can be derived from the significantly higher grain loss at the outer limits of the characteristic curve. However, corresponding to all simplifications of the numerical model, the abstraction of the DEM particles, the variety of parameters and all initial uncertainties, it can be concluded that Fig. 5 is the fundamental prove of the method for the application to separation process.

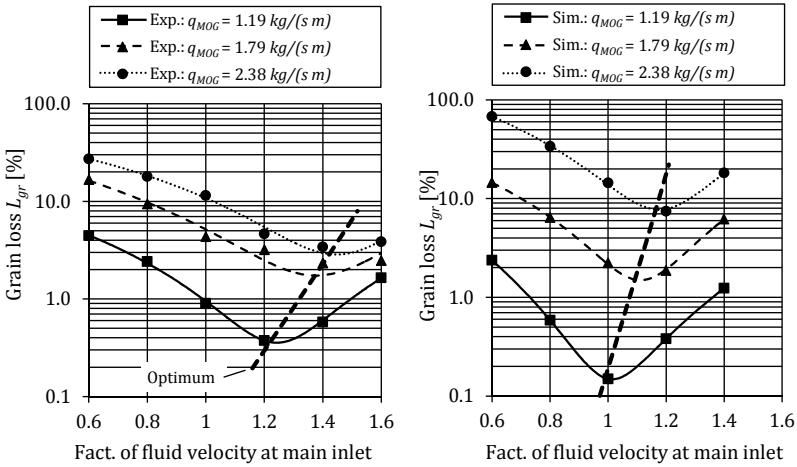

Fig. 5: Interaction of relative MOG feedrate and fluid velocity at main inlet on grain loss. Comparison of experimental results (left) and numerical results (right). Factor of fluid velocity represents factor of fan turning speed to nominal speed.

Conclusions and future work

The coupled CFD-DEM approach is suitable to simulate the separation process of grain and MOG in combine harvester cleaning devices. The distribution of size of DEM MOG particles is of major influence to grain loss. The applied moisture model produces plausible results but still needs to be validated by experimental results. Further the simulation appears to be more

sensitive to changes of air volume flow than the experiment. At present, tailored drag coefficients for the DEM grain and straw particles are determined by advanced CFD simulations.

References

[1] Rademacher, T. (2011): „Druschfruchternte - Wettbewerb der Systeme nimmt zu.“ *Eilbote (13)*, pp. 10-13.

[2] Zhao, Y. (2002): *Einfluss mechanischer und pneumatischer Parameter auf die Leistungsfähigkeit von Reinigungsanlagen im Mähdrescher. Dissertation.* Hohenheim, VDI/MEG Forschungsbericht Agrartechnik 387.

[3] Hübner, R. (1999): *Entwicklung eines Modells zur Auslegung einer rotierenden Reinigungseinrichtung im Mähdrescher, Dissertation.* TU Dresden.

[4] Beck, T. (1992): *Meßverfahren zur Beurteilung des Stoffeigenschaftseinflusses auf die Leistung der Trennprozesse im Mähdrescher.* Dissertation, Stuttgart-Hohenheim: VDI-Verlag GmbH.

[5] Zhu, H.P., Z.Y. Zhou, R.Y. Yang, und A.B. Yu. (2008): „Discrete particle simulation of particulate systems: A review of major applications and findings.“ *Chemical Engineering Science*, pp. 5728-5770.

[6] Lu, G., J.R. Third, and C.R. Müller (2015): "Discrete element models for non-spherical particle systems: From theoretical developments to applications." *Chemical Engineering Science 127*, pp. 425-465.

[7] Freye, T. (1980): *Untersuchungen zur Trennung von Korn-Spreu-Gemischen durch die Reinigungsanlage des Mähdreschers.* Dissertation, Stuttgart-Hohenheim: im Selbstverlag.

[8] Schwarz, M., J. Pförtner, P. Mümken, und S. Böttinger (2012): „Gutbewegungsvorgänge auf dem Vorbereitungsboden, Erfahrungen mit der DEM-Software PASIMODO.“ *VDI-Berichte Nr. 2173*, pp. 363-369.

[9] Lenaerts, B., Aertsen, T., Tijskens, E., De Ketelaere, B., Ramon, H., De Baerdemaeker, J. and Saeys, W. (2014): „Simulation of grain–straw separation by Discrete Element Modeling with bendable straw particles.“ *Computers and Electronics in Agriculture 101*, pp. 24-33.

[10] Pförtner, J., and S. Böttinger (2013): "Validierungsstrategie für DEM-Modelle von Mähdrescherbaugruppen." *VDI-MEG Kolloquium Landtechnik (40) Hohenheim 12./13.Sept.*, pp. 27-32.

[11] Pförtner, J., S. Böttinger, M. Schwarz, and L. Schürmann (2016): "Simulation des Entmischungsprozesses von Korn und Kurzstroh." *Tagungsband der 74. Internationalen Tagung Landtechnik LAND.TECHNIK Köln.*

[12] Ma, Z., Y. Li, and L. Xu (2015): "Discrete-element method simulation of agricultural particles' motion in variable-amplitude screen box." *Computers and Electronics in Agriculture 118*, pp. 92-99.

[13] Li, H., Y. Li, and F. Gao (2012): "CFD-DEM Simulation of material motion in air- and screen cleaning device." *Computers and Electronics in Agriculture (88)*,pp. 111-119.

[14] Prüfer, A., J. Englisch, M. Schultze, and T. Meinel (2014): "ADALS – Beitrag zur DEM-Partikelsimulation in der Landmaschinentechnik." *Landtechnik 69 (4)*, pp. 180-184.

[15] Korn, C., Herlitzius, T. (2014): Strömungssimulation als Entwicklungswerkzeug in der Mähdruschtechnik – Potential, Numerische Verfahren und Validierung. *VDI Bericht* 2226, VDI-MEG Tagung LAND.TECHNIK, Berlin.

[16] Srivastava, A.K., W.T. Mahoney, and N.L. West (1990): "The effect of crop properties on combine performance." *Transactions of ASAE 33 (1)*, pp. 63-72.

[17] Huisman, W. (1978): „Moisture content, coefficient of friction and modulus of elasticity of straw in relation to walker losses in a combine harvester." *ASAE Publication 1-78*, pp. 25-29.

Acknowledgment

The computations were performed on the Bull HPC-Cluster of the Centre of Information Services and High Performance Computing (ZIH) of the Technical University of Dresden. Special thanks for the generous allocation of computer time.

A new discrete element model (DEM) for maize

Dipl.-Ing. **Ádám Kovács**, Prof. Dr.-Ing. **István J. Jóri**,
Dr.-Ing. **György Kerényi**,
Budapest University of Technologies and Economics,
Budapest, Hungary

Abstract

Numerical modelling of agricultural crops is becoming much more widespread but there is no suitable simulation method that could predict the interactions among fibrous agricultural materials (stalks and stems) and machine parts. Our study focuses on the developing of a new discrete element model (DEM) for maize to analyze the complex phenomena in a corn head, particularly during harvesting. The first step, formation of the suitable, therefore new, DEM geometrical model is presented in this paper.

1. Introduction

One of the most efficient testing methods for agricultural machine designers is the in-situ experiments, however, due to the seasonal characteristics of agricultural products these tests are usually limited in time and often prove to be very expensive.

Numerical modelling of agricultural crops is becoming much more widespread but there is no suitable simulation method that could predict the interactions among fibrous agricultural materials (stalks and stems) and machine parts.

A discrete element model (DEM) contains separated, discrete particles which have independent degrees of freedom and the model can simulate finite rotations and translations, connections can break and new connections can come about in the model [1].

Maize (*Zea mays*) is one of the most cultivated crop of the world: almost 900 million metric tons of corn were produced in 2016 [2]. Maize is mainly used for forage (40%), ethanol production (30%) and human consumption (10%) [3, 4].

Consequently, our study focuses on the development of a detailed DEM model for maize to analyze the complex phenomena in a corn head, particularly during harvesting. The first step, formation of the suitable DEM geometrical model is presented in this paper.

2. Theory and background

Maize is mainly harvested by forage and combine harvesters. In a combine harvester, the maize plant is mainly processed by the corn head, only the maize ears are conveyed into the

machine for further processing. Based on observations of 13 commercial corn heads the following major phenomena take place during harvesting: transversal compression, flexural load and free cut on the stalk; collision of maize ears. The maize stalk and ear are mainly involved into the harvesting process, so the biological structure of these parts will be explained.

The maize stalk, constituted of nodes and internodes, provides the highest mechanical resistance against external loading [5]. The cross section of an internode has a rind-core (skin-pith) structure, see on Fig. 1. It has an elliptical shape and there is usually a groove in its longitudinal direction. In contrast, the cross section of a node is close to circular and there are usually wrinkles on its surface. Thanks to the different orientations of tissues there is higher resistance against transversal loadings near to the nodes [5]. Two typical phenomena can be observed during bending of stems: ovalisation and buckling. Relation could not be observed among the presence of the core and other physical parameters of the stalk [6]. The shape of a maize ear can be divided into three segments: lower segment, where the shank joins to the cob and a diameter is gradually increasing; middle segment, where the diameter is roughly constant and the upper segment, where the diameter is slightly decreasing [7].

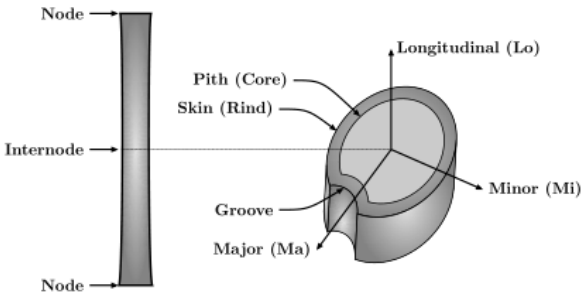

Fig. 1: Structure of an internode

To model the shape of stems and stalks chain of spheres, enhanced chain of spheres, hollow structure and solid body DEM geometrical structures were reported [8]. By using cylinders or capsules, a segmented virtual stem model was created to analyze bending and compression on stems [9, 10]. To analyze overlaid cut in disc mowers, the stem model was formed by chain of spheres [11]. A DEM for maize ears was defined for analyzing corn threshing process [7]. In this model, the maize cob and kernels were separately defined.

3. Materials and methods

For our study EDEM 2017.2 (DEM Solutions Ltd., Edinburgh) discrete element software was selected. In a bonded DEM model, particles represent the geometrical models and a bond structure represents the mechanical model. After consideration of available bonded contact models, the Timoshenko-Beam-Bonded model was chosen for our study [12].

After taking into account the biological traits of maize and phenomena during harvesting in-situ and laboratorial measurements and observations were established to analyze the physical parameters of maize.

The measured data were analyzed by mathematical and statistical methods to find correlation among them. Based on the results a calculation method was created to define the parameters for the DEM geometrical model.

By using possible DEM formations for stems and stalks, a hybrid geometrical model was defined by using chain of spheres, solid and hollow geometrical models to analyze phenomena in a corn head.

4. Experimental results

The analyzed parts of maize were exactly defined, see on Fig. 2. Section “A” contains the most important parts of the stalk and the maize ear with the shank. Here, the internodes and nodes provide the highest resistance against external loads, their bending behavior plays an important role in losses. Another important part of the stalk is the shank that holds the maize ear thus it has a significant effect on gathering. In section “B”, parts don’t play an important role in losses but they provide significant resistance during processing. In section “C”, stalk parts provide very low resistance against external loads.

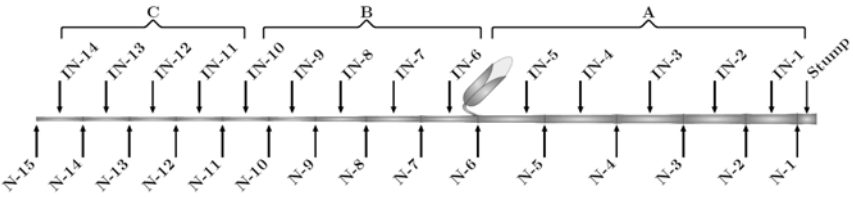

Fig. 2: Definition of a maize stalk (N: node; IN: internode)

Samples (type: Sufavor FAO 360, Saaten-Union Hungária Kft) were collected from the middle region of Hungary in October 2016. However, the number of internodes and nodes was

14 and 15 on each stalk, respectively, the upper part of the stalk, section 'C', was usually broken, thus, results about the first ten internodes and nodes will be presented here.

Based on 10 samples, the average main diameter of the first node was 28.5 ± 1.4 mm (P=0.05) and among the specified diameters (δ) and positions (p) of nodes and internodes linear correlations were found, see on Fig. 3.

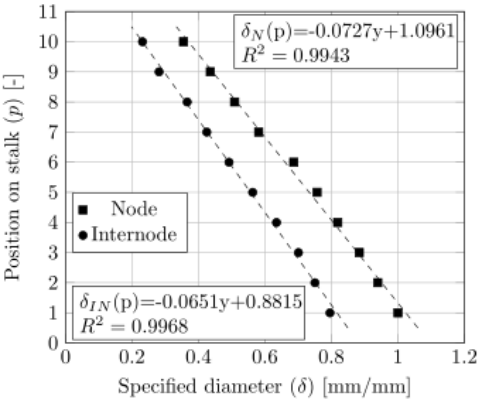

Fig. 3: Specified diameter of nodes and internodes

The average length of ten internodes was 1510 ± 128 mm (P=0.05). The relationship among the specified lengths (λ) and positions (p) can be defined by three linear equations on Fig. 4.

According to our observations, there were two maize ears on each stalk: a fully matured and a rudimental one. Our measurements and observations focused on the fully matured one.

Two positions of maize ear were observed: hanging and standing. Based on 100 observed plants, 59% of the plants had hanging maize ears with broken shanks, hence, experimental results will be explained for hanging maize ears.

Based on 20 samples, the position of center of mass (CM) of hanging maize ears was 92.9 ± 5.1 cm (P=0.05) from the ground and 10.1 ± 1.3 cm (P=0.05) from the center of the stalk. The main diameter and length of hanging maize ears were 47.6 ± 0.9 mm (P=0.05) and 169.8 ± 8.7 mm (P=0.05), respectively.

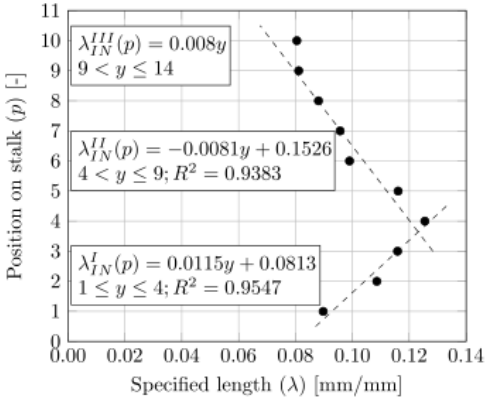

Fig. 4: Specified length of internodes

The size of the shank impacts on the ear gathering force essentially. Based on 20 samples its diameter and length were 10.6 ± 0.4 (P=0.05) mm and 115.8 ± 15.7 (P=0.05) mm, respectively.

To model the shape of the ears an image based analysis was conducted on 20 samples. In this process, an axis symmetric property of the maize ears was assumed. Based on the curvature of maize ears, the centers of mass could be calculated and an ideal ear shape can be formulated, as shown on Fig. 5.

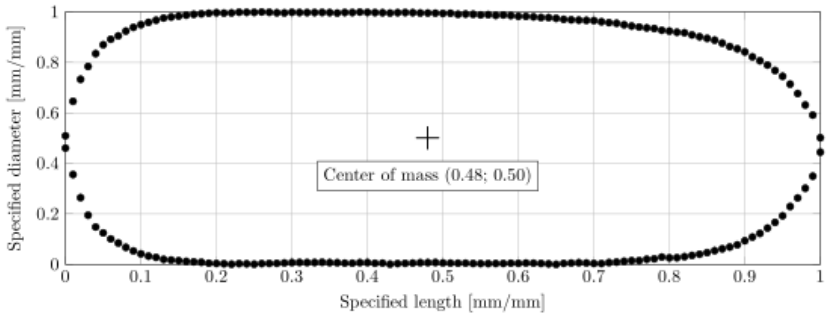

Fig. 5: Ideal shape and average center of mass of maize ears

5. Model formation

During the model formation hollow, solid and chain of spheres geometrical structures were used to create each parts of the model. Based on the importance and role of maize parts during harvesting, their geometrical structure is more or less detailed in our model, as shown on Fig. 6. In the stalk model, all cross sections of nodes and internodes are circular while special traits (groove, wrinkle) and core of internodes were neglected.

The root and soil-root connection was approached by chain of spheres geometrical model that is situated in a conical geometry to provide relaxation against external bending loads. The stump is modelled by a hollow structure with 18 particles in one cross section.

From the 1st to the 10th, nodes were modelled by a solid geometrical structure in which particles were composed in one circular layer of particles that is made up of 19 particles: 12 in the outer circle, 6 in the middle circle and 1 in the center. This model provides higher resistance against external loading near the nodes. Above the 10th node, nodes were modelled by larger spherical particles.

From the 1st to the 6th, internodes were modelled by hollow geometrical structure. In a cross section of internode, particles were composed in one circular layer that is made up of 18 particles. This model provides a good possibility to model the typical failure modes (buckling and ovalisation) of internodes. Between the 7th and 10th, internodes were modelled by hollow geometrical structure but there are 12 particles in each circular layer. Above 10th, internodes were created by chain of spheres geometrical model.

The shape of the shank was formed in such a way that it can carry a hanging ear by using chain of spheres model. It is impossible to model this broken condition of the shank so a curved shape with unbroken bonds was created.

The geometrical model of the maize ear is one particle that is formed by several sphere surfaces. The previously described ideal shape of the maize ears (Fig. 5) was approached by 25 sphere surfaces, supposing that the maize ears are axis symmetric. This detailed maize ear model provides a good possibility to analyze interaction among maize ear and parts of the machine. The maize ear was situated in such a way that its center of the mass was near the same as the results from the measures.

To define the physical properties of DEM geometrical structure a calculation method was created based on the experimental results. Four initial parameters (main diameter of the first node, length of the first ten internodes, main diameter and length of maize ear) can be chosen while the others (properties of shank; properties of ear position and shape) are the same as the measured average ones. Based on the chosen parameters, the geometrical parameters of the real plant parts can be calculated based on the experimental results (Fig. 3 and 4).

If the physical parameters of the real plant are known then the physical parameters of the DEM model can also be calculated by geometrical equations related to the geometrical structure of each part.

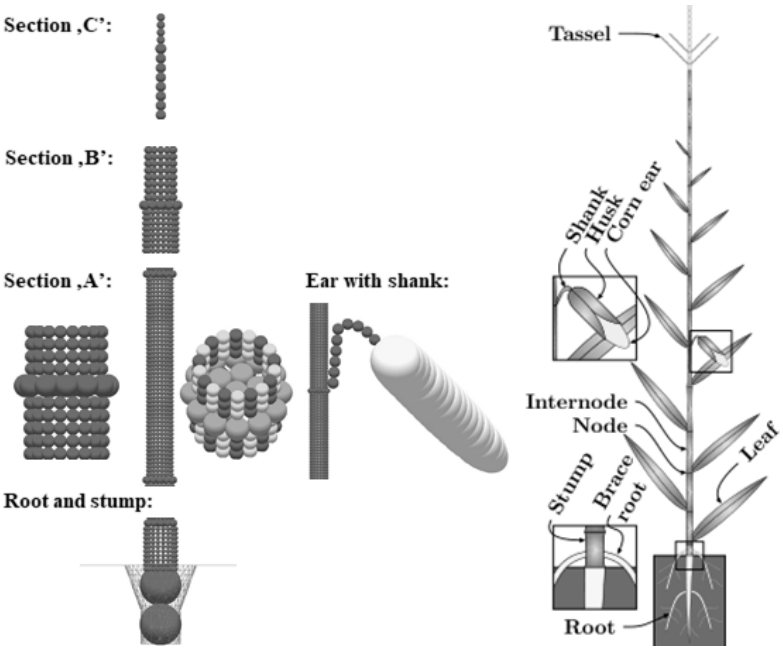

Fig. 6: DEM geometrical model for maize

6. Conclusion

A numerical and experimental study of physical properties of maize was undertaken using discrete element method (DEM) in order to simulate harvesting process by a combine harvester. Based on in-situ and laboratorial experiments correlation among the main physical properties of maize were analyzed. A new DEM geometrical model was formed and a calculation method was defined to create this model. The following conclusions could be drawn:

1. the main parts of maize plant that have a significant importance during harvesting were defined;
2. experimental method was established to measure and analyze the significant physical properties of a maize plant;
3. a new, more detailed DEM geometrical model was formulated by using different possible geometrical structures for modelling stems and stalks;

4. a calculation method was created and verified to integrate physical properties of maize plant into the DEM geometrical model;
5. the more detailed DEM geometrical model is suitable to analyze losses, working quality and efficiency of parts of a corn head.

In the future, the discrete element bonded model will be added to the model and its parameters will be calibrated based on experimental results from transversal compression, three-point bending and dynamic cutting on maize stalks. The current calculation method will be extended to model the natural diversity of physical traits of maize plant.

References

[1] Cundall, P. A.; Hart, R. D.: Numerical Modeling of Discontinua. Analysis and Design Methods, No. 1993 (1993) pp. 231-243.

[2] USDA, FAS Grain: World Markets and Trade, Jan. 12, 2017.

[3] USDA, ERS Feed Outlook, Jan. 17, 2017.

[4] ProExporter Network, Crop Year Ending Aug. 31, 2017.

[5] Robertson, D. J.; Smith, L. S.; Cook, D. D.: On measuring the bending strength of septate grass stems. American Journal of Botany 102(1) (2015) pp. 5-11.

[6] Leblicq, T.; Vanmaercke S.; Ramon H.; Saeys W.: Mechanical analysis of the bending behaviour of plant stems. Biosystems Engineering 129 (2015) pp. 87-99.

[7] Yu Y.; Fu H.; Yu J.: DEM-based simulation of the corn threshing process." Advanced Powder Technology, No. 26 (5) (2015) pp. 1400-1409.

[8] Jünemann, D.; Kemper, S.; Frerichs, L.: Simulation of stalks in agricultural processes – applications of the discrete element method. Landtechnik 68(3) (2013) pp. 164-167.

[9] Leblicq, T.; Smeets, B.; Ramon H.; Saeys W.: A discrete element approach for modelling the compression of crop stems. Computers and electronics in agriculture 123 (2016) pp. 80-88.

[10] Leblicq, T.; Vanmaercke S.; Ramon H.; Saeys W.: Mechanical analysis of the bending behaviour of plant stems. Biosystems Engineering 129 (2015) pp. 87-99.

[11] Kemper, S.; Lang, T.; Frerichs, L.: The overlaid cut in a disc mower – results from field tests and simulation. Landtechnik 69(4) (2014) pp. 171-175.

[12] Brown, N. J.; Chen, J-F.; Ooi, J. Y.: A bond model for DEM simulation of cementitious materials and deformable structures." Granular Matter, No. 16 (2014) pp. 299–311.

Modelling method for analyzing grain harvesting concepts

Florian Peters, M.Sc., Prof. Dr.-Ing. **Hubert Korte**,
Faculty of Agricultural Sciences and Landscape Architecture,
University of Applied Sciences, Osnabrueck;
Dr.-Ing. **Ralf Bölling**,
CLAAS Selbstfahrende Erntemaschinen GmbH, Harsewinkel

Abstract

This paper presents a method for analyzing grain harvesting concepts. As a first step, the impact of harvesting concepts on the process chain are explained. Changes in harvesting process chains affect the crop flow management. On this account, a design method is developed to model the harvesting procedure. This method is based on a modular structure containing different system levels, which provides the opportunity to configure variable process chains. The evaluation method forms the basis to define the behavior of processes and machines. Furthermore, the performance of the process chain is determined. Considering the energy consumption, the machine costs and the process time deducted from the performance, the harvest operating costs are quantified. The combination of these methods is used for analyzing modifications and illustrating the potential of different harvesting concepts. Different types of modifications on every level of the system can be assessed by the method. Possible applications include the analysis of changes in machine concepts, the verification of suitability of different concepts regarding environmental factors and the composition of completely new harvesting concepts.

1. Introduction

In the area of agricultural economy and research different machines and harvesting concepts for grain harvesting are discussed (Fig. 1). Some of these concepts are practically used and examined, for example the “Kompakternte” [1] or the McLeod harvest system [2]. Others are theoretical visions like harvesting swarms of self-propelled cutterbars in combination with a stationary threshing machine [3].

Modifications of machines and harvesting concepts lead to changes in the design of process chains. Those changes influence each processing step, the combination and the connection between the processes. Thus, the crop flow management is affected. In general terms, the

way of harvesting is redefined. In order to analyze the effects of modifications, a method is needed which designs the structure and evaluates process chains.

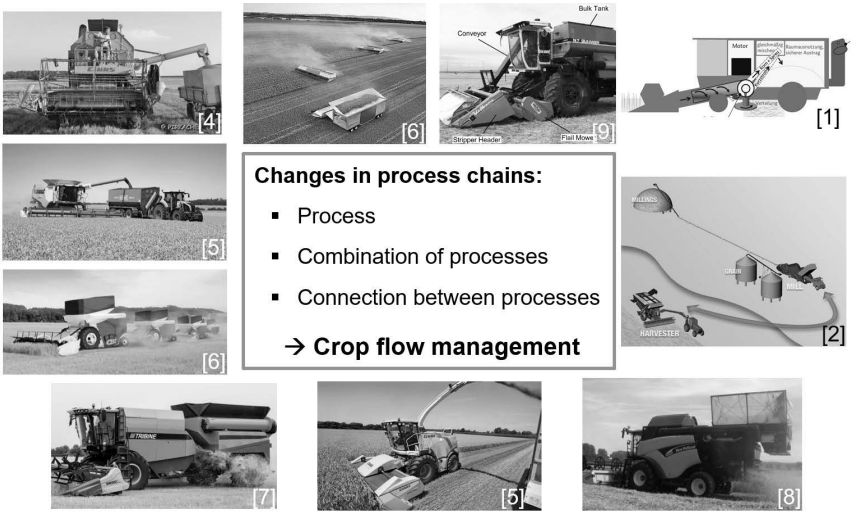

Fig. 1: Examples of harvesting concepts

2. Design method

A method to design the structure of harvesting processes systematically is developed. This method uses different system levels with variant modules in each subsystem. The composition of these modules defines the process chain. The following list describes the system levels in accordance with their degree of detail in a hierarchical order:

- Agricultural company
- Production system
- Machine system
- Machine
- Component
- Parameter

The aim of the method is to design crop flow. Consequently, it describes the crops journey from the field to the final destination, i.e. the agricultural company. Therefore, the procedures of material transformation are considered. Since harvesting process chains are similar to industrial process chains, their elementary functions can be used to illustrate harvesting concepts. An industrial process chain is a combination of logistics and production

technologies. The procedures of logistics and production technology are divided in qualitative and spatiotemporal transformations [10]. In the presented method, the system level “component” takes these procedures into account. Variant modules of this subsystem express the behavior of material handling. In general, crop flow operations are storing, moving and processing. These operations are equal to the components. They represent elementary processes of harvesting concepts. Their function is characterized by construction, setting and crop parameters. Components form the basis of a machine. As a subsystem they are integrated into a stationary, semi-stationary or mobile machine type. On the next level of detail different machine types work together and build a machine system. Within the machine system the connection between the individual machines is defined. Depending on the storage capacity the machines cooperate in different dimensions, i.e. continuously, discontinuously or independently. A harvesting process represents one section of the annual cycle in a crop production system. Soil tillage, cultivation, fertilization and crop protection complete the cycle of the production system. Various production processes, such as land cultivation and livestock production, are business units in an agricultural company.
Due to the modular structure, this method provides the opportunity to configure variable process chains. Different machine and harvesting concepts can be designed by modifying different elements, namely the type of component, the arrangement and number of components per machine, the type of machine as well as the number and connections of the machines.

3. Evaluation method

Based on the previous methodological approach a method for evaluating harvesting concepts is generated. The evaluating procedure takes the behavior of the elementary processes within the machines into account. Additionally, the cooperation of machines and their mutual influence is considered. Subsequently, the process chains are assessed by different criteria, namely their performance in the area of efficiency, their energy consumption and the total cost of harvesting.

In a first step, the characteristic operating conditions for each machine type of the machine system are determined. In a conventional grain harvesting procedure different machine types are involved, such as the combine harvester, grain cart and transport vehicle. The conditions describe the behavior of a single machine in the process chain.

In the following common conditions of a combine harvester are illustrated (Fig. 2). These comprise harvesting (1), unloading (2), simultaneous harvesting and unloading (3), turning at the headland (4), waiting for the grain cart (5), driving in-field (6) and on-road (7).

Fig. 2: Example – Characteristic operating conditions of a combine harvester

In a second step the status for every component in each operating condition is specified. The status indicates how the machine performs in the different situations. It consists of the elementary processes for material transformation as well as the ground drive and system parts. During harvesting (1) the threshing, separating and cleaning unit operate. Meanwhile the unloading auger does not work and the ground drive moves with the given velocity. In contrast, the status of the unloading auger changes when simultaneous harvesting and unloading (3) is the operating condition. Throughout the headland turn (4) the elementary processes operate without load in idle function.

The throughput of crop flow is considered in order to detail the status of the components. For each component, mathematical models are integrated. The model is a function of construction, setting and crop parameters. As a result, the models describe the separation of the processing components and the power requirements.

Each individual component has a performance potential. Within the machine, the components are connected and work simultaneously. Consequently, the process with the lowest performance affects the process chain and reduces its potential.

The principle of performance reduction among cooperating components can be transferred to the machine system. Their mutual influence is caused by the cooperation of machines. Thereby, the connection of the machines is significant. By definition, independent working machines are not affected. Thus, they can make use of the installed machine performance. In contrast, continuous and discontinuous connections could reduce the throughput capacity. The impacts can be divided into two kinds of reduction. On the one hand, there are

interferences during the crop flow transfer between the machines because the involved components of both machines depend on each other. Theoretically, they operate as one machine. For that reason, the lowest performance determines the process chain. On the other hand, the coordination of machines effects waiting times as the storage of crop flow limits the working procedure. Hence, machines have to wait for another machine to transfer crop flow in order to continue the working procedure.

These regulations are valid for every cooperation of processes and machines and define their performances as well as the performance of the whole harvesting process chain (Fig. 3). Based on the performance, the process times for each component status is determined considering the characteristic operation condition.

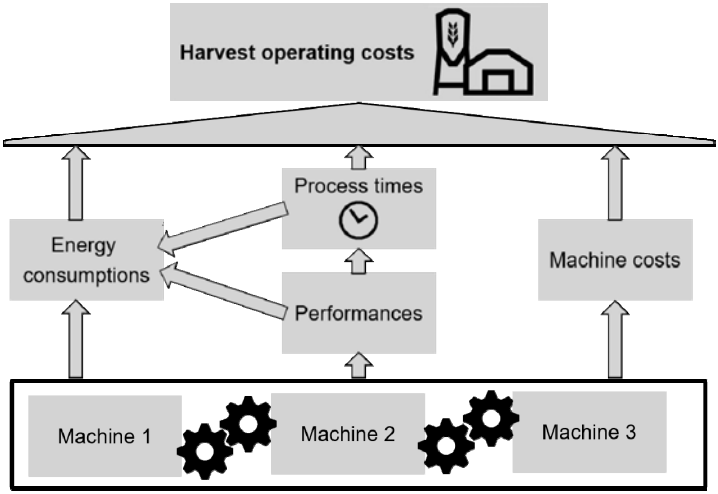

Fig. 3: Schematic illustration of the evaluation method

Moreover, the process times, the performances and the power requirement models form the basis to calculate the energy consumption of the process chain. The machine costs are the summation of acquisition and operating cost. Acquisition costs include depreciation and interest rates. The operation costs encompass, for example, insurance, service, repair and lubricants. Finally, the wage and energy cost are calculated and added to the machine costs. This sum yields the harvest operating costs. The specific harvest operating costs are quantified by the ratio of total costs to the amount of harvested crop or harvested land.

4. Result

The modelling method provides the opportunity to evaluate modifications and their influences on the process chain. There are different analytical perspectives. First, the application of the method supports the evaluation of alterations within the machinery concept. For instance, the setting parameters of the threshing unit can be changed. Thereby, the separation process and the power requirement are influenced. Thus, the machine and the machine system are affected. As a consequence, there are changes in performance and energy consumption which leads to changes in the overall harvest operating costs. Concluding, changes on every level of the system can be assessed by the method. Second, alterations regarding environmental factors, such as distance between field and final destination, field size or crop yield, can be analyzed. Therefore, the prevailing conditions of the agricultural company are taken into account when assessing the suitability of different concepts. Third, the composition of the whole process chain can be examined, i.e. completely new harvesting concepts can be analyzed and compared.

5. Conclusion and outlook

The combination of the presented methods is used for analyzing harvesting concepts and for illustrating their potentials. The result can support decision making with regard to the development of machinery. Future work will focus on applying the modelling method in order to compare harvesting concept, e.g. a comparison between the conventional concept of combine harvester, “Kompakternte” and the theoretical visions such as harvesting swarms of self-propelled cutterbars in combination with a stationary threshing machine. Moreover, further development of the method is needed in order to evaluate the concepts’ consequences on the entire cycle of the production system.

6. Reference

[1] Rumpler, J.: Innovation SpreuStroh – Neue Perspektiven mit neuen Verfahren. Auftaktveranstaltung Innovationsforum SpreuStroh, Malschwitz 01/21/2016.

[2] N.N.: McLeod Harvest – The world´s Premier Harvesting System. Presentation. Available from: http://home.cc.umanitoba.ca/~carlberg/MCLEODWHOLE.ppt?bcsi_scan_71efa5f77394d2ae=qYQgQ/qpMuF8bQ5b3wfaDM7BO5pFAAAArDoT6A==:1 (Accessed 08/18/2017).

[3] Herlitzius, T.; Mueller, H.; Kranke, G.; Witting, H.; Wolf, J.: Concept Study of a Self Propelled Harvester versus a modular System. VDI-MEG Tagung LAND.TECHNIK AgEng 2011, Hannover 11th-12th November 2011, S.69-75.

[4] Pirkacher, R. Available from: http://www.agrartechnik-im-einsatz.de/de/index.php?page=view_picture&id=681931 (Accessed 08/18/2017).

[5] CLAAS. Available from: http://www.claas.de/unternehmen/presse/downloadcenter. (Accessed 08/18/2017).

[6] TU Dresden, Agrarsystemtechnik. Available from: www.agrarsystemtechnik.tu-dresden.de (Accessed 11/05/2015).

[7] Law, J.: Articulated 27-tonne capacity Tribine combine harvester tipped for Australian market. Available from: http://www.weeklytimesnow.com.au/machine/articulated-27tonne-capacity-tribine-combine-harvester-tipped-for-australian-market/news-story/c39063a24411a0669f74525ef41e698c (Accessed 08/18/2017).

[8] Marti, F. et al.: Sammlung von Spreu und Kurzstroh – Ergebnisse und Erfahrungen aus 3 Jahren Projektarbeit an der HAFL. Berner Fachhochschule. Presentation, Tänikoner Agrartechniktage 06/20/2013.

[9] Siemens, M. C.; Hulick D.E.: A new grain harvesting system for single-pass grain harvest, biomass collection, crop residue sizing, and grain segregation. Transactions of the ASABE, Vol. 51(5), S. 1519-1527, 2008.

[10] Pfohl, H.-Ch.: Logistiksysteme – Betriebswirtschaftliche Grundlagen. Darmstadt: Springer Verlag, 2010.

Telematics and Big Data Analytics – An Effective Way to Quantify Fuel Saving Potentials

A Proof of Concept by the Joint Research Project EKoTech

M.Sc. **B. Köber-Fleck**, M.Sc**. P. Ahlbrand**,
CLAAS KGaA mbH, Harsewinkel;
Prof. Dr.-Ing. **S. Böttinger**,
University of Hohenheim, Stuttgart;
Prof. Dr.-Ing. **H. Korte**,
University of Applied Sciences, Osnabrück

Abstract

In the 21st century, humanity face two important topics that concern future developments: Climate change and Big Data. On the one hand, climate change is a global challenge that can only be handled successfully with well-designed systematic and cross-industry mitigation strategies. On the other hand, Big Data offers tools, which enable us to identify potentials for efficiency gains in process chains.

This paper describes a Proof of Concept to use telematics data from agricultural machinery to detect fuel saving potentials. The work was carried out in the joint research project EKoTech 'Efficient fuel use in agricultural technology'. It aims to evaluate saving potentials in selected agricultural process chains in the period from 1990 to 2030. It is a cross-industry approach working with project partners of competitive manufacturers, agricultural operators, and research institutes. Consequently, a high variety of data sources have to be analysed and merged. Furthermore, the concept has to pay attention to data privacy rights and confidentiality of industry data.

With the Proof of Concept, the team wants to find out if the 'Cross-Industry Standard Process for Data Mining 1.0' (CRISP-DM 1.0) methodology is according with the requirements of the project as a guideline for data analytics.

Motivation

With regard to the 2014 synthesis report of the Intergovernmental Panel on Climate Change (IPCC), there are large uncertainties concerning CO_2 emissions from agriculture, forestry,

and other land use (AFOLU) [1]. Furthermore, AFOLU has a share of 24 % out of 49 Gt CO_2-eq total greenhouse gas emissions of all economic sectors. The intention of the EKoTech project is to show that the innovative power of the agricultural industry has the possibility to contribute to a reduction of CO_2 emissions. Big Data analytics based on telematics machine data is chosen as a tool to fulfil the ambitious requirements of the cross-industry approach.

EKoTech approach

The EKoTech research project is structured in seven working packages shown in Figure 1 [2].

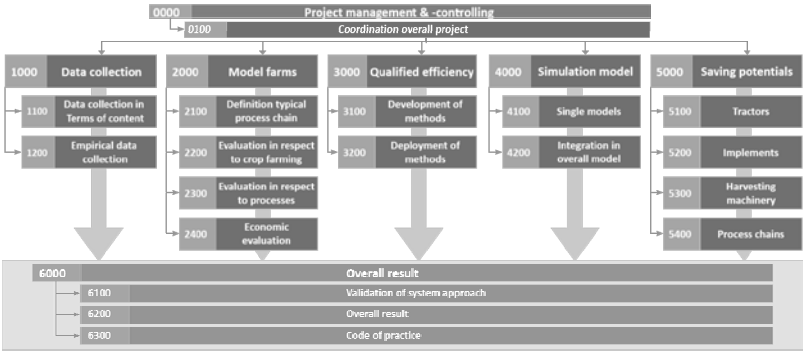

Fig. 1: EKoTech structure of working packages [2]

The project team is facing different challenges, which are jeopardizing the project's targets.

The first challenge is, to define the typical mechanisation chains for different farms for the initial year 1990. The project partner Thuenen Institut in Braunschweig is instructing this task.

The second challenge is to identify those innovations, which have changed fuel efficiency up to 2017. Subsequently, future saving potentials have to be identified and quantified based on selected innovations until 2030.

One possibility to achieve significant results is the quantification of the saving potentials based on machine data from machines working under conditions related to real life machine use. However, all these analytics have to be done in a competitive environment. Consequently, the industry partners need a common procedure to work on these tasks in-house first, with all available data and competences. Then, the industry partners come together for workshops to develop an outcome that is aligned with all industry partners. In the

next step, these results are evaluated together with the project partners from the research institutes and an interface to the simulation models has to be created.

EKoTech Determination of Fuel Efficiency Potentials

Fuel efficiency gains are the use of a lower amount of fuel to provide the same level of output [3]. The Proof of Concept focuses on the task to benchmark existing and foreseeable innovations between 1990 and 2030 with a positive impact on fuel efficiency and to make a qualitative and quantitative evaluation of those with significant efficiency potentials. With regard to the project's targets, fuel efficiency is defined in the pure sense as the direct energy consumption of farm machinery in crop production. The efficiency is related to the output, defined as harvested tons of wheat, maize or grass silage per hectare. Figure 2 shows the four areas, which will impact the future fuel savings and have to be considered in the project:

1. Technologies, which are available in the market until 2017 and the developments of their take rates until 2030
2. Operator support systems, which enhance the operator's competence in all levels of machine usage, making a fully usage of the installed machine capacity possible
3. The availability of technical solutions to improve the preconditions for the change to a more efficient agronomic system. One example is the change from conventional cropping to systems such as strip tillage or controlled traffic farming
4. The expected market launch of future innovations from 2017 to 2030 including alternative fuels.

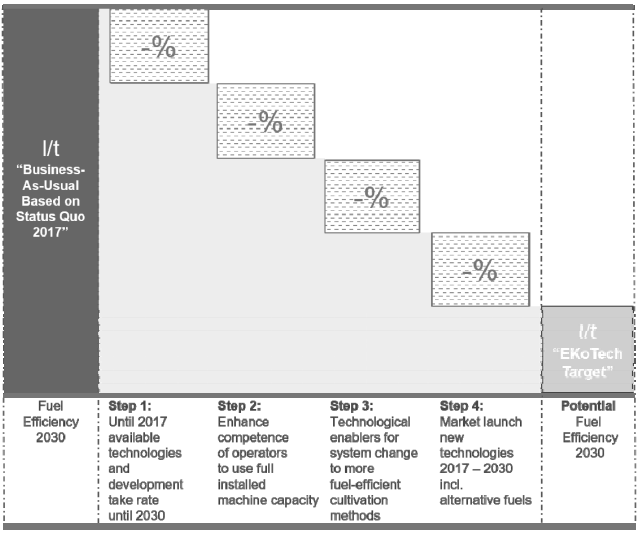

Fig. 2: Four steps to potential fuel efficiency after full abatement 2030

With the Proof of Concept, Step 1 is in focus. The selected criteria are typical farms in Germany, wheat production, harvesting and the fuel savings especially for combines. The other process steps of wheat production, as well as maize and grassland will follow in the ongoing studies of the project team.

Proof of Concept

Target of the Proof of Concept is to test, if the data source of telematics data in combination with Big Data analytics is a possible way to quantify fuel saving potentials. As a methodology CRISP – DM 1.0 was chosen. There is evidence to suggest that this combination fulfils the ambitious project requirements. CRISP-DM 1.0 is structured in six phases shown in Figure 3 [4].

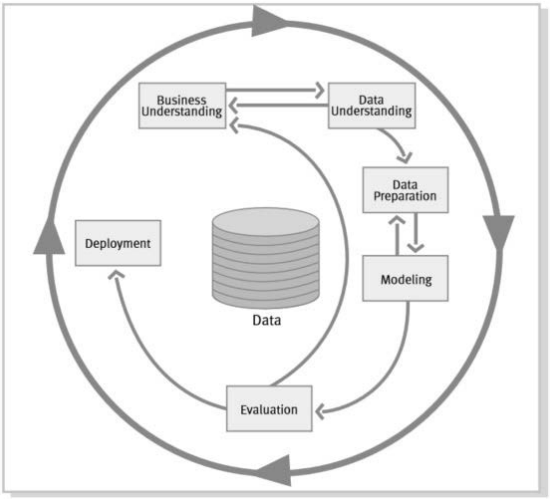

Fig. 3: Phases of CRISP-DM 1.0 model [4]

The initial phase focuses on understanding the project objectives and requirements. Therefore, the project team defined a standardised survey for the key data of innovations. To provide an overview of the results of the evaluation by the industry partners the so called 'Innovation Cards' summarise the results. The aim is to obtain a common understanding about innovations with fuel saving potentials and to estimate the potentials by profound data analytics. This paper presents the application of different CRISP-DM 1.0 aspects based on two examples.

The first one is 'rubber tracked undercarriages'. This technology is an enabler for subsequent fuel efficient soil processing, such as non-ploughing cultivation concepts. Furthermore, the realisation of the saving potentials is not depending on the driver's skills. Nevertheless, harvest conditions such as precipitation and soil type are influencing the degree of efficiency. The target was to find out, if a sufficient telematics data set is available to compare wheel and rubber tracked undercarriages for the same machine type. With the available data source, it was possible to use anonymised and pseudonymised telematics data of CLAAS combines in Middle and Western Europe. For the definition of the combine type, the results of interviews with farmers in three typical regions in Germany were used. They represent wheat production in 'Western Pomerania', 'Magdeburger Börde' and the 'Cologne-Aachen-Lowlands'. The farm sizes vary from 250 to 1,300 hectares with an average yield level of

nine tonnes per hectare in wheat. The considered specifications of the defined typical combines are an installed engine power from 430 to 610 horse power and the use of wheels or rubber tracked undercarriages. Further specifications such as working width are available for more detailed analytics. To choose the data set for the corresponding CLAAS combine types, the characteristics are translated in the company specific combine nomenclature. After the first data cleansing loop, only 12 % of the initial database was still available for the comparison of fuel consumption from rubber tracked undercarriage and wheel machines. The analysis was possible for two typical combine types due to the need for a sufficient machine population to pay attention to data privacy and statistical needs. For the typical combine type of Western Pomerania, the chosen data set was not sufficient. In Figure 4 the distribution of machines is shown in detail.

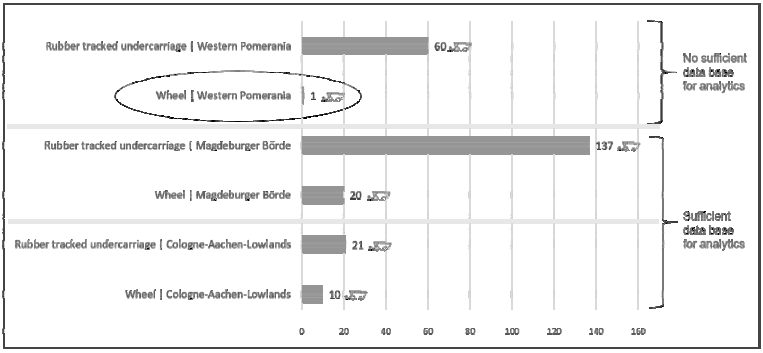

Fig. 4: Example of available data based on a selection of typical machines for wheat harvest to compare fuel consumption with rubber tracked undercarriage or wheel machines

For the machine populations equipped with rubber tracked undercarriage a significant lower fuel consumption was calculated by comparing the median. Further data cleansing steps will be done in the ongoing studies of the project team.

The second innovation is the automation product CEMOS AUTOMATIC. To take full advantage of the steadily increasing installed capacity of modern combines, there is a need to invest in their automation. In the future, the role of the machine operator will shift more and more from the classic worker to a manager who monitors the automated work processes. The Innovation Card ‘CEMOS AUTOMATIC‘ with more details is shown in Figure 5.

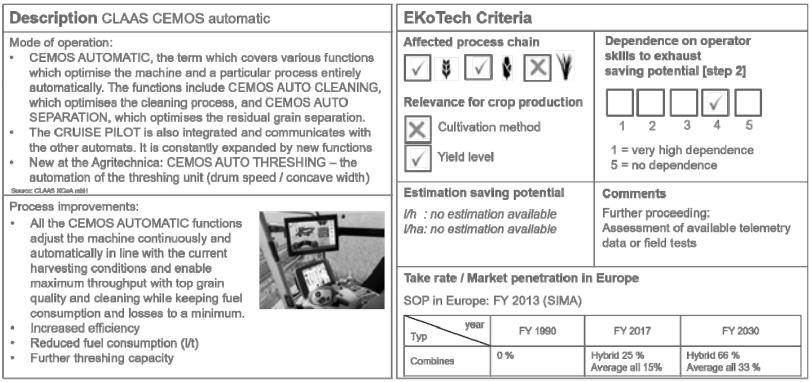

Fig. 5: The Innovation Card example 'CEMOS AUTOMATIC'

Furthermore, Figure 6 shows the comparison of the geographical location of typical EKoTech areas for wheat production and the machine populations of CLAAS combines equipped with Cruise Pilot, CEMOS including Cruise Pilot, and without any driver assistance systems.

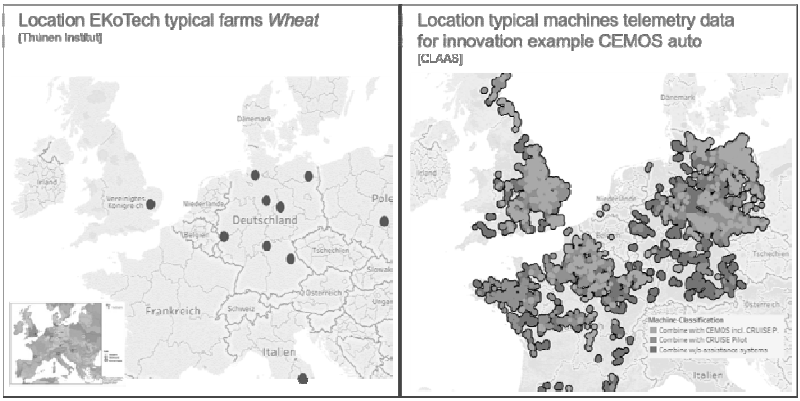

Fig. 6: Comparison of geographical location of EKoTech typical farms for wheat production and CLAAS combine population with and without driver assistance systems

The data set contains up to 130,000 threshing hours of 1,500 machines before data cleansing and afterwards 78,600 threshing hours of 734 machines. Based on the results

of the telemetry data analysis, CEMOS AUTOMATIC delivers a performance increase of between 15 to 18 %. More details are shown in Figure 7**.**

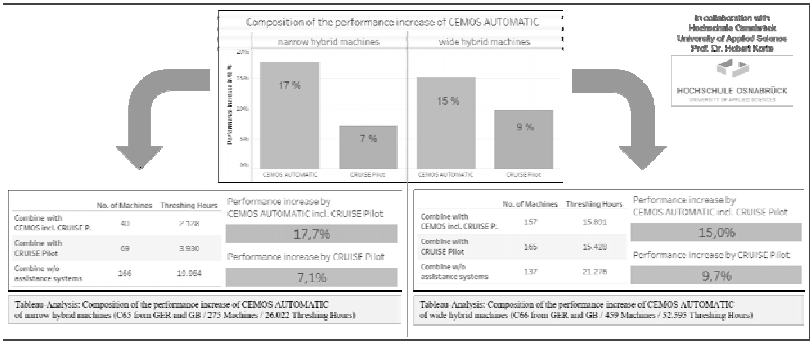

Fig. 7: Results composition of the performance increase of 'CEMOS AUTOMATIC'

Additionally, conclusive results show a significant difference in throughput between machines with CEMOS AUTOMATIC and/or CRUISE PILOT versus machines without any driver assistance system. The throughput increase improves the efficiency of the machine, which also reduces fuel consumption and thus machinery costs.

For the deployment of the Proof of Concept results, the next step is to transfer the data into the simulation models of the EKoTech project. Furthermore, experts from the cooperating research institutes and farmers are going to validate them. Finally, the development of take rates of these innovations from their market entry until 2017 have to be worked out. The results will become the estimation base of take rates in the period from 2017 to 2030.

Summary and outlook

The results of the study support the hypothesis that telematics and Big Data analytics offer an effective possibility to quantify fuel saving potentials, based on large quantities of real machines and not just single trials. Nevertheless, the data cleansing process is essential to make sure that the results are representing the fuel savings under real life conditions. The data analysts always have to keep in mind that the data collection is not executed under test conditions. For example, only a low proportion of the data collecting sensors are self-calibrating. Consequently, the data quality is depending on the reliability of the machine operator. Furthermore, the availability of a sufficient data set for the comparison of different feature specifications for one type of combine is not self-evident and has to be verified for every single case.

The principal advantage is the utilization of an extensive machine data volume in various real harvest conditions, in different geographical regions, and in different periods. This means in theory a very authentic data set is used. It could become more representative for the total combine fleet operating in the selected regions than results under test conditions with a small machine population and few threshing hours. Furthermore, the positive development of take rates of telemetry systems for combines improves the size of the machine population. This will increase the likelihood to get sufficient machine populations for very specific queries, as the EKoTech project targets require them.

The authors like to thank the Federal Ministry of Food and Agriculture (BMEL) for supporting this research project based on a decision of the Parliament of the Federal Republic of Germany via the Federal Office for Agriculture and Food (BLE) under the innovation support program.

References

[1] IPCC, 2014: Climate Change 2014: Synthesis Report. Contribution of Working Groups I, II and III to the Fifth Assessment Report of the Intergovernmental Panel on Climate Change [Core Writing Team, R.K. Pachauri and L.A. Meyer (eds.)]. IPCC, Geneva, Switzerland, 151 pp

[2] Fleck, B., Nacke, E., Böttinger, S., Frerichs, L. and Hanke, S.: Der Weg zur freiwilligen Selbstverpflichtung der europäischen Landtechnikindustrie zur Reduktion von CO2-Emissionen. Tagung Landtechnik AgEg, 19./20.11.2014 Berlin. In: VDI-MEG, VDI-Bericht Nr. 2226. Düsseldorf: VDI: VDI Verlag (2014), p.301-308

[3] OECD, Improvement Energy Efficiency in the Agro-food Chain, OECD Green Growth Studies, OECD Publishing, Paris, http://dx.doi.org/10.1787/9789264278530-en (2017)

[4] CRISP-DM Consortium: CRISP-DM 1.0: Step-by-step data mining guide (2000).

Development of energy requirements of tractors and implements

M.Sc. **Julian Schwehn**, Dipl.-Ing. **Steffen Häberle**,
Prof. Dr.-Ing. **Stefan Böttinger**, University of Hohenheim, Stuttgart

Abstract

The efficient use of the limited supply of resources and the reduction of harmful greenhouse gases are key challenges in the 21st century. To reach sophisticated climate directives stated by legislative power, the search for saving potentials throughout all branches is necessary. Finding technologies and strategies along the process chain in agriculture is the aim of the joint research project “EKoTech – Efficient fuel use in agricultural technology”. The further aim of the project is to give recommendations for action towards farmers and manufactures for a further application of saving potentials. To show already reached savings and to build up a database for the project, a comprehensive research of literature is done at the Institute of Agricultural Engineering at the University of Hohenheim. This article shows an extract of the research and discusses first results of the evaluation.

Motivation

Global population has been increasing crucially since the middle of the 20th century expecting ten billion humans in 2050 with need for food [1]. Furthermore, the usage of conventional commodities e.g. oil and gas as our primary source of energy, has also been increasing for a considerable time. Significant changes within this development in both fields are not expected in the near future. To provide food for the growing humanity, the need for another increase in productivity, and following expenditure of resources, is inevitable. However, associated with the consumption of conventional commodities are the emissions of climate-relevant gases. These so-called anthropogenic greenhouse gas emissions have effects on the natural greenhouse effect. The accumulation of additional greenhouse gases caused by humankind is presumable one factor of climate change [2]. Therefore, conventional natural resources are limited in their usage, making the search for reasonable alternatives significant. Until traditional carriers of energy are going to be substituted comprehensively by alternative sources, the aim should be the efficient usage of available conventional resources. In 2008, the legislative power of the European Union prescribed core demands for a Europe-wide climate and energy policy. The aim is to increase the energy efficiency until 2030 by

27 % and to lower greenhouse gas emissions by 40 % referred to 1990 [3]. To reach the proclaimed aims, it is necessary to find saving potentials throughout all industries. The forecasted saving potential in agriculture is at 1.1 to 4.3 $GtCO_2e$ per year [4].

In recent years, the focus of agricultural engineering has been on the engine of tractors and self-propelled machinery. The effort was to fulfil the regulatory limitations of exhaust gas emissions, limiting innovations in other areas and further reductions of harmful emissions through other technologies. Finding further technologies and strategies along the process chain to reduce the fuel and energy consumption of tractors and implements, is the focus of the joint research project “EKoTech” funded by the Federal Ministry of Food and Agriculture in Germany. The joint venture of manufactures of farm machinery and several research institutions are trying to determine already reached reductions in fuel consumption and to find potentialities of further savings, using conventional farms and a simulation model. The aim is to define and analyse options for further reductions of the specific fuel consumption in agriculture and to develop recommendations for action towards farmers and manufactures for further savings.

Procedure in EKoTech

The project is subdivided in several working packages with different tasks and aims. An accurate literature research is done to detect already reached savings in fuel consumption since 1990 and to get the latest data of energy and fuel consumption of current project-relevant machines. Average farm models in nine selected soil-climate regions over Germany and six all over Europe are built up through extensive interviews and group discussions. The aim is to develop representative farms with region-specific characteristics and conditions. The consideration of Europe-wide regions helps to gain expertise and to avoid inefficient recommendations for actions for farmers. To detect further saving potentials within the cultivation systems of wheat, maize and grassland until 2030, single-machine models of project-relevant machines are built up, as well as a process model to simulate different sub steps in the process chain of the selected cultivation system. The further task of the simulation model is to fill detected gaps in the database. Potential future savings are qualitatively and quantitatively detected in another working package that consists of several manufactures.

Data collection in EKoTech

The conduction and responsibility of the data collection within the EKoTech project is done at the Institute of Agricultural Engineering of the University of Hohenheim. The KTBL (Advisory

board of Technique and Construction in Agriculture), the 'Johann-Heinrich von Thünen-Institute' and the manufactures who participate support the work. The working package aims to detect energy requirements and fuel consumptions for project-relevant machines of 2016 (content data collection) and to show the development since 1990 (empiric data collection). With the collected data, a database is built up using the software tool Microsoft Access. Figure 1 shows the graphical illustration of the working package together with several inputs from other project partners and working packages. The overview displays the further usage of the collected data in the single-machine model, the general model and the extension of already existing databases located at project partners e.g. the KTBL.

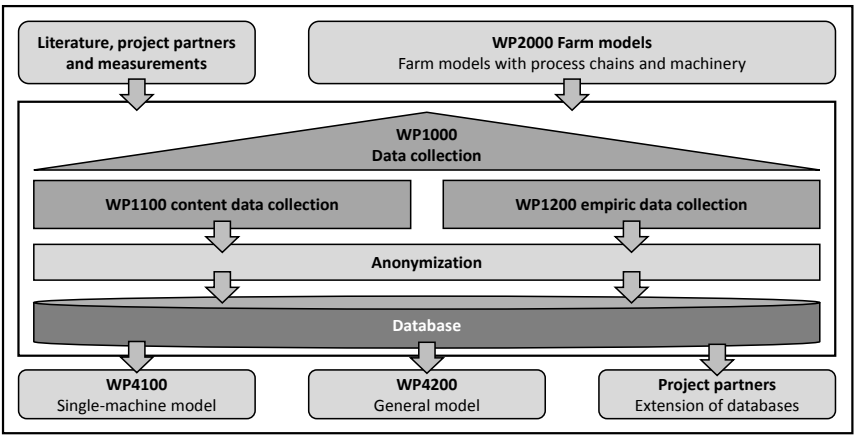

Fig.1: Graphical illustration of the working package "Data collection"

A core demand of the working package is the anonymization of the collected data. By using average tractors and implements in the following simulation model, the back tracing of an implement to a certain manufacturer is not possible.

Development of the fuel consumption of tractors

The fuel consumption of a tractor is an essential factor of variable costs, which refer to a farm's machinery costs. Therefore, the fuel consumption can be used as a parameter to compare different machinery. Furthermore, the importance of environmentalism and the endeavour to a further reduce of different harmful emissions has been increasing. With the long-term comparison of tested tractors, it is possible to make statements about the development in technology and efficiency.

On a worldwide perspective, there are different test procedures in action. The OECD Code 2 standard test is one of the most used test procedures for a tractor's approval. The procedure consists of a power take-off test and three different tests, which are necessary for approval:

- Main power take-off and five extra points for calculating fuel consumption characteristics
- Hydraulic power and lifting force
- Drawbar power and fuel consumption (unballasted tractors)

A one-hour lasting test is conducted to verify the claimed maximum performance. The engine is heated up over an adequately lasting warming-up period for the power of the engine to become stabilised. The allowed variation of power during six readings is set at 2 %. After the maximum power test, a test at full load and varying speed is performed (full load curve), following a test at varying loads (limiting curve). In order to make statements about the engine's fuel consumption, five additional points in partial load operation are conducted [5]. In a summary of 926 tested tractors under conditions of the OECD Code 2 standard at the Nebraska-Tractor-Test laboratory, KIM [6] shows the development of the specific fuel consumption from 1959 to 2002. The curves in Figure 2 show a swaying progression throughout all power classes, but also a general reduction from about 15 % from 1959 until the beginning of 1990. After 1990, the curves show an almost steady course.

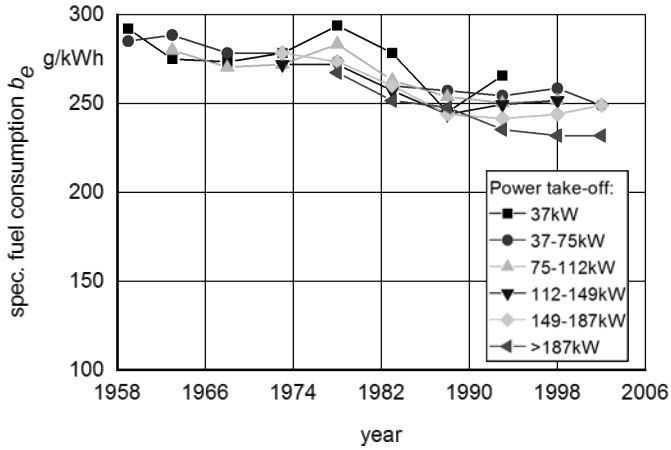

Fig. 2: Development of specific fuel consumption tested with OECD Code 2 standard [6]

The illustrated Figure 2 also indicates that along with an increasing power of the tested tractors comes a higher reduction of the specific fuel consumption. In reality, the operation points of the engine near the full load or limiting curve can be graded as rare. To make statements about real life fuel consumptions of tractors, part load areas of the engine characteristics are important. The so-called PowerMix of the German Society of Agriculture (DLG) consists of twelve different part-cycles. They are derived from different tasks that occur in process chains of several agricultural systems all over Germany. The aim is to obtain nearly realistic specific fuel consumptions of tractors to compare them under different operating conditions. By use of a draught power measuring vehicle, different load profiles under similar conditions are imprinted on the tractor. Imprinted parameters are tractive power, power take-off and hydraulic power in single mode and in combination. Figure 3 shows the evaluation of 45 tested tractors with the DLG PowerMix. The figure displays the specific fuel consumption over power classes and emission standards.

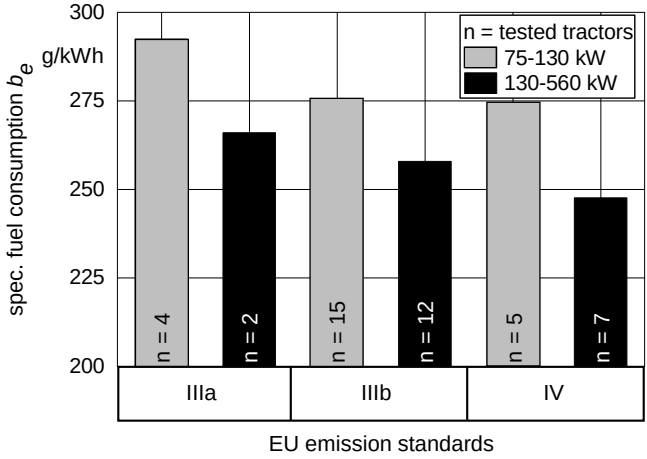

Fig. 3: Development of specific fuel consumptions over EU emission standards for non-road engines

The evaluation shows an almost similar trend as Figure 2. With higher power classes comes a lower specific fuel consumption. In the power class from 75 to 130 kW is from EU stage IIIB to EU stage IV almost none reduction visible.

Development of the energy requirements of implements

To display the development of energy requirements of implements, tractive force or tractive power as parameter for comparison is chosen. However, to compare different measurements, other parameters like soil type or soil moisture are needed in addition. Those secondary parameters are often described superficially. Gaps in the database are the consequence, making consistent evaluations difficult. To fill the gaps in the database, different approaches on tractive force or tractive power calculations are researched. In the next step, calculated values are compared with measurements. Researched calculation models are models from the ASABE, Gorjatschkin and the KTBL. The approach described in this article is by Gorjatschkin and it is used to calculate tractive forces for ploughs [7]:

$$F_Z = b \cdot t \cdot (k + e \cdot v^2)$$

The working width *b* is a fixed factor with 1 meter, as measured values of tractive force are also converted into a specific tractive force per meter. The working depth *t* varies with different measurements. Working speed *v* is weighted by square. *k* and *e* are empirically determined values. Parameter *k* (kN/m^2) covers the soil as a factor, *e* (kNs^2/m^4) characterises the applied working tool.

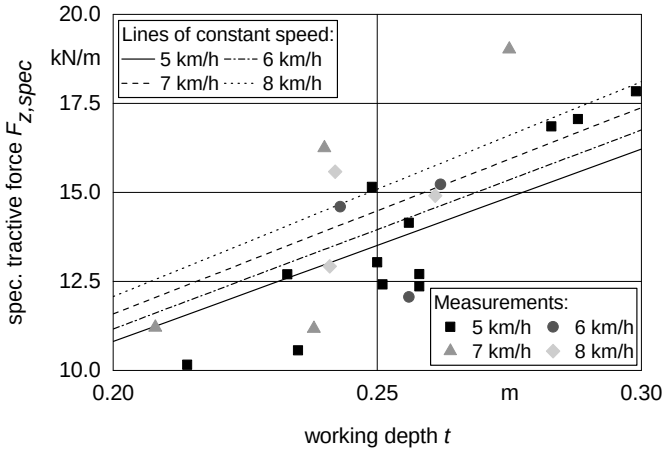

Fig. 4: Comparison between calculated specific tractive force (kN/m) with the equation of Gorjatschkin (*k*= 50 kN/m^2, e= 2.5 kNs^2/m^4) and real measurements [8]

Figure 4 shows a comparison between the calculated values from the Gorjatschkin equation and measurements with ploughs on silty loam in different working depths. Different forms of workings tools on the utilised ploughs are not considered. *k* is fixed at a value of 50 kN/m^2 covering the silty loam, *e* is fixed at a value of 2.1 kNs^2/m^4. The graphic shows the calculated constant lines of working speed compared with 22 data points recorded during different experiments. The mean deviation between calculated and measured data is at 0.48 kN/m at a speed of 5 km/h. Greater deviation cannot be explained due to missing stated boundary conditions (soil type, soil moisture) in the test reports.

Besides the equation of Gorjatschkin, further approaches like ASABE and KTBL are researched and compared with measurements within the EKoTech project. Furthermore, different implements like cultivators and (short) disk harrows are considered. To compare calculated values with real data, databases of currently 91 data points for ploughs, 76 measurements for cultivators and 22 data points for (short) disc harrows are available. Most of the data was collected at the DLG in Groß-Umstadt. Within the EKoTech project, test reports from the repository where gathered and digitalised.

Summary and outlook

Defining options for a further reduction of fuel consumption in agriculture and giving recommendations for action for farmers and manufactures is the aim of the joint research project EKoTech. At the Institute of Agricultural Engineering at the University of Hohenheim, a comprehensive research of literature is done to show already reached potentials of saving and to build up a database to make a statement about energy requirements and fuel consumption of project-relevant tractors and implements. Different worldwide-engaged test standards are used to compare tractors regarding their specific fuel consumption. To fill up gaps in the database of the implements, different approaches for calculating tractive force are considered and compared with researched measurements. The next step within the project is the planning of field tests to measure missing data detected in the implements' database.

'The project is supported by funds of the Federal Ministry of Food and Agriculture (BMEL) based on a decision of the Parliament of the Federal Republic of Germany via the Federal Office for Agriculture and Food (BLE) under the innovation support programme.'

References

[1] United Nations: World Population Prospects - The 2015 Revision. Key findings and Advance Tables. Department of Economic and Social Affairs. United Nations, p. 2-2, 2015.

[2] Matthes, F.C.: Klimawandel und Klimaschutz. Informationen zur politischen Bildung (2008) No. 287.

[3] Europäische Kommission: Mitteilung der Kommission an das Europäische Parlament, den Rat, den Europäischen Wirtschafts- und Sozialausschuss und den Ausschuss der Regionen - Ein Rahmen für die Klima- und Energiepolitik im Zeitraum 2020-2030, Brüssel, 2014.

[4] Berning, F.: CO_2 - nicht nur der Motor macht's. topagrar (2013) No. 7, p. 108-111.

[5] Organisation for Economic Co-operation and Development: Code 2 - OECD Standard Code for the Official Testing of Agricultural and Forestry Tractor Performance, p. 11-13, 2016.

[6] Kim, K.U., L.L. Bashford and B.T. Sampson: Improvement of Tractor performance. Applied Engineering in Agriculture 21 (2005) No. 6, p. 949-954.

[7] Gorjatschkin, W.P.: Theorie des Pfluges - Grundlagen zu einer systematischen Berechnung der Pflüge. Moskau: Industrie Verlag AG 1927.

[8] Deutsche Landwirtschafts-Gesellschaft e.V. - Fachbereich Landtechnik: Prüfberichte Gruppe 3a. DLG Prüfberichte, 1985-1993.

Advancement of the Hohenheim Tractor Model – Adaption on current demands

M. Sc. **Arwid Meiners**, Dipl.-Ing. **Steffen Häberle**,
Prof. Dr.-Ing. **Stefan Böttinger**, University of Hohenheim, Stuttgart

Abstract

The joint research project ,,Efficient fuel use in agricultural technology'' (EKoTech), which started in 2016, has the objective to identify strategies and technologies proposing an increase of energy efficiency thus reducing fuel consumption and exhaust gas emissions. The holistic approach is to define potentials by analysing entire agricultural process chains. The aim is to derive recommendations for owners, users and manufacturers of agricultural machinery. One tool being used to meet the project's challenges is the Hohenheim Tractor Model for calculating absolute fuel consumption. It is developed further and therefore has to be enhanced by validated implement models. These models have to be adapted for fitting the project requirements. This paper thereby outlines a method for simulating machines and machine combinations. As an advancement of the simulation model according to Schreiber [1], first approaches are discussed for the tyre-soil model. This concerns the demand for reproducing large tyres of today's technology and dimensions.

Motivation

The climate and energy policy objectives of the European Union passed in 2014 extend the three key demands that have already been defined in 2008 [2]. Within the observation horizon up to 2030 a reduction of greenhouse gas emissions by 40 % is demanded besides an extension of renewable energies and an increase in energy efficiency by 27 % each referred to 1990 [3,4].

Since increasing tightening of thresholds for harmful emissions after having introduced emissions legislation for agricultural machinery the full potential of agricultural engineering development capacities is inhibited regarding innovations and in consequence the competitive environment. A discussion of thresholds for climate-damaging emissions such as CO_2 like in automotive industry can be seen as a possible further step by the legislative. The CEMA (European Committee of Associations of Manufacturers of Agricultural Machinery) aspires a holistic approach to a voluntary commitment as first presented in [5] for highlighting alternatives to legal regulations.

An initial step on this way is the joint research project EKoTech funded by the Federal Ministry of Food and Agriculture and accompanied by the Federal Office for Agriculture and Food. In various work packages, the involved consortium partners from industry and university together compile the objectives achieved since 1990 and the achievable innovation potentials concerning fuel savings in agricultural machinery and process chains up to 2030. Results will be action recommendations towards the agricultural engineering industry and the utilization of machinery in agriculture. [6]

Methodological approach in EKoTech

The fuel saving potentials in 2030 are derived from the fuel consumption of the process chains within the cultivation systems wheat, maize and grassland for model farms by accounting to the reference year 1990. The fuel consumption is referenced to the quantity of crop harvested. Thus the criterion ,,litres fuel per unit grain equivalent'' results for evaluation. The model farms are defined from the identified soil-climate regions in Germany and relevant regions of the EU. Each of them is represented by a typical, virtual farm which is formed as the average of the respective core production region and is characterized by certain information such as area structure, machine equipment and yields. Their elaboration is part of a separate work package. [5,7]

Besides extensive scientific literature research for data acquisition, simulation models are built up to determine the fuel consumption of agricultural process chains. The objective is to quantify

- technical influencing factors,
- structural conditions and
- organizational relations

regarding their influence on fuel consumption. The task is to fill in any data gaps for the reference year 1990, to set the current status in 2016 and to determine the fuel consumption in 2030 considering the innovation potentials worked out. For this purpose, two types of simulation models are established. The Institute of Mobile Machines and Commercial Vehicles of the Technische Universität Braunschweig develops a model for simulating the procedure and usage of machines and machine combinations in the process chains as specified on the model farms. The results, so-called operational profiles, contain the partial times of each different subtask in hours based on KTBL-scheme [8] (Advisory board for Technique and Construction in Agriculture) for each step of the process chain (e.g. seed bed preparation, seeding, fertilizing). The simulation models for single machines, as they are developed at the In-

stitute of Agricultural Engineering at the University of Hohenheim, provide the fuel consumption in litres per hour related to each partial time. The calculation of both results occurs within the superordinate overall simulation model. A summation over the whole process chain in all cultivation systems of the respective model farm leads to the total fuel consumption.

Simulation models for single machines

For the determination of fuel consumption simulation models of the single machines used in each of the process steps are required. They calculate the consumption in litres per hour and enable to consider technical influencing factors on a component-based level. In principle, they can be assigned to three different categories with exemplary machines:

- Vehicle: Tractor, truck
- Implement: Plough, rotary harrow, baler
- Self-propelled machine: Combine harvester, forage harvester, wheel loader

As an approach for these simulation models, the Hohenheim Tractor Model based on Schreiber [1] is enhanced regarding the project objectives. In most cases, the tractor is taken into account combined with an implement. The schematic structure shown in figure 1 highlights how such a machine combination is compound from two submodels.

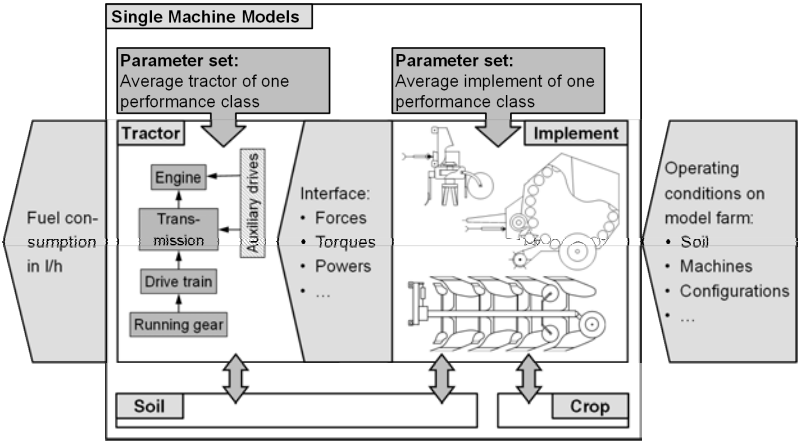

Fig. 1: Schematic structure of the single machine models

The submodel of the implement provides all relevant physical parameters for a particular application transferring these to the tractor in a predefined interface. Based on this the sub-

model of the tractor, consisting of the basic components running gear, drivetrain, transmission and engine, calculates an absolute fuel consumption. An interaction model is intended between the abstractly modelled soil and the running gear of the tractor and implement and with the attached tools of the implement. The operating conditions on the model farms form the input variables of the model including soil information (type of soil, moisture content, soil condition), the type of the utilized machines (e.g. standard tractor with a rotary harrow), the performance class (e.g. 75-111 kW and 3 m) and certain boundary conditions respectively parameter settings (e.g. pitch, working depth, PTO speed). The simulated tractors and implements each represent the average machine of a specific performance class, which is based on the KTBL approach [9]. In accordance to the input variables, a parameter set for the models is chosen. For a selected machine combination, the fuel consumption of all subtasks defined within the machine's operational profile is output.

The modular development of the models in Matlab Simulink largely follows the functional components. In addition, it is differentiated between drive (hydraulical, mechanical and electrical) and tractive power at the implement. Thus, it is possible to replace the characteristic values or diagrams deposited in the parameter set by alternative approaches.

The variety of machines to be simulated requires a component-specific, differently intensive modelling. According to the project objectives, a uniform level of detail is not reasonable. Therefore, the machines are subdivided into functionally connected components in a first step. For a typical application an expert-based assessment of the power distribution between the components is carried out supported by literature research, cf. figure 2.

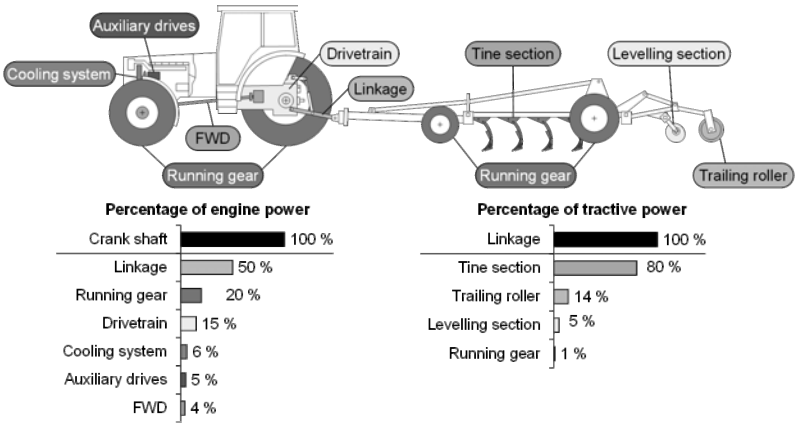

Fig. 2: Power distribution at a tractor implement combination while cultivation

An additional estimation of the potential for future energy savings at these components opens up the field of action for innovations and justifies a more or less detailed modelling. Therefore, the model of a trailing roller at the cultivator or the rotary harrow can be kept simple, whereas the running gear of the tractor requires a more in-depth treatment.

Advancement of the Hohenheim Tractor Model

The current status of the Hohenheim Tractor Model needs an extension to simulate the running gears of current and future tractors, as shown in [10]. This concerns the integration of rubber belt gears and the verification of the capability to reproduce current tyre dimensions. The latter is discussed below.

The tyre-soil model to determine drawbar pull/slip-curves for each single wheel of the tractor is evolved as a regression model upon a database from Steinkampf [11]. To define the tyre it requires the width and the rolling radius which can be derived from the tyre designation and furthermore the tyre pressure. The resulting regression parameter abstractedly represents the contact area. A detailed description can be found in [12]. However, with rolling radii of more than 0.9 m and 0.8 m tyre width the model reaches the limits of its outdated database. The tyre dimensions for standard tractors according to KTBL [9], summarized in table 1, are beyond the previously researched range.

Table 1: Tyre dimensions for standard tractors beyond the scope of the Hohenheim Tractor Model, based on [9]

Performance class	Tyre dimension
112 - 129 kW	650/65 R 38
130 - 167 kW	620/70 R 42
168 - 184 kW	650/65 R 42
185 - 300 kW	710/70 R 42

The approach discussed in [10] proposes a reduction of tyre dimensions beyond the scope to the largest tyre size displayable. However, a comparison to measurements shows deviations especially with high and low slip values. The effect of an extrapolation of the regression equations to reproduce the tyre dimensions listed above presents figure 3. Compared to the largest tyre 20.8 R 38 examined by Steinkampf [11] the computed curves show almost the same course for slip values up to 20 %. However, larger tyre sizes result in a higher κ_{max} under equal soil conditions. In this case, the maximum difference for the tyre 710/70 R 42 is

moderate by $\Delta\kappa$ = 0,03 which corresponds with the expected influence. The effect of different soil conditions with a tyre 710/70 R 42 is shown in figure 4 (left). Even for extreme assumptions, like on asphalt, an extreme but not an unrealistic curve results. A first alignment of that operating condition with measurements conducted by Schulze-Zumkley [13] is also highlighted in figure 4 (right).

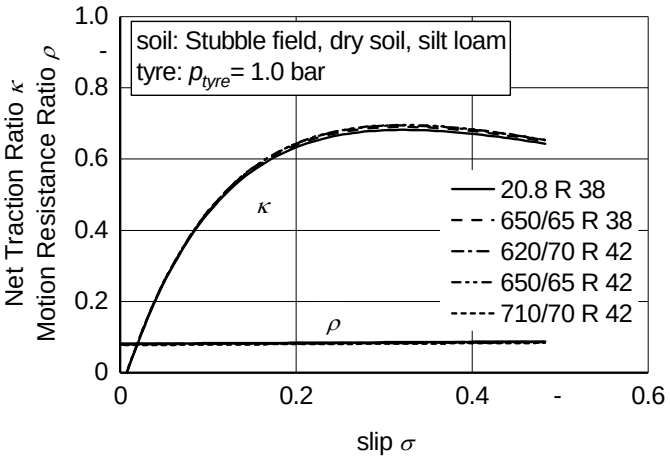

Fig. 3: Simulated net traction and motion resistance ratio over slip for tyre dimensions beyond the scope of the Hohenheim Tractor Model

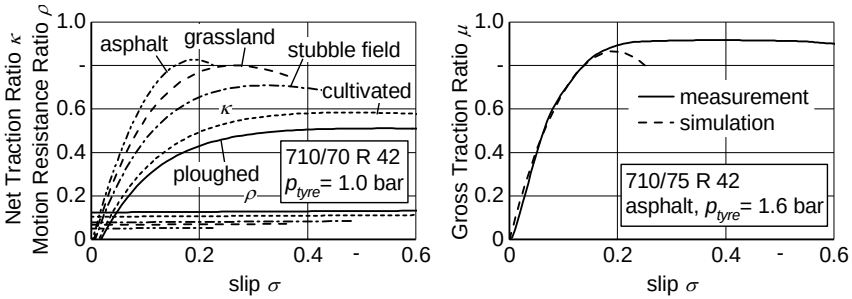

Fig. 4: Simulated net traction and motion resistance ratio (left) and simulated gross traction ratio in comparison to measurements by [13] (right)

Comparing to the measured gross traction ratio of a tyre 710/75 R 42 on asphalt good results can be gained with the simulation model especially for the aspired operating range at low slip values. For higher slip rates the simulation remains at a lower gross traction ratio. Furthermore the distinct decrease after having reached the maximum gross traction ratio cannot be proved in the measurements, the same behaviour as emphasized in [10] on deformable ground. A slight modification of the regression equations therefore has to be considered. Overall, the capacity of the tyre-soil model for simulating large tyre dimensions can be classified as realistic. With certain limits an application beyond its scope is therefore possible when extrapolating the equations. An alignment with measured curves, particularly on deformable ground, must show in which extent an adjustment of the regression is necessary.

The planned measurements will be conducted similar to [13] using a test tractor equipped with 2 measuring rims at the rear and one at the front axle. Additionally a dynamometer is mounted to the three point hitch measuring the drawbar pull introduced by a second tractor constantly decelerating the test tractors. Thus, it will be possible to determine the drawbar pull/slip-curves for the whole vehicle as well as for each single tyre. Performing this method on various soils will provide a sufficient data basis for estimating an adjustment of Schreiber's regression equations.

Summary and outlook

Within the project EKoTech, simulation models are developed for calculating the fuel consumption of agricultural process chains. These are composed of two types of models, one for modelling the procedure and usage of machines and machine combinations in the process chains and one for simulating the single machines utilised. The Hohenheim Tractor Model is applied to the single machines in the project and is enhanced for this purpose. The development of a huge variety of additional models for implements requires the presented methodology to determine a component-specific degree of detail. At the tractor, the focus is on the tyre-soil model. It is shown that an extrapolation of the underlying regressions allows to simulate present tyre dimensions. The alignment with measurements will be a further step. Measurement series for drawbar pull/slip-curves on deformable ground of the tyre dimensions listed above at a complete vehicle are therefore planned. A subsequent adaption of the regression will update the running gear model to a current state of the art.

‘The project is supported by funds of the Federal Ministry of Food and Agriculture (BMEL) based on a decision of the Parliament of the Federal Republic of Germany via the Federal Office for Agriculture and Food (BLE) under the innovation support programme.’

References

[1] Schreiber, M.: Kraftstoffverbrauch beim Einsatz von Ackerschleppern im besonderen Hinblick auf CO_2- Emissionen. Dissertation Universität Hohenheim, Forschungsbericht Agrartechnik des Arbeitskreises Forschung und Lehre der VDI-MEG, No. 442. Aachen: Shaker 2006.

[2] Bundesministerium für Umwelt, Naturschutz, Bau und Reaktorsicherheit: Klimaschutz in Zahlen, 2015.

[3] Europäische Kommission: Mitteilung der Kommission an das Europäische Parlament, den Rat, den Europäischen Wirtschafts- und Sozialausschuss und den Ausschuss der Regionen - Ein Rahmen für die Klima- und Energiepolitik im Zeitraum 2020-2030, Brüssel, 2014.

[4] Europäischer Rat: European Council (23 and 24 October 2014) Conclusions. EUCO 169/14, 2014.

[5] Fleck, B., E. Nacke, S. Böttinger, L. Frerichs and S. Hanke: Der Weg zur freiwilligen Selbstverpflichtung der europäischen Landtechnikindustrie zur Reduktion von CO2-Emissionen. Tagung Landtechnik AgEng, 19./20.11.2014 Berlin. In: VDI-MEG, VDI-Berichte Nr. 2226. Düsseldorf: VDI-Verlag 2014, p. 301-308.

[6] Decker, M.: Effiziente Kraftstoffnutzung in der AgrarTechnik - EKoTech. In: L. Frerichs. , Jahrbuch Agrartechnik 2016. Braunschweig: Institut für mobile Maschinen und Nutzfahrzeuge 2017, p. 22-29.

[7] Hanke, S., L. Frerichs, B. Fleck and E. Nacke: Methode zur Ermittlung der CO2-Emissionen von Landmaschinen in einer Verfahrenskette. Tagung Landtechnik, 19./20.11.2014 Berlin. In: VDI-MEG, VDI-Berichte Nr. 2226. Düsseldorf: VDI Verlag 2014, p. 309-314.

[8] Winkler, B. and J. Frisch: Weiterentwicklung der Zeitgliederung für landwirtschaftliche Arbeiten. 19. Arbeitswissenschaftliches Kolloquium des VDI-MEG Arbeitskreis Arbeitswissenschaften im Landbau, 11./12.03.2014 Dresden. In: Leibniz-Institut für Agrartechnik Potsdam-Bornim e. V. (ATB), Bornimer Agrartechnische Berichte, Heft 81. 2014, p. 14-21.

[9] KTBL (ed.): Betriebsplanung Landwirtschaft 2016/17 - Daten für die Betriebsplanung in der Landwirtschaft. 2016.

[10] Weisbrodt, J.: Der Claas Xerion als selbsfahrende Säeinheit - Potentialanalyse für verschiedene Anbauregionen anhand eines Simulationmodells. Dissertation Universität Hohenheim, 2016, Forschungsbericht Agrartechnik des Arbeitskreises Forschung und Lehre der VDI-MEG, No. 564. Aachen: Shaker 2016.

[11] Steinkampf, H. and G. Jahns: Betriebseigenschaften von Ackerschlepperreifen bei unterschiedlichen Einsatzbedingungen. Landbauforschung Völkenrode (1986), p. 1-427.

[12] Schreiber, M. and H.D. Kutzbach: Influence of soil and tire parameters on traction. Research in Agricultural Engeneering 54 (2008) No. 2, p. 43-49.

[13] Schulze Zumkley, H.: Reifenparameterermittlung aus Fahrversuchen mit einem Ackerschlepper unter besonderer Berücksichtigung des Hohenheimer Reifenmodells. Dissertation Universität Stuttgart, 2016, Forschungsbericht Agrartechnik des Arbeitskreises Forschung und Lehre der VDI-MEG, No. 571. Aachen: Shaker 2017.

Definition of a test method to evaluate vibrations acting on a tractor driver

Dr. **Jürgen Karner**,
Josephinum Research, Wieselburg;
DI **Christof Danner**, DI **Andreas Kerschbaumer**,
AVL List GmbH, Graz, Österreich;
DI **Heinrich Prankl**,
Francisco Josephinum / BLT, Wieselburg

Abstract

Tractors are universal machines in agriculture. They are used off- and on-road with attached trailers or implements, or operated on the farm site. Increasing speeds result in high chassis accelerations, e.g. on rough tracks and roads, affect the health of the driver.

In case of machine operation by employees, the compliance with minimum health and safety requirements is mandatory. The regulations (e.g. Directive 2002/44/EC [1]) oblige to evaluate the exposure of workers to the risks arising from vibration. Daily exposure limit values for vibrations, as well as the sensors, signal-filters and evaluation formulas to be used are defined by the regulations, but they lack a specification of defined driving conditions. According to the codes, the measurements shall be carried out under “normal operation”, but a tractor´s operating range is incredibly versatile [2]. Previous tests were carried out typically without implements [3, 4]. So an objective test method “Wieselburg vibration test-cycle” with specified driving cycles including ballast settings has been developed. The method enables benchmarks between tractors and provides input for tractor development (e.g. suspension setup) under different driving conditions.

Competent authorities can use the tool and the procedure to evaluate the whole-body-vibrations or create own test cycles based on the measurements of individual events.

1 Introduction

The DLG PowerMix is a widely recognized and accepted method for evaluating fuel consumption. The described cycles were taken as reference drives and slightly adapted in terms of vehicle speed and load situation (ballast, axle loads etc.), supplemented with transportation drives. For the repeatability of the test drives the ISO 5008 [5] smooth and rough tracks and adjacent tarmac are used. The tests are performed with unloaded tractors and with ballast, wherein the ballast substitutes the vertical drawbar load or implement load in hitch-up position.

The total range of standard-tractors was divided into 7 classes and corresponding ballast loads are based on statistical analysis of tractor data.
For measurements and data processing the modified tool AVL DRIVE™ was used. Based on the vibration evaluation permissible operation times and numerical values were calculated.
Furthermore, a range of 4WD tractors provided by CNH Industrial was used to analyse parameters which might influence the results. Finally, several tractors from different manufacturers with 75-110 kW nominal power have been used in the evaluation.

2 Methodology

2.1 Measuring equipment

The tool AVL-DRIVE™ is utilised for the measurements. The tractor's CAN-bus signals, vertical front axle-acceleration and the accelerations on the seat-pad are used to derive the exposure limit values. The triggering and matching of the corresponding events are performed automatically by the software. The evaluation is done according to the root-mean-square method described in ISO 2631-1 [6]. The resulting values (in time units) are also converted to a rating (0 to 10 points), whereas the number of seven shall indicate the legislative borderline of eight hours of exposure.

2.2 Development of the test cycle and test events

As the field of application of tractors is so versatile, the test cycle has to define appropriate driving conditions in order to limit the variety and complexity of testing. The test procedure includes ten "events", each representing a certain speed and track, hitch position and ballast attached at the rear. Each event is repeated five times, as recommended by ISO 5008. The analysis of certain events provides input for tractor development (e.g. suspension setup). For overall comparisons of different tractor-models a single numerical rating (0-10) and a permissible operating time are calculated. For tractor development, individual events can be analysed for vibration comfort optimization, e.g. suspension setup.

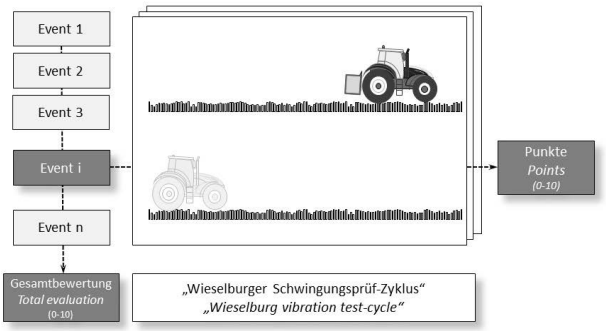

Fig. 1: The Wieselburg vibration test-cycle consists of ten events, each representing different driving conditions

Figure 1 shows that not only the whole test cycle can be evaluated, but also individual events. Each event is repeated five times, as recommended by ISO 5008. Prior to the definition of the individual events, several variables which might affect the vibration behaviour were analysed using different tractors. Especially driving speed, ballast, ballast position and driver's weight was investigated with different tractors.

The basic tests were executed with the following tractors:

Case Puma 210	Steyr CVT 6160	Case Maxxum 150	Steyr Multi 4115 tier4i
Steyr Multi 4115 tier4f	Case CVX 185	New Holland T7.270	

For the purpose of these investigations the tractors were driven w/o ballast at speeds from 8 to 16 kph over the 100 m (smooth) ISO track and with ballast at 8 to 20 kph. The 35 m (rough) track was driven at 4 to 8 kph including ballast.

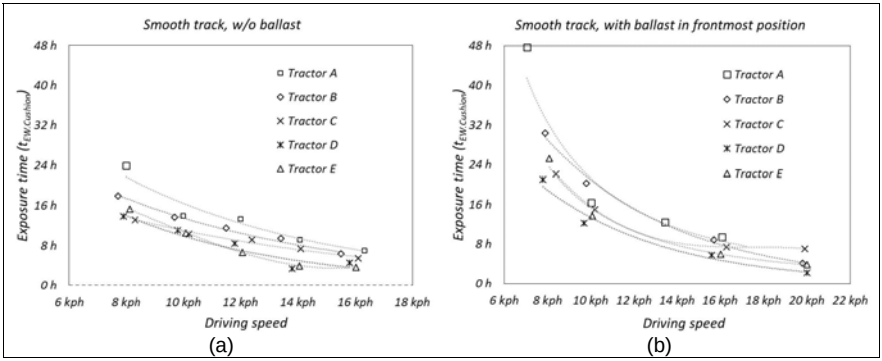

Fig. 2: Influence of the driving speed over the 100 m ISO track without ballast (a) and with ballast attached at the rear linkage of the tractor (b)

Unsurprisingly the vibration level measured on the seat-cushion increases at higher speeds. Consequently, the permissible exposure time decreases. Tractor A would enable an operation of 8 hours up to 15 kph (empty, Figure 2a) and up to approx. 17 kph with ballast of about 1 500 kg at the rear linkage (Figure 2b).

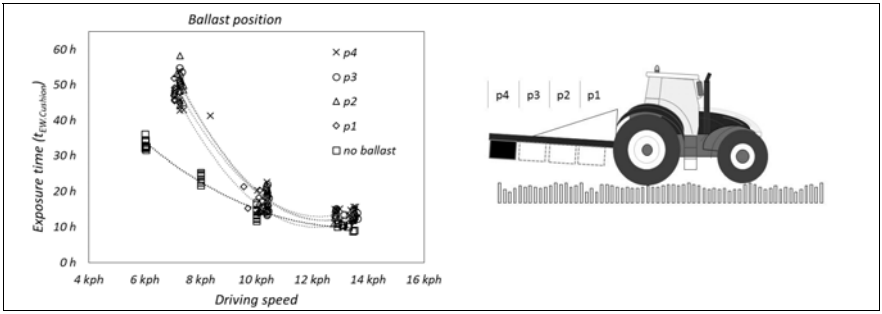

Fig. 3: Influence of ballast and position

The influence of the ballast position was studied in four different distances to the three-point linkage (position p1 frontmost - p4 rearmost). Figure 3 shows that the ballasted tractor outperforms the empty tractor and enables longer operation times. The ballast puts more weight onto the rear axle and therefore relieves the front axle. The large-sized rear tyres comprise good vibration damping behaviour. The position of ballast (p1, p2, p3 or p4) has minor influence. The results of empty and ballasted tractor converge with increasing speed (typically between 14 to 16 kph). The driver weight has no significant influence on the results.

2.3 Definition of Test Cycle

The driving speeds are basically derived from the DLG PowerMix, with minor changes (Table 1). The operations with plough, cultivator and mower are imitated with 9, 12 and 15 kph on the smooth track (100 m). The rear axle load with the implement in working position in-field is nearly the same as with the empty tractor on track. Therefore no ballast will be attached. Baler, manure spreader and loader wagon put specific drawbar load onto the tractor. This load is simulated by ballast on the three-point-linkage with driving speeds from 9 to 15 kph and an additional transport event (cart track) with 20 kph.

Headland turning is done with lifted implements. The driving event is performed with 5 kph and ballast on the rougher track (35 m).

Two road transportation events were added with 40/50 kph (depending on the rated velocity), empty and ballasted. The test is performed on a tarmac surface next to the ISO-tracks, with a single impulse. This is induced by wooden three-layer formwork panels (2 000 x 500 x 27 mm), fixed onto the tarmac.

Table 1: Overview of test events

	Events	Track	Ballast	Speeds	Hitch
1, 2, 3	e.g. plough, cultivator, mower in working position	smooth	no	9, 12, 15 kph	down
4, 5, 6	e.g. baler, manure spreader, loader wagon	smooth	Ballast (simulate drawbar load)	9, 12, 15 kph	up
7	Transport (cart track)	smooth	yes	20 kph	up
8	Headland turning (implement up)	rough	Ballast (simulate lifted implement)	5 kph	up
9	Transport	tarmac	no	40 or 50 kph	down
10	Transport	tarmac	yes	40 or 50 kph	up

Based on statistical analysis of 114 tractor models seven power-classes were defined. By the help of regression analysis the mean empty load and wheel base were derived [7].

Table 2: Tractor classes

	I	II	III	IV	V	VI	VII
Nominal engine power (in kW)	≤ 55	≤ 74	≤ 110	≤ 147	≤ 184	≤ 220	>220
Ballast used for test (in kg)	440	592	880	1 176	1 472	1 760	1 760

The nominal power was taken as reference for the calculation of the ballast weight because it is the engine power that determines the size of the implement (e.g. working width) a farmer usually chooses, not the weight of the tractor.

The ballast weight was chosen in order to fulfil legal requirements (in Austria: 20 % of the empty weight onto the front axle) and to comply with the maximum load capacity.

The analysis showed that the rear lifting force increases with the power of tractors up to about 180 kW. Beyond that power-value, the lifting force is rather constant as trailed implements are commonly used. Therefore the ballast is the same for tractors in classes VI and VII (Table 2).

3 Results and Discussion

For the latest tests the following machinery was used: John Deere 6130 R, Claas Arion 530, New Holland T5.120, Lindner Lintrac 90, Fendt 313 Vario.

All these tractors cover class III, using ballast of 880 kg for any model. Table 3 shows the results of class III tractors.

Table 3: Test results from tractor class III

	Units	Limit for 8h working time	Tractor F	Tractor G	Tractor H	Tractor I	Tractor J
$a_{eff.cushion}$	m/s²	1.15	1.23	1.14	1.12	1.24	1.22
$t_{eff.cushion}$	hrs.	8	7.02	8.12	8.45	6.84	7.15
AVL-DRIVE™ Rating	pts.	7.0	6.51	7.03	7.11	6.42	6.57

The measured effective accelerations values on the seat cushion showed similar values. For an eight hour working day a limit of 1.15 m/s² must not be exceeded. Two models turned out to be slightly below this value, three above. Therefore the permissible working duration shall be restricted to exposure times below eight hours. Higher acceleration leads to shorter expo-

sure time. The numerical AVL-DRIVE™ Rating equals seven points with an effective acceleration of 1.15 m/s² or an exposure time of 8 hours.
Consequently, the AVL-DRIVE™ Rating is above seven for two models, and below seven for the remaining three.

4 Summary and Outlook

The presented test method defines driving conditions for whole-body-vibration measurements on agricultural tractors. Seven power-classes were defined. Some test drives shall also be carried out with ballast attached to the rear three-point-linkage. Therefore, the ballast levels were proposed for each power-class. A further set of tractors will be tested in every power-class to enable the creation of a database for detailed benchmarks of tractors. The "Wieselburg vibration test-cycle" could be basis for a standardization process.

Acknowledgements

The authors thank CNH Industrial, Lindner Traktorenwerke, ACA Center Roher, Esch.Technik GmbH, Heindl Landtechnik GmbH, and Raiffeisen-Lagerhaus Mostviertel Mitte eGen for providing tractors for the tests.

References

[1] Directive 2002/44/EC of the European Parliament and of the Council of 25 June 2002 on the minimum health and safety requirements regarding the exposure of workers to the risks arising from physical agents (vibration)

[2] Schrottmaier, J., Lechner, B. (1986): Untersuchungen zur EG-Fahrersitzprüfung. Forschungsberichte der Bundesanstalt für Landtechnik, Wieselburg. Heft 16, Februar 1986

[3] Scarlett, A.J., Price, J.S., Stayner, R.M. (2007): Whole-body vibration: Evaluation of emissions and exposure levels arising from agricultural tractors. Journal of Terramechanics 44 (2007), S. 65-73

[4] Schrottmaier, J., Nadlinger, M. (2000): Untersuchung und Optimierung der schwingungstechnischen Eigenschaften von Traktoren mit gefederter Vorderachse und gefederter Fahrerkabine. 58. VDI-MEG-Tagung Landtechnik, 10.-11. Oktober 2000, Münster

[5] ISO 5008:2002: Agricultural wheeled tractors and field machinery – Measurement of whole-body vibration of the operator. International Organisation for Standardisation, 2002

[6] ISO 2631-1:1997: Mechanical vibration and shock – Evaluation of human exposure to whole-body vibration – Part 1: General requirements. International Organisation for Standardisation, 1997

[7] Karner, J. (2017): Analysis of Power and Dimensions of European Tractors. GSTF Journal on Agricultural Engineering (JAE) Vol.3 No.1, 2017

Driving comfort analysis of an agricultural tractor with the Hohenheim Tyre Model on complex tracks

Alexander Bürger, M.Sc., Prof. Dr.-Ing. **Stefan Böttinger**,
University of Hohenheim, Stuttgart

Abstract

The driving comfort of agricultural tractors – meaning the driver's isolation from whole-body vibrations – is increasingly targeted by legislation and vehicle manufacturers. To increase the efficiency of the development process, virtual methods based on the objective evaluation of vibration values can be used. This paper presents a method to objectively evaluate the driving comfort of an agricultural tractor with a multi-body simulation model. The evaluation is exemplarily based on international standards such as the ISO 2631-1 standard for the evaluation of whole-body vibrations and the EU Delegated Regulation 1322/2014 for the evaluation of driving seats. A standard roadway referred to by the ISO 5008 standard is used as vehicle excitation. A special focus is set on the ability of the Hohenheim Tyre Model to generate the force inputs of the vehicle multi-body model as exact as possible. The investigations presented are summarised by validation measurements on a smoother track standard roadway with a test tractor. The measurements and the simulation results show a good correlation in both time and frequency domain.

Introduction

Agricultural tractors are increasingly used for a wide variety of tasks, including traditional farming tasks as well as heavy transport tasks with farming or construction background. On the one hand, the driving safety of these vehicles has to be ensured with respect to the controllability during severe driving manoeuvres. One the other hand, the occupational safety of the driver – especially his isolation from whole body vibrations – is focussed by legislation [1-3]. The latter requirement is usually summarised by the term driving comfort.

During the state of the art development process of these machines, the evaluation of driving comfort parameters mostly requires prototypes of the driving seat, the driver's cabin or the whole vehicle. Subjective impressions of the driver can hardly be linked to measureable vibration values [4,5]. This fact supports the development of reproducible virtual test methods. Accompanying the design process of a tractor, simulation models of these vehicles can

nowadays easily by established. They can then be used to evaluate vehicle parameters regarding the driving safety or the driving comfort without the need of physical prototypes.
For a higher reproducibility of driving comfort investigations and to refer to standardised vehicle and driver's cabin excitations, standard roadways are used [6]. These state demanding requirements on the tyre model used for the simulation process, which needs to reproduce the force excitations based on a high frequency of road elevation changes and very sharp transitions precisely. Due to its adaptive footprint approach, the Hohenheim Tyre Model [7,8] is generally able to handle complex road profiles. Validation results have already been presented for single discrete obstacles like pulses, steps or ramps for single wheel and whole vehicle passages [7]. Its application for consecutive elevation changes on tracks like the ISO 5008 smoother track [6] is investigated in this paper.

Virtual driving comfort evaluation method

To virtually evaluate the driving comfort of an agricultural tractor, a multi-body simulation model of a Fendt 313 Vario is set up in cooperation with the manufacturer, figure 1. This tractor is available at the Institute of Agricultural Engineering at the University of Hohenheim for experimental and virtual investigations regarding driving dynamics and driving comfort. The frequency response system of this vehicle consists of various rigid bodies (chassis, front axle, driver's cabin, driving seat and driver), which are connected via joints and force element.

Fig. 1: Multi-body simulation model of the Fendt 313 Vario test tractor on ISO 5008 smoother track standard roadway

Key element of the simulation model is the Hohenheim Tyre Model. The tyre model acts as force element between the road surface and the vehicle. The geometric variations of the road

elevation as well as the friction conditions result in certain deflections of the tyres and therefore certain force generations. These forces have to be reproduced as exactly as possible in both time and frequency domain.

The Hohenheim Tyre Model is characterised by a fully physical approach, figure 2. Various spokes, which are arranged on a certain angular sector with a spacing of 2° to 3°, are equipped with Voigt-Kelvin elements in radial, tangential and lateral direction. Depending on the underlying force transmission principles, they are defined as linear or non-linear elements. Important for its application on rough road surfaces is the tyre-surface-interaction. It is based on an adaptive footprint approach. The road surface – including discontinuous transitions between neighbouring surface segments – are scanned via 1 to 5 scan points per spoke. Based on the undeformed length of each spoke, the deflections in radial, tangential and lateral direction are calculated and used as inputs for the force elements in the particular directions. The force transmission between the tyre and the road surface is based on a stick-slip approach. Interradial springs connecting two adjacent spokes are also very important for driving comfort investigations on rough road surfaces. These elements reproduce the swallowing rate of the tyre by affecting the prevenient and following spokes during a deflection process on an obstacle. [7]

To calculate the tyre forces in longitudinal F_x, lateral F_y and vertical direction F_z as well as the tyre torques M_x, M_y and M_z, the tyre model is provided with the input quantities longitudinal and lateral wheel hub velocities v_x and v_y, distance between wheel hub and road surface h_{Hub}, camber angle β and the angular velocities around the lateral and vertical axis ω_y and ω_z. All 19 fully physical tyre parameters were determined on the institute's tyre test stands during earlier research [7] and amended for additional lateral force transmission principles [8].

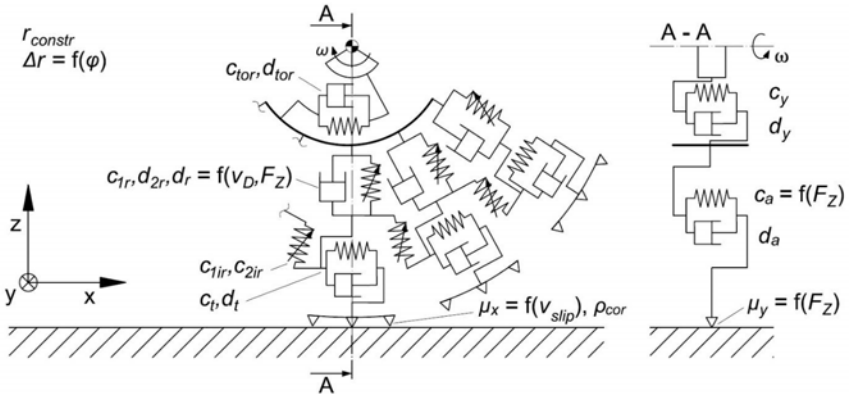

Fig. 2: Structure and parameters of the Hohenheim Tyre Model, according to [7]

The forces and torques calculated by the tyre model and induced into the multi-body model of the test tractor are transferred by the rigid bodies as well as force elements like the front axle or driver's cabin suspension. Eventually, the driver's cabin and the driving seat as well as the driver experience a certain excitation referring to the initial road excitation. These excitations are usually measured as accelerations in longitudinal (direction of travel), lateral (left hand side regarding the direction of travel) and vertical (upwards) direction.

The ISO 2631-1 international standard objectively evaluates the driver's exposure to whole-body vibration [1]. Regarding the threat of damage of certain human organs, the acceleration signals in longitudinal, lateral and vertical direction on the seat surface are weighted and averaged using an rms-value. Finally, the three average values are combined in a single metric *a*, equation 1.

$$a = \sqrt{(1.4 \cdot a_{xw})^2 + \left(1.4 \cdot a_{yw}\right)^2 + a_{zw}^2} \qquad \text{Eq. 1}$$

On the one hand, this objective factor can be used to compare different vehicles under reproducible test conditions, relative to the consequences of the vibration exposure. On the other hand, it provides a quantity to classify the extent of vibration exposure on the driver.

A second metric to evaluate driving comfort is presented in the Delegated Regulation 1322/2014 by the European Union [3]. Here the focus is set on the evaluation of the driving seat. Hence, the vertical weighted and averaged acceleration values at the seat attachment

point a_{wF}* and on the driving seat a_{wS} are set into relation to evaluate the reduction of vibration exposure via the metric V_a, equation 2.

$$V_a = \frac{a_{wS}}{a_{wF}^*} \qquad \text{Eq. 2}$$

To ensure reproducible boundary conditions, a standard roadway referring to the ISO 5008 smoother track [6] is used in the investigations presented. For standard conditions, this road profile is passed with a driving velocity of v_D = 12 km/h and a tyre inflation pressure of p_i = 1.2 bar. To evaluate the driving comfort based on ISO 2631-1 and EU 1322/2014, the multi-body model of the test tractor is additionally equipped with acceleration sensors at the seat attachment and the seat surface.

Validation results

The simulation model is validated by comparing the simulation results to measurements on a real ISO 5008 smoother track. For this reason, a Fendt 313 Vario test tractor is instrumented at the Institute of Agricultural Engineering, figure 3. Three measuring rims are installed at the two rear wheels and the right front wheel to measure the wheel hub forces F_x, F_y and F_z. The measuring principle is based on measuring spoke deformations with strain gauges arranged in different full bridges [9]. Additionally, the test tractor's chassis is equipped with an inertia measuring unit (IMU) below the vehicle's centre of gravity, an optical Correvit S-400 velocity sensor below the rear axle, a steering angle sensor and an angular sensor on the front axle suspension rocker. For driving comfort evaluation purposes, one-dimensional acceleration sensors are placed on the front and rear axle and the seat attachment point. A three-dimensional acceleration sensor is attached directly below the driver on the seat cushion. Last, the position and movement of the driver cabin is measured by two angular sensors at the rear cabin guides and a wire-actuated encoder parallel to the right front bushing of the cabin.

Fig. 3: Test drive with instrumented test tractor on ISO 5008 smoother track

Exemplarily, a test run on an ISO 5008 smoother track surface is evaluated for a vehicle total mass of m = 9090 kg (1150 kg front and 1800 kg rear ballast weights, 40/60 weight distribution), a tyre inflation pressure of p_i = 1.2 bar and a driving velocity of v_D = 12 km/h. As the road surface only excites the vehicle through the tyre contact patches in longitudinal and vertical direction, the transmitted longitudinal and vertical tyre forces are analysed first of all. The transient force responses during the measurement and the simulation are compared using separate error measures for the magnitude error ε_m and the phase error ε_p, together forming a comprehensive error ε_c [10].

For a better optical comparability of the force responses in the time domain, only a 5 s excerpt out of an approximately 30 s test drive is visualised, figure 4. Especially the simulated vertical wheel hub forces F_z show a good correlation with the measurements at the measuring rims. This is shown by a maximum magnitude error of $\varepsilon_{m,z,max}$ = 2.2 %, a maximum phase error of $\varepsilon_{p,z,max}$ = 1.6 % and a resulting comprehensive error of $\varepsilon_{c,z,max}$ = 2.7 % for the whole test duration. The longitudinal wheel hub forces F_x show slightly larger errors, based on larger force fluctuations during the measurements. These mainly result in the differing longitudinal control elements (driving velocity control) in the simulation and on the test tractor, which have to be improved for further investigations.

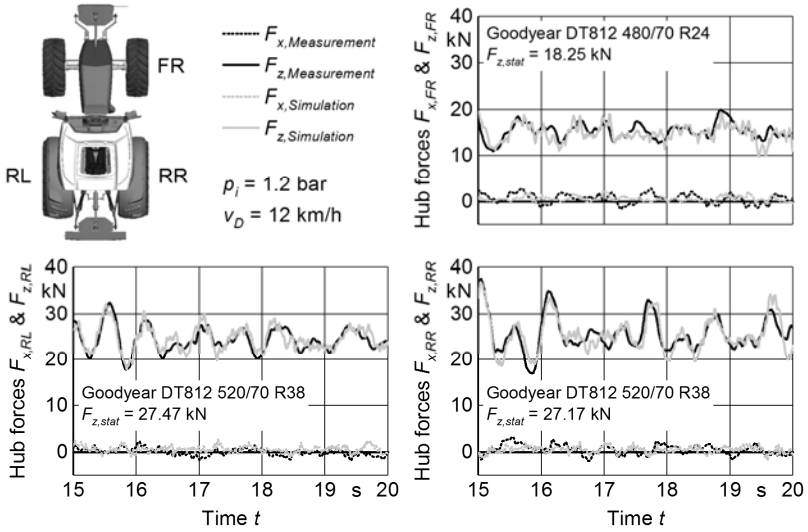

Fig. 4: Time excerpt of the longitudinal and vertical wheel hub forces F_x and F_z during ISO 5008 smoother track test in the time domain

Additionally, the conformity of the vertical force response is shown in the frequency domain, figure 5. As presented in earlier research at the Institute of Agricultural Engineering, an amplitude spectrum (AS) peak hold diagram with Hanning windowing (2.048 s period, 50 % overlap) is used for this purpose [7,11]. Only the front right tyre shows larger deviation between measurements and simulation results. It is noticeable, that the lug pair frequencies of the rear (13.1 Hz) and front tyres (15.9 Hz) cannot be determined from the measurements and are obviously without a strong influence on the vehicle's driving comfort.

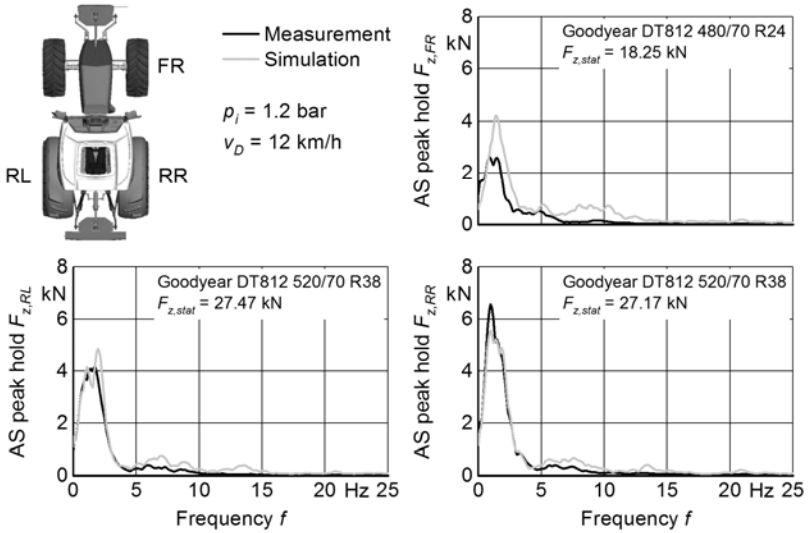

Fig. 5: Vertical hub forces F_z during ISO 5008 smoother track test in the frequency domain (amplitude spectra peak hold)

Summing up, the driving comfort evaluation values based on ISO 2631-1 and EU 1322/2014 are determined from the measurements and the simulation results, table 1. The deviations of approximately 3 to 6 % reinforce the validity of the virtual driving comfort evaluation method presented in this paper. It has to be stated though, that evaluation metrics like the ISO 2631-1 standard are less significant for the validation process, as the acceleration components in the different directions can compensate each other's errors. Single direction metrics have therefore to be more closely investigated and taken into account.

Table 1: Driving comfort evaluation parameters based on measurement and simulation

Standard	Parameter	Measurement	Simulation	Deviation
ISO 2631-1	a	1.4786 m/s²	1.4334 m/s²	-3.06 %
EU 1322/2014	V_a	0.8565	0.9064	5.83 %

Summary and outlook

The improvement of the driving comfort of agricultural tractors becomes more important with rising customer demands and operative and legislative requirements. Virtual evaluation methods make the development process of these vehicles faster and more efficient. This

paper presents a virtual driving comfort evaluation method based on a multi-body model of a tractor in combination with the Hohenheim Tyre Model, which was especially developed for large agricultural tyres. For reproducible boundary conditions, a ISO 5008 smoother track is used as vehicle excitation. The model is validated with measurements on a test tractor on a respective road surface. The wheel hub forces as main excitation calculated by the simulation show a good correlation with the measurements in both time and frequency domain. The correlation in the time domain is objectively measured with separate magnitude and phase error metrics. The whole-body vibration evaluation based on ISO 2631-1 and EU 1322/2014 also shows little deviation between approximately 3 and 6 %.

In combination with earlier published results [12], the model and method presented will serve as virtual development platform at the Institute of Agricultural Engineering. Different undercarriage systems will be investigated according to their influence in the driving safety and the driving comfort of agricultural tractors. These investigations will include different front wheel suspensions as well as suspended rear axles on tractors built in standard architecture (cabin over the rear axle, 40/60 weight distribution). Ultimately, the potential of this architecture in comparison to the possibilities of tractors built in trac-architecture (cabin in the vehicle centre, 50/50 weight distribution) [13] will be virtually determined. Furthermore, the analysis of active suspension systems is another possible field of model application.

References

[1] -,-: ISO 2631-1: Mechanical vibration and shock – Evaluation of human exposure to whole-body vibrations – Part 1: General requirements. 1985

[2] -,-: Regulation (EU) No 167/2013 of the European Parliament and of the Council of 5 February 2013 on the approval and market surveillance of agricultural and forestry vehicles. Official Journal of the European Union 167 2013

[3] -,-: Commission delegated regulation (EU) No 1322/2014 of 19 September 2014 supplementing and amending Regulation (EU) No 167/2013 of the European Parliament and of the Council with regard to vehicle construction and general requirements for the approval of agricultural and forestry vehicles. Official Journal of the European Union 1322 2014

[4] Böttinger, S., J. Haberland, C. Brinkmann and S. Jantzen: Driving Comfort with Agricultural Tractors – State of the Art and Objectification of the Evaluation. In: Proceedings of the 10th European Conference of the ISTVS, Budapest, October 3-6 2006, CD-ROM

[5] Haberland, J., C. Brinkmann and S. Böttinger: Driver comfort of agricultural tractors – subjective and objective methods of assessment. In: vieweg technology forum (Eds.), 7th Stuttgart International Symposium, Automotive and Engine Technology, Volume 1, Stuttgart, March 20-21 2007, Friedr. Vieweg & Sohn Verlag, Wiesbaden, pp. 233-250

[6] -,-: ISO 5008: Agricultural wheeled tractors and field machinery – Measurement of whole-body vibration of the operator. 1979

[7] Witzel, P.: Ein validiertes Reifenmodell zur Simulation des fahrdynamischen und fahrkomfortrelevanten Verhaltens von Ackerschlepperreifen bei Hindernisüberfahrt. Dissertation University of Stuttgart, 2015, Forschungsbericht Agrartechnik des Arbeitskreises Forschung und Lehre der Max-Eyth-Gesellschaft Agrartechnik im VDI No. 548. Aachen: Shaker Verlag 2015

[8] Bürger, A., S.Böttinger and P. Witzel: Simulation of wheel load fluctuations and the effect on the lateral force transmission in the tyre contact patch. In: VDI-MEG: Tagung Landtechnik 2016, Cologne, November 22-23 2016. Düsseldorf: VDI-Verlag 2016, pp. 283-292

[9] Späth, R.: Dynamische Kräfte an Standardtraktoren und ihre Wirkungen auf den Rumpf. Dissertation Technical University of Munich, 2003, VDI Fortschritt-Berichte Reihe 14, No. 115. Düsseldorf: VDI-Verlag 2003

[10] Geers, T. L.: Objective Error Measure for the Comparison of Calculated and Measured Transient Response Histories. Shock and Vibration Bulletin 54, Part 2, 1984, pp. 99-107

[11] Brinkmann, C.: Experimental Investigation on Tractor Tire Vibration Properties. Dissertation University of Stuttgart, 2016, Forschungsbericht Agrartechnik des Arbeitskreises Forschung und Lehre der Max-Eyth-Gesellschaft Agrartechnik im VDI No. 573. Aachen: Shaker Verlag 2017

[12] Bürger, A. and S. Böttinger: Modelling of high volume agricultural tyres for driving dynamics investigations. In: 17th Stuttgart International Symposium Automotive and Engine Technology Volume 1, Stuttgart, March 14-15 2017. Wiesbaden: Springer Fachmedien GmbH 2017, pp. 91-105

[13] Hoppe, U.: Einfluss der Hinterachsfederung auf die Fahrdynamik von Traktoren. Dissertation Technical University of Berlin, 2007, Forschungsberichte aus dem Fachgebiet Konstruktion von Maschinensystemen. Duisburg & Köln: WiKu-Verlag Dr. Stein 2007

Control concepts for ride comfort improvements of harvesting machines with large headers

M. Eng. **Benedikt Jung**, John Deere GmbH & Co. KG, Kaiserslautern;
Dr. **Byron Miller**, Deere & Company, Waterloo;
Prof. Dr.-Ing. habil. **Thomas Herlitzius**, TU Dresden;

Abstract

A crucial part in feeding the ever growing world population is a significant productivity increase of existing agricultural machinery. Besides the engine power, also the vehicle weight, the grain tank capacity, and the cutting width of the front-end equipment is steadily increasing. With the giant headers, it has become essential to use header control systems which help to maintain a constant height of the front-end equipment above ground.

This paper discusses potential solution approaches for reducing the undesired effects of harvesting machine dynamics and names structural limitations. Two concepts for improving the ride comfort and the header height control performance are presented, which do not require major hardware design changes.

Within the first concept demonstrated, it is investigated if a command shaper can be used to proactively suppress self- induced vehicle oscillations. Within the second concept, it is examined whether the inclusion of the vehicle speed as additional control variable can improve the vehicle stability. Results from simulations and field tests are presented in order to give insights in the improvement potential.

System Overview and Solution Approaches

Nowadays self-propelled harvesting machines have unsuspended axles. Unless the machines are equipped with tracks, they are equipped with large and soft agricultural tires with a very low damping ratio. As a consequence, excited vehicle oscillations only subside slowly. A result is a poor ride comfort and a degraded header height control performance, since the slowly subsiding vehicle oscillations are also present at the header tip and have to be compensated by the header controller. The undesired vehicle oscillations are excited in three different ways. First, they are excited by driving over uneven terrain. Second, they are excited by height adjustments of the heavy harvesting heads in use. Third, they are excited by vehicle speed changes since the harvesting machines have a relatively high centre of gravity.

The greatest reduction in ride comfort and the poorest header control performance can be observed if the harvesting machine is excited close to its resonance frequencies. Conversely,

the greatest ride comfort improvement and header control performance can be obtained if the resonance frequencies of the harvesting machine are either not excited, or strongly dampened. Table 1 depicts calculated values for the decoupled pitch and heave natural frequency and according damping ratios of a combine harvester at an exemplary operating point.

Table 1: Relevant natural frequencies and damping ratios of a combine harvester at an exemplary operating point

type of motion	ω_0 [rad/s]	D [-]
heave	10.7	0.11
pitch	8.2	0.08

Since it is a stated goal that no major design changes should be performed, a reduction of the vehicle oscillations can only be obtained by either using additional control variables, or by modification of existing control loops. Within the following, only the pitch oscillations of the vehicle are addressed. Hereto, one has to identify suitable actuators on the machine that have an impact on the vehicle pitch. Fig. 1 presents the sideview of a self-propelled forage harvester and illustrates potential machine motions impacting the vehicle pitch.

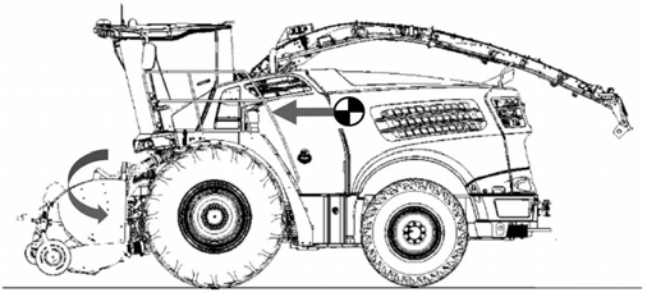

Fig. 1: Sideview of a self-propelled forage harvester, Potential machine actuations impacting the vehicle oscillations

Most obvious is the rotation of the frontend equipment relative to the harvesting machine. Especially large headers have a giant moment of inertia. The motion is realized by actuation of the hydraulic cylinder located between the feederhouse and the chassis. Further on, the vehicle pitch is affected by vehicle speed changes. When accelerating, the machine pitches backwards. When braking, the machine pitches forwards. The inclusion of the vehicle speed

as additional control variable is examined later in this paper. First, the potential of height adjustments of the frontend equipment is investigated.

Proactive vehicle oscillation suppression

As mentioned earlier, height adjustments of the harvesting head excite pitch oscillations. The potential of improving the header control performance by feedback control changes is examined in great detail by XIE et al. [1]. Within her research, she finds that a significant improvement cannot be obtained by feedback control only. XIE names the under-actuation of the system and the non- collocation of sensors and actuators as the main problems, which make it difficult to move the closed loop poles far away from their open loop locations. A different approach to deal with under-actuated systems is called command shaping. Instead of overwriting the machine dynamics or modifying system parameters, command shaping targets to pro-actively suppress self-induced machine oscillations. The working principle of an early command shaping method, known as posicast control, is shown in Fig. 2.

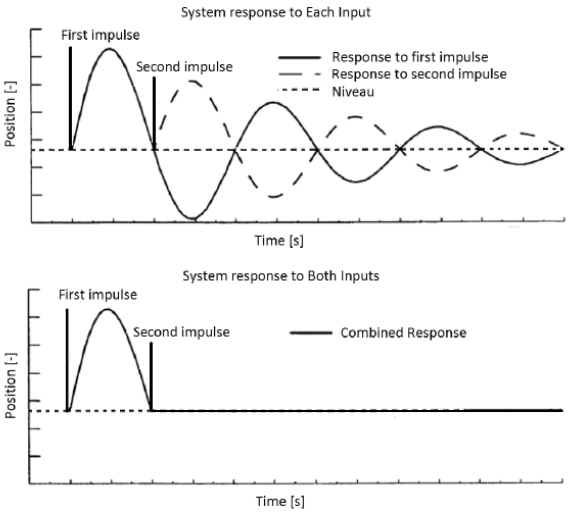

Fig. 2: Posicast control working principle, as shown in [3]

This method takes a baseline command and delays part of the command before giving it to the system. The delayed part cancels out the vibration induced by the portion of the baseline command that is not delayed [2]. The shaper used within the posicast method can be summarized as

$$\begin{bmatrix} A_j \\ t_j \end{bmatrix} = \begin{bmatrix} \frac{1}{1+K} & \frac{K}{1+K} \\ 0 & 0.5 \cdot T_d \end{bmatrix}$$

$$\text{with } K = \frac{-D \cdot \pi}{e^{\sqrt{1-D^2}}},$$

$$\text{and } T_d = \frac{2 \cdot \pi}{\omega_0 \cdot \sqrt{1-D^2}}.$$

As can be seen, the delay times t_j between the impulses, and the amplitudes A_j of the impulses only depends on the natural frequency and damping ratio of the oscillation to be suppressed. Fig. 3 shows a comparison on how the header of the test machine returns to the desired setpoint after a manual header position overwrite with and without command shaping. It can be clearly seen that the command shaper has a positive impact on the settling time of header-induced pitch oscillation after a setpoint change.

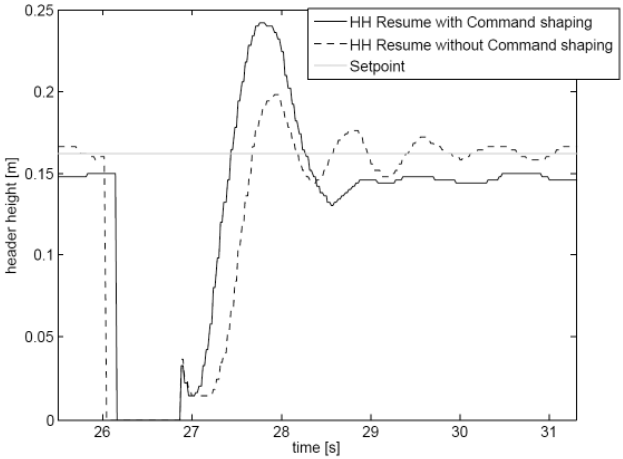

Fig. 3: Comparison of header height resume with and without command shaping, Exemplary response

A challenge in using command shaping techniques exists for systems with a time-varying natural frequency and damping ratio. This is true for self- propelled forage harvesters and combine harvesters. Especially for combine harvesters, the dynamic properties vary significantly during operation due to the changing grain tank fill level. One solution to this is the use of more robust shapers, which come with a penalty in reaction time. Another solution is the

use of an adaptive command shaping approach, which adapts to the change in natural frequency and damping ratio. Unless self-induced vehicle oscillations can be suppressed well with command shaping approaches, vehicle oscillations excited by uneven terrain are challenging since the baseline command of the excitation is unknown.

The vehicle speed as additional control variable

The second concept to be examined is the inclusion of the vehicle speed as additional control variable. The vehicle speed is made available as additional control variable by enhancement of the existing vehicle speed control loop, as it is shown in Fig. 4.

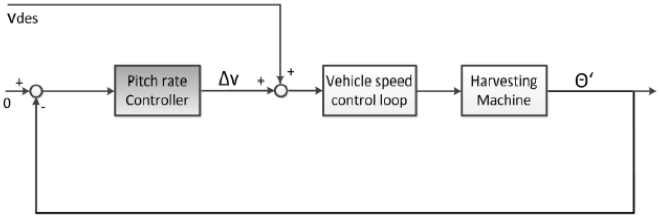

Fig. 4: Enhanced vehicle speed control loop

The validation of the concept is done in the simulation environment by the example of a combine harvester using the artificial test track shown in Fig. 5.

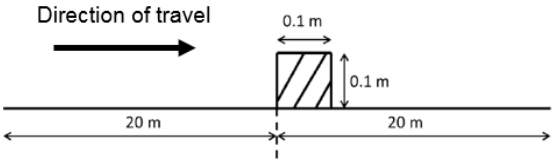

Fig. 5: Test track layout for simulation-assisted concept validation

The gain $k_P = 0$ in Fig. 6 represents the behaviour of the current speed control loop without inclusion of the vehicle speed as additional control variable. It can be seen that the deviation of the cutterbar height is greatest for the case $k_P = 0$, and decreases for increasing proportional gains. Fig. 7 depicts the resulting change in vehicle speed, which is increasing with increasing proportional gains. To choose an appropriate gain for the pitch rate controller requires the consideration of aspects limiting the viable range of vehicle speed changes. One of the limiting aspects is the acceleration acting on the operator in the cabin due to the additional vehicle speed adjustments. Another limiting aspect is the quality of harvest,

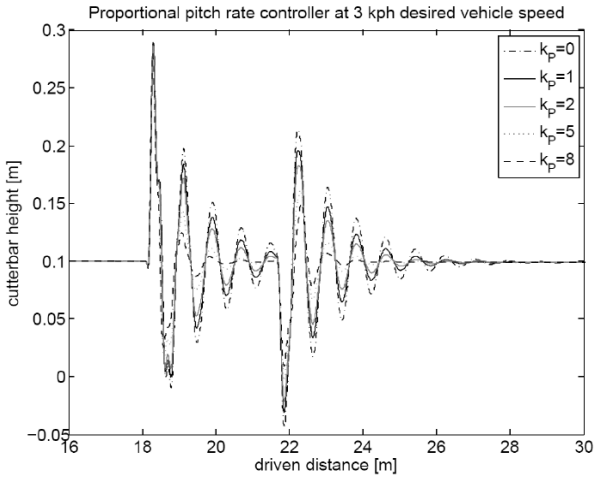

Fig. 6: Comparison of the cutterbar height over the driven distance obtained with different pitch rate controller gains

demanding for a constant crop flow to be fed into the machine. Vehicle speed adjustments result in a variation of the crop flow.

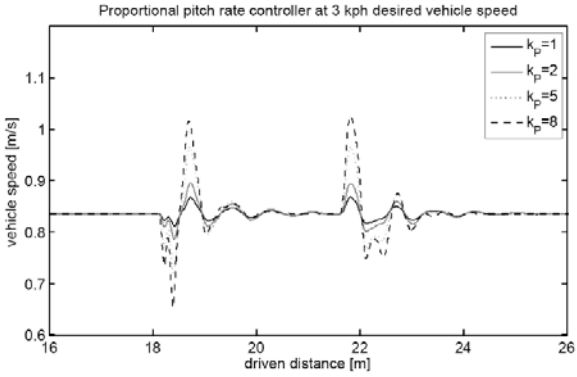

Fig. 7: Comparison of the vehicle speed over the driven distance obtained with different pitch rate controller gains

Summary

Within this paper, solution approaches for improving the ride comfort of self-propelled harvesting machines are discussed and two concepts, which do not require major hardware changes, are presented. The first concept relies on the modification of existing control loops. The second concept relies on the inclusion of an additional control variable. The improvement potential is demonstrated with results from field tests and simulations.

References

[1] Xie, Y. and Alleyne, A. G. and Greer, A. and Denault, D.: Fundamental limits in combine harvester header height control. American Control Conference 2011

[2] Singhose, W.: Command shaping for flexible systems: A review of the first 50 years. International Journal Of Precision Engineering And Manufacturing, Vol. 10, No. 4, 2009, pp.153 -168

[3] Singer, N. C. and Seering, W. P.: Preshaping command inputs to reduce system vibration. ASME Journal of Dynamic Systems, Measurement and Control, Vol. 112, 1990

Evaluation of a Suspension Concept of a Hydropneumatic Full Suspended Tractor with Focus on the Dymnamics in Combination with Implements

Dipl.-Ing. **Maximilian Sieting**, Dr.-Ing**. Jan Krüger**,
Prof. Dr.-Ing. **Henning J. Meyer**, Technische Universität Berlin, Berlin

Abstract

The advantages of a full suspension of the axles of a tractor regarding the ride comfort and the driving safety can be shown on the basis of the dynamic behavior of the vehicle on different road surfaces for a passive and a semi-active chassis suspension or a chassis-cab suspension. In order to keep the implement on the tractor as unaffected from the dynamics of the vehicle structure as possible, some manufacturers pursue a concept in which the rear three-point linkage is connected to the hydropneumatic sprung rear axle of the vehicle. Due to this type of connection, a partial decoupling between the implement and the vehicle body is achieved, but the advantage of a sprung rear wheel axle is somewhat diminished because of the transferred mass of the rear three-point linkage (and the implement) onto the rear axle. To provide the full potential of a fully sprung tractor with respect to e.g. the wheel-to-ground contact during travel, it would be advantageous to keep the axle mass as low as possible.

In a current project, the dynamic properties of a fully-sprung test tractor (TUB-Trac) are investigated with special focus on the combination with an attachment. The central objective is to evaluate the applicability of this vehicle concept for the various tasks in the agricultural and municipal sector. This is carried out using a plane multi-body simulation model, validated by measurement results that is built to calculate a large range of system parameter variations. The evaluation will be based on a direct assessment of the dynamic behavior of the TUB-Trac and on comparing its properties with those of its basis, the MB-Trac.

In this manuscript, some parts of this work will be described and an exemplary comparison of three different chassis concepts (including the TUB-Trac) based on simulation results will be discussed.

1. Introduction

At the Technische Universität Berlin, an experimental tractor (TUB-Trac) based on a MERCEDES MB-Trac was developed to investigate the vehicle concept of a fully sprung tractor with a hydropneumatic chassis suspension. Both the front and rear axles were equipped with a double-acting hydropneumatic suspension, in which the damping can be

continuously adjusted by means of a proportional valve that allows a semi-active control [1]. The scientific research that was carried out in the course of developing the TUB-Trac focused on the driving behavior and the influence of a controlled suspension.

The general objective of this project was to improve the driving comfort as well as the associated conflict between driving safety and driving comfort. An important result of this work is that a significant improvement in driving comfort and driving safety can be achieved with a rear axle suspension and that further improvements in driving comfort using a semi-actively regulated suspension can only be achieved if the control systems used for this purpose have sufficiently low response times. In order to resolve the conflict of objectives (driving safety and driving comfort), the interplay of the regulated chassis suspension with a likewise controlled cab suspension was investigated and the potential of this approach to improve the vehicle system was shown [2].

A special feature of the TUB-Trac in comparison to other tractors with a rear axle suspension is the connection of the rear three-point linkage and thus the connection of rear attachments. The hydraulically actuated three-point linkage of the TUB-Trac is attached directly to the sprung frame and not to the rear axle, resulting in a relatively small mass of the rear axle of the TUB-Trac. For this purpose, the entire mass of a rear-mounted implement is transferred trough the upper structure to the wheels of the TUB-Trac via the front and rear suspension. As a result, the TUB-Trac - independently of its mass distribution - has a different dynamic behavior than the tractors available on the market.

Until now, the impact of rear attached masses and the operating forces introduced via the rear three-point linkage have not been investigated for the vehicle concept of the TUB-Trac. A basic question, which arises from the consideration of the TUB-Trac-implement-system, is to what extent the vehicle concept is suited to fulfill the various tasks of work for which a tractor is normally designed. The aim of this work is to examine the vehicle concept of the TUB-Trac with regard to carrying and using rear-mounted attachments.

2. Objective and Approach

A general assessment of the vehicle concept of the TUB-Trac for agricultural use as an universal working machine is, as a whole, difficult and in the context of a single work not viable. Therefore, the work presented here is limited to the assessment of the vertical-dynamic behavior of the single-track vehicle model at constant speeds with regard to attachments and the rear-wheel driving dynamics. The basic tool of the work is a plane multi-body model of the TUB-Trac, validated by tests on the TUB-Trac and used for a comprehensive analysis of its system behavior. The simulation model, which is calculated with MATLAB, is designed in

such a way that relevant vehicle and environmental parameters can be varied efficiently. The following basic relationships and influencing variables are to be investigated:

1. Basic vertical dynamics of the vehicle with and without a rear attached mass
2. Vertical dynamics in soil processing with a mounted plough
3. Possibilities to improve the vertical-dynamic behavior of the TUB-Trac

3. Simulation Modell of the TUB-Trac

The basic vertical-dynamic behavior of the TUB-Trac is calculated using the planar multi-body model according to Fig. 1.

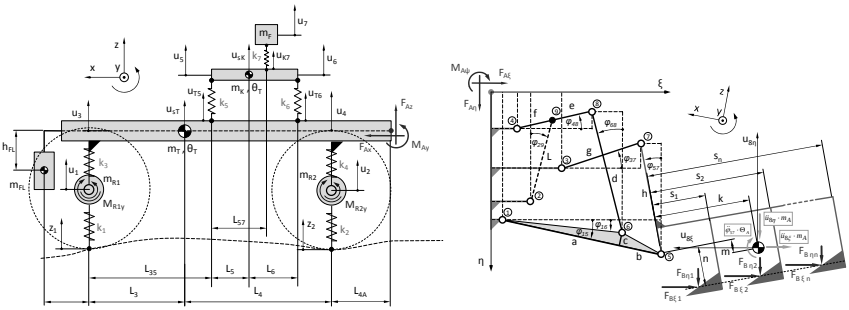

Fig. 1: Plane multi-body model of the TUB-Trac and the rear three-point linkage with a mounted plough

The planar, kinematic model according to Fig. 1 is used to model the rear three-point linkage, with the kinematics described by transfer functions. The coupling of the tractor model with that of the rear three-point linkage is carried out by using the cutting loads at the fictitious connecting point A of the tractor.

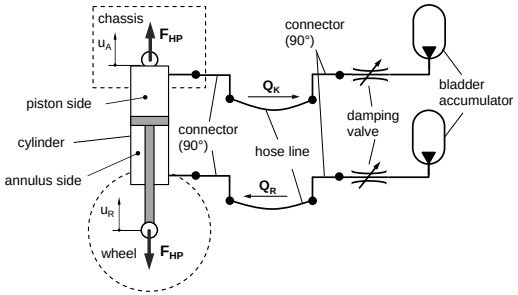

Fig. 2: Schematic model of the hydro-pneumatic suspension system of the TUB-Trac

The hydro-pneumatic chassis suspension was modeled as shown in Fig. 2. For this step, all important hydraulic resistances of the system as well as the dynamics of the damping valves were taken into account.

As mentioned above, the model was validated using test results. This allows a good representation of the vertical dynamic behavior of the TUB-Trac. By way of example Fig. 3 shows the calculated and measured values of the rms-value of the rear axle and chassis acceleration and the dynamic wheel-load coefficient for the adjustable damping levels ("PV" values: 3 very high, 9 very low damping) of the TUB-Trac based on the ISO smoother track [3] with a driving speed of 10 km/h.

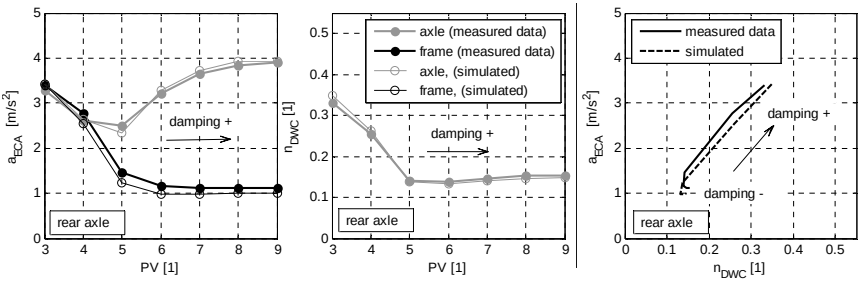

Fig. 3: Comparison of the calculated effective-value of the axle and chassis acceleration (a_{ECA}) and the dynamic wheel-load coefficient (n_{DWC}) based on simulation and measured data of the TUB-Trac (Track: smoother-Track, 10km/h, synchronous excitation (without implement))

The comparison of simulation and measurement results shows a good consistency of the results, which also can be shown in a comparable manner for the vehicle with attachments, as well as for the time domain of the accelerations and the suspension travel.

4. Simulation of the vertical dynamics of the TUB-Trac and comparison with other tractor models

The analysis of the vertical dynamics of the TUB-Trac using measured values or simulation results raises the question of how the TUB-Trac behaves in comparison to other tractors. However, a direct comparison with other vehicles is difficult for several reasons. On the one hand, a comparable vehicle would have to be modeled in a similar modeling depth, which is often not possible due to the unavailability of required data. On the other hand, it is usually not appropriate to compare different vehicle concepts if different requirements and targets determine the technical implementation of the vehicles. Consequently, the following compari-

sons will be based on vehicle models whose basic design (mass distribution, geometry) corresponds to that of the TUB-Trac, and which differ only by the connection of the axles and the rear three-point linkage. Here, three models (A, B, C) depicted in Fig. 4 are presented.

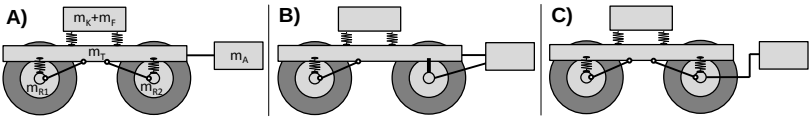

Fig. 4: Schematic structure of the compared tractor models

Model A represents the basic model of the TUB-Trac in its basic set-up. Model B represents the TUB-Trac with a rigid rear axle and model C shows a full-suspension vehicle with an attachment of the rear three-point linkage on the sprung rear axle. Thus, the model C corresponds to the unladen state of model A.

The comparison of the vehicle models is based on the effective values of the chassis accelerations and the dynamic wheel-load coefficient, which are plotted in a diagram (conflict diagram) and are abbreviated as ECA or DWC in the following. The starting point for the comparison of the models represents the conflict diagram of the TUB-Trac in the unladen state shown in Fig. 5. In this diagram, the calculated effective accelerations (ECA) of the front and rear structure as well as the dynamic wheel-load coefficient (DWC) were plotted for three different preload pressures (min.: 50 bar, basic set-up: 69 bar, max.: 180 bar) of the hydropneumatic suspension.

The preload pressure represents the static pressure in the piston side of the suspension cylinder of the unladen vehicle. The exemplary preload pressures of 50 and 180 bar correspond approximately to the permissible upper and lower limit of the preload pressures so that the load limit of the installed hydraulic components of the TUB-Trac using the available spring travel is not exceeded.

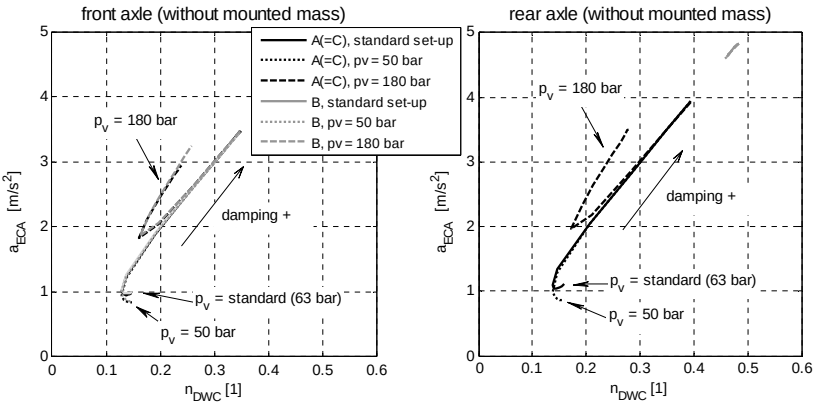

Fig. 5 Conflict diagram of the TUB-Trac (model A=C) and B for different damping and minimal and maximal permissible preload pressures (50 - 180 bar); ISO smoother track, V = 10 km/h

Looking at the left diagram of Fig. 6 which shows the conflict curves of the front chassis of the models A (= C) and B, it is demonstrated that these have almost identical shapes. Very high damping (curve start: top right) result in high acceleration and dynamic wheel-load coefficients. If the damping decreases, the ECA and the DWC also sink, regardless of the preload pressure. Only when the damping falls below a certain value the curves separate significantly. From this point, the ECA and the DWC of the chassis set-up with high preload pressure rise abruptly while they continue to decrease for the chassis with low preload pressure. In the latter case, the dynamic wheel-load coefficients increase again only with very low damping.

Similar patterns result for the rear part of the tractor model A (= C), due to the approximately symmetrical structure of the vehicle. Only the calculated ECA and DWC of model B are much higher due to the rigid rear axle attachment. Interestingly, the rigid rear axle has almost no effect on the shape of the front ECA and DWC for the road excitation considered here. It also demonstrates that a soft suspension and a correspondingly adapted damping improve the driving comfort as well as the wheel-ground contact for the road excitation considered here. However, it must be taken into account that a very soft suspension adjustment is usually unfavorable in terms of driving situations such as evasive maneuvers, braking processes, excitation through obstacles or a rough terrain.

To show the effect of an exemplified rear mounted mass of approx. 1000 kg on the characteristics of the ECA and the DWC of the TUB-Trac (model A) with its basic set-up, the calculated conflict curves for the laden and unladen model are compared in the conflict diagram of Fig. 6.

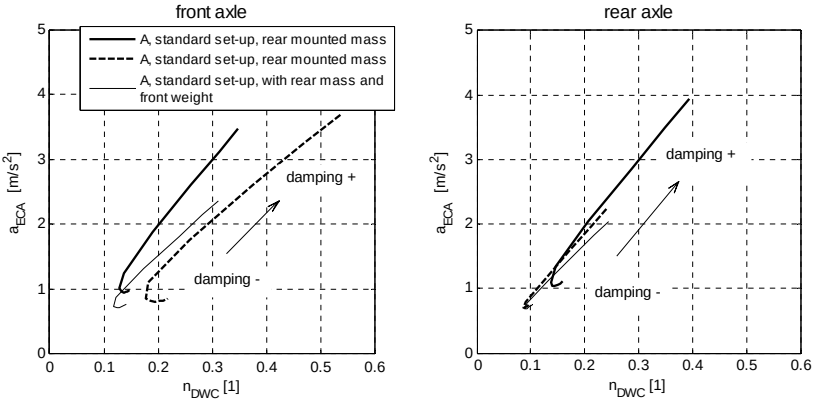

Fig. 6: Conflict diagram of the TUB-Trac (Model A) with standard set-up, with and without rear mounted mass; ISO smoother track, V = 10 km/h

By carrying a rear mounted mass the DWC of the front part of the TUB-Trac (model A) is increased because of the decreasing static wheel contact force whereas the effective chassis acceleration is only slightly affected. The rear part of the TUB-Trac is - as expected - affected more strongly by the mounting. In this simulation example, both the ECA and the DWC decrease significantly, which can in principle be regarded as positive.

The effect of an additional front attached mass is shown by the thin line in Fig. 6, using 1000 kg as an example mass. Due to the increase of the static wheel contact force of the front axle, the DWC of the front axle can be reduced. But also the ECA decreases, especially for higher damping values. However, the front attached mass has no particularly strong effect on the ECA and the DWC of the rear part of the tractor

Finally, the conflict curves of models A, B and C with a rear attached mass and rear-front-mass combination are compared in Fig. 7. For model C, a lower chassis damping leads to higher ECA than for models A and B. Overall, the DWC of the front axles have comparable values for all models. Because of the rigid axle connection, the DWC of the rear part of the tractor are significantly higher for model B than for models A and C. If only the DWC and the

ECA were used as an evaluation criterion, the chassis of model A would have the most favorable characteristics for all influencing variables that are considered in this example.

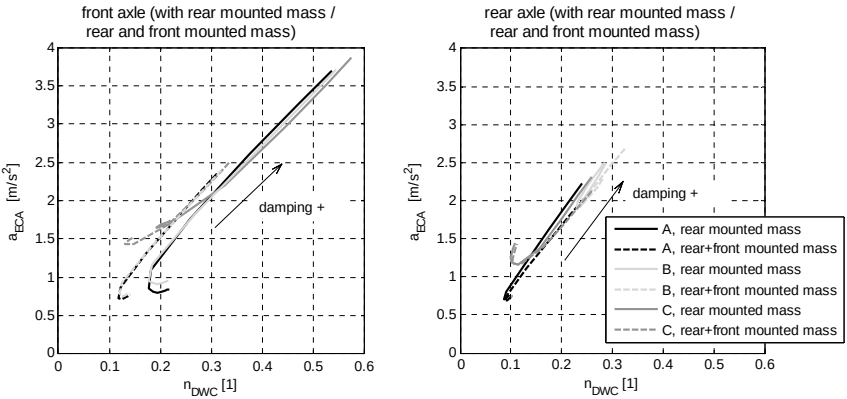

Fig. 7: Conflict diagram of models A, B, and C with standard set-up, with rear mounted mass respectively rear and front mounted mass; ISO smoother track, V = 10 km/h

Conclusion

The exemplary simulation results provided in this paper show a few possibilities offered by the underlying work to analyze the vertical dynamics of tractors. More specifically, an example simulation was introduced, which suggests a possible advantage of the chassis concept of the TUB-Trac in terms of the resulting chassis accelerations and the wheel-ground contact when attaching masses on the tractor such as implements. Further studies that are required to evaluate and improve the performance of the TUB-Trac are an integral part of the current work.

References

[1] HAMMES, Stephan: Entwicklung eines semi-aktiven Federungssystems für hydropneumatisch vollgefederte Traktoren. Dissertation. 1., Aufl. Aachen : Shaker, 2011 (Forschungsbericht Agrartechnik des Arbeitskreises Forschung und Lehre der Max-Eyth-Gesellschaft Agrartechnik im VDI (VDI-MEG) 502)

[2] KRÜGER, Jan: Kombinierte Regelung semi-aktiver Kabinen- und Aufbaufederungen zur Verbesserung von Komfort und Fahrsicherheit mobiler Arbeitsmaschinen. Dissertation. 1. Aufl. Aachen : Shaker, 2017 (Forschungsbericht Agrartechnik des Arbeitskreises Forschung und Lehre der Max-Eyth-Gesellschaft Agrartechnik im VDI (VDI-MEG) 568)

[3] ISO 5008:2002-07. 2002-07. Agricultural wheeled tractors and field machinery - Measurement of whole-body vibration of the operator

Efficient development by automatic calibration of tractor transmission control units

Dipl.-Ing. **Christopher Körtgen**, Institute for Machine Elements and Machine Design of RWTH Aachen University (IME), Aachen;
Gabriele Morandi, CNH Industrial, Modena;
Univ.-Prof. Dr.-Ing. **Georg Jacobs**, **Achim Kramer** M.Sc., IME, Aachen

Abstract

In this paper a software tool to reduce the resources for a calibration of a transmission control unit is presented. This has been reached by transferring the currently used manual parameterization to an automatic process. The automatic process is defined as a mathematical optimization problem and is split into three elements, the tractor behavior which represents the longitudinal dynamic of the tractor, the rating of the driving behavior by an appropriate algorithm which substitutes the subjective rating of a test driver and the multi-criterial optimization algorithm which chooses systematically new sets of parameters based on the driving behavior-rating. The development steps, the validation and the calibration results of the software tool are discussed in this paper.

Introduction

In the middle of the twenty-first century, the demand for food will be 70% higher than today. Due to limited available and suitable land, the necessary growth in production cannot be achieved by expanding the cultivated land, but by increasing the yield. Therefore, the existing land must be farmed more precisely. The working process quality is dependent on the precisely controllable tractor speed, which is widely achieved by modern power split transmissions. Optimizing the vehicle speed requires the appropriate selection of the ratio by choosing the mechanical gear and the swivel angle of the hydraulic pump by the transmission control unit (TCU) of the tractor. To achieve optimal behavior of the tractor, the TCU must be calibrated towards proper interaction of the mechanic, electric and hydraulic components. This calibration process must be carried out for each tractor model and repeated for every significant change of the drive train (e.g. introduction of a new engine generation). New engines are being developed on a regular basis driven by stricter international laws regarding allowable pollutant emissions.

Currently, the calibration of the TCU is done mainly manually, which means it is based on the subjective driving perception of an experienced calibration engineer on a test vehicle. The multiple parameters of the TCU will be optimized one after another to achieve the demanded driving behavior.

The frequent repetitions of this process as well as the high number of parameters which have to be optimized by the same repetitive technique, qualify the TCU calibration process for automation. This means that the mentioned manual steps to achieve a calibrated TCU must be transferred into a software environment. The automatic calibration process will substitute the driving tests with driving behavior simulations, the subjective rating of the driving behavior by the calibration engineer with an objective rating algorithm and the TCU parameter selection with an optimization algorithm.

In this paper, the development steps to achieve an automatic calibration process and the transfer to a software tool are shown. The validation of the software tool is described. Finally, results of the software tool on the tractor will be presented and discussed. The results demonstrate the benefit of the automatic calibration process.

Automatic calibration of a powersplit tractor transmission

In the beginning the main steps to achieve an automatic calibration is described. The calibration of the parameters of a TCU can be divided into three functions: the driving maneuvers, the classification of the driving behavior as well as the calculation of the new transmission parameters. Each of these functions must be automatically processed in a computer-assisted manner in order to be able to perform the entire transmission calibration automatically. There are two possibilities to quantify the driving behavior of the tractor automated. The first option is the simulation of the driving behavior in a tractor simulation model and the second option is the testing of the real tractor on a test bench. In the next step the driving behavior is analyzed and evaluated. For this purpose, characteristic values are developed which describe the desired driving behavior of the tractor. An example of such a characteristic value is the time required to reach a desired velocity. In the last step, improved transmission parameters are determined based on the evaluation of the driving behavior by a suitable algorithm [1,2]. For this purpose, a certain number of maneuvers with different transmission parameters are used as the basis. A repetition of the maneuvers with new and better transmission parameters and a subsequent evaluation of the driving behavior with the new transmission parameters result in further optimization parameters. By implementing this optimization into a loop it will produce better transmission parameters with every loop cycle. When the desired driving behavior has been achieved the loop will be stopped. The transmission parameters from the

final loop are submitted to the automatically calibrated parameter set for the transmission. Up to here, the development of the automatic calibration process is finished, but it is not suited yet for straightforward usage in industrial environments. The next step is the transfer of the process to a usable software tool for industrial environments.

Calibration Tool

In order to make the described automatic transmission calibration usable in industrial environments, the determined algorithms and evaluations are transferred into a simple and flexible calibration tool. It must be taken into account that the maneuvers of the tractor can be performed in a software environment as well as on the real tractor. The real tractor can be driven on a test stand or even on a test track. The tool should be used in all the described cases and therefore requires standardized interfaces (see Figure 1, input and output arrows). The input interface for example collects the driving behavior measurement data of the tractor or the simulation. The output interface defines and triggers (not on the test track, because of safety reasons) the desired maneuvers and transmits the transmission parameters to the TCU (software or real TCU). With this standardized interfaces the tool can be used in all the described cases.

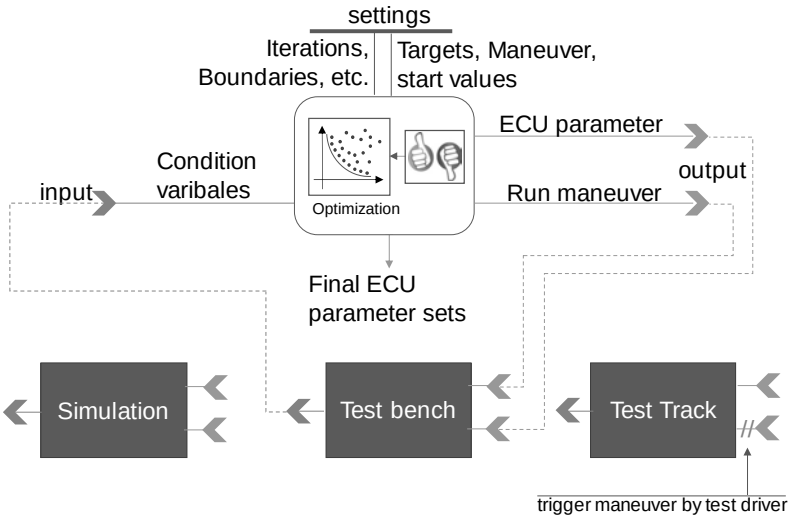

Fig. 1: Automatic calibration tool structure with standardized inputs and outputs

The cost of the transmission tuning in the simulation is much lower than that on a test stand because of fewer necessary resources. Therefore, a combination of simulation [3,4] and test rig calibration is used for resource-conserving transmission calibration. To benefit from the explained process, the transfer of calibration results from simulation calibration to test rig calibration is necessary. The results of each calibration loop are saved by the calibration tool and can be loaded into a different environment This not only enables the possibility of a resource efficient calibration but also a fail save option to continue a calibration if a test is abandoned. All the described functions can be controlled via a graphical user interface, which simplifies the learning of the tool. It is afterward applied to a real tractor to demonstrate its capabilities.

Tests

The capabilities of the automatic transmission calibration tool is validated by means of test rig tests. For this purpose, the institute's own 1MW dynamometer is used. The test setup is shown in figure 2.

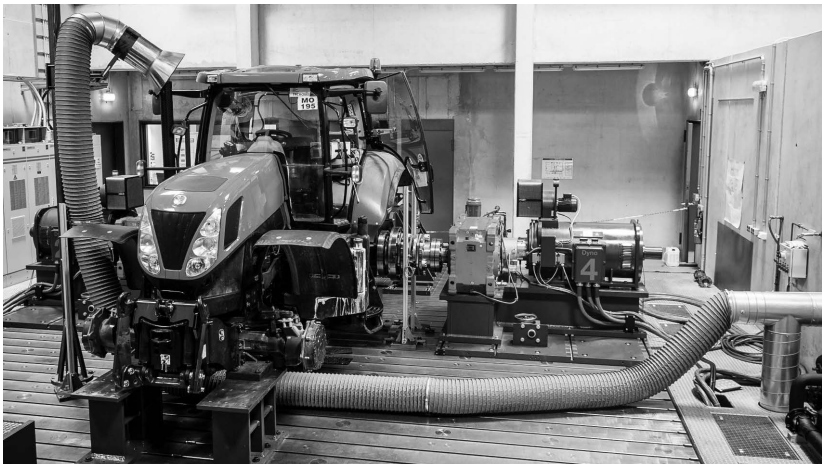

Fig. 2: Tractor Test Bench: Setup of the automatic calibration of the real tractor

The tractor is driven by the internal combustion engine. Two electric dynamometers with an additional gearbox are connected to the wheel hub of the tractor and apply the wheel based loads. The control of the tractor and the specification of the driving maneuvers are controlled by real-time hardware. Here, the desired maneuvers are automatically performed and the associated wheel loads are calculated by considering inertia, drag and work tasks. This can

be used to simulate various attachments, trailer loads or maneuvers. With this setup the new transmission parameters are validated in a wide range. The calibration tool automatically defines and starts the maneuvers, evaluates the results, determines new parameters which are automatically transferred to the tractor and used for the next maneuvers.

Results

The results of the tests are shown in the diagram below (figure 3). It shows a part of a typical driving cycle with different acceleration processes towards different target speeds. This driving cycle was carried out with different transmission parameters, which leads to deviating driving behavior and thus to different accelerations. The different transmission parameters are all part of one automatic transmission calibration process. The starting point of the transmission calibration is the red measurement curve. This shows a very slow acceleration and an unstable control behavior when reaching the target speed (overshoot). With every calibration loop pass the acceleration improves with simultaneous remaining stable control behavior. The automatic transmission calibration optimizes the various acceleration processes towards different target speeds at the same time and can also take different tractor attachments and weights into account.

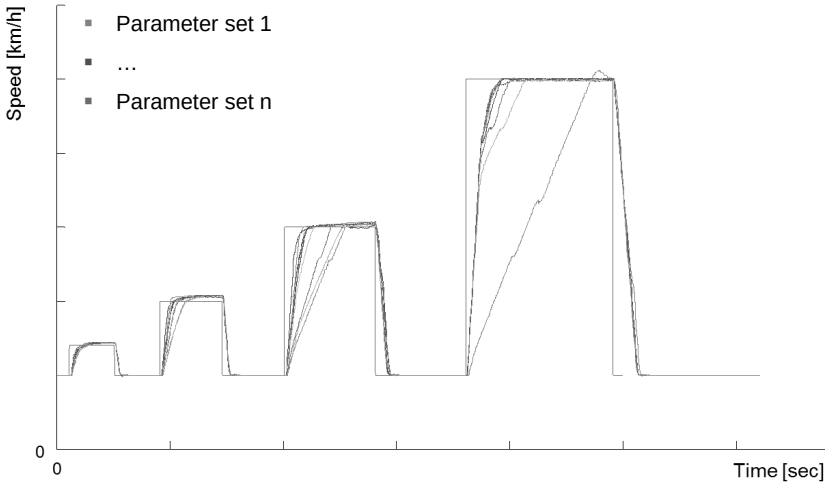

Fig. 3: Automatic calibration results of a typical driving cycle with different acceleration processes

The driving behavior of the tractor after the automatic transmission adjustment is comparable to the driving behavior of the serial tractor and could be achieved with reduced resource usage. The results are achieved within a day of testing and without the interaction of a person. The manual calibration process last usually around 2 weeks. Both durations are not considering the setup of the tractor for the test track or the setup of the test bench.

Conclusion

This paper shows an automatic transmission calibration tool. The results of this tool are applied on a power split transmission of a tractor. To transfer the current manual calibration process to an automatic calibration process the manual process is split into three elements. The first element is the driving behavior, the second element is the driving behavior rating and the third element is the optimization by choosing new parameter sets. In the previous process the driving behavior is represented by physical tractor tests and the rating and optimization is done by the calibration engineer in a manual, experience based manner. To automate this process, these three elements are transferred to a software environment. The longitudinal dynamic of the tractor is represented by a tractor simulation, the driving behavior-rating algorithm substitutes the subjective rating of a test driver and the optimization algorithm systematically chooses new sets of parameters based on the driving behavior-rating. These software elements are connected together to form an optimization loop, which is used for the automatic parametrization process of the transmission control unit. Afterwards, this process is transferred into a usable software tool for industrial environments and different use cases such as simulations, test bench tests or driving tests as well as combinations out of these three. A validation of the software tool was done on a dynamometer test bench and has shown promising results. With the automatic transmission calibration tool the resources of the transmission calibration could be reduced to one day of test rig testing and with this the development process of new tractors becomes more cost effective.

[1] Deb, K., Pratap, A., Agarwal, S., Meyarivan, T.: A Fast Elitist Multi-objective Genetic Algorithm: NSGA-II, IEEE Transactions on Evolutionary Computation 6, 2002.

[2] Kahlbau, S.: Mehrkriterielle Optimierung des Schaltablaufs von Automatikgetrieben, Dissertation der Brandenburgischen Technischen Universität, Cottbus, 2013.

[3] Matthies, F.: Beitrag zur Modellbildung von Antriebssträngen für Fahrbarkeitsuntersuchungen, Dissertation der TU Berlin, Berlin, 2013.

[4] Körtgen, C.; Morandi, G.; Jacobs, G.; Straßburger, F.: Automatisierte Parametrierung der Getriebesteuerung eines leistungsverzweigten Getriebes. ATK, Aachen, 2015.

Determining saving potentials in a tractor drivetrain using a simulation model and measured operating data

M.Sc. **Kerstin Ritters**, Dipl.-Ing. **Philipp Winkelhahn**,
Prof. Dr. **Ludger Frerichs**,
Institute of Mobile Machines and Commercial Vehicles,
Technische Universität Braunschweig;
Dipl.-Ing. (FH) **Bastian Kriebel**, CLAAS KGaA mbH, Harsewinkel

Abstract

To increase the efficiency of tractors purposefully, it is beneficial to analyse the power flow and thereby to identify significant sources of losses in the powertrain for different operating states. The use of simulation models is appropriate to be able to recognise losses already in an early development stage. To find potentials for energy savings in the real use of the tractor, it is essential to simulate typical application cases with representative loads. For this, a high number of data sets for different operation modes must be analysed. After identifying critical power sinks, counter-measures can be developed and implemented into the simulation model. Since those measures may influence the tractor speed, it is necessary to transfer the time-based model and input data to path-based ones. The path-based simulation results can be compared and a quantitative effect of the measure can be assumed.

1. Introduction and motivation

The minimisation of fuel consumption in applications with attached implements is a matter of special importance for the development of tractors. The manufacturers take optimisation measures both on component level and system level to increase the efficiency in the entire powertrain. For this purpose, the knowledge of typical cases of operation and performance requirements of each single consumer is fundamental.

In the scope of a research project, a modular simulation model of a tractor drivetrain was built up and validated. As input data for the model, measurement data of real machines is used, so that realistic load profiles can be simulated. Representative data sets have to be extracted from of a high number of measurements. To investigate the effect of technical optimisation measures with the model, it is necessary to transfer both model and inputs from time-based to path-based. As an example, simulation results with different driving velocities will be shown.

2. Simulation model

The simulation model, which was built up, represents the drive train of a Claas Xerion 4000 with a nominal engine power of 308 kW and the power split transmission ZF ECCOM 5.0 Overdrive. The main structure and components of the model were presented in 2016 [1]. Focus of this paper will be on its validation.

The model is built up in Matlab/Simulink, using the Simscape Toolbox. To be able to change single drivetrain components, the model is designed modularly. Besides the physical components, like engine, transmission or axes, there are some control and calculation blocks. The model inputs include driver requests, demands of power units and auxiliary consumers, environmental conditions and the drag force of the implement. Most of the inputs are derived from data, which were recorded on machines in real applications with a frequency of 1 Hz. That means, quite realistic scenarios can be simulated and analysed. In this data, the drag force, which has a high influence on the power demand of the tractor, is not included. To determine the forces, a controller is defined, which uses the drag forces as manipulated variable to obtain the same power request at the tractor engine as it was measured, see figure 1.

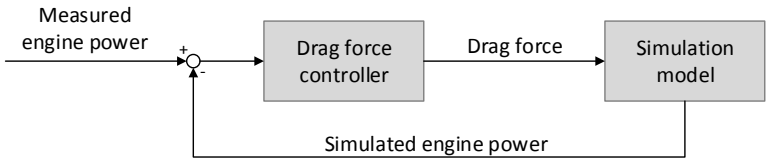

Fig. 1: Block diagram of the drag force control unit

The validation of the simulation model is based on measurements, which were done by the Deutsche Landwirtschafts-Gesellschaft (DLG) in the course of the DLG-Powermix [2]. The main advantages of that data are, the drag force was measured and the fuel consumption was detected very precisely. By using the DLG-data, it is possible to validate the model in three steps:

- Validation of losses and fuel consumption without drivetrain control unit and drag force control unit
- Validation of drivetrain control unit without drag force control unit
- Validation of drag force control unit (whole model)

In this paper, only the results of the last step are shown. The main value for the evaluation of the simulation model is the specific fuel consumption of the tractor, as long as the driving task is fulfilled. Since the built up model is able to represent every challenge of the Power-

mix, the specific fuel consumption can be used as evaluation parameter. The simulation results and the measurement of the DLG are compared in figure 2.

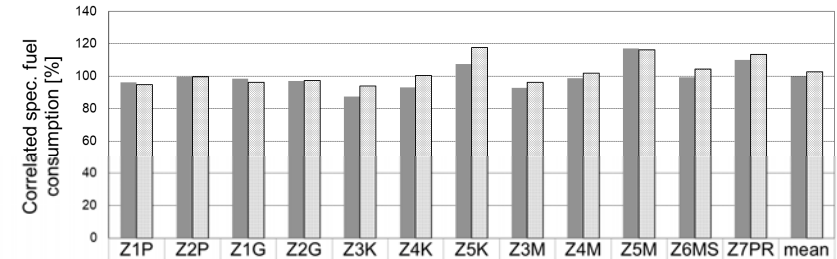

	Z1P	Z2P	Z1G	Z2G	Z3K	Z4K	Z5K	Z3M	Z4M	Z5M	Z6MS	Z7PR	mean
DLG	96,23	99,62	98,49	96,98	87,55	93,21	107,5	92,83	98,87	117	99,25	110,2	100
Simulation	94,8	99,7	96,3	97,5	94,1	100,7	117,7	96,3	102,0	116,2	104,5	113,6	102,8

Fig. 2: Comparison of the specific fuel consumption between measurement and simulation of the DLG Powermix cycle (cycle definition in [2])

With a mean deviation of 2.8 %, the simulation model produces very good results. The main reasons for the differences are, the DLG-Powermix is performed on a test track, which contains curves, but the simulation model at present does not include transverse dynamics. Furthermore, the data basis for the calculation of some components losses is limited, hence, in some operating points the losses are represented only vaguely. Nonetheless, the model can be used to do further investigations on the power flow in the drivetrain and to show potentials for the reduction of fuel consumption.

3. Application cases

With the validated simulation model, different applications can be analysed. In this paper, two different applications are considered: soil tillage with only pulling tasks and liquid manure application with a combination of pulling tasks and hydraulic power requirements (pump fixed to transmission-pto).

To find representative data sets of the tractor, a high number of data files is necessary. For both applications about 2500 data sets on two machines were analysed. Each data set and measurement begins when the tractor is turned on and it ends when it is turned off. The data was recorded over a period of 1.5 years. It can be assumed that both machines were used either for soil tillage or liquid manure application solely, but there is no information about the attached implement.

The recorded data contains approximately 160 values from the CAN bus, which were logged with a constant frequency of 1 Hz. For the considered applications, the frequency is suffi-

cient, since quasi-stationary operation modes will be analysed. For the soil tillage, four different operation modes will be distinguished: the transport journey to the field, the working process itself, the turning and standstill. The liquid manure application can be divided into journey, application and refilling of the slurry tank.

The data evaluation was automated by a Matlab script. At first, a list of all data sets is generated, which contains, inter alia, the name and the size of each file. The file size is proportional to the recorded time and in a first step all data sets, which contain only a small amount of data, can be removed from the list. If all data sets, which are smaller than 1 MB (approx. 38 minutes of recorded time), are removed, there are 660 files left. In the next step, the data of those 660 files is loaded to the Matlab workspace. Depending on the required hydraulic power, it can be differentiated between soil tillage and liquid manure application data sets. For each application, a new list of files is generated. To identify the single operation modes, the conditions in table 1 are used. Data sets, which cannot be assigned to any application or operation mode, or where data was not recorded correctly, are deleted from the list and not taken into account in the further steps.

Table 1: Conditions to identify operation modes

Application	**Operation mode**	**Condition**
Soil tillage	Standstill	Velocity < 0.5 km/h
	Journey	Velocity > 15 km/h, 3-point hitch position >= 50 %
	Turning	Front steering angle > 50 %
	Working	3-point hitch position < 50 %
Liquid manure application	Journey	Hydraulic power < 5 kW
	Refilling	Hydraulic power >= 5 kW , velocity < 1 km/h
	Application	Hydraulic power >= 5 kW, velocity >= 1 km/h

When the operation modes are identified, the percentage of time of each mode can be determined. Furthermore, the mean values of specific data, like the velocity, the power of the engine or the hydraulic power, can be calculated. Now, for each application those mean values and the average proportional time is known. In the last step, the average values are compared to the values of each file and the reference data sets can be identified. For the best sets a data sheet with main information is created and the user can finally choose out of a small number of preselected data sets manually.

4. Time-based and path-based model and data

The procedure of determining saving potentials with the simulation model can be seen in figure 3. With the representative data set, which is directly derived from the measurements, it is possible to analyse typical power flows in the tractor drivetrain. For this purpose, a time-based simulation is sufficient. The power flow reveals losses in the drivetrain, which may be reduced by optimisation measures. Those measures could be taken on component level or system level or they could optimise the operation strategy. Depending on the measure, the speed of the tractor might change and by that, the power demand changes as well. To take this into account, it is necessary to transfer the time-based data to path-based data.

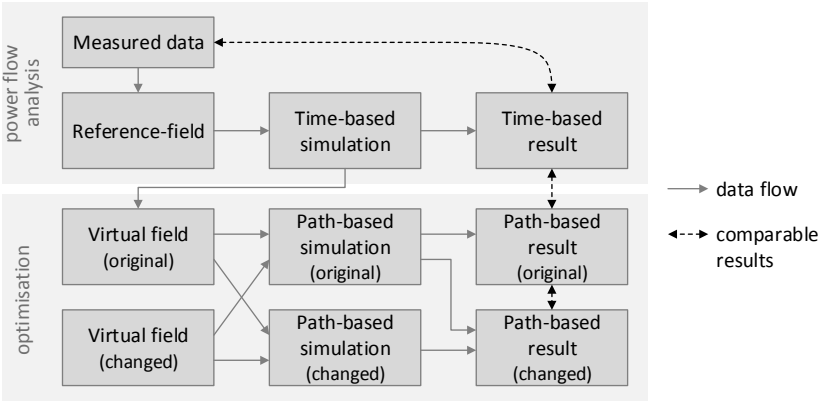

Fig. 3: Approach to determine and estimate saving potentials by use of the simulation model

To show the need of the path-based simulation, an exemplary result of a measure can be seen in figure 4. The tractor performs soil tillage with a high engine load. If the needed time to cultivate a field is not decisively, the tractor speed can be reduced to save fuel [3]. Therefore, in figure 4 the original path-based result (grey) and the result with a reduced velocity demand (black) are shown. Since the tractor speed is reduced, it needs more time to drive the same track and the power requirements decrease due to the lower speed. With the lower speed, the fuel consumption per area is reduced by 2.5%.

5. Conclusion and outlook

Based on data, which was measured with two system tractors in different applications over a period of 1.5 years, representative data sets can be found and automatically analysed. For

this, the applications and operation modes within an application are identified by certain conditions, like current velocity, power requirements or position of 3-point hitch or wheels. For each operation mode an average velocity and engine power requirement can be calculated and used as reference value. Finally, the data sets can be compared to the mean values and by this a reference data set can be found.

With the reference field and a simulation model of the tractor, typical operation points can be analysed with regard to the power flow and losses in the drivetrain. To show saving potentials by measures, which may affect the driving speed and the drag forces, the original time-based model and model inputs are transferred to path-based ones.

In the next step, the power flow and power losses will be analysed by use of the simulation model and the representative data sets. Based on the results of the analysis, different optimisation measures will be developed and implemented into the model. With the results, the effect of the measures can be estimated.

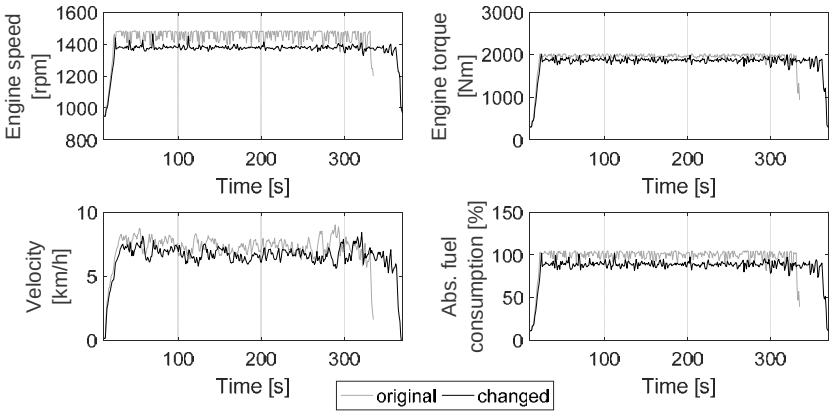

Fig. 4: Path-based simulation results for soil tillage with original speed demand and 90% speed demand

6. References

[1] Winkelhahn, P., Frerichs, L., Kriebel, B.: Antriebsstrangmodellierung am Beispiel eines Systemtraktors, VDI-MEG Tagung LAND.TECHNIK 2016, Köln 22.-23.11.2016, S. 99-104

[2] http://www.dlg.org/vehicletechnology.html, accessed 08.08.2017

[3] Schreiber, M.: Kraftstoffverbrauch beim Einsatz von Ackerschleppern im besonderen Hinblick auf CO_2-Emissionen, Universität Hohenheim Diss. 2006

Testing and Benchmarking a Powertrain with Independent Wheel Control for Heavy Machinery

Dipl.-Ing. **Danilo Engelmann**,
M.Sc. **Marcel Reinhold Unger**,
Prof. Dr.-Ing. **Marcus Geimer**,
Karlsruher Institut für Technologie Karlsruhe

Abstract

This paper treats about “Line Traction 3” (LT3), which is a mechatronic driveline for heavy machinery like agricultural tractors, combines, or wheel loaders. LT3 is expected to improve the performance and augment new functions to the existing ones of conventional drivelines. For testing and validating this assumption for LT3 and similar driveline systems, we introduce “MOBiL” , a hardware-in-the-loop method adapted for mobile machinery. The MOBiL method will be explained to bring out the differences in modelling and test procedures compared to on-road hardware-in-the-loop methods. Then, we will present the validation of the LT3 driveline in an agricultural context by using the MOBiL method. A discussion of the relevant results obtained for tractors and wheel loaders will be followed by a final summary.

Motivation for independent wheel control

Mobile machinery are machines with the capability to work and drive. Both functions are propelled via separate powertrains, each of them having significant power flows. This is the definition according to [1] (Fig.1).
Continuous efforts are being made to optimized these two powertrains. They interact to fulfil the tasks of the vehicle. The driveline itself is adapted for each machine and its special uses. Besides the efforts to reduce losses, engineers also are trying to augment the functionalities of the drivelines in such a way that the machine fits precisely into their intended tasks. In the field of agricultural engineering, this often means to not only improve efficiency, but also to

optimize the traction of tractors, combines, or wheel loaders. In most cases, these are conflicting objectives [1].

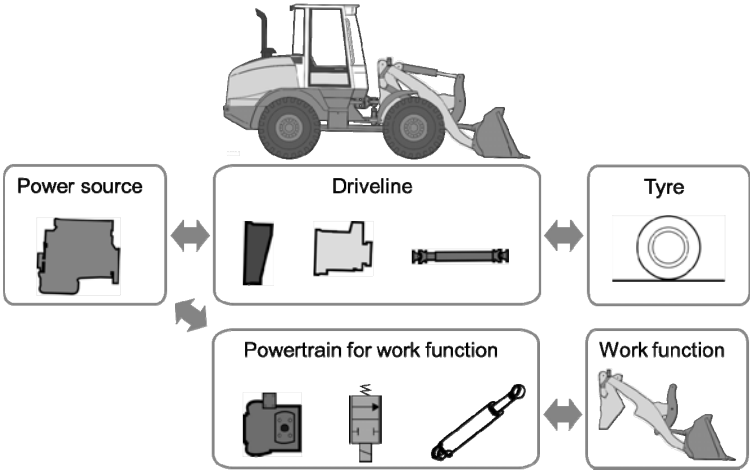

Fig. 1: Generic mobile machine with powertrains

To give an example, mechanical drivelines provide high efficiency, but under poor traction conditions, only the amount of torque of the wheel with the poorest traction can be transmitted to all other wheels. To avoid loss of traction, state-of-the art heavy machines have the possibility to lock their differentials or, like in the case of tractors and wheel loaders, the longitudinal distribution is equipped only with a fixed gear stage acting like a locked differential. This mode of operation causes problems in that each wheel runs at one and the same speed, and turning corners with the vehicle causes tensions in the driveline [2] or forced slip on the tyres. Hence, the requirement arises to drive each wheel separately and independently from the other ones. One possible way is to design vehicles with hydraulic or electric wheel hub drives. In this case, each wheel has his own motor to drive it. However, also such kind of driveline needs gear boxes/stages when used in mobile machinery to provide the wheels with the required torque. In addition, drivelines of that type have more losses under certain circumstances e.g., in the case of a mechanical equivalent and an increased unsprung mass, especially when the possible estimated power for each wheel is near to the system power of the vehicle due to the high mass of the required motors.

In conclusion, a possible solution to obtaining an efficient driveline with maximum traction would be a mechanically locked driveline with the same characteristics as those of wheel hub

drives. Such driveline would transfer the maximum amount of torque to the wheels at maximum efficiency without building up tensions or slip by driving through curves.

Mechatronics allows to control each wheel on mechanical drivelines

The Linetraction 3 (LT3) driveline is the attempt to meet the requirements set out in the previous chapter. It is a mechanical driveline which could be propelled by any kind of engine or motor. It is quite similar to conventional drivelines but there are no differentials, thus it behaves like a locked powertrain providing the maximum traction in every driving situation. However, with the differentials being absent, the driveline needs a new possibility of realizing different speeds of the wheels when cornering to avoid tensions and slip. This is achieved by means of superposition gears in the lateral distribution of each driven wheel. Due to the missing mechanical control abilities of the differentials, it is necessary to control the superposition of the speeds separately by a dedicated electrical control unit (ECU).[3]
In the case of conventional drivetrains using differentials, the relevant strategy and behaviour are determined by the design of the gears of the differentials. With the control of the driveline by an ECU, more than one possible strategy can be implemented depending on the driving situation or driver input via human machine interfaces (HMI) [4]. The mechanical driveline parts represent the mechanical basic system, which uses hardware or software sensors, information processing in the form of an ECU, and actuators for the superposition gears and hence fulfils the requirements of a mechatronic system according to the definition given in VDI 2206 [5].

From X in the loop to the MOBiL method

According to the V-model defined in VDI 2206, which is also used in the LT3 development process, it is necessary to have a method to appropriately validate the properties once defined at the stage of system design. One commonly used validation method is the XiL concept. In this validation concept, for each step at the integration stage of the V model, validated models are used for validating the respective unit under testing. This method was first introduced in 2008 [6].
The use of validated models is essential to this method, since they replace the physically not existing or not available systems that interact with the physical system under testing. Depending on the integration level at which analyses are carried out, more or less detailed models are needed.[7]

The use of validated models of the simulated system is a key point. Normally, these models are built up in the macro cycle of the V-model following the modelling section starting during the system design phase and continuously supporting the development process.

MOBiL - A test method optimized for mobile machinery

The XiL method is a powerful tool for validation. It is often used in the passenger car industry during development processes. The original concept of XiL, however, has to be adapted for application to the investigation of heavy machinery. As stated above, mobile machines have the capability to drive and work, with both functions being propelled via separate powertrains. Hence, it is necessary to augment the existing work frame of XiL, for example for realizing the parallel structure of powertrains known from real machines.
The MOBiL method is adapted to these needs of mobile machinery.
It allows to build up a structure combined from simulation models and real units under testing. These systems, real or simulated, interact as would the systems in the real setup. [8]

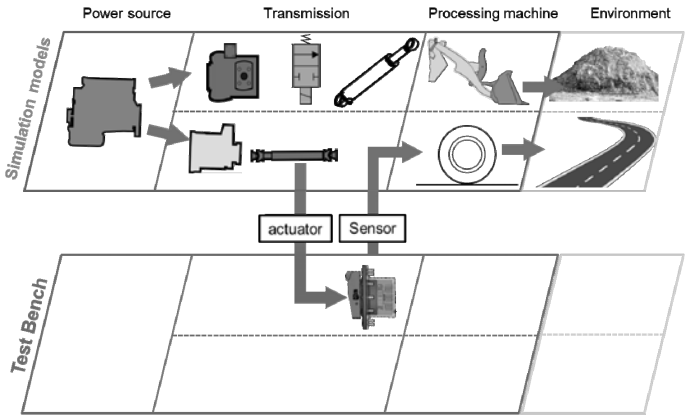

Fig. 2: “MOBiL“ effect chain for LT3

This is how work function and driveline interact, e.g. in wheel loaders: When the wheel loader shovel penetrates a bulk pile, it generates forces and interacts with the chassis which then causes a dynamic shift in axle load influencing the driveline situation driveline (Fig.2). The same is valid for e.g., tractors pulling a plough.

A second important point is to train the operator for the MOBiL method: He will no longer act only as driver as in the case of XiL but must be able to act as machine operator. The operator closes the machine control loop to enable the machine to fulfil the work task.[8]
This means that the computer-generated operator needs to be enhanced for operating work and driveline by acting like a realistic machine operator. For human operators, this implies that the typical machinery HMIs and visualisation have to be implemented to correctly close the control loop of the machine against the operator.

Testing the line traction 3 driveline with MOBiL

The basic function of the superposition gears, as the essential elements in the LT3 driveline, was tested successfully in a first project. This means that the validation was successful at the subsystem level according to VDI 2206. [4]
The next step is the validation in a vehicle such as a tractor, combine, or wheel loader.
Equipping a machine of each kind, however, would cause major costs and a big effort of time. Here, a validation method like MOBiL can exert a “frontloading” effect on the project. Frontloading means that validation of the functions and the proof of concept for each type of machinery can be achieved within a shorter period of time at lower costs.[8]
As mentioned before, the aim is to test the line traction superposition gear during typical driving situations in mobile machines.

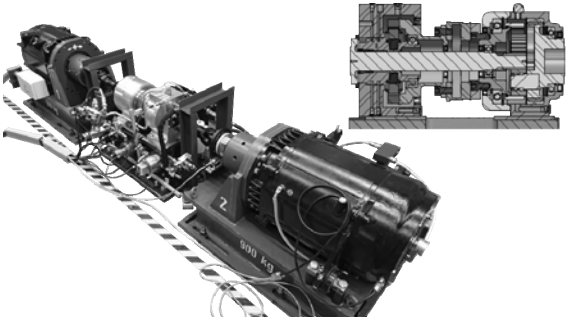

Fig. 3: Line Traction 3 unit on the test bench, and section of the LT3 unit

The superposition gear, here the unit under testing, is implemented with an own ECU on the test bench. The electric machines of the test bench drive and break the unit according to the values calculated by the real-time computer on which the simulation models run. The test bench machines and the control unit of the LT3 unit communicate via high- speed CAN bus

with the real-time computer. Hence, the same unit can be tested as if mounted on different machines only by changing the machine model on the real-time computer (Fig. 3).[8]

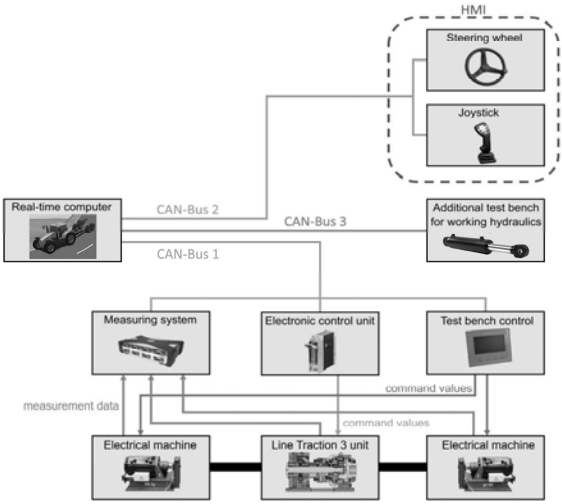

Fig. 4: MOBiL test bench architecture

Also, different control strategies can be tested easily by chancing the settings on the ECU of the unit or chancing the CAN communication between the real-time computer and the ECU.
In addition, the interaction of human machine operators with potential new assistance systems can be tested through the new degrees of freedom of the driveline.

Validation of Line Traction 3 Driveline

A first step to proving the concept is to validate the algorithm which calculates the necessary differential speeds for each wheel (Fig.5). It should be able to calculate the correct speeds without building up forced slip.

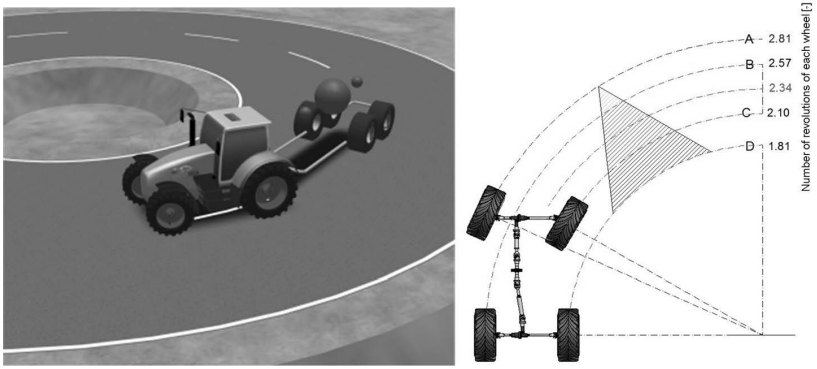

Fig. 5: Right: Tractor model during steering, and left: Calculated differential speeds

The tested LT3 unit (speed controlled) is compared in Figure 6 with other simulated drivetrains in which the operator tries with a wheel loader to reach 20 km/h in a curve with a curve radius of 10 m and a constant μ =1.. The locked differential is not able to produce the necessary differential speed for the wheels, and suffers a high slip. The differential and both LT3 drivelines are able to compensate the wheel speeds. As seen, both of the possible control modes for the LT3 driveline fulfil their intended purpose. After testing the basic functions, more advanced strategies which use the ability to control each wheel independently can be investigated. One possible strategy is yaw control, for example to optimize and improve avoiding manoeuvres (Fig 7). To improve turning manoeuvres, the skid steer mode could be combined with the normal steering to reduce the turning radius of the vehicle, as seen in Figure 8.

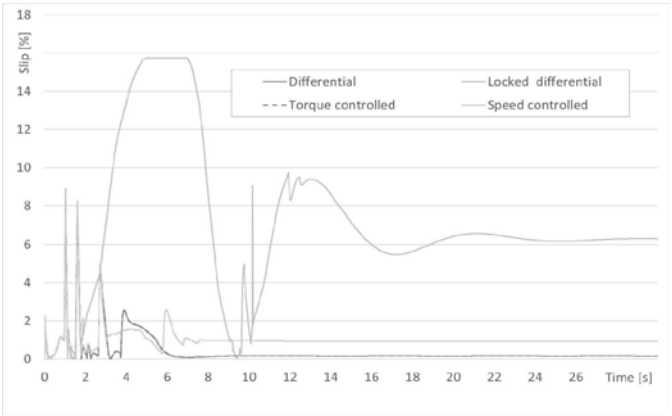

Fig. 6: The diagram shows slip over time for different drivelines

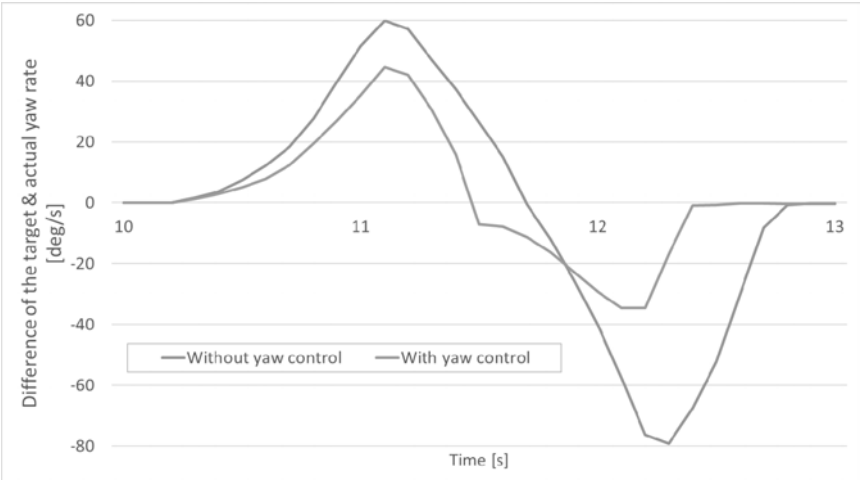

Fig. 7: Yaw rate difference with and without yaw control

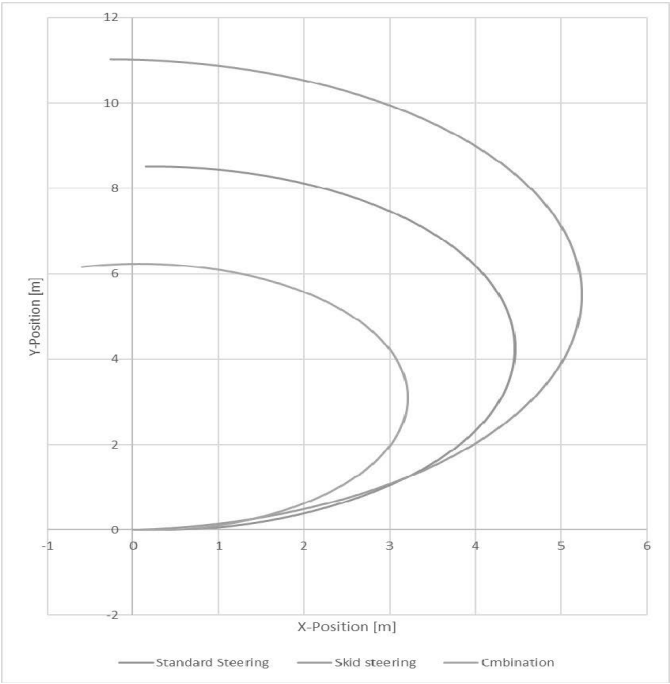

Fig. 8: Turning radii with different steering types

Summary & Outlook

The MOBiL method is the first attempt to introduce XiL validation also to the field of mobile machinery. It allows to test the components and subsystems in a holistic way. In the present LT3 project, MOBiL helps to achieve a massive frontloading in the development process because it allows to test the LT3 units in different generic types of mobile machines due to the use of validated simulation models so that no physical prototypes are needed. This reduces costs, now and in future projects. The MOBiL method allows an early proof of concept at the level of in-vehicle use. Now, customized and representative cycles and scenarios for each machine type in the context of LT3 can be developed and tested to provide a realistic work scenario for each machine. This will continue to show the advantages of mechatronic drivelines such as LT3. It also provides the possibility now to test critical driving situations of the machines to achieve an improvement in such dangerous situations without risking damage to the machines or life of the operator. In addition, the interaction of

the machine with the operator can be investigated and the results obtained allow taking a deeper look into the field of HMi.

Acknowledgement:

The authors would like to thank the Federal Ministry for Economic Affairs and Energy for funding the project based on a decision by the German Bundestag. Special thanks also go to ifm electronic for supporting the project.

References

[1] Geimer, M. u. Pohlandt, C.: Grundlagen mobiler Arbeitsmaschinen. Karlsruher Schriftenreihe Fahrzeugsystemtechnik, Bd. 22. Karlsruhe, Hannover, Karlsruhe: KIT Scientific Publishing; Technische Informationsbibliothek u. Universitätsbibliothek 2014

[2] Huber, A.: Ermittlung von prozessabhängigen Lastkollektiven eines hydrostatischen Fahrantriebsstrangs am Beispiel eines Teleskopladers. Zugl.: Karlsruhe, KIT, Diss., 2010. Karlsruher Schriftenreihe Fahrzeugsystemtechnik, Bd. 2. Karlsruhe, Hannover: KIT Scientific Publishing; Technische Informationsbibliothek u. Universitätsbibliothek 2010

[3] Engelmann, D., Müller, J., Müller, W. u. Geimer, M.: Anforderungen an den Antriebsstrang eines schweren Nutzfahrzeugs. ATZoffhighway 8 (2015) 2, S. 26–37

[4] Engelmann, D., Müller, W. u. Geimer, M.: Project “Line Traction 3” - Mechanical driveline with active wheel hubs. In: Getriebe in Fahrzeugen. Triebstrang, Integration, Elektrifizierung : mit Fachausstellung = Drivetrain for vehicles 2016 ; drivetrain, integration, electrification : with exibition. VDI-Berichte, Bd. 2276. Düsseldorf: VDI Verlag GmbH 2016, S. 731–742

[5] VDI-Richtlinien VDI 2206. *Entwicklungsmethodik für mechatronische Systeme*

[6] Düser, T., Ott, S. u. Albers, A.: X-in-the-Loop als integrierte Entwicklungsumgebung von komplexen Antriebssystemen. In: 8.Tagung Hardware-in the- Loop-Simulation Haus der Technik,. Kassel 2008

[7] Düser, T.: X-in-the-Loop - ein durchgängiges Validierungsframework für die Fahrzeugentwicklung am Beispiel von Antriebsstrangfunktionen und Fahrerassistenzsystemen. 2010

[8] Brinkshulte, L., Engelmann, D., Geimer, M. u. Iwanicki, M.: MOBiL. Eine auf mobile Arbeitsmaschinen optimierte Prüfmethode. Hybride und energieeffiziente Antriebe für mobile Arbeitsmaschinen. 6. Fachtagung, 15. Februar 2017, Karlsruhe. Karlsruher Schriftenreihe Fahrzeugsystemtechnik, Band 50. Karlsruhe: KIT Scientific Publishing 2017, S. 173–194

Development of a high performance continuously variable drive for mobile agricultural and construction machinery

Dr.-Ing. **Falk Hantschack**, GKN Walterscheid Getriebe GmbH, Sohland;
Dr.-Ing. **Robert Rahmfeld**, Dipl.-Ing. **Jens Bagusch**,
Danfoss Power Solutions GmbH & Co. OHG, Neumünster;
M.Sc. **Andreas Meyer**, Kramer-Werke GmbH, Pfullendorf;
Dipl.-Ing. **Egbert Dohm**, GKN Walterscheid GmbH, Lohmar

Abstract

The development of mobile agricultural and construction machinery is more and more driven by the enhancement of machine performance, optimization of system efficiency and increase of user comfort. GKN Walterscheid, Danfoss Power Solutions and Wacker Neuson recognized this market demand and have developed a high performance continuously variable drive in a close cooperation approach. GKN took the responsibility for the design, the manufacturing and the test bench validation while Danfoss supplied the hydraulic components and provided technical support and expertise regarding system integration and vehicle start up. Wacker Neuson took the responsibility for functional and durability testing in the vehicle. The new hydrostatic propel drive is be able to transfer a power of 130 kW and be suitable for vehicles with corner power demand up to 1000 kW. Although this high performance step hat to be realized, the dimensions had to be kept comparable to the existing drive line systems. This has been achieved by using a new 370cc bent axis motor kit, based on the high efficient 45° synch joint technology. The large conversion range of the 45° technology makes it possible to drive through the entire machine speed range without shift process. This offers on the one hand high user comfort and on the other hand advantages from the energy efficiency point of view. Especially power management systems which need consider the full vehicle approach can take advantage of this single motor solution. Enhanced efficiency can be achieved by using the dry case capabilities of the new unit. Furthermore the integration of the standard bent axis motor family controls and loop-flushing components reduced the required development effort and time, and offers various control options with a perfect fit to available controller and software interfaces.

1. Motivation, requirements for a new propel drive for mobile agricultural and construction machinery

Mobile working machines place ever higher demands on their propel drive. The fields of application of telehandlers and wheeled loaders have become so divers that now large distances are travelled, heavy loads pulled and high-dynamic and long Y-cycles are realized in material handling at the same time. A high traction force, efficient driving at high speeds and good dynamics are thus indispensable customer requirements for state-of-the-art propel drives.

In the past, continuously variable hydrostatic propel drives have become established on smaller compact machines that ensure efficient control of the working task at hand, and convince through their harmonious working cycle. For machinery with a higher tare weight from 7.5t and outputs of up to 130 kW, a classical hydrostatic solution with one motor and one pump is not yet feasible. This is where hydrodynamic converters, manual transmissions, and transfer cases for two motors with a switch-off are currently being used -- along with an increased usage of shift-on-fly solutions. Time and again, engineers consider power-split solutions in this range of performance. The Wacker Neuson Group was unhappy with this situation. On the one hand, it is possible to use the torque converter technology and thus not be able to take advantage of a hydrostatic drive, or to accept a trade-off for continuously variably operation. This trade-off is, however, unfavourable in certain operating conditions, and is also subject to wear and tear through repeated shifting processes. Power-split solutions are not available at present and, in this performance segment, they would hardly be economically justifiable for the customer.

Customer needs for:

- High traction forces of up to 8.5t,
- High speeds of 40 km/h while maintaining traction force,
- High efficiency at typical working cycles
- Very good reversibility
- And unconditional reliability

are demanding the development of new solutions for the propel drive of Wacker Neuson machinery. Along with the partners GKN and Danfoss, a new propel drive solution has been developed for this range of performance that will perfectly meet customer needs while maintaining the benefits of a hydrostatic drive at full continuously variably operation.

2. Underlying technology: a 45° wide angel axial-piston machine

The 45° bent axis technology from Danfoss is well established in the market for CVT transmissions. To meet the trend to bigger machines with higher power requirements, Danfoss extended the 45° portfolio by a new rotating group with 370cc/rev.

Kit Design

The Danfoss 45° rotating group design is based on the sync-joint-technology known from Danfoss 32° bent axis motors. The 45° technology offers superior efficiency compared to any available rotating group worldwide. In addition, the rotating group is designed for dry case operation (no oil in the housing around the unit), which reduces the churning losses. The overall peak efficiency is at 97%.

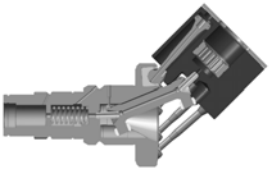

Fig. 1: 45° Rotating Group for ICVD

Table 1: Parameters of 370cc Rotating Group

Key Design Parameters 370cc Rotating Group	
Displacement	370cc
Max. angle	45°
Max. working pressure	550 bar
Rated application pressure	420 bar
Rated flow	551 l/min

Traditional bent axis motor designs utilize a valve-segment design (Fig. 2) for the connection between the rotating parts and the non-moving housing. This design allows a maximum angle range of approx. 0°-32°. Use of larger angles requires a yoke-design (Fig. 3), which can swivel from 0° to 45° in positive and negative direction. Using yokes also allow bigger cross sections which reduces the pressure drop (losses).

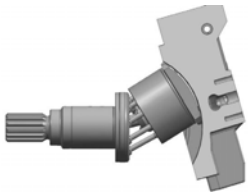

Fig. 2: Valve segment design

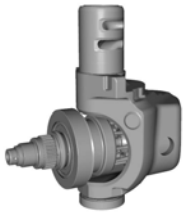

Fig. 3: Yoke Design with 45° Rotation Group

The large max. angle of 45° allows a seamless driving till final vehicle speed without shifting at a high-performance level. Image 4 shows some simulation results of rotation groups with different max. angles. 45° technology allow to drive the final vehicle speed (here at 4000rpm) with larger angles which leads to lower power losses. Power losses can be reduced even more by using the dry case technology and dead volume optimization [1][2].

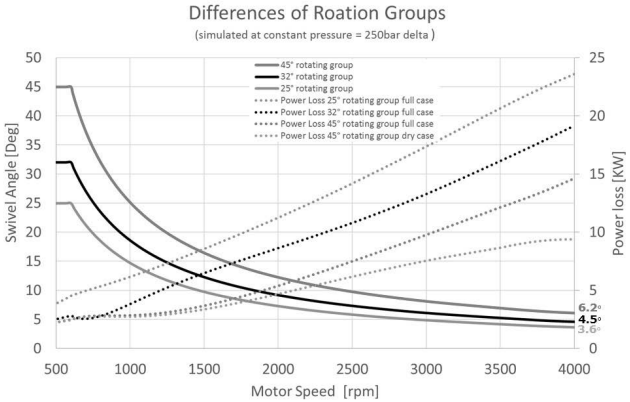

Fig. 4: 45° Differences of Rotation Groups

3. Constructional design of the drive

The newly developed continuously variable propel drive is based on a single-motor concept while using the wide-angle rotating group with a displacement of 370cc. The proven construction variant of combining motor and gearbox in one housing, represented by the well-known ICVD drive with a 233cc displacement, has been retained. The integrated gearbox, on the one hand, provides for the compact design of an output for the front and rear axles with

only one output shaft and, on the other hand, the adaptation of maximum output speed and output torque within a gear ratio of i = 0.96 to 1.67.

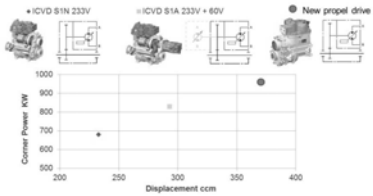

Fig. 5: Maximum performance range compared to existing ICVD wide-angle drives

The propel drive has been designed for a maximum output of 130kW and is available for vehicles with a maximum power requirement (theoretical performance at maximum engine speed and maximum torque) of 1,000kW. See table 2 for a complete overview of all technical data. See Fig. for a comparison of the new 370cc drive with present wide-angle drives in terms of maximum performance. This shows that the new single-motor concept with a higher displacement makes it possible to achieve a significantly higher maximum performance than with previous two-motor solutions. An increase in displacement to 370cc without taking up any significant extra installation space was impossible in the present design of the ICVD drives due to the nearly unchanged installation conditions in the target vehicles with their higher demands on traction force. A revision of all components was necessary to achieve a higher performance density. The drive's compactness has been increased, and the specific ratio of maximum-performance-to-weight could be raised by 11% from 0.55 kW/kg to 0.51 kW/kg compared to the ICVD S1A-233v+60V.

Using only a single engine results in a high overall efficiency of the propel drive. In particular, the load-independent splashing and drag losses of a second engine, additional antifriction bearings and clutches for engagement functions or power-shift transmission stages have been completely eliminated. There are no losses through engagements within the slip range of friction-based shifting clutches. See the complete design of the propel drive is shown in 6. The wide-angle bent-axis device is in a proven manner mounted, guided, and supplied with pressure oil in a swivel yoke. The swivel yoke is deflected with high pressure by a servo piston located in the bearing cover.

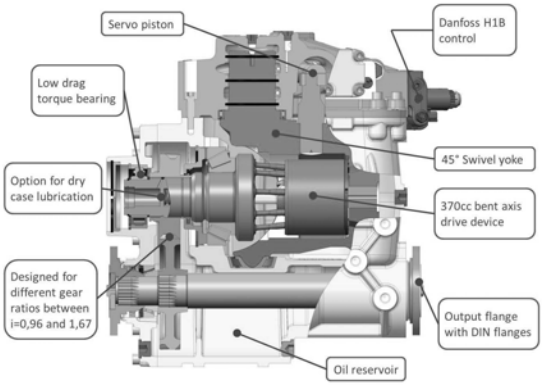

Fig. 6: Design of the new 370cc propel drive

The bearing of the drive shaft also meets the requirement of a high overall efficiency. In addition to the tapered roller bearing, dissipating axial force, a cylindrical roller bearing with a lower loss is being used. Further potential for increasing efficiency offers the reduction of splashing losses in particular on the drive shaft. In such a dry-case version, leakage oil is extracted, and the bearing of the drive shaft and the engine itself are supplied with injection lubrication as necessary. The drive shaft itself has already been designed for this kind of lubrication.

Only the overall behaviour of the power train, consisting of a fully hydrostatic gearbox and a diesel engine is crucial for the performance and efficiency of the driven vehicle. The propel drive must be optimally integrated into the control behaviour of the power train in order to enable Automotive Driving or Best Point Control. For this purpose, all control or software capabilities of existing bent-axis engines should be utilized without restrictions. Therefore, we fell back upon the proven Danfoss H1B control unit for proportional pressure control and pressure limitation. The position feedback to the swivel angle has been realized mechanically. The controllability of a H1B motor are possible as well with the new propel drive. The utilization of a valve component produced in a substantially higher quantity additionally increases system reliability and improves maintainability.

Table 2: Parameters of 370cc Rotating Group

Key Design Parameters of the new 370cc propel drive	
Displacement	370cc
Ratio range	0,96 – 1,76
Max. pressure difference	480 bar
Max. peak pressure	510 bar
Max. torque at *i*=1 and 450bar	2650 Nm
Max. output speed at *i*=1	3700 rpm
Dimensions L x W x H	523 x 372 x 565 mm
Weight	approx. 210 kg

4. Control and Regulation for Optimum Driving Behaviour

GKN and Danfoss decided to take as much advantage from technical synergies as possible. Instead of developing a new control system for the ICVD 370 and to guarantee a reliable controllability at a high-performance level, the electro-proportional controls known from Danfoss H1B-Motors have been integrated into the new transmission. By using existing and proven technology from series production it was possible to significantly reduce the development time of the transmission.

Danfoss high-pressure motor controls offer a highly dynamic behaviour and making the ICVD370 controllable like a standard hydraulic motor, such as H1B. All control functions are integrated in a separate assembly, which simplifies the overall design and guarantees a good serviceability.

The H1B-Controls are optimized for electronic controls (e.g. Danfoss PLUS+1®) and can be integrated into various software architectures.

Initially available Controls

- Electric proportional de-energized min. Displacement with BPD* and PCOR**
- Electric proportional de-energized min. Displacement with BPD* and PPCOR***
- Electric proportional de-energized min. Displacement

5. Summary and Outlook

Based on the 45° bent axis technology and the proven concept of motor and gearbox combination a propel drive was developed in a power range that was not available before. The whole development was driven to achieve higher traction forces in combination with a higher

grade of efficiency. The new design of the propel drive offers future possibilities to improve the efficiency with a concentrate lubricant injection in combination with leakage oil extraction for the rotating group and the gear stage in a dry case solution. Furthermore all control and software options on a common H1 hydrostatic drive train can be used with this propel drive to by the integration of the electro-proportional control caps from the Danfoss H1B-Motors. Best point control, the usage of the diesel engine in working point with the optimum of efficiency can be used with this new propel drive.

The series production of the ICVD 370 started already and the new propel drive will be used in the large telehandler models of Kramer and the largest wheel loaders of Kramer, Weidemann and the whole Wacker Neuson Group.

[1] Göllner, W., 2017, Auslegungskriterien und Potentiale für hydromechanisch leistungsverzweigte Getriebe, 17. Antriebstechnisches Kolloquium, ATK, Aachen

[2] Göllner, W., 2017, The design of powersplit transmissions using new technologies of hydrostatic components, 2017 Bath/ASME Symposium on Fluid Power and Motion Control, FPMC2017, Sarasota

[3] Schumacher, A., 2011, Best Point Control – Energetisches Einsparpotential eines Antriebstrang Managementsystems, 1 Conference Transmissions in Mobile Machines, Friedrichshafen

[4] Kruth, R., 2014, Analysis and optimization of a drive line system using the example of an agricultural telehandler, International Conference on Agriculture Engineering, Berlin

Counting seeds in air seeders

Dipl.-Ing. **Sebastian Meyer zu Hoberge**,
Dipl.-Ing. **Martin Liebich**,
Dipl.-Ing. **Paulo Martella**,
Müller-Elektronik GmbH & Co. KG, Salzkotten

Abstract

This article describes Müller-Elektronik´s seed counting sensor for air seeders, the AIRidium® Sensor. The sensor assembly uses piezo electric technology in combination with analog and digital signal processing methods to deliver highly accurate counting results at seed frequencies of up to 10,000 bouncing events per row and second.

Introduction

Sensor data is the basis for every precision farming application. Since the introduction of air seeders in agricultural processes, a weight-based manually performed procedure was chosen for calibrating the transmission ratio of the metering unit. From an agricultural point of view, a seeds per area value is much more sensible than using the weight per 1,000 seeds, fertility of the seed, a calibration factor, and weight-based values for estimating the seed rate. With this approach, calibration and the required repetition of this process take a lot of time. Therefore, automation in this area aims to increase the performance of the overall seeding process.

While several companies started to integrate switches on the air seeder to start and stop the calibration process without having to walk between the seeder and the seeder control display in the tractor cab, the company Amazone even integrated a small display on the seeder to control the whole process directly while standing beside the metering unit [1]. As a solution with higher automation, the company Lemken introduced a system that works online with a bypass and an integrated scale [2]. But all of these systems are based on the weight of a sample and are not capable of online measurement.

Müller-Elektronik's approach was to develop a robust seed flow sensor that is capable of measuring the seed flow with high accuracy. The scope of the project also included gathering online information about the lateral and longitudinal distribution of the seed.

Design and functionality of the sensor

The piezoelectric sensor is based on a contact measurement principle. Every single grain has to collide with the baffle plate of the sensor element in order to achieve optimal counting accuracy. The inner cone serves to focus the seed flow towards the centre of the sensitive impact plate. The angle of the elbow corresponds to the average impact angle of the seeds (see Fig. 1).

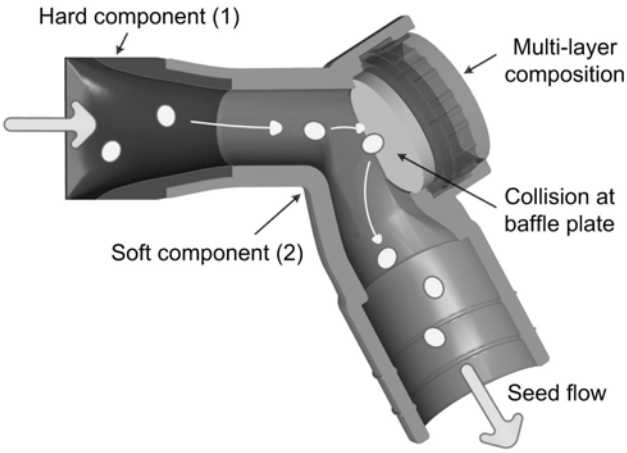

Fig. 1: Piezoelectric sensor for detecting seeds in airstreams

The hard component (1) of the inlet can be adapted to the mechanical interfaces of the different distribution heads and can substitute the existing fixture of the seed tube. The soft component (2) of the multifunctional sensor housing absorbs forces and vibrations, and supports the seed tube at the outlet. The pressure-grouted multi-layer composition ensures short and significant sensor signals [3].

Due to the short reaction time of the piezoelectric ceramic and the special multi-layer composition, this device can reliably count up to 10,000 equal and equidistant hits per second. The sensitivity is high enough to detect even small seeds like canola very accurately.

Another big advantage compared to common sensors is the self-cleaning effect and the wear-resistant sensor plate. As a result, this passive sensor is a ruggedized element, maintenance-free and very well suited for the rough environmental conditions in air seeders.

Operational capability of the electronic evaluation system

The complete signal processing is carried out in a central Electronic Control Unit. Up to 20 sensors can be connected to an evaluation electronic. The ECU is encapsulated with casting resin and installed directly under the distribution unit, well-sheltered from environmental conditions.

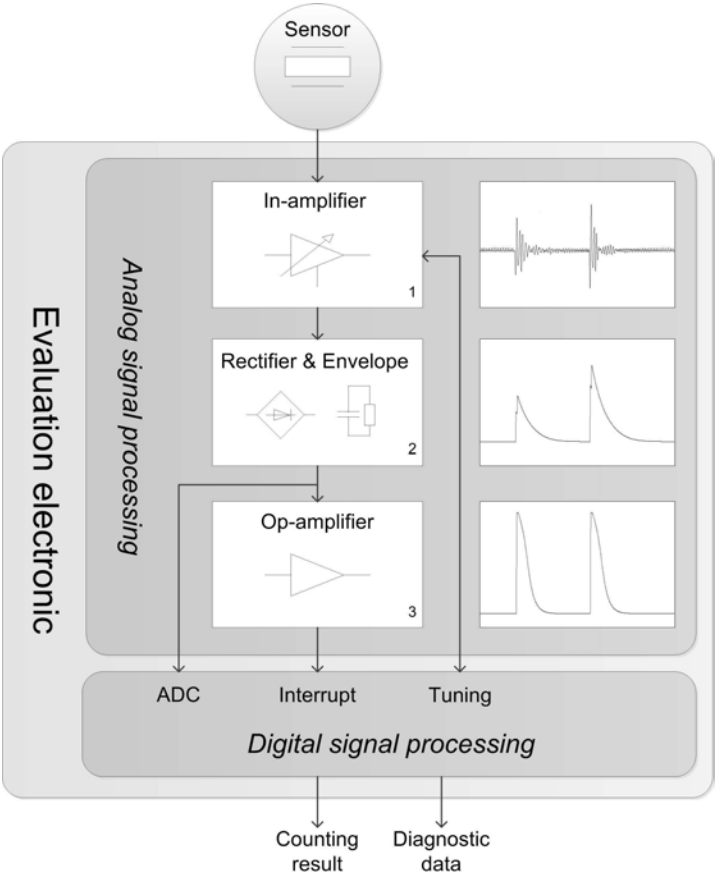

Fig. 2: Block diagram of the signal processing exemplary for one sensor input

Each sensor input has analog signal processing with independent automatic sensitivity adjustment. Various seed types, different air velocities and output rates lead to variable kinetic energies of the grain. The signal strengths differ even more because the impact angles and

the material properties of the seed types also have an influence. The adaptive sensitivity adjustment is an important performance feature to handle all of these different operating conditions. Additionally, calibration of the sensors at the factory is not necessary.

Figure 2 shows the analog pre-processing simplified in 3 steps and the interface to the digital signal processing. The instrumentation amplifier increases the alternating sensor signal according to the initial sensitivity setting. Afterwards, in step 2 the signal is rectified and an envelope is formed. The third logic part consists of a multi-stage operational amplifier that converts each envelope of a collision event into a binary counting pulse. Every single interrupt of these counting pulses triggers the analog-to-digital converter (ADC) to measure the peak value of the envelope within a few micro seconds. Because of the variation of the signal amplitudes, an arithmetic mean for averaging the peak values is used as a control variable. The time required to adjust the sensitivity depends on the environmental conditions, the sample size for averaging, the control deviation at the beginning, and also on the seed rate. In order to reduce this time period, a set of configuration parameters can be used to improve the starting point.

Based on our experience and the probability of information loss, the resolution of each sensor evaluation unit is only limited to a counting dead time of 125 µs, which still allows a detection of 8,000 equidistant hits per second. The cascadable evaluation circuit can be adapted to different distribution unit sizes and seed row numbers. Another advantage is the reduced number of participants on the CAN bus to achieve lower bus loads. The ECUs can be addressed and updated on the field. There are also many diagnostic functions, like the built-in self test for checking the connection of the passive sensor elements. The existing CAN protocol allows easy integration of the AIRidium® system into the application of the seeder. The central evaluation electronic system significantly reduces the overall system costs and permits simple and very flexible integration of the sensor system into existing control systems.

Sensor system embedded in the seeder application

The AIRidium® system has been integrated into several air seeder applications. The Implement Control Unit (ICU) communicates with the AIRidium® ECUs on a separate sub bus that is independent of the ISOBUS. In the tractor cab, the user can interact with customized application software that is shown on a display. The display exchanges data with the ICU through the ISOBUS. The AIRidium® ECUs gather data for every single grain of seed that collides on the sensors. The ICU receives the seed frequency for every single row. The cycle time can be adjusted with respect to the bus load, for example, from seeds per 10 ms to

seeds per 1 sec. The collected data, such as the lateral and longitudinal seed distribution, can be mapped in a farm management information system (FMIS). In addition, it is conceivable to use the sensor data to find the best working point of the air seeder to achieve better seed distribution.

Different visualization methods can be used to monitor the operating behavior. Warning limits can be defined to indicate if there is a blockage or other problems on a row. Blockage in a tube can be detected very rapidly, because the kinetic energy drops by the square of the seed velocity. Therefore, blockages can be detected even before the seed flow drops down completely.

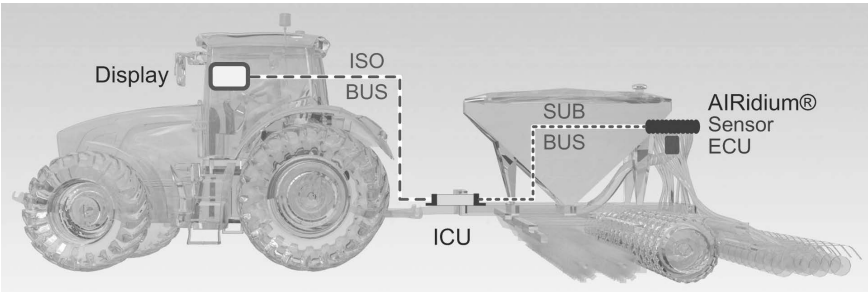

Fig. 3: Air seeder equipped with the AIRidium® system

The most important information is the number of seeds per revolution of the metering unit. With precise counting of the seeds and knowledge of the rotational speed of the metering unit there is no need for the conventional manual calibration test. The output rate can be entered as seeds/m² and dynamic blockage limits can be used depending on the output rate.

It is not possible to compensate one-time and non-recurring effects like a short-term bridging over the metering unit or a leaf in a metering cell. But the prolonged changing of influencing factors such as the fill level in the hopper, flow properties of the seed, seed weights or changing the seed offers a high potential for the improvement of precision seeding. All of these exemplified influencing variables can modify the calibration factor in seeds per revolution. The main advantage of a seed counting system is to measure these kinds of deviations and to provide a reliable control variable for regulating the metering unit [4].

The application offers a choice of different seed types. By selecting the seed type, the ICU transmits the corresponding configuration parameter settings to the AIRidium® ECU. The stored settings refer to a seed database that is continuously enhanced. To achieve the maximum accuracy, the sensitivity can also be adjusted by fine tuning. For new or unknown seeds, an automatic calibration for a given target value is also feasible.

Experience from test facilities and field tests

Each AIRidium® component has to pass an acceptance inspection under stable and reproducible conditions. OEM-related test facilities are used to validate the counting accuracy under more realistic conditions. The counting behavior for the different seed types has been reviewed under various air speeds and output rates.

The AIRidium® system was successfully tested with different seed types such as canola, milo, wheat, barley, triticale, rye, oats, peas, soybeans, and corn. Each seed type was precisely detected. The positive results obtained at the test facilities were reproduced with the implements on the field. Most seeds were counted with standard settings and good counting accuracies. The AIRidium® sensor has proven its worth even with canola under rough and dusty conditions. The counting accuracy for canola is high enough to regulate the metering unit based on the “seeds per revolution” control variable. Today, a multitude of implements are equipped with AIRidium®. The seeding of canola is based on the counting results and is carried out without a calibration test. The working widths of the test implements range from 3 m to 18 m, equipped with 20 to 72 sensors. The AIRidium® system has also been used in a single seed precise control system [5].

Summary and outlook

The AIRidium® system complies with the high technical requirements and economic aspects. Thanks to the high resolution, it is possible to count up to 8,000 hits per second with each sensor element. It is the first maintenance-free sensor system for counting seeds in air seeders with high counting accuracies for very different seed types. The configuration parameters for the sensitivity adjustment are currently determined by Müller-Elektronik and stored in a seed database. In the future, these manual steps have to be eliminated to improve the usability in practice and to further increase the degree of automation.

[1] Neunaber, M.: Amazone Cirrus 03 mit TwinTerminal. Profi-Neuheiten 2014.

[2] Giesen, G.: Automatische Abdrehprobe zur Saatguteinstellung von pneumatischen Drillmaschinen. LEMKEN GmbH & Co. KG, Alpen. Neuheitenanmeldung zur Agritechnica 2015.

[3] EU-P 3 060 035

[4] EU-P 3 008 988

[5] Rothmund, M., Haselhoff, A., Baum, D., Petr, V.: Approach for a single seed precise control system for small grains based on piezo-electric and optical sensors. Land.Technik 2014, pp. 215-221

Defining the dynamic performance of a no-till seeder by measuring the geo-referenced seeding depth

M.Sc. **G. M. Sharipov**, Dr. **D. S. Paraforos**,
Prof. Dr. **H. W. Griepentrog**,
University of Hohenheim, Stuttgart;
M.Sc. **C. Gall**,
AMAZONEN-Werke H. Dreyer GmbH & Co. KG, Hasbergen

Abstract

Retaining a precise seeding depth throughout the entire seeding operation is one of the biggest challenges especially in no-till seeding. Harsh and variable soil conditions as well as high driving speeds are the reasons for unstable coulter movements and unsatisfactory seed placements. The first stage of this challenge requires to describe the seeder dynamic response to soil conditions along with the corresponding seeding depth variation. In the present paper, the performance of one coulter assembly and its dynamic response to soil surface profile was captured by a combination of different sensors placed at a sensor-frame and the assembly. After the operation, the position of each single seed within a specified section was georeferenced, to calculate the absolute seeding depth. The introduced methodology for the absolute georeferenced seeding depth was validated with the ground truth seeding depth measured from seedlings after emergence. The comparison indicated small differences of 0.9 mm between the mean values and 0.2 mm between standard deviations of absolute georeferenced seeding depth. Future work will focus on to reduce the vertical dynamics of the coulters.

Introduction

The performance of a no-till seeder, in terms of seeding depth, is an important factor in achieving reliable seed germination and plant emergence and hence to achieve a significant effect on grain yield [1]. However, this requires a seeder that interacts appropriately with harsh soil conditions like compacted soil and plant residues at high forward speeds, with the purpose of placing seeds at the desired depth [2]. Since the seeding depth variation is considerably affected by the machine dynamic response to soil surface undulations, the relationship between the seeder dynamics and its performance plays a very important role in optimising the dynamic behaviour of the seeder for keeping a precise seeding depth.

The seeder dynamic responses to soil surface undulations can be characterised by the reaction forces on the coulter that have a significant influence on the mean seeding depth. The reaction forces on a coulter can be described with its horizontal and vertical components [3]. In the present study, the total reaction forces, arising on the coulter assembly, were introduced by the vertical, horizontal, and profile impact forces, since a packer wheel is attached for different depth settings [4]. Using up-to-date sensors with a high accuracy like a robotic total station have been introduced [5] to measure georeferenced position of seeds and to analyse depth variations, which offers the possibility of describing and evaluating the seeder performance with the corresponding motion dynamics.

A project was set up to optimise a no-till seeder, in terms of vertical motion stability, for reducing the variation of seeding depth under realistic high-capacity performance. With the aim to assess the performance quality of the seeder, this paper presents the new methodology for determining absolute georeferenced seeding depth with the corresponding dynamics of the seeder and validation of the methodology by comparing its results with the measurements of the ground truth seeding depth (hypocotyl).

Materials and Methods

A 12-row no-till seeder with 25 cm inter-row distance (AMAZONEN-Werke H. Dreyer GmbH & Co. KG, Hasbergen, Germany) and a 6210R 156.6 kW tractor (John Deere, Moline, Illinois, USA) were employed, to perform the seeding operations. To measure the field surface profiles and the machine dynamics parameters, i.e. accelerations, displacements, and tilting information, a metal bracket that carried all the necessary sensors was developed and mounted on the main frame of the seeder (Figure 1). Multiple sensors were placed on both the sensor bracket and one of the coulter assemblies. An SPS930 total station (Trimble, Sunnyvale, USA) provided the in-field absolute geo-referenced position of the main frame of the seeder by tracking a Trimble MT900 prism fixed on the developed sensor-frame. The vertical displacements of the coulter assembly was detected using a DT50 laser range finder (SICK AG, Waldkirch, Germany) attached on the developed sensor-frame. The real-time tilting information (roll-pitch-yaw) of the seeder main frame and the coulter assembly were acquired from two VN-100 inertial measurement units (IMUs) (VectorNav, Dallas, USA) fixed on the sensor-frame and the plate, respectively. To measure the vertical and surface profile impact forces, three linear 350 Ohm DY41-1.5 - Strain Gauges with two parallel measuring grids (HBM GmbH, Darmstadt, Germany) were attached at three points on one coulter assembly. The developed software in Microsoft Visual Studio C# 2010 [6] for recording and storing the data from the total station, the laser pointer and the two IMUs, had a multi-thread

architecture, thus making possible a parallel data acquisition. To store the data from the stain gauges, a QuantumX-MX840B (HBM GmbH, Darmstadt, Germany) data acquisition system with eight channels was used. More information can be found in [7] regarding the utilised sensors and data acquisition systems.

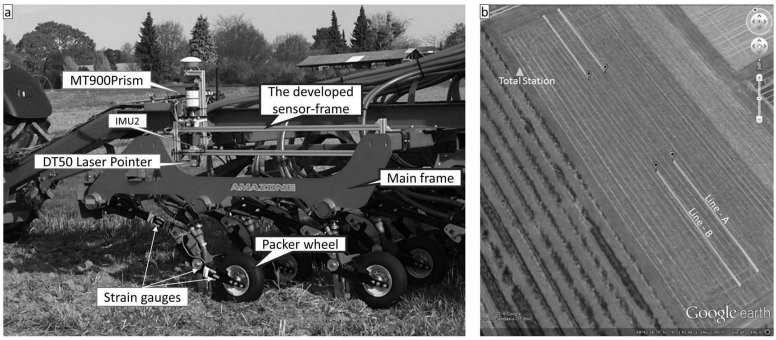

Fig. 1: (a) The developed sensor frame mounted on the no-till direct seeder and (b) a satellite image of the field where the measurements were performed. Lines A and B depict the specified paths of the examined coulter assembly.

All field experiments were carried out at the “Heidfeldhof”, a research farm of the University of Hohenheim (48°42´39.28´´N, 9°11´47.19´´E). The soil at the field was slightly stagnic luvisol with 9.4% sand, 68.1% silt, and 22.6% clay [8]. Field experiments for seeding wheat (*triticum aestivum* L.) were performed to obtain surface profiles, forces and machine dynamic parameters, like vertical accelerations and displacements, under stubble field condition. For all dynamic measurements, the operation speed of the tractor was set constant at 10 km h^{-1} and the target seeding depth was adjusted to 50 mm. After accomplishing seeding for acquiring machine dynamics and surface profiles, a measurement was carried out to measure the position of every single seed (Figure 2a) and thus, to calculate absolute georeferenced seeding depth. A 20 m furrow (Figure 1b, red colour in Line - A) was carefully opened by hand to reveal 352 seeds without disturbing their position on the seedbed. Next, the total station using the MT1000-G prism and a 2 m poll provided every seed 3D position in the same coordinate system as the acquired surface profile. The correctness of the introduced methodology for obtaining the georeferenced seeding depth was validated by comparing the results with the ground truth seeding depth by measuring the hypocotyl length (Figure 2b) that was conducted on a parallel row (Figure 1b, green colour in Line - B).

Results and Discussion

The geo-referenced seed positions and the corresponding surface profile of the selected 20 m are presented in Figure 3a. The combination of the geo-referenced seed positions and the

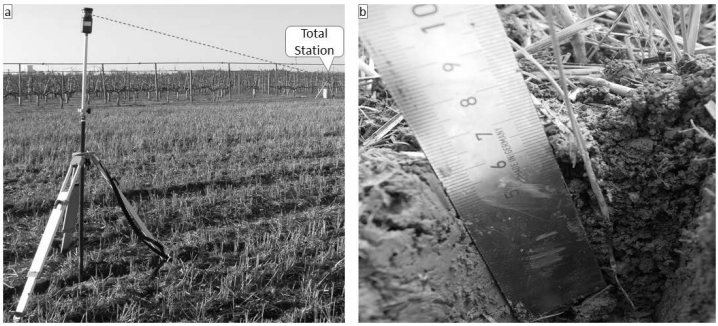

Fig. 2: Measuring the (a) geo-referenced seeds after seeding and the (b) ground truth seeding depth after field emergence (hypocotyl).

profile, which were employed to calculate the absolute georeferenced seeding depth, is illustrated in Figure 3b. The corresponding vertical forces and the profile impact forces were extracted from the measured strain and can be seen in Figure 3c, and d, respectively. The relation between the forces and the variation of seeding depth was introduced by correlating spatial frequency contents.

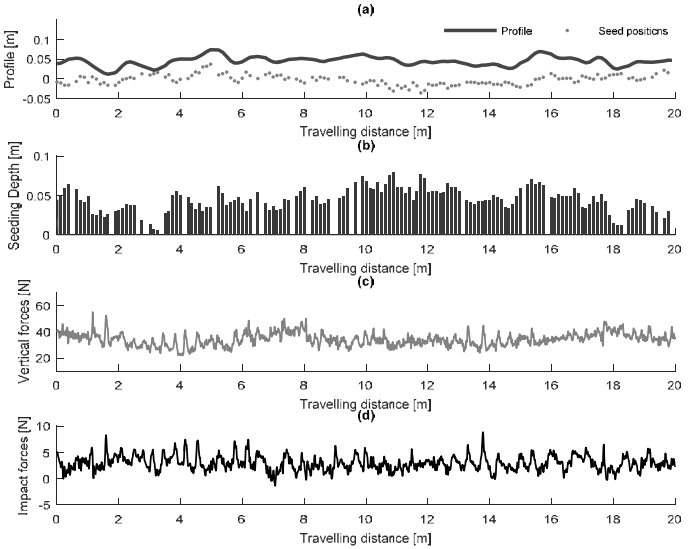

Fig. 3: (a) Georeferenced seed positions with the corresponding surface profile, (b) absolute seeding depth and the corresponding (c) vertical and (d) impact forces.

The comparisons between the georeferenced and ground truth seeding depth were based on statistics of the both seeding depths measurements. The frequency histograms of the geo-referenced and ground truth seeding depth are presented in Figure 4a, and b, respectively.

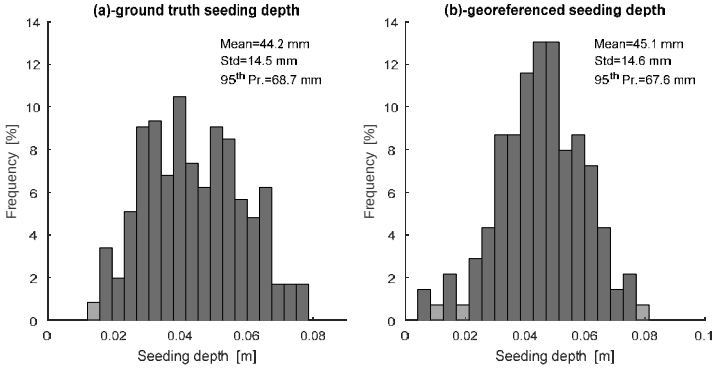

Fig.4: Frequency histograms of the seeding depth measured from (a) hypocotyl of seedlings and from (b) geo-referenced seed positions and surface profiles.

The analyses of the statistics depicted that the minimum and maximum seeding depth were 14.2 mm and 77 mm for ground truth depth measurement and 12 mm and 83 mm for the geo-referenced seeding depth that show discrepancies of 2.2 mm and 6 mm between minimums and maximums, respectively. The mean values of both the ground truth seeding depth and the geo-referenced seeding depth were equally close to the target seeding depth of 50 mm with a small discrepancy of 0.9 mm. The difference between the standard deviations was also not significant with 0.2 mm difference. This means that in both measurements, the variation of the seeding depth was evenly close to its mean value. In addition, 95th percentile of the ground truth seeding depth samples varied below 68.7 mm. This value was 67.6 mm for the geo-referenced seeding depth samples.

The Kruskal-Wallis non-parametric analysis resulted that all data originated from the same population and the dataset of the georeferenced seeding depth variation was significantly different from the one for the ground truth seeding depth variation.

Conclusion

A new methodology for measuring seed positions in absolute geo-referenced coordinates was used and proposed to assess the seeding depth variation. The correctness of the methodology was verified by comparing its statistics with the measurement statistics of seeding depth measured from hypocotyl length of seedlings. The comparison analysis indicate that the introduced methodology adequately results in measuring the seeding depth.

Acknowledgement

The authors gratefully acknowledge the financial support provided by GA nr 213-2723/001–001–EM Action2 TIMUR (Training of Individuals through Mobility to EU from the Uzbek Republic) project. The project was conducted at the Max-Eyth Endowed Chair (Instrumentation & Test Engineering) at Hohenheim University (Stuttgart, Germany), which is partly grant funded by the Deutsche Landwirtschafts-Gesellschaft (DLG) e.V.

Reference

[1] R. Derpsch *et al.*, “Why do we need to standardize no-tillage research?,” *Soil Tillage Res.*, vol. 137, pp. 16–22, 2014.

[2] D. F. B. Collins, “Effect of soil characteristics, seeding depth, operating speed, and opener design on draft force during direct seeding,” *Soil Tillage Res.*, vol. 39, no. 3–4, pp. 199–211, 1996.

[3] a. Abo Al-Kheer, M. Eid, Y. Aoues, a. El-Hami, M. G. Kharmanda, and a. M. Mouazen, “Theoretical analysis of the spatial variability in tillage forces for fatigue analysis of tillage machines,” *J. Terramechanics*, vol. 48, no. 4, pp. 285–295, 2011.

[4] G. M. Sharipov, D. S. Paraforos, and H. W. Griepentrog, “Modelling and simulation of the dynamic performance of a no-till seeding assembly with a semi-active damper,” *Comput. Electron. Agric.*, vol. 139, pp. 187–197, 2017.

[5] D. S. Paraforos, M. Reutemann, G. Sharipov, R. Werner, and H. W. Griepentrog, “Total station data assessment using an industrial robotic arm for dynamic 3D in-field positioning with sub-centimetre accuracy,” *Comput. Electron. Agric.*, 2017.

[6] D. S. Paraforos, H. W. Griepentrog, and S. G. Vougioukas, “Country road and field surface profiles acquisition, modelling and synthetic realisation for evaluating fatigue life of agricultural machinery,” *J. Terramechanics*, vol. 63, pp. 1–12, 2016.

[7] G. M. Sharipov, D. S. Paraforos, A. Pulatov, and H. W. Griepentrog, “Dynamic performance of a no-till seeding assembly,” *Biosyst. Eng.*, vol. 158, pp. 64–75, 2017.

[8] P. Högy, C. Poll, S. Marhan, E. Kandeler, and A. Fangmeier, “Impacts of temperature increase and change in precipitation pattern on crop yield and yield quality of barley,” *Food Chem.*, vol. 136, no. 3–4, pp. 1470–1477, 2013.

Reasons of irregularity of seed's distribution in the divider heads of air-seeders

Dr. **Andrii Yatskul**,
Chaire Agro-Machinisme et Nouvelles Technologies,
UniLaSalle – 19, Beauvais, France ;
Dr. **Jean-Pierre Lemiere**,
UMR PAM, Agrosup Dijon, Dijon Cedex, France

Abstract

Modern seeding equipment must allow to cultivate sizeable areas efficiently and finalize the seeding in a short amount of time. Air-seeder is a solution for a fast seeding: seeds are conveyed from the high-capacity seed hopper to the coulter-bar by an air-stream. Taking into account the complexity of this type of seed drills, they stay little-studied. Few developments have been done on divider headers responsible of distribution accuracy. This paper deals with a study on the influence of divider head geometry and functioning conditions on the seed's distribution accuracy. Moreover, observation of the seed's behaviour is done using a high-speed camera system. These experimental results allowed proposals of hypothesis about the parameters influencing the final result, necessary for future divider heads design.

Keywords: Air-seeder, distribution accuracy, divider head, distribution manifold, head geometry, seed distribution, air-delivery system

Introduction

Air-seeding is a well-known principle since the 1960's [17]. Air-seeders (are equipped with an air-delivery system, for transporting the metered seeding material from a main storage hopper to the soil openers, located on a tillage implement, in single or multiple air lines. The important technical benefits of air-seeders as high autonomy (in terms of hopper filling), manoeuvrability, productivity, easy loading and adjustment, have to withstand following shortcomings: low transverse distribution accuracy, seed damage, frequent risks of clogging and high energy consumption.

Commonly, the distribution accuracy of the seeding material between the seed rows is evaluated with a coefficient variation coefficient (ISO-7256/2) [14]. According to agrotechnical requirements, the variation coefficient of a seed distribution must be lower than 5 % for cereal seed and lower than 10 % for fertilizers [4, 16] in order to avoid the consequences

on the yield. The first divider had a smooth surface tower and a CV is in the range of 15-27 % [11, 17]. By using the vertical tower with the concentric corrugations, creating an additional turbulence, it resulted in huge improvements, with a CV of around 4-8 % [17]. Some manufacturers use the towers with radially punched bosses on the side of the vertical tube. In the world patent database, a lot of interesting technical solutions of divider heads are proposed, with no proof of their practical efficiency however. The majority of known researches remained mostly empirical tests and statement of facts: acceptable solution or unacceptable with a lack of fundamental analysis and descriptive physical models of a distribution process [1, 2, 5, 6, 7, 10, 12, 15, 17]. We are aiming to determine the influence of main divider head functioning conditions (as the air velocity and the material flow rate) and elbow on the seed's distribution accuracy. The complete study is presented in [19].

Materials and methods for studies on experimental setup

The study was carried out on a specific experimental setup Fig.1 within the company Kuhn SA in France. We used the (i.e. hopper mounted to the front of the tractor) Kuhn TF1500 front hopper in combination with the 20 outlet divider head already manufactured for use with air-seeders such as the KUHN Venta 3000. The airline was substituted by the straight horizontal airline with a transparent section between the injector and the elbow. Once the seeds expelled by the metering unit (2) from the frontal hopper (1), they were picked-up by the air flow provided by the blower (4) in the injector (3). They were transported in the flexible pipe (5) towards the elbow (6) through a vertical tower with the concentric corrugations (9) and divider head (8). The material flow rate was controlled by Kuhn's electronic terminal ISOBUS VT50.

During the test, the seeds were collected and weighed from each individual outlet at various material and air rates. All outlets were numbered. It was decided that the influence of the most commonly encountered functioning factors, leading to clogging or to a breach of the distribution quality should be investigated. In order to eliminate any metering irregularities due to the start and to the end of metering, trial duration lasted 2 minutes. Each trail was undertaken in a threefold repetition. Air velocity was measured on the straight part of the loaded airline using Pitot tubes according to [9] by universal micro-manometers Testo 512. In order to estimate the distribution accuracy and compare its value to the agronomy requirements, we used the common notion of variation coefficient (CV) according to (ISO 7256/2) [14]:

$$CV = \frac{Standard\ deviation\ of\ sample\ mass\ (g)}{Average\ sample\ mass\ (g)} \times 100\% \quad (1)$$

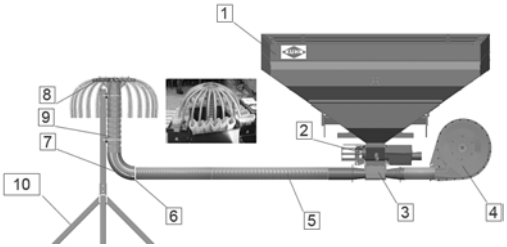

(a) (b)

Fig. 1: (a) Experimental setup.

Results and discussions

Influence of the air velocity and the material flow rate on the distribution accuracy

This series of experiments aimed to estimate the coefficient of variation (CV) as a function of air velocity and material flowrate. This CV varies depending on different combinations for a given seeding material type and a given distribution head (table 1). Material flow rate corresponded to the real seeding material rate (for example 12.5 g s^{-1} per outlet corresponds to 220 kg ha^{-1} for a 3m working width (20 rows) at a forward speed of 10 km h^{-1}). We noticed that for given flow rate the CV does not change proportionally to the air velocity. The best distribution accuracy for a given flow rate can only be obtained for a precise and definite air velocity value. It could be useful to present the relationship between the distribution accuracy, air velocity and material flowrate in a three-dimensional graph (figure 5) using Matlab R2014b. We noticed that for given flow rate the CV does not change proportionally to the air velocity. The best distribution accuracy for a given flow rate can only be obtained for a precise and definite air velocity value Fig. 1. It is obvious that there is a relationship between these parameters and particle behaviour inside a divider head.

Table 1: Coefficient of variation as a function of air velocity and material flow rate.

	Material flowrate per outlet, g s^{-1}				
Air velocity, m s^{-1}	5	8	12.5	15	30
30	9.10	8.17	5.18	4.62	9.56
	9.42	8.13	5.29	4.61	9.34
	9.11	8.24	5.31	4.53	9.46
26	8.06	6.04	4.94	8.58	11.14
	8.19	6.12	5.01	8.46	11.22
	7.93	6.19	5.01	8.64	11.11
20	6.41	4.27	9.19	14.38	16.52
	6.31	4.19	9.33	14.45	16.71
	6.35	4.21	9.26	14.37	16.47

As it was shown in [17], the air-seeder distribution system must ensure not only the particles conveyed, but also the agro-technical requirements concerning the supply regularity and highest quality distribution between seeding rows. In order to insure the constant flow without any pulsation and any clogging, to increase the air velocity appears sufficient, but needs a deeper study, according to our results.

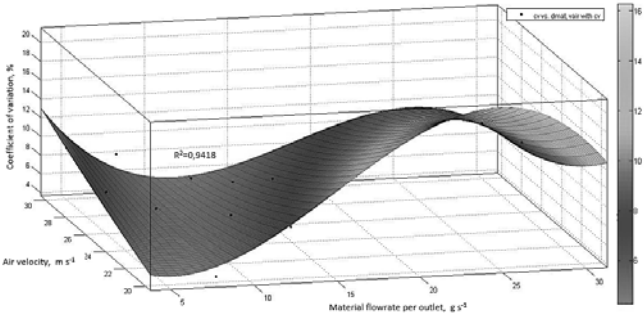

Fig. 2: Influence of the air velocity and the material flow rate on the distribution accuracy.

The air provides its energy to the particles' acceleration. As the kinetic energy of particles increases they follow the air flow direction. At the same time, the air with a low velocity cannot produce a sufficient aerodynamic action to stabilize the particles and give them the right direction. Thus in the case of a low air velocity, the direction of the particles are conditioned

by their initial direction due to rebounds, centrifugal force, collisions between particles etc. When regarding the results of the figure 4.1, we could affirm that for a given material flow rate, there is an optimal air velocity ensuring the highest distribution accuracy. In addition, an air velocity value greater than 34-39 m s^{-1} could induce seed damages [20]. These damages could reduce the seed resistance to diseases and decrease the future yield.

Importance of the elbow

The movement of air-seeds flow in the elbow is one of the most complex parts of the distribution system. The changes of direction from horizontal to vertical are combined with numerous structural changes in the flow, causing important pressure drops [8, 13, 20]. High-speed video analysis allows us to certify the structural changes affecting not only the air (local redistribution of velocities and pressures), but also the particle flow. In all cases, we noted the collision with the exterior wall of the elbow. The particle velocity decreases significantly. For example, for seeds having a speed of 9-15 m s^{-1} before the elbow, it falls to 3-6 m s^{-1} in the downstream. The velocity decreasing is compensated by the air-flow energy, accelerating the particles. The dotted red zone (Fig. 3, a) is a very troubled area. Here the particles collide iteratively with the walls and other particles agitated in the air vortexes. Near the exterior wall of the elbow we noticed a local increasing of the flow concentration and particles spinning angular velocity.

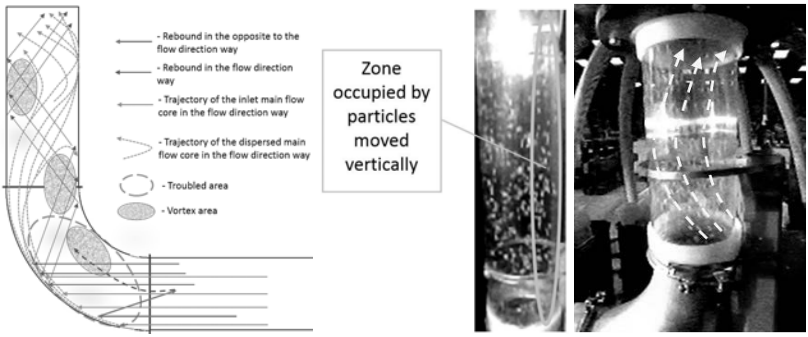

(a) (b)

Fig. 3: (a), Trajectory of particles in the elbow and in the tower (b), Frame from high-speed video of particles outgoing from the elbow and moving through the tower.

Hence, each collision with the elbow could have two possible outcomes (Fig. 3, a): the particles continue to follow the exterior wall of the elbow, or they begin an intensive saltatory movement (Fig. 3, b). It is the major outcome. Moreover, when the air velocity is reduced according to the minimum conveying velocity, the particles tend to slide on the elbow side vertically. Furthermore, the increasing of the air velocity implies more intensive rebounds. This movement, which is characteristic of particle flow core. In the first case, the distribution field orientation is defined by the last particle orientation, generally after the last rebound. Returning to the question of optimal air velocity ensuring the best distribution accuracy, we could say that for a given dividing device and a given material flow rate we could find an air velocity, when at the dividing instance the particles velocity horizontal component will have the minimal value. So, the influence of the last rebound will be minimal.

After the elbow the flow tries to acquire the typical structure for straight pipes. For that, the flow needs some transition distance. This distance is a function of the elbow "stiffness", of the air velocity and of the flow concentration. After the collision with the wall, particles move obliquely upwards until the next collision with the tower wall in 30-45 cm. As the distance increases, the particles disperse in the tower cross-section.

Conclusions

In this paper, an essential part of fundamental study [19] has been proposed for the functioning of an air-seeder with a vertical type divider head. For each divider head and for a given material flow rate of a given seed species, there is an air velocity ensuring the best distribution accuracy. It is due to the saltatory movement of the particles' flow core. Further work could lead to the reduction of the overall dimensions of the divider head and of its height. In order to improve the distribution accuracy, further work must focus on the removal of impacts in the elbow (make elbow lighter or install a deflecting and guiding elements) or its disposition. It would be useful to carry out a study on a horizontal-type divider head.

Acknowledgments

The authors would address their kind regards to the Kuhn SA company for providing the experimental equipment and financial support.

References

[1] Allam, R. K. and Wiens, E. H. (1981). Air Seeder Testing, ASAE/CSAE Paper No. 81-323, Prairie Agric. Machinery Inst., Lethbridge, Alberta.

[2] Astahov V.S. (2007). Mechanical and technological fundamentals of the air-seeding having a centralized distribution system. (Астахов В.С. Механико-технологические основы посева сельскохозяйственных культур сеялками с пневматическими системами группового дозирования: Дис. докт. техн. наук. Горки) D. of Science thesis. Gorki, Byelorussia, 377 p.

[3] Bourges, G., & Medina, M. (2012). Air-seeds flow analysis in a distributor head of an" air drill" seeder. In Ist International Symposium on CFD Applications in Agriculture 1008 (pp. 259-264).

[4] Buzenkov G. M., Ma S.A. (1976). Crop seeding machines. (Бузенков Г.М., Ма С.А. Машины для посева сельскохозяйственных культур. Машиностроение) Moscow, 270p.

[5] DLG. (2009) Amazonen-werke H. Dreyer GmbH & Co. KG. Anbau-Bestellkombination AD-P 303 Super/KG 3000/KW 580. Ablagequalität und Handhabung. DLG-Prüfbericht 5720F. Deutsche Landwirtschafts-Gesellschaft. Groß-Umstadt. Deutschland 6p.

[6] Gierz, Ł., & Kęska, W. (2011). Badania laboratoryjne nad rozdziałem strumienia nasion w głowicy siewnika pneumatycznego. Inżynieria Rolnicza, 15, 117-125.

[7] Heege, H. J., & Zähres, W. (1975). Pneumatische Saatgutzuteilung bei Sämaschinen. *Grundlagen der Landtechnik*, *25*(4). pp. 111-115.

[8] Idelchik, I. E. Handbook of Hydraulic Resistance, (2005). Jaico Publishing House; 3 edition, 816p.

[9] Lefebvre, J. (1986) - Mesure des débits et des vitesses des fluides. Masson.

[10] Kumar V., Divaker C. & Durairaj C., (2000). Influence of Head Geometry on the butive Performance of Air assisted Seed Drills. *J. agric. Engng. Res.*, 75, pp. 81-95.

[11] Mahlstedt, J., & Heege, H. J. (1972). Die pneumatische Zuteilung von Getreide in Sämaschinen. *Grundlagen der Landtechnik*, *vol. 22 (1972) no. 2, pp. 33—38.*

[12] McKay M. E., 1979 Performance Characteristics of Pneumatic Drills: Transverse Distribution. Numéro 45 de Agricultural engineering reports. University of Melbourne, Department of Civil Engineering. 1979. 22 p.

[13] Mills, D. (2013). *Pneumatic conveying design guide*. Butterworth-Heinemann, 650p.

[14] Norma, ISO 7256/2, (1984). Sowing equipment-Test methods-Seed drills for sowing in lines.

[15] Pippig, G. (1978). Prallteilung von Saatgut-Luft-Gemischen in vertikalen und geneigten Förderleitungen mit kreisrundem Querschnitt. *agrartechnik*, *28*(8).

[16] Spaar, D., 2008. Crops: cultivation, harvesting and processing. (Зерновые культуры. Выращивание, уборка, доработка и использование. ООО ≪DLV АГРОДЕЛО≫,) Moscow, Russia, 656 p.

[17] Weiste, H. (2013) The ACCORD PNEUMATIC-System: From invention to worldwide application, Landwirtschaftsverlag GmbH, Münster-Hiltrup. Germany, 224p.

[18] Yatskul, A. I., Lemière, J. P. (2014). Experimental determination of flow concentration for pneumatic conveying systems of air-seeders. INMATEH-Agricultural Engineering, 44(3).

[19] Yatskul, A., Lemiere, J. P., & Cointault, F. (2017). Influence of the divider head functioning conditions and geometry on the seed's distribution accuracy of the air-seeder. *Biosystems Engineering*, *161*, 120-134.

[20] Zuev, F.G., (1976). Pneumatic conveying on crop processing industries. (Зуев Ф.Г. Пневматическое транспортирование на зерноперерабатывающих предприятиях.- М.: Колос). Moscow, 344p.

Development and Utilization of a Planter Automatic Downforce Evaluation Test Stand to quantify System Response and Accuracy

Dr. **Ajay Sharda**, Assistant Professor,
Ryan Strasser, Graduate Research Assistant,
Kanas State University, Manhattan, USA;
Dr. **Matthias Rothmund**, Team Lead F&E, Systems Engineer,
Horsch Maschinen GmbH, Schwandorf

Abstract

In recent years, newer precision planters have seen integration of automatically controlled row unit downforce systems to reduce soil compaction, maintain proper seeding depth and control row unit ride quality. By keeping planter row unit downforce properly applied, a more uniform emergence and increased yield potential can be obtained. However, little knowledge exists to understand downforce system response and accuracy during scenarios typically occuring during field operation. Therefore, the study was conducted with two key objectives to study were to 1) develop a lab-based test stand to evaluate downforce system response time, accuracy, and downforce load distribution between the gage wheels, opening discs, and closing wheels; and 2) evaluate an automatic downforce system using test stand under simulated real-field scenarios. A downforce system test stand was designed with the capabilities of changing row unit vertical travel as well as load distributions between the planter row unit's gage wheels, opening discs, and closing wheels. The test stand was developed after assessing field operation of a planter with automatic downforce system operated on multiple fields. Simulation scenario were developed to 1) operate planter at varying speeds with uniform soil type and moisture; and 2) operate on soil with varying resistance due to texture and/or moisture changes. Real-time field data was used to develop simulation test files with target disc loading conditions. A custom LabVIEW program was developed to operate the downforce test stand's pneumatic valves and record data from the test stand and row unit sensors using a National Instruments (NI) CRio Chassis. The LabVIEW program could also read control commands from *.txt file, henceforth referred to as a simulation file, to actuate desired disc loads through the disc loading mechanism and platform height through the platform height control mechanism. The program would read the simulation file containing target values of disc load and platform height, parse the data fields and send it correspond-

ing control loops. The control loops would used the simulation file data as a target load or distance height setting while reading pressure transducer and ultrasonic sensor data for current load of the disc cylinder and current height of the test stand, respectively. A National Instruments cRIO Chassis and C series modules were used to control the test stand and record data from the test stand at 10 Hz. Results from different scenarios exhibited that the test planter's automatic downforce control system maintained the target gauge wheel load setting of 38 kgf ±- 22.7 kgf for more than 94% of the time. The downforce control system was able to manage gauge wheel load with disc load variations up to 68 kgf within 1.3 sec and load variation upto 22 kgf within 0.5 sec. Overall, the planter downforce control system ability to maintain target gauge wheel loads at varying speeds and soil texture variation within 0.5 to 1.3 s suggested appropriate control for precision planter.

Introduction

In recent years, great improvements have been made in row crop planter design. Many of these improvements were focused around seed metering and delivery to the in-soil furrow and the ability to maintain proper seed spacing. Accurate seed placement is critical for uniform spacing, achieving target population, and providing optimum yield potential (Zhao and Chen, 2015). In addition to spacing seed, uniform depth is a vital parameter for achieving uniform emergence (Nielsen, 2004). With increases in seed metering accuracy, other areas of the planter must be addressed to further improve seed placement and take full advantage of these highly accurate seed meters.

On a typical planter row unit, there are three main soil-engaging components; the closing wheels, gauge wheels, and opening discs. The gauge wheels ride across the field surface to prevent the opening discs from penetrating deeper than the seed depth setting. To keep the gauge wheel in contact with the soil, vertical downward force must be applied to the row unit until the proper seed depth is reached, the gauge wheels have reached a target load, and the press wheels are in full contact with the ground. At a certain depth setting, the opening discs will only require a specific amount of downforce to reach the set seeding depth. The required disc load changes with soil type, texture, moisture, and terrain, so overall applied downforce must be adjusted (Sharda et al., 2017). By adjusting the applied downforce, a target gauge wheel load can be maintained that prevents overloading or under loading of the gauge wheels that could cause compaction or improper seeding depths. Because soil texture and moisture throughout a field affect required disc loading, trends in soil moisture and texture can be mapped using soil EC measurements (Grisso et al., 2009), and used to infer changes in disc loading that will occur.

Currently, no method has been developed to statistically evaluate the automatic downforce control systems on row crop planters. With limited tests to evaluate planter downforce systems, additional studies are needed to better understand how automatic downforce control systems respond as well as the effects of changes in opening disc loading and their effects on gauge wheel loading. To evaluate the response and accuracy of these automatic hydraulic downforce systems and better understand the relationship between the opening disc loading and gauge wheel loading, this study was designed with three objectives, 1) develop a test stand to statically evaluate planter hydraulic downforce systems within a lab-based environment; 2) evaluate test stand operational performance and capabilities; and 3) quantify hydraulic planter downforce control system response to simulated soil and terrain changes

Methodology

Downforce Test Stand Capabilities

To analyze the accuracy and response of hydraulic downforce control systems under real-world field scenarios, a downforce test stand was designed, constructed, and evaluated. The test stand was designed to support the load of a Horsch Maestro (Horsch Maschinen GmbH, Schwandorf, Germany) seeding row unit and withstand the additional load added through the hydraulic system during automatic downforce control system (Horsch Maschinen GmbH, Schwandorf, Germany) operation. The row unit operation was controlled using a Horsch field computer connected to the planter electric control unit, hence forth referred to as an ECU, (Horsch Maschinen GmbH, Schwandorf, Germany) through the planter's ISOBUS.

The test stand consisted of a horizontal, suspended platform, of a scissor-lift type design to support and engage with the row unit. The test stand has the capability to separately load the planter row unit's gauge wheels and opening discs as well as the ability to change the row unit's operating height using pneumatic controls. The row unit's gauge wheel placement and dimensions, row unit weight, and magnitude of load that the hydraulic downforce system applied was derived from the manufacturer's product literature, drawings and personal meetings. Based on row unit weight and hydraulic downforce system capability, the test stand was designed for a maximum load capacity of 4454 N. Additionally, the test stand incorporates a vertical travel mechanism to raise and lower the height of the platform and a disc loading mechanism to simulate soil resistance so that the planter's downforce system feedback and response can be gathered.

Data Collection and Test Stand Control

A custom LabVIEW program (Labview, 2014) was developed to operate the downforce test stand's pneumatic valves and record data from the test stand and row unit sensors using a National Instruments (NI) CRio Chassis. On the test stand, the total downforce load was measured using a S-type load cell (Part no. 1631-03C, PCB piezotronics, Depew, NY, USA). Gage wheel load was measured through a 9810 N load cell (Part no. J4-1000, Fliegel, AgrarTechnic GmbH, Mühldorf, Germany) mounted on the planter row unit. Row unit hydraulic pressure and hydraulic supply pressure were measured through two hydraulic pressure sensors, (HAD 844L-A-0250-161, Hydac, Glendale Heights, IL, USA). Opening disc cylinder pressure and airbag pressure were measured through two pneumatic pressure sensors, (Part no. 1502881EZ100PSIG, PCB Piezotronics, Depew, NY, USA). Instantaneous test stand height was measured using an ultrasonic distance sensor, (Part no. UR18.DA0-11119994, Baumer, Southington, CT, USA). Among all the sensors, the gauge wheel load cell and one hydraulic oil pressure sensor were located on the planter row unit itself. To obtain the PWM duty cycle sent from the planter ECU to the automatic downforce hydraulic control block, the ECU signal wire was tapped and the signal sent to the NI 9403 module. The LabVIEW program counts the time that the PWM signal is high vs. low to calculate the duty cycle. The PWM signal produced by the planter ECU represents the automatic downforce control system's output. Several NI C-series modules (NI 9476, 9205, 9221, 9205, 9203) in the CRio chassis provided digital and analog inputs and outputs to interface with the various valves and sensors. The LabVIEW program read control commands from a *.txt file, henceforth referred to as a simulation file, to actuate desired disc loads through the disc loading mechanism and platform height through the platform height control mechanism. The program read the simulation file containing target values of disc load and platform height, parsed the data fields, and sent it to the corresponding control loops. The control loops used the simulation file data as a target load or height setting while reading pressure transducer and ultrasonic sensor data for current load of the disc cylinder and current height of the test stand, respectively. If the difference between the set value and actual value was above a set threshold, the control loop would adjust the pneumatic component up or down to achieve the desired load setting. A flow diagram of the program's operation is outlined in Figure 1.

The program included a main data display screen to observe real-time critical parameters during test stand operation. Real-time values displayed were total stand load, disc load, gage wheel load, press wheel load setting, hydraulic oil pressure in several key locations, and the duty cycle of the planter's ECU Pulse Width Modulation (PWM) output that controlled

the planter's hydraulic downforce. The screen also contains operator controls to start and stop downforce test simulations.

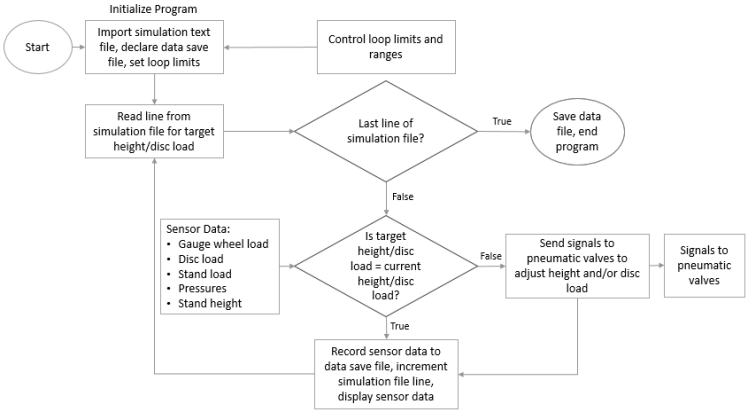

Fig. 1: LabVIEW program logic flow diagram

Field Data Simulations

After evaluating the operational capabilities of the downforce test stand, several scenarios were chosen from operational field data to be simulated and analyzed on the downforce test stand for automatic downforce system evaluation. The scenarios were chosen with varying and dynamic opening disc load variability, which would change the gauge wheel/disc load distribution and demand automatic downforce system actuation. The field data included information on real-time gauge wheel load and hydraulic pressure. To derive real-time disc load, it was assumed that the total downforce applied is equivalent to the sum of gauge wheel load, disc load and closing wheel load. Total downforce load is the sum of row unit weight and applied hydraulic load.

To collect the total downforce applied at different hydraulic pressures, the downforce test stand was set to maintain a constant row unit ride height while the hydraulic pressure output was changed using the planter's diagnostic screen. A linear regression was fitted between row unit cylinder hydraulic pressure and total downforce. The results show the relationship between the applied row unit hydraulic pressure and the total load applied and the intercept of the equation represents the weight of the row unit. The regression equation was used to calculate total downforce from real-time hydraulic pressure data during simulation tests.

Experimental Design

Three field scenarios were selected with the planter travelling at 7.2, 9.7, and 12 kph, henceforth referred to as S1, S2, and S3 “Disc loading at Planting speeds” in order to quantify the automatic downforce system response and accuracy at maintaining target gauge wheel load during varying planting speeds. The second set of simulation scenarios were from data strips representing a planter traversing from a section of the field with a heavier soil texture to a lighter soil texture represented by changes in soil EC. Data from two planting speeds of 7.2 kph and 9.7 kph with the planter moving through a varying soil texture were selected to generate simulation text files, henceforth referred to as S4 and S5 respectively “Disc loading on Varying Soil Textures”. Finally, the third simulation scenario was selected with the planter operating on a field edge with a rocky/hard clay soil that produced highly variable disc loading. The planter was operating at 9.7 kph and the simulation will be referred as S6, “Disc Loading on Rocky-Hard soil Zone”.

Data Analysis

Real-time gauge wheel load, from our simulated scenarios, was analyzed to gather the accuracy and response of the automatic downforce control system. Data was analyzed to quantify the percent time that the gauge wheel load was maintained within ranges of ± 89, ±156, and ±223 N of the target gauge wheel load setting by the automatic downforce controller. These ranges were chosen to represent three levels of downforce operation, selecting a range that describes how well the downforce system would work in a particular field would be dependent on a particular producer’s preference. The response time was the difference in time from when the gauge wheel load went outside the desired ±223 N range due to dynamic disc load deviation, and the time when the gauge wheel load returned within ±223 N of target load. To determine the automatic downforce controller’s ability to respond to different disc load variations, three disc load change events were selected. The selected disc load change events occurred during the speed simulations, soil type change simulations and the headlands hard clay/rocky simulation. The events represent disc load changes of 223, 412, and 677 N.

Results and Discussion

The results for each scenario were evaluated to quantify the effects of speed and soil texture on downforce system operation and response. For each scenario, the percent time of each test that the planter remained within a target gauge wheel load range was calculated. Also

calculated was the response time of the automatic downforce system to several disc load change events.

Disc loading at Planting speeds Scenario

Results for S1, S2, and S3 indicated that the downforce control system maintained target gauge wheel load within ±89, ±156, and ±223 N for an average of 72%, 92%, and 99% of the 7.2 kph test respectively. Similar results were observed for simulation of the planter operating at 9.7 kph where load was within target ranges of ±89, ±156, and ±223 N for an average of 61.71, 88.68, and 99.00% of the test, respectively, and 12 kph, where load was within target ranges of ±89, ±156, and ±223 N for an average of 89.02, 99.86, and 100% of the test, respectively. The results suggested that the control system could maintain target gauge wheel loads within tighter ranges for a longer duration of time with the planter operating at higher speeds, Table 1. Although, from a producer perspective, gauge wheel load within ±223 N of target may be satisfactory. If the goal is to maintain a tighter range, such as ±156 N, then future work needs to be conducted to optimize the control system response with varying speeds.

Table 1. Summary of the planter's ability to maintain target gauge wheel load during simulated scenarios

Simulation Scenario	Percent of test time within ranges		
	±89 N	±156 N	±223 N
S1	72%	92%	99%
S2	62%	89%	99%
S3	89%	100%	100%
S4	77%	94%	100%
S5	80%	90%	96%
S6	60%	847%	94%

Disc loading on Varying Soil Texture Scenario

The results for the S4 and S5 simulation tests indicated that the automatic downforce controller maintained gauge wheel load within ±89, ±156, and ±223 N of target load for 77%, 94%, and 100% of the test, respectively with the planter traveling at 9.7 kph. Whereas at 7.2 kph, the planter maintained gauge wheel load within ±89, ±156, and ±223 N of target gauge wheel load for 80%, 90%, and 96% of the test, respectively. The simulation results exhibited that

the planter, when traversing through varying soil textures, had disc load variations of larger magnitude thus creating a greater control demand.

Disc Loading on Rocky-Hard soil Zone Scenario

The simulation conducted representing a planter crossing through a field's headlands that contained a hard/packed clay with some rocks indicated that the planter's automatic downforce control system maintained gauge wheel loading within ± 89, ±156, and ±223 N of the target load for 60%, 84%, and 94% of the test, respectively, Figure 2.

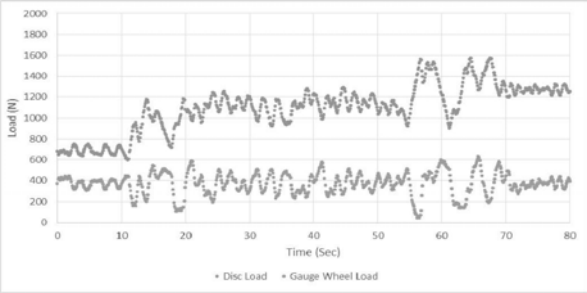

Fig. 2: S6 Simulation results of planter experiencing a headland with a hard, rocky clay

Conclusion

The main conclusions of this study were:

1. The test stand was able to conduct planter downforce control system evaluation using real-word field data.
2. The test planter's automatic downforce control system maintained the target gauge wheel load setting of 373±223 N for more than 94% of the time during all simulations.
3. The downforce control system was able to manage gauge wheel load with disc load variations up to 667 N within 1.3 sec.

References

Nielsen, R. L. (2005). Effect of Plant Spacing Variability on Corn Grain Yield. Retrieved June 12, 2017, from http://www.agry.purdue.edu/ext/corn/research/psv/Update2004.html.

Sharda, A., Fulton, J., Badua, S., Griffin, T., Ciampitti, I., & Haag, L. (2017). Planter downforce technology for uniform seed depth. K-State Extension. Retrieved from http://www.bookstore.ksre.ksu.edu/pubs/MF3331.pdf.

Zhao, S., & Chen, Y. (2015). Seed Distribution in Soil and its Effects on Early Plant Growth. Applied Engineering in Agriculture, 415-423. doi:10.13031/aea.31.10846.

Grisso, R., M. Alley, D. Holshouser, and W. Thomason. (2009). Precision farming tools: Soil electrical conductivity. Virginia Cooperative Extension. Retrieved from https://pubs.ext.vt.edu/442/442-508/442-508_pdf.pdf.

Biomethane as tractor fuel

Opportunities for customer, manufacturer or climate

Dr. **Petri Hannukainen**, Dr. **Rafael Åman**,
Agco Corporation, Suolahti, Finland

Abstract

Farming is today dependent on fossil energy. Agricultural machinery uses mostly fossil diesel as engine fuel. Also heating and electrics of farm facilities are direct energy consumption of food production that is at least partly based on fossil energy. Production of agrochemicals consume large amount of energy which is mostly produced by fossil fuel. Additionally, agrochemicals use many raw materials that have limited natural resources, like phosphorus. In general, the whole food production chain, including machinery, heating and electrics of farm facilities, production of agrochemicals, is at least partly based on fossil energy.

Due to increased usage and unit costs, energy has become a major cost of food production. Thereby energy consumption as overall is important to optimize in food production to guarantee its viability but also sustainability. Nowadays the CO_2 emissions of non-road mobile machinery (NRMM) are not controlled by legislation. However, the machines' fuel efficiency is important marketing factor that drives the development. Reduction potential of CO_2 emission when using combustion engine as main energy source of vehicle is limited to rather modest ratio. Development in different components and vehicle operation can gain some improvement in total efficiency. By switching to the renewable fuel the reduction in CO_2 emissions reduction can be dramatic.

This paper considers different aspects of the farm energy consumption and how biogas production can influence to it. Specifically, how tractor operation can benefit of renewable natural gas (RNG – also biomethane) availability. Finally, the experiences of Agco/Valtra on tractors running on RNG are discussed.

Background of alternative fuels and Valtra dual fuel RNG tractor prototypes

In the past several alternative fuel options have been suggested to replace the fossil fuels. Ethanol has been probably the most potential candidate together with different biodiesel products. Recently, RNG upgraded from biogas has been under big interest to be used as an

alternative vehicle fuel. Today, most manufacturers offer passenger cars that are able to use CNG and RNG.

In the 70's and other oil crisis the fuel substitutes were considered to improve energy security and to stabilize prices. Later on, the possibility to reduce the local pollution, especially reduction of noxious exhaust emissions, was the driving force. Lately, the focus has changed to the global environmental problems and climatic issues, which has brought emphasis on biofuels due to their ability to reduce the greenhouse gases (GHG). When biofuels are considered, the policy related to agriculture and labour has a strong position [1].

For company Valtra the RNG operated tractors are not the first proposed products that use renewable fuel. A prototype of tractor running on wood gas (Fig. 1, LHS) was developed by Valmet – former brand name of Valtra. Anyhow, this product newer reached the market.

At the end of 70's ethanol production was increasing in Brazil and large sugar beet farms wanted to use ethanol also as fuel for their own tractors. This started a development project by company Valmet do Brazil in South America to provide a solution for tractor to use ethanol as fuel. A dual-fuel engine that used small amount of diesel to ignite ethanol fuel due to compression was developed together with company MWM. Tractors called Alcool Valmet (Fig. 1, RHS) were sold 1700 units during 1983-1986, until the oil price went down and the interest in use ethanol as tractor fuel disappeared [3].

Fig. 1: LHS: Wood gas operated *Valmet* tractor running on field [2].
RHS: Ethanol operated *Alcool Valmet* tractors in 80's in South America [3]

Biodiesel has been under development for a long time. Also Valtra has had projects in 90's to test 1st generation biodiesel (FAME) to be used as tractor fuel. In current models maximum of 10% blend of FAME is accepted. Additionally, 2nd generation biodiesel (advanced biofuels)

according to standard EN15940:2016 is accepted as 100% blend for current products. Examples of advanced biofuels are NexBTL® by Neste and BioVerno® by UPM [4,5].

Biogas production has increased in Europe since 2005 very rapidly as can be seen in Fig. 2, LHS. Germany is clearly the biggest producer. In Fig. 2, RHS, can be seen that the number of biogas plants in Europe increased from 16,834 to 17,376 in 2015 (+3%). Some countries achieved significant increase such as the United Kingdom (77 additional plants / 17% growth), Belgium (20 / 11%) and the Netherlands (16 / 6%). In terms of biogas production, national associations and third-party observers quantify the total amount of electricity produced from biogas at 60.6 TWh, a number that corresponds to the annual consumption of 13.9 million European households [7].

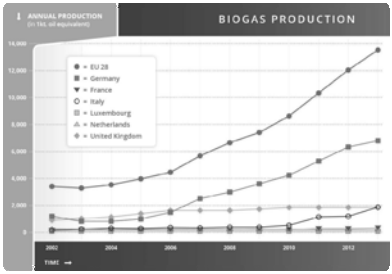

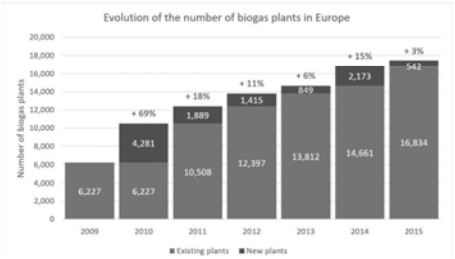

Fig. 2: LHS: Evolution of biogas production in European countries, [6].
RHS: Evolution of the number of biogas plants in Europe from 2009 to 2015 [7]

In 2015, there were 92 new biogas upgrading units commissioned which continues the steady growth of the RNG sector. Germany remains a leader in the sector, with 185 RNG plants. A few countries achieved significant growth, such as the United Kingdom (+43 new plants), France (+12), Switzerland (+11), Germany (+7) and Denmark (+6). These numbers reflect a clear development in Europe, showing that the biogas industry is a mature one.It can be then expected that these positive trends will continue in the short future [6]. In RNG production Sweden is clear dominant. In 2014 Sweden used appr. 50% of produced biogas as upgraded automotive fuel [8].

Increasing production of biogas was the main driver for Valtra to introduce a RNG operated tractor prototype. It was primarily intended for customers who have the domestic biogas production at own farm. First prototype of dual fuel RNG tractor was introduced in 2010 by Valtra at Borgeby Fältdagar [9] in Sweden. Since 2010 several units of RNG operated tractors has been manufactured to be used, for example, in different research projects to

collect information about usability and benefits of the solution. The two projects that Valtra has participated were the MEKA project in Sweden and BiomeTrak project in Germany. Target with prototypes has been to provide a tractor that is able to operate on RNG without major practical disadvantages from user point of view, meaning visibility, engine power or possibility to use different implements. First generation RNG tractor prototypes used in above-mentioned projects were not optimized with respect to engine exhaust emissions. This need to be noted when observing project results.

Data collection and demonstration of solution usability

Aim in participation to research projects has been to study feasibility and also partly environmental aspects of proposed solution. Valtra has provided four RNG driven tractor prototypes to the projects. This chapter briefly describes the scope of projects as well major findings.

MEKA project in Sweden

MEKA (Metandiesel Efter Konvertering av Arbertsmaskiner – "*Methane-diesel Retrofit of Non-Road Machinery")* project was performed between 2012-2015 by Swedish Board of Agriculture and the Swedish Transport Agency. Background in project was the recognized fact that diesel is predominant fuel used in NRMM. On the other hand, long term goal in Swedish vehicle fleet has been set to be independent of fossil fuels by 2030. Alternative fuels are used only in margin by this sector. Dual fuel operation using methane and diesel is a technology that has been deemed as having good potential [10]. At the time project was started, dual fuel NRMM vehicles did not exist in the market. One major reason for this has been lack of regulations to perform type approval for such machinery. Thereby one target of project was to provide information and knowledge to develop coming regulations to enable also development of dual fuel technology for NRMM.

MEKA project evaluated three different tractor prototypes, two Valtra N101 (1st gen.) and one Valtra N123 (2nd gen.) tractors. Project tested tractors in practical work conditions but also in laboratory environment. Additionally, project used portable emission measurement system (PEMS) to track tractor emissions during real working conditions. Four different loading cycles were performed during PEMS measurements to replicate different operation scenarios:

- Heavy transient work i.e. driving on country road with heavy trailer
- Heavy constant work i.e. field land cultivation

- Light transient work i.e. light transport on road and front loader work at farm
- Light constant work i.e. included grass mowing

MEKA project concluded that dual fuel tractors performed well through tests. Results showed small, in average ~4%, fuel cost benefit during dual-fuel operation when compared to diesel operation. Average of Swedish fuel prices from 2010-2014 was used for calculation. Project calculated climate impact of machines and results presented that dual fuel operation gained 15-30% decrease in climate impact with 1st generation N101 prototypes and up to 40% decrease with 2nd generation N123. The N123 had more developed software in ECU to control engine methane feed. Finally, project concluded that third party's system for retrofitting dual fuel for tractors is not recommended. This is due to the fact that conversion requires extensive adaptation of the engine and a good deal of commitment from the engine manufacturer to find solutions that can offer real climate benefits.

Figure 3. shows total climate impact of N123 tractor with different fuel options during different loading cycles based on PEMS measurements.

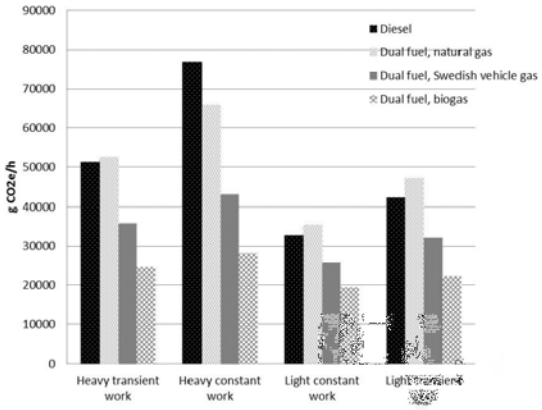

Fig. 3: Total climate impact for each loading cycle with N123 RNG tractor [10]

Even the prototypes used within project has not had development focus on emissions and fuel efficiency, in dual-fuel mode we can see clear improvement on climate effect. As fuel in calculations the biogas or Swedish vehicle gas (SVG) were used. The SVG is a mixture of fossil CNG and RNG, with blend of 40/60% ratio that project assumed respectively.

BioMekTrak project in Germany

BioMekTrak project was performed during 2014-2016 by Technology and Support Center (TFZ) in Straubing. Target of project was to collect experiences of RNG operated tractor in real working conditions as well perform emission testing for tractor prototype, see Fig. 4 [11]. Project used one Valtra N101 for testing. Testing was performed in two ways, emission and performance tests in laboratory based on non-road static cycle (NRSC) with eight stationary operation points. Field testing covered 620h of different types of practical field work.

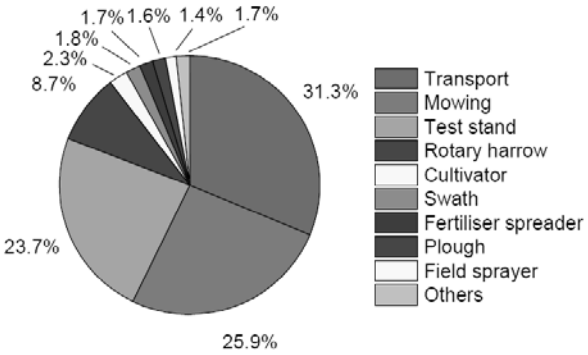

Fig. 4: Distribution of tractor operations in field testing [11].

Project conclusions were supplementary to results from MEKA project. Tractor practical operation was found to be good and users were mostly satisfied. Although, operational range in dual fuel mode was found to be quite limited and require gas filling station nearby in daily use. Tractor prototype tested at TFZ was first generation prototype, in which engine exhaust emissions were not optimized. Especially, HC emissions were found to be higher in dual-fuel mode than in diesel mode. On the same time a large potential to reduce them only by changing ECU control and optimization of oxidation catalyst was concluded. The NOx emissions were found to be slightly smaller in dual-fuel operation. Finally project outlined that with further development on dual-fuel tractor, biomethane could be a sustainable, alternative fuel option for agricultural tractors [11].

Opportunities in production of biogas and RNG in Agriculture

Energy consumption in farming and in food production can be divided into two categories, indirect and direct. Direct consumption is the part which is more visible to the customer and

thereby easier to affect as well. Figure 5 shows major distribution of farm energy demand [12].

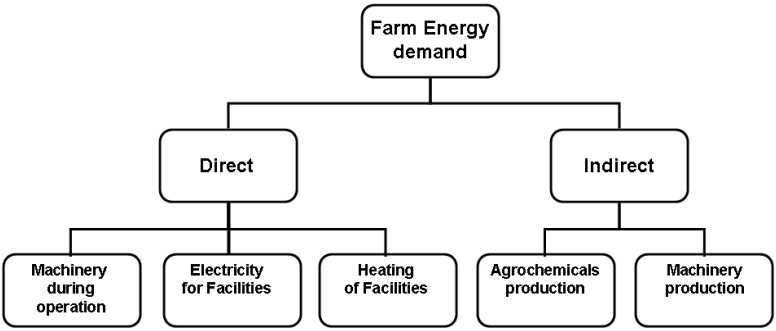

Fig. 5: Farm energy demand [12].

Biogas and RNG production provides many different aspects to improve sustainability and economy of farming and also support energy independency of farm. It could create new income for farms if energy is sold outside. On the other hand, increasing costs of fertilizers has resulted to situation where big portion of farm income is used to cover this expense. Biogas production enables to recycle nutrients, to decrease amount of purchased fertilizers and is a good opportunity to increase yield in organic farm. In Europe, organic farming is continuously increasing while average of organic crop production was 6.2% of land area and Austria is leading country with 20% [13].

One example of taking advance of different aspects in biogas production is Palopuro Agroecological Symbiosis (AES) that resulted from research project of nutrient, energy and climate efficient way of producing food. Palopuro AES is based on organic farm of 385 hectares. The yield from green manure grasses is harvested and taken to the dry digestion plant together with horse and hen manure. The plant produces energy for farm as well RNG for own machinery and to be sold outside. Digestion residue is taken back to the arable land as fertilizer. The recycling of biomass through biogasification reduces the loss of nutrients. Digestion residue can be targeted more accurately than green manure as fertilizer which besides involving less environment problems improves yield [14].

Tractor or other farm machinery fuel consumption is considered as part of direct energy consumption. The farm can cut direct energy cost by replacing all or part of machinery fuel with own produced RNG. As MEKA project reported [10], even by using purchased RNG it is

possible to reduce fuel cost of tractor compared to diesel operation. Anyhow, if fuel is coming from own production this economical benefit can be even higher.

Based on observations from MEKA and BioMektrak projects as well Palopuro AES studies it can be stated that production of biogas and RNG can have positive impact in many forms to farm energy demand. Direct energy consumption can be compensated by using biogas for heating and electricity of facilities and RNG as machinery fuel. Also portion of indirect consumption can be reduced by replacing the agrochemicals with biogas digestion residues.

A global aim is to reduce GHG emissions. E.g. EU has set targets to reduce GHG emissions with 20% by 2020 and with 40% by 2030 when compared to 1990 level. Even higher (80%) long term target is set by 2050 [15]. These targets have already led to actions in automotive sector where passenger cars' CO_2 emissions have reduced greatly. On the other hand, there are many discussions ongoing whether targets for vehicles should be local or global. For example, electric cars are locally emission-free. But if electricity is produced with fossil fuel, total emissions of driving can be even higher than for gasoline. In Fig. 6 is presented a comparison of *well-to-wheel* emissions for some renewable fuels compared to diesel and gasoline.

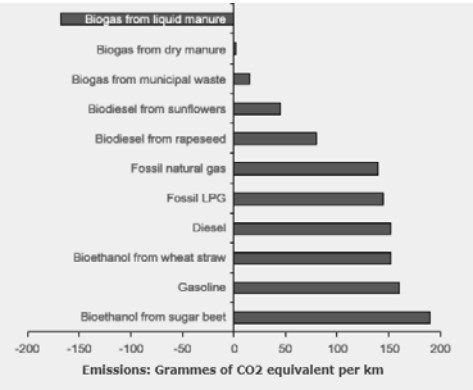

Fig. 6:. Comparison of *well-to-wheel* emissions of biofuels [16]

Emission regulations for NRMM basically follow few steps behind on-highway regulations. On-highway and passenger car regulations aim to reduce local emissions, which is reasonable as these vehicles are often used with large intensity in dense populated areas. Anyhow, agricultural vehicles are typically used in rural areas where normally less pollution exists, than in urban areas. Thereby, it could be worth of considering if emission regulation

for such machinery should be directed more to take into account global emissions instead of local ones. As results from MEKA project showed, even with prototype tractors the climate effect of tractor was greatly improved by using RNG in dual fuel operation compared to diesel operation. Improvement of GHG emission by 40% is such a high number that it would be extremely difficult to achieve in other means, like increasing the diesel operated vehicle efficiency at same amount. Thereby using RNG gives good opportunity to improve climate effect of agricultural machinery.

Conclusion

In this paper the background of Agco/Valtra development related to renewable fuels in tractors was introduced. The results of two research projects that tested RNG operated tractors were presented. As major results, the tractors were operating well during tests in practical work condition. Also, even tested tractors were prototypes they gave positive feedback about environmental effects when using RNG as tractor fuel. Additionally, RNG operation gained small improvement to direct fuel cost of tractor operation. Paper also discussed other benefits that biogas and RNG production can offer for food production. It can improve farms economy and thereby secure local food production. It also can have positive effect more globally by changing farm energy usage from fossil based more towards renewable based. Other positive climate effects can be achieved by replacing fossil fertilizers with biogas plant residues. To start production of RNG will not be beneficial if only used as tractor fuel. But in creating complete food production value chain to be more economical and sustainable it tractor running on RNG plays very important role.

Acknowledgement

Authors would like to thank all research personnel in MEKA and BioMeTrak projects. A major contribution related to RNG tractor development in past decade has been given by Mr. Tapio Riipinen from Afcon Oy. Finally, authors want to dedicate this paper to memory of Mr. Hannu Niskanen, who made remarkable career at Valtra tractors in different positions and countries during 1971-2011. Mr. Niskanen published several books related to tractor technology as well documenting history of Valtra company and products. One of last projects Mr. Niskanen started before retirement was the development of RNG operated tractor.

References

[1] Murtonen, T. & Aakko-Saksa, P. *Alternative fuels with heavy-duty engines and vehicles*. VTT working papers 128, 2009.

[2] Niskanen, H. 1998. *Munktellista Valtraan: Pohjoismaisen traktorin menestystarina jatkuu* (In Finnish). Valtra, Finland, 1998. ISBN: 952-90-9990-8.

[3] Niskanen, H. *60 vuotta Valtran värikkäitä vaiheita* (In Finnish), Valtra, Finland, 2010. ISBN 978-951-98599-5-8.

[4] UPM BioVerno: A renewable fuel from Finland. Available in: http://www.upmbiofuels.com/products/Pages/Default.aspx [Referred Aug. 9, 2017]

[5] Neste Oil produces renewable fuel with innovative technology. Available in: http://www.bioeconomy.fi/neste-oil-produces-renewable-fuel-with-innovative-technology/ [Referred Aug. 9, 2017]

[6] What is Biogas. Available in: http://www.lee.lu/index.php/en/biogas [Referred Aug. 9, 2017]

[7] EBA launches 6th edition of the Statistical Report of the European Biogas Association. Available in: http://european-biogas.eu/2016/12/21/eba-launches-6th-edition-of-the-statistical-report-of-the-european-biogas-association/ [Referred Aug. 9, 2017]

[8] IEA bioenergy task 37, Country report Sweden. Available in: http://task37.ieabioenergy.com/country-reports.html [Referred Aug 24, 2017]

[9] Borgeby Fältdagar in Sweden. Available in: https://www.borgebyfaltdagar.se/?page=facts_ about_borgeby_faltdagar& p=2024&m=1645 [Referred Aug. 9, 2017]

[10] Einarson, E., Törnquist, S., Enghag, O. & Lundström, E. *Biogas operation in Non-Road Machinery*. Final report from the MEKA project. Swedish Transport Agency, 2016. ISSN 1102-3007.

[11] Mautner, S., Emberger, P., Thuneke, K. & Remmele, E. *Emissions- und Betriebsverhalten eines Biomethantraktors mit Zündstrahlmotor* (in German).Technology and Support Center (TFZ), Germany, 2017.

[12] Pichlmaier B., Hannukainen P. & Godbole R. *A Global Approach to Energy Efficiency*, VDI Landtechnik 71, pp 495-505, Germany, 2013.

[13] Organic crop area on the rise in the EU. Eurostat news release 208/2016. Available in: http://ec.europa.eu/eurostat/documents/2995521/7709498/5-25102016-BP-EN.pdf/cee89f9e-023b-4470-ba23-61a9893d34c8 [Referred Aug 25, 2017]

[14] Helenius, J., Koppelmäki, K. & Virkkunen, E. *Agroecological symbiosis in nutrient and energy self-sufficient food production*. Ministry of environment report 18/2017, ISBN Nid.:978-952-11-4715-9, Finland, 2017.

[15] European commission climate strategies & targets. Available in: https://ec.europa.eu/clima/policies/strategies_en [Referred Aug 24, 2017]

[16] Organic power. Available in: http://www.organic-power.co.uk/biomethane_compared_to_other_fuels.aspx [Referred Aug 24, 2017]

Conventional and Novel, New Approaches to Creating High-Density Biomass Bales

Dr. **Kevin J. Shinners**, **Joshua C. Friede**, **Joshua R. McAfee**, **Daniel E. Flick**, **Nolan C. Lacy**, **Cyrus M. Nigon**,
University of Wisconsin, Madison, WI US

ABSTRACT

The costs for harvest, aggregation, storage, and transport of dry biomass are all impacted by bale density. Manufacturers are now offering high-density (HD) balers to meet demands to lower biomass feedstock costs. Field evaluation of HD balers was conducted to quantify achievable bale density and subsequent specific energy consumption (SEC) required to bale common biomass crops. Maximum bale densities were 180 and 240 (kg DM)·m^{-3}, for wheat straw and switchgrass, respectively. Baling SEC increased as a second-order polynomial function of bale density. Although conventional plungerhead balers can create HD bales, the balers are expensive and baling is power intensive, requiring large tractors. We propose an alternative approach where HD bales are created by reshaping and recompressing low-density square or round bales. Pressure-density relationships show that HD recompressed bales can be created with much lower energy requirements than by conventional methods. An alternative, novel approach to creating HD large-square bales by continuous compaction using an auger with compressing rollers was developed and field evaluated. With this technology, square (80 x 80 cm) wheat straw bales in excess of 180 (kg DM)·m^{-3} were produced with the auger baler which is much less complex and lighter weight than a conventional plungerhead baler.

INTRODUCTION

The large-square bale (LSBe) is currently the most common package used to harvest and store biomass feedstocks, primarily because it produces the greatest package density. Bale density has been identified as having the greatest impact on feedstock harvest costs [1]. To achieve legal transport weight limits in many countries, the LSBe density should be about 240 kg·m^{-3} [2]. Using conventional balers, LSBe densities of only 145 to 200 kg·m^{-3} have been reported for switchgrass, wheat straw and maize residue [3-6]. To produce higher-density bales, manufacturers have modified large-square balers (LSBr) to produce greater bale-face pressure by increasing resistance to bale movement through longer bale chambers and greater chamber convergence. Although greater density can be achieved, increased

harvest costs due to the more expensive baler, larger tractor required and higher operating costs (fuel, stronger twine, etc.) may overwhelm cost saving in storage and transport [7].

After almost four decades of improvements, the LSBr design is now highly optimized and a marvel of agricultural engineering. But densification by a reciprocating plungerhead may have reached practical limits. Greater bale density is achieved by applying higher pressure to the bale face, but the pressure-density relationship is a power function. After initial void reduction and consolidation, large increases in pressure only produce small incremental density improvements. When applied over the large area of the bale face, even relatively low pressures of 700 kPa will generate tremendous forces and torques which requires heavy frame members, robust driveline components, and large flywheels. Current LSBr use a reciprocating plungerhead with typical frequency of 40 to 50 strokes per minute. Power requirements for densification in this manner are high because of the relatively high-frequency of the tremendous applied loads. What is proposed here are several alternatives that could offer methods to create bale densities even greater than those produced by current LSBr technology, but requiring less power and lighter, simpler machines.

HIGH-DENSITY BALING WITH CONVENTIONAL BALERS

Conventional LSBr have difficulty achieving densities greater than 200 $kg \cdot m^{-3}$ for biomass crops [3-6], which is not sufficient for weight-limited transport. We investigated the ability of a HD baler (Krone 1290 HDP XC) to create bales that could achieve weight-limited transport. Assuming bales would be shipped at 85% DM, maximum bale densities achieved were greater than 240 $kg \cdot m^{-3}$ for switchgrass, reed canarygrass, maize residue, and sorghum but not for wheat straw (max. of 200 $kg \cdot m^{-3}$). Total SEC required from the tractor engine to make bales at the maximum density was 9 to 18 $kJ \cdot (kg\ DM)^{-1}$, depending on crop type and yield. Baling SEC increased as a second-order polynomial function of bale density. Precutting increased bale density by 4 to 10% and increased total SEC by 11 to 21%.

RECOMPRESSION AND RESHAPING BALES

Recompressing and resizing square bales is sometimes used to improve transport efficiency, especially for high-quality bales that will be transported long-distances or exported overseas [8]. This process is often done in capital-intensive industrial facilities located off-farm. The added costs of transport prior to recompression may be economical with high-value animal feeds like lucerne but not with low-value biomass feedstocks. What is proposed here is on-board recompression and reshaping of both large-square and large-round biomass bales. In this embodiment, low-density bales would be produced by low-cost conventional baler

mechanisms and then the bale would be delivered to an on-board or trailed recompressor. Densification, reshaping and resizing of the first bale would occur in the 30 to 60 s while the next bale is formed. Although densification forces are large, these forces can be applied over a relatively long time so specific energy requirements are much less compared to those required by conventional high-density balers. Current tractors have more than adequate hydraulic flow and pressure to produce the needed forces with reasonable size cylinders. Ingenious designs that place cylinders in tension would reduce required frame size and weight. After densification, there may be sufficient dwell time available for material stress relaxation, allowing the material to lose some of its resiliency before the bale is restrained [9]. Reducing recoil forces reduces bale expansion, maintains achieved density, and allows for lower-cost restraining material to be used. In our research, recompressing LSBe produced re-expanded bale densities of 279 and 282 (kg DM)·m^{-3} for wheat straw and switchgrass, respectively. When compression occurred over less than 25 s, specific energy was less than 1.1 kJ·(kg DM)$^{-1}$. The total force applied by the restraints to prevent bale re-expansion was more than twice that required for HD LSBe.

An alternative recompressed bale system has been proposed that uses a large-round bale (LRBe) for initial harvest and packaging and then uses a reshaping and recompression process to improve bale density, cross-section and transport efficiency [10-11]. We developed a bi-axial recompression system [10] conducted as a three-stage progression: vertical reshaping to cuboid shape, followed by vertical and then horizontal densification (fig. 1). Densities of 240 (kg DM)·m^{-3} was achieved with common biomass crops but density decreased 19 to 30% due to re-expansion after strapping and release of pressure. Recompression over 15 to 20 s required less than 1.0 kJ·(kg DM)$^{-1}$.

An important design aspect of an on-board recompressor is how initial density and the desired final bale size affect the required size of low-density bale before recompression (fig. 2). Low initial density reduces baler costs but increases the size and cost of the recompressor. If a 1.3 m final LSBe length is desired from a single compression charge, then very low initial bale density may be unrealistic due to the required length of the recompressor chamber. Alternatives such as multiple recompression charges or combining two recompressed bales are potential solutions but will add to design complexity. A successful recompressor design will balance the baler cost savings due to low initial density requirements with the size and complexity of the recompressor.

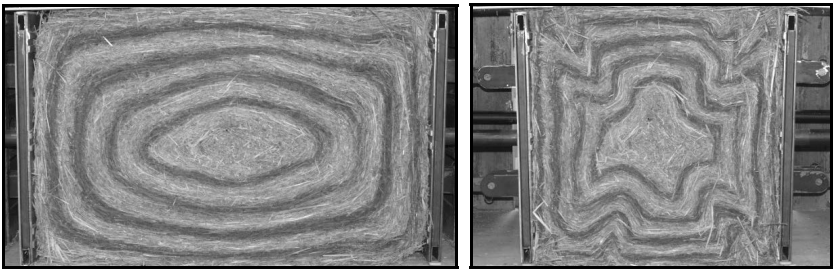

Fig. 1: Concentric rings flattened during vertical reshaping and compression (top). During horizontal compression, material will shear and fold along the bale diagonals where the shear stress is greatest (bottom). After [10].

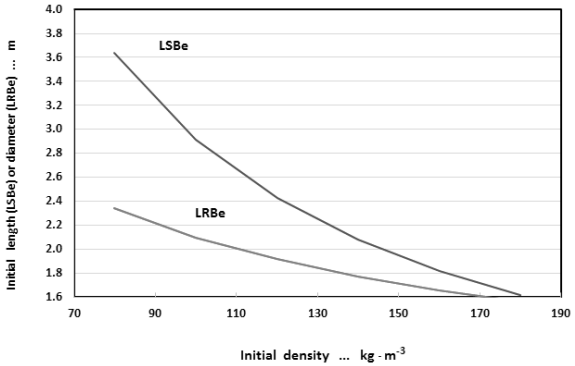

Fig. 2. Initial bale density versus required initial length (for LSBe) or diameter (for LRBe) to achieve 240 kg·m^{-3} final density. LSBe final length is 1.3 m and LRBe final dimensions are a 1.2 m cube.

CONTINUOUS HIGH-DENSITY COMPACTION WITH AN AUGER BALER CONCEPT

Conventional plungerhead balers intermittently compress flakes into a converging bale chamber and compression takes place at relatively high-frequency. We are investigating an alternative baling concept that replaces the discontinuously compressing plungerhead with a continuous feeding auger with a set of conical rollers at the end (fig. 3).

The auger lays thin layers onto the bale face and the rollers flatten the crop as it is laid onto the face. A converging bale chamber with square 80 x 80 cm cross-section is used to complete bale densification. Axial force on the auger is measured and a feedback control system is used to alter tension panel pressure to maintain a target auger compression force. Challenges with this approach include achieving a square bale cross-section from a round auger and segmenting the continuous crop stream into discrete bales. Careful application of auger strippers in the barrel was needed to push crop to all four corners of the chamber [12]. The pivoting bale separation arms are used to cut the bale into discrete lengths and clear a path for the needles to supply twine to the knotters. Bale densities of 230 to 250 (kg DM)·m^{-3} have been achieved with crops like switchgrass and maize residue. Baler SEC was typically less than 5 kJ·(kg DM)$^{-1}$, comparable to that of a LRBr. The baler mass is 5400 kg, considerably lighter than a LSBr producing similar bale dimensions. The combination of thin-layers and flattened crop help produce high bale densities with a machine that is potentially simpler and more cost effective than a conventional baler.

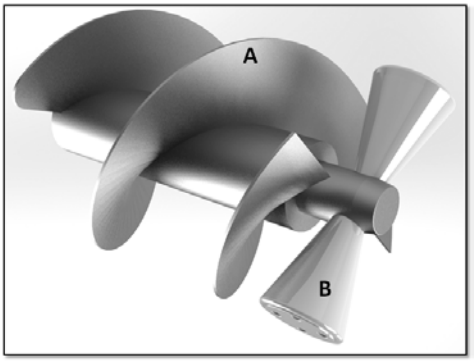

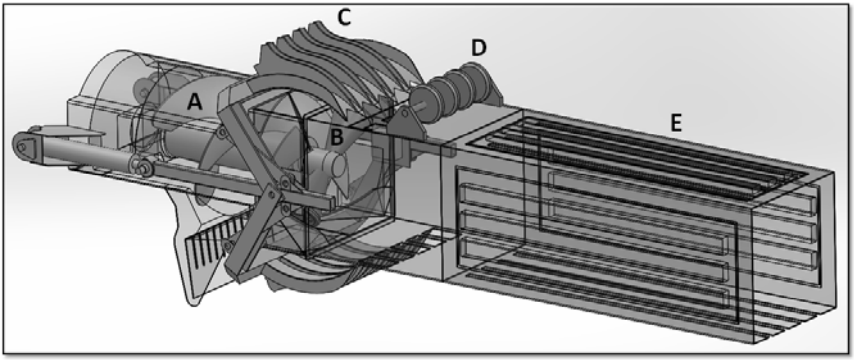

Fig. 3: Auger baler concept consisting of (A) feeding auger; (B) compressing rollers; (C) bale separation system; (D) knotters; (E) converging bale chamber.

ACKNOWLEDGEMENTS

This research was partially sponsored by the University of Wisconsin College of Agriculture and Life Sciences, CenUSA, a research project funded by the Agriculture and Food Research Initiative Competitive Grant No. 2011-68005-30411 from the USDA National Institute of Food and Agriculture, and USDA National Institute of Food and Agriculture, Hatch Project No. WIS01721. We also acknowledge the financial, material or technical support of DuPont Biosciences, John Deere Ottumwa Works, and Krone North America.

REFERENCES

[1] Kenney, K. L., J.R. Hess, N.A. Stevens, W.A. Smith, I.J. Bonner, D.J. Muth. 2014. Biomass Logistics. Bioprocessing of Renewable Resources to Commodity Bioproducts, 29-42.

[2] Miao, Z., Phillips, J. W., Grift, T. E., & Mathanker, S. K. (2013). Energy and pressure requirement for compression of Miscanthus giganteus to an extreme density. Biosyst. Eng., 114(1), 21-25.

[3] Cundiff, J. S., & Marsh, L. S. (1996). Harvest and storage costs for bales of switchgrass in the southeastern U.S. Bioresour. Tech.,56(1), 95-101.

[4] Kemmerer, B. D., & Liu, J. (2010). Spring switchgrass harvest with a New Holland large square baler. ASABE Paper No. 1009029. St. Joseph, MI: ASABE.

[5] Shinners, K. J., Binversie, B. N., Muck, R. E., & Weimer, P. J. (2007). Comparison of wet and dry corn stover harvest and storage. Biomass Bioenergy, 31(4), 211-221.

[6] Shinners, K. J., Boettcher, G. C., Muck, R. E., Weimer, P. J., & Casler, M. D. (2010). Harvest and storage of two perennial grasses as biomass feedstocks. Trans. ASABE, 3(2), 359-370.

[7] Sokhansanj, S., Webb, E., & Turhollow, A. (2014). Cost impacts of producing high-density bales during biomass harvest. ASABE Paper No. 141912320. St. Joseph, MI: ASABE.

[8] Beauchemin, K. A., & Rode, L. M. (1994). Compressed baled alfalfa hay for primiparous and multiparous dairy cows. Journal of Dairy Science, 77(4), 1003-1012.

[9] Ast, G. (1987). Apparatus and method for recompressing bales of fibrous material. U.S. Patent 4,676,153.

[10] Lacy, N.C. and K.J. Shinners. (2016). Reshaping and recompressing round biomass bales. Trans. ASABE. 59(4): 795-802.

[11] Olander, B. D. (2014). Giant round baler compressor. U.S. Patent No. 8,833,247.

[12] Sibley, D.A., and D.R. Dolberg. (1996). Specially shaped auger compactor housing section for effecting even distribution of material into bale-forming chamber having rectangular cross section. U.S. Patent 5,535,669.

New Techniques for Mobile Pelletisation

Kai Lüpping M.Eng,
Maschinenfabrik Bernard KRONE GmbH & Co. KG, Spelle

Abstract

The technique for producing pellets had already been developed more than 100 years ago. In the 1960s, farmers already started to produce briquettes on the field. Until today, two pressing principles have well established in the pellet production market. Some pelleting presses are equipped with ring cavities, others have flat ones. One or more rollers push the material into the pressing channels. There are more possibilities to produce pellets although the variant with pellets made from straw has never played an important role even though pellets have several advantages over straw bales.

A straw bale is a piece good that means that each bale must be considered individually. Pellets however can be considered as bulk goods. This offers automation possibilities when using straw, e. g. when feeding animals or in terms of energetic use.

Pellets are especially well-suited for bedding since they are really easy to portion and also absorb more water than straw coming from bales. If the grinding of crops, which is standard nowadays, is waived, the structure is preserved. The result is an particularly high-quality bedding combined with minimum efforts.

Other disadvantages of pellets were the difficult transportation of bales as well as the complex production. First, straw must have been collected from the field. After delivering it to a stationary pelletising unit the bales are cut, shredded and finally pellets are produced. The new technique allows to collect material directly from the field. Next, it is fed to the pellet press rollers which produce pellets out of the straw.

Thanks to this innovative pressing principle of the KRONE Premos 5000 the crop processing can start immediately. The teeth on the first pellet press roller run synchronously over the pressing channels of the second roller. Thus, a closed pressing chamber is guaranteed for each pressing channel.

Short transport ways in pellet production and use result in great economic benefits. Just taking into account the straw recovery 60 euros can be saved. In addition, energy is saved since there is no need to pre-shred the straw when pelletising. Real cost benefits are offered to the end customer thanks to the automatic usage possibilities of pellets.

State of technology in terms of pelletisation

The production of pellets is not a new technique. There are patents which are more than 100 years old [1]. At that time, pellets were produced by means of two rollers. One roller pushed the material with its teeth in the gap of the other roller. Both rollers were alternately equipped with a tooth and a gap.

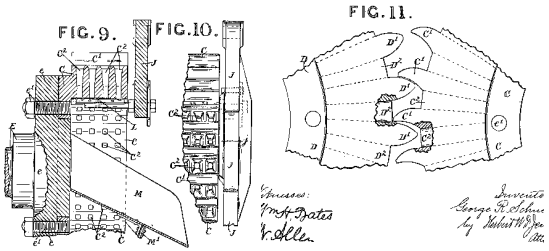

Fig. 1: Pelletisation 1914 [1]

Over the years new ideas on pelletisation were generated, e. g. a method including augers [2] which are similar to the extruders for plastic used nowadays.
Around the year 1966, John Deere developed a press which was able to produce briquettes on the field. Briquettes are larger than pellets and are likely to have a lower density.

Fig. 2: John Deere Hay Cuber [3]

Finally, techniques using pan grinding presses have established themselves [4]. A distinction must be made between two systems. The rollers of the flat die press run over a perforated disc. The second system operates with ring cavities. One or several rollers roll on a perforated ring. Doing this, the rollers position firmly at one spot while the ring cavity is

driven. The material to be pressed is fed between the rollers. The finished pellets growing on the outside are cut to a defined length.

Advantages and application of pellets

The better handling is the main advantage of pellets over straw bales. A straw bale is a piece good that means that each bale must be considered individually. Although several bales can be transported at the same time each individual bale is considered. Pellets, however, are bulk goods. Here, straw is treated as a mass product which means that not each pellet is counted separately. Thus, feed systems are able to transport straw automatically and make it available for final consumption thanks to current technology.

Another great advantage is the high bulk density of pellets. On average, square balers nowadays press straw with a bulk density of 160 kg/m³ to 200 kg/m³. For pellets, a bulk density of more than 600 kg/m³ can be expected. This saves transport and storage expenses. Comparing this density with the one of high-pressure bales, the difference is even clearer, as shown in fig. 3.

Fig. 3: Advantages of pellets [5]

The application areas for pellets are very versatile. One of the most obvious is combustion. In some countries, the combustion of straw pellets is commonplace. Power stations have been adapted to this kind of use. Besides coal and oil, the power station in Amager (Denmark) is also able to combust straw pellets.

Pellets are also added to animal feed. Thanks to the pellets straw can be added to the feed automatically and is an alternative to bran which is used as a fibre additive nowadays. Furthermore, the bedding for animals is another application field of pellets. Due to their simple handling they are ideal for bedding but also for the removal of excrements. Another positive feature is the reduced dust load when bedding. In addition, pellets have a better

absorption power than bales. Water can be better absorbed due to the short straw pieces and due to the wax layer which was damaged during the pressing process.

Fig. 4: Applications of pellets [5]

Premos 5000 technology

The PREMOS pellet harvester introduces a new innovative technique. A pick-up takes up crops that are transferred to the crop conveyor by the feed rotor. Next, the crops are guided under the bottom pellet press roller. Then, it is fed from behind to both rollers. Unlike traditional pelleting presses, the crops are not pre-crushed. So the straw structure remains the same. The straw is drawn in by both pellet press rollers. Alternately, one roller is equipped lengthwise with pressure rings and pressing channels. The material is pressed by the pressure ring of one roller into the pressing channel of the second roller. The pressure rings are provided with teeth.

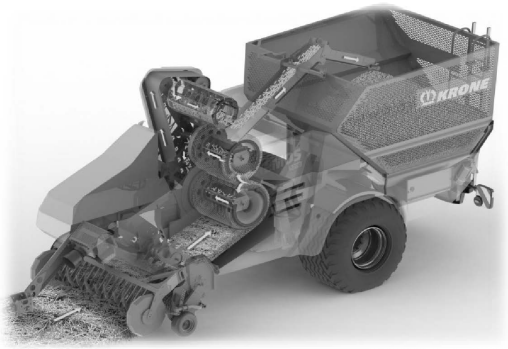

Fig. 5: Premos cut view [5]

Their tips position on the surfaces between the single pressing channels. As a result, a closed pressing space develops (fig. 6). The tooth root between the teeth has a round shape. One more innovative aspect is that the tooth does not enter the pressing channel funnel. No forces are generated between the tooth flanks and the pressing channel. As a consequence, the amount of energy needed is significantly reduced.

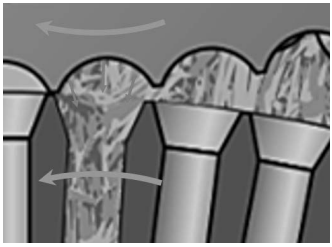

Fig. 6: Compression [5]

After the material has left the pressing channel it is cut to an adjustable length inside the pellet press rollers. Augers pass it on to an elevator from where it goes to a rotating screen. The screened material falls back onto the crop conveyor. By means of an additional conveyor belt the pellets reach the hopper.

The finished pellets have a temperature of approx. 80 °C. They are cooled both in the pellet press rollers and hopper so that they achieve their final strength. Due to favourable evaporation conditions water is extracted from the pellets.

Economic constraints

An economic benefit of the PREMOS compared with traditional pelletising systems is the fast conversion process from straw to pellet. A PREMOS machine just measures a way of 4 metres from the pick-up collecting straw to the pressed finished pellet. Also traditional systems start with taking up straw from the field. The costs are the same here but subsequent costs for the bale chain are saved when working with a PREMOS machine. Money is not only saved when pressing and loading: there are no further transport and storage costs for post-shredding. These costs of approx. 60 euros per tonne are significant. Working with the PREMOS, some steps in the pelletising process are not required anymore. There is no pre-shredding process which is usually done by hammer mills. These consume a large amount of energy in today's pelletising machines.

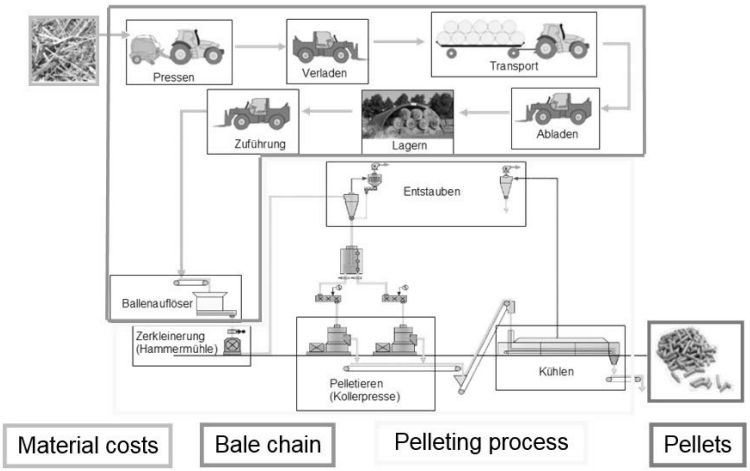

Fig. 7: Traditional pelletising

There is always the question whether it is sensible to compress straw with 400 HP and a throughput of 5 tonnes per hour or if it is better to burn the diesel. Five tonnes of straw have a calorific value of approx. 24,500 kWh. A tractor consumes less than 100 l/h. This is a calorific value of 990 kWh. Comparing these values results in an energy use of less than 4 % during pelletising.

Another great benefit of the PREMOS is that it can be used stationary. Instead of the pick-up a bale shredding system can be installed. This system shreds square bales and feeds them to the machine. This allows to postpone field operations to times of reduced work loads. This

is of particular interest for regions with just a few operating days for pressing straw or a short period of working time on the fields.

[1] US 1127925 A
[2] US2910726 A
[3] Youtube
[4] EP0201052 A2
[5] Krone
[6] de.wikipedia.org/wiki/Kraftwerk_Amager

Field performance of a novel mower-chipper for the harvest of short rotation coppices

Dr.-Ing. **Ralf Pecenka**, Dr.-Ing. **Detlef Ehlert**, Dr. **Thomas Hoffmann**,
Leibniz-Institut für Agrartechnik und Bioökonomie, Potsdam

Abstract

Restrictions in availability and performance of equipment as well as high cost of harvest equipment for wood from agriculture produced in plantations of short rotation coppices (e.g. poplar, willow or black locust) are still a limiting factors for the further growth of this branch in agriculture. Three different harvest systems – two of them based on modified forage harvester and one mower-chipper - have been investigated during the harvest of poplar and black locust in season 2015/2016 in Germany. Although there are major differences in machine design, requirements to the layout of plantations, maximum harvestable tree size and performance of machines for SRC-harvest, no major differences in the effective material capacity (EMC) between forage harvester based solutions and the mower-chipper (EMC ~16 odt h^{-1}) could be observed during the test. Wood chips produced with the investigated forage harvesters fulfilled the requirements for chips of class P16 … P31, but with a higher content of fines (>10%). In contrast, the wood chips produced with the mower-chipper have been much coarser, fulfilling the requirements for chips of class P31 to P45, with a very low content of fines (< 7 % d.b. black locust, < 5% d.b. poplar). All tested harvesters showed reliable operation under practice conditions and are commercially available.

Introduction

Woody biomass from agriculture is a promising source for non-fossil energy. Cropping fast growing trees on agricultural land is connected to several environmental advantages such as low demand for mineral fertilisers, a drastic reduction in use of chemicals for plant protection, an increase in biodiversity due to extensive agricultural practices and carbon storage due to the establishment of large root systems in the soil [1, 2]. Poplar, willow and black locust are typical varieties of such fast growing trees respectively short rotation coppices (SRC). After planting the trees in a properly designed planting scheme with regular spacing, the SRC-plantations are typically harvested every two to six years without replanting. According to present experience such plantations maintain their productivity for at least 25 years. In dependence to tree variety, soil conditions and local climate typical long term yields from 8 to 15 odt ha^{-1} yr^{-1} can be expected [3].

Despite of many years of research and development in the SRC-sector, there are still several problems in cultivation and mechanization of the SRC-process chain, particularly caused by the lack of knowledge and machinery. In particular cost-efficient harvest and high dry matter losses during storage are still matters of much concern. Although a lot of new harvest machines were developed and tested during the last 30 years, only a few have exceeded prototype stage. Analysing the process chain for SRC, it can be concluded that high investment costs for suitable harvest equipment, low flexibility of harvest solutions regarding variety and cultivation scenario as well as high machine weight accompanied by problems regarding limited trafficabillity of the fields at harvest time are some of the most important obstructions at present [4].

As a result, approx. 30 % of the total production costs are located in the process steps of harvest and transport alone, assuming optimal harvest conditions. At present, direct-chipping respectively cut-and-chip lines seem to be most cost-efficient for harvest of SRC, and modification of forage harvesters is a promising option (Fig. 1) [5]. But for economic operation of these expensive harvest systems cultivation areas of more than 300 ha are required [6]. A further disadvantage of harvesting SRC with forage harvesters is the limited length of the wood chips. Previous experiments and investigations of wood chip storage have shown that bigger particles (chip length of more than 50 mm) can be advantages for long term storage due to improved drying by natural air ventilation [7, 8, 9].

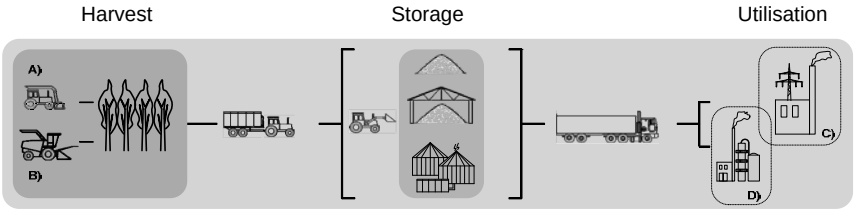

A) Harvest with mower-chipper
B) Harvest with forage harvester
C) Energetic use
D) Use for materials

Fig. 1: Process chain for cut-and-chip harvest, storage and utilisation of wood chips from SRC

The Leibniz Institute for Agricultural Engineering and Bioeconomy (ATB) has developed a simple and low weight tractor-mounted mower-chipper for medium sized standard tractors (150-250 kW) [10]. The machine has been intensively tested and optimized during the harvest seasons from 2014 to 2015.The commercial machine (MH 130) has been presented at

the Agritechnica 2015 and is marketed now by the Kluge GmbH from Königswartha/Saxonia, Germany. For the evaluation of this harvest system under practice conditions, harvest performance data from harvest tests with the mower-chipper MH-130 and two different forage harvester solutions have been analysed and compared in season 2015/2016.

Materials and Methods

The different machine concepts for SRC-harvest with cut-and-chip lines are shown in Fig. 2 and 3. Whereas the mower-chipper solutions process the trees in their natural vertical position (Fig. 2), forager harvesters have to push them to a horizontal position after cutting from the plant stand (Fig. 3). Connected to this are limitations in planting density, tree age resp. stem diameter for harvest with forage harvesters (Tab. 1). In return, forage harvester can harvest also plantations with double rows (e.g. typical for SRC-willow), whereas mower-chippers are limited to single row plantions.

Fig. 2: Fendt 930 tractor with mower-chipper MH-130 from Kluge GmbH

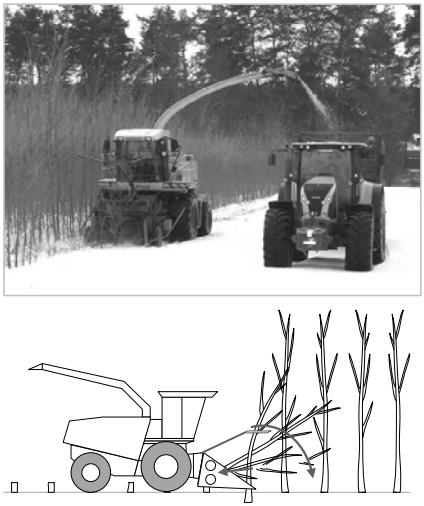

Fig. 3: Claas Jaguar 870 forage harvester with HSAB-header

During the field tests three different harvest systems have been investigated in detail:

- A Claas Jaguar 870 forage harvester with a HSAB-header MK IV and a standard chipping drum for harvest of fine chips (class P16)

- A Claas Jaguar 900 forage harvester with a Wimatec-header HV 1400 and a modified chipping drum for harvest of middle size chips (class P31)
- A mower-chipper MH130 from Kluge with a Fendt 930 tractor for harvest of middle size and coarse chips (P31 … P45)

The machines have been tested on fields in the county of Brandenburg from January to February 2016. Table 1 gives an overview of the relevant machine data and Table 2 shows the details of the field tests.

Table 1: Machine data of the tested harvest systems for SRC

Parameter	**Harvest technology**		
	1	2	3
Basic machine	Class Jaguar 870	Class Jaguar 900	Fendt 930
Power (kW)	350	480	300
Header	MK IV	HV 1400	MH 130
Max. stem diameter	< 15 cm	<15 cm	20 cm
Planting layout	Single and double row	Single and double row	Single

Table 2: Field data for 8 different SRC-harvest test in season 2015/16

Parameter	Field test							
	1	2	3	4	5	6	7	8
Harvest system	Claas Jaguar 870 with MK IV [1]			Claas Jaguar 900 with HV 1400 [2]			Fendt 930 with MH 130 [3]	
Date of harvest	Jan 2016			Jan 2016			Feb 2016	
Location [4]	SB			SM	DE	TR	MA	EL
Tree species	Poplar							Black locust
Clone	Max 1-4							?
Root age (years)	4	4	4	5	4	4	4	4
Stem age (years)	4	4	4	5	4	4	4	4
Average diameter (cm)	5.8	5.0	5.1	5.7	5.0	6.1	7.0	5.6
Planting design	Single row, ~8300 trees ha^{-1}							
Net size (ha)	5.25	7.25	5.98	1.6	3.9	3.4	2.84	0.98
Yield (odt ha^{-1} yr^{-1}) [5]	6.2	4.2	5.1	3.1	4.0	4.4	11.3	4.8
Harvested biomass, total (odt)	130.6	121.8	121.8	25.2	62.3	60.5	127.9	18.9
Harvested biomass (odt ha^{-1})	24.9	16.8	20.4	15.7	16.0	17.8	45.0	19.3

[1] Henriksson Salix AB, Eslöv/Sweden

[2] wimatec MATTES GmbH, Ostrach/Germany

[3] Kluge GmbH, Königswartha/Germany

[4] SB … Strausberg, SM … Schmergow, DE … Derwitz, TR … Trechwitz, MA … Massen, EL … Elsterwerda

[5] odt … oven dry ton respectively dry matter based ton

Results

The field tests have shown that the choice of harvester is only one of the important factors influencing the overall performance of the whole harvest chain. Other important factors are e.g. experience of the driver, field conditions (trafficability, stem diameter, size of headlands), organisation and transport chain. Although bigger differences in harvest capacities have been observed between the single field tests, the average material capacity of the mower

chipper system was comparable to the average capacity of forage harvester based solutions during the tests (15.5 resp. 15.8 odt h-1), Tab. 3.

Table 3: Performance data from 8 different SRC-harvest test in season 2015/16

Parameter	Field test							
	1	2	3	4	5	6	7	8
Harvest system	Claas Jaguar 870 with MK IV			Claas Jaguar 900 with HV 1400			Fendt 900 with MH 130	
Tree species	Poplar							Black locust
Machine capacity								
Effective field capacity [2] (ha h^{-1})	0.51	1.25	1.37	0.54	0.82	0.63	0.36	0.78
Effective material capacity [2] (t h^{-1})	28.8	50.7	63.6	20.9	30.5	25.2	36.2	24.0
Effective material capacity (odt h^{-1}) [3]	12.7	21.1	28.0	8.5	13.2	11.1	16.0	15.0
Average eff. material capacity (odt h^{-1})	20.6			10.9			15.5	
	15.8						15.5	
Machine productivity								
Share of productive times (%)	48	31	49	32	64	60	38	49
Machine breakdown (%)	2	13	6	27	0	7	19	14
Average share of productive times (%)	43			52			43	
Average share of machine breakdown (%)	7			12			17	

[1] SB … Strausberg, SM … Schmergow, DE … Derwitz, TR … Trechwitz, MA … Massen, EL … Elsterwerda

[2] harvested acreage or mass per working hour including times for waiting, repair etc.

[3] odt … oven dry ton respectively dry matter based ton

The MK IV system is a SRC-header based on more than 15 years of experience from harvest of willow and poplar from SRC. Whereas the HV1400 header and the MH 130 mower-chipper are new solutions offering some innovative features such as direct mechanical connection of all drives at the HV 1400 header and adjustable chip length as well as the possibil-

ity to harvest much bigger trees (up to 20 cm stem diameter) with the MH 130. The share of machine breakdown times for these new solutions is still 5 to 10 % points higher. According to the experiences from the practice test in 2015 and 2016 it can be concluded, that both new systems are market ready. It can be expected that the observed problems can be solved by minor modifications of the relevant machine components.

Figure 4 shows the distribution of particle sizes produced with the three different harvesters. The forage harvester based solutions are designed to produce fine chips (class P16 … P31). In dependence to the adjustment of the intake and the chipper drum the HV1400 system produced a higher share of bigger wood chips compared to the MK IV system. However, both harvesters showed a relatively high amount of fines in the produced chips (> 10 %).

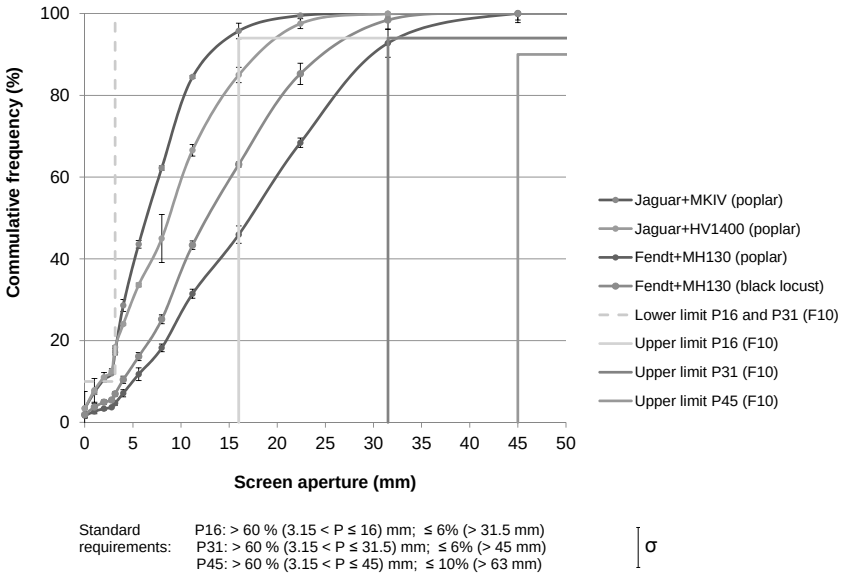

Fig. 4: Particle size distribution of the wood chips produced during SRC-harvest 2015/16

The MH130 harvester offers the opportunity to change the chipping length in a wide range between 40 to 120 mm. During the test, the cutting length was adjusted to 75 mm. Consequently, the produced chips have been much coarser (class P31 … P45) than the chips produced with the forage harvesters. Furthermore, the content of fines was much smaller (<7%

d.b., black locust resp. < 5% d.b. poplar). The differences in stem diameter at cutting height, wood structure and the high content of branches for black locust are seen as the main factors leading to the observed differences in the particle size distribution of poplar and black locust.

References

[1] Balasus A, Bischoff WA, Schwarz A, Scholz V, Kern J. 2012. Nitrogen fluxes during the initial stage of willows and poplars in short-rotation coppices. Journal of Plant Nutrition and Soil Science 175(5):729-738.

[2] Hellebrand HJ, Strähle M, Scholz V, Kern J. 2010. Soil carbon, soil nitrate, and soil emissions of nitrous oxide during cultivatio n of energy crops. Nutrient Cycling in Agroecosystems 87(2):175-186.

[3] Scholz V, Ehlert D, Hoffmann T, Kern J, Pecenka R. 2011. Cultivation, harvest and storage of short rotation coppice - long-term field trials, environmental effects and optimisation potentials. Journal fo Agricultural Machinery Science 7(2):205-210.

[4] Pecenka R, Ehlert D, Lenz H. 2014. Efficient harvest lines for Short Rotation Coppices (SRC) in agriculture and agroforestry. Agronomy Research 12(1):151-160.

[5] Vanbeveren SPP, Spinelli R, Eisenbies M, Schweier J, Mola-Yudego B, Magagnotti N, Acuna M, Dimitriou I, Ceulemans R. 2017. Mechanised harvesting of short-rotation coppices. Renewable & Sustainable Energy Reviews 76:90-104.

[6] Scholz V, Eckel H, Hartmann S. 2009. Verfahren und Kosten der Energieholzproduktion auf landwirtschaftlichen Flächen. KTBL-Schrift: Die Landwirtschaft als Energieerzeuger 476:67-80.

[7] Horváth Z, Marosvölgyi B, Idler C, Pecenka R, Lenz H. 2012. Storage problems of poplar chips from short rotation plantations with special emphasis on fungal development. Acta Silvatica et Lignaria Hungarica 8(1):123-132.

[8] Lenz H, Idler C, Hartung E, Pecenka R. 2015. Open-air storage of fine and coarse wood chips of poplar from short rotation coppice in covered piles. Biomass and Bioenergy 83:269-277.

[9] Pecenka R, Lenz H, Idler C, Daries W, Ehlert D. 2014. Development of bio-physical properties during storage of poplar chips from 15 ha test fields. Biomass & Bioenergy 65:13-19.

[10] Ehlert D, Pecenka R, Wiehe J. 2012. New principle of a mower-chipper for short rotation coppices. Landtechnik 67(5):332-337.

Real driving emissions of tractors during field work and on the test stand

M.Sc., Dipl.-Ing. **J. Ettl**, Dr. **K. Thuneke**, Dr. **E. Remmele**,
Dr.-Ing. **P. Emberger**, M.Sc., Dipl.-Ing. (FH) **G. Huber**, TFZ Straubing;
Prof. Dr. **H. Bernhardt**, TU München

Abstract

Exhaust gas emission limits from non-road mobile machinery (NRMM) such as tractors, excavators or loaders have been increasingly tightened in recent years. But there is only little knowledge about the emission behaviour under real-life operating conditions of diesel and rapeseed oil fuel compatible tractors of the latest emission stage IV. Besides mitigation of greenhouse gas (GHG) emissions from agricultural machines, also other limited and not limited exhaust gas emission components are relevant, to perform optimization processes entirely. Considering this, comprehensive knowledge is necessary about real emission behaviour of mobile machinery. By using a portable emission measurement system PEMS Semtech Ecostar, which was set up in a sturdy box for off-road use, the emission components NO_X, CO, HC and CO_2 as well as the exhaust mass flow are measured. In this work a methodology is suggested to transfer in-field recorded engine parameters of ploughing into test cycles. The test cycles are applied at the tractor, which is connected to an eddy current brake with its PTO shaft. A high congruency in emission behaviour between in-field recorded and on the test stand replicated values can be observed for three repetitions. The specific emission values for all measurements with rapeseed oil fuel are under the limit values for test cycles according to the EU Regulation 2016/1628 or ISO 8178. Furthermore, regarding results neither significant differences between the use of rapeseed oil and diesel fuel nor divergences of PEMS and stationary gas analysers are recognized. Further investigations should clarify whether the method is applicable to further tractors and other tractor works.

1. Introduction

Exhaust gas emission limits for non-road mobile machinery (NRMM), like tractors, excavators or loaders have been increasingly tightened in the European Union (EU) during recent years. Emission testing for type-approval is performed on dismounted engines on the engine test bench by applying the non-road steady state test cycle (NRSC) as well as the non-road transient test cycle (NRTC) like ISO 8178. Since both test cycles do not represent actual conditions in the field properly, monitoring of real driving emissions (RDE) by using portable emission measurement systems (PEMS) is proposed with upcoming EU exhaust emission stage V in the year 2019. On the other hand, portable emission measurement systems are associated with considerable technical and economic expenses as well as a reduced repeatability in contrast to the test stand. For recurrent determination of emissions during tractor life without engine dismounting, measurements by eddy current brakes connected to the tractor PTO shaft have become more common [1][2][3]. A sophisticated method would be beneficial to evaluate emission behaviour and fuel consumption for specific tractor works under real driving conditions. Such a method could simplify optimization processes of mobile agricultural machinery in terms of emissions, efficiency and environmental sustainability. Due to significant greenhouse gas (GHG) emission reduction potential of more than 59 % and to guarantee national food production sovereignty, rapeseed oil fuel is a reasonable alternative to fossil diesel fuel for agricultural machines [4][5]. However, there is only little knowledge about the emission behaviour of diesel and rapeseed oil fuel compatible tractors of the latest emission stage IV under real-life operating conditions.

2. Purpose

With a portable emission measurement system (PEMS) gaseous emissions such as nitrogen oxides (NO_X), carbon monoxide (CO), hydrocarbons (HC), carbon dioxide (CO_2) and the exhaust gas mass flow (Q_M) should be recorded during field work. Additionally actually monitored field operation characteristics should be transferred to a tractor PTO test stand control, where they serve as default values for generating work specific test cycles. Emission results from theses practice derived test cycles should be evaluated and compared to the emission values during field operation with PEMS and of legal based test cycles.

3. Approach

Fig. 1 shows in-field emission measurements with a Fendt Vario 724 S4 tractor connected to a 5-furrow Pöttinger Servo 45 Plus plough. The tractor is compatible for rapeseed oil and diesel fuel operation while the engine control unit (ECU) settings remain unchanged for optimised diesel operation. The tractor is equipped with a Deutz TCD 6.1 L6 engine (exhaust gas emission stage IV) and features an exhaust gas recirculation (EGR) as well as an exhaust gas after-treatment system (EAT) comprising a diesel oxidation catalyst (DOC), a diesel particle filter (DPF) and a selective catalytic reduction (SCR). The in-field exhaust gas emissions are detected with a Semtech Ecostar PEMS of the company Sensors Inc. The PEMS combines NDUV, NDIR, FID as well as an exhaust gas mass flow meter. All analysers are mounted in a dust and water proof housing on the front linkage of the tractor. The ECU parameters engine speed (n_{CAN}) in min^{-1} and actual engine-percent torque (M_{CAN}) in % are monitored from the CAN bus according to SAE J1939. The total 8.5 h measurement time was carried out in three repetitions with 2.9 h, 3.2 h und 2.4 h at an average ambient temperature of 8 °C.

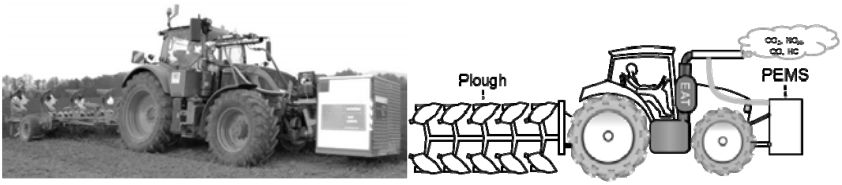

Fig. 1: Rapeseed oil fuelled Fendt 724 S4 with PEMS during ploughing

The emission measurements at the tractor test stand (Fig. 2) are performed with the same engine speed (n_{CAN}) and torque (M_{CAN}) profile as the previous in-field measurements.

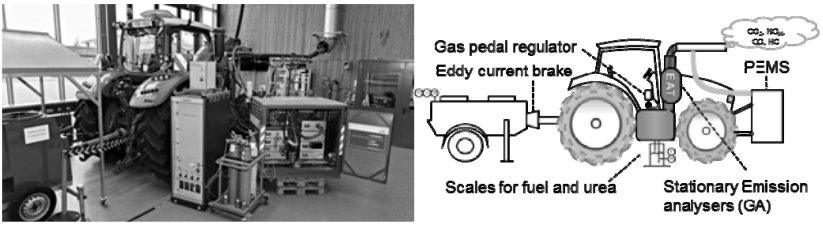

Fig. 2: Setup for emission measurements at the tractor test stand

Therefore PTO speed and torque as well as engine speed (n_{CAN}) and torque (M_{CAN}) from the CAN bus values are measured at 130 different levels within the engine map and a linear fit curve for the speed and a three-dimensional fit curve for torque are computed. The resulting functions are used to transfer test cycles with recorded CAN bus data of actual engine speed (n_{CAN}) and torque (M_{CAN}) values into target values for the gas pedal regulator and the EGGERS PT 301 MES eddy current brake on the test stand. The ploughing test cycle is started after the tractor was conditioned to the same coolant temperature (of 41 °C, 67 °C and 66 °C) as at the beginning of the in-field emission measurements. The average ambient temperature at the tractor test stand (16 °C) was higher compared to the measurements on the field. Lower temperatures at the test stand were not possible to reach for longer.

At the tractor test stand the limited exhaust gas emission components nitrogen oxides (NO_X), carbon monoxide (CO) and hydrocarbons (HC) are recorded by both, the PEMS and the AVL SESAM 4 stationary gas analysis system (including FTIR, FID and PMD). The exhaust gas mass flow (Q_M) is calculated according to ISO 8178 on basis of fuel consumption, which was measured by continuous weighing of an external fuel tank using a Mettler-Toledo KB60.2 platform scale. Measurements are conducted in accordance with ISO 8178 by the application of a steady state [3] and a transient test cycle, latter modified by generating mean values of aggregated spans over 10 seconds of the original NRTC for type approvals on engine test benches [1]. Measurements of the emission behaviour were conducted with rapeseed oil fuel (fuel standard DIN 51605) and diesel fuel (according to CEC RF-06-03).

4. Results

Engine and emission data from measurements over 8.5 h ploughing in the field were evaluated and resulting field-work profiles successfully transferred to the tractor test stand. Fig. 3 shows the high degree of accordance between in-field recorded and on the test stand replicated values for n_{CAN} and M_{CAN} with regression coefficients (R^2) over 98 %. The deviations mainly occur in transient phases during the turning on the headland. Due to the inertia of the tractor system, not all peaks of n_{CAN} and M_{CAN} could be reproduced. Furthermore, at idle on the test stand the rotational mass of the eddy current brake and the tractor PTO gear box require additional torque compared to the field.

Despite many influencing factors, the emission behaviour of the tractor at the tractor test stand was well reproducible with a high conformity for the measured NO_X and CO_2 emission concentrations and the exhaust gas mass flow.

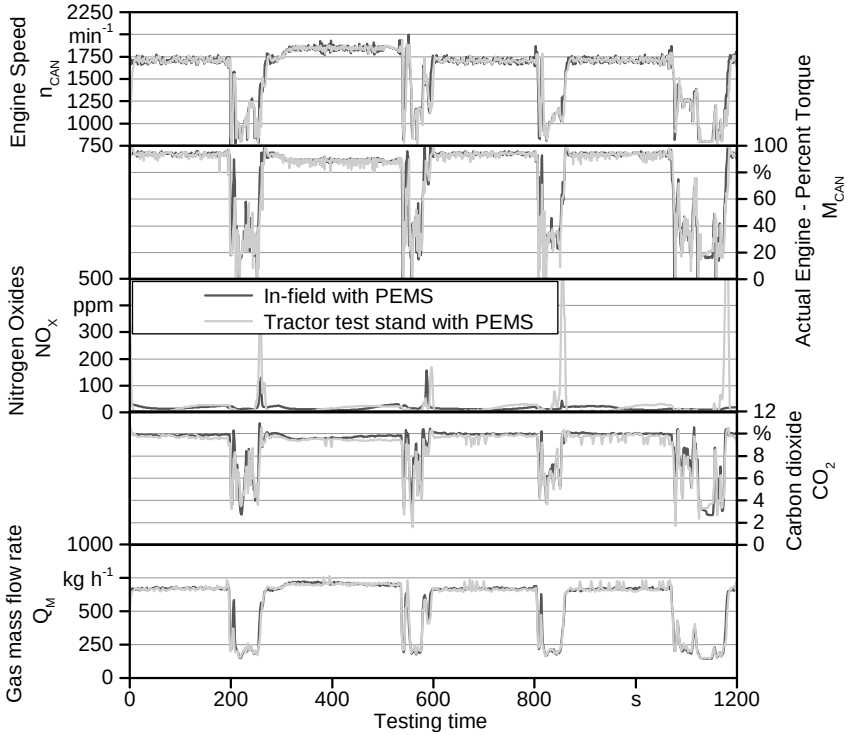

Fig. 3: Engine speed, torque, NO_X, CO_2 and Q_M values during a 1200 second long segment of ploughing, recorded in-field and replicated at the tractor test stand with PEMS

In-field and during the test cycle on the test stand the NO_X emissions are mostly far below 50 ppm. Some higher peaks of NO_X emissions occur shortly after the transient turning process during the insertion of the plough into the soil. These NO_X peaks arise more frequently at the tractor test stand than in the field. The reason therefore might be the 8 K higher ambient temperature with possibly higher NO_X emissions before the EAT and a sudden increase of the gas mass flow rate, which can diminish the NO_X conversion rate at this situation. However, the median and the average values between in-field recorded and on the test stand replicated values for NO_X, CO_2 and Q_M differ only slightly over the entire measuring period of 8.5 h. The box plot in Fig. 4 shows this results with rapeseed oil fuel. The box includes the upper and lower quartiles, the whiskers indicate the 95th and the 5th percentile and the average values are displayed as honeycomb-shaped dots.

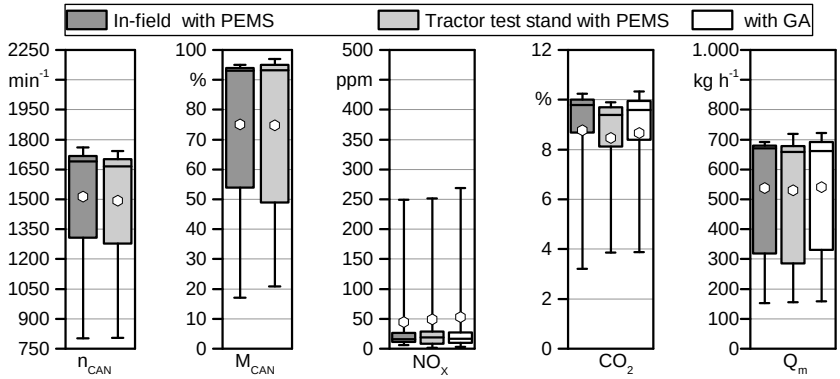

Fig. 4: Distribution of engine speed, torque and exhaust emission concentrations measured in-field with PEMS and at the tractor test stand with PEMS and stationary gas analysers (GA)

Despite of different measuring principles and the accuracy of the analysers the results with PEMS are rather equal to the stationary gas analysers (GA). This is also reflected in the results of the specific NO_X emissions related to the power at the PTO shaft in Fig. 5.

Fig. 5 shows the specific NO_X emissions with rapeseed oil fuel during ploughing in the field and at the tractor test stand as well as the results of the 10 s NRTC and the NRSC with rapeseed oil and diesel fuel.

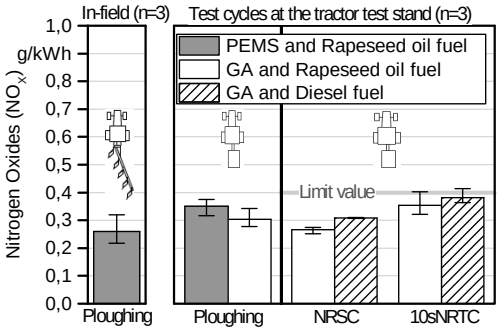

Fig. 5: Specific NO_X emissions during ploughing in the field and the derived ploughing test cycle at the tractor test stand as well as during the test cycles of ISO 8178 with rapeseed oil and diesel (n = 3)

The increase of 0.09 g/kWh NO_X during ploughing at the test stand compared to the in-field measurement may have been caused by the different ambient temperatures or by the deviations in speed and torque control. Beside the ambient parameters also different conditions of the engine (such as injector deposits or wear) or of the EAT (such as urea deposits in the SCR system or load-state of the DPF) could have influenced the results. Nevertheless, the specific NO_X emission values of all measurements with rapeseed oil fuel are below the limit value of 0.4 g/kWh for the NRSC and NRTC according to the EU regulation 2016/1628. During ploughing with PEMS the average NO_X emissions were lower than during the 10 s NRTC at the tractor test stand. Reasons therefore are that the actual tractor works with a plough are usually much less dynamic and demand more engine power than the legal transient test cycle (NRTC). A significant difference between the use of rapeseed oil and diesel fuel cannot be recognized. During all measurements the DOC mostly reduces HC and CO significantly under 10 ppm. The resulting low level of specific emissions under 0.6 g/kWh CO and 0.005 g/kWh HC during ploughing, in the NRSC and 10 s NRTC are far below the legal limit values of 5.0 g/kWh for CO and 0.19 g/kWh for HC.

5. Conclusions and Outlook

The engine data during RDE measurements can be transferred successfully to the tractor test stand, where a high congruency in emission behaviour can be observed for three repetitions. The results can help to determine work specific real world emissions and emission factors of agricultural mobile machinery, operated with various fuels. Besides the use of a rather complex PEMS on board of the tractor a different approach is suggested to ascertain quasi real world emissions on a tractor PTO test stand, where comprehensive data derived from practice operated vehicle fleets can be included. Applying this method the development of propulsion systems that are compatible with sustainable biofuels and optimisation processes can be more effective to improve air quality and reduce greenhouse gas emissions. Further investigations should clarify whether the method is applicable to different tractors and other tractor works.

Acknowledgements

The authors would like to thank the Bavarian Ministry of Economic Affairs and Media, Energy and Technology for funding the project, BayWa AG for providing the tractor and the state owned farm Mainkofen for the excellent cooperation during RDE measurements.

References

[1] ETTL J, BERNHARDT H, THUNEKE K, EMBERGER P, REMMELE E (2016): Transient emission and fuel consumption measurements on plant oil tractors. Landtechnik 2016;71(2):44–54.

[2] ETTL J, HUBER G, BERNHARDT H, THUNEKE K. (2016): Real Emissions of a Plant Oil Compatible Tractor: Measured by PEMS and on the Tractor Test Stand. ATZ offhighway 2016;9(11):46–51

[3] EMBERGER P, LANDIS M, KRAMMER K, PRANKL H, SCHAUFLER H, SCHIESS I ET AL. (2011): Measurement of emissions of a tractor — round robin test of ART, FJ-BLT and TFZ. Landtechnik 2011;66(1):56–9.

[4] ENGELMANN K, DRESSLER D, HAAS R, REMMELE E, THUNEKE K. (2017): Climate protection by rapeseed oil fuel. Straubing: Technologie- und Förderzentrum im Kompetenzzentrum für Nachwachsende Rohstoffe (TFZ)

[5] REMMELE E, ECKEL H, WIDMANN B. (2014): Regenerative Energieträger und alternative Antriebskonzepte für mobile Arbeitsmaschinen. Landtechnik;69(5):256–9.

Efficiency Optimization by Using “Vehicle in the Loop” Test Methodology

Dipl.-Ing. (FH) **Waldemar Stark**, M.Sc. **Claudia Pieke**,
John Deere GmbH & Co KG, Mannheim

Abstract

The DLG PowerMix test was conducted on a real test track and public roads. Currently the DLG PowerMix test is running on the vehicle test bench. This benchmark test evaluates the fuel consumption of tractors in different operating and driving conditions. The John Deere Product Verification & Validation group has applied and implemented a “Vehicle in the Loop” methodology, also called “model-based”, to run those tests on a new 4WD powertrain test bed with active electric dynamometers mounted on all axles and PTO plus a hydraulic load unit.

The test environment allows the replication of customer applications by using topographic road profiles, modeled trailers and implements in a real time environment. The vehicle is set on stationary stands with wheel hub dynamometers. The vehicle dynamic characteristics are modeled as a multi body system complemented by tire models.

This setup takes into account all relevant environmental effects influencing the overall fuel consumption in different operating scenarios and allows the real-time investigation of various vehicle performance specifications.

The main advantage is the reduction of development time and cost because it is now possible to evaluate drive strategies and vehicle efficiency concepts in a well-controlled laboratory environment. Furthermore, the deep cross linking of vehicle hardware and simulation platform allows a realistic maneuver based testing for vehicle optimization with excellent correlation to real world customer applications in an early development stage. This underlines Deere’s efforts in optimizing efficiency and performance of our products.

Motivation

The primary purpose of agricultural tractors, especially those in the middle to high power ranges, is to perform drawbar, PTO and hydraulic work. The efficiency of a tractor is measured by the amount of work accomplished relative to the cost incurred in getting the work done.

The ideal tractor converts all the energy from the fuel into useful work at the drawbar, PTO and hydraulic system. In practice, most of the potential energy is lost in the conversion of

chemical energy to mechanical energy, along with losses from the engine through the drivetrain and finally through the tractive device (Fig. 1).

Efficient operation of farm tractors includes: (1) maximizing the fuel efficiency of the engine and drivetrain, (2) maximizing the tractive advantage of the traction devices, an increase in useful PTO work, providing high hydraulic load capability and (3) selecting an optimum travel speed for a given tractor-implement system.

The understanding and prediction of tractor efficient operation is a major goal of the tractor developer. It is necessary to determine the vehicle performance in theory and by lab verification in order to predict the tractor performance in the field to meet the customer requirements.

Traditionally, the validation of the global vehicle targets takes place after the integration of the real vehicle components late in the development process. This typical trend always stands in the way of the need to get the knowledge about the tractor performance with focus on the customer requirements as early as possible in the development process.

DLG PowerMix test is one of the most important test routines for the determination of the tractor efficency; however, performing a PowerMix test at the DLG requires a fully functional tractor, which typically is available only very late during a development program. As a result DLG PowerMix fuel consumption data is available only very late in the development program when most of the design is already frozen. This has been identified as a gap. In order to close the gap it is desired to predict DLG PowerMix fuel consumption data at an early development stage. Thus, the replication of the DLG PowerMix Test in a laboratory environment has been identified as an effective solution for evaluation of the complete tractor efficiency.

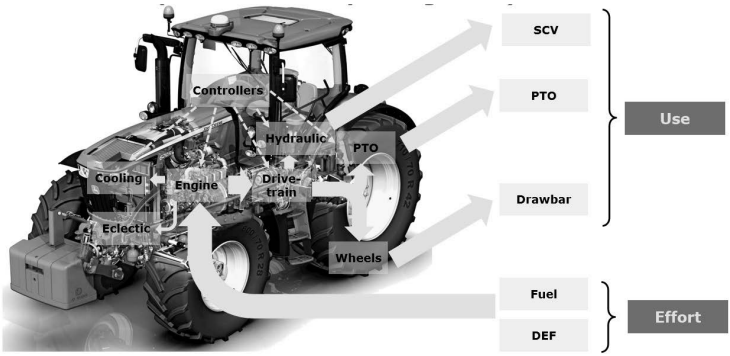

Fig. 1: Energy flow distribution in the tractor.

DLG PowerMix Overview

The DLG PowerMix test procedure is a transient fuel consumption test, which consists of 13 cycles replicating tractor field and transport applications [1], [2]. During the cycles the tractor is loaded by a drawbar load vehicle, a PTO dynamometer (Dyno) and hydraulic load unit according to the cycle requirement. At transport test the draw bar load is determined by scalable trailer weight. The tractor load in this case, is scaled based on stationary PTO power measurement during the stationary PTO test.

This method allows testing tractors with different power ratings with comparable load factors. Table 1 shows an overview of the 13 cycles.

Table 1: DLG Power Mix test cycle overview.

Cycle Number	Abbreviation	Description	Classification	Vehicle Speed [km/h]	PTO Speed [rpm]	Duration [sec]
1	Z1P	100% Ploughing	Heavy drawbar work	9	-	250
2	Z1G	100% Cultivating	Heavy drawbar work	12	-	250
3	Z2P	60% Plough	Medium drawbar work	9	-	250
4	Z2G	60% Cultivating	Medium drawbar work	12	-	250
5	Z3K	100% Rotary Harrow	Heavy PTO work	6	900	250
6	Z3M	100% Mowing	Heavy PTO work	16	900	250
7	Z4K	70% Rotary Harrow	Medium PTO work	6	900	250
8	Z4M	70% Mowing	Medium PTO work	16	900	250
9	Z5K	40% Rotary Harrow	Light PTO work	6	900	250
10	Z5M	40% Mowing	Light PTO work	16	900	250
11	Z6MS	Manure Spreading	Drawbar, PTO, and hydraulic work	7	1000	500
12	Z7PR	Baling	Drawbar, PTO, and hydraulic work	10	1000	500
13	Z8T	Transport	Drawbar work	-	-	-

The PowerMix field test is performed at the DLG test center in Groß-Umstadt, Germany on an outside track and transport test on public road. This test is considered as a method to determine fuel consumption data under real field and transport applications, which allows the comparison of different tractors models.

Presently, the DLG PowerMix test has received a fundamental modification. With this modification DLG realized the vision “Field to the Rig” and brought the PowerMix test from the test-track to the test-rig. This matter created a new challenge, a better understanding of the impacts on the end results of the DLG PowerMix.

Signal-based versus Maneuver-based Testing

Up to now the standard test methodology applied on dyno test rigs is a time-based measurement and replication of load signals for the powertrain, PTO and hydraulic systems of the tractor. The measured or even artificially generated load signals are replicated on the test bed using fast control loops.

The signal-based methodology works well if the unit-under-test does not significantly influence the amplitude and shape of the replicated load signals. For a detailed analysis of vehicle efficiency the complex behavior of the overall system of tractor and trailer or implement with the road or field has to be considered. The determination of load profiles before test execution for active powertrains and other vehicle systems is not possible anymore. Therefore the maneuver-based methodology uses a detailed and validated vehicle model. All test runs are defined by the selected vehicle configuration including trailer or implement, a selected road topology and a well-defined sequence of maneuver steps for the driver.

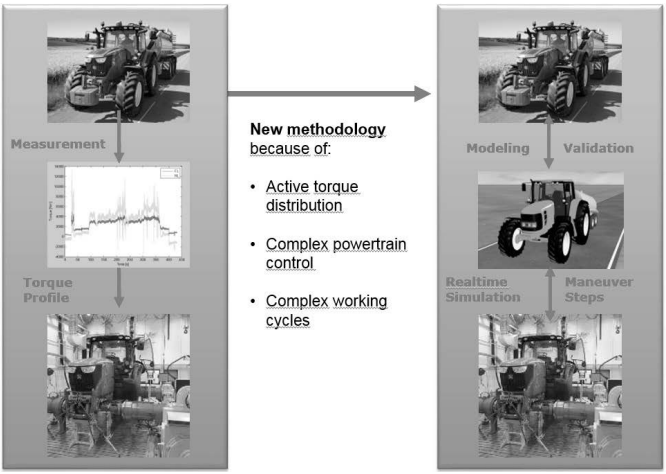

Fig. 2: Test methodologies at the vehicle test rig.

System Layout of the Test Bed

The Unit under test is installed on a new 4WD powertrain test bed with active electric dynamometers mounted on the axles and PTO plus a hydraulic load unit.

The different signals of the real powertrain are measured at each axle and provided to the virtual wheels of the tractor. The interaction of the complete tractor with trailer, road and environment is simulated in the virtual world. The resulting wheel speed is controlled back in the real world with each dyno module. The simulation platform uses a detailed real-time multi-body model for wheels, chassis, cabin, trailer and implements. All multi-body components are described by its geometrical size and physical parameters like weight, inertia and COG. The tractor / trailer combination is driving on the defined three-dimensional road with defined

attributes like friction, roughness or soil type. The fuel consumption of the real powertrain is measured with high precision and evaluated for all tested variants and test runs as shown in Fig. 3.

Unlike the replication of load profiles, the tire loads are not calculated in advance. Instead, the maneuvers are defined and the driving physics, e.g. tire physics (rolling resistance, slip, etc.) and momentum of the trailer are calculated online and in real time. Test description and test object are clearly separated. The advantage: once implemented, the maneuvers can be used for different vehicles. The 3D online visualization with a connection to Google Earth gives an overview on the current progress of the tests.

Currently a robust and efficient process to parameterize the detailed vehicle models from component design data and measurements is introduced.

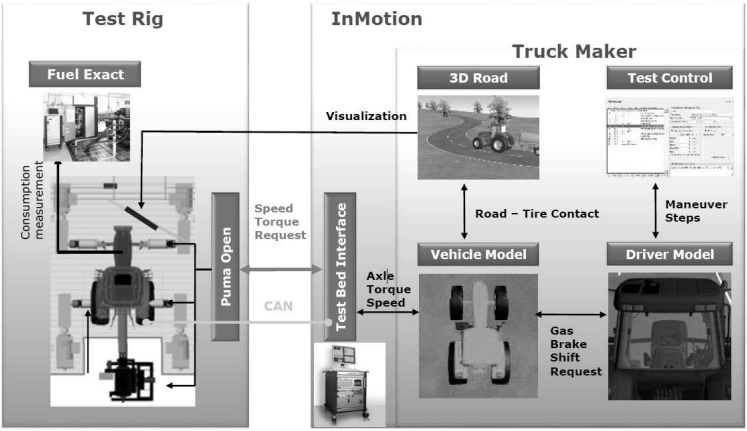

Fig. 3: Systems on the vehicle test bed.

Results

In order to recognize the deviation between the two test methods a deep analysis of the Power Mix1.0 concerning to noise parameters were carried out. Through the refinement of the vehicle model, maneuvers and test ambient parameters it was possible to get the good correlation between the DLG vs. the model based testing. A comparative test series has shown that the fuel consumption measurement result shows an accuracy within 2% compared to official DLG results. This accuracy lies within the standard deviation of real-world tests. In addition, the scatter band of the results (measurement noise) on the test bed is smaller than in real-world operation.

A contributor to the deviation which has been identified, is the tire road contact simulation. One way to reduce the deviation is a tire pretest, in order to determinate the most important parameters individually for each test candidate. However, for comparative testing the accuracy is considered sufficient.

The Fig. 4 and Fig. 5 shows comparison of corner parameters measured at the DLG and on the test rig with model based test method.

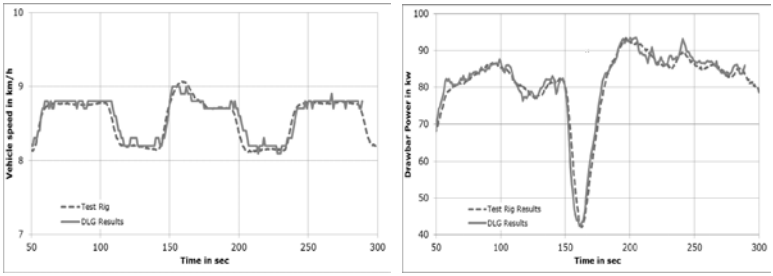

Fig.4: Test results comparison DLG vs Model based testing in Draw Bar Power Mix cycle.

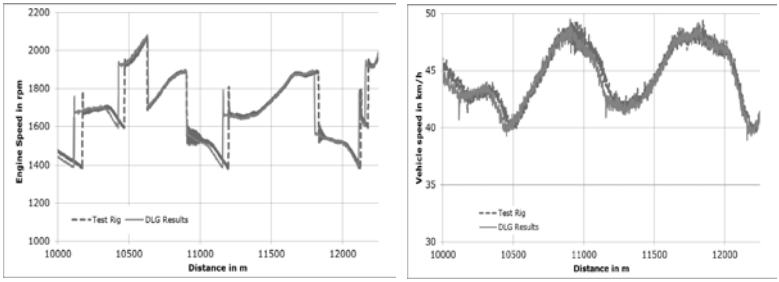

Fig. 5: Test results comparison DLG vs Model based testing at Transport test (Hill cycle).

Conclusion

The “vehicle in the loop” test methodology in the laboratory is a powerful and application representative opportunity to investigate and predict the tractor efficiency concerning to fuel consumption data during a tractor development program.

The following advantages of the new testing procedure can be noted:

- Expensive, time-consuming and weather-dependent on-site tests can be reduced to a minimum.
- Comprehensive fuel measurements in customer use cases show savings potential.

- Fuel consumption results can be predicted accurately earlier than before. The risk of failing to meet the specification requirements is reduced.
- If variant diversity increases, representative boundary samples can be identified and using the model-driven approach.
- The test solution is open, flexible, and extendable. Model-based testing is future-proof and will advance developments in the area of electrification and automation.

[1]. Degrell O., Ferstein T.: der DLG-PowerMix – methodic und Funktionalität. VDI Tagung Land technik, Hannover, Nov. 2003

[2] Degrell O., Ferstein T.: DLG powerMix – ein praxis orientierter Tractortes. VDI Tagung Land Technik, Hannover Nov. 2005

[3] Zoz F., Grisso, R.: Traction and Tractor Performance. ASAE Distinguished Lecture Series #27, 2003

[4] Back P., Hodel B., Pirro P., Stark W.: Replication of the DLG PowerMix tractor fuel consumption test in a laboratory environment. VDI Tagung Land Technik, Hannover Nov. 20011

[5] Pieke, C., Stark W., Pfister F., Schyr C.: DLG-PowerMix auf dem Leistungsprüfstand. ATZ (2017).

[6] http://www.dlg.org/Traktoren.html

Agricultural Tire Energy Efficiency test method and dedicated equipment to measure the fuel consumption and traction of agricultural tires under real field conditions

Kornél Szalay, **László Kovács**, **Gábor Bércesi**, **István Oldal**, NAIK MGI,Hungary;
Emmanuel Piron, IRSTEA, France;
Julien Charlat, **Thierry Joly**, **Clement Poncet**, **Florence Tran**, Michelin, France

Abstract

The ENTAM as the European Network of Testing stations of Agricultural Machines and equipment has settled up a new ENTAM Technical Working Group in order to draft a common methodology to test the agricultural tire energy efficiency, in close cooperation with Michelin. The aim was to find a compromise between easiness and representativeness of the measurements, with reproducible records carried out on real agricultural fields, in standardized soil conditions. In this paper a novel dedicated equipment is presented which uniquely provides possibility to measure dimensionless tire performance indices in a standardized way. The equipment covers a wide range of tire dimensions and is capable of applying large vertical loads and drive torques. It will play a key role to determine optimal tire settings and decisively contribute to profitable and sustainable agricultural practices.

Introduction

Global background

Sustainability, sustainable development are well-known terms which have many, sometimes rather different definitions. The very basic topics and related challenges are common. They all agree that climate change, energy and fossil fuel scarcity have high importance in this regard. Reduction of greenhouse gas emission and fuel consumption are two of those key elements. Agricultural production plays decisive role in the sustainable future so energy efficiency of agricultural machines is getting more and more important.

Mobile machinery and the pneumatic tires in particular play a very significant role in this context. For a tractor, one third of the mechanical energy delivered by transmissions to the wheels is lost. Some energy is lost in soil compaction, by tire slippage, and by rubber viscoelasticity. The remaining two-thirds are used for pulling, carrying and traction.

Studies have been published evaluating the specific contribution of the engine, the transmission, or the tires on the fuel consumption performance. The role of a tire to the fuel consumption in the field is significantly determined by its tractive efficiency as defined in ASABE, D497 (2009).

The tractive efficiency can be evaluated, based on physical variables that can be measured directly at the wheel centre, namely the drive torque (T), the rotation speed of the wheel (ω), the net traction force (NT), the actual travel speed (V), the vertical load in the contact patch area (W). Some analytical vehicles and laboratory equipment conceptually composed of a chassis and a tested wheel were developed in the past, in order to record "on-the-go" measurements of these variables. Although, no standard test exists so far, so as to evaluate the performance of the tires under real working conditions, on the field. In 2011 according to this new requirement the 9th ENTAM Technical Working Group has been established in order to draft a common methodology to test the “Agricultural Tire Energy Efficiency”.

The working concept of a novel dedicated test equipment had been laid down to uniquely provide possibility to measure dimensionless tire performance indices in a standardized way and to form the basis of a tire-only energy performance. The equipment and the standardized test method have been jointly and gradually developed by the NARIC Hungarian Institute of Agricultural Engineering (MGI) and the Michelin Tire Company, in cooperation with the IRSTEA National Research Institute of Science and Technology for Environment and Agriculture. The name of the equipment had been created as an acronym based on the possible application fields of the unique single wheel tester: FAST^2. In this paper the authors wish to present a review of the technical capacities of the latest prototype of the new equipment, designed to be large enough to test the biggest agricultural tires of today and the coming years.

Stakes & aims

Key economical stakes for farmers are productivity and fuel consumption. The tires contribute decisively to these stakes through traction and energetic efficiency. Tire deformation, soil deformation and tire slippage have a large impact on tire energy loss mechanisms. It is therefore fundamental to reproduce pertinently tire/soil interaction. The aims of the FAST2 machine project are to provide a tool to be able to evaluate traction and energetic efficiency of tire alone in the field, independently of the vehicle and in real soil conditions. The technical challenges for the project team are to achieve both good measurement accuracy and machine sturdiness, to be able to perform tests in field conditions.

ENTAM test method

Method

A common methodology for testing agricultural tire energy efficiency has been set up by the ENTAM network, as described in [1]. This test method allows coming up with a dimensionless tire-only energy performance index called PLI (Pull Loss Index). Formula for calculating PLI is shown in Figure 1.

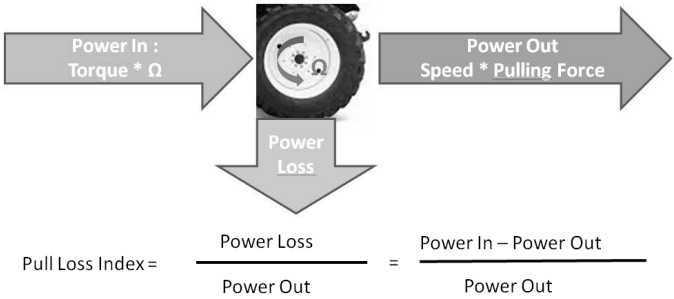

Fig. 1: formula for calculation of PLI

For example, having a PLI value of 50% for a given tire means: if the power requirement at the drawbar is 100 kW, then 150 kW of power is needed at the wheel axle.

Results presented in section [2] were obtained following ENTAM test protocol, namely by respecting – among others - 3 criteria on the soil:

- texture: clay, silt, sand resp. between 5 and 15%, 10 and 30%, 55 and 75%,
- moisture content (water mass / dry mass) between 10 and 14%,
- cone index value (according to ASABE EP542 and ASABE S313 [4, 5]) between 0.5 and 0.9 MPa.

Example of ENTAM test method results: comparison of 4 dimensions in 2016

Following previous studies performed in the years before [1], many experiments were conducted in 2016 at IRSTEA Montoldre place, by use of IRSTEA single wheel tester shown in Figure 2.

Fig. 2: IRSTEA single wheel tester performing a tire efficiency test in a field

The ability to sort tires using the ENTAM test method has been specifically addressed during the study and test plan included repeatability, field characteristics and field preparation influences. Four different tires, from Tire 1 to Tire 4 on the graph, were evaluated using each manufacturer recommendations for inflation pressure, regarding the applied load. For each tire and test configuration, 4 different measurements were carried out successively using increasing traction coefficients (defined as the ratio pull force over vertical force) from 0.1 to 0.4 by step of 0.1, and following ENTAM test recommendation (data collection on 4 successive zones during an up-down round trip in the field). Each tire has been tested 2 times on random places in the same field, and tire 2 has also been tested in another field, and in the same place as both first evaluations, but after a new soil preparation (Fig. 3).

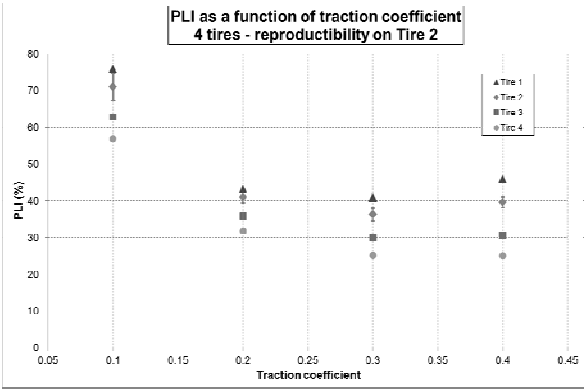

Fig. 3: Results using 4 different tires, 4 different traction coefficients for each tire. Reproducibility for tire 2 is presented using error bars.

Results obtained show the robustness of the method and its ability to sort different tires. Whatever the traction coefficient is on the global range, the global sort stays the same. Reproducibility results presented for tire 2 are based on a Student test. The magnitude of the error bar is smaller than the difference between tires. As a consequence, the difference between tires is significant since the error bar takes into account field effect, in-the field test position and successive soil preparations.

FAST^2 Machine

Specifications of the FAST2 machine

The main specifications of FAST2 machine are:

- Tire diameter : 1460 to 2500 mm
- Tire width : 311 to 973 mm
- Tire seat : 30 to 50 inches
- Net traction : - 1000 to 7200 daN
- Vertical load : 2000 to 12000 daN
- Torque : -1250 to 9000 daN.m
- Travel speed in field : up to 15 m/h
- Wheel rotation speed : up to 9 rad/s
- Tire slip ratio : up to 25%

The FAST2 machine enables to get 4 types of results:

- PLI and CLI indexes with ENTAM test method
- Traction efficiency curve
- Moving resistance

Global description of the machine

The FAST2 machine is a self-propelling vehicle with a measurement post to test tire only. The following 3D model illustrates the complete structure of FAST2 with the measurement system situated in the middle (Fig. 4).

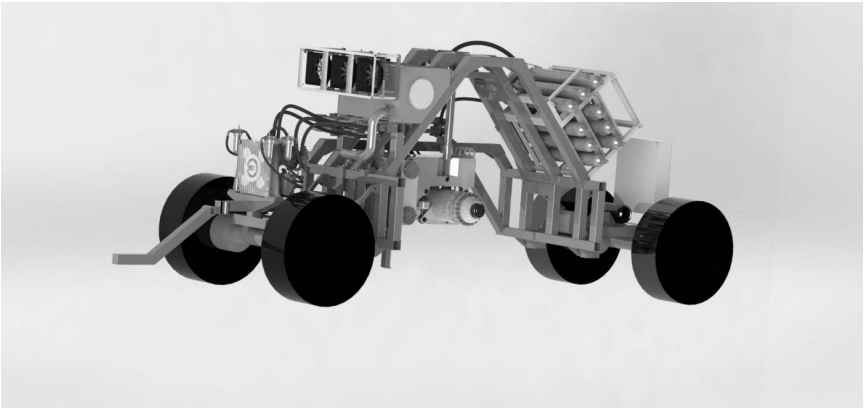

Fig. 4: The 3D model of the equipment.

Principle of measurement of FAST² machine

In order to have the ability to sort tires based on the ENTAM test method accurate and repeatable measurements are needed of drive torque (T), the rotation speed of the wheel (ω), the net traction force (NT), the actual travel speed (V), the vertical load in the contact patch area (W). A new isostatic measurement principle has been designed (Fig. 5). Key elements of the configuration are high accuracy 1 direction load cells. Traction force (NT) is measured by load cell 1 (LC1). Vertical load is measured by LC2, LC3, LC4. The calculation of NT and W are done with the following simple formulas:

$$NT = LC1 \qquad W = LC2 + LC3 + LC4$$

In addition to the 1D load cells a torque measuring flange is built into the spindle to accurately measure the drive torque (T). Traction force (NT) and vertical load (W) are measured by load cells. In addition to the 1D load cells a torque measuring flange is built into the spindle to accurately measure the drive torque (T).

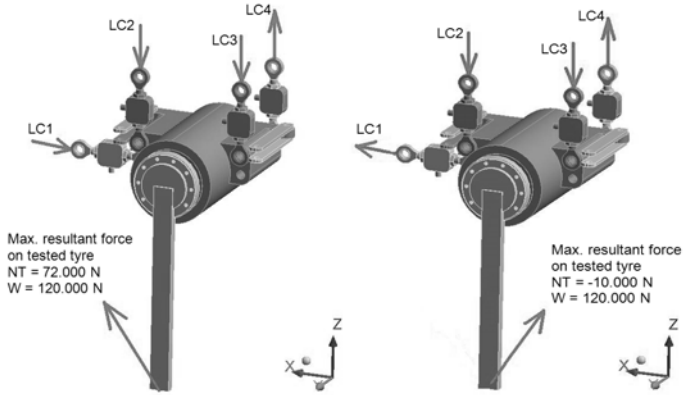

Fig. 5: Isostatic measurement system: Forces in case of drive (left) and brake modes (right).

Principle of kinematic of FAST2 machine

The FAST^2 can be used for tests in field in “self propelled double axle” configuration (Fig. 6). The whole mass of FAST^2 lies on the trailer’s front and rear axles. The tested wheel is situated between the front and rear shaft of the trailer. In general, the tractor controls the trajectory (direction) of the equipment. The front and rear axles are steerable. Through the PTO the tractor drives four hydraulic pumps which provide hydrostatic drive for the tested wheel in the middle, the four peripheral wheels through gearboxes and also feed the two hydraulic cylinders. One is to set the measuring position other is to express the vertical load on the tested wheel. Testing wheel is centred to the tractor’s axle. The driving force delivered by the tested wheel is counteracted by the peripheral wheels based on the desired test mode. In case the measured wheel is driven (drive mode) the four peripheral wheels are broke. In case the measured wheel is broke (brake mode) the four peripheral wheels are driven. The drive of the measured wheel and the peripheral wheels are both hydrostatic, driven by two separate hydraulic circles but pumps are mechanically connected. With adequate control the extra traction force awaken on the tested wheel (NT) is available to drive the peripheral wheels – it saves the energy. A part of the energy used for braking is used for driving (patent pending). The efficiency of energy reuse depends mostly on the slip ratio of the wheels (tested wheel and peripheral wheels). The travel speed of FAST^2 is controlled through the regulation of the four peripheral wheels speed.

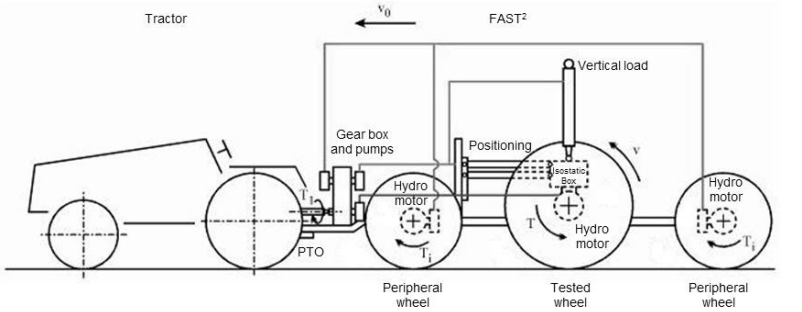

Fig. 6: “Self-propelled double axle” configuration (drive mode).

Green and red lines illustrate the active hydrostatic drivelines. Blue line represents the oil flow to feed the hydraulic cylinders to set the desirable measuring position and to provide vertical loads on the tested wheel.

CONCLUSION & PROSPECTS

The first measurement results showed high potential in performing tire-only measurements under field conditions. In order to assure the desired accuracy and quality of the collected dataset a new measurement principle has been designed. The equipment’s new design has been finished and currently the manufacturing phase is under finalization period. The completion of the test equipment is end of 2017. With the fully operational prototype the first field tests will be carried out in early 2018. The unique features of FAST^2 will make possible to test the biggest agricultural tires (tires with diameters up to 2.5 m and width up to 0.90 m; vertical loads up to 120000N, traction force from -10000N to +72000N) even under extreme usage conditions (speeds up to 15 km.h^{-1} up to 40% slip ratio in the field) or on the road, driving or braking torque of the tested tire up to 90000 Nm). In the coming years, this test equipment will be used to strengthen the understanding of the basics of the tire performance, depending on the tire design (tire construction; tire tread), the various types of soft soils, and the usage conditions (vertical load; inflation pressure; applied driving torque and resulting slip rate). FAST^2 can be a useful test equipment to enforce the standard test methods for performances that are key factors in minimizing the environmental impact of mechanized agriculture. FAST^2 can contribute to a standard test for fuel consumption in the field. Following the 1st field tests for reception, the FAST^2 machine will be available to perform test the tests described in this paper (PLI/CLI, traction efficiency curve, moving resistance) for external customers, under operation of trained ENTAM Network institutes.

Acknowledgement

Authors would like to express their gratitude to all colleagues from NAIK MGI, IRSTEA and Michelin, who have contributed in the project. Special thanks go to:

- From NAIK MGI: Márk Szente, Bakk János, István Keppler
- From Michelin: Patrick Vervaet, Matthieu Vandemoortele
- From IRSTEA: Denis Miclet

Their theoretical and practical knowledge, experience and support provided during all these years are strongly appreciated.

References

1. [ASABE; EP542 (R2009)]: "Procedures for Using and Reporting Data Obtained with the Soil Cone Penetrometer"
2. [ASABE; S313]; "Soil Cone Penetrometer"
3. [ASABE, D497] "Agricultural Machinery Management Data" 2009.
4. [Dessèvre, D. (2010): A review of the main effects of the tires and their usage, on the fuel consumption of agricultural tractors. EurAgEng 2010.
5. [Forissier, J.F.] Methodological precautions for tractor fuel consumption's measurement Land Technik – AgEng 2009.
6. [G Fancello, M. Szente, K. Szalay, L. Kocsis, E. Piron, A. Marionneau] New experimental method for measuring the energy efficiency of tires in real condition on tractors. VDI AgEng 2013.
7. [Giulio Fancello, Márk Szente, László Kovács, László Kocsis, Kornél Szalay, Emmanuel Piron, Denis Miclet and Philippe Héritier] Agricultural Tire Energy Efficiency test method link with specific fuel consumption for measuring the efficiency of agricultural tires under real conditions on tractors**,** VDI AgEng 2015.
8. [Kassai, Zs. and Szente, M]: Complex comparison of tractor transmission systems between Continuously Variable Transmission and Powershift Transmission. VDI-MEG 2005.
9. [Szalay K., Szente M., Kovács L., Kocsis L., Bablena A., Bércesi G., Piron E., Miclet D., Héritier P., Fancello G.] Agricultural tire energy efficiency tests: a commitment toward a sustainable agricultural production, AgEng 2016.
10. [Szente, M.; Kriston, S.; Forissier, J. F.] A New Single Wheel Tester – Global Traction and Motion Resistance Measuring System, EurAgEng 2010.
11. [Andreas A., Hans-Joachim T.] DLG powermix chassis dynamometer – the field on a test bench, VDI AgEng 2015

Field test validation as part of the development of a narrow track tractor

Dipl.-Ing. Agr. **Jürgen Mengele**, AGCO Fendt GmbH, Marktoberdorf

Abstract

In the smaller power range from 70 to 110 horsepower tractors, AGCO Fendt has set standards for absolutely high technology in the area of specialty tractors with the 200 series V/F/P. This narrow track tractor has clearly defined requirements regarding the overall dimensions of the tractor, the different mounting possibilities of implements for an outstanding number of different applications and the highly integrated operation possibilities for high customer satisfaction and high productivity.

This article initially focuses on the different variants of the 200 Vario specialty tractors and will subsequently describe the different mounting areas for the implements. In the course of reaching emission stage EU 3B the opportunity was used to integrate new innovative technologies to increase the performance of the tractor. These new technologies within these models provide a daily benefit for the customer and meet the expectations of the market for permanent increase of efficiency.

Extensive field tests of several thousands of hours verify the engineering design and ensure durability and reliability for the required lifecycle under specific conditions. Particularly with regard to the huge number of special types of applications and implements of these tractors it is important to do intensive tests in the field. Test farmers and test drivers evaluated the improvements and accompanied the development process up to the series solution. The major targets to reach a higher performance level and to cover reliability and durability of the complete tractor were achieved.

1. Different model variants of the 200 Vario specialty tractors

Since the launch of the 200 V/F/P series this tractor and its variants have been well known for highest performance in the area of specialty tractors. Depending on the variant, it has special specifications.

The V model- variant

The 200 V model variant is the tractor for vineyards for row spacing from 1.50 to 2.20 m. The tractor has a smallest possible outer width of 1.07 m. It was specially designed for this kind of operations and is the smallest variant.

1.2. The F model variant

The F model variant is an ideal tractor for fruit and wine growing with a wider spacing between the rows from 1.90 to 3.00 m. The tractor has an outer width beginning at 1.32 m. It is also used in vegetable growing and hothouse operations.

The P model variant

For hops and fruit growing, or in very wide vineyards the P variant is the ideal tractor for the customer. In row widths from 2.20 to 5 m the tractor fits the requirements, starting with an outer width at 1.68 m. Based on this it is possible to mount a wide, more comfortable cabin. This specialty tractor has wider axles and higher lifting capacity at the three point linkage front and rear.

2. Different mounting areas

The Fendt Vario specialty tractors differ in the number of mounting areas compared to a standard tractor. Beside the front and rear linkage it is possible to mount implements in the middle of the tractor. This inter axle mounted implements like cultivator or tillage tools allow a highly accurate operation of implements very close to the plant. Also cultivation in the row between the plants is possible. This became very popular in the past years. This development was, among other, caused by the controversial public discussion about the intensive usage of glyphosate. It gives the wine grower the tool to control weeds without chemicals or even to reduce the use of them significantly. The inter axle mounted implements are also ideally suited for operations with economical implement combinations. This saves not only operation time and machine costs, it also increases working quality by reducing driving tracks and soil compaction.

On the front linkage the implement can be mounted in the lower links and top link when the implement should be moved with the three point linkage but also can be mounted fixed with bolts on an adapter frame at the front of the tractor. This gives the operator a very stiff and close attachment of the implement which is important for accurate work, for example with trimmers. This kind of attachment also has major advantages in weight distribution and maneuverability, making driving easier in difficult terrain.

The rear point linkage at the V/F variants could be equipped with swinging power lift. It allows a lateral and tilt adjustment as well as swinging and lock with the push of a button. The tilt can be monitored via tilt indicator in the cab. The implement can be adjusted perfectly to the row and to the underground.

3. Improvements and adaptations

The 200 V/F/P tractors with their **C**ontinuously **V**ariable **T**ransmission (CVT), their powerful hydraulics, their perfectly ergonomical workplace, flat floor cabin and their unique detail solutions have set new standards in efficiency, ride comfort and overall profitability since their launch in 2009. But also at top technology, customers always ask for further developments to fulfil their higher demands for an advanced usage of the tractor.

3.1 Technical development goals

To fulfil the expectations of the customers and operators following items were determined:

Retaining basic concept of the tractor as compact as possible

No constraints as to the visibility and manoeuvrability

Robust and reliable exhaust after treatment system, meeting all the specific operation conditions of the specialty tractor

No loss of high power density and compactness of the machine design

Improvement of the cost-to-benefit ratio

3.2 Installation and field validation of the Exhaust After Treatment (EAT) system

With the introduction of technical innovations on the 200 V/F/P it was also necessary to comply with the current emission stage EU 3b. The installation situation of the cooled external Exhaust Gas Regulation (EGR) and the Diesel Oxidation catalyst (DOC) is shown in figure 1.

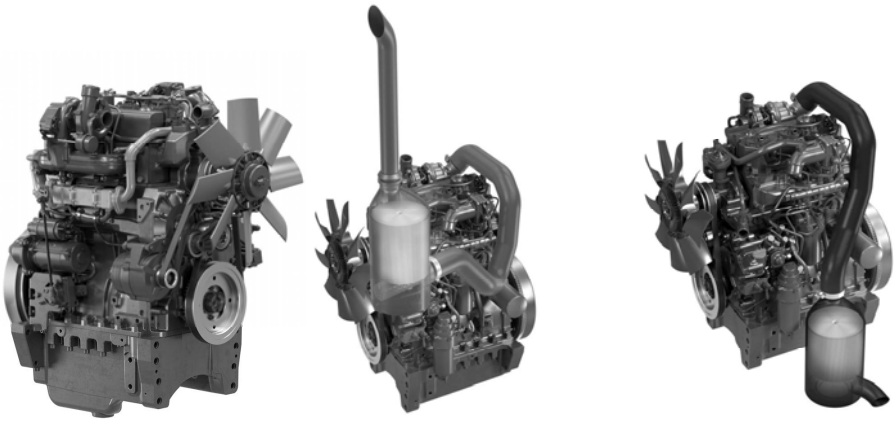

Fig. 1: Installation of EGR (left) and DOC at top position (middle) and at bottom position (right)

This installation has an impact to the tractor. Especially with regard to the DOC it is recommendable to choose its position considering the additional required space. When the operator wants to use the inter axle mounted area he will choose the DOC to be fitted at the top as

shown in figure 1 in the middle. With this installation situation intensive mounting tests were made in the field with a big number of implements for center mounting area. It was not the first priority to get many field test hours. It was a functional field test to get a validation regarding the fitting accuracy of the implements at this mounting area. Many implement manufactures were involved in these researches and a few changes were made within the development process up to series production.

A new EAT system has not only an impact regarding the additional required space for the components; it has also influence on the characteristics of the engine run and at least an influence on the controls of the engine in tandem with the CVT. The CVT offers the operator a tremendous benefit. But this benefit is not only a matter of the CVT, it is a matter of perfect interaction between engine and transmission. With the new EAT System multiple field tests were done to cover the perfect interaction between these components. Especially the very high number of implements cause highly differing effects and loads on the tractor. Many different implements or implement combinations strain the tractor simultaneously at drive train, PTO and hydraulics. Here it is even more important that the engine runs dynamically. On steep slopes in the vineyard the speed has to be adapted without jerking and interruptions. The engine controller has to regulate to needed power and torque precisely. Interruptions and jerking will lead to bad driving comfort and at least to higher fuel consumption. Feedback from operators and our own test drivers helped to reach the performance level that was convincing for this high end product.

3.3 Field validation of the reversible engine fan

Especially front implements like trimmers or cane pruner in the vineyard often lead to a massive quantity of leaves and other plant residues on the hood of the tractor. Figure 2 shows this situation while trimming the vine rows. This causes a massive decrease of the cooling capacity and the operator has to clean the fan grills several times a day. With a reversible engine fan it is possible to clean the fan grill without leaving the cab. The air flow direction switches when the fan blades are turning. Time period for reversing and time while reversing can be easily adjusted in multifunction display. Reversing is possible at full engine speed and at full load. Field tests were done in vineyards with one row and over row trimmers, leaf strippers and cane pruner. It is important to validate the system not only at one place and at one time. Conditions for the deposit of leaves differ not only with the development stage of the vine. Grape varieties, the kind of vine cultivation, growing systems, stock formation and also the weather conditions have an influence on this. Therefore it is important to catch the worst combinations in the field while testing to reach the target of a functional system even at

the worst operation conditions. While testing in the field several improvements e.g. at the hood were made to come to a series solution.
The result of a reversible fan is a permanently clean fan grill that creates a time saving, as well as offers a clean cooling package that at least results in a better fuel economy.

Fig. 2: Plant residues at the fan grill while trimming vineyards

3.4 Field validation of the ultrasonic guidance system

To bring the well-known benefits of guidance systems also to the vineyard, hops or fruit farmers, AGCO Fendt integrated a pre-fitted guidance system into the 200 V/F/P Model. The guidance system via open interface is based on the ISOBUS TIM functionality (Tractor Implement Management) promoted by the Agricultural Industry Electronics Foundation (AEF).
When the conformity test for TIM is available, all other guidance systems which meet the test can be installed. The so-called “TIM Guidance ready” feature at Fendt includes the complete wiring in the cab, steering controller, front axle steering angle sensors, the safety system and also the control panel for pre- activation and activation of the guidance system.
Customers can choose between two different guidance systems and can retrofit them. First one: Guidance with GPS receiver for positioning of the tractor. Second one: Guidance with ultrasonic sensors to steer the tractor in plantation or vineyard on the basis of an existing plant population. This is explained here more precisely:
The front mounted ultrasonic sensors calculate the actual distance to the rows and the tractor follows the adjusted distance to the rows/ plants. When the tractor is driven with two or more implements in combination a guidance system relieves strain for the driver. He can focus his concentration on the implements and their precise adjustment. But in in a plantation like a vineyard it is so important to drive precisely on the way line. A deviation from the way line in the row will lead to damage in the plantation most of the times.

Field tests with ultrasonic sensors were made in different growth phases of the plants. While scanning the leaf wall or the rows in fruit plantings with ultrasonic sensors it is important to reduce external influences as far as possible. Due to the field test validation, steering settings and software were changed, the cover of the sensors was modified and positions of sensors were changed a few times to achieve the best performance in scanning the row. When operating e.g. with a trimmer, it is very important that after trimming the leaf wall is straight without waves. Otherwise, the tractor will follow this contour at subsequent trimmer runs. Good covers and fenders for the sensors against plant residue, optimal adjustment possibilities of the sensors and also good driver training for this adjustments are mandatory.

4. Overall field test validation

To meet the targets of the development of the tractor, it is not only necessary to test single improvements on the tractor in functional tests. It is also necessary to expose the complete tractor to intensive and endurance testing in the field. All features and new technologies together will be tested combined in the field. Even the best team play of all components of a tractor is extremely important for highest customer satisfaction. The best integration into the architecture and a holistic view with the involvement of all different implements and their operation strategies will lead to success. The test tractors have to be operated by a large number of different persons. Different countries have also different methods of growing their plants. Implements or conditions like the steepness in the field differ from region to region and from country to country. So it is important to check all these variations with international field testing. The test tractors of the 200 V/F/P series have in the meanwhile summed up more than 10,000 operating hours and will be built Q4/2017 in series production.

5. Conclusion

With the emission level EU 3B the 200 V/F/P is equipped with new technologies that helps the customer to reach a better cost to benefit ratio and to get the best performance ever. The field tests of this new emission stage and of the new technologies are a very important part of the development process. Besides the granting of lab test results it is essential to get feedback from the field and the daily work with the tractor. Especially with this tractor series and its variants it is challenging to meet all expectations of the customer. An outstanding number of different implements and mounting areas, a cutting edge in compactness, manoeuvrability and driver comfort lead to an intensive field test to reach superior performance and highest efficiency.

Integrated wheel load measurement for tractors

M.Sc. **Michael Peeters**, Dr.-Ing. **Viktor Kloster**,
Dr.-Ing. **Thomas Fedde**, CLAAS Tractor, Paderborn;
Prof. Dr. **Ludger Frerichs**, Institute of mobile Machines and Commercial Vehicles, Technische Universität Braunschweig

Abstract

Soil protection and increase in traction performance with optimized fuel consumption are main drivers in tractor developments today. A minimum axle load is the sweet spot for soil protection, whereas a certain weight is necessary to achieve the requested traction force. Therefore, the axle loads should be transferred via a large contact area to the soil. On the one hand there is the need to distribute the tractor weight proportional to the ratio of tire sizes to the driven axles. On the other hand the tire inflation pressure should be set to the smallest allowed value for soil protection, restricted by the overload capacity of the tire.

Today, axle loads can only be measured in static condition by means of scale without traction forces. Due to unknown vertical and horizontal forces transferred from the implement to the tractor, the dynamic axle loads while working can only be estimated. This complicates the choice of the operator for the right ballasting and the right tire inflation pressure.

Therefore, a holistic measuring concept is presented, based on [1], which allows compensation of disturbance variables and providing additional signals to determine machine weight each time. The sensors are integrated into kinematics of suspended frontaxles and geometries of rigid rear axles. At the rear, the axle shafts are used as sensor elements. In the front the hydropneumatic suspension system is used. Resulting strains to the axles out of static and dynamic vertical forces can be measured and evaluated. The measured axle loads and the front/rear load distribution can be displayed to the driver and used for further assistant systems for tractor operation.

1. Motivation

The new approach is to measure the real tire loads under dynamic conditions. With known dynamic axle loads the operator gets useful hints for the right setting of ballasting and tire inflation pressure. But dynamic axle loads depend on many ambient conditions. Tire individual wheel load is influenced by vertical, horizontal and lateral forces. Vertical forces on tires are driven by the Center of Gravity (CoG) and the weight of the empty machine as well as

ballasting weights and acting forces from implements to the machine. Also inclinations in longitudinal and lateral direction of the vehicle will influence the dynamic wheel loads. Due to vertical and drag forces transferred from an implement to the tractor, the dynamic wheel and axle loads vary extremely while a working process. In any situation the tire loads respective the axle loads have to be measured to enable tire overload protection. Thus there is the possibility, to drive the tire in its optimum for traction force and/or soil protection.

Because of the variability of force application points in the rear of a tractor (Figure 1), to connect implements or ballasting weights, the most sensible measurement points are on the axle body or axle shaft. All resulting forces have to be carried by the axles respectively the tire-soil-contact.

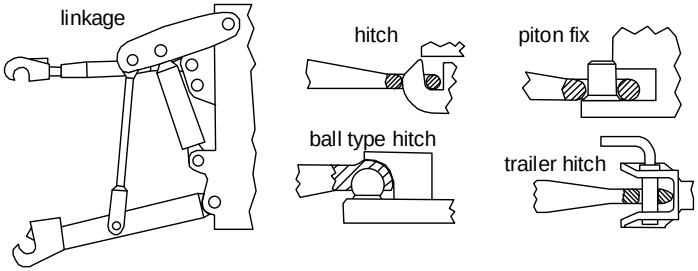

Fig. 1: Exemplary connection points in the rear of a tractor for implements or weights

Today the minimal tire inflation pressure given by the tire manufacturer in form of tire load tables includes a factor to compensate dynamic tire load effects. With consistently detected dynamic axle loads the allowed settings could also be optimized.

2. State of the Art

Different methods for an integrated measurement of axle loads for commercial and agricultural machines are known, but only few are used in serial applications. In WO 2013/104981 A1 [2] and in [3] assemblies are described for rigid axles. The bending of the axle housing in the consequence of the effective wheel load is measured by resistance strain gauges. A similar system, which also uses the bending of the axle housing as active principal, is used for an overload protection system for telehandlers [4]. Instead of resistance strain gauges a distance measurement is realized via capacitive sensors.

The patent DE 102009025494°A1 [5] describes an ultrasound sensor which is installed in the rim to measure the distance between rim and tire. With known tire inflation pressure and individual tables given by the tire manufacturers it should be possible to estimate the wheel

load. In WO 2017/042265 A1 [6] an axle load measurement via distance measurement between axle housing and wheel flange is described.

For suspended axles several systems are used, all of them are based on similar active principals. Pressures in hydraulic, pneumatic or hydropneumatic suspension systems are measured and calculated via cross-sectional areas into forces. In DE 10029332 B4 [7] it is described for pneumatic axle suspensions for commercial vehicles and trailers. Pichlmaier [8] and DE 102015206369 A1 [9] show the axle load measurement for hydropneumatic suspended axles of tractors via pressure measurement at the suspension cylinder.

Späth [10] developed measurement wheels which allow the measurement of forces for all three degrees of freedom. Kistler GmbH [11] develops measurement wheels which can detect torques for all degrees of freedom additional to the forces. Wieckhorst [1] presented, based on DE 102013110311 A1 [12], a traction sensing element. This uses passive magnetostrictive sensors, assembled on the shaft of the rigid rear axle, to quantify vertical and horizontal tire forces as well as the driving torque.

3. Sensing Principals

For suspended front axles a measurement system like known from Pichlmaier [8] or according to the patent [9] can be used. Dependent on the axle kinematics, the hydropneumatic spring damper system and the number of cylinders several pressure sensors are needed to calculate active cylinder forces. For prestressed systems a pressure sensor for each piston chamber and ring chamber is needed. In Figure 2 the principal is shown for the simplest case, a suspended axle with one cylinder.

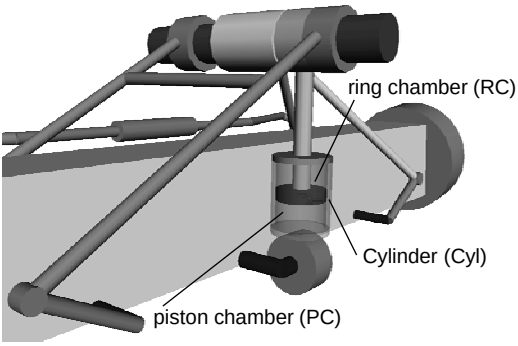

$$F_{RC} = p_{RC} \cdot A_{RC} \quad (1)$$

$$F_{PC} = p_{PC} \cdot A_{PC} \quad (2)$$

$$F_{Cyl} = F_{PC} - F_{RC} \quad (3)$$

$$F_{Const} = (m_{axle} + m_{tires}) \cdot g \quad (4)$$

$$F_{Axle} = F_{Cyl} + F_{Const} \quad (5)$$

F: force	m: mass
A: area	g : gravity
p: pressure	

Fig. 2: Calculation of axle load of suspended axles with one cylinder

On rigid rear axles forces can be measured via active magnetostriction. A magnetic field induced into a ferromagnetic part leads to a change of the length of this part, caused by the Joule Effect. The Weiss Areas orientate more or less in direction of the magnetic field, shown in Figure 3. The other way around, a length variation due to acting forces affect the magnetic field induced on the part. This effect is called Villari Effect. Both effects belongs to the magnetostrictive effects.

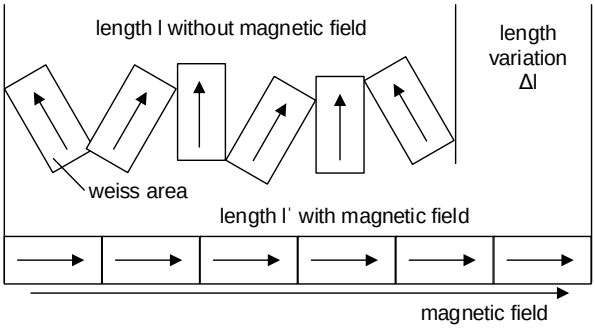

Fig. 3: Joule-Effect: Length variation of a ferromagnetic part caused by a magnetic field [13]

Magnetostriction needs two sensing elements. The primary sensing element is a ferromagnetic part like a shaft, the secondary sensing element is the sensor head. The needed magnetic field can be coded to the ferromagnetic part or otherwise a sensor head has got a field coil or a Magnetization-Yoke to produce a non-permanent magnetic field. To measure the intensity of the magnetic field sensing coils are used.

Strains on the primary sensing element effectuate length variations of the part, the orientation of the Weiss Areas are thereby influenced [13]. To detect changes in the magnetic field out of strains in the consequence of bending moments, the potential between two sensing coils, H_1 and H_2 (Figure 4), is compared. For unstressed parts the potential is zero. If the principal stress axis σ_1 of the bending force is aligned with the magnetic field between field and sensing coil H_1, the potential is higher than in the orthogonal direction between field coil and H_2. The orientation of the induced magnetic field ensures automatically that the sensor is not influenced by stresses due to the torsional moment, because the principal stress axis for the torque changes the magnetic field for H_1 and H_2 in the same level.

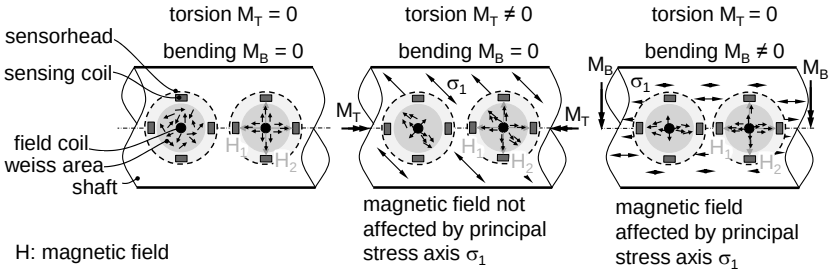

Fig. 4: Functionality of a magnetostrictive bending sensor

4. Sensing Unit

To get the real front axle load, masses of the unsuspended parts of the front axle, mainly dominated by the axle body and the tires, must be added to the detected cylinder force, seen in equation (4) and (5). The cylinder force is affected by friction of sealings between piston/cylinder and piston rod/cylinder. Stick-slip-effect in the cylinders sealings, influenced by lubrication, can disturb the pressure level in static conditions. Also the friction in every joint of the axle kinematics influence the determined cylinder force, but in this concept it is less than the sealing friction. For static conditions only a small part of the chassis weight is carried by the kinematic elements of a suspended axle, the dominating weight is carried by the hydraulic cylinder. With locked 4 wheel drive clutch the kinematic construction of the axle also transfers drag forces, so the joint friction raises. Pichlmaier [8] found an impact of 0.25 % of the identified cylinder forces due to all friction elements. This is less in dynamic conditions.

As an enhancement of the passive magnetostrictive sensor presented by Wieckhorst [1], for the integrated wheel load measurement at the rear axle active magnetostrictive sensors are used. Biggest advantage of active magnetostrictive sensor is a not needed magnetic coding of the primary sensing element, in this case the axle shaft.

For the active magnetostriction it is necessary, that the primary sensing element is a ferromagnetic material, surface hardened and it should be degaussed for a less noisy signal along the circumferential. Residual magnetization in the material downgrades the quality of the induced magnetic field and the measured signal gets worse through this disturbance. To correct the signal, especially to get valid values in static conditions, an absolute angle sensor allows an angle-dependent compensation. An integrated distance sensor compensates disturbances out of rotational non-uniformities and bending of the axleshaft, also the signal is compensated against changes in temperature.

A sensor using this physical principal can be installed on top of the axle shaft, mounted directly in the axle housing or using a retrofit adapter in front of the axle housing, see Figure 5. An absolute angle sensor is mounted on the axle shaft. Pressure sensors can be installed in the pipes for the suspension cylinders or directly at the hydraulic block for the suspension system. Inclination sensors are installed on the tractor frame and are just influenced by a less number of accelerations.

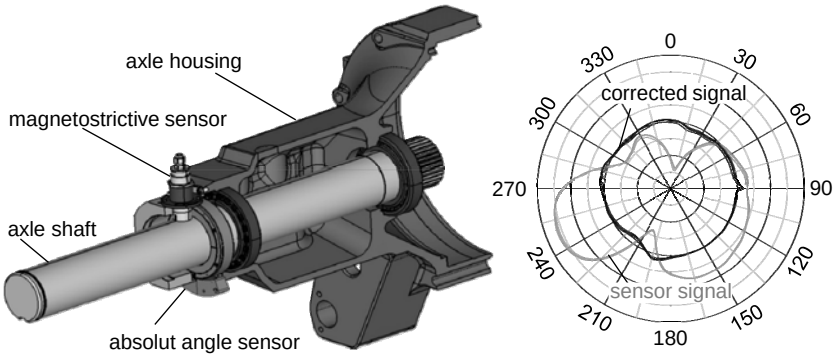

Fig. 5: Sensor assembly in the rear axle housing and signal correction via an absolute angle sensor

5. Validation

For the measurement system of suspended axles the axle load and the calculated cylinder force must show a constant offset due to the unsuspended masses, like shown in the equations in Figure 2, and because of friction, as mentioned above. Figure 6 shows measurements of a tractor in field-test, equipped with wheel force transducers of Kistler and pressure sensors in the suspension cylinder. The calculated difference between the sum of the vertical forces of the front wheels and the determined cylinder force is approximately constant, hence the theory from Figure 2 is validated for dynamic conditions. In standstill it is recommended to measure after deactivation and activation of the suspension system for minimization of influences from stick-slip-effect.

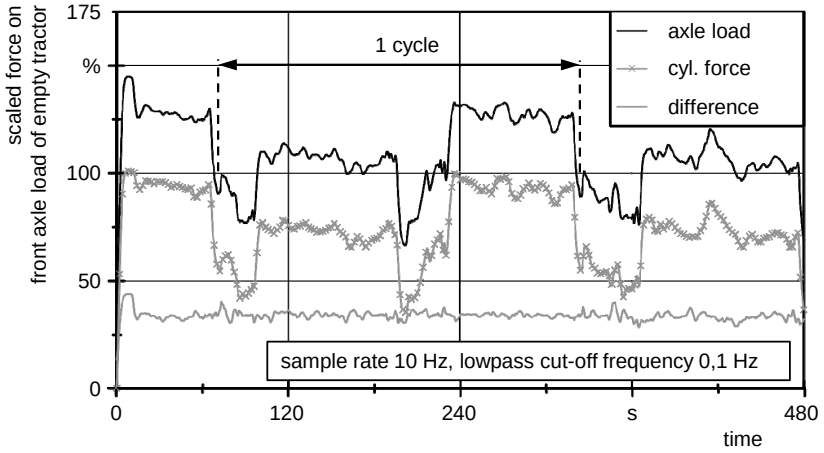

Fig. 6: Difference of axle load and calculated cylinder force, measured with an Axion 840 equipped with a 6 furrow plough and 1500 kg front ballast

For the rear axle sensors first validation measurements were carried out with a minimized sensor unit, without angle sensor and only on the right side of the machine. The calibration of the sensor was done with variable axle loads in static conditions by means of scale and verified for dynamic conditions by slowly driving with constant velocity on a flat area. In this case, the axle load is about the same compared to standstill.

In field-tests with a semi-mounted cultivator changes of the axle load balance can be seen as differences between field work process and headland turning process (Figure 7).

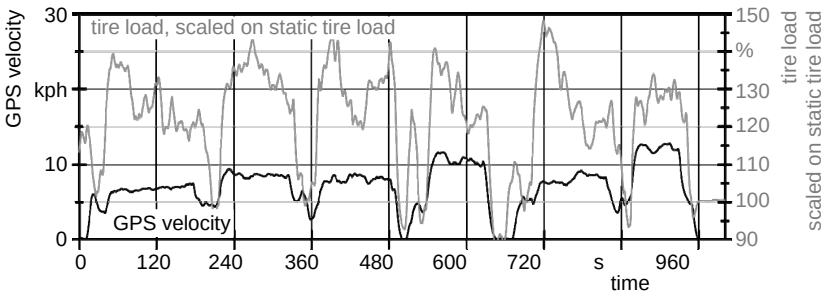

Fig. 7: Load on the rear right tire of an Arion 550 equipped with a semi-mounted cultivator and 900 kg front ballast

The cultivator transfers vertical force to the tractor due to its own weight. The vertical forces rises while working because of process forces, hence the axle load rises, too. The signals are lowpass filtered and the residual magnetization influence is approximately compensated. As mentioned above for static measurements the signal needs an angle depended compensation.

6. Conclusion

To support tractor operators for the right machine settings in reference to ballasting and tire inflation pressure an integrated axle load measurement system is presented. Acting with sensors in the rear, using the Villary Effect, and determine the pressure status of the suspended front axle all tractor axle loads can be determined.

References

[1] Wieckhorst, J., Fedde, T., Frerichs, L., Fiedler, G.: A Tractive Sensor. VDI-Berichte Nr. 2251. Düsseldorf: VDI-Verlag, 2015, S.219-226

[2] Patent: WO 2013/104981 A1. AGCO International GmbH. 2013

[3] Rempfer, M.: Grundlagen der automatischen Reifenluftdruckverstellung bei Traktoren. TU München. Dissertation. 2003

[4] Overload warning, brochure, Elektro-Bau-Elemente GmbH, Leinfelden-Echterdingen http://www.ebe-gmbh.de/resources/load/Overload_warning_EN.pdf, 25.07.2017

[5] Patent: DE 102009025494 A1. Grasdorf Wennekamp GmbH, 2011

[6] Patent: WO 2017/042265 A1. AGCO International GmbH. 2017

[7] Patent: DE 10029332 B4. Continental AG. 2007

[8] Pichlmaier, B. R.: Traktionsmanagement für Traktoren. TU München. Dissertation. 2012

[9] Patent: DE 102015206369 A1. Deere & Company. 2016

[10] Späth, R.: Dynamische Kräfte an Standardtraktoren und ihre Wirkungen auf den Rumpf. TU München. Dissertation. 2003

[11] Schulze Zumkley, H., Böttinger, S.: Modular measuring wheels for high horsepower tractors. VDI-Berichte Nr. 2060. Düsseldorf: VDI-Verlag, 2009, S.33-39

[12] Patent: DE 102013110311 A1. CLAAS Tractor SAS. 2015

[13] Hering, E.; Schönfelder, G.: Sensoren in Wissenschaft und Technik. Vieweg+Teubner Verlag, Wiesbaden: 2012

A Traction Field Test – Real Time Tire Soil Parameters of a Tractor in Tillage Applications

Dipl.-Ing. **Jan Wieckhorst**, Dr.-Ing. **Thomas Fedde**,
CLAAS Tractor, Paderborn;
Prof. Dr. **Ludger Frerichs**, Institute of Mobile Machines and Commercial Vehicles, Technische Universität Braunschweig

Abstract

The losses occurring in the tire soil contact dominate the system efficiency of a tractor in tillage applications. The user can influence these traction losses by varying ballasting and the tire inflation pressures of the tractor. However, even for experienced users it is difficult to find the right setup due to missing information on dynamic axle loads and tractive efficiency. At the AgEng Conference 2015, a sensor concept for crucial tire soil parameters, which can be integrated in the rigid rear axle of a tractor, was presented [1]. The test bench results were promising.

In 2016, the prototype sensor was installed at one rear axle shaft of a tractor and has been used for field tests in different tillage applications. The focus of these field tests was to find out if the prototype sensor has the potential to be used for online optimization of the tire inflation pressure, based on the dynamic wheel load and tractive efficiency. The impact of the boundary conditions on the tire inflation pressure that leads to max tractive efficiency was surprising. The dry conditions during stubble cultivation in northern Germany in summer 2016 led to interesting results, which are discussed in this presentation.

1. Motivation

The tire inflation pressure of a tractor does not only have an impact on soil compaction on agricultural soils, but also on the tractive efficiency in traction applications. This is something that is well known and has already been discussed in [1]. The general rule today is to reduce the tire inflation pressure as much as possible in order to reduce soil compaction and to increase the tractive efficiency whilst working on agricultural soils. The deflation of the tires is limited by the tire load capacity. The tire load capacity is the technically permissible vertical wheel force which depends on the tire inflation pressure. The corresponding tire load tables are published by tire manufacturers. However, measurements made in the past show for some conditions the lowest tire inflation pressure is not necessarily the most efficient [2] [3]. This means an automatic central tire inflation system has not only to ensure that the tire

inflation pressure is adjusted according to the actual tire load, but has also to do an online optimization of the tractive efficiency, if efficiency is the optimization goal.

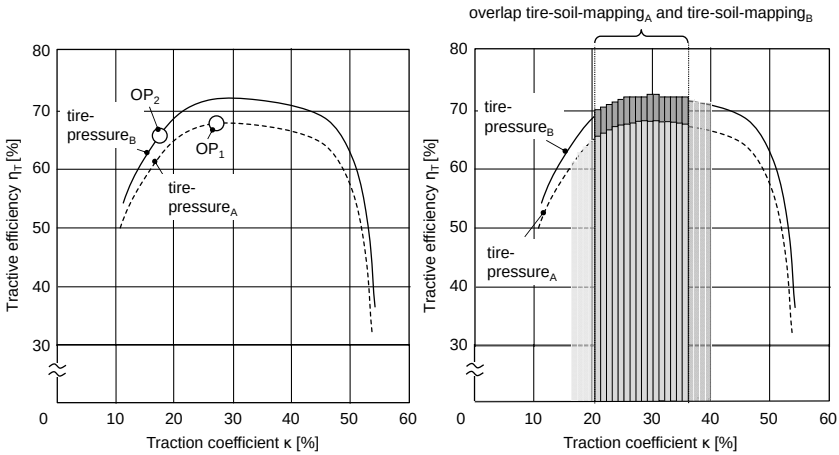

Fig. 1: Comparison of two tire pressure settings regarding tractive efficiency

In Figure 1 the tractive efficiency is plotted over the traction coefficient in a tire soil mapping. In order to optimize the tractive efficiency, simply comparing the actual tractive efficiencies at different tire pressures is not sufficient, as shown in Figure 1 on the left. Two exemplary curves for two different tire inflation pressures A and B are compared. Operating point 1 in the left diagram leads to the maximum tractive efficiency that is possible for tire pressure A at a traction coefficient of 28%, whilst operating point 2 on the curve of tire pressure B does not, as the traction coefficient of 18% is too low. The tractive efficiency in operating point 1 is higher than the tractive efficiency in operating point 2, so simply comparing these two tractive efficiencies without taking into account the traction coefficient, would lead to the misinterpretation that tire pressure A leads to higher tractive efficiencies than tire pressure B. Comparing the tractive efficiencies of different tire pressures at different traction coefficients might occur, for example, when working uphill and downhill on a field. Operating point 1 represents the tractor working uphill, whilst operating point 2 represents the tractor working downhill with a lower traction force at the wheel and hence a lower traction coefficient than whilst working uphill. In order to find the most efficient tire pressure, the automatic tire control system needs to generate and compare tire soil mappings for different tire inflation pressures. The diagram on the right side of figure 1 shows the comparison of two tire soil mappings that have been generated by classifying the tractive efficiency over the traction

coefficient. The evaluation of the overlapping areas of both mappings allows the comparison of different tire pressures in regards to tractive efficiency, whilst avoiding the comparison of operating points that are located at completely different traction coefficients within the mappings.

2. Tractor Drivetrain with Integrated Traction Sensor

The prototype tractor that has been used for the field tests was equipped with all sensors necessary to generate real time tire soil mappings at one of the rear wheels of the tractor (figure 3). The tractive efficiency equals the quotient of the output power and the input power of the wheel:

$$\eta_{Traction} = P_{out}/P_{In}$$

The input power is calculated as the product of the angular velocity of the wheel and the wheel torque:

$$P_{In} = \omega_{wheel} \cdot T_{y,wheel}$$

The angular velocity of the rear wheel is calculated from the speed sensor at the bevel gear shaft in the drivetrain that is also used for calculating the theoretical working speed of the tractor (w/o slip). This means, that cornering and inhomogeneous traction conditions at the rear axle of the tractor cause a problem, as the calculated speed might differ from the actual rear wheel speed when the rear differential is not locked. In order to avoid this problem, all measurements have been performed whilst driving straight and with homogenous traction conditions on a flat surface. The wheel torque is measured with an improved traction sensor based on the sensor presented in [1]. The output power of the wheel is calculated as the product of the traction force of the wheel and the working speed:

$$P_{out} = v_x \cdot F_{T,wheel}$$

The working speed is measured by a GPS sensor that is mounted to the structure of the tractor. The traction force of the wheel is measured by the traction sensor. The traction coefficient is calculated by dividing the actual traction force of the wheel by the actual vertical wheel load. Both values are measured by the traction sensor:

$$\kappa = F_{T,wheel}/F_{z,wheel}$$

In order to validate the traction sensor, the tractor has also been equipped with a ball-type hitch that has been prepared by applying resistance strain gauges to provide reference values for the draft force of the tractor.

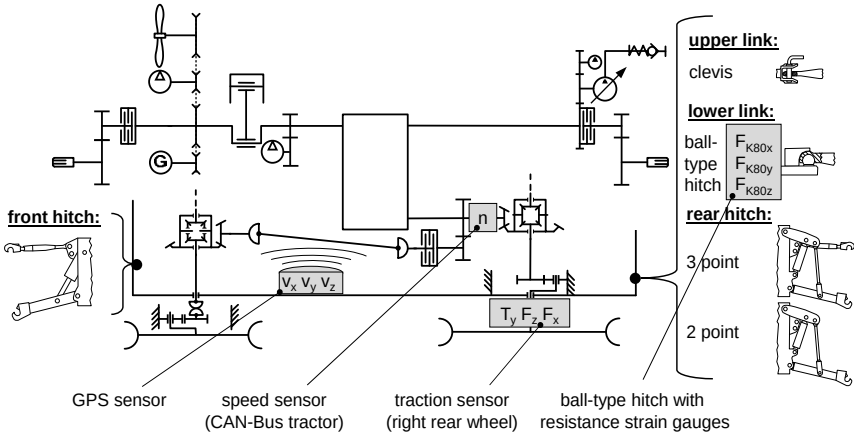

Fig. 2: Sensor overview of tractor for traction field tests

3. Validation of the Sensor Performance within the Tractor

After finishing the test bench phase [1] and installing the traction sensor in the tractor, tests have been made in order to validate the sensor performance. The signal for the vertical wheel force has been tested by comparing the signal of the traction sensor with the value given by a weighing plate. Figure 4 shows the signal for the vertical and the horizontal wheel force of the traction sensor over time whilst lifting a rear weight, and the measuring values of the weighing plate under the right rear wheel (accuracy +/- 0.25 kN). The rear weight is lifted up after 10 seconds and lowered down after 30 seconds. The deviation between the signal of the traction sensor for the vertical wheel force and the values of the weighing plate is less than 0.5 kN. The signal of the traction sensor for the horizontal wheel force shows only a small influence of the vertical force of less than 0.2 kN.

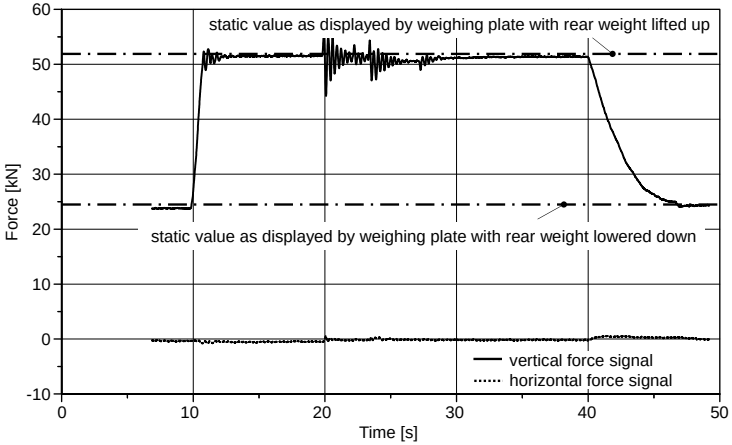

Fig. 3: Validation of traction sensor signal for vertical wheel force

In order to validate the signal of the traction sensor for the horizontal wheel force, a draft force measurement was made with a braking trailer on tarmac. The braking trailer has two retarder axles with four brake torque settings each. The four wheel drive of the tractor was not activated during the measurement and the tire pressure on both axles was set to 1.6 bar. In the upper diagram in figure 5, the signal of the traction sensor for the horizontal wheel force and the signal of the ball-type hitch are plotted over time. The draft force signal of the hitch has been divided by two, for an easy comparison with the wheel force signal of the traction sensor. In the lower diagram in figure 5 the corresponding driving speed is plotted, which is 9 km/h throughout the whole measurement (activated cruise control). Both retarder axles of the braking trailer are activated on stage 4 at the beginning of the measurement. One of the retarder axles is deactivated after 35 seconds. The signal of the traction sensor for the horizontal wheel force and the signal of the hitch match quite well. The raw and the filtered deviation of both signals are plotted in the diagram in the middle of figure 5. At the beginning of the measurement, when both retarders are fully activated, the wheel force measured by the traction sensor is 0.21kN higher than the signal of the hitch. This is plausible as the rear wheel has not only to overcome the pulling force of the braking trailer, but also the rolling resistance of the front wheel. The rolling resisitance on tarmac is between 1.5 % and 3 % and the calculated front axle load of the tractor under pull is 24 kN, which results in a rolling resistance force between 0.19 kN and 0.38 kN per front wheel. After the deactivation of one of the retarder axles, the deviation increases up to 0.71 kN. The reason is

that during the calibration of the traction sensor priority was given to the main working range, which leads to less accuracy for low traction forces.

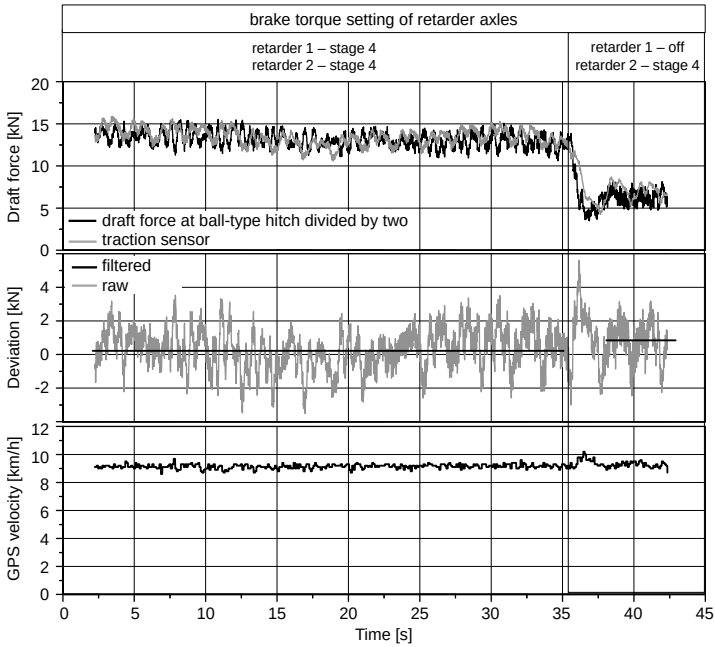

Fig. 4: Validation of traction sensor signal for horizontal wheel force on tarmac

4. Field Tests

All of the field tests were made in Lower Saxony in Germany in summer and autumn 2016. Figure 6 shows an exemplary comparison of four tire soil mappings that have been generated with different tire pressures, whilst performing flat stubble cultivation with a chisel plow on the same field and on the same day. The position of the three point hitch has been adjusted after all tire pressures changes in order to compensate the impact of the tire inflation pressure on the diameter of the tires and to keep the working depth constant. The tractive efficiency was classified over the traction coefficient. The operating range for all tire inflation pressure settings within the tire soil mapping is between 10% and 30% of traction coefficient. The tractive efficiency is still increasing over the traction coefficient in this area. The sweet spot of maximal tractive efficiency at traction coefficients over 30% was not reached, as the weight of the tractor was too high for the low pulling force demand of the chisel plow with the flat working depth setting. The tire pressure was modified in 4 steps from

0.7 bar to 1.0 bar. The tire load capacity has not been exceeded in any of these measurements. Changing the tire inflation pressure had an impact on the relative position of the tire soil mappings to each other. The tire soil mapping of the 0.8 bar measurement reaches the highest tractive efficiencies between 60% at 14% of traction coefficient and 78 % at 26 % of traction coefficient. The 0.9 bar measurement follows with 58 % tractive efficiency at a traction coefficient of 11 % and 72 % efficiency at a traction coefficient of 25 %. The lowest tire inflation pressure leads to a significantly lower tractive efficiency between 44 % at a traction coefficient of 15 % and 69 % at a traction coefficient of 32 %. The highest tire inflation pressure of 1.0 bar leads to the lowest tractive efficiencies of 32 % at 9 % of traction coefficient and 57 % at 28 % of traction coefficient.

The fact that the lowest pressure is not necessarily the most efficient was indicated by Rempfer [2] and Wettemann [3]. The offset of up to 9 % of tractive efficiency caused by a change of tire inflation pressure of only 0.1 bar is surprisingly high. However, the comparison of the tire soil mappings that have been generated by calculating the tractive efficiency and the traction coefficient from the sensor values allows the evaluation of the tire pressure regarding their energy saving potential.

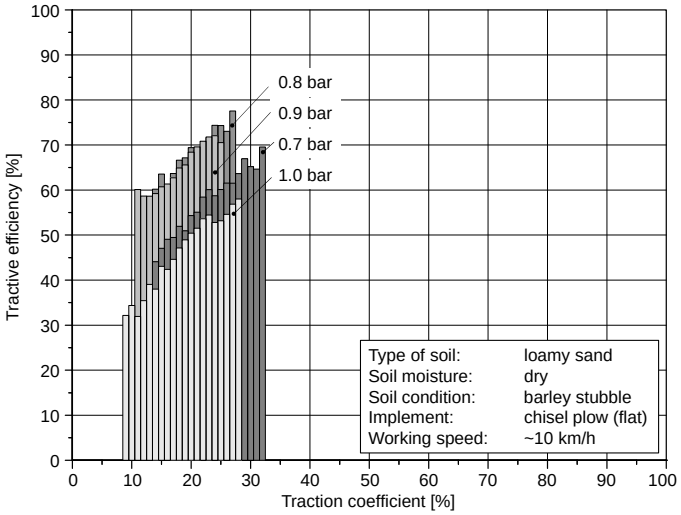

Fig. 5: Real time tire soil mappings for different tire inflation pressures whilst stubble cultivation on loamy sand

5. Summary and Conclusion

The improved traction sensor that is based on the sensor presented in [1] has successfully been installed in a tractor for field testing. The field tests with the traction sensor confirm the fact that the lowest tire inflation pressure is not necessarily the most efficient. The big impact of only small tire inflation pressure changes on the tractive efficiency is surprising. The tire soil mappings generated by classifying the tractive efficiency over the traction coefficient allow the evaluation of different tire inflation pressures regarding the tractive efficiency.

References

[1] Wieckhorst, J., Fedde, T., Frerichs, L., Fiedler, G.: A Tractive Sensor – Integrated Measurement of Tire Soil Parameters for Tractors. VDI-Berichte Nr. 2251. Düsseldorf: VDI-Verlag, 2015, S.219-226

[2] Rempfer, M.: Grundlagen der automatischen Reifendruckeinstellung bei Traktoren. Dissertation. Düsseldorf: VDI Verlag 2003

[3] Wettemann, P.: Ackern mit weniger Diesel. Neue Landwirtschaft (2012) 4, pp.67-70

Influence of the Drive Train and Chassis on Power Shift Operations in Standard Tractors

M.Sc. **Christian Birkmann**, Dr.-Ing. **Thomas Fedde**,
CLAAS Tractor, Paderborn;
Prof. Dr. **Ludger Frerichs**, Institute of Mobile Machines and Commercial Vehicles, Technische Universität Braunschweig

Abstract

The first partial power shift and full power shift transmissions for standard tractors were developed in the 1950s with mechanic and hydrostatic gearshift actuation systems [1], [2], [3]. These partial power shift transmissions usually had a two speed planetary drive in serial arrangement with a synchronized gearbox, whereas the full power shift transmissions consisted of a serial arrangement of several planetary drives with mechanic and hydrostatic gearshift actuation systems.

Today, electro-hydraulic gearshift actuation systems are state of the art and offer a wide range of opportunities to optimize power shift behavior and therefore handling comfort. On the other hand the number of setting parameters increases. To achieve an efficient transmission application process it is useful to have a general understanding of the influence of the dynamic tractor drive train and chassis behavior on power shift operations.

The influence is analyzed with the help of a complete tractor simulation model which is based on a given tractor. The resulting effects are evaluated by transmission output speed and torque.

1. Power Shift Transmissions for Standard Tractors

Till the end of the 1980s, partial and full power shift transmission concepts were unpopular in Europe [4]. Today, there are existing various numbers of different partial power shift transmissions as well as few full power shift transmissions. Partial power shift transmissions are offering two to eight power shifted ratios, combined with a synchronized range box, whereas full power shift transmissions offer 16 to 23 power shifted ratios [4]. Moreover, it became more likely to use a counter shaft design instead of planetary drives. To reduce the number of spur or planetary gears, the transmissions are designed as “grouped” transmissions with a serial arrangement of several sub-transmissions. Each sub-transmission offers two or more ratios. The resulting number of ratios is the product of the ratios per sub-transmission. This

leads to transmissions with a high amount of ratios, consisting of less spur or planetary gears [4]. But the demands on the gear shift actuation system increase with the number of sub-transmissions, especially for gear shifts involving several sub-transmissions. The basic power shift operation within one sub-transmission, including one engaging and one releasing clutch, is called a “one swop” gear shift. If two sub-transmissions are involved it will be called a “two swop” gear shift and so on. It is obvious that full power shift transmissions require such “multi-swop” gear shifts including several sub-transmissions. The same applies to some partial power shift transmissions, too.

2. Basic Power Shift Operation (“One Swop”)

Depending on the shift direction (up and down) and the torque flow direction (pulling and pushing) it is common to define four different shift conditions. Theoretically, an up-shift under pulling condition acts like a down-shift under pushing condition. The same applies for the other two conditions. Therefore, it is sufficient just to deal with up- and down-shifts under pulling condition. Regardless of the shifting direction, a basic power shift operation, consisting of one engaging and one releasing clutch, can be explained with the help of a simplified drive train model (Figure 1). It consists of two parallel power flow paths, each including one clutch and offering different ratios between the engine and the load. In case of slipping clutches during the power shift operation the drive train is divided in two dynamic subsystems. The first one includes inertia and stiffness of the engine and the primary transmission. The second one covers the secondary part of the transmission and the load.

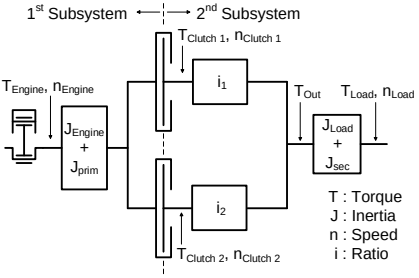

Fig. 1: Simplified drive train model (“one swop”) based on [5]

Figure 2 shows the corresponding “one swop” power up shift process including several phases. It consists of a preparation phase, a torque transfer phase, a synchronization phase and a finalization phase. In the preparation phase the theoretical torque of the engaged

clutch is reduced by releasing the safety pressure against slippage. In addition, the hydraulic chamber of the other clutch is filled until the kiss-point with the friction plates is reached. During the torque transfer the power flow path changes from one gear ratio to the other, but no speed synchronization occurs. This is done by engaging the former disengaged clutch until it carries the applied torque. It is important that the former engaged clutch is fully released at the end of the phase and therefore it is continuously disengaged during the whole phase. The output torque decreases due to the changed gear ratio. In the synchronization phase the differential speed of the new engaged clutch is reduced by “overtorque” of the clutch and/or by engine torque control. If engine torque control is used the output torque remains nearly constant, whereas “overtorque” of the engaged clutch leads to an output torque increase. For comfortable down- shifts the order of torque transfer phase and synchronization phase must be interchanged. In the finalization phase the theoretical torque of the new engaged clutch increases by reapplying the safety pressure.

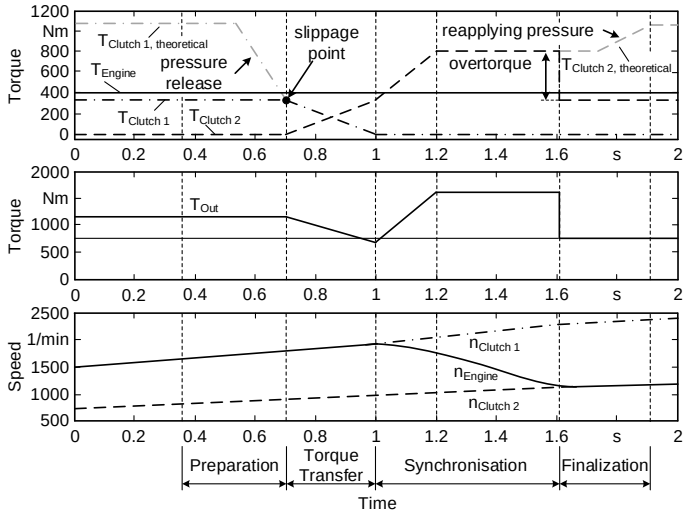

Fig. 2: Basic power up-shift process without engine torque control based on [5]

To perform comfortable power shifts, it is important to sense the transferred torque of the transmission at least during the preparation phase. This can be done by estimation, by torque sensors, by detecting differential speed while carefully releasing the engaged clutch until the slippage point is reached, or by a combination of these methods. Among these, only

the method of detecting differential speed gives the exact correlation between hydraulic pressure and required clutch torque. Therefore, this method is required for the final pressure release before starting the torque transfer or synchronization phase. It is used to control the differential speeds during the synchronization phase, too. Unfortunately, this method is influenced by the dynamic behavior of the drive train and the chassis.

3. Tractor Drive Train and Chassis Model

In order to analyze the influence of the drive train and chassis on the differential speed detection and therefore on the power shift operation itself, a complete tractor model optional with two and four wheel drive (2WD, 4WD) is created. The drive train model includes transmission and axle ratio, inertia and stiffness plus tire slippage, inertia and stiffness. The chassis model includes the component masses, a suspended front axle, a suspended cabin plus seat as well as dynamic axle load distribution. The drive train and chassis models are created with the help of AMESim and used in co-simulation with a Matlab model for the transmission controller.

To get a better understanding of the resulting effects, the main influencing components like inertia und stiffness are illustrated as a rough schematic drive train model (Figure 3). For simplicity reasons only one involved power shift clutch is shown.

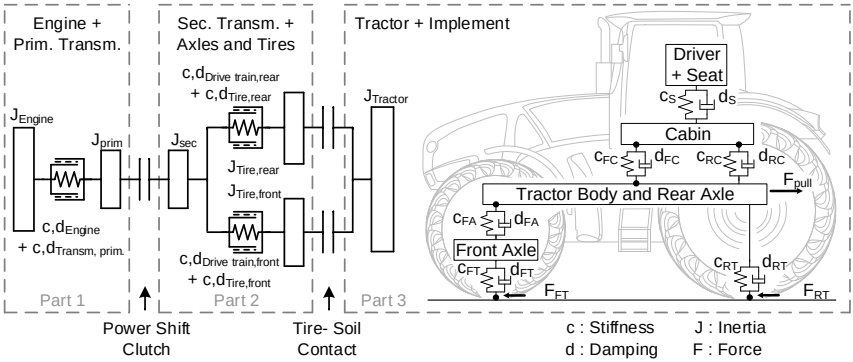

Fig. 3: Schematic tractor drive train and chassis model

It can be seen, that the model consist of three dynamic parts which are divided by the power shift clutch and the tire-soil contact of the front and rear axle. Part 1 represents the engine plus the primary part of the transmission. Part 2 includes the secondary part of the transmis-

sion as well as the front and rear axle drive train plus tires. Part 3 represents the longitudinal and vertical tractor and implement behavior. The AMESim drive train model is more detailed with regard to inertia and stiffness distribution. In addition, part 3 of the model, representing the tractor and implement behavior, consists of a detailed 2D chassis model (Figure 3).

Figure 4 helps to explain how the method of differential speed detection is influenced by the primary and secondary inertia connected to the clutch. While reducing the torque capacity of the clutch by reducing hydraulic pressure, the clutch will start to slip after a certain time. If the differential speed between primary and secondary clutch side exceeds a threshold value, the slippage is detected. At this point the pressure reduction will stop and the clutch torque capacity remains constant. If the stiffness between secondary clutch inertia and tire inertia is high, they can be seen as one huge inertia, decelerating or accelerating slowly. But in a tractor the stiffness of the tires and the axle drive train are low. Therefore, the torsion angle between secondary clutch inertia and tire inertia is high. In case of clutch slippage the tension releases and the small secondary clutch inertia decelerates or accelerates faster than the bigger tire inertia. This effect can result in quicker differential speed detection (Figure 4). As a consequence the slippage torque of the clutch remains on a higher level.

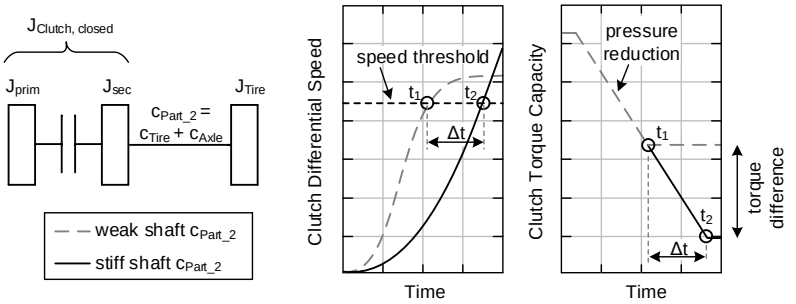

Fig. 4: Influence of shaft stiffness on differential speed detection

In a real tractor this stiffness is depending on the drive train configuration and the tires which can also vary in size and pressure. Moreover, if 4WD is engaged, the stiffness will be defined by the front and rear axle drive train, superposed by the influence of the front axle lead. In an optimal case the stiffness is the sum of both, but as the load and slip ratio of the front and rear axle vary, the resulting stiffness varies, too. Depending on the axle load distribution the stiffness is more similar to the front or the rear axle drive train.

4. Results of the Simulation Model

In Figure 5 the results of the tractor simulation model are shown as transmission output speed and torque during a power shift operation. The comparison includes simulations with 2WD and 4WD, as well as with concrete and clayey/sandy soil. With regard to the provided shift algorithm a power shift on concrete with 4WD results in the highest output torques and longest clutch synchronization time. With 2WD the synchronization time is shorter and therefore the torque peak is lower. The main reason is that the tire slippage of a 2WD tractor increases much earlier during the reengagement of the clutch than in a 4WD tractor. As a result the synchronization point is reached earlier and the peak torque reduces.

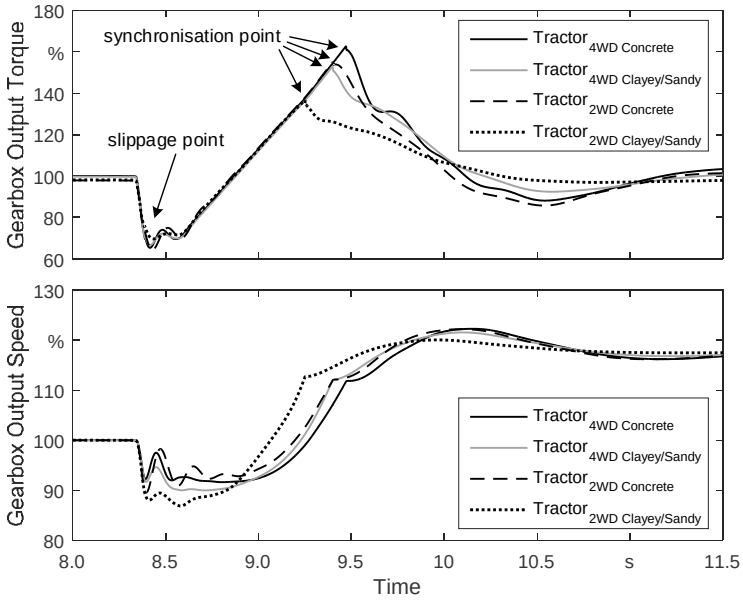

Fig. 5: Simulated transmission output speed and torque during a power shift operation

The effect of a weaker drive train of a 2WD tractor compared to a 4WD tractor should result in earlier differential speed detection and therefore in a higher torque level at the slippage point, but it can be seen that the influence on the torque level is very small. Additional investigations with different tire stiffness support this conclusion.

The influence of different traction coefficient curves can be stronger than the influence of an engaged four-wheel drive, whereas the effect is very similar. A smooth traction coefficient curve like for clayey/sandy soil leads to an earlier synchronization based on higher tire slippage and therefore to less jerky shifts.

5. Summary and Conclusion

In order to investigate power shift operations a detailed simulation model of a tractor is created. The model includes the complete tractor drive train plus chassis behavior. The simulation results show a remarkable influence of the chassis and drive train configuration on the power shift behavior, whereas the main reason is based on different tire-soil interaction. As a next step the simulations need to be validated with real tractor measurements.

References

[1] Erwin, R.L.; O'Harrow, C.T.: Tractor Transmission Responds to Finger-Tip Control. Agricultural Engineering 40 (1959) 4, pp. 198-203 and 207

[2] Buckingham, F.: The Shift in Transmissions. Implement & Tractor 77 (1962) 12, pp. 32-36 and 92-95

[3] Harris, K.C.; Jensen, K.J.: John Deere Power Shift Transmission. Construction and Industrial Machinery Meeting, 9.-12. Spet.1963, SAE paper 739A

[4] Renius, K. Th.: Globale Getriebekonzepte für Traktoren. ATZ offhighway (2014) 8, pp.16-29

[5] Fischer, R.; Jürgens, G.; Kücükay, F.; Najork, R.; Pollak, B.: Das Getriebebuch. Wien: Springer 2012

‘2 in 1 tire’ technology to allow maximal efficiency of the transmission chain in both road and field usage

Ing. **Patrick Vervaet**, Ing. **Marc Gandillet**,
Michelin , Clermont-Ferrand, France

Abstract

The tire and the tire/soil interaction play a major role in the efficiency of the transmission chain of a tractor as, in field usage, it is frequent that, due to rolling resistance of the tire, slippage and sinkage of the tire in the soil, more than 30% of the power available at the axle is not transmitted to the ground. In recent years, 2 key technologies have been developed to optimize this situation: Central Tire Inflation Systems and low pressure tires (IF and VF)

The new Michelin EvoBib technology allows a breakthrough compared to the current art. It consists of a tire that, under the action of a Central Tire Inflation System, drastically changes its shape to adapt its performances from road to field.

For field usage, this tire increases its effective tread width by a ‘hinge’ effect in the sidewall. The contact patch surface is increased by more than 20% compared to a similar tire at the same pressure. Depending on the soil conditions, it brings a potential increase of 20 to 50% of traction force at a given slip ratio.

For road usage, the tire presents a narrower tread and its design is completely different from the ‘V-lug shape’ of the classical agricultural tires. In this case, the rolling resistance of the tire is reduced by some 15% compared to classical tire at the same pressure; the comfort and wear performances are also optimized.

Furthermore, this tire needs less ballast to transmit tractive effort, and could therefore lead to a new design of ‘lighter’ high power vehicles allowing better soil preservation and less fuel consumption

State of the art

On agricultural tractors, the tire is a key component in the transmission chain between the engine and the soil. The main parameters to optimize its Tractive Efficiency (defined as the ration Output Power/Input Power) are

- Pressure optimization: it is a compromise as lowering the pressure brings a longer footprint and a smaller sinkage of the tire in the soil but increase the energy dissipated in the deflection of the tire (Rolling Resistance)

- Ballasting: the weight applied on the tire is a key parameter for the optimization of tractive efficiency as it has been established by previous studies that, with classical tires, the maximal Tractive Efficiency is obtained at a level of Net traction Ratio (traction effort divided by the load applied on the tire) around 40% (1)
- Tire design: for example, the radial technology, with the functional differentiation between the sidewall and the belt has allowed an homogeneous repartition of stresses in the contact patch and thus more efficient transmission

However, many studies have showed that the level of Tractive Efficiency of a tractor tire (part of the power brought at the wheel that is transmitted to the ground) is lower than 70% on most kind of soils (1)

An ENTAM workgroup has defined a method to measure the Tire Efficiency in soft soil. This efficiency in defined in a 'PullLoss Index (PLI) characteristic (2)

EvoBib Technology

The technology developed differentiates from previous art by the fact that the tire presents 2 completely different shapes depending of its usage. The activation of the change of shape is obtained by change of pressure through, for example, the usage of a Central Tire Inflation System.

The first shape is designed to optimize the tire for road or hard soil usage. Compared to the 'classical V lug' agricultural tire, the width of the tread in contact with the ground is narrower and present a higher 'rubber vs. void' ratio, with a 'quasi-continuous' tread profile at the centre. It is reached when high pressure level (over 2/3 of the nominal tire pressure) is activated through CTIS

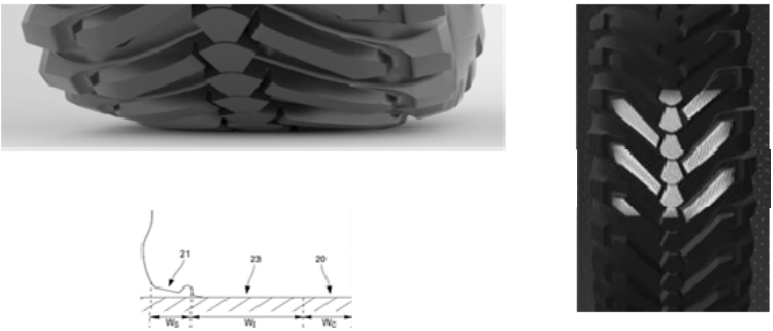

Fig. 1: Tire shape and contact patch in 'Road' configuration

The second shape is designed to optimize the tyre for field, or soft soil usage. In this case, the contact patch is much wider than in a classical tyre. The ‘shoulder’ part of the tread, is specifically designed with a low ‘rubber vs. void’ ratio. This shape is obtained when low pressure level is activated.

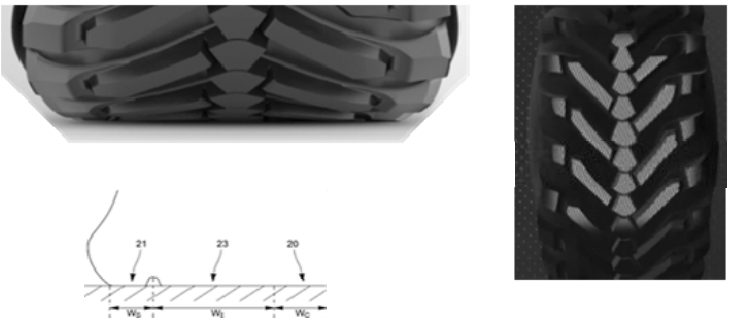

Fig. 2: Tire shape and contact patch in ’Field’ configuration

The key challenge was to keep, in both shapes, a homogeneous repartition of stress in the contact patch. It is well known that the key benefit of the radial technology is to allow, through a functional separation of the ‘tread’ and ‘sidewall’ zones of the tyre, a robust and homogeneous contact patch. However, this radial structure used to structurally ‘fix’ the width of the contact patch independently from the load and pressure applied.

The EvoBib technology suppress this limit by the combination of an innovative tread profile and of a carcass and belt structure in which the rigidities are scaled in such a way that the ‘shoulder’ (zone ‘A’ in figure 3) behave like a sidewall at high pressure and like a tread at low pressure.

With those technologies and the help of high level 3D Finite Element analysis, we could obtain an homogeneity of stresses in the contact patches in both conditions.

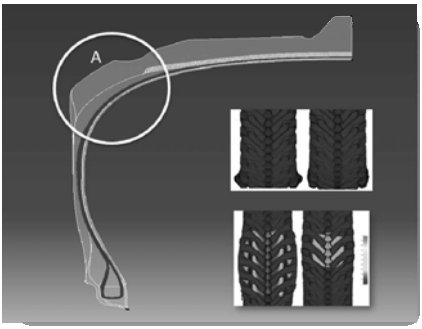

Fig. 3: ‘Shoulder’ zone and map of stresses in contact patch in road and field configuration

Key Performances

Through this technology, significant gains are obtained in various performances of the tire

- ***Soil Compaction***: in field configuration, the surface of the contact patch obtained is 20% bigger than with classical tire for the same level of load and pressure. This, of course limits the impact of the tire on soil compaction
- ***Traction:*** the increased width in soft soil, associated with a lower sinkage of the tire in the soil due to the bigger footprint brings a higher capacity of the tire to transmit high tractive efforts.
    - This performance can be measured in a test were 2 tractors are linked by a drawbar in which the stress is measured. The front tractor tries to accelerate while the second maintain the speed constant. Simultaneously, the stress in the drawbar and the slip ratio of the tires of the front tractor are measured. After analyse, we build ‘slip/traction curves’ showing the ability of a set of tire to generate a traction effort at a given slip ratio

Fig4 show the results of such a test. With the EvoBib, we observed, for the same load and pressure, gains of tractive effort in a range of +20 to +50% for slip ratio around 10% which is the range of slip ratio usually considered as optimal for tractive efficiency

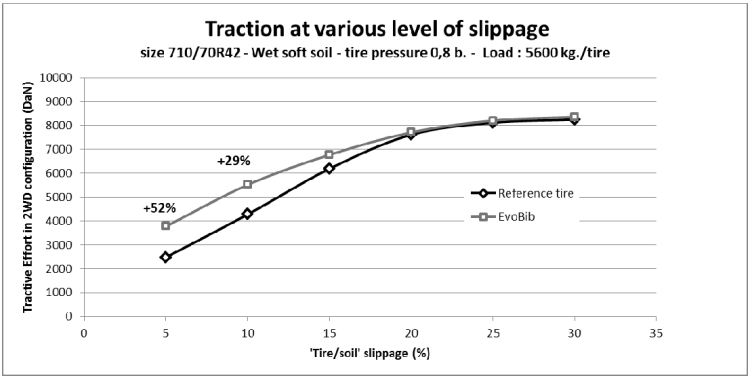

Fig. 4: Traction efforts obtained at various slip level: comparison between EvoBib technology and the best tires of the previous art (AxioBib)

- ***Rolling Resistance***: this characteristic can be expressed as a trailing force proportional to the load applied on the tire when rolling on a hard surface. On tires dedicated to agricultural usage, it is often in the range of 20 kg./ton. (it is to be noted that this level is much higher than in passenger cars and truck tires as, on agricultural usages, an important focus is given to the flexibility of the tire) The limitation of the tread width in contact with the ground in road usage leads to a reduction of Rolling resistance of the tire of over 15% for a given load and pressure.
- ***Driving comfort*** : The specific design of the tread in road configuration, with the suppression of the 'lug ends' in the central zone leads to a limitation of the vibrations transmitted and an higher steering rigidity

Impact on vehicle design

In the state of the art, many studies have confirmed an optimal Pull Loss Index of the tyre at a NTR (Net traction Ratio = Net traction divided by the dynamic load applied on the tire) of around 40%(2)(5) . With the EvoBib technology, we observed that this optimum value is highly increased, at value significantly over 50%. We also observed significant improvement in the maximal tractive efficiency. This means an opening to significant changes in the tractor design

3 directions might be followed

- Use a given vehicle for a more intensive work
    - For example, the usage of VF710/70 R42 and VF600/70R30 EvoBib tyres, brings an additional available power at the drawbar of over 20 HP on a 300 HP tractor
- Use a smaller engine on a given vehicle for the same work
    - The same work at the drawbar may be performed on the same tractor with a needed power at the engine reduced by some 15%

- Use a lighter vehicle to transmit the same power
    - With the increase of optimal NTR from 40 to over 50%, it allows to have a lighter tractor to perform the same traction performance. For a given engine power, it has been estimated a possibility of 10% vehicle weight reduction (from change of ballast or vehicle design) with an increased effective traction. This allows additional gains on soil compaction and fuel economy.

[1] F.Zoz and R.Grisso : '*Traction and tractor performance*' ASAE distinguished lectures series, tractor design 27, 2003

[2] G.Fancello, K.Szalay : 'Agricultural Tyre Energy Efficiency test method, link with specific fuel consumption for measuring the efficiency of agricultural tyres under real conditions on tractors' AgEng, VdI 2015

[3] B.Pichlmaier : '*Traktionsmanagement fur traktoren*' Dissertation. Technische Universität Munchen, 2012

[4] F.Zoz and J.Wiley : '*A theoretical basis for tractor ballasting recommandation'* ISTVS conference may 1995

[5] Brixius W.W. : Traction prediction equations for Bias Ply Tires. ASAE Paper 87-1622 (1987)

[6] Dessèvre, D. (2010): A review of the main effects of the tires and their usage, on the fuel consumption of agricultural tractors. EurAgEng 2010.

Redundant Communication in Daisy Chains for Improved Diagnostics and System Reliability in Seeders and Planters

Dr. **Matthias Rothmund**, Dr. **Sebastian Villwock**, **Philipp Pollinger**,
HORSCH Maschinen GmbH, Schwandorf

Abstract

Multiple row modules, section modules, nozzle controllers are often connected in CAN-based daisy chains in application bars of seeders, planters, sprayers. By single wire or connector faults, the whole daisy chain is not operable anymore and failure locations are not easy to detect. Redundant communication for CAN busses was introduced a long time ago, but existing approaches do not cover harness faults that we commonly see in agricultural applications. In this project a redundant communication system for daisy chains was developed with only one physical CAN bus but a redundant connection to two CAN controllers of the master ECU.

1. Problem and objectives

In several types of agricultural equipment a set of uniform controllers is combined to a daisy chain mostly connected by a CAN bus. This applies for instance for row controllers in planters and also for section or nozzle controllers in sprayers. All controllers are typically connected with one CAN controller of the central implement ECU. Generally, the power supply wires for the controllers are located in the same cable as the CAN bus wires. Often, there is an additional electrical control wire used to assign a specific address to each controller to determine its position in the daisy chain.

In case of a connection fault of CAN bus, it is no longer possible to effectively run the daisy chain based system. This is at least the case for that part of the daisy chain after the fault location, but quite often not possible at all due to missing CAN bus termination. It is obvious that it will be for the same reason difficult to localize the faulty part inside the daisy chain and it will be even harder if the failure is caused by a loose contact.

The general approach to reach higher system availability is to introduce redundant communication. But the specific solution has to deal with specific requirements in our equipment. The objectives in our project were to really cover the common faults that we frequently see while

machines are working in the field and to still allow operation in case of a single fault in CAN communication as well as an instantaneous diagnose of the problem.

2. State of the art

José Rufino [1] describes two different approaches for physical CAN bus redundancy. The first one is a redundant physical layer consisting of a Primary and a Secondary in which the CAN interface of a connected ECU (Node) has only one CAN-Controller, but with an upstream Media Selector. This media selector has the technical ability to detect failures on the Primary bus and switches to Secondary bus if necessary. This offers high network availability and protocol transparency, but is not able to handle all bus errors. The second approach is a redundant bus topology with two CAN controllers in each CAN interface which he calls full space-redundancy. This offers also a high network availability and additionally a broader coverage of faults, but it requires a software-based redundancy management and causes protocol processing overheads. Finally, Rufino [1] describes a combination of both approaches with fully redundant CAN communication by separate CAN controllers in which each physical channel has again a primary and secondary bus with a Media Selector component in the CAN interface. This results in very high fault coverage and very high network availability. For all described approaches, specific hardware is needed. In doing so, for full space-redundancy ECUs with multiple CAN interfaces could be used which are common today.

However, all approaches are dealing with faults on the controller or electronic level only. In agricultural equipment, we quite often have another kind of mechanically induced issues like connector or cable problems which result in loose contacts or disconnections. This could of course be improved by introducing separate harnesses for full redundant channels, which makes it expensive and also results in more cables to handle in a machine or equipment. Maryanka et al. [2] propose to use the electrical power line inside a vehicle as redundant CAN communication channel. This has the advantage that especially in new developed architectures no or not many additional harnesses are needed. However, there are still additional connectors needed and also specific hardware components to process CAN traffic from the power line. Moreover, in our specific daisy chain topologies where we mainly need redundant communication, sometimes the power lines are integrated in the same harness as the CAN cables.

3. Technical approach

The following explanations are based on an existing project to develop a more robust communication system for daisy chained row modules in a seeder or planter. In our approach, there is no additional physical CAN communication channel provided. In a classic CAN based daisy chain, a number of uniform nodes (for instance row modules) and one main ECU to control daisy chain nodes is connected to the bus. We now additionally connect a second separate CAN interface of the main ECU to the same bus, while topology-wise the CAN cable physically connects to one main ECU CAN interface before and to the other after the daisy chain (fig. 1).

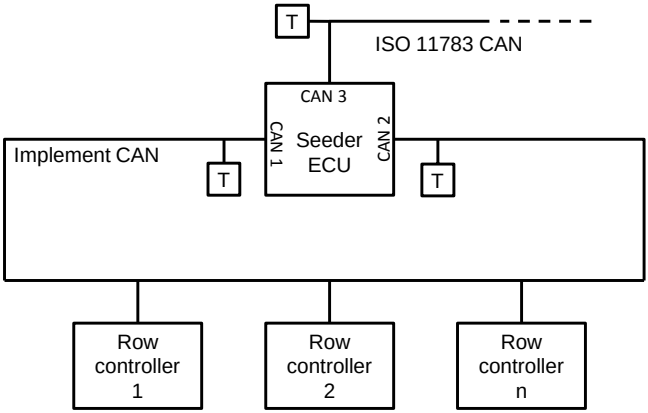

Fig. 1: Schematic bus topology for redundant communication over one physical CAN bus

In any case of interruption caused by harness or connector defects, the idea is according to figure 1 to communicate from two sides to reach all nodes ‘left’ from the defective location with CAN interface 1 of the seeder ECU and all nodes ‘right’ from it with CAN interface 2. Of course, this requires a bus disjunction and termination management at each row controller, because in case of a loose contact or interruption of the physical bus, the remaining parts of the CAN bus are not terminated and likely not functional anymore.

Two different approaches can be looked at to resolve this inside the nodes. In both cases, the CAN bus has to be physically fed through the daisy chain ECUs with an in and an out connector and the stub to the CAN controller has to branch off inside the ECU housing.

The first alternative is to have one physical bus where all daisy chain ECUs are connected and which can be disjoined between the in and out connectors of the ECUs with electronic

switches in CAN high and low wires. At the same time terminators on both sides of the switches have to be switched on to establish a functional communication bus between the seeder ECU and the last daisy chain ECU before the defective location on both sides (fig. 2). One main disadvantage of this approach is the specific hardware that is needed to disjoin the bus and switch terminators. Also the software logic to detect defective locations by dis- and re-joining daisy chain nodes one by one from both sides is quite complex and thus is expected to be error-prone.

The second alternative is to have two separate CAN controllers on each daisy chain ECU and to always establish a new physical bus between two nodes (fig. 2). This way, in case of a fault between two modules, the communication between all other nodes - partly from left and partly from right side - stays functional without further actions.

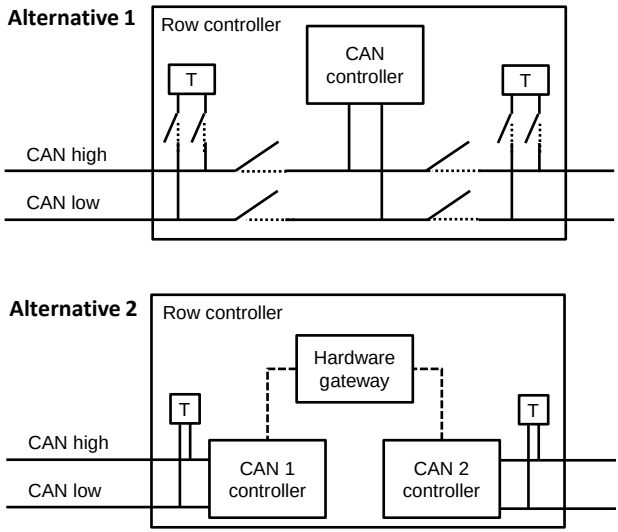

Fig. 2: Schemes of CAN architectures inside daisy chain ECUs with one (alternative 1) and two (alternative 2) CAN interfaces

A disadvantage of alternative 2 is the latency caused by CAN message forwarding inside the node from CAN 1 to CAN 2. By hardware gating this is expected to be reduced to about 1 ms per daisy chain node.

4. Results and discussion

From a technical point of view, both drafted hardware solutions are possible to be realized. In doing so, alternative 1 causes more software and testing efforts to develop the basic software layer which is responsible for CAN bus separation and termination and detection of fault locations. It is the preferable solution for time critical requirements in terms of parallel processes like row switching for section control. For alternative 2 at least 1 ms delay should to be calculated between one row or nozzle and the next one in case all rows are commanded at once.

In a first step, a row module according to alternative 2 was developed using a hardware gateway to transfer messages from the receiving to the sending CAN controller. The ‘direction’ of communication depends on which is currently the sending CAN interface of the seeder ECU. An excerpt of an oscilloscope recording is contained in figure 3. It shows cascading of the messages from one CAN bus to the next one respectively from one row module to the next one.

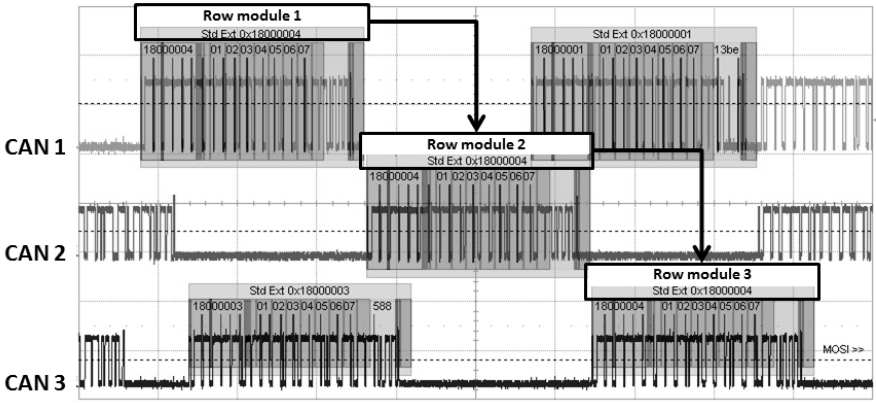

Fig 3.: Oscilloscope record of a message cascade on three independent CAN busses in three sequent row modules

In this case under lab conditions and without any additional bus load, not more than the theoretical latency caused by the message length of a CAN message with 29bit identifier and 8 data bytes (~700 µs) was measured. As long as there are no other messages on the ‚receiving‘ bus, the time consumption for hardware gating is insignificant. As soon as other mes-

sages on this specific row module bus are blocking forwarding at the hardware gate, the latency will increase depending on the bus load.

In normal work mode, CAN 1 of the seeder ECU sends ‘from left side’ into the daisy chain of row modules which is located in the application bar. In case one module cannot communicate to the next one right side anymore, hardware gating will be stopped inside this module and parallel communication will be started from CAN 2 of the seeder ECU. This way, a parallel, identical CAN messaging is realized from both sides of the daisy chain. In case of one defect between two modules, still the whole application bar can operate (fig. 4, case 1). In case of a defect inside one module, either the whole bar or all modules except the defective one can operate depending on the kind of error (fig. 4, case 2). If there is more than one fault along the daisy chain, the system can still operate till the modules before the first defect on each side from left and from right of the chain (fig. 4, case 3).

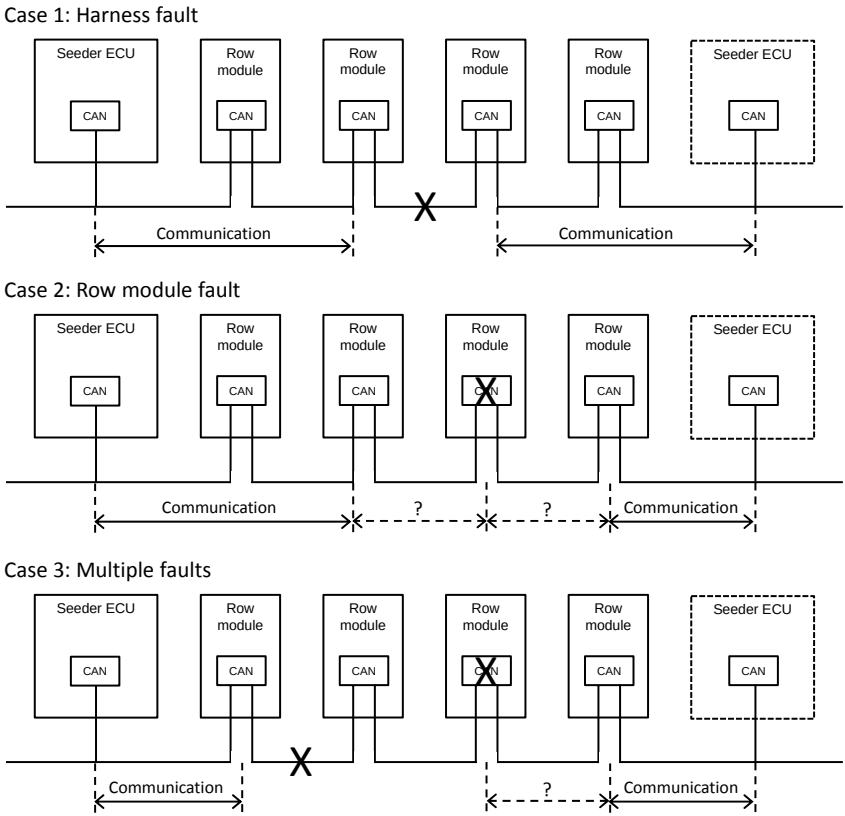

Fig. 4: Fault scenarios and resulting communication for redundant CAN on one physical layer

The CAN addressing of daisy chain nodes is normally resolved by an additional wire and a high/low output on the CAN-out side and an high/low input on the CAN-in side. As the communication can now change its direction in case of a communication interruption, this wire could be optionally connected to one input and one output on both CAN sides of each module and to two in- and outputs each at the seeder ECU (fig. 5). This way, addressing could also be triggered from both sides, but it requires robust software logic to handle addresses and row allocation which is essential for applications with geometric dependencies like section control.

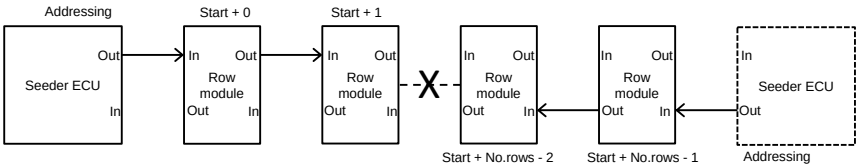

Fig. 5: CAN addressing ability from both daisy chain ends in case of a disconnect fault

To ensure the ability of further operation in case of a disconnection inside the daisy chain by wire or connector or module fault, electronic power is also provided by two outputs which are wired to both sides of the daisy chain.

5. Conclusion

The developed system will allow continued operation in case of many harness or connector defects. Detection and proper system reaction in case of a loose contact which causes short-time breakages requires robust software logics and has to be approved in practical testing. Latencies in the chosen CAN architecture can cause imprecise results especially in sectional control applications with many seed rows or sprayer nozzles. Also timing issues in request-response communication between distributed CAN nodes can be expected, especially at higher bus loads when time delays are not systematic and cannot be calculated in advance. In this case the architecture presented as alternative 1 in this paper will be an option, but causes more development efforts. Generally, it will turn out over time if the costs and efforts for redundant communication systems in agricultural equipment are justifiable by high improvements in terms of robustness and availability in critical work load situations of our customers. Potentially, other measures like harness installation design and robust connectors are also suitable to improve system availability. Definitely, the chosen approach for redundant communication allows fast and focussed diagnostics of CAN issues inside a daisy chain. HORSCH is going to introduce redundant daisy chain communication in a pre-series planter model from 2018.

[1] J. Rufino: Redundant CAN Architectures for Dependable Communication, CSTC Technical Report RT-97-07, 1997

[2] Y. Maryanka, O. Amrani, A. Rubin: The Vehicle Power Line as a Redundant Channel for CAN Communication, http://yamar.com/articles_text/plc-as-redundant-can/, 8/4/2017

Extending ISO 11783 for four wheel steering and implement steering

Dr.-Ing. **Timo Oksanen**, Aalto University, Finland

Abstract

The current ISO 11783 standard supports guidance communication between a guidance system and a tractor with a single actuator, but nothing more. In this paper, the developed concepts to extend the ISO 11783 standards are presented, to cover a) four-wheel steering of tractor, b) implement steering and c) interchange of steering system parameters. The developed concepts are backwards compatible with the current standard that is desirable for product development and management. The concepts are scalable and flexible, for future extensions (like chained implements). The concepts do not limit to any specific navigation principles but allow interchange of relevant variables that generalize any system, both tractors and implements. Opportunities of ISO 11783 towards support of four-wheel steering and implement steering are discussed and proposed plus interchange of relevant parameters. For the future, it is important and relevant not to design the communication around any specific algorithms but generalize in order to standardize only the communication interface, not the method of guidance.

Introduction

ISO 11783 standard series known as the base for ISOBUS compatible equipment is widely in use by dozens of manufacturers aiming at global compatibility. The first step in ISOBUS was to interconnect implement ECU to tractor cabin using a common user interface device and the next step was to integrate automation, like variable rate application or section control to the tractor-implement system. The next step would be to integrate navigation systems, using ISOBUS. The current ISO 11783 standard supports only guidance communication between a guidance system and a tractor with a single actuator (like front wheel steering).

Considering navigation needs of modern tractor-implement system, one degree of freedom is not sufficient for the accurate guidance of vehicle system. On the other hand, the tractor may be equipped with four-wheel steering, like Claas or JCB tractors, or the implement may contain steering units, like Grimme harvesters or Orthman planters. Using four-wheel steering or

combined tractor-implement steering would allow using two degrees of freedom that enables more precise control of both lateral tracking error and heading error of the desired part of the implement. However, the current ISO 11783 is limited to only tractor steering with one actuator so there is no standard way to interconnect systems.

On the other hand, the guidance systems could utilize the added degrees of freedom in many ways, not only in the mainland operation to increase accuracy but also in the headland for more agile turning. Sophisticated control algorithms are able to control multiple steering actuators at the same time, like front wheel steering of tractor plus drawbar joint angle for trailed implement steering, presented by Backman et al. [7].

Practical scenario

Automatic guidance based on GNSS sensors can be installed on tractors either by the tractor manufacturer at the factory or it can be added as an add-on later. Even with factory-installed automatic guidance systems, the manufacturer of guidance system is often other than the tractor itself, even if the integration is done by the tractor manufacturer. For the reason, a guidance system is one component of multi-brand system, which consists of tractor, connected implements, GNSS and the guidance system. As ISOBUS was developed specifically to tackle the challenges of multi-brand systems and plug-and-play, it is natural to consider the interconnection of guidance system and steering units via ISOBUS, even if not being mandatory channel. Below, it is assumed that tractor is manufactured by brand A, implement by brand B and guidance system by brand C.

Plug-and-play is a key requirement for farming machinery, as the system is integrated not earlier than in the farm and it may not be assumed more skills to do the integration than one needs to interconnect an auxiliary device to the computer with USB. Any other approach except plug-and-play for interconnecting modular systems does not make sense, as the number of combinations of different implement models and tractor models is so large that no one could keep up the system, not even within a single full liner.

Commanding steering over the current ISOBUS

The current ISO 11783 standard series (parts 7 and 9) supports commanding of the steering actuator of the tractor over ISOBUS using remote control messages. The steering actuator is typically an electronic directional valve that drives the hydraulic steering cylinder. In the standard, curvature is used to abstract the steering actuators and various kinematics of tractors,

like front-wheel steering, rear-wheel steering, articulated steering or crawler tractors. Hence, guidance system needs to command only the desired curvature of the tractor and the steering unit of tractor converts it to the steering angle or to differential drive ratio. Symmetrically, the steering unit broadcasts the current measured curvature to ISO network, which is not measured in a sense of motion but against theoretical railroad model without any slip.

However, even if the guidance system is able to command and read the curvature, it lacks the information of steering dynamics, as there is no standard way to communicate e.g. lag of steering, maximum rate of steering or even maximum mechanically possible curvature. Therefore, installing a guidance system in plug-and-play manner is not possible, but requires some tweaking and tuning, to be stable and accurate.

Four wheel steering

Tractors with four wheel steering can be commanded using the current ISOBUS curvature command and it is up to the manufacturer or user to select whether the desired curvature is actuated by using front, or rear or both steering actuators. Thus, even if being a functional approach, a tractor with two degrees-of-freedom (DoF) for steering is commanded by single set point and the other DoF is not utilized in path tracking. Furthermore, if user changes the steering mode, the guidance system is unaware of this change and path tracking accuracy changes remarkably.

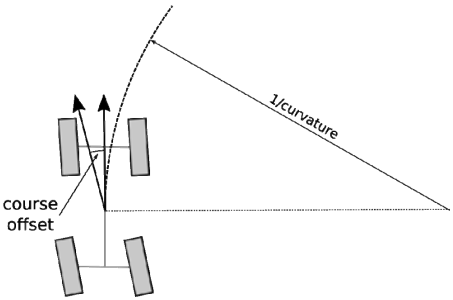

Fig. 1: Definition of course offset in conjunction with curvature, for four wheel steering.

Hence, commanding four wheel steering requires something in addition to the curvature. The proposed additional commanded value is *course offset*, see Figure 1. If curvature set is zero, the course offset steers all wheels to the same angle, defined by course offset. If curvature is

non-zero, solution to compute front and rear steer angles requires more equations, unique conversion formula exists. Hence, the guidance system is able to control both lateral steering along the path by using course offset variable and heading by using curvature variable.

Implement steering

In this context, we define implement steering as a capability to manoeuvre tractor-connected implement on the implement side, to follow the path. In implement steering, the movement is partially limited by the tractor and its trajectory, but within some range the implement may steer itself into better position. For hitch mounted implements, side-shifter actuators may be used to move the functional point in the implement frame (like sowing units). For trailed implements, both side-shifter in drawbar, actively actuated joint in the drawbar, or steered wheels / coulters may be used. In some implements the range of movement may be limited to +/- 50 cm, while in some mowers / rakes the movement may be several meters sideways.

Guidance system commanding both the tractor and the implement is desired as the implement only steering would require an operator to use substantial effort to steer the tractor. As the desired path is common for the tractor and connected implement, the standard should support the idea of combined guidance system that commands both the tractor and implement [9]. In ISOBUS systems, this would be realized in multi-brand systems like presented in Figure 2. However, the standard defines only the interfaces, so it does not exclude the pattern of separated guidance systems.

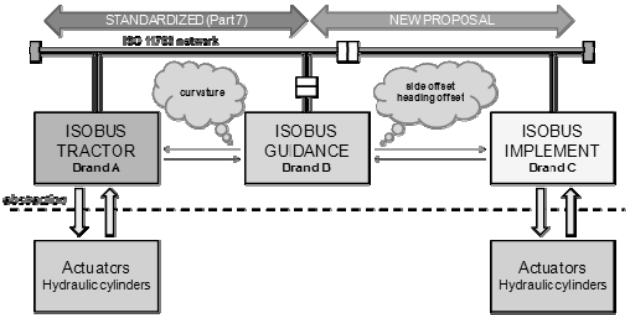

Fig. 2: Guidance over ISOBUS for tractor and implement, architecture. [8]

Due to plug-and-play requirements, the interface for implement steering must be something more abstract than the current position of a hydraulic cylinder, as otherwise guidance sys-

tems have to contain kinematic models of every single equipment manufactured in the world, in order to know how the position of hydraulic cylinder affects the guidance objective.

For tractor control, curvature was originally selected as the control variable. Curvature presents a nice level of abstraction, as guidance system does not need to know the kinematics of the tractor and guidance system may be easily moved from one tractor to the other and the interface is rather simple for a tractor manufacturer to realize.

However, as implements are connected to the tractor and the tractor controls the movement of the connected system in the field (including curvature), curvature is not an option for implement side abstraction. Even if curvature is not an option, something similar in terms of abstraction level is required.

Oksanen & Backman [6] have proposed an *Abstract implement* model as a solution for this. Abstract implement is a kinematic model that can be fitted to any kind of implement. Abstract implement is simple defined as three joints and two links between those plus some coordinate systems that are used to define the position of the functional point and a possible GNSS receiver.

After defining abstract implement and its parameters, the control variable (corresponding to curvature on the tractor side) is needed. Oksanen & Backman [6] define the control variable as side offset, which is very simple to calculate for one degree-of-freedom implements and examples are presented to show how to calculate it for implements having two degrees-of-freedom, like a potato harvester with both drawbar steering and rear wheel steering. In addition to the side offset as control variable, another control variable, optional variable, is heading offset, which is to be used in case implement has two actuators. Utilisation of both the side offset and heading offset control variables simultaneously allows the guidance system to control a long potato harvester along curved ridges so that intake follows ridges laterally and intake orientation is along the ridges.

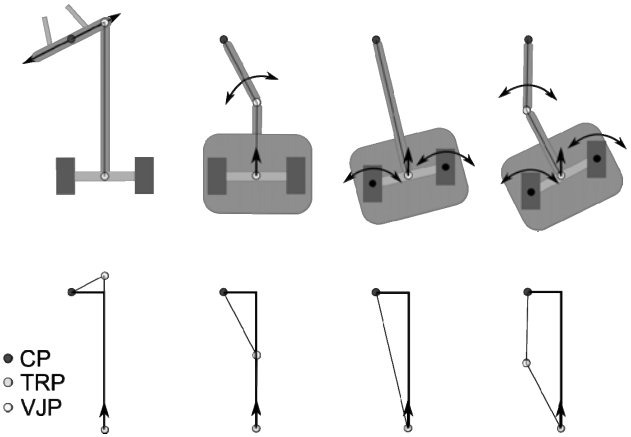

Fig. 3: Abstraction of implement; on top some physical implements are visible, on top the physical appearance is hidden, otherwise the same. Blue dot represents Connection Point (CP) to the tractor (or to preceding implement), green dot represent True Rotational Point (TRP) and yellow dot is defined as Virtual Joint Point (VJP), which appears in some cases in conjunction with real joint. All four examples follow the tractor exactly in the same manner, as the relative position of TRP and CP is the same - guidance system does not need to know the real physical implementation, only the dimensions of abstract implement including VJP. [6]

Parameters and transfer of those

The extension of communicating steering system parameters to the guidance system would enable more advanced navigation and true plug-and-play of the guidance system. The required parameters of steering are: a) the maximum curvature (steering angle), b) the maximum course offset, c) the maximum change rate of curvature / course offset and finally d) the lag and delay (of first order dynamic model) of curvature / course offset. Alone, approximate values of these would open doors for true plug-and-play, even if some parameters may be time-dependent, like due to engine revs or temperature.

To transfer the parameters of tractor steering, constants, from the steering system to the guidance system, a standard method is required. The parameter pool consists of a list of parameters. Two schemas are available in the standards for this: to follow the object pool approach used in ISO 11783-6 [1] for virtual terminal parameters, or NMEA2000 [4] or SAE

J1939 multipacket [5]. Virtual terminal kind of object pool allows hierarchical representation, a tree of parameters instead of a list, while NMEA2000 or SAE J1939 multipacket model is remarkably simpler for the implement.

For implement steering, the same pattern should be used, sketched by Oksanen & Backman [8] presenting the concept of Implement Guidance Parameter Pool (IGPP). IGPP consists of 22 listed parameters, defining not only lag and delay (of first order dynamic model) for side and heading offset, but also the relative coordinates of TRP, VJP etc. However, implement steering is defined in another way and there may be more than one implement connected and the control variables are remarkably different, so parameter pool structures should be differentiated in a way that one list/pool type for tractor steering parameters and another for implement steering.

The steering & guidance parameter communication should be kept separated from ISO Task Controller protocol, as the guidance pattern sketched in Figure 2 should be operable without Task Controller.

Remote control messages in the future

Meanwhile, ISO 11783 communication methods for the remote control of tractor subsystems are under development, from earlier known as ISO 11783 Class 3 Tractor ECU, to ISOBUS TIM system. TIM (Tractor Implement Management), defined by AEF (Agricultural Industry Electronics Foundation) is replacing earlier ISO 11783 Class 3 to improve liability risks, embedding functional safety requirements and considering product life time processes for compatibility. However, the signals transferred between parts of ISOBUS system are more or less the same as earlier.

The guidance concepts presented in this paper are compatible with the latest communication patterns that make the real time communication safer, in terms of functional safety and security. Integrating implement steering, four wheel steering and steering system parameter transfer would allow better plug-and-play for guidance systems while TIM is defining the backbone for communication.

Conclusions

The extended interface does not only make the development and testing process of guidance systems easier, but also aims at better plug-and-play experience at farm level. Plug-

and-play is a crucial built-in feature of ISOBUS and the extensions of the standard may not cause any risk on that.

[1] ISO IS 11783-6. Tractors and machinery for agriculture and forestry — Serial control and communications data network — Part 6: Virtual terminal. International Organization for Standardization, Geneva, Switzerland, 2014.

[2] ISO IS 11783-7. Tractors and machinery for agriculture and forestry — Serial control and communications data network — Part 7: Implement messages application layer. International Organization for Standardization, Geneva, Switzerland, 2009.

[3] ISO IS 11783-9. Tractors and machinery for agriculture and forestry — Serial control and communications data network — Part 9: Tractor ECU. International Organization for Standardization, Geneva, Switzerland, 2012.

[4] NMEA: NMEA2000 - Standard for Serial-Data Networking of Marine Electronic Devices. National Marine Electronics Association: 2015.

[5] SAE: Surface vehicle recommended practice, SAE J1939. 2015.

[6] Oksanen, T. and Backman, J.: Standardization proposal on Implement guidance for ISO 11783 compatible tractor-implement systems. Aalto University: Aaltodoc series Working papers 2015.

[7] Backman, J., Oksanen, T. and Visala, A.: Navigation system for agricultural machines: nonlinear model predictive path tracking. Computers and Electronics in Agriculture, 82, 2012, pp. 32–43.

[8] Oksanen, T. and Backman, J: Implement Guidance model for ISO 11783 standard. Proc. of 5th IFAC International Conference Agricontrol 2016. IFAC-PapersOnLine 49(16), 2016, pp. 33-38.

[9] Backman, J., Oksanen, T. and Visala, A.: Applicability of the ISO 11783 network in a distributed combined guidance system for agricultural machines. Biosystems Engineering, Vol. 114(3), 2013, pp. 306–317.

ISOBUS Automation – On the Road to TIM

How to secure liability for open TIM systems

Dr.-Ing. **Georg Happich**, AGCO GmbH, Marktoberdorf;
Dipl.-Ing. **Hans Jürgen Nissen**, John Deere GmbH & Co. KG,
John Deere Werk Mannheim

Abstract

A large topic in the Ag industry today is the discussion about the introduction of an open Tractor Implement Management (TIM) system, whereby the implement is given the control to set tractor functions (e.g. the implement requests a specific ground speed, hitch position, hydraulic valves oil flow, …). The Agricultural Industry Electronics Foundation (AEF) has taken the challenge to lead this discussion towards a standardized solution based on ISOBUS protocols and technologies. After presenting the general concepts of the open Tractor Implement Control system during the VDI LAND.TECHNIK conferences in 2013 and 2014 ([5], [6]) the following paper presents the actual state of work of this AEF Project.

1. Motivation and Introduction

While ISOBUS [2] enables interoperability of electronic-based products across manufacturers in the agricultural market, the focus of the industry today is to reach a higher level of automation in such open multi-brand systems. This automation allows further process optimization and/or reduction of operator fatigue in this rapidly growing system complexity. Tractors provide multiple energy outlets like hydraulic valves or PTOs, but also ground speed, steering and hitches. While attachments and implements bring process specific knowledge utilizing the power of the tractors. A natural next step is of course to have the implements control the power outlets. More and more manufacturers started to provide proprietary solutions in past years for example balers control the ground speed and hydraulic valves. Even when they utilize the ISOBUS messaging to give the implements access to the tractor functions, they still do not provide open usage across manufacturers. This is driven by safety and liability aspects in combination with missing or unclear specification. Product-liability forces the manufacturers to ensure that only known and well tested product combinations can be used in the field. Therefore manufacturers perform joint testing with each possible counterpart to ensure safe operation before they release a product to the market.

In 2012 the AEF took the challenge to standardize the interaction between tractors and attachments towards a modular self-propelled machine in an open ISOBUS solution that meets the safety and liability concerns of the individual participants. While the definition of the required ISOBUS messaging and safety requirements appear to be known, it is the standardisation work to provide the means to ensure only known and trusted equipment can work together in the field which is a new challenge for the AEF experts.

2. Objectives of the AEF project team

TIM systems are destined to be distributed on a wide scale as automated systems assisting the operator in the effective use of the machinery. Such system architecture brings a new level of complexity and responsibility with respect to safety and liability, as more than one manufacturer is involved in the overall system. The AEF Project Team “Functional Safety” encountered several areas of liability risks, once manufacturers enter such a multi-brand automation system. Based on this identification the AEF decided to create the project team “ISOBUS Automation” to develop and define methods and processes, to ensure that the industry wide liability risk for the manufacturers is reduced to an acceptable level. The processes and methods are formulated in an AEF Guideline [4], and shall include all needed aspects of state-of-the-art normative and several AEF Guidelines [1].

In the meantime the scope of project team “ISOBUS Automation” has been enlarged, as the overall concept of reducing liability risks affects the work of other AEF project teams, such as the “Conformance Test”, “Engineering and Implementation”, “Service and Diagnostics”, “Communication and Marketing”, and “Wireless Infield Communication”. Driving the coordination of TIM relevant attributes within these project teams requires the need for open lines of communication between teams.

3. Technical Concept

The technical concept implies that products ensure AEF compliance with usage of a digital authentication process.

3.1 General Concept

Each TIM product must perform and pass an AEF Conformance Test in order to get a digital certificate from the AEF. The digital certificate will be included into the production software payload of each series components’ electronic control unit (ECU). The digital certificate ensures that the TIM counterpart of each component can check for AEF conformance as well as

the AEF tested functions that the component supports. To reduce the system start-up time the related authentication checks need to take two different options:

- Full weight Authentication (FwA): When two TIM components get plugged together for the first time, a complete authentication needs to be executed to introduce the products to each other.
- Light weight Authentication (LwA): With the FwA both components share a specific secret, so that on additional start-ups both only validate this secret. While the FwA takes several seconds (up to a minute), the LwA brings the system back to operation within a few seconds (e.g. after an unintended engine stall).

Once a component's certificate needs to be revoked due to e.g. functional misbehaviour, responsible manufacturers have means to revoke the certificate with usage of the so called Certificate Revocation List (CRL). The CRL may be placed as part of the software payload of each component. Once a certificate is listed on the CRL of an ECU, this specific ECU will not work with a component containing the revoked certificate. The CRL is managed and generated by the AEF, while the manufacturers include it in their products.

3.2 Certificate Hierarchy and Public Key Infrastructure

In detail, when a FwA is performed, each counterpart is not only checking the validity of one single certificate, but of a complete certificate chain. This mechanism ensures via a given certificate hierarchy, that only instances approved by the AEF (so called Certificate Authorities, CA's) are allowed to issue certificates.

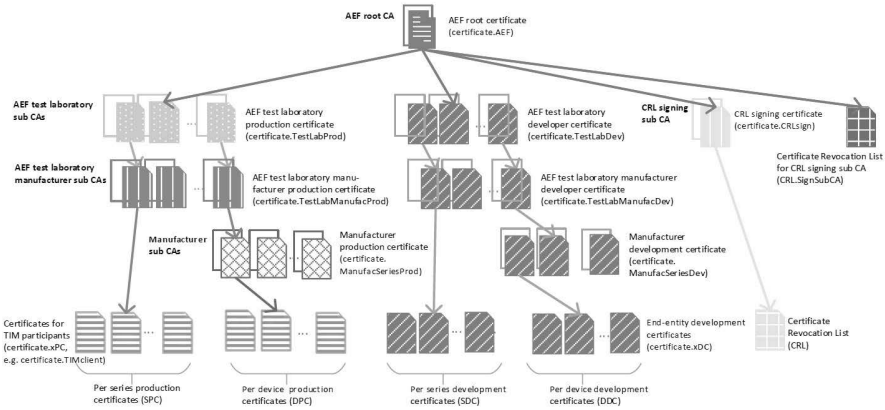

Fig. 1: TIM Certificate hierarchy

The hierarchy concept is depicted in Fig. 1. At the very top level the AEF is the owner of the root CA and the root certificate. Both in combination act as a trust anchor for the whole certificate chain. Underneath the root CA four instances are shown (counted from left to right):

- The first (outer left) branch depicts the series production certificate and CA chain.
- The second branch (diagonal stripes) is an equal twin of the first and represents the optional chain for development certificates (a development certificate is utilised by manufacturers when in development or field trial season, but have not yet passed the conformance test [6]).
- The third branch only contains the CRL as an end-entity and the relevant signing CA.
- The forth branch – only as a spare – contains another CRL as a revocation container, designed for the case if a CRL gets compromised and needs to be revoked as well.

The following section refers only to the first (outer left) branch. The AEF allows test labs to generate certificates. This implies technically, that the test labs act as a so called subsidiary (sub-) CA's. Each sub-CA has a certificate containing its identity and its own public key, and is signed by the root certificate.

In order to be able to react on manufacturers' mistakes, the AEF decided to add another sub-CA on the laboratories' level (technically underneath the labs' sub-CA). Revoking this "AEF test laboratory manufacturer sub-CA's" certificate (see Fig. 1) implies that ALL certificates of this manufacturer under this laboratory are instantaneously invalid once an updated CRL is considered.

The next level may directly represent the end-entity certificates (bottom layer with horizontal stripes in the leftmost branch – e.g. one certificate for a given SW version). Optionally a manufacturer may decide to work with individual certificates per machine or product. In this case the respective SW version is represented by an intermediate layer, the Manufacturer Sub CA (thin crosslines), while the individual certificates are listed underneath.

3.3 Authentication in the field

The general concept describes that the FwA as well as the LwA are designed to validate the TIM counterpart's integrity. The FwA consists of three phases:

- Phase 1: the certificate chain is exchanged over the ISOBUS. All certificates are to be exchanged to validate the authenticity of all certificates. The first phase guarantees, that both TIM server and TIM client are in possession of an authentic certificate.
  During phase 1 the certificates are also checked against the CRL.
- Phase 2: In this phase a mutual Elliptic Curve Diffie-Hellmann (ECDH) Key Exchange is performed. The ECDH allows for a mutual computation of a shared secret with us-

age of the received public and the own private key. The secret together with the certificate serial number is to be stored on the device for usage in the LwA start-ups.

- Phase 3: A block Cipher-based Message Authentication Code (CMAC) is used to verify the mutual possession of the shared secret.

The LwA consists of the certificate exchange and the CMAC verification of the common shared secret (stored during phase 2 of the FwA).

3.4 Safety considerations

Reaching a respectively required level of functional safety is defined in various differing standards, such as ISO 25119 or IEC 61508. In order to define a stable foundation for distributed electronical systems, the AEF team “Functional Safety” aligned on a basic set of safety rules valid for ALL TIM systems [3]. Fulfilling the safety rules is a mandatory condition for a TIM component. A manufacturer has to declare his conformance to these AEF definitions when he applies for the AEF conformance test for his TIM product.

4. The road to TIM

The AEF committed itself to define an open standard for TIM implementations based on ISOBUS with setting up the project team “ISOBUS Automation”. The question of “how to verify integrity and to deal with liability?” is close to being answered with AEF Guideline 023 “ISOBUS Automation Principles” [4]. To facilitate the implementation, to reduce the time-to-market, and to deal with common experience of recent ISOBUS function development, the following sections give an overview of the next steps and open items before TIM is able to enter the market.

4.1 Road Obstacles and Mitigation Methods

A common disadvantage of some ISOBUS implementations – e.g. the Virtual Terminal (VT) implementations – is that there are countless different interpretations and implementations of ISOBUS functions. The introduction of a common Conformance Test as common sense within the industry has improved the situation in recent years, but still the overall costs of the countless developments for the whole industry remains as an unspoken burden. As the TIM authentication is indeed a standardised process and needs to be exactly the same for the whole industry, the AEF decided to order a **common authentication stack** from an external provider. The authentication stack is specified to not depend on specific operating systems (OS’s) or hardware platforms, as far as economically justifiable.

To enable the TIM product authentication all certificates need to be derived from the same root (Fig. 1: TIM Certificate hierarchyFig. 1). Therefore the AEF decided to invest in a common

infrastructure to get certificates, signatures, and key pairs. This infrastructure is technically called “**Public Key Infrastructure**” (PKI). The PKI will be integrated in the well-known AEF ISOBUS database.

As a matter of definition, for TIM the **conformance test** is a mandatory condition. Without successful completion of the AEF conformance test, no certificate will be in place and no open TIM implementation will be available. This implies a major change that the AEF has to deal with: until now the AEF conformance test acts as an instance to assign a seal of quality; for TIM the conformance test is one instance to enable functionality, and needs to act as a trust and liability anchor. The “ISOBUS Automation” team is working with the “Conformance Test” team to enhance the TIM conformance test accordingly.

4.2 Testing of Authentication

While the “ISOBUS Automation” team decided to form a liaison with the “Conformance Test” team for working on the TIM conformance test, the project team has also formed an internal subteam working on the validation of the common authentication stack (Auth.Lib). Within this subteam representatives of more than 8 leading manufacturers are working on individual integrations and implementations of the common Auth.Lib, in order to validate the quality, usability and transferability of the library. To validate interoperability of the implementations, the “ISOBUS Automation” team has been organising special TIM Plugfests. As this work is ongoing and the TIM Plugfest is scheduled after the editorial deadline of this article, the presentation during the conference will be used to show major experiences of the integration tests. The Auth.Lib is scheduled to be delivered by the end of 2017.

4.3 Functional Trials in the field

An open topic now is the scheduling of field tests with TIM functionalities. Until this point the major focus of the “ISOBUS Automation” team has been to work on the definition and technical specification of the authentication as a successor for TIM functions. In the field customers will see the authentication as a mandatory condition for working with TIM systems, but it is the quality of TIM systems that will drive or decline further progress and future perspective of modular self-propelled machinery.

Thus the “ISOBUS Automation” team identified a major need to combine field test power of the whole industry in order to deliver a system architecture that is flexible, scalable and – most important – brand independent to assure higher efficiency in the field.

5. Conclusion and Outlook

The given article gives an overview of the current state of the AEF development towards releasing TIM as an Operator Assistance system. The technical concept consists of a digital authentication process used for ensuring an acceptable level of liability for the individual manufacturer providing TIM equipment. The article deals with several non-specific topics and decisions the AEF and the AEF “ISOBUS Automation” team needed to follow in order to facilitate the industry-wide development of such modular self-propelled machinery in the field. Several decisions have already been taken and/or the progress of those issues is promising (PKI, Auth.Lib, common safety goals). Other issues still imply a challenge (progress of conformance test, functional testing and validation) for a contemporary introduction of TIM products to the market. Although the technical concept – in details the specification in form of the AEF Guideline 023 – will be set to a FDIS-State (AEF Final Draft International Guideline) in late 2017, both conformance test development and functional testing may affect the guideline retroactively.

For the “ISOBUS Automation” team – and the whole AEF – the focus of work for the next months will and need to be finalizing the Auth.Lib work, and concentrating on both the conformance test development as well as the functional testing.

The implementation and testing of the TIM concept and related infrastructure is in progress by major industry players in the “ISOBUS Automation” team. However, the expectation is that more interested manufacturers join this activity in the upcoming years to deliver an attractive fleet of TIM products to our customers and in parallel share the infrastructure costs between a larger number of players. The overall goal of the group is to reach production level implementation in 2018.

[1] www.aef-online.org

[2] ISOBUS consists of ISO11783 part 1 to 14 and AEF specific additions formulated in AEF guidelines, which can be obtained under [1]

[3] AEF Functional Safety Guideline: The AEF guideline “AEF 007 FDIG 0.48 ISOBUS – ISOBUS Automation” summarizes the safety aspects of TIM systems. The document can be obtained under **Fehler! Verweisquelle konnte nicht gefunden werden.**.

[4] AEF ISOBUS Automation Guideline: The AEF guideline “AEF 023 DIG 0.07 ISOBUS – ISOBUS Automation Principles” summarizes the AEF security concept and the TIM related processes and methods. The document can be obtained under [1].

[5] VDI LAND.TECHNIK 2013 – “AEF ISOBUS Automation – State of the Discussion”; presented by Dipl.-Ing. Florian Ahlers, AgBRAIN GmbH, Osnabrück and Dipl.-Ing. Hans Jürgen Nissen, John Deere GmbH & Co. KG, John Deere Werk Mannheim

[6] VDI LAND.TECHNIK 2014 – “AEF ISOBUS Automation – Status and Progress Report”; presented by Dipl.-Ing. Hans Jürgen Nissen, John Deere GmbH & Co. KG, John Deere Werk Mannheim and Dipl.-Ing. Florian Ahlers, AgBRAIN GmbH, Osnabrück

Challenges of digital revolution

How the AEF plans to manage interoperability

Dipl.-Ing. **Norbert Schlingmann**,
Agricultural Industry Electronics Foundation AEF e.V., Frankfurt;
Dipl.-Inf. **Hannes Schallermayer**, FarmFacts GmbH, Pfarrkirchen;
M.Sc. **Johann Witte**, Müller Elektronik, Salzkotten;
Dipl.-Ing. Computer Science **Christophe Gossard**, John Deere, Mannheim

Abstract

Initially, the main focus of AEF was the implementation and further development of the ISO-BUS standard (ISO 11783) which governs electronics and data exchange between different farm machines (e.g. tractor – farm implement).

With the digital revolution in farming unfolding, the AEF's scope of work is no longer limited to ISOBUS only, but has been expanded to cover additional areas of critical importance for Digital Farming such as:

- Farm Management Information Systems (FMIS)
- Wireless in-field communication
- High-Speed ISOBUS
- Electric drives
- Camera systems

This document will provide an overview of the status quo for data exchange with the different interfaces and describes the activities of AEF. In conclusion, it will show what has to be done to fulfil customer needs and how to manage the EU expectations.

Standards for data exchange

The data exchange standards between mobile farm equipment and farm management systems (or data management systems) are standardized in ISO11783, Parts 10 & 11. AEF is working on guidelines which define clear interfaces by using ISOXML and the new extended FMIS data interface referred as "EFDI".

Part 10 of ISO11783 describes the XML file format with about 60 potential elements for content like, client, farm, part field, polygon, worker or device. This file format enables a FMIS to send an order to a MICS (mobile information control system), a Taskcontroller can understand the job and can command a device. While the job is running, a Taskcontroller can log

all the activities and can send back a finished task to the FMIS with all totals and information. All the required values in this process (e.g. fertilizer in mass per area, yield, fuel…) are standardized in Part 11 of ISO11783, currently about 525 entries.

The data transport process has changed. To have a USB stick with data at the end of the day is no longer adequate because of:

1. Machines are working for long periods in the fields and no longer returning to the farm at the end of the day. No data would be available to check tasks and values in this case.
2. Sometimes it's necessary to send new orders to the still working machines in the field: Consequence: Not possible.
3. In addition the farmers need the currents field and machine status which is also not possible currently.

In all these examples, and there are more, the task data fileset via USB stick is no longer useful. Therefore communications between devices directly wireless to a server or a cloud system in real time is necessary and has to be standardized.

With this understanding of the current needs in the market, the AEF started the development of a new data transmission system, called EFDI (Extended FMIS Data Interface). The "FMIS" project team analysed the benefits of the different current file formats and protocols used in business to determine the best direction to proceed. The team is working on a guideline and preparing prototypes for testing. This new standard is very flexible and can send a fragment of the logfile every second or a whole task set of the day as well, without any data media.

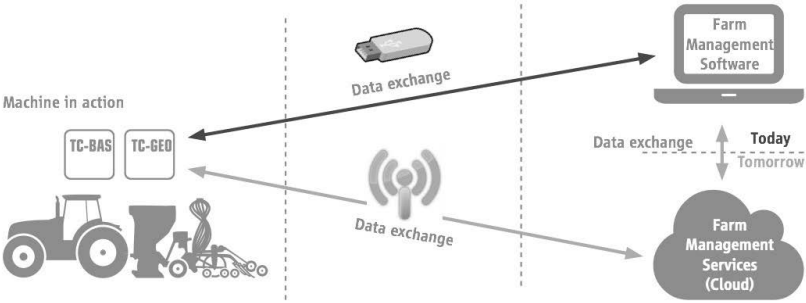

Fig. 1: Date exchange with USB stick and EFDI protocol using wireless communication

AEF is creating an absolute new valuable standard to support modern systems from machine-to-machine, over machine-to-FMIS up to cloud-to-cloud communication.

Collaboration with AgGateway

AEF has joined forces with AgGateway to define the process for data exchange, future-proof and adapt it to the needs of Digital Farming.

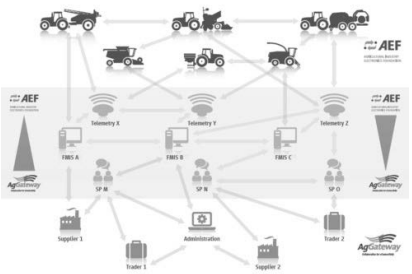

Apart from the fact that both AEF and AgGateway are active in developing sector-specific standards and guidelines, the value of cooperation lies in pooling different areas of expertise and knowledge. This allows both to cover the entire landscape of Digital Farming.

Fig. 2: Respective areas of expertise of AEF and AgGateway. Areas of cooperation are highlighted in the shaded area.

Interfaces for interoperability

In addition to existing communication solutions for agricultural machinery like ISOBUS, based on the ISO11783, radio based machine-to-machine communication is another step towards digital revolution in farming. Compared to automotive markets, usage of agriculture machinery in areas with low population density and therefore bad cellular coverage are boundary conditions for our machine-to-machine radio interface.

Even though more than 90% of the world population today is connected via cell phone based technologies, only 30% of the landscape is covered by cellular radio and even less with 3G or above [1].

Most of the agrarian used areas come with a low bandwidth or no cellular coverage. According to use cases there is a big gap between control oriented applications like Tractor-Implement-Mananagement with tough real time requirements and more data oriented aspects like sharing of process data or diagnostic sessions.

In addition to this, the mix of different brands of agricultural machines is a restraint for backend-based cellular communication services. Due to these facts, there is a general demand for the standardization of a wireless direct machine-to-machine communication for agricultural in field usage.

Fig. 3: Worldwide mobile communication overview

In order to cover different use cases such as platooning of vehicles, A-B lines or coverage map sharing, remote display applications and camera access, a wireless connection with a range of at least some hundred meters and worldwide availability of technology and radio frequency is necessary.

The physical layer of a WiFi based communication approach shall represent the basis for the AEF project team “WIC” (Wireless in-field communication). The use of existing technologies 802.11-based Wifi standards will be evaluated. In addition, the car-to-car standard 802.11p is in scope as a suitable radio technology. In general, the system architecture will allow adding additional upcoming communication standards like 5G with suitable efforts.

But tunnelling a CAN message through an IP-based communication network raises high demands on safety, security and real-time behaviour. There are some concepts how to use IP based communication standards with CAN message frames. Within these concepts the trade off between connection oriented (TCP/IP) and connection less (UDP) approaches is discussed. But the Ag industry and project team WIC comes with some requirements which are not covered by commercially available solutions, therefore there is no solution available out of the box [4&5].

In order to enhance the performance of agricultural processes, even functionalities like Task-Controler-Log or Tractor-Implement-Management (TIM) are not only in scope but driving this development as key issues.

A key-based authentication process in combination with encrypted communication shall ensure the reliability of the data exchange between different market participants.
A common software library called “WIC core application” is one part of the work outcome of the AEF project team. It will cover the basis functionalities and reduce the development cost for each individual company. The WIC core application will come with an API for basic services like network setup or service discovery and will provide this functionality to some kind of vendor specific application. Due to the provision of this piece of common software, issues with interoperability and time to market can be minimized.

How to manage the initiatives of the European Commission

The European Commission started the initiative, Internet of Things (IoT), by launching the Alliance for Internet of Things Innovation (AIOTI) in 2015. This has created a vibrant IoT ecosystem in Europe, and aims notably at breaking silos between vertical IoT application areas.
The main goal of the European Commission is, that citizens will be able to simply plug-in an IoT device to get data from all kind of objects or vehicles, like weather stations, home refrigerators, telecommunication units or from agriculture machinery to obtain information and data independently. However, the necessary infrastructure has to be in place and the interfaces to e.g. agricultural machines have to be defined.

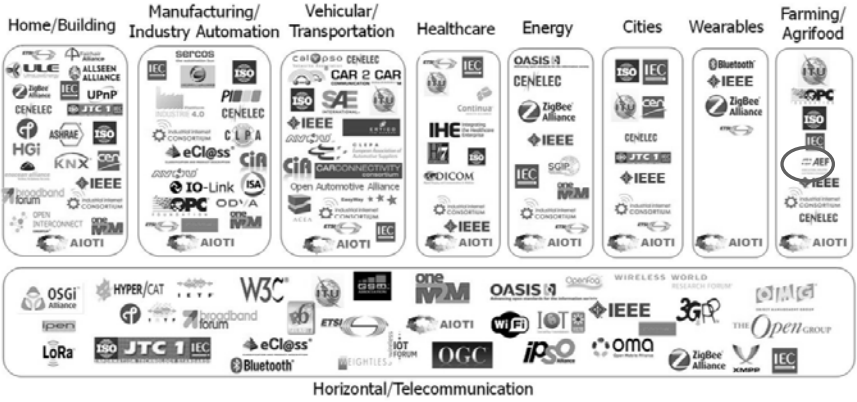

Fig. 4: AEF within IoT landscape vertical domain „Farming/Agrifood [2]

The Ag industry, which is located inside AIOTI landscape “Farming/Agrifood” vertical application area, should be part of the definition phase. It will be the AEF and its member companies to deal with it. The main goal is to use existing infrastructure that was developed by AEF

member companies, as well as solutions for safety and security related issues. The collaboration with AIOTI bodies is one of the challenges AEF and the Ag industry have in common. Converting AEF guidelines into standards where the Ag sector can leverage what they have developed so far. Therefore, it is important to be part of this initiative and play an active role.
Without a consolidation between the vertical and horizontal domains, it can not be considered a benefit from the sector, and silos will remain. The Agricultural Industry Electronics Foundation already provides a gateway to exchange information between all the platforms within the agriculture industry.
Security and safety would also need to be addressed across. AEF should be the "consolidated hub" for the agriculture industry. It is planned to create a real demonstration to show the data interaction between the other sectors and the agriculture industry. Collaboration with ETSI (European Telecommunications Standards Institute) is expected, when CEMA manages the input from the different actors of the market.
AEF prepared and project proposal as a pilot with ETSI (Fig. 4). It describes the use case what have to be done if a slow moving machines enters a road. Reduction of accidents between agriculture machinery and cars is one of the major goals.

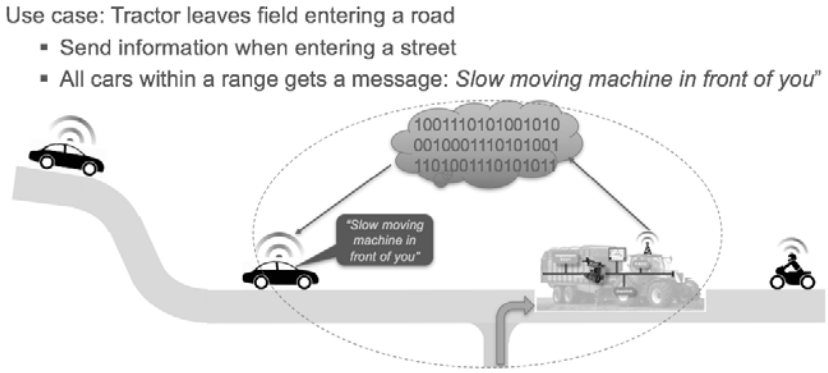

Fig. 5: Defined project to reduce accidents between fast moving vehicles and agriculture machinery.

Conclusion

Using existing infrastructure and defined interfaces like ISO-XML and the new EFDI protocol is the basis to manage interoperability. Data interaction from machine-to-machine or from machine-to-cloud based solutions have to be organized. The AEF and its project teams have a vison of how to manage this challenge. EFDI to transfer data during machine operability is

on the way, new wireless communication channels to transfer data from machine-to-machine as well. Initiatives like IoT are a challenge for the Ag industry and can be managed by using existing and new standards.

Together with its member companies, the AEF is willing to manage the challenges of the digital revolution. The Ag industry manufacturers have to integrate new technology based on these standards to allow interconnectivity between manufacturers and farmers. Data has to be easely managed for improved usage by the end customer. He expects to get easy access all times to all data to optimize his field and machines operations. In the end he must stay connected.

References

[1] ICTFactsFigures2016

[2] Source: http://www.aioti.org

[3] Source: http://www.kammerath.net/weltweit-mobiles-internet.html

[4] The future of CAN / CANOpen and the industrial Ethernet challenge by Wielfried Voss

[5] CAN frames trough IP Networks by Mark Gerber CAN Newsletter 3/2015

Design of Laboratory Environment for Development of Cleaning System Automation

M.Sc. **D. Hermann**, AGCO Research & Advanced Engineering Global Harvest, Randers, and Technical University of Denmark;
Ph.D. **F. Schøler**, B.Sc. **M. L. Bilde**, AGCO Research & Advanced Engineering Global Harvest, Randers;
Prof. **N. A. Andersen**, Prof. **O. Ravn**, Technical University of Denmark

Abstract

This paper addresses the design of a laboratory environment for research and development activities used for automating the cleaning process in a combine harvester. The aim is to facilitate closed-loop automation test runs with extended duration. By utilising individual MOG and grain feeding units as well as recirculating the biomass material any combination of these occurring in an actual field can be simulated in the laboratory.

1. Introduction

Development of a closed-loop control system for fan speed and sieve openings in a combine harvester cleaning system requires extensive test with material collection for system modelling as well as sensor and control scheme verification. Acquiring material samples during actual field tests are often subject to large variations due to varying local field conditions causing low repeatability. Additionally it is not possible to control the cleaning throughput of material other than grain (MOG) during field experiments, which is the dominant variable for grain loss.

Previous laboratory setups had limited total test time either due to length of the conveyor belt using manual material distribution or due to reservoir capacity using automated feeding.

It was shown by [6] that it was possible to build a MOG feeding system with a high repeatability (R^2=0.99). Later [7] showed that the cleaning loss could be continuously measured as an absolute quantity by collecting all the residue flow continuously and post cleaning a subflow in a cyclone separator.

By complementing field data collection with laboratory data collection one avoids the dependency on machine availability and limited harvest windows as well as variations from whether, crop and local field conditions. The laboratory provides a solid basis for elementary verification with a large number of material samples and high repeatability, which is difficult to acquire during field experiments. Performance evaluation and control scheme comparison is

advantageously conducted in the laboratory, where after the final verification and robustness to varying biological parameters should be conducted in the field.

This paper will present the design of a system able to continuously feed grain and MOG material to a cleaning system. An analysis of the required excitation variables and measurement variables is given in Section 2. Design of the material feeding unit, material recirculation, test stand and sampling is described in Section 3. Results for feeding accuracy as well as a comparison between laboratory and field data is provided in Section 4.

2. Analysis

2.1 Cleaning System Optimisation Goals

The cleaning process is a complex process with tightly coupled interdependencies. Hence, it is important to sample the grain and MOG components of the residue (grain loss), tailings and clean grain material flows. The material samples are used to investigate actuator, material and sensor interdependencies for model generation and performance evaluation [5].

2.2 System Excitation

The MOG throughput and moisture content are the dominant non-controllable extrinsic parameters affecting the separation performance in the cleaning system [1, 2, 3, 4]. The continuous feeding unit should reproduce the variations in local crop conditions to provide any combination of MOG and grain within the nominal range for the cleaning system. However on-line excitation of the moisture content in grain and MOG is not practical, hence all material must be affected prior to any test.

2.3 Design of Experiments

Design of experiments is crucial in the evaluation process of different control methodologies and for parameter tuning. Hence the possibility to repeat sequences with equivalent excitation of total throughput and material composition provide a solid foundation for performance evaluation. The continuous flow test facilities will primarily be used for these categories

Single run: cleaning system performance evaluation and modelling

Continuous run: long duration runs for closed-loop automation testing

For single test runs the grain and MOG reservoirs should contain sufficient biomass to complete a 2 minute test. For long automation test runs it is not practical to increase the reservoir size accordingly, hence the biomass material will be re-circulate to extend the test duration.

3. Laboratory Design

The aim is to design laboratory test facilities that allow control of total material throughput and MOG ratio in a controllable environment with high repeatability.

3.1 Cleaning System

The cleaning system is mounted in a frame facilitating lateral and longitudinal excitation using a single pivot point in the front end and two vertical actuated points in the left and right rear end. The test stand is additionally equipped with a yield sensor, moisture sensor, grain quality sensor, infra-red tailings volume sensor as well as impact type sensors for loss, tailings and upper sieve distribution.

3.2 Biomass Feeding

The largest single challenge in the overall laboratory setup is to provide continuous MOG feeding, as the MOG material is challenging to handle and easily can build up in lumps at various locations causing material blockage. However [6] showed good performance with a novel concept for MOG feeding, where the MOG in the feeding unit was constantly kept in motion and the provided throughput depends on the speed of the feeding chain conveyor and the opening to a scraper conveyor. A somewhat similar concept is utilised in design of the MOG feeder, Fig. 1. A constant relationship between the conveyor speed and the MOG feeding rate can be maintained when the MOG feeding buffer level is kept within a specified range.

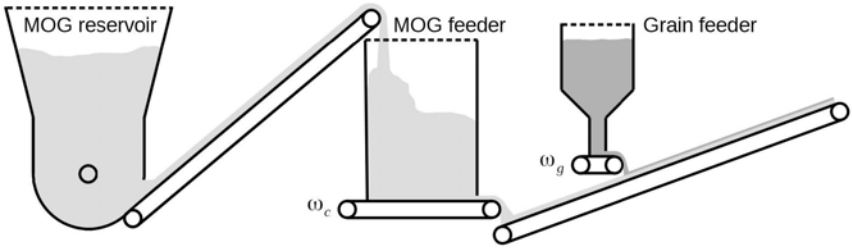

Fig. 1: Feeding system for grain and MOG biomass.

The grain feeding unit is designed as a large grain tank with a funnel shaped bottom where the material layer is kept at a constant height. The grain throughput is proportional to the conveyor belt speed. The grain material is delivered on top of the MOG layer before the final conveyor belt is feeding material into the cleaning system.

3.3 Material Recirculation

A material re-circulating system is designed in order to extend the run time for automation testing, see Fig. 2. The MOG reservoir, MOG feeder and grain feeder are the individual units forming the overall biomass feeding system in Fig. 1. The re-circulation system consists of the residue collection unit located after the cleaning system as well as the MOG and grain return conveyor belts that transport the material back to the MOG and grain reservoirs respectively. When running single tests, the continuous mode can be used to clean the material by feeding the material grain or MOG reservoirs individually through the cleaning system at a low throughput where a high separation performance obtained. Fine cut straw is used to simulate the MOG material instead of collecting actual MOG consisting of chaff and straw pieces, as these are not available in the required quantities for laboratory testing.

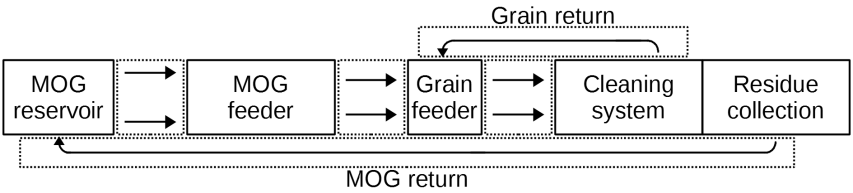

Fig. 2: Overall continuous laboratory material flow with material recirculation.

3.4 Material Sampling

When the cleaning system has reached steady-state in single run mode material samples are acquired from the residue, tailings and clean grain material flows. The sampling system is designed so material samples can be acquired in continuous mode during automation tests as well, in order to compare performance improvements for the automation system.

4. Results

The MOG and grain feeding units are evaluated by sampling material on the conveyor belts just before the cleaning system with sample lengths of 1m. The results are shown in Fig. 3, where a coefficient of determination of R^2=0.99 and R^2=1.00 are obtained for the MOG and grain feeder respectively. The accuracy is considered satisfactory.

In order the verify that the laboratory environment represents actual field experiments, the aim is to see the similar trends from actuators to material flow and from material flow to sensor readings. It is not expected to obtain an exact match of the measured material flows between field and laboratory experiments, as these are known to vary significantly from field to field due to various non-observable biological parameters.

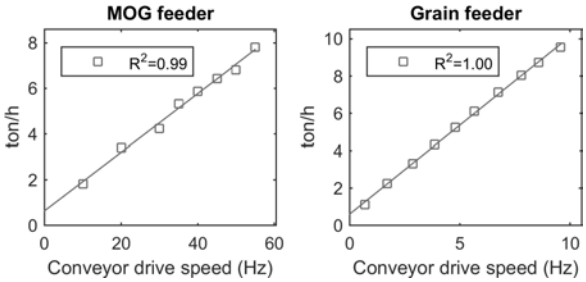

Fig. 3: Evaluation of feeding system for grain and MOG biomass.

In Fig. 4 an example for comparison of grain loss, tailings grain and tailings MOG material flows are shown as a dependency of fan speed at a similar throughput.

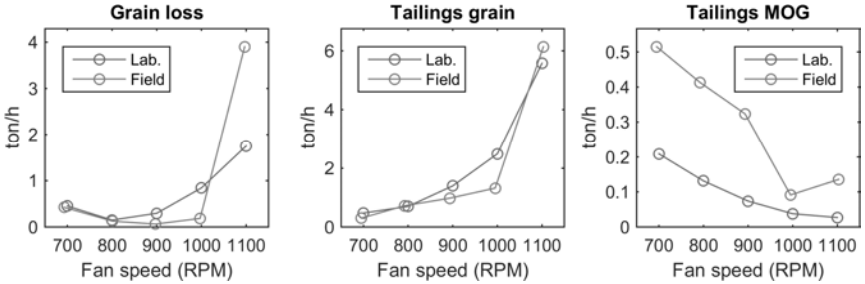

Fig. 4: Comparison of field and laboratory test results.

Each point represents a 10s material sample. It is vital that the three dominant phases of “packed bed”, “fluidised” and “air borne” described by [3] are obtainable. The “packed bed” occurs at low fan speeds where the grain kernels are travelling on top of a MOG mat on the upper sieve (sloughing loss), “fluidised” where the grain loss is lowest and the “air borne” phase where the kernels become air borne, hence not segregated though the upper sieve (blowing loss). The three phases are present in both the field and laboratory data. For the tailings grain and MOG throughput an exponential increase and a roughly linear decrease dependency to fan speed are represented respectively in both the field and laboratory data.

5. Conclusion

An analysis of the laboratory set-up required for closed-loop automation test was conducted, showing the need to run short tests for performance evaluation, modelling and sensor evaluation as well as long duration runs for closed-loop automation testing and verification.

The overall design of the biomass feeding system and cleaning system test stand with material sampling and re-circulation was described. The biomass feeding showed a reasonable good accuracy with a coefficient of determination at R^2=0.99 and R^2=1.00 for MOG and grain respectively.

Evaluation of trends for grain loss, tailings grain and tailings MOG dependency on fan speed showed good resemblance between acquired material samples from field and laboratory.

The continuous cleaning system laboratory facilities are expected to provide a significant advantage in the design and verification process for state of the art automated cleaning systems as well as future generations to come.

Literature

[1] Miu, P.: Combine Harvesters Theory, Modeling, and Design. CRC Press, 2016

[2] Creassaerts, G., Saeys, W., Missotten, B. and De Baerdemaeker, J.: A generic input selection methodology for identification of the cleaning process on a combine harvester, Part I. Biosystems Engineering, volume 98, 2007, 10pp. 166-175

[3] Freye, T.: Untersuchungen zur Trennung von Korn-Spreu-Gemischen durch die Reinigungsanlage des Mähdreschers. Ph.D. Thesis. Universität Hohenheim,1980

[4] Fliege, L.: Einfluss der Hangneigung auf die Leistungsfähigkeit von Reinigungsanlagen im Mähdrescher. Ph.D. Thesis. Universität Hohenheim 2010

[5] Hermann, D., Bilde, M. L., Andersen, N. A. and Ravn, O.: A Framework for Semi-Automated Generation of a Virtual Combine Harvester. IFAC-papers online, volume 49-16, 2016, 6pp. 55-60

[6] Schwarz, M.: Gutzuführungskonzept für Laboruntersuchungen von Mähdrescherreinigungseinrichtungen. Landtechnik, 2010, 4pp. 376-379

[7] Schwarz, M.: Kornverlusterfassung an Getreidevorreinigern. Landtechnik, 2012, 5pp. 42-46

Online determination of hectolitre mass during threshing by analyzing air-filled pore volume in grain fills

J. Berberich, Dr. **R. Tölle**, Prof. **U. Schmidt**,
Humboldt-Universität zu Berlin, Berlin;
M. Huth, M.Sc., promethano GmbH, Berlin;
Dr. **A. Feiffer**, feiffer-consult, Sondershausen

Abstract

Determination of hectolitre mass is a traditional and wide spread method to get fast information about grain quality. Using various analyzing methods in different countries can refer to divergent results of the analysis. Furthermore, determination of hectolitre mass is influenced by ambient conditions like environment and operators. Because of the necessary weighing process and the vibrations during harvest, it is not possible to determine hectolitre mass during threshing directly on a combine harvester. For this case, another option to analyze grain quality online could be image analysis of grain geometry. This is still expensive and a lot of computing work is needed to use it on a harvester. That is why a new method has been developed by Humboldt-Universität zu Berlin and the promethano GmbH, Berlin. Instead of weights, air-filled pore volume in grain fills is determined to indicate hectolitre mass with this method. First trials with an air pycnometre show that both parameters correlate with each other. The use of an air pycnometre seems to be possible on a combine harvester, too. By effecting controlled vibrations additionally to the combine's vibrations, standardized conditions are secure with every measurement. Thus it is possible to get reliable results about the hectolitre mass online on the combine harvester.

Key words: Grain Quality, Hectolitre Mass, On-combine monitoring, Air-filled Pore Volume

Introduction

Traditionally determination of hectolitre weight is a fast and wide spread method to get information about grain quality in agriculture. Farmers as like as grain trading companies still use test weight to make a decision about the quality of the grain. [1]

There are different methods for hectolitre mass determination all over the world. Various measurements refer to different results. [2] Furthermore, it is not possible to determine test

weight online on a combine harvester due to vibrations and the necessary weighing process. Another possibility to assess grain quality quickly, is the optical analysis of grain. With this method, grain shapes and optical anomalies can be evaluated. [3] This method generates good results but a lot of computing work is necessary and the technique is expensive.

In comparison, air-filled pore volume measurements cannot directly determine the weights or shapes of porous materials or fillings but their cavities. [4] These cavities can help to get information about the components of a filling without weighing.

Materials and methods

For evaluation of the relation between hectolitre mass and air-filled pore volume, grain samples from different fields and regions in Germany were analysed. The samples came from farmers and grain traders in Baden-Wuerttemberg, Bavaria and Thuringia. They were taken in 2016. Up to analysis, they were stored under dry and dark conditions inside airtight containers to avoid metabolic changes.

The experimental setup consisted of a chondrometre (Hecto, Pfeuffer), an analytical balance (PCB 3500-2, Kern) and an air pycnometre with analyzation unit (promethano). First the kernels were filled into the chondrometre as given. Then the upper and lower parts of the chondrometre were divided by the dedicated cut off slide. Afterwards, the lower part with the kernels was put into the airtight chamber of the air pycnometre (Fig. 1 and **Fig. 2**) and the analysis of the pycnometre started. In the following, the lower part of the chondrometre was taken out of the chamber and the kernels were weight to determine the test weight.

Fig. 1: Lower part of the chondrometre inside the air pycnometre.

Fig. 2: Air pycnometre, closed airtight.

Results

Fig. 3 shows an indirect proportionality between test weight and air-filled pore volume of grain kernels. High hectolitre mass refers to low air-filled pore volume and vice versa.

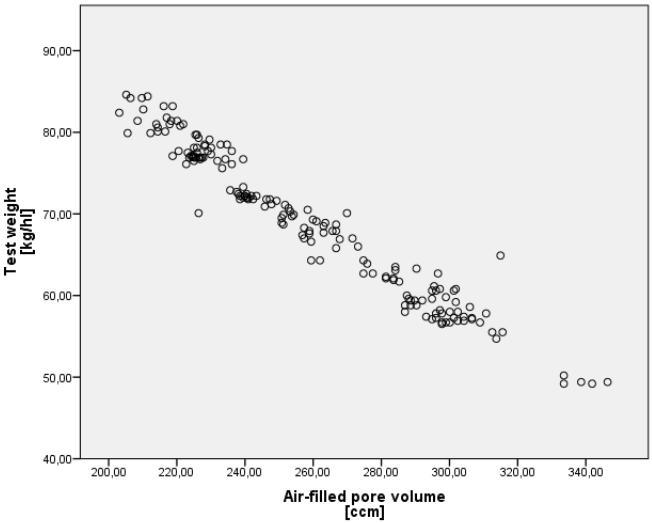

Fig. 3: Relation between air-filled pore volume and test weight of grain.

Different species induce various air-filled pore volumes (**Fig. 4**). Oat shows the highest air-filled pore volume, followed by barley and wheat. Rye and durum seed's air-filled pore volume is located in the middle of the wheat kernels. Rape seed shows similar air-filled pore volumes as rye, with some samples, inducing the smallest air-filled pore volume of all samples.

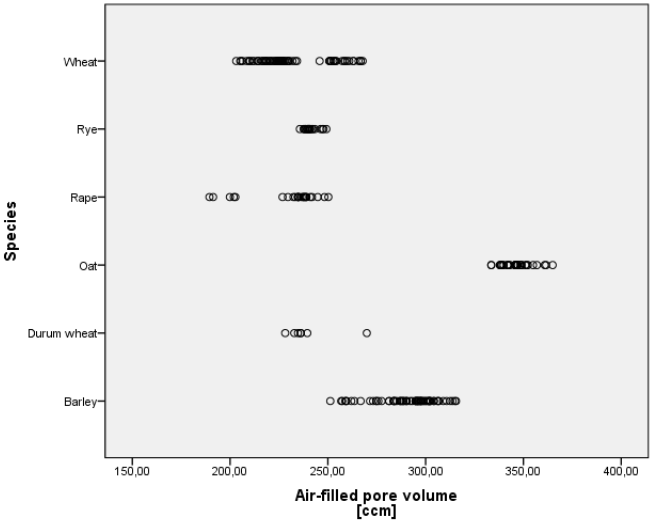

Fig. 4: Air-filled pore volume of different species.

Discussion

High test weight is associated to high yield. [5] Therefore determination on combine harvesters is interesting to get fast information about the quality of the grain. As seen in **Fig. 3**, hectolitre mass can also be determined indirectly by air-filled pore volume. **Fig. 4** shows, that various species refer to different air-filled pore volumes. Both findings can be used for on-combine analysis of grain. Kernels of different grain species have diverse geometry. Perfect sphere packing led to air-filled pore volume of 26 %. [6] As seen in **Fig. 4**, oat refers to the highest air-filled pore volume. These kernels are not as round as spheres and cannot arrange inside the measuring cylinder close to each other. [7] As a result, high air-filled pore volume can be observed. By observing pressure drop trajectory, it might be also possible to figure out whether there are small pores but many or big ones and few. This measuring sys-

tem can give information about stock or awns inside the sample and help to adjust the threshing system.
Vibrations on a combine harvester will affect the measuring system and results. For this reason, controlled vibrations during the measurement process are necessary. Further investigation is needed to evaluate the force of the vibration unit.

Outlook

Based on current knowledge, test weight could give information about grain and threshing quality on the combine harvester. Due to the necessary weighing process and the vibrations during threshing, it is not possible to determine hectolitre mass on-combine, yet. First results of the laboratory experiments with an air pycnometre show promising results regarding determination of test weight indirectly.
In future, on-combine determination of air-filled pore volume in grain fills will give fast information for farmers and grain traders. Threshing processes can be optimized and threshing grade can be increased.

Acknowledgements

Our special thanks goes to the Mr. Henning Kuper for his assistance during the experiments. Furthermore, we want to thank all farmers and grain traders for the grain samples.
The project is supported by funds of the German Government's Special Purpose Fund held at Landwirtschaftliche Rentenbank and the Federal Agency of Agriculture and Food (BLE).

References

1. Lee M, Lerohl M, Unterschultz J (2000) Buyer preferences for durum wheat: a stated preference approach. The International Food and Agribusiness Management Review 3(3): 353–366. doi: 10.1016/S1096-7508(01)00053-2
2. Manley M, Engelbrecht ML, Williams PC et al. (2009) Assessment of variance in the measurement of hectolitre mass of wheat, using equipment from different grain producing and exporting countries. Biosystems Engineering 103(2): 176–186. doi: 10.1016/j.biosystemseng.2009.02.018
3. Berberich J, Risius H, Huth M et al. (2012) Investigation of continous imaging analysis of grain quality on a combine harvester. Infomation Technology, Automation and Precision Farming. International Conference of Agricultural Engineering - CIGR-AgEng 2012: Agriculture and Engineering for a Healthier Life, Valencia, Spain, 8-12 July 2012
4. Scheffer F, Schachtschabel P (2010) Lehrbuch der Bodenkunde, 16. Spektrum, Akad-Verl., Heidelberg
5. Lockwood JF (1960) Flour Milling, 4th edn. Henry Simon Ltd, Stockport
6. Kittel C (2013) Einführung in die Festkörperphysik/Symmetriemodelle der 32 Kristallklassen zum Selbstbau: Einführung in die Festkörperphysik, Auflage: unveränderte Auflage. Oldenbourg Wissenschaftsverlag, München
7. Donev A, Cisse I, Sachs D et al. (2004) Improving the Density of Jammed Disordered Packings Using Ellipsoids. Science 303(5660): 990–993. doi: 10.1126/science.1093010

A hand-held measuring device for identifying the sharpness of knives in agricultural machinery

Prof. Dr. **Karl Wild**, M.Sc. **Torsten Schmiedel**,
Zentrum für angewandte Forschung und Technologie an der University of Applied Sciences Dresden;
Dipl.-Ing. (FH) **Daniela Geißler**, Dresden Elektronik GmbH;
Dr. **Josef Rottmeier**, Ingenieurbüro Rottmeier, Erding

Abstract

For detecting the sharpness of knives, which are employed in agricultural cutting and chopping processes, a hand-held measuring device was developed. The measurement method is based on detecting the force which is necessary to cut through a test medium. As test medium a stranded wire is used. The detected values for the required forces are transmitted via Bluetooth to a smartphone. On the smartphone an app is running. It utilizes the embedded calibration model for the individual knife types and calculates the sharpness. Afterwards the results are shown on the display and the user is informed whether the knife has to be sharpened or replaced.

1 Introduction

In agriculture cutting processes play an important role. Material is chopped intensively especially during harvesting operations e.g. when maize is chopped. So, the required energy is enormous. It mainly depends on the sharpness of the employed knives. In a forage chopper, dull knives lead to a power requirement which is about twice as high as with sharp knives [1]. In addition, sharp knives are essential for ensuring a high harvest or cutting quality. Therefore, dull knives have to be sharpened or replaced. On the other hand the sharpening or grinding process or the replacement of knives are time-intensive operations. Also, grinding reduces the durability of a knife. Hence, the grinding process or a knife exchange should be performed only if the knife is really dull or worn out. For this reason the sharpness of knives has to be detected. Currently, in agricultural operations this is carried out by auxiliary variables without any measuring device. Therefore, the sharpness is detected very inaccurately [2], [3].

In the past different approaches have been made for measuring the sharpness of knives in the forage chopper. They are based on inductive, optical, vibrational / acoustical or force measuring methods [4], [5], [6], [7]. Up to now there is no system available which can be bought by a farmer. For detecting the knife sharpness in other machinery like balers, self-loading wagon or mowers, no research work or available products are known. Thus, the objective of a research project was the development of a hand-held measuring device to determine the sharpness of knives in various agricultural machines with a sufficient accuracy.

2 Principle of Operation

The applied method for the developed device is based on the measurement of the force, which is necessary to cut through the insulation layer of a wire. The sharper a knife the less force is required. On the wire a voltage is applied. As soon as the knife has passed through the insulation layer and hits the inside conductor a short is caused. The short is detected by the device electronics and therefore the end of a measurement of the force is determined very accurately.

For selecting the most suitable wire a large number of tests have been carried out on a universal testing machine. Different rigid and stranded wires with various insulation thicknesses and insulation materials were compared. A large amount of influencing parameters on the measuring method were identified and quantified. In Fig. 1 a magnified cross section of a stranded wire and a typical test curve are demonstrated.

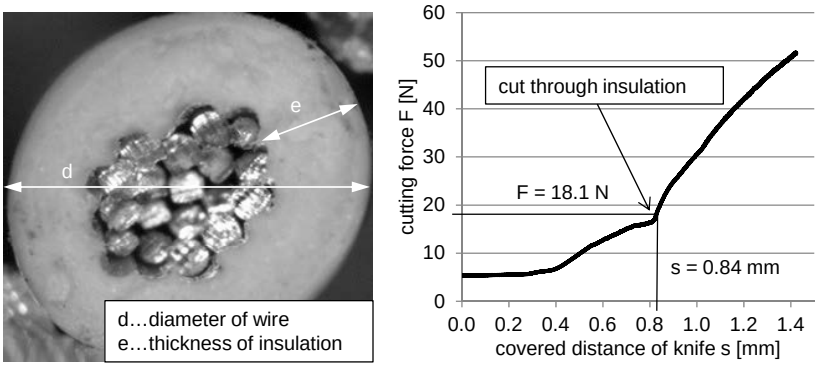

(a) (b)

Fig. 1: Cross section of a stranded wire (a) and correlation between covered distance of knife s and cutting force F of the cut through an insulation (b); (stranded wire with PVC insulation, d = 1.4 mm, e = 0.3 mm, radius of cutting edge r = 0.1 mm)

As shown in Fig. 1b, the required cutting force is not increasing constantly. Also, different phases can be seen: from s = 0.0 mm to s = 0.4 mm the stranded wire is squeezed by the knife. After that the knife cuts into the insulation material until it reaches the conductor in the wire at s = 0.84 mm. All this makes it necessary to analyze the time of the short to identify the end of the cut through the insulation material.

Due to temperature dependences of wire insulation materials this parameter was investigated, too (Tab. 1).

Tab. 1: Cutting force and relative standard deviation as affected by the ambient temperature (wire with PVC insulation; e = 0.2 mm)

Temperature [°C]	Force [N]	Rel. standard deviation [%]
-10.0	46.2	11.3
24.0	33.7	9.5
55.0	17.7	8.7

It can be seen that for insulation material made out of PVC the cutting force is significantly temperature-dependent. Therefore, a wire with PVC insulation requires temperature compensation.

To determine the required forces for different degrees of sharpness (expressed by the radius of the cutting edge “r”), numerous experiments were performed on the universal testing machine. Thus, correlations between the cutting force F, the cutting edge r of the knife and the wire characteristics could be established (Fig. 2).

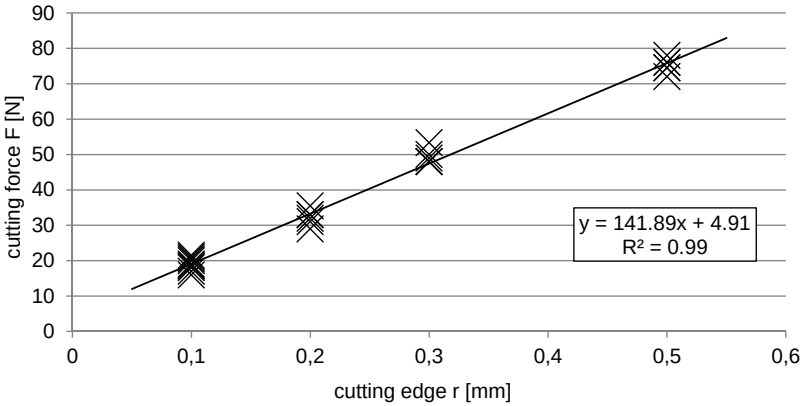

Fig. 2: Measured cutting force F for cutting through the insulation of a wire compared to the cutting edge radius r (number of replications: 6; stranded wire with PVC insulation, d = 1.4 mm, e = 0.3 mm)

The results show that the detected cutting forces are a good indicator for the knife sharpness. Therefore, the operation principle was implemented in measuring device.

3 Technical implementation

The research and development work led to a compact, hand-held, and cost-efficient measuring device. It is designed in such a way that the knives can be tested in a mounted state. A time-consuming disassembly is not necessary. The measuring device is built up of a handlebar and a sensing head (Fig. 3).

The sensing head includes a feeder, which consists of two ellipsoid rotating rolls. The rolls are rotating when the level on the handlebar is operated. With it the sensing head is drawn towards a knife for detecting the sharpness (Fig. 4a). The mechanics of the feeder ensure a reproducible and constant feeding translation. This is helpful for knives which are not easy to access (e.g. in a forage chopper). Inside the feeder there is the measuring unit with the wire which rests on a load cell. In addition, there is a second measuring unit at the front end of the

sensing head (Fig. 4b). This is used for detecting the sharpness when there is not enough space for the roller based feeder (e. g. in balers or self- loading trailers).

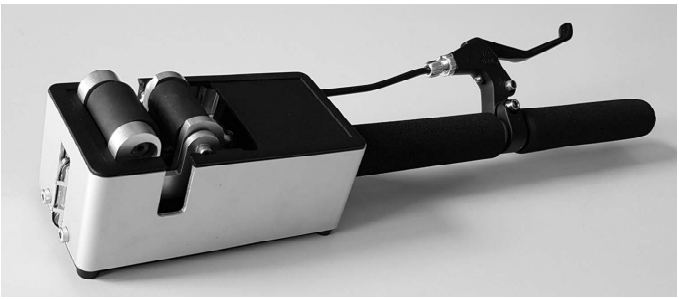

Fig. 3: Measuring device for sharpness measurements

(a) (b)

Fig. 4: Roller infeed application for investigating a kitchen knife (a) and front end application for investigating a mower knife (b)

By not cutting the wire completely for a force measurement, there are no single pieces. The used strand pieces are still on one string. Consequently, they are wound up on a coil inside the sensing head and do not pollute the environment.

Additional, a thermocouple is integrated in the sensing head. It detects the temperature of the wire which is necessary to calculate a correction factor for eliminating the temperature influence.

The measured force and temperature values are transmitted via Bluetooth to a smartphone with an app for handling the data (Fig. 4a). The developed app contains calibration models for different kind of knives and employs statistical methods for calculating the desired sharpness information (Fig. 5).

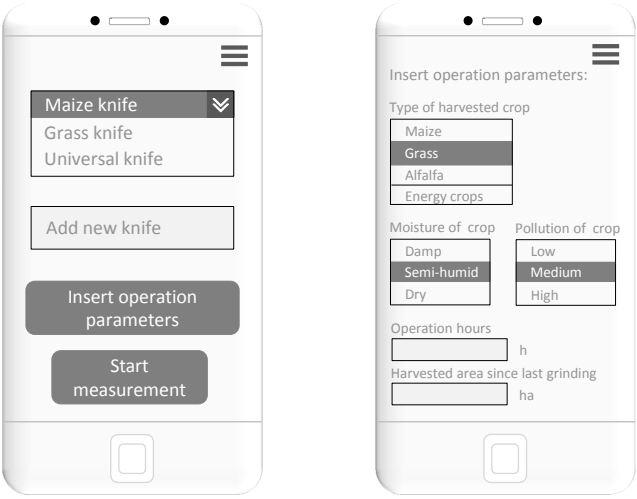

(a) (b)

Fig. 5: Smartphone interface to submit the type of knife (a) and operation parameters (b)

Also, the app informs the user as soon as a sufficient number of individual measurements for a knife is gained. Finally, the user gets the information about the sharpness status of the knife with a high accuracy and the recommendation whether he has to sharpen / replace the knife or not.

Fig. 6 shows the results of a test in practice. The measured force values of two different self-loading trailer knives at eight different spots are presented.

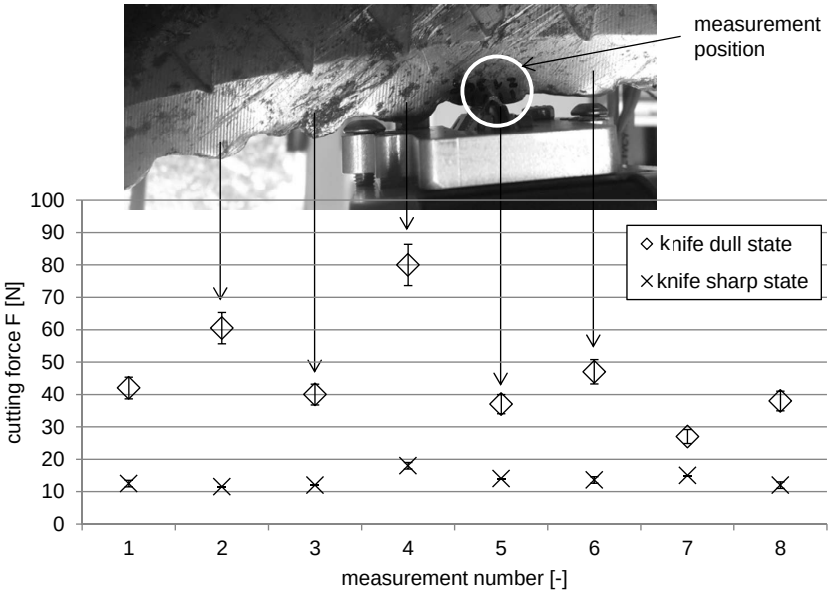

Fig. 6: Required cutting force F and standard deviation to cut through the insulation of a wire as affected by the sharpness state of two different knives of a self-loading trailer (number of replications: 6)

A significant difference between a sharp knife and a knife used after grinding can be seen. The low values for the standard deviations demonstrate a good repetition for the measurements. Also, it becomes obvious that a dull knife has a much higher variation in the sharpness than a freshly grinded knife. This is the main reason for employing statistical methods in order to receive a meaningful information about the sharpness status of a complete knife.

In addition, the calibration models have to determine the boundaries between the individual degrees of sharpness respectively dull state. For any type of knife, this procedure can be calibrated and stored by the smartphone interface.

4 Conclusions

Employing the force for cutting through the insulation of a wire is a useful method for detecting the sharpness of a knife. Based on this method a mobile, hand-held and cost-efficient measuring device could be developed. In combination with a smartphone app it can be employed for detecting the sharpness status of knives in all kinds of agricultural machinery e.g. forage harvesters, balers or self-loading trailers. The next step is to generate measurement data and more calibration models in order to ensure universal applicability for various types of knives.

5 Acknowledgement

This research and development project was funded by the Federal Ministry for Economic Affairs and Energy (BMWi) on the basis of a decision by the German Parliament.

6 References

[1] McClure, J. R.; Hall, L. D.: Sharpening apparatus for forage harvester knives, Patent US 5172521 A, 1992.

[2] Herlitzius, T.; Becherer, U.; Teichmann, J.: Messer von Feldhäckslern zum richtigen Zeitpunkt schleifen – Grundlagenuntersuchungen, LANDTECHNIK– Agricultural Engineering, vol. 64, no. 2, 2009, pp. 131-133.

[3] Wild, K.; Walther, V.; Schueller, J. K.: Reducing fuel consumption for chopping maize with a self-propelling forage harvester, VDI-Berichte 2060, Düsseldorf: VDI Verlag, 2009, pp. 405-410.

[4] Graff, E. A.; Podhorecki, M. J.: Apparatus and method for non-contact measurement of the edge sharpness of a knife, Patent US 5196800 A, 1993.

[5] Heinrich, A.; Bernhardt, G.: Messverfahren zur Feststellung des Schärfezustandes der Paarung Häckslermesser/Gegenschneide eines Feldhäckslers, VDI/MEG Tagung Landtechnik, Halle 2002, VDI-Berichte 1716, Düsseldorf: VDI Verlag, pp. 325-330.

[6] Kormann, G.: Harvesting machine comprising a monitoring device for monitoring the sharpness of cutting blades and/or their distance to a counter-cutter, US 20050072135 A1, 2005.

[7] Siebald, H.; Hensel, O.; Benke, F.; Merbach, L.; Walther, C.; Kirchner, S. M.; Huster J.: Real-time acoustic monitoring of cutting blade sharpness in agricultural machinery, IEEE/ASME Transactions on Mechatronics, no. 99, 2017, pp. 1-10.

4-row potato harvester based on a mirrored product flow concept

B. Eng. **Dirk-Jan Stapel**,
GRIMME Landmaschinenfabrik GmbH & Co. KG, Damme

Abstract

4-row potato harvesters are only built based on a “straight product flow” nowadays. GRIMME took the challenge of building a 4-row self-propelled harvester Based on the “SE” concept. Big challenges were to get the 4-row machine within road regulation dimensions, getting the weight distribution right and to pass obstacles in the field.

Building the machine based on a mirrored product flow gave us the necessary capacity, putting the bunker on the rear axle the right weight distribution, folding the cleaners to get in road dimensions and integrating a crab steering for more soil Protection and passing obstacles in the field. GRIMME will present the new Concept with the VENTOR 4150 on Agritechnica 2017.

Background

In the field of potato harvesting there are two main concepts for the product flow: the ‘straight product flow’ concept with overloading cart elevator or ring elevator on one hand and the side elevator (SE) concept on the other hand. The SE harvesting principle was invented and patented by GRIMME in 1991 [1]. At the time being, it is the most often sold principle worldwide [2].

A tremendous growth has been observed for the market of self-propelled 4-row potato harvesters during the last ten years [2]. However, until now only self-propelled 4-row potato harvesters following the ‘straight product flow’ concept have been commercially available to the market. In order to fill this gap GRIMME has developed a self-propelled 4-row potato harvester following the SE principle.

Basic principle of the SE concept

The ‘SE’ harvester principle is based on an inclined side elevator system. The side elevator system is a combination of a sieving web with a diviner web on top (Figure 1, Point 1). This system combines three functions. The first is sieving, second is separation of haulms and the third is transportation of the product to the upper deck of the machine. Next, the product flow is passed to separator units (Figure 1, Point 2) transporting it out of the diviner web. The second separator (Figure 1, Point 3) conveys the product to the picking table (Figure 1, Point 4), which transfers the potatoes in the Bunker (Figure 1, Point 5).

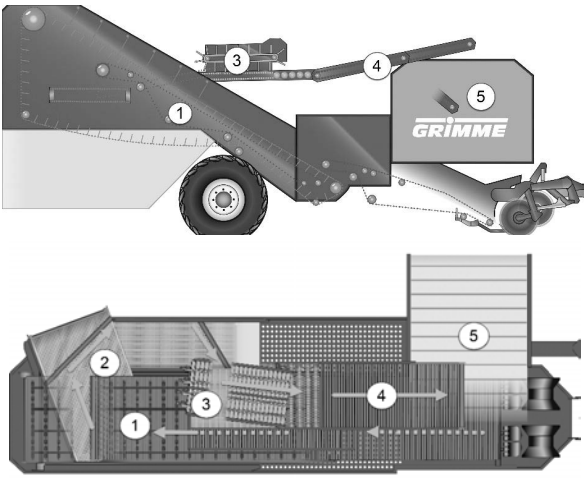

Fig.1: 2-row SE product flow in a trailed harvester

Idea behind the new 4-row Product flow.

The central idea behind the new concept is to mirror two SE-like 2-row machines and combine them into one 4-row machine. This sounds quite simple, but leads to a number of challenges. The concept of the 4-row product flow is sketched in Figure 2. First, there is a 4 row intake web (Figure 2, Point 1) followed by the inclined side elevator (Figure 2, Point 2). Starting from the second web, the product flow is separately led to two different sides of the machine and processed on the 'mirrored' separators (Figure 2, Point 3). In case of trailed machines following the SE concept, the product flow now turns to the front of the machine. However, in this case for the 4-row concept the product flow turns to the back of the machine. The second set of separators returns the product streams from the sides of the machine to the middle of the machine (Figure 2, Point 4) and reunites the separated product streams on the bunker-filling elevator. The bunker-filling elevator (Figure 2, Point 5) transfers the potatoes into the bunker centered in the back of the machine.

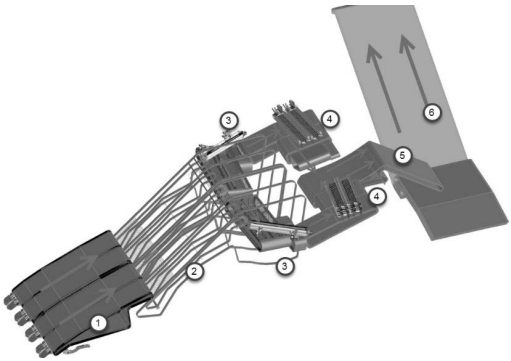

Fig. 2: New 4-row product flow

Challenges during development.

As mentioned, a number of challenges had to be addressed during the development of the machine.

Weight:

A serious challenge of the concept was finding an optimal weight distribution for the machine. One of the major requirements for potato harvesters is keeping the first sieving web relatively flat in order to prevent the potatoes from rolling back. Another major requirement for this ma-

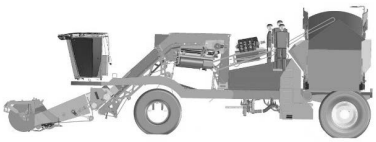
Fig. 3: 4-row SF concept

chine was a bunker capacity of 15 tons. For carrying the bunker load and the machine weight, two huge axles were required. The front axle had to be placed under the first main web in order to have a huge front axle together with keeping the webs flat. Consequently, the front axle is situated almost in the middle of the machine (Figure 3). With front axle in this position and rear axle almost completely at the back of the machine, it was imperative to place a huge part of the weight at the back of the machine.

Road Regulation

Mirroring two machines and combining them in to a single machine would be simple - if there were no restrictions regarding machine size for road transportation. However, under this aspect the SE principle has one serious disadvantage. It is unavoidable, that the product flow has to leave of the inclined side elevator (Figure 2, Point 3) sidewards. As the first two webs (Figure 1, Points 1 and 2) have a width of approx. 1500 mm in a trailed 2-row harvester, a web width of around 3000 mm was needed in order to meet the requirement of doubling the sieving capacity with respect to a 2-row harvester. This in combination with separators conveying side wards out of the side elevator brought up two major challenges. How to get the dimensions of such a system within the allowable range of road regulation, particularly when considering machine width? And, how to pass obstacles and field boundaries while harvesting (Figure 4)?

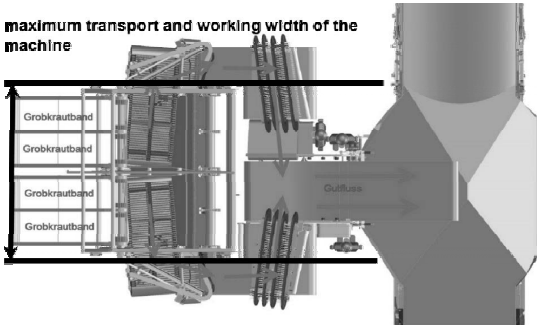

Fig. 4: Road Limitation

One of the first conceptual ideas was to reduce the width of the sieving area in the front. However, given the fact that reducing width in this area is a tremendous reduction of cleaning capacity, this option was discarded early. The idea of folding the separators came up. Folding is a complicated issue, particularly with respect to collisions between parts. A major requirement was having a folding system with least turning points and changes on collision possible. For folding the separators around the side elevator, the first and second separator are divided and separately folded. Targeting a simple folding system, conceptual design of it took a plenty of effort. It resulted in a satisfactory, easy solution: The first separator folds into the diviner web (Figure 5) by two turning points. The cylinders folding this separator are working with a master / slave system. It folds the system with only one hydraulic function in and out of the diviner web. Due to the master / slave principle, malfunctions of the system due to wrong setup or incorrect operation are inherently avoided. The second separator has only one turning point. It is guided into its respective position by only one cylinder.

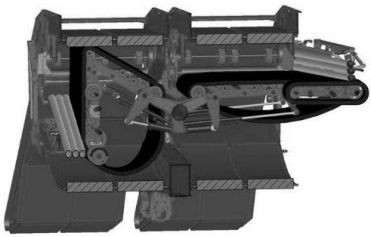

Fig. 5: left a folded 1st separator, at the right a unfolded 1st separator

.

Passing obstacles in the field

The third major challenge was passing obstacles in the field with a total width exceeding the working width of the machine on both sides (Figure 4). Even in case of walls, trees or electric pylons on the side of the field, it must be possible to harvest the rows closed to the side.

The solution for this issue was letting the machine drive in crab steering, so the complete back of the machine would move to a side (Figure 6) and the unfolded separators move behind the intake. This feature brings a second very important advantage. As the front and rear wheels of the machine drive in separate tracks, the harvested field is rolled over evenly and

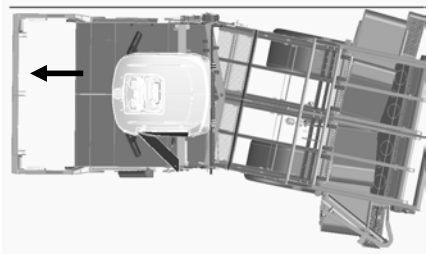

Fig. 6: passing Boundaries in the field

unwanted soil compaction due to multiple passes of wheels in identical tracks are avoided.
Bending a machine with a full-width product flow for crap steering is another novelty of the concept. However, again it brought some very challenging issues. To understand the problem it is important to know that for getting the product flow to the upper deck of the machine, its height had to be increased continuously. All part of the web system flat or even with decreasing height (for example drops) are causing extra length for the machine in total. Another very important issue is keeping drops in the web system - wherever required - as small as possible, as potatoes are very sensitive to drops. The first draft for the design of a swivel point in a sieving web system in order to be able to drive in crab steering mode, can be seen in Figure 7.

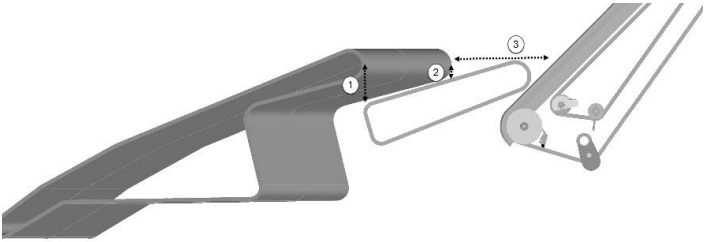

Fig. 7: First idea of a crab steering solution

The easiest way is to pick two webs lying horizontally and swivel them avoiding the difference seen at point 1 and 2 in Figure 7. However, the height difference between left and right implies that the drop at the left side is much higher than on the right side. This is not acceptable. To avoid this drop a flat web is needed. However, in a web system, it is not
possible to switch from flat to steep in one web. The reason is that there had to be rollers on top of the web, i.e., in the product flow damaging the potatoes. Consequently, an extra drop is required to switch from a flat web to a steep web. However, in case of this machine a flat intermediate web and an extra drop would have increased the machine length by more than 1000 mm.

Another solution for a swivel point in the machine without increasing machine length was searched. It was found in the simple solution of making the second web bendable itself such that the frame directly compensates the length difference. In Figure 8 can be seen how the frame of the Side elevator (Figure 8, Point 2) swivels with the first main web (Figure 8, Point 1). E.g., if the intake moves to the right side, the right side of the web system gets a little steeper and moves back meanwhile the left side gets a little flatter and moves to the front. Point 3 in Figure 1 depicts that the frame has a flexible construction. This solution allows machine bending causing only 300 mm of machine length. Further, it does not require another web and is extremely simple in its working manner.

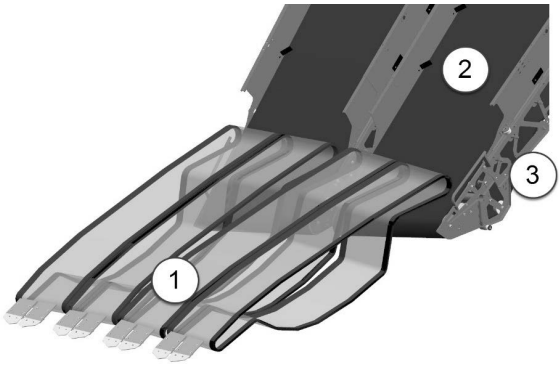

Fig. 8: swiveling 1st main web and side elevator

Conclusion

The combination of the mirrored product flow, a foldable separator system and the crab steering solution replaces 2 trailed machines without compromises and allows building a machine that meets road regulation requirements. For the numerous novel solutions, GRIMME was able to claim several patents [3] on the mentioned new concepts.

After several years of testing this concept, GRIMME will present the VENTOR 4150 on this year's Agritechnica.

Fig.8: Ventor 4150 in the field

References

[1] Johannes Welp; Kartoffelerntemaschine; EP 0 212 174 B1

[2] GRIMME Landmaschinenfabrik GmbH & Co. KG

[3] Dettmer Franz-Josef; Feldkämper, Stefan; Maschine zum Ernten von Hackfrüchten; DE102014015834A1

[4] Dettmer Franz-Josef; Bellersen, Werner; Hackfruchterntemaschine; DE102014015835A1

Calculation of the losses in series-hybrid powertrains

Prof. Dr.-Ing. Dipl.-Wirt. Ing. **Roland Schmetz**,
Rhine-Waal University of Applied Sciences, Cleves

Abstract

Regarding agricultural tractors, the efficiency of electric series-hybrid powertrains is often depicted as worse than the efficiency of mechanic-hydraulic power-split powertrains. For verification, the losses of an electric series-hybrid powertrain of 150 kW power are for example calculated and compared with the losses of a typical mechanic-hydraulic power-split powertrain of the same power. The comparison of the losses shows that the electric series-hybrid powertrain clearly exceeds the efficiency of the comparative mechanic-hydraulic power-split powertrain in the main work range and that there is still potential for improvement.

Background

In recent literature on mobile machines, especially on agricultural tractors, the efficiency of electric series-hybrid powertrains (ESHP) is often reported to be worse than the efficiency of mechanic-hydraulic power-split powertrains (MHPSP) **[1, 2, 3]**. According to **[4]** the efficiency of electric machines is so high that the efficiency of a mechanic-electric power-split powertrain (MEPSP) is worse than that of an ESHP even for a 50 kW-tractor (which is proved in **[5]**), but the efficiency of an MHPSP for the same tractor is still 5% higher than that of an ESHP. All these statements are in contradiction to the overwhelming knowledge on electric and hydraulic propulsion. This contradiction is to be investigated by an example-ESHP with 150 kW power. For this purpose, a general model of a typical MHPSP is defined, and the limits for the investigation are fixed. Then, the losses of the comparative powertrain are calculated and verified. In two further steps the analysis of the single components of the ESHP as well as the approximate calculations of the losses caused by them are carried out. From the subsequent comparison, the core statements of this paper are derived.

Modeling

Although classic vehicle manufacturers prefer parallel hybrid, electric power-split or series-hybrid powertrains with electric single-wheel drives, here the ESHP is based on powertrains, as they are used in vehicles with an external energy supply (for example trolleybuses, trams, also those with inductive energy supplies, and Siemens-eHighway trucks or as range-

extenders in battery electric vehicles). However, the advantage of certain systems depends very much on their particular application. According to **[6]** an ESHP is the most suitable for larger agricultural tractors, if advantageous also in combination with drive axles. On base of further calculations and in contradiction to [3], it can also be shown that electric single-wheel drives are not advantageous for standard tractors. Main advantages of ESHPs for larger tractors are:

- Very good integration into existing tractor concepts
- Very good suitability for electric machines of high efficiency
- Very good utilization of electric machines and power electronics
- Very good controllability of the powertrain
- Cost-effective solution with a very good ratio of technical to economic value

The powertrain of the ELTRAC® (the first tractor with an ESHP using modern inverter technology **[7]**) according to the left part of **Fig. 1** is the best way to calculate the losses in an ESHP and to compare it with an MHPSP. It has a typical tractor engine and a typical final drive unit, consisting of a bevel and a differential gear, two planetary gears for the rear wheels and a power take-off to the front axle, which is not shown. In case of rectilinear driving, the differential gear can be assumed to be at standstill or locked and therefore be neglected. Both the tractor engine and the final drive are interchangeable with conventional tractors. If the savings according to [6, 7], which can be achieved beyond the efficiency level of an ESHP, are not considered, only the unit in the balance limit (consisting of the electric machines, the rectifier and the inverter) and the two-stage gearbox outside still require adequate counterparts. Thus, the model of the MHPSP requires the same assemblies as the medium-sized Agco-Fendt Vario-tractors whose data are readily available (right part of Fig. 1). With regard to the presence of comparable two-stage gearboxes in both powertrains, these can also be clamped out. Finally, this provides good comparability and allows the reduction of the comparison to the two units in the balance limits.

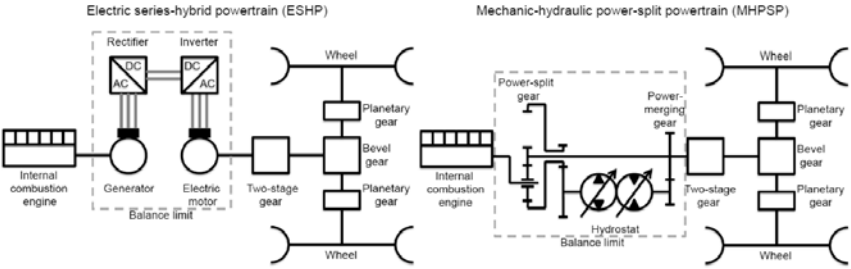

Fig. 1: Electric series-hybrid and mechanic-hydraulic power-split powertrains

Rough calculation of the losses in the comparative powertrain

The efficiency of the MHPSP is $\eta_{MHPSP} = [S \bullet \eta_M + (1 - S) \bullet \eta_H]$. The split factor S ($0 \leq S \leq 1$) gives the proportion of the mechanically transmitted power and the term (1 - S) the proportion of the hydraulically transmitted power. The efficiencies η_M and η_H take the losses in the M(echanic) and H(ydraulic) branches into account. An efficiency of 97% for the split gear (planetary gear with a driven arm, three internal meshing contacts and a drive-through shaft) and an overhead of 1% for pressure lubrication, oil splashing and friction (e.g. by bearings and seals) lead to $\eta_M = \sim 0.97 \bullet 0.99 = \sim 0.96$. The efficiency η_H is made up of the mechanical losses $\eta_{H\text{-}M(echanic)}$ in the hydraulic branch, the volumetric and hydro-mechanical losses of the pump and the motor of the hydrostat, as well as the effort for the auxiliary units to $\eta_H = \eta_{H\text{-}M} \bullet \eta_{Vol(umetric)\text{-}P(ump)} \bullet \eta_{H(ydro)M(echanic)\text{-}P} \bullet \eta_{Vol\text{-}M(otor)} \bullet \eta_{HM\text{-}M} \bullet \eta_A$. An efficiency of 98% for the split gear (planetary gear with one driven arm and three external meshing contacts) and 99% for each out of the two spur gear sets (hydrostat reducer and power merging gear set) and an 1% cut for pressure lubrication, oil splashing and friction lead to $\eta_{H\text{-}M} = \sim 0.98 \bullet 0.99 \bullet 0.99 \bullet 0.99 = \sim 0.95$. The efficiency of the auxiliary units of the hydraulic branch, such as the losses of the charge pump and the overload protection as well as the filter and flushing circuits of the hydrostat, is considered by the efficiency $\eta_A = 98\%$. The losses of the fans of the radiator circuit are not taken into account. However, the efficiency of the hydrostat has yet to be determined. According to [2], the best efficiency of a hydrostat is 96% at its peak. A closer look, however, reveals that this efficiency was not determined due to the ISO 4409-standard, since the measurements were performed with a single (two-shaft) electric motor (thus with a fixed displacement ratio). In addition, impacts by auxiliaries were neglected and the oil ISO-VG 11 was used instead of ISO-VG 46, which is recommended for the hydrostat of the comparative powertrain. Because of these deficiencies, real efficiencies of hydrostats are lower. According to other sources, even high efficient hydrostats have only efficiencies of 90% at their peaks **[**1, **8, 9]**. Therefore a (still high) hydrostat efficiency $\eta_{Hydrostat} = \eta_{Vol\text{-}P} \bullet \eta_{HM\text{-}P} \bullet \eta_{Vol\text{-}M} \bullet \eta_{HM\text{-}M} = \sim 0.9$ is applied here. Then the efficiencies are $\eta_H = 0.95 \bullet 0.9 \bullet 0.98 = 0.84$ for the hydraulic branch and $\eta_{MHPSP} = [S \bullet 0.96 + (1 - S) \bullet 0.84]$ for the MHPSP in the balance limit. Depending on the split factor S, the resulting efficiencies of the MHPSP are shown in **Table 1**. The main working range of a tractor is usually $S \approx 0.25$ with high engine utilization and the maximum transport speed is usually $S \approx 1$ with significantly reduced engine utilization. The maximum transmissible power close to $S \approx 0$ is limited by the size of the hydrostat. It is not taken into account that the efficiency is also adversely affected by the unavoidable idle losses of the hydrostat even at S = 1. In addition, operating ranges with positive ($S < 0$) and negative ($S > 1$) circulating power are not considered. The above

calculations are confirmed by performance tests carried out by the German Agricultural Society's test center in Groß-Umstadt. There, a maximum tractive power of 137.5 kW corresponding to an efficiency of 0.78 was measured for an Agco-Fendt Vario-tractor 724 with a powertrain according to Fig. 2 and a maximum engine output of 176.4 kW at 1700 rpm **[10]**. If this efficiency is corrected by the losses of the two-stage gearbox and the final drive, which is about 6 to 7% according to [3], a good match is obtained with the calculated efficiency in the main working range, where the maximum drag power should appear.

Table 1: Calculated efficiencies of the MHPSP

Split factor S	Efficiency η_{MHPSP}
0	0,84
0,25	0,87
0,5	0,90
0,75	0,93
1	0,96

Components of the electric series-hybrid powertrain

Electric machines

Due to content restrictions, the electric machines cannot be described in detail here. But it is important to know that the former CEMEP (the European Committee of Manufacturers of Electric Machines) EFF efficiency classes were restricted to electric machines up to 90 kW. This may be one of many reasons why larger electric machines have received little attention in powertrains for off-road applications for long periods of time, despite their ability to deliver constant power with high efficiency across large operating ranges, if operated in combination with a suitable inverter (thus in IES1 or IES2-systems due to EN 50598-2). Since 2011, in the European Union the new IE efficiency classes according to IEC 60034-30:2009 (IEC: International Electrotechnical Commission) apply for electric machines up to a power of 375 kW. Due to this standard the new IE3-types (more efficient than the former EFF1-electric machines) were introduced, followed up by an amendment (IEC 60034-30-1:2014) defining a new IE4-standard, mentioning already a future IE5-standard, expanding the application range for standard electric motors to powers from 0.12 to 1000 kW, as well as making information about part load-efficiencies mandatory (**Fig. 2**). It should be noted, that the full-load efficiencies slightly increase with increasing speed (see efficiencies at 60 Hz frequency instead of 50 Hz) or by stepping down to 75% load. With regard to the standard, here the (minimum) required efficiency of 95.6% can be applied to the electric motor. In contrast,

asynchronous generators are rarely used in ESHPs. Synchronous generators are more common, which have a slightly higher efficiency of about 96% at a power of 150 kW.

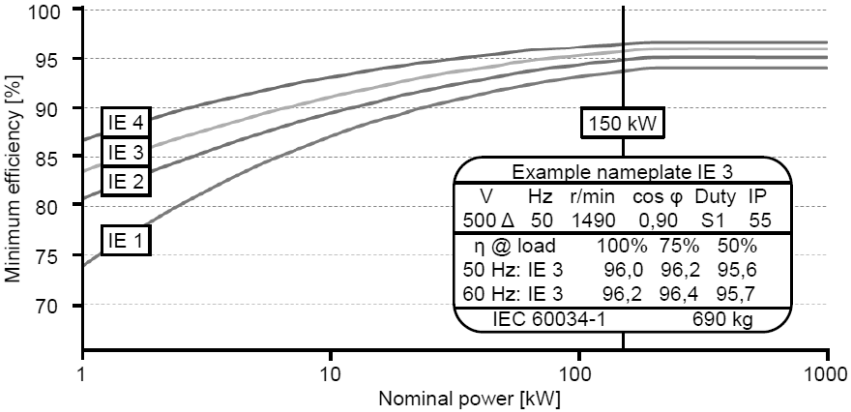

Fig. 2: IE classification for 50 Hz 4-pole electric motors according to IEC 60034-30-1:2014

Power processing unit (PPU)

The most common configuration of the PPU of an ESHP (without energy recovery if braking) is shown in **Fig. 3**. The PPU contains a rectifier, a DC-link with smoothing capacitor(s) and a brake resistor, and an inverter with six IGBTs with free-wheeling diodes. The two IGBTs with free-wheeling diodes required for each phase are available as a ready-to-use module (or all six IGBTs as six-pack) whose gates only have to be connected to a low-power driver unit. This unit generates width-modulated pulses depending on the operating state. Another IGBT is required for the actuation of the brake resistor. In line with a controlled three-phase AC-synchronous generator an uncontrolled rectifier can be used. Most commonly this is a B(ridge)6-rectifier consisting of six power-diodes arranged as bridges from each single phase to the two lines of the DC-link. A typical power-diode characteristic is shown in the lower left part of Fig. 3. When a single-phase AC-current of 100 A with a voltage of 500 V is rectified, the losses while conducting during the positive half-wave are about 100 W and while blocking during the negative half-wave about 7 W (for a power-diode like IR-1N2067). It should be noted, that a B6-rectifier cannot pass the full available power. This is expressed by the so-called power factor λ_R which is 0.955 for a B6-rectifier. This means that a generator must be designed for an apparent power of approximately 157.1 kVA for a supply of 150 kW power to a DC-link via a B6-rectifier despite the much lower losses of its diodes. In special applications, AC-currents with more than three phases can be generated and rectifiers with

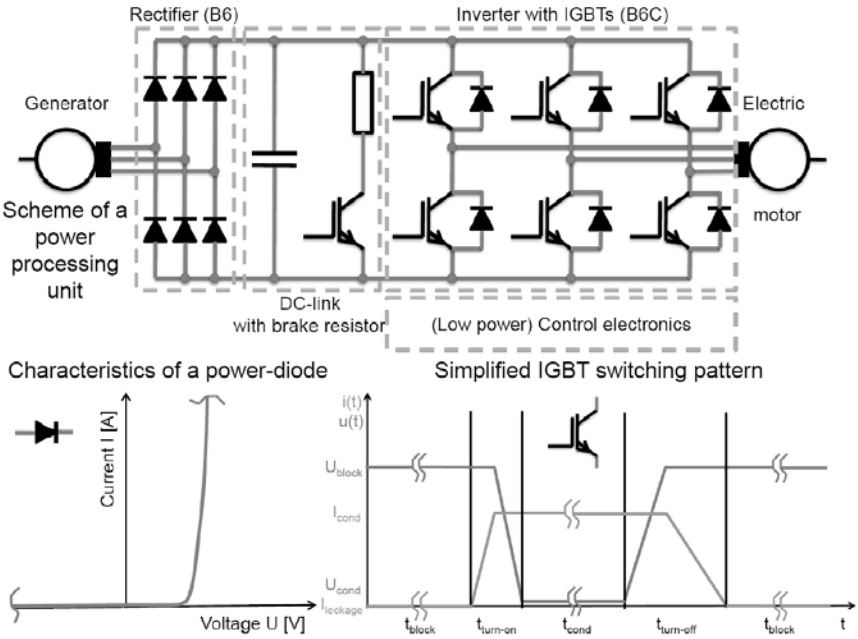

Fig. 3: Power Processing Unit

more than six pulses can be used. Then, the current from the DC-link is converted again by an inverter to a three-phase AC-current, but now with its amplitude and frequency adjustable. The simplified switching pattern of a single IGBT of such an inverter is illustrated in the lower right part of Fig. 3. When switching an IGBT, the voltage and the current do not change immediately. In reality, short delays occur, before the voltage falls from the blocking voltage U_{block} to the on-state voltage U_{cond} of the IGBT at the end of the switch-on operation, as well as rises vice-versa from the on-state voltage U_{cond} to the blocking voltage U_{block} at the end of the switch-off operation **[11]**. A free-wheeling diode is required in order to avoid voltage peaks in the reverse direction, which occur during the switch-off of inductive loads like here. As a result, a significantly higher loss occurs during the switching of an IGBT in contrast to a passive power-diode. Typical switching (or modulation) frequencies of the IGBTs in inverters for AC-asynchronous motors of a size like here are 1 to 4 kHz. With regard to these losses, the losses during conduction and blocking are only slightly higher than in the case of a power-diode. In addition, driving the M(etal) O(xide) S(emiconductor)-gate of an IGBT also requires electrical power that has to be taken into account. But, in relation to the base or gate

power, which conventional semiconductors require, this power is low. For rough calculations of the losses in ESHPs, the simplified switching pattern of an IGBT shown in Fig. 6 is sufficient. For a closer inspection the Infineon-dimensioning tool IPOSIM and its technical documentation **[12]** can be used. Typical values for the following calculation are taken from datasheets like for those of Infineon IGBT-modules FF200R12KT4 or IGBT-six-packs FS200R12KT4R.

Rough calculation of the losses in the electric series hybrid powertrain

The input power of the ESHP is $P_{I(nternal)C(ombustion)E(ngine)}$ = 150 kW. The nominal power of the generator is calculated for a voltage of $U_{G(enerator)}$ = 500 V 3~ (Δ) and an efficiency of η_G = 0.958 to $P_G = P_{ICE} \bullet \eta_G$ = 143.7 kW = $3 \bullet U_G \bullet I_G/\sqrt{3}$ (→ I_G = 165.9 A). Assuming (for the most critical case) the equivalents of one power-diode per phase as permanently conducting and of the remaining power-diode as permanently blocking, the losses in the B6-rectifier are $P_{R(ectifier)\text{-}loss} = 3 \bullet U_{D\text{-}loss} \bullet (I_G/\sqrt{3}) + 3 \bullet U_G \bullet I_{D\text{-}leakage}$ = 308.4 W. Thus, the output power of the B6-rectifier is P_R = 143.4 kW and its efficiency η_R = 0.998. Furthermore, in the DC-link the voltage is $U_{DC(\text{-}link)} = U_G \bullet \sqrt{2}$ = 500 V • √2 = 707 V and the current is $I_{DC} = P_R/U_{DC}$ = 202.8 A. The losses caused by leakages of the DC-link capacitor(s) and the IGBT for the actuation of the brake resistor can be neglected in the case of a rough calculation since they are below 10 W. Furthermore, the IGBT is only actuated in case of sudden braking processes, while the kinetic energy set free in the comparative MHPSP is deleted by mechanical brakes. The typical power demand of a single driver unit is $P_{G(ate)E(mitter)}$ = 60 W @ I_{cond} = 120 A during actuation of the IGBT-gate. Again, assuming (for the most critical case) one IGBT per phase as permanently on and the remaining IGBT as permanently off, the maximum conduction time per IGBT is $t_{cond} < 50\%$ of a full period ($t_{cond} \leq (T/2) - t_{turn\text{-}on} - t_{turn\text{-}off}$) and the minimum blocking time per IGBT is $t_{block} \geq 50\%$ of a full period ($t_{block} \geq T/2$). This results in inverter losses of $P_{I(nverter)\text{-}loss} = f \bullet [6 \bullet 0.5 \bullet U_I \bullet (I_{DC}/\sqrt{3}) \bullet (t_{turn\text{-}on} + t_{turn\text{-}off}) + 6 \bullet U_{cond} \bullet (I_{DC}/\sqrt{3}) \bullet t_{cond} + 6 \bullet P_{GE} \bullet (T/2) + 6 \bullet U_I \bullet I_{leakage} \bullet t_{block}$. With $(T/2) = t_{turn\text{-}on} + t_{cond} + t_{turn\text{-}off} = t_{block} = 1/(2 \bullet f)$ and the most critical pulse width modulation frequency of f = 4 kHz and $U_I = U_{DC}/\sqrt{2}$ the maximum inverter losses are $P_{I\text{-}loss}$ = 1190 W. Thus, the output power of the inverter is P_I = 142.2 kW and its efficiency η_I = 0.992. Although the power factor of an inverter can usually be controlled close to $\lambda_I = 1$, it should be noted, that an inverter in an application like here needs an overload capacity of a factor two, which is fulfilled for the semiconductor-types mentioned above. Taking that into account, the nominal power of the three-phase asynchronous motor, which is operated with the output voltage of the converter U_I = 500 V 3~ and has an efficiency of $\eta_{E(lektric\ motor)}$ = 0.956 as given earlier, can then be calculated to $P_E = P_I \bullet \eta_E$ =

135.9 kW. Furthermore, any additional losses caused by auxiliaries like pumps for a liquid cooling of the electric machines and the PPU are considered by the efficiency $\eta_A = 0.99$. Then the overall efficiency of the ESHP is $\eta_{S(erial\ hybrid)} = \eta_G \bullet \eta_R \bullet \eta_I \bullet \eta_E \bullet \eta_A = 0.958 \bullet 0.998 \bullet 0.992 \bullet 0.956 \bullet 0.99 = 0.9$. Thus the ESHP clearly exceeds the efficiency of the comparative MHPSP in the main work range.

Conclusions

From the comparison of the ESHP investigated with the comparative MHPSP, the following statements can be derived:

- An ESHP of 150 kW power clearly exceeds the efficiency of the comparative MHPSP in the main working range.
- By the use of more efficient (e.g. IE4) electric machines and further optimized inverters (e.g. by the use of silicon-carbide made semiconductors) further improvements in efficiency of ESHPs are still possible.

References

[1] Renius, K. T. and Resch, R.: Continuously Variable Tractor Transmissions: ASAE Publication No. 913C0305, pp. 14-22

[2] Rahmfeld, R. and Skirde, E.: Efficiency Measurement and Modelling: 7th International Fluid Power Conference Aachen 2010: Proceedings Vol III, pp. 53-66

[3] Geimer, M. and Renius, K. T.: Motoren und Getriebe bei Traktoren: Frerichs, L. (ed.): Yearbook Agricultural Engineering Vol. 24, Braunschweig: 2012, pp. 69-77

[4] Morselli, R.: Electrification in Ag: 5th International Colloquium Electrical Drives in Agricultural Machines: Herlitzius, T. (ed.): Dresden 2014

[5] Schmetz, R.: Überschlägige Berechnung der Verluste in serienhybriden Antrieben: Geimer, M. and Synek, P. (ed.): Karlsruher Schriftenreihe Vol. 30, 2015, pp. 141-160

[6] Schmetz, R.: Elektrische Traktorantriebe: ATK 2011, pp. 77-101

[7] Schmetz, R. and Kett, J.: Neue Produkttechnologien im Traktorenbau, insbesondere elektromechanische Traktorgetriebe. VDI-Report 1449. Düsseldorf: VDI-Verlag 1998

[8] Kohmäscher, T.: Modellbildung, Analyse und Auslegung hydrostatischer Antriebsstrangkonzepte. RWTH Aachen Diss. 2008

[9] Murrenhoff, H.: Grundlagen der Fluidtechnik. Aachen: Shaker-Verlag 2012

[10] Wilmer, H.: (K)Ein teurer Spaß. Profi 25 (2013) 1 pp. 12-18

[11] Mohan, N., Undeland, T. and Robbins, W.: Power Electronics. Minneapolis: Wiley 2003

[12] IPOSIM, technical documentation. Infineon Technologies AG, Warburg 2006

Method for load-based evaluation of machines using the example of a tractor

M.Sc. **Florian Balbach**, Dr. **Eberhard Nacke**,
CLAAS KGaA mbH, Harsewinkel;
Prof. Dr.-Ing. **Stefan Böttinger**, Universität Hohenheim, Stuttgart

Abstract

Tractors are multipurpose machines. Each farming operation with the tractor applies different loads on different components of the drivetrain. The variation of these loads is not considered by today's hour meters and makes the precise evaluation of the actual physical tractor condition difficult. This weakness demands for a new evaluation method taking into account different load parameters. This approach uses pseudo damage calculation. The load spectrum that a tractor is exposed to during heavy pull has been recorded and was compared to a reference load spectrum known from literature. The resulting load factor for the drivetrain shows higher loads on the tested machine in comparison to a reference load spectrum. Due to this new load factor a tractor operation hour can be compared to a reference operation hour. Condensing a tractor's load history enables precise tractor validation, flexible maintenance and optimization of tractor setup.

1. Introduction

Tractors play an important role on agricultural farms. Yearly utilization depends on farm size and many other factors. Application spectra of mid-size tractors vary a lot while large-size tractors are mostly used for heavy tillage or power take-off (pto) applications only. However, since hour meters only count operation hours, there is no indication about stress factors that a tractor may have seen during its lifetime. Old tractors often were equipped with mechanical engine speed-synchronous driven tractor meters. With this technique engine operation at idle speed has been weighted lower than tractor operation at engine nominal speed. For example 1 hour of operation at 1,500 min^{-1} engine speed was counted as 1 maintenance hour, operation at engine nominal speed was counted as 1.4 maintenance hours. Preventive or corrective maintenance is still state of the art for agricultural machines. However, approaches based on condition monitoring lead to better material usage and result in higher up-time rates. At the same time condition monitoring based approaches require individual sensors that need to be set up and are adding product cost. An alternative to the condition monitoring based approach is the estimation of the tractor condition by load evaluation. This can be done either with already installed or additional sensors [1; 2].

For these reasons there is a definite need to develop a method for a factor calculation that is load-based. This load factor should be calculated separately for major tractor sub-assemblies and sub-components. Further condensing of these separate load factors into one all-encompassing machine load factor should be considered. In contrast to other approaches to predict remaining lifetime [3], the new method should combine past loads in an objective and transparent way.

2. Fatigue and Fatigue Damage Hypothesis

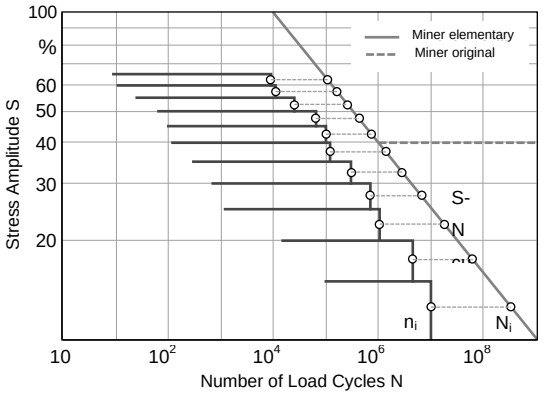

$$D = \sum_{i=1}^{k} \frac{n_i}{N_i}$$

10

Fig. 1: Linear damage accumulation hypothesis: S-N curve and Miner's rule

Mobile working machines always had to deal with the conflict of a high durability requirement and a demand for low weight. This led to the application of the fatigue strength concept. Basics of fatigue testing go back to August Wöhler [4], who developed a procedure for standardized material testing. By applying periodic loads with equal amplitudes the number of load cycles to material failure can be determined. The repetition of this testing procedure with increasing amplitude values generates a component's Wöhler curve (S-N curve) as shown in Figure 1. It is defined by the stress amplitude (S) and the number of load cycles (N) and is depicted in a graph in double-logarithmic scale. A typical S-N curve is composed of the area of low cycle fatigue $N \leq 10^4$ cycles, the area of finite life fatigue strength $N = 10^5$ and the knee point to endurance limit at $N_D \geq 10^6$ [5; 4].

Drivetrains of mobile working machines are confronted with stochastic loads. To convert varying loads over time into one overall damage factor, the application of a damage accumulation hypotheses becomes necessary. According to DIN 3990/6 [6] damage accumulation hypothesis can be separated into linear, non-linear and relative methods, while the linear method is mostly used for agricultural machinery [5]. These damage accumulation hypotheses assume equal damage contribution from equal loads and no influence of load sequence. For calculation of the overall damage, load cycles of one load class are compared with the corresponding point on the S-N curve. By the ratio of potential load cycles N_i and applied load cycles n_i, an overall damage D is calculated as shown in Eq. (1). If $D \geq 1$ a components failure is expected statistically [6].

3. Load Spectrum in Agriculture

Long-term measurements need to be classified in order to condense information. Speed synchronous classification is recommended for cyclic loads as they appear on gears. Load amplitudes are summarized in classes of identical width resulting in a histogram. By summing up the individual classes, starting at the bottom with the lowest class, a cumulative load distribution − the load spectrum −, shown in Figure 2 can be generated. Semi logarithmic axes for frequency distribution are state of the art [4; 5]. Load spectra for tractors are separated into engine and drive wheel side. Measurements can be standardized by means of Eq. (2a) or (2b) to be comparable between different tractors [5; 7].

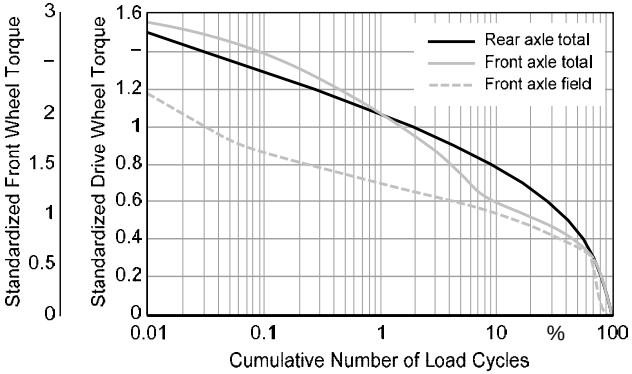

Fig. 2: Standardized tractor lifetime load spectrum for drive wheels and front axle [5; 7]

$$\frac{T_{Drive\ wheel}}{m_{net\ weight} * g * r_{Drive\ wheel}} \quad (2a) \qquad \frac{T_{Front\ wheel}}{m_{Front\ wheel} * g * r_{Front\ wheel}} \quad (2b)$$

4. Materials and Method

To verify the approach a mechanical front wheel drive (MFWD) tractor (135 kW, ECE R 120) with continuous variable transmission (CVT) was used for measurements. Figure 3 shows the layout of the drivetrain and sensor positions. Torque was measured with calibrated strain gauges. The field test sample rate was 1 Hz which showed sufficient accuracy during previous long-term measurements. According to the updated “Kuratorium für Technik und Bauwesen in der Landwirtschaft” (KTBL) working time classification from Reith et al. [8], measurements have been reduced to execution time t11 and turning time t12 so that fault time t2 and non-productive time t3 didn’t need to be analyzed. Engine data was divided into 10 load classes, transmission and drive axles into 18 classes. Negative torque as seen during push in forward or pull in reverse operation was not considered. This simplification is possible because tractors mostly operate in the forward direction and both flanks of the gear tooth are designed for the same lifetime [9].

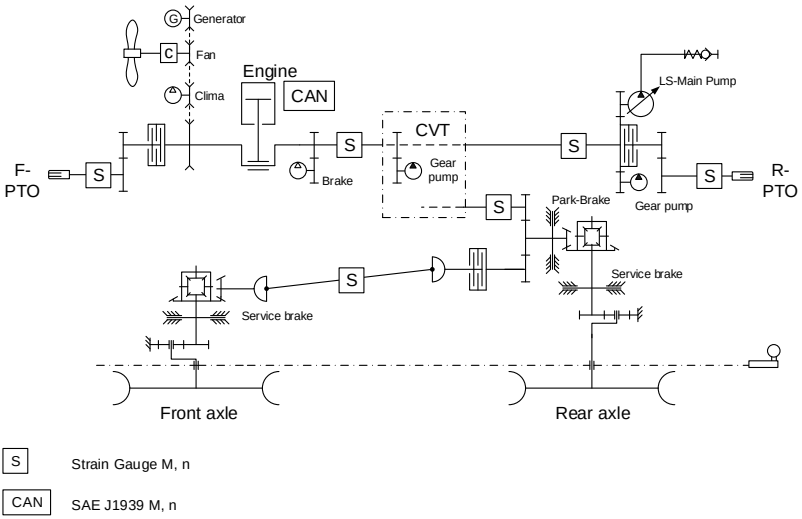

Fig. 3: Drivetrain layout of testing machine, MFWD tractor, 135 kW

Measurements were taken with strain gauges at the assembly level as shown in Figure 3. This enabled the calculation of power flow within the drivetrain, displayed in Figure 4. On the drive wheel side all signals were converted into drive wheel forces. For statistical certainty all measurements were repeated and finally aggregated to a load spectrum, e.g. heavy pull

gearbox output. Due to standardization with Eq. (3) the data is comparable with data from other machines.

$$LF = \frac{\sum_{i=1}^{k} L_{Test_i}}{\sum_{i=1}^{k} L_{Reference_i}} \qquad (3)$$

The drive wheel and front axle load spectra, published by Renius [5] and Meiners [7], are used as reference for the calculation of load factors (LF). Load spectra are not constant amplitude fatigue tests and therefore cannot be compared directly. Nevertheless, reference and application load spectrum should be compared. Therefore a pseudo damage calculation is used to calculate individual loads (L), analog to the calculation of D from Eq. 1 to the previously described fatigue damage accumulation hypothesis by Palmgren-Miner.

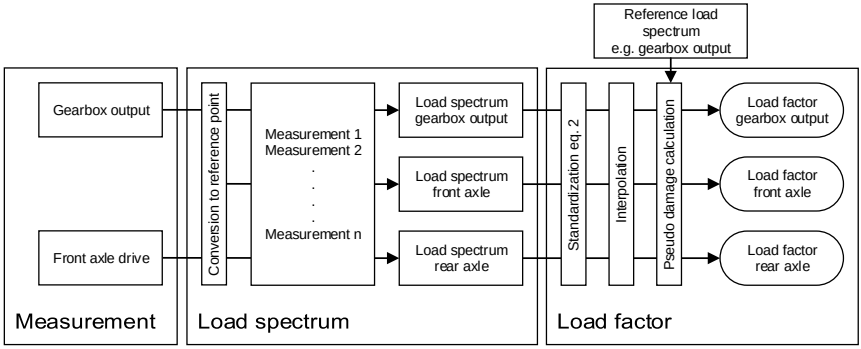

Fig. 4: Procedure of load based machine evaluation

Since it is difficult to determine the S-N curve for real component assemblies, a fictive S-N curve with a slope exponent from the “Forschungskuratorium Maschinenbau” (FKM)-guideline for ferrous and cast materials is used [10]. While the Miner’s rule assumes $D \leq 1$, pseudo damage scenarios can reach higher damage sums. Because the fictive S-N curve is only used to relate different load classes to each other, L can reach values ≥ 1. Measured load spectrum and reference load spectrum are compared to the same fictive S-N curve, which makes the absolute position of the curve irrelevant. Analysis is done in analogy to the Miner’s rule. Calculation of quotients of load sums from Eq. 3 result in a dimensionless number which is called load factor. The LF is calculated individually for each assembly. An all-encompassing tractor LF can be generated by individual weighting of assemblies.

5. Results and Discussion

The drive wheel load spectrum of a tractor with CVT has been measured during 5 days of heavy pull operation and reduced to t11 and t12 which covers 6.18 h of field work. Results are shown in Figure 5. Curve 1a represents the overall tractor load spectrum, curve 2a the front axle and curve 3a the rear axle. All curves are standardized and related to the driving wheel. The reference curves 1b-3b are adapted from Renius' 10,000 h tractor lifetime and Meiners' front axle load spectrum [5; 7]. The original curves have been developed for tractors with manual transmission and clutch operation and show higher portions of load peaks compared to curves from CVT tractors. Load peaks in CVT tractors mostly come from field work. For this reason the original curve has been reduced by 0.8. The measured curves are shifted more to the right side of the load spectra which means higher loads at higher number of load cycles. Curves measured below 10 % frequency have lower gradients than the reference curves due to missing load peaks of clutch and shifting operation.

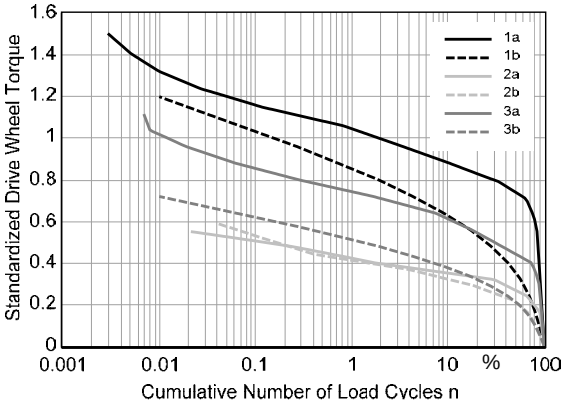

Fig. 5: Standardized load spectrum of a heavy pull application for drive wheel side with reference load spectrum, adopted from [5; 7]. 1a = Overall load spectrum, 1b = Overall reference, 2a = Front axle, 2b = Front axle reference, 3a = Rear axle, 3b = Rear axle reference.

Assuming tractor axle load distribution of 40 % front axle load, a slope exponent for iron and cast materials of k = 5, and an axle efficiency of $\eta_{front\ axle} = 0.93$ and $\eta_{rear\ axle} = 0.95$ in the previously described pseudo calculation results in the following LFs:

- Tractor overall load spectrum (Gearbox output): 4.52
- Front axle load spectrum: 0.89
- Rear axle load spectrum: 7.59

These LFs provide means to weight tractor operation hours. For example 1 hour of heavy pull operation under these condition equals 7.59 “standard” operation hours for the rear axle. In other words, a tractor which was designed to resist 10,000 h of the rear axle reference spectrum 3b, shown in Figure 5, would have reached its expected lifetime on the rear axle after $\frac{10{,}000\ \text{h}}{7.59}$=1,317 h. This shows a high load on the whole tractor during heavy pull applications. But these LFs are calculated only for the effective time frames t11 and t12 of field work [8] which cause the highest loads on the tractor. Idle times at low loads due to fault time t2 and non-productive time t3 also contribute to the tractor lifetime load spectrum and increase the overall tractor operation hours.

6. Conclusions

With the example of ploughing a new method has been introduced to evaluate the actual physical condition of tractor assemblies by comparing past loads to a reference load spectrum. The author uses load spectra from literature as reference and performs a pseudo damage calculation. Ideally the reference load spectra equal those used for assembly design. Further applications and analysis of engine and pto will follow. The method needs a reliable and low cost torque measurement to become adopted by tractor series production. Promising approaches have been shown by Wieckhorst et al. [11]. Calculated LF can help to gain transparency and relate tractor operation hours to a reference operation hour. This provides additional information of past tractor loads and gives the opportunity to evaluate tractors more precisely by considering the real stress the tractor experienced.

References

[1] • Boog, M.: Steigerung der Verfügbarkeit mobiler Arbeitsmaschinen durch Betriebslasterfassung und Fehleridentifikation an hydrostatischen Verdrängereinheiten. Dissertation KIT Karlsruhe 2010, Karlsruher Schriftenreihe Fahrzeugsystemtechnik, Reihe 4. Karlsruhe 2010.

[2] -,-: DIN 31051: Grundlagen der Instandhaltung. Berlin: Beuth-Verlag, 2010.

[3] Rice, T. D.; Janasek, C. G.; McKinzie, K. K. and Ziskovsky, D. J.: Arbeitszyklusaufzeichnungssystem und Verfahren zum Schätzen des Schadens und der verbleibenden Lebensdauer von Antriebsstrangkomponenten. German Patent Application. DE 102015214357A1, 04.02.2016.

[4] • Radaj, D.: Ermüdungsfestigkeit. Berlin/ Heidelberg: Springer-Verlag 2003.

[5] • Renius, K. T.: Last- und Fahrgeschwindigkeitskollektive als Dimensionierungsgrundlagen für die Fahrgetriebe von Ackerschleppern. Düsseldorf: VDI-Verlag 1976.

[6] -,-: ISO 6336-6: Calculation of load capacity of spur and helical gears: Calculation of service life under variable load. Geneva: ISO-Verlag, 2006.

[7] Meiners, H.-H.: Die Beanspruchung einzelner Schlepperaggregate bei unterschiedlichen landwirtschaftlichen Arbeiten. Landtechnik 39 (1984) No. 10. pp. 438–441.

[8] Reith, S.; Frisch, J. and Winkler, B.: Revision of the Working Time Classification to Optimize Work Processes in Modern Agriculture. Chemical Engineering Transactions 58 (2017) in print.

[9] Biller, R. H.: Ermittlung von Gesamt-Lastkollektiven für Ackerschlepper. Grundlagen der Landtechnik 31 (1981) No. 1. pp. 16-22.

[10] -,-: Rechnerischer Festigkeitsnachweis für Maschinenbauteile aus Stahl, Eisenguss- und Aluminiumwerkstoffen. Frankfurt am Main: VDMA-Verlag, 2012.

[11] Wieckhorst, J.; Fedde, T., Frerichs, L. and Fiedler, G.: Integrated Measurement of Tire Soil Parameters for Tractors. In: VDI/MEG-Tagung Landtechnik 6./7.11.2015 Hannover. In VDI-Berichte 2251. Düsseldorf: VDI-Verlag 2015, pp. 219–226.

Predict the unpredictable

Benefits and limits of machine data analytics and component health prediction

Daniel Hast, **Benjamin Rosenbaum**, Bosch Rexroth AG, Dortmund

Abstract

Vehicle uptime during the lifecycle largely depends on the right component design as well as timely maintenance and service. From an engineering perspective, the basis for replacing guesswork by prediction is precise knowledge of both the load cycles and wear conditions of the vehicle and its components. Monitoring load cycles, trends, deviations and structural borne sound and their correlation to component fatigue data are today's tools to gather instantaneous insights to machine health beyond common tracking of machine hours. To collect and analyze these data automatically along with the necessary modelling of product knowledge becomes much easier within a connected solution. Moreover, it is applicable to entire fleets instead of single "wired" vehicles. In this contribution, we highlight engineering procedures and algorithms for connectivity supported analytics to predict component health and residual lifetime. Besides lifetime prediction, these comprehensively processed smart data sets also deliver engineering-ready real world specs for next generation vehicles to R&D departments.

The challenge: Thrusting assumptions by knowledge to optimize lifecycle cost

The lifecycle of machines along with facilitating productivity brings forth lifecycle cost from engineering, operation, maintenance and more stages. The cost at each stage of the lifecycle are typically associated to each other [1]. An example for this is the overdesign of components that shall ensure low maintenance cost and high durability. While reducing operational cost this gives rise to cost in production and engineering. The common approach to keep those cost at a reasonable level is based on experience and assumptions, such as for the common definition of maintenance intervals based on operating hours. If more knowledge was available, more robust and less risky decisions could be made. If for example, the health status of a machine and its components was known at every time, maintenance could be optimized in terms of cost and risk. Boosting knowledge requires the mapping of technical knowledge into models and the acquisition of machine data [2]. In the following, we propose a set of appropriate modelling techniques and show how this becomes

possible in a connected infrastructure for mobile machine components. In this frame, we focus on predictive diagnosis as prerequisite for condition based predictive maintenance and on the beneficial aspects of enhanced knowledge in the perspective of engineering. Regarding the global variety of machinery and operational conditions in addition, the existence of limitations in terms of predictive statements becomes self-evident. Beyond the proposition of Bosch Rexroth's framework for prediction, we will also illustrate some of the limitations of predictive statements that are known nowadays.

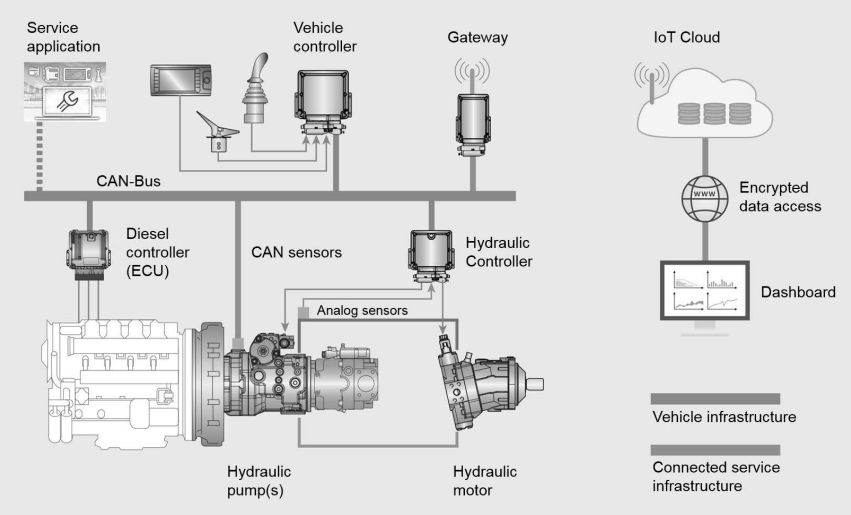

Fig.1: Basic structure of a connected hydrostatic drivetrain in a mobile machine

As a basis for our considerations, **Fig.1** shows the basic structure of a connected hydrostatic drivetrain in a mobile machine to which we refer to as the Internet of Things (IoT) infrastructure in the future.

Boosting knowledge representation by joining models and data

Four groups of basic techniques to join machine data and engineering knowledge form the framework of our analytics. **Fig. 2** provides an overview of these groups, incorporating load-cycle evaluation, analysis of structure-borne noise, trend analysis and functional diagnosis. By comparing measured load cycles with reliability models, the statistically remaining useful lifetime, for instance for the main bearing of a pump, can be determined [2]. In addition, load collective data recorded in the field are utilizable as a sound basis for future product

generations. The structure-borne noise evaluation by e.g. pattern recognition algorithms complements the analysis methods and allows for insight to mechanical changes throughout the lifecycle [4].

Fig. 2: Foundational analytics techniques for predictive diagnosis in PredictDrivetrain

The cloud-based storage of historical data makes it possible to observe and analyze long-term trends. The analysis of trends in known signs of damage allows for predicting when failure is likely to occur [1]. Functional diagnosis helps to recognize known faults, which are identified with the help of diagnostic algorithms based on local operating data history [3]. The execution of evaluation algorithms can take place spread out over different levels (domain controllers, gateway, and cloud) to overcome limitations in terms of data transfer and computational requirements.

Predictive diagnosis of machine components

PredictDrivetrain is a smart service by Bosch Rexroth that automatically processes sensor data and provides the basis for predictive maintenance [1]. The goal is to exploit the full potential of machine components and at the same time identify wear-induced faults before they cause failure. Our approach combines product and application expertise with diagnosis and data-mining analytics to detect and to predict fatigue and wear trends [3]. In order to employ the beneficial properties of the available resources, we work within a connected infrastructure with distributed intelligence for networking components along the entire data processing chain – from the single sensor to the cloud. The IoT infrastructure along with PredictDrivetrain ensures that appropriate maintenance action can be foreseen and triggered appropriately. The infrastructure comprises three main elements: An application-specific set of sensors to process the relevant operating data, high-performance electronics with local software components to monitor machine characteristics and a comprehensive, cloud-based smart service that incorporate the analytics. The service evaluates sensor data acquired directly or indirectly at the machine subsystems such as the hydraulic travel drive or the diesel engine (Figure 1). Based on this data, analysis methods calculate the current condition and the remaining expected service life of the components. While in operation, load cycles are calculated and processed as input to durability models of the components for example

[2]. Deviations from normal behavior are also determined as well as local and global trends. Furthermore, pattern recognition models evaluate structure-borne noise signatures [4]. The current component health status is determined by blending the results of all these techniques. The results are either displayed to the user via a web-based dashboard or made available using predefined interfaces and protocols via inter-cloud services. The distributed computing blends into existing connectivity solutions in every part of the infrastructure. Thanks to modular design and the usage of open standards, various evaluation functions are available at the different system levels. By that, important information about the condition of the hydraulic components can also be adapted in the operating strategy according to the respective scenario.

Gaining knowledge in an engineering perspective

A solution that acquires the loads of a single vehicle or multiple vehicles within a fleet and generates detailed evaluations of load data is Bosch Rexroth's smart service NextGenSpec [1]. This significantly simplifies design and dimensioning of vehicle components for future generations of the vehicle. The service relies on the available sensor signals in the vehicle and utilizes physical models that represent the relation between loads and the sensor signals. The captured scenarios are differing in their scope of load data as well as in their accuracy. For example, highly precise statements about the drive torque can be derived with the help of pressure signals in the hydraulic drivetrain. A 5-axis inertia sensor is required to describe the full system loads such as the dynamic load of radial and axial tire forces in the case of a wheel driven vehicle. For vehicles with varying vehicle weight, like a combine harvester with integrated grain tank, a fill level sensor helps to improve accuracy. Additional knowledge can be achieved by further signals such as travel speed, pressure or tank volume as well as the geographical position of the vehicle. From the sensor data, the forces at the wheel contact points are determined as a first step. From these, the mechanical stress of various components in the drivetrain can be estimated using normal geometric relations. The load data can be prepared for the user in different ways.

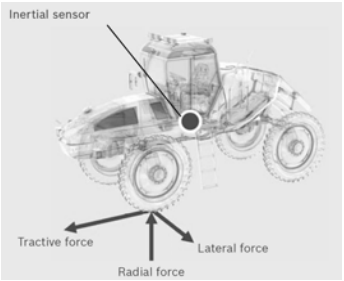

Fig. 3: Derivation of tire contact forces

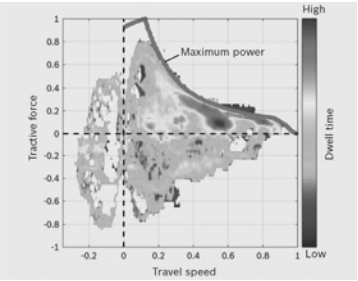

Fig. 4: Travel drive 2D histogram

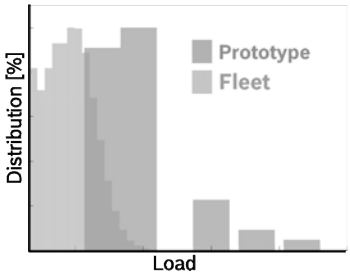

Fig. 5: Stress collectives of a prototype compared to fleet average.

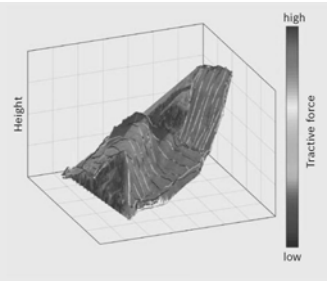

Fig. 6: Geo-mapping of the vehicle load

For example, the load distribution in a travel drive diagram can be directly displayed (**Fig. 4**) and incorporated for reliability calculations. Those are possible with the help of material fatigue curves. The correlation of load data with geographical information allows for geo-mapping of the recorded load data. This facilitates the validation of field data in order to take into account regional influences (**Fig. 6**) and the collection of knowledge from whole fleets (**Fig. 5**). Detailed knowledge, incorporated during the engineering phase allows for avoiding under- or oversized components and hence for efficient design and dimensioning.

Recent limitations of predictive statements

Predictive statements, concerning the health status of machines or concerning the load distribution for future product generations are limited in general [1]. Recent limitations are due to many influences, such as statistical or numerical issues as well as incomplete observations for example. In this contribution, we display the limitations of model-based analytics with the example of the machine traction force.

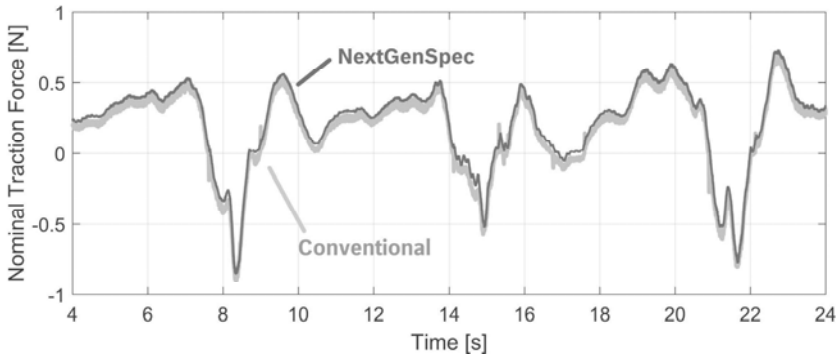

Fig. 7: Comparing conventional measurement of traction force to NextGenSpec Results

Consider here the direct and costly measurement using a strain gauge applied wheel force transducer compared to a model based method, based on pressure measurements [1]. **Fig. 7** shows, that within a representative drive-cycle, the deviation between the directly measured signal and the signal determined by NextGenSpec is below 5%. This deviation is due to unknown environment variables in the computation such as hose expansion or magnetic hysteresis of control valves. Although, model-based predictive statements are limited nowadays, the advantages of more representative results as displayed in Figure 5, and lower cost commonly justifies their utilization and make them a powerful tool to thrust assumptions by knowledge.

Conclusions

The combination of machine data and deep product knowledge enables more efficient design and maintenance. Due to recent developments, mobile machines are prepared to be a part of the internet of things and to host smart services. Those lead to reduced cost over the entire machine life cycle.

- By predicting upcoming faults in machine components, PredictDrivetrain provides the basis for predictive maintenance. This enables service just in time, which prevents unforeseen outage and allows for efficient exploitation of resources.
- The allocation of detailed and engineering-ready data, which is core of NextGenSpec, enables drastically simplified and deterministic design and dimensioning of vehicle components. Furthermore, the service accelerates the validation of prototypes.

The smart services PredictDrivetrain and NextGenSpec by Bosch Rexroth can be joined with any cloud-based solution via open interfaces, which is the basis for easy scaling from a prototype to whole fleets.

References

[1] Glasbrenner, P., Beuter, B., Hast D. and Gombos, A.: Smart services – Added Value throughout the complete life cycle; Perspectives and Dialogue: Next level of Safety, Efficiency and Automation, MOBILE 2017, Augsburg (2017), Bosch Rexroth AG, pp. 133-141

[2] Boog, M.: Steigerung der Verfügbarkeit mobiler Arbeitsmaschinen durch Betriebslasterfassung und Fehleridentifikation an hydrostatischen Verdrängereinheiten. Karlsruhe Institute of Technology (KIT) Diss. 2010

[3] Hast D., Findeisen R. and Streif S.: Detection and isolation of parametric faults in hydraulic pumps using a set-based approach and quantitative-qualitative fault specifications. Control Engineering Practice 40 (July 2015), pp. 61-70

[4] Torikka, T.: Bewertung von Analyseverfahren zur Zustandsüberwachung einer Axialkolbenpumpe. RWTH Aachen Diss. 2011

Tablet App to control safety critical functions on farming machines

Dipl.-Ing. **Kai Oetzel**, CLAAS E-Systems, Dissen a.T.W.

Abstract

Since the introduction of the first iPhone in 2007 and the first iPad in 2010 the utilization of smart devices became common in large parts of private and professional life.

A continuously growing number of apps in the agricultural sector support the farmer in different areas and activities of his business. Smartphones and tablets are found today in nearly each cabin of an agricultural machine. Farmers are using smart devices to communicate with each other, control logistics, check the weather or document their activities on the go.

Because of the high number of smart device already utilized in agriculture, farmers raised the question, why they cannot use their existing tablets also to control working machines as a replacement for dedicated control terminals.

Following this demand, CLAAS developed a concept, how to utilize a tablet app as user interface to control agricultural machines attached to a tractor. The developers needed to overcome several technical challenges as part of this concept:

- A consumer tablet has not interface to the CAN Bus of the machine. Thus, a additional hardware as gateway between the CAN bus of the machine interface and the tablet needs to be developed.
- To control machines regardless of their brand, the tablet app needs to follow the ISO 11783 (ISOBUS) standard.
- Machine functions operated by the tablet app maybe harmful for the operator or people near to the machine. Thus, the tablet app needs to comply with functional safety guidelines of the AEF based on the ISO 25119

As a result of this effort an ISO 11783 compatible universal terminal (ISO UT) was realized as tablet app and an additional hardware component (CLAAS wireless interface) that connects the tablet to CAN bus of the machine.

1. Functions of a ISO Universal Terminal (UT) according to ISO 11783

The ISO 11783 „Tractors and machinery for agriculture and forestry – Serial control and communications data network“ or short “ISOBUS” is a standard to define a communication protocol between tractors or other self-propelled machine and implements attached.

One part of the standard provides a protocol for agricultural machines to be controlled by the machine operator via a universal terminal that also implements the ISO 11783. The terminal works similar to a web browser displaying graphical information (data mask and soft keys) of the attached implement and transfers user interactions on soft keys and certain parts of the data mask back to the implement. For a better usability the ISOBUS standard allows the universal terminal to assign certain machine interactions from the terminal to haptic elements like switches, joysticks or buttons which also have to follow the ISO 11783. These elements are called auxiliary devices (AUX).

Additionally the ISO 11783 provides a data format that allows data exchange between the "ISOBUS" on the machine and the farm management information system (FMIS). This exchange comprises mainly data related to work records of jobs operated by the machines (e.g. machine counters, amounts, totals, working time, GPS tracks etc.). Because this data format is based on the XML standard it is called "ISOXML".

Fig. 1 shows all components according to the ISO 11783 on the machine.

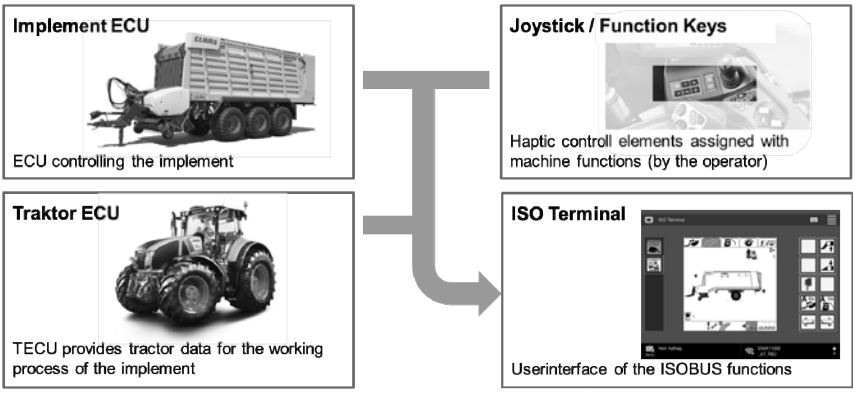

Fig. 1: Components of the ISOBUS

2. Motivation for the realization of an ISO terminal as tablet app

Due to the fact that tablet computers are common companions for farmers and machine operators also in the cabin of a tractor, CLAAS had the idea to provide machine operation as a tablet app.

Beside the idea of re using a device that is already in the farmer's hand, a tablet computer provides several benefits compared to dedicated ISO terminal devices:

- Simplify maintenance and failure identification at the implement through wireless operation
- Wireless exchange of job data with FMIS (Farm Management Information System)
- Machines are online with no extra effort -> Farming 4.0
- High tablet computer population in the farming sector (e.g. controlling/observing biogas plants, fleet management, checking weather forecast etc.)
- Big screen with high resolution and touch operation at comparable low price (consumer device)

3. Functional safety requirements to an ISO universal terminal

Since an ISO universal terminal can be used to control every implement that follows the ISOBUS standard it is obvious that this can also cover implements which can do harm to people near to it in case of wrong operation of malfunction.

Because of this potential risk manufacturers of agricultural machines are supposed to follow the standard ISO 25119 “Tractors and machinery for agriculture and forestry -- Safety-related parts of control systems”. The ISO 25119 provides a classification of machine functions in terms of:

- Potential harm: S0 (No significant injuries) to S3 (Life-threatening injuries)
- Exposure to the hazardous event: E0 (Improbable) to E4 (Frequently)
- Possible avoidance of harm: C0 (Easily controllable) to C3 (none)

After rating each of these aspects the results will be used to calculate the “agricultural performance level” ($AgPL_R$). The $AgPL_R$ provides a set of values (a, b, c, d, e) where “*a”* is lowest and “*e”* is the highest level.

Each $AgPL_R$ requires a special set of measures that need to be considered while constructing and implementing the electronic control function of the rated feature. These measures are derived from the determination of:

- Hardware Category (HW Cat.): 1, 2, 3, 4
- Diagnostic coverage (DC): low, medium, high
- Software requirements level (SRL): B, 1, 2, 3
- Mean Time To dangerous Channel Failure ($MTTF_{dC}$): low, medium, high

The relation between the AgPL, HW Cat, DC, $MTTF_{dc}$ und SRL is shown in **Fig. 2**

AgPL	Software Requirement Level (SRL)				
a	1	B	B	B	B
b	2	1	B	B	B
c		2	1	1	1
d			2	2	2
e					3
HW Cat.	Cat. B	Cat. 1	Cat. 2	Cat. 3	Cat. 4
DC	low	medium	medium	medium	high

$MTTF_{dC}$=low $MTTF_{dC}$=medium $MTTF_{dC}$=high

Fig. 2: Relation between the AgPL, HW Cat, DC, $MTTF_{dC}$ und SRL

Fig. 2 makes it obvious that e.g. an AgPL=b can be reached either with SRL=2, HW Cat.=B, DC=low, $MTTF_{dC}$=medium or with SRL=B, HW Cat.= 2, DC= medium, $MTTF_{dC}$=low. Thus increasing e.g. the software requirements level gives the opportunity to decrease the hardware category. This fact is especially important when designing a control unit as part of a safety critical function utilizing a consumer hardware like a tablet computer.

Because an ISO universal terminal may be part of the safety critical path of a function with AgPL=a and higher as the control unit for the operator, the AEF (Agricultural Industry Electronics Foundation) created a guideline [1] how to apply the ISO 25119.
The guideline defines that an ISO universal terminal can only be used as control unit for safety critical features with the maximum of AgPL=b. It may be used for AgPL=c, but only with an additional hardware control unit provided by the machine manufacturer (e.g. switch). For AgPL=d and AgPL=e an ISO universal terminal cannot be used. Here the machine manufacturer needs to provide a separate control unit, designed specifically to meet the AgPL of this machine function.

4. Realization of the AEF guideline for the ISO 25119 with a tablet app

Before answering the question if and how the AEF guideline for the ISO 25119 can be met with an ISO universal terminal realized on a consumer device the side conditions have to be made clearer.

For systems with $AgPL_R$<=b where an ISO universal terminal is part of the complete system as control unit the AEF guideline defines the parameters as in **Fig. 3**.

	Complete system	ISO Universal Terminal
Hardware category:	Cat = 2	Cat = 1
Software requirement level:	SRL = B	
Diagnostic coverage:	DC = medium, 60% ≤DC < 90%	
Mean time to failure	MTTFd= low, ≥3 years	MTTFd= mittel, ≥10 years

Fig. 3: Requirements for the complete system with $AgPL_R$ <= b

After analyzing if HW Cat.=1, SRL=B, DC=Medium and $MTTF_{dC}$=medium can be realized with a consumer device we found the result in **Fig. 4**.

The analysis in **Fig. 4** made clear, that an ISO universal tablet can only be realized on a consumer device with an additional hardware component that provides an appropriate HW Cat., SRL, DC and $MTTF_{dC}$.

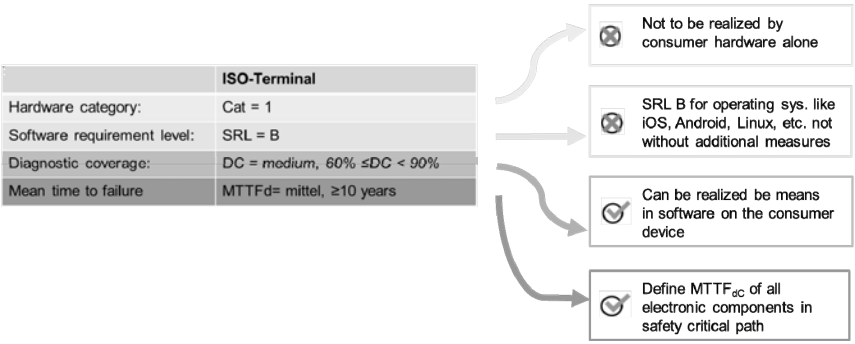

Fig. 4: Determination of safety parameters for realization on consumer device

5. CLAAS Universal Terminal on Tablet (CUTT)

After the clarification that an additional hardware is required to fulfill the functional safety requirements with an ISO universal terminal on a consumer tablet the complete system needed to be designed. The hardware component was called CLAAS wireless interface (CWI).
In the first design approach the CWI has the following main functions:

- Bridge the ISOBUS data from the CAN bus on the machine over WLAN to the tablet
- Realize a control unit for the consumer tablet and cut the ISOBUS connection when necessary.

To come to a complete set of safety requirements for both the CWI and the software on the consumer tablet, two steps where performed:

1. The definition of system boundaries
2. A failure mode and effects analysis (FMEA)

With the results from the FMEA all technical safety requirements could be developed according to a structured process illustrated in **Fig. 5**.

Fig. 5: Proceeding for the development of the safety concept for the CUTT

The resulting safety architecture could fulfill all functional safety requirements.

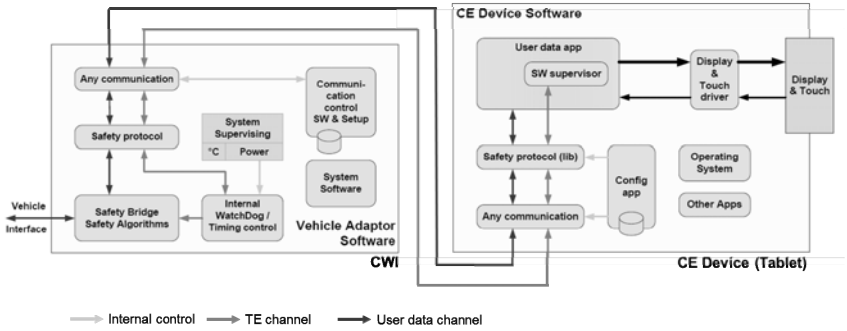

Fig. 6: Safety architecture

6. Summary and outlook

Opportunities and benefits:

- The operation of implements and the acquisition of job data with a tablet offers a high value for the customer compared to conventional terminals (online connection)
- The tablet solution is attractively priced. The customer can re use existing hardware.
- The possibility of software updates via appstores allows fast release cycles.
- The customer participates in the fast advancement of tablets and can always use actual hardware.

Disadvantages:

- Ensuring a deterministic runtime behavior on OS such as iOS or Android is only possible to a limited extent.
- Implementation effort: additional hardware, assurance of SRL 1, specific challenges of CE Device OS

Risks:

- Changes in CE Device OS (e.g. annual iOS updates) and possible bugs cannot be foreseen.

References

[1] AEF Guideline ISO 25119 Chapter 6.1, page 2 & chapter 6.2, page 3

On-line monitoring of nutrients (NPK) in liquid manure by a nuclear magnetic resonance (NMR) sensor installed at a slurry spreader

Post doc **Morten K. Sørensen**[1], Research Engineer, Ph.D. **Michael Beyer**[2], CEO **Ole Jensen**[2], Scientific Engineer, Ph.D. **Oleg N. Bakharev**[1], Dean **Niels Chr. Nielsen**[1], Senior Advisor **Tavs Nyord**[3],

[1] Interdisciplinary Nanoscience Center (iNANO) and Department of Chemistry, Aarhus University, Aarhus,Denmark;
[2]NanoNord A/S, Skjernvej 4A, Aalborg Ø, Denmark;
[3]Department of Engineering, Aarhus University, Aarhus, Denmark

Abstract

Knowledge of the actual content of nitrogen, phosphorus, and potassium (NPK) in animal liquid manure (slurry) is highly important to optimize crop production and avoid environmental pollution when slurry is spread on agricultural fields. Here, we present a mobile, low-field nuclear magnetic resonance (NMR) sensor suitable for on-line monitoring of the NPK content in animal slurry as an alternative to crude estimates or tedious non-specific, off-site laboratory analysis. The sensor is based on ^{14}N, ^{17}O, ^{31}P, and ^{39}K NMR employing a digital NMR instrument with a 1.5 T permanent magnet (Halbach type). This setup enables direct detection of ammonium N, total P, and K, and indirect evaluation of the organic N content, covering all practical components of NPK in animal slurry. In correlation laboratory studies, the obtained NMR measurements show good agreement with reference measurements from commercial laboratories, and with the sensor mounted on a commercial Samson PGV 20 slurry tanker, the sensor performance have been demonstrated both when the tanker was standing still and moving as during normal operation.

Background

Huge amounts of animal slurry (liquid manure) are produced from intensive livestock farming every year. Generally, animal slurry is applied as fertilizer to agricultural fields, which implies a possible source to pollution of the environment if overdosed. In order to optimize plant yields and minimize environmental effects, it is of immense importance to know the actual composition of the slurry and thus be able to apply the right amounts of nutrients on the fields. Some of the most important parameters are the contents of ammonium N, total N, total

P, and K. In general, the content of NPK in animal slurry is highly variable depending on animal type, feeding strategy, season, storage conditions, and sedimentation in storage tanks which imply highly inhomogeneous distributions even in the same tank of slurry. Chemical characterization using standard laboratory methods at the best, only provides averaged information masking intrinsic big variations, and they are time consuming, costly, impractical, and in particular measurements of total N and total P contents are demanding due to essential pre-degradation of the solid fractions. Therefore, the amount of NPK nutrients delivered to the fields through spreading of animal slurry is today mainly determined on the basis of standard values based on general information on animal and housing type, without accurate knowledge of the potential fertilizer value or environmental impact.

Addressing these challenges, we propose a nuclear magnetic resonance (NMR) sensor suitable for on-line monitoring of NPK in animal slurry directly at, for example, slurry spreaders, slurry trucks during transportation, or in storage tanks. This sensor should be seen in context of previous extensive research in rapid monitoring of nutrient values which mainly have led to methods relying on measurements of electric conductivity[1–3] or near-infrared spectroscopy[4-6]. Opposed to these techniques, NMR offers direct measurements of NPK in all types of animal slurries without any sensitive parts in contact with the slurry media and without calibration requirements on the user side or choice of slurry type before measurement.

Material and method

The essential parts of the NMR sensor for NPK monitoring is shown in Fig. 1a (prototype version), and consists of a cylindrical Halbach magnet with a static magnetic field of 1.5 T, a digital field-programmable gate array (FPGA) console, a 400 W power amplifier, and a shielded probe with a radio-frequency (rf) solenoid coil with an inner diameter of 9.2 mm. To minimize drift of the permanent magnetic field, the hardware is assembled in a temperature-controlled cabinet with a fixed temperature stabilized to a deviation of less than about ± 0.1 °C. Further details for the laboratory prototype are given in Ref. 7-8.

While the sensor setup is suitable for measurements with the sample flowing directly in the probe bore, for demonstration purposes we used test samples in tubes of perfluoroalkoxy alkane (PFA) with an outer/inner diameter of 9/8 mm and a sample length of about 120 mm as shown in Fig. 1b.

To unravel the organic fraction of nitrogen, we apply ^{17}O NMR. We assume that the ^{17}O NMR intensity is correlated to the content of water and thus dry matter, and based on laboratory analysis of different animal slurries the content of organic N correlates well to the dry matter content[8]. Following this, the content of organic N can be evaluated from the ^{17}O NMR signal,

and the total N content in the animal slurry is obtainable as the sum of ammonium N and organic N.

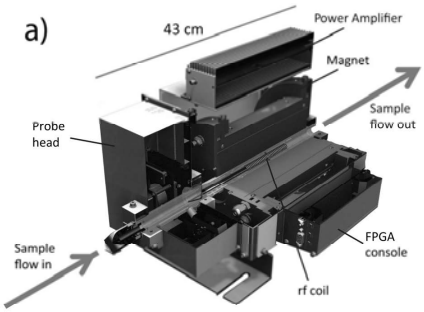

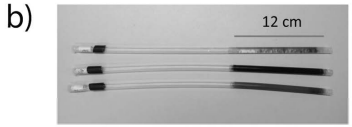

c)

	Spin	Abundance	Sensitivity	Frequency
^{14}N	1	99.6%	1.01	4.6 MHz
^{17}O	5/2	0.037%	0.011	8.7 MHz
^{31}P	1/2	100%	66.3	26.0 MHz
^{39}K	3/2	93.1%	0.473	3.0 MHz

Fig. 1: (a) Illustration of the NMR sensor with the probe bore and NMR coil in the centre of a compact setup with magnet, probe, FPGA, and power amplifier shown around it. (b) Three examples of the sample tubes with animal slurry (samples 1, 8, and 9 defined in SI) used for demonstration. (c) Table of characteristics for the four relevant isotopes, including nuclear spins, natural abundances, NMR sensitivities relative to 1000 for ^{1}H, and the resonance frequencies at 1.5 T. Adapted from Ref. 8.

To demonstrate the performance of the proposed NMR sensor for measurements of NPK in animal slurry, we performed ^{14}N, ^{17}O, ^{31}P, and ^{39}K NMR measurements of 40 test samples in the laboratory, and corresponding commercial NPK analyses were obtained from five external laboratories for comparison with currently common practice. Samples of 16 animal slurries were collected from Danish farms and biogas plants, and included five slurries from cattle, five from pigs, three from mink, and three anaerobically co-digested slurries from biogas plants. Care was taken to find different slurries to ensure a good representation of such slurries in general. Duplicate samples were made for all 16 slurries to give 32 slurry samples. In

addition, eight NPK solutions of NH_4Cl, K_2HPO_4, KH_2PO_4, and KCl dissolved in water were included to yield a total of 40 samples (see details and an overview of all samples in Ref (. Aliquots of each sample were packed in PFA tubes (inner diameter 8 mm, and sample length 120 mm) for NMR experiments, and in 500-1000 ml containers for external laboratory analysis. All samples were kept cold (2-5 °C), and the sample containers for the laboratories were sent with cooling items in insulated boxes. Laboratory results were obtained for dry matter, ammonium N, total N, total P, K, and pH. Half of the samples (with randomized sample numbers) were sent for laboratory analysis three weeks after analysis of the first samples.

For field trials, a new generalized commercial version of the sensor (Tveskaeg NMR sensor by Nanonord A/S) was mounted on a commercial Samson PGV20 slurry tanker. This sensor enables full-automatic detection of all relevant isotopes on the sensor without manual actions. To demonstrate the performance and robustness of the NMR sensor during field operation, NPK measurements with this setup were performed for comparison of stationary NMR measurements (connected to wall power outlet) and field measurements (power from tractor) with the sensor running on a slurry spreader in operation. For the latter, measurements were performed both with the tractor/spreader standing still and while driving at a bumpy ground.

Results

While the mean values of ammonium N, total N, total P, K, and pH analyzed at the five different commercial laboratories showed no significant difference between duplicate samples, considerable uncertainties were observed on the individual laboratory results.[8] Based on the results for all samples, standard deviations between individual measurements and the mean of the measurements for each sample were 0.25 g/l for ammonium N, 0.19 g/l for organic N (without the eight samples of NPK solutions), 0.18 g/l for total P, and 0.16 g/l for K. Generally, large deviations on external laboratory analysis are particular observed for organic N and total P in the slurries following large solid fractions and challenging subsampling at the laboratories due to the inhomogeneous distributions of the nutrients (in turn, this emphasizes the need of on-site analysis of a relative large fraction of the slurry as enabled by an on-line NMR sensor). Results obtained at the NMR sensor showed good agreement with the mean results from the five commercial laboratories. For the set of 40 smaples the standard deviation between NMR and laboratory results were 0.28 g/L for ammonium N, 0.26 g/L for organic N, 0.20 g/L for total P, and 0.51 g/L for K (see Fig. 2).[8]

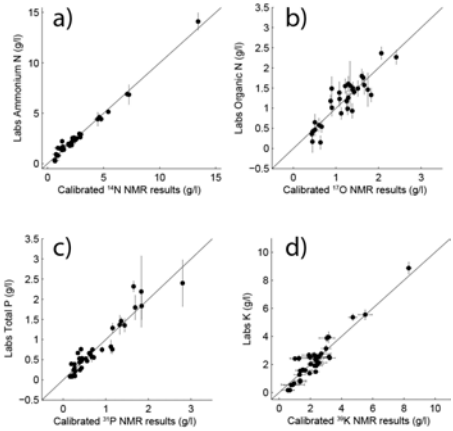

Fig. 2: Calibrated NMR intensities (horizontal) correlated to reference measurements from commercial laboratories (vertical). (a) ^{14}N NMR versus ammonium N, (b) ^{17}O NMR versus organic N obtained as total N minus ammonium N, (c) ^{31}P NMR versus total P, and (d) ^{39}K NMR versus K content. Vertical error bars show the obtained standard deviations on the laboratory analysis, whereas the horizontal error bars plotted for a) and d) show the standard deviations obtained for measurements at five and six NMR sensors, respectively. Vertical (a,b,c,d) and horizontal (a,d) error bars are plotted for all data points although some are to small to be visible. Adapted from Ref. 8.

Aiming at a measurement time of about 5 minutes, the precision was estimated for on-line measurements utilizing the full sample volume. Based on the present results we found standard deviations of 0.23 g/l for ammonium N, 0.27 g/l for organic N, 0.20 g/l for P, and 0.76 g/l for K with effective measuring times of 3.7 min for ammonium N, 3.5 min for organic N, 3.3 min for P, and 4.4 min for K.[8] In comparison, for ammonium N, organic N, and P, these deviations on the NMR results are similar to the deviations on the individual laboratory results.

Field trials showed no significant difference in NMR measurements whether analysis where performed in a stationary (laboratory) environment or with the sensor operating at a driving slurry spreader. For visualization, Figure 3a shows a series of NPK measurements performed with the NMR sensor under various conditions (stationary, on spreader, and on spreader while driving), whereas Fig. 3b illustrates the position of the installed sensor in the cabinet on the side of the spreader.

Full-scale evaluation of the accuracy and precision including automatic sampling from the tank of the spreader are planned in near future.

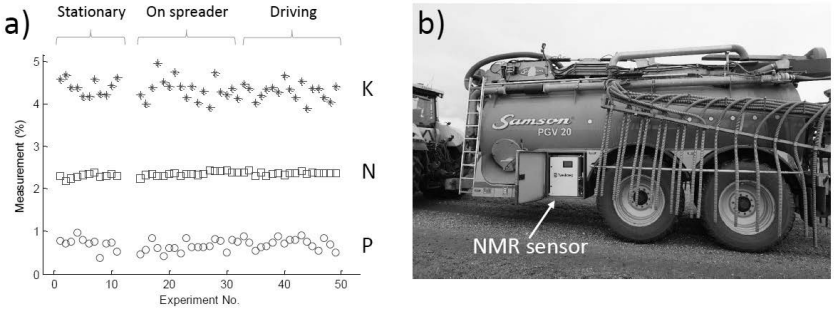

Fig. 3: Measurements with NMR sensor installed at slurry spreader. (a) ^{14}N NMR (sqaures), ^{39}K NMR (stars), and ^{31}P NMR (circles) measurements of NH4-N, K, and P, respectively. Several measurements were performed in three different scenaria as indicated above the plot; 'Stationary' with the sensor connected to wall power outlet, 'On spreader' with the sensor installed at the spreader with power from tractor, and 'Driving' with the additional condition of driving with the spreader/tractor simulating a typical work situation. Each measurement was here performed over 15 s for N, 28 s for K, and 26 s for P using an NPK test-sample solution. (b) Picture of the NMR sensor in operation at slurry spreader.

Conclusion

We have developed a robust, multinuclear NMR sensor suitable for on-line analysis of NPK in animal slurry. Measurements of the ammonium N, organic N, total P, and K contents have been demonstrated in good agreement with external laboratory analysis, and the performance of the sensor when installed on an operating slurry spreader have demonstrated showing no loss compared to laboratory tests.

[1] Yagüe, M. R.; Quílez, D. *J. Environ. Qual.* **2012**, *41*, 893–900.

[2] Provolo, G.; Martínez-Suller, L. *Bioresour. Technol.* **2007**, *98*, 3235–3242.

[3] Moral, R.; Perez-Murcia, M. D.; Perez-Espinosa, A.; Moreno-Caselles, J.; Paredes, C. *Waste Manag.* **2005**, *25*, 719–725.

[4] Reeves, J. B.; Van Kessel, J. S. *J. Dairy Sci.* **2000**, *83*, 1829–1836.

[5] Sørensen, L. K.; Sørensen, P.; Birkmose, T. S. *Soil Sci. Soc. Am. J.* **2007**, *71*, 1398–1405.

[6] Chen, L.; Xing, L.; Han, L. *J. Environ. Qual.* **2013**, *42*, 1015–1028.

[7] Sørensen, M. K.; Vinding, M. S.; Bakharev, O. N.; Nesgaard, T.; Jensen, O.; Nielsen, N. C. *Anal. Chem.* **2014**, *86*, 7205–7208.

[8] Sørensen, M.K.; Jensen, O.; Bakharev, O.N.; Nyord, T.; Nielsen, N.C. *Anal. Chem.* **2015**, 87, 6446-6450.

STEP-Water: Information Tool on Sprayer Technology for Water Protection

A way to support sustainable and socially acceptable chemical application

Dr. **P. Hloben**, Deere & Co, Mannheim;
J. C. Rousseau, Berthoud, Belleville;
T. Bals, Micron Sprayers, Bromyard;
Dr. **I. Hostens**, CEMA, Brussels;
Prof. **P. Balsari**, Univ. of Turin, Turin;
Dr. **M. Röttele**, Better Decision; Kandern,
S. Rutherford, ECPA, Brussels

Abstract

An information tool for sprayer technology assessment has been developed by sprayer manufacturers (CEMA) and the crop protection industry (ECPA) as a joined initiative. It aims to provide relevant information for farmers, advisers and other stakeholders with regard to available sprayer technologies, which can serve as enablers to help prevent losses of pesticides to water.

Introduction

The reduction of Plant Protection Product (PPP) losses to surface water is a challenging task for the current intensive agriculture production. The recent issues related to the protection of pollinators, spray drift and its impact on health of inhabitants who live close to farm filed has raised the public interest and stronger the demand to transform the application of agriculture chemicals from an intensive way into a sustainable one. Results from the several studies [1] have shown that optimized sprayer technology can be a key enabler to reduce the risk of PPP losses to water. With the amendment of the EU Machinery Directive in 2009, the aspect of environmental protection has been strengthened. However, the awareness of the role, sprayer technologies can play in terms of water protection still need to be improved. An information tool for sprayer technology assessment has been developed by sprayer manufacturers (CEMA) and the crop protection industry (ECPA) as a joined initiative. It aims to provide relevant information for farmers, advisers and other stakeholders with regard to available sprayer technologies.

Easy Access to Information

Until now, the EU farmers or advisers had very limited access to the objective information about:

- The available sprayer technologies which represent the state of the art and which contributes to prevention of spray liquid losses to the environment water to the information when e.g. purchasing new sprayer, or with regard to upgrading sprayers – retrofitting.

- The information about retrofittability. Not every technology is retrofittable due to boundaries of the legal obligations and complexity. The tool provides information which technology can be retrofittable and under which conditions.

- The minimum legal requirements for sprayers. The tool list technologies obligatory for sprayers when following European standards (CEN) and Global standards (ISO) to comply with the European legislation. This provides the users an understanding of the requirements written in standards and a legal certainty that that they operate a compliant sprayer.

The STEP-water tool allows an instant and free access to the relevant information (see Fig.1).

Fig. 1: Step-Water: Home page with testimonials blocks

Step-Water Tool Structure

The information tool is available online via a web site in several languages and is organized in two modules: a) Field Crop Sprayers and b) Bush & Tree Crop Sprayers (see Fig. 2).

Fig. 2: Step-Water: Selection of the sprayer type – Field and Bush & Tree Crops sprayers

For each type, users are guided through a menu of technology areas which were selected as the biggest sources of the emission of the spray liquid or the concentrated plant protection product. The key areas are: **Filling**, **Internal and External Cleaning**, **Spray Losses**, and **Remnants**. Each technology area is evaluated by about 10 questions. An information “Why” - to use the technology and “What” the technology means is provided.

For each key area there is available a list of the respective technologies, which are categorized as follows:

i) **Required:** (technologies obligatory for sprayers when following European standards (CEN) and Global standards (ISO) to comply with the European legislation.

ii) **Strongly recommended:** these technologies are not currently obligatory, but they are very important to protect water, and may become mandatory in the future.

iii) **Recommended:** In this category technologies are indicated which should be considered by farmers when purchasing a new sprayer. These technologies represent the latest state of the art e.g. variable rate nozzles, active boom control systems or new close transfer systems which allows fast incorporation of concentrated chemicals into the spray tank.

For each technology a short explanation is given including the reasoning with regard to different requirements and recommendations (see Fig. 3). Users of the information tool can indicate if the required technology is available on an existing sprayer, or is intended to be included on a new sprayer.

Fig. 3: Step-Water: Example of list of available technologies for “Internal Cleaning” area

The Assessment and Reports

A summary list of technologies already present on a sprayer with their categorization is available as a quantitative result which can be used for the further considerations. Following rating can be achieved:

- **Sprayer does not meet the current standard requirements –** One or more “Required” requirements for the sprayers were not selected. The sprayer is not compliant with latest standards which represents the state of the art. The user is asked to update his/her sprayer and advised about the retrofittability.

- **Satisfactory** – all of the required minimum standards are met.
- **Good** - the sprayer is equipped with all relevant required technologies and with the some of the strongly recommend (20 -70%)* and recommended (20-50%)* technologies.
- **Excellent** - the sprayer is equipped with all relevant required technologies and with the majority of the strongly recommend (> 70%)* or recommended (>50%)* technologies.

*Percentage of positively answered questions.

In addition, relevant information with regard to upgrading of sprayers – retrofitting – is included (See Fig. 4). Here is important to mention that from a technical point of view much is possible. However in order to stay within the boundaries of the legal obligations, depending on the features a number of factors need to be taken into consideration. The retrofitting should generally not be done by users of the sprayer, particularly when more is required than a simple fitting of a part e.g. low drift spray nozzle. The accredited and/or expert organisations can organise themselves to obtain the necessary tools and expertise and to make a revised risk assessment of the retrofitted sprayer. Additionally they can cover the related legal responsibilities and liabilities.

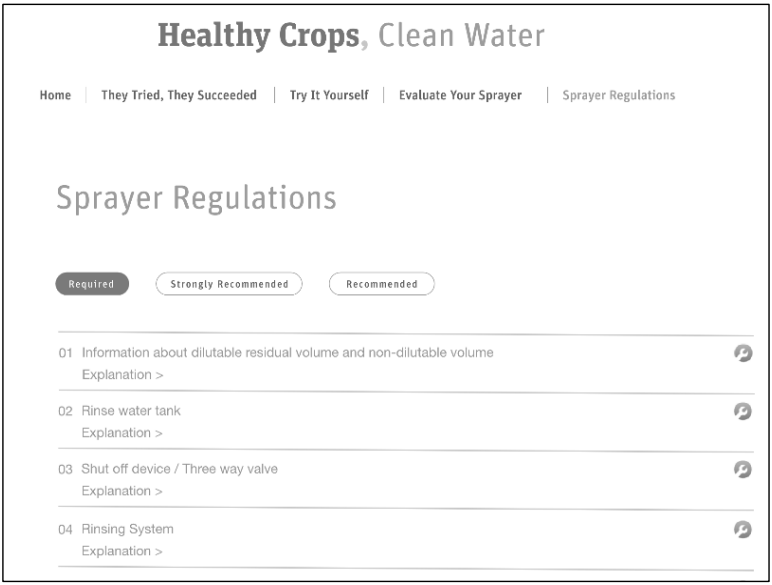

Fig. 4: Step-Water: Example of the report with the indication for retrofittability.

Summary

By focusing on new and existing sprayers it is expected that the information tool will contribute to the overall improvement of water protection by sprayers, and help farmers to assess whether their sprayers are compliant with current EU regulations. There are certain benefits for the farmers when using the tool. First of all it identifies the most effective spraying technology while minimizing negative effects which contributes to savings of chemicals and input costs. Next the protection of water against spray drift and run-off pollution is improved which will leads to more sustainable and socially accepted crop protection.

The principle and the basic idea of this information tool may be applicable also for the other types of agriculture technology like fertilizers applicators or planters which deals with the emissions of chemicals.

[1] Cemagref and TOPPS partners: Proposal on a sustainable strategy to avoid point sources pollution of water with plant protection products, 2008

A system for online control of a rotary harrow using soil roughness detection based on stereo vision

DI **Peter Riegler-Nurscher**, DI Dr. **Jürgen Karner**,
Josephinum Research, Wieselburg;
BSc **Josef Huber**, DI Dr. **Gerhard Moitzi**,
Ass.Prof. DI Dr. **Helmut Wagentristl**, University of Natural Resources and Life Sciences, Vienna, Austria;
DI (FH) **Markus Hofinger**, Pöttinger Landtechnik GmbH, Grieskirchen;
DI **Heinrich Prankl**, Francisco Josephinum / BLT, Wieselburg

Abstract

In conventional soil cultivation, a seed drill combination with a rotary harrow is the standard method for sowing grain. The aim is to create a crumbly seedbed to achieve a homogenous high field emergence. The quality of the seed bed is dependent on machine parameters like working depth, driving speed, PTO rotating speed and the geometry of the harrow tines and soil properties. We propose a method based on a stereo vision system which is able to observe the working result (e.g. roughness) of a seed drill combination visually. The real-time automatic control of the rotary harrow machine parameters is based on the soil roughness indices of the vision system. A closed-loop control continuously affects the roughness (variations due to natural soil properties) by changing PTO- and driving speed. Different seedbed roughness conditions were produced with different PTO and driving speed on two soil conditions. For the evaluation of the relationship between the roughness and aggregate size of the soil, a sieve analysis was performed and compared to the roughness index computed with the proposed vision system. To enable a transfer into a robust practical system, we assessed the different external influences, like dust, vibrations, residue cover etc., on the vision system.

1. Introduction

It is very important to control the roughness of a seedbed to increase plant emergence and to reduce the risk of soil erosion. For the regulation of the tillage operation it is required to measure the tillage results accurately in motion. In recent years many machine vision based methods have been published. All these methods share the reconstruction of the soil surface into a point cloud. Methods using a laser scanner (see [1] and [2]) are very accurate at this task, but also very expensive due to the hardware needed. Stereo camera systems on the other hand are passive, in principle motion insensitive and relatively cheap. The results on

stereo camera based soil roughness measurements published in [3] and [4] are very promising. Therefore the stereo camera principle was selected for our application.

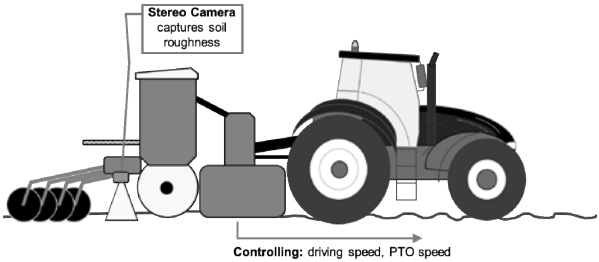

Fig. 1: Concept of the control system

Figure 1 shows the principle of our measuring and control system and the mounting position of the camera. Soil roughness is influenced by soil cloddiness and soil surface deformations. So we compared results from a sieve analysis with the measured roughness, shown in Section 4.

2. Roughness measurements

The roughness estimation is based on a stereo camera setup. To get an accurate reconstruction of the soil surface, the cameras are calibrated. First, the intrinsic parameters (focal length and principle point) of each camera are estimated. Afterwards, the extrinsic parameters, like the 3D transformation between the two camera centres, are calculated. The hardware setup of the two cameras should be as stable as possible to reduce geometric deformations which change the extrinsic parameters. However, during the tests over a time period of two years we did not observe such changes. All computations are done on a single board computer.

2.1 The estimation pipeline

The stereo camera captures two images (see Figure 3 a and b) with a baseline of 50 mm between the sensor centres. Figure 2 shows the processing pipeline which gets two input images and delivers a resulting roughness value. In the first step, stereo correspondences between the two images are matched. This is done by the block matching algorithm provided in OpenCV [5] by K. Konolige. The block matching algorithm delivers a disparity map (see Figure 3 c) which can be converted into a point cloud (see Figure 3 d) by using the camera calibration parameters. The scaling of the resulting point cloud is defined by the calibration and was chosen in mm. The resulting point cloud is not dense, where the density is depend-

ent on the image quality. For quantification of the image quality *q* the ratio of found correspondences to image size in pixels is used. The value of *q* ranges from 0, which implies that no correspondences were found, to 1 which indicates that all possible correspondences are found. This image quality value *q* in combination with the driving speed enables the system to detect errors during the measurement.

In a next step, different parameters can be calculated from the point cloud, for example surface normals or height measurements. Finally, a roughness value is estimated from the point cloud parameters. We chose a variant of the *RC* index proposed in [4] and also used in [3], which can be computed very efficiently. To eliminate the roughness pattern produced by the roller, the roughness is estimated in two different directions with RC_x and RC_y (see [4]). This results in a higher roughness transversal to the driving direction RC_y compared to the roughness along the driving direction RC_x (equation see [4]). Only correct depth measurements from the stereo algorithm, without interpolation, are used for the calculation of the *RC* values. The captured area per sample is about 60 cm x 40 cm. To increase the captured area we calculate a sliding mean window over several sample points.

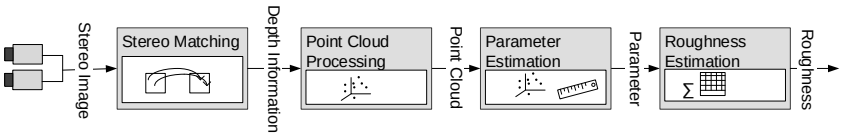

Fig. 2: Pipeline of the roughness estimation algorithm

The maximal framerate of the camera is 60 fps, but due to the high computation time the actual sampling rate is much lower.

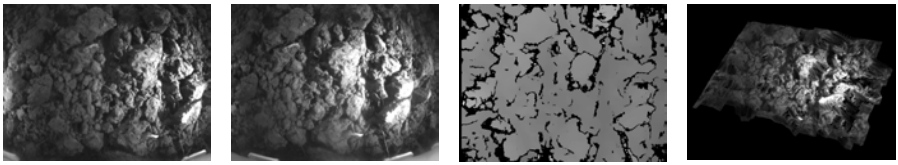

a) b) c) d)

Fig. 3: a) left camera image; b) right camera image; c) disparity map; d) reconstructed point cloud (Digital Elevation Model, DEM)

2.2 Environmental influences

The main challenge of getting a practical and robust system is to cope with environmental influences during the camera measurements. The camera image is inherently noisy, but the

signal to noise ratio increases with good lighting conditions. Therefore we added additional headlights which illuminate the soil surface with visible light. Additional lighting not only increases the image quality on cloudy days, it also enables night operations and decreases the need for a high dynamic range on shiny conditions. At very dry conditions like in July 2017 the rotary harrow produced dusty conditions. The influence of dust is reduced by the rear roller of the rotary harrow, which blocks much dust produced by the tines. At increased driving speed the dust clouds are blown away. The headlights, which shine on the soil in a shallow angle, increase the visibility of the soil surface through the dusty atmosphere. Depending on soil texture and soil moisture the rear roller lifts soil clods at a certain speed and the lifted soil decreases the image quality.

The algorithm filters unlikely spikes and speckles from the depth map. This filtering mainly affects plant residue. The system inherently is not able to measure the soil roughness at very high residue cover. Effects of vibrations have not been observed. The exposure time of the camera is about 1 - 5 milliseconds and is therefore not influenced by low frequency movements of the rotary harrow.

2.3 Sieve analysis

For evaluation purposes, we conducted sieve analyses at two locations. The extracted soil sample size was about 25 x 25 cm and 5 – 7 cm in depth. The sieve grid sizes were 40, 20, 10, 5, 2.5 and 1.25 mm. The measured masses were combined to a mean weighted diameter (MWD, equation see [6]) and compared to the measured roughness at the sample position. The results are shown in Section 4.1.

3. PTO and speed control

An ISOBUS Class 3 application was developed to change driving speed and PTO speed of the tractor by the implement (rotary harrow). The controller is based on a proportional control system. The desired roughness of the field R_{ref} is selected by the operator. The camera images are fed into the single board computer, which calculates the current roughness. The roughness value R_{act} is passed on to the implement ECU of the rotary harrow. The control loop is shown in Figure 4. The implement ECU estimates the control error and sends ISOBUS (Class 3) commands to change the PTO speed and/or the driving speed. Additionally, a hysteresis was introduced to reduce the influence of small changes in soil roughness.

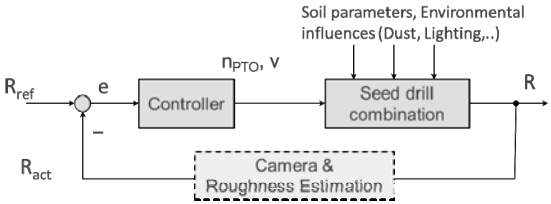

Fig. 4: Control loop; R_{act} denotes the soil roughness captured by the stereo camera and R_{ref} the roughness selected by the user. The goal is to reduce the error e between R_{ref} and R_{act} by changing the PTO speed n_{PTO} and/or the driving speed v.

Currently there are three modes implemented: controlling just PTO speed, controlling just driving speed or controlling both simultaneously.

4. Evaluation

We estimated the correlation between the roughness measurements of the camera system and the measured clod diameter of the sieve analysis (see 4.1). To assess the working intensity of the rotary harrow we compared the machine parameters to the measured roughness (see 4.2).

4.1 Comparison of soil roughness to weighted mean clod diameter (Sieve analysis)

Table 1: Correlation between measured soil roughness and weighted mean clod diameter

	Location 1: Groß Enzersdorf, AT	Location 2: Krummnussbaum, AT
Pearson correlation between mean clod diameter and soil roughness	0.54989	0.65702
Statistical significance two-tailed	0.000024	0.000080
N	52	30
Soil: % sand; % silt, % clay	36; 44; 20 (silty loam)	10; 70; 20 (loamy silt)
Date	24th August 2016	3rd November 2016

Table 1 shows the correlation between the results of the sieve analysis and the roughness measurements. The lower correlation at location 1 can be described by a lower range of roughness values. At location 1 the sample position was determined by GPS. This increases the uncertainty of the measurement due to the GPS-Error. At location 2 the roughness was estimated at the exact position where the sieve analysis sample was taken.

4.2 Comparison of soil roughness to rotary harrow tine speed

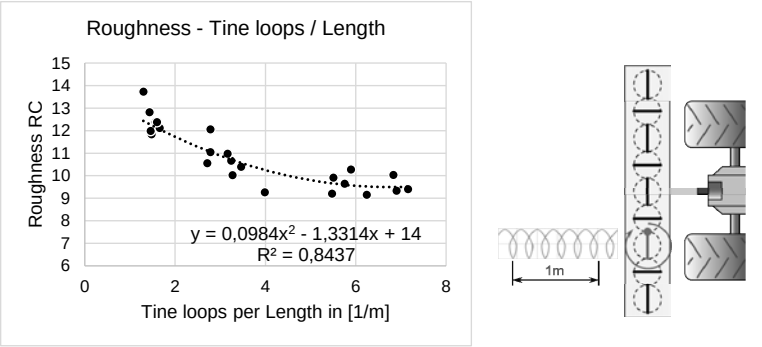

Fig. 5: Comparison of soil roughness to rotary harrow tine speed. Each point equals the mean value of one track. N = 24. The left image shows the tine loops per metre soil.

For these tests the PTO speed was held constant at 300, 540 and 1000 min^{-1}. The test took place at location 2 (Krummnussbaum, AT). The driving speed was estimated via GPS. The value of the x axis equals single-tine rotational speed divided by driving speed (rpm/(m/s)), representing tine loops per metre. As expected, the roughness decreases with increased intensity of the working process (see Figure 5).

5. Summary and Outlook

The goal of seedbed preparation is a crumbly seedbed to achieve high field emergence. The proposed method based on stereo vision is able to observe the field roughness visually. The measured value is used to control the machine parameters of a seed drill combination to get a homogeneous result. The system is able to operate at any lighting conditions, also during night time. A segmentation of the soil clods could increase the correlation to the weighted mean diameter of the clods.

Acknowledgements

The Project is funded by the Austrian Federal Ministry of Transport, Innovation and Technology (BMVIT) under the program "Bridge 1" between November 2015 and December 2017. We would like to thank CNH Industrial for providing the ISOBUS Class 3 enabled tractor. We also thank the farmers Josef Huber, Peter Prankl, Thomas Riegler and Stefan Riegler-Nurscher for providing fields for our tests.

References

[1] Turner, R., Panciera, R., Tanase, M. A., Lowell, K., Hacker, J. M., & Walker, J. P. (2014): Estimation of soil surface roughness of agricultural soils using airborne LiDAR. Remote Sensing of Environment, 140, 107–117

[2] Zhixiong, L., Nan, C., Perdok, U. D., & Hoogmoed, W. B. (2005): Characterisation of soil profile roughness. Biosystems Engineering, 91(3), 369–377

[3] Riegler, T., Rechberger, C., Handler, F., & Prankl, H. (2014): Image processing system for evaluation of tillage quality. Landtechnik.

[4] Taconet, O.; Ciarletti, V. (2007): Estimating soil roughness indices on a ridge-and-furrow surface using stereo photogrammetry. Soil and Tillage Research 93, pp. 64–76

[5] OpenCV Library, http://opencv.org/

[6] Kirchmeier, H, Geischeder, R. Demmel, M. (2005): Bearbeitungseffekt und Leistungsbedarf von Kreiseleggen mit unterschiedlicher Kreiselgeometrien. Landtechnik 60 (4), pp.196-197

Development of a tillage-machine for seed-bed cultivation of heavy soils

Dipl.-Ing. **M. Marsel**, Dipl.-Ing. **T. Bögel**,
Prof. Dr.-Ing. habil. **T. Herlitzius**, Technische Universität Dresden;
M.Eng. **Bernd Neunkirchen**, Antriebstechnik-Roth GmbH;
Dipl.-Ing. **H. Eidam**, Dipl.-Ing. (FH) **T. Sander**,
Eidam Landtechnik GmbH, Lößnitz

Abstract

Soils with a high fraction of clay, so called heavy soils, offer high crop yields for farmers, but the problem is the short time range to do tillage respectively seed-bed cultivation. Therefore implements with high draft force requirements providing limited seed-bed quality. A new implement with active tools should be developed, which reduces the traction force up to generating propulsion and do well quality seed-bed cultivation in one transition. This machine unites the process of subsoiling, pre-crushing, deep-compacting and fine-crushing in two active powered working stages with different tools. Therefore, new working tools for each section were developed and tested in field. The generation of propulsion with these new tools was validated by different working results of subsoiling and pre-crushing in dependence of the slip ratio. The tool combination has proven the potential to work effectively for seed-bed cultivation of heavy soils.

1. Introduction

In Germany six to eight percent of the arable area contains so called heavy soils which are characterized by a high fraction of clay. The good water-holding capacity of these soils leads to high fertility and increased crop yields, but the possibility of tillage is very weather-dependent.

Today seed-bed cultivation machinery is usually pulled by tractor and powered by the PTO. Available machines like harrows have only moderate satisfying work-efficiency on heavy soils. High fuel consumption and deficiencies in seed-bed quality are typical. The consequences are multiple transitions accompanied by soil compaction to get the desired process result.

Project objective of a consortium of TU Dresden in cooperation with Roth Antriebstechnik GmbH and Eidam Landtechnik GmbH is the development of an active powered implement for seed-bed cultivation of heavy soils. Therefore, Roth Antriebstechnik will develop the whole drive train with the transmission control and Eidam Landtechnik a new frame structure which is optimized for compressive forces. This implement should increase the efficiency of seed-bed cultivation with lowering the draft force consumption and achieve a good seed-bed quality by one transition. The machine is useable for plowed and unplowed heavy soils as well as soils with biomass residuals like grass or stubble.

Already In the 1980s TU Dresden tried to develop a self-propelled machine called SABEMA for seed-bed cultivation especially for plowed heavy soils. This machine consisted of a modified tractor with a front and a rear implement. The tractor was able to lift up to be carried from implements. The propulsion was realized from the front implement with modified tooth packer tools. The steering was possible with articulated kinematics between the tractor and the attachments. At this time the possibility to realize variable drives was limited to mechanical components, so the full potential of this development could not be reached. The research results of this project delivered the basics for the development of the new implement.

2. Working tools for the implement

The implement to be developed has to do different tasks along the process of cultivation. First the soil has to be subsoiled, pre-crushed and deep-compacted with a depth of 125 mm. This step generates a loosened ground with big soil aggregates. Next the ground has to be crushed and mixed in a depth of ca. 40 … 60 mm to get the right packing density for drilling. To reduce negative effects like erosion of the fine-crushed soil, it has to be re-compacted.
The machine generating propulsion to get lower draft force consumption, achieved by form enclosure between working tools and soil with additional positive slip. Through the superposition from a rotational and a translational movement, the outer sections of the working tool describe an extended cycloid. These movement allows that the tool braces against little “earth dams” and cause a force to push forward. The number of work elements, the tool diameter and the slip are important parameters for generating a propulsive force. The slip should be constant in relation to the tractors velocity to get the best result of crushing, compacting and generating propulsion. Therefore, a variable drive train is required to control the speed of the working tools. For this reason Roth Antriebstechnik will develop an innovative drive train which is powered by PTO. This CVT allows to variate the speeds of the different working sections to adjust a perfect work-quality and efficiency depending on the velocity.

The cultivation processing of the new machine is divided into two working-sections. The first stage realizes the functions of subsoiling, pre-crushing, deep-compacting, generating propulsion and bracing. Therefore, new and optimized tools where developed shown as in Figure 1. The designation of the tools is composed of two numbers. The first describes the working-section, the second is a consecutive number.

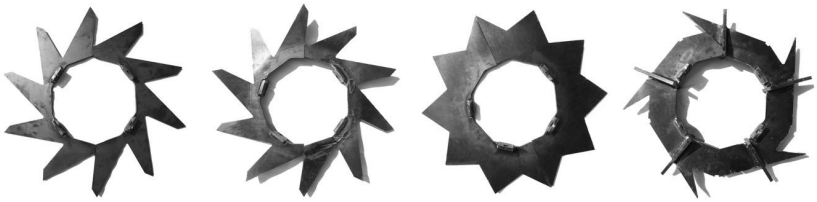

1-1 *1-2* *1-3* *1-4*

Fig. 1: Prototype tools of working-section one

All tools have the same outer diameter and the same number of work elements. The first tool 1-1, a modified tooth packer, where developed in the end of the 1980s by Baur [1]. This tool is characterized by a compromise of generating propulsion, deep-compacting and subsoiling. Tool 1-2 is a variation of the first. The tilted work elements are increasing the function of subsoiling and the working width of one tool by less generation of propulsion. The next tool 1-3 is a standard star packer. According to the studies of Kranz, a result is that the normal star packer tool is suitable to generating propulsion, but the results of subsoiling and deep-compacting are of lower quality [2]. The concept tool 1-4 is a combination of two active elements. The spikes in radial orientation should realize a lower penetration resistance into the soil and the axial v-shaped elements should generating high propulsion through their width and the more active form enclosure.
The result of working-section one is a deep compacted and pre-crushed soil with an aggregate diameter of ca. 120 mm or less.

Working-section two of the implement should realize the functions of fine-crushing (soil aggregate diameters less than 40 mm) and rear-compacting. Therefore, three tool concepts where created shown in Figure 2.

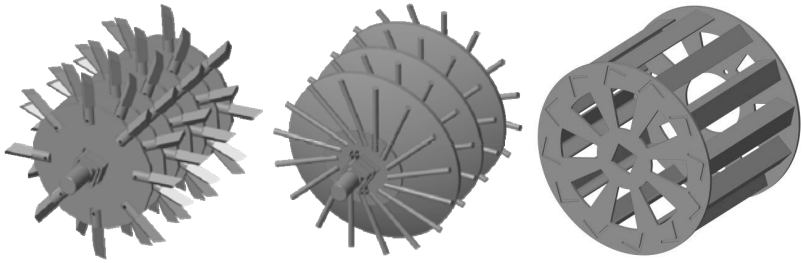

2-1 *2-2* *2-3*

Fig. 2: Prototype rotors of working-section two

Prototype tool 2-1 is a fast turning rotary tiller. This tool is well performing in fine-crushing, but is expected to have the highest power consumption of the three variants. The crushing is based on cutting, beating and impacting effects. The high power consumption is due to the side effect of accelerating and raising soil aggregates without the effect of crushing. Two rotor variants were used, one with straight tillage tools and the other with tilted working elements by 10 degree to increase the working width. Tool 2-2 is a combination of passive and active working elements. The passive rolling lens packer represents a narrowing gap. The active rotary tiller tool is pushing soil aggregates through this gap. Thrust-push-forces are crushing the soil aggregate energy-efficiently supported by the relative movement between active and passive parts. Power consumption of this tool is lower compared to the rotary tiller while producing a good crushing effect. The third tool concept 2-3 is an active angle bar roller. This tool was developed in the 1980s by Konzack [3]. It is characterized by very low draft force requirements with the potential of generating propulsion at higher slips ratios and an acceptable fine-crushing result with the ability of re-compacting.

The result of working-section two is a prepared seed-bed with the majority of soil aggregates at a diameter of less than 40 mm.

3. Field test results

Currently a functional prototype machine with a working width of one meter exists. The current variable drive train is realized with a permanent magnet synchronous motor (PMSM) with an integrated inverter from STW. The speed of the e-machine is controlled by tractor's velocity and a predefined constant slip using a master-ECU and communicated via CAN to the STW power electronics.

Field tests on heavy floodplain soils were done to validate the general machine concept and the characteristics of each tool. During these tests of the different working tools power consumption and propelling force were measured. The following figures show representative results for the working tool 1-3 of working-section one.

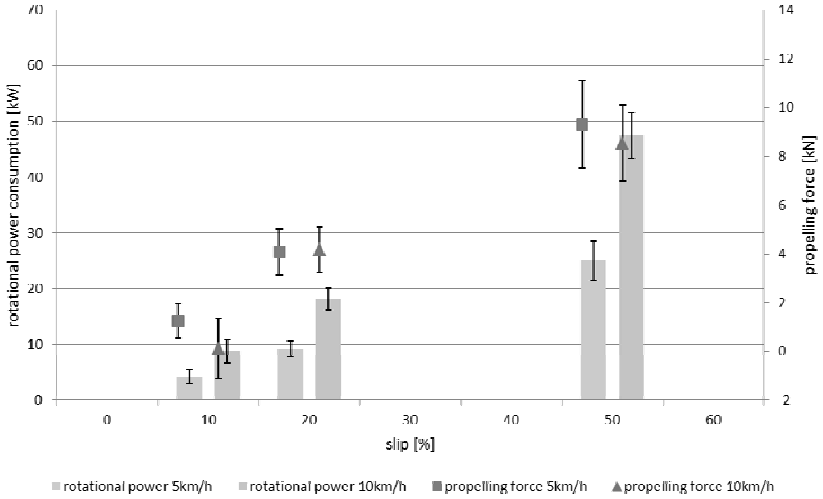

Fig. 3: Relationship of rotational power consumption and propelling force depending on slip of the tool 1-3

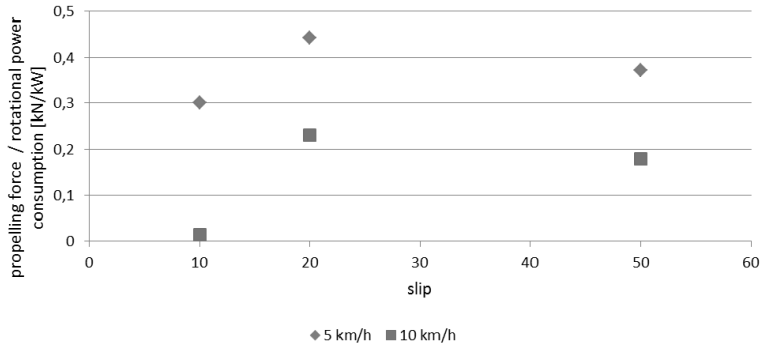

Fig. 4: Ratio of propelling force to rotational power consumption depending on slip of the tool 1-3

Figure 3 shows the relationship of power consumption, slip and propelling force. It can be seen that the tool is generating propulsion. The magnitude of the propelling force depends on the slip and the ground speed of the tractor. The power consumption increases linearly with higher slip and higher velocity. Figure 4 shows the ratio of propelling force to power consumption depending on slip. Only a small range of slip (here about 20 percent) is optimal for energy effective generation of propulsion.

The working results in subsoiling, pre-crushing and deep-compacting are different for the working tools in section one at the same slip ratio. The best results of the tested slip ratios delivered the modified tooth packer tool 1-2. The tool 1-3 has only acceptable working results at slip lower than 10 percent or beyond 50 percent. The concept tool 1-4 has the problem of clogging. The axial elements hold the soil back preventing the working elements from penetrating into the ground deep enough.

4. Conclusion

The first field tests confirmed the design intent of the tools of working-section one and the ability to generate propulsion while showing similar and acceptable working results. A constant slip in dependence of the tractor's velocity was realized using a variable drive train. The field tests show an optimal and energy efficient slip range for the tools about 20 percent.

The Working-section one of the new implement provides a subsoiled and pre-crushed ground with aggregate diameter less than 120 mm. The following working-section two has to realize a ready seed-bed with the processes of fine-crushing and re-compacting. Tools for this working section still have to be validated in field tests as well as the adjustment of the working parameter from the two process stages to realize the requirement for a well-prepared seed-bed in one transition. With the new implement the potential of reducing draft force as well as fuel consumption for the tillage of heavy soils can be expected.

References

[1] Baur, Andreas: Untersuchungen zu aktiv rotierenden, scheibenförmigen Werkzeugen für die Verdichtung und Zerteilung des Bodens; Dissertation; TU Dresden; 1981

[2] Kranz, Jörg: Untersuchungen an kinematisch gekoppelten treibenden und getriebenen Werkzeugen mit horizontalen Drehachsen zur mit dem Pflug kombinierten Saatbettbereitung; Dissertation; TU Dresden; 1986

[3] Konzack, Joachim: Untersuchungen zum Einfluss ausgewählter Konstruktions- und Betriebsparameter rollender Werkzeuge auf den Energieaufwand beim Verdichten und Zerkleinern des Bodens nach der wendenden Grundbodenbearbeitung; Dissertation; TU Dresden; 1981

Development of a Sprayer Performance Diagnostic Tool for Better Management Practices of In-Field Spraying Operations

C. A. Shearer, **J. D. Luck**, **J. T. Evans**,
University of Nebraska-Lincoln, Lincoln, NE., USA

Abstract

Chemical application is a prevalent crop management practice used worldwide. The EPA reported 5,821 million of pounds of pesticide active ingredient used at the producer level worldwide in 2012 [1]. With the increase of herbicide resistant weeds and other environmental concerns, it is continually important to ensure pesticides are applied at proper application rates. Research efforts were aimed to aid in the reduction of over- and under-application through development of a program to improve sprayer operator feedback. Real-time sprayer analytics data were recorded, paired with corresponding Geographic Information System (GIS) points, and processed with the resulting program to produce high resolution sprayer coverage maps and application error analysis reports. The resulting reports showed significant sprayer errors not commonly found in current sprayer feedback.

Introduction and Background

While sprayer technologies have advanced greatly over the past decade and a half, chemical application errors are still prominent in many in-field operations. Over-application of pesticides can cause harm to the crop, reducing yield, and result in added pollution to the environment. Under-application of pesticides fails to control pests within the field, again lowering crop yields, and causing profit loss for the producer. Current operator feedback from in-field pesticide application operations conveys limited information and often times does not allow the operator to visualize a true representation of their performance. Farm Management Information Systems (FMIS) typically do not account for overlap, varying application rates across the width of the spray boom during turns, or off-rate errors due to controller response. A central Kentucky case study showed three fields, all of which had only 25% to 36% of the field areas receiving within ±10% of the target application rate, in large part due to the aforementioned errors [2]. The focus of the efforts were development of improved mapping systems and product distribution summaries that would allow operators to make better-informed decisions leading to improved management practices during spraying operations.

The development of an improved coverage mapping software would provide strong support for producers in regards to technology decision making. A 2010 Luck et al. study's results showed a significant reduction in over-application of chemicals when an automatic boom section control was introduced to a sprayer [3]. Results from the case study showed a 50% reduction of overlap over-application from the previous season using manual section control (12.4% over-application) to the following season with automatic boom section control introduced (6.2% over-application). Another study conducted by Luck et al. suggested a strong relationship between the field shape factor of perimeter-to-area ratio (*P/A*) and overlap error [4]. Errors were found to increase as the field *P/A* increased, the more inclusions and concavities a field exhibits the more error due to section control shut off was observed. The need for improved spray application mapping was also highlighted in orchard settings as a tool for verification of field operations [5]. Development of improved mapping systems and product distribution summaries would aid operators in their decision making regarding whether advanced sprayer technologies are justifiable for their fields. In addition, better management practices maybe come obvious through examining the sprayer error reports.

Goals and Objectives

The overarching goal of the research efforts was to develop a user-friendly tool to aid in development of improved management practices of sprayer operators. The necessary objectives for reaching this goal were: 1) to develop a program to create higher resolution as-applied maps; and 2) utilize the same program be able to identify, locate, and quantify potential off-target and off-rate errors after field spraying operations.

Methods

Research efforts focused on meeting the above-mentioned objectives lead to the development of the Pesticide Application Coverage Tool (PACT) based in MATLAB. The PACT program was developed to process real-time sprayer performance data and generate high resolution coverage maps and quantified error reports.

Data Collection

To simplify the development of the PACT program, initial dataset input formats were restricted to two forms. The first dataset option for the program was a controller area network (CAN) bus-based data collection service offered by Farmobile (Farmobile, Inc.; Overland Park, KS), where real-time sprayer performance data was output into a shapefile containing the necessary information for the PACT software. GIS data points provided in the Farmobile

files came from an integrated Global Positioning System (GPS) antenna operating with Wide Area Augmentation System (WAAS) level accuracy. The second input dataset form consisted of text files from KVASER (Kvaser, Inc.; Mission Viejo, CA) CAN message loggers. Raw CAN messages were read and recorded by a KVASER Memorator Pro 2xHS v2 data logger, messages were processed through a database and decoded messages were output in a chronological text file handled by the PACT program. KVASER logged GIS data received from the GPS receiver were real time kinematic (RTK) corrected values.

Program Functionality

A real-time sprayer performance dataset paired with accompanying GIS data were combined with user defined sprayer set-up parameters to produce as-applied maps as well as informational reports containing quantitative post-application error information. The raw input dataset, as well as user-supplied sprayer set-up information, are defined via the graphical user interface (GUI) in the MATLAB environment (Figure1). Real-time sprayer performance data necessary for program operation consisted of GPS-defined location with an accompanying timestamp, boom section status (i.e., on or off), and either a flowrate or pressure reading for the boom which was used to calculate each section's respective application rate. Contingent on the real-time sprayer performance data file type the various metrics were concatenated with the closest common timestamp. The dataset was then resampled to a 2 Hz frequency, or next highest possible frequency if data is not available at a 2 Hz rate (i.e., 1 Hz).

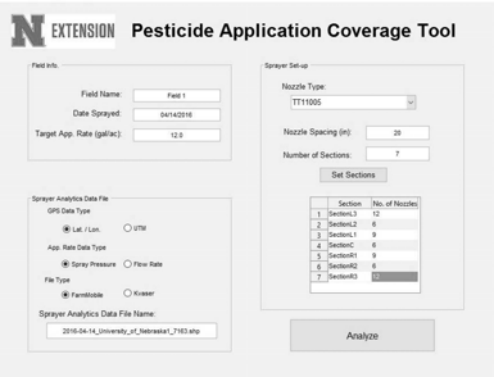

Fig. 1: Graphical user interface for program user to real-time sprayer performance data and sprayer set-up parameters.

Using the information provided regarding the sprayers setup, projected locations were calculated for each individual boom section at each sprayer location point using basic geometric relationships. The section locations were then paired with the section on/off status values to eliminate boom section locations marked with an off value. Remaining section location points and the boom section widths were used to generate coverage polygons spanning from the current point to the next. A calculated flow rate value (from pressure readings and nozzle type) or recorded flow rate value was used to apply an associated application rate value for each plotted polygon. Individual boom section flow rate values were deemed to offer limited additional benefits for the sprayer feedback. A single flow rate value was used at each sprayer position and assumed to be uniform across all sections along the width of the boom.

Off-target error locations were identified as sharing overlapping polygons for multiple sprayer passes. When an overlap was identified, the polygon area values were adjusted accordingly and the application rates summed together in the overlapped region. Off-rate errors (e.g., from turning) were identified based on the amount of area covered by each boom section compared with the amount of area covered by the middle most boom section(s). Remaining errors identified in the field were attributed to spray rate controller response errors, most likely due to speed changes or boom section actuation. The final spray application data were compiled in the forms of as-applied maps and an easy to read report format with quantitative values for the various errors.

GUI

The GUI was created in a MATLAB environment to improve usability for end users. The end design required minimal input in an easy to understand format which consisted of three main sections. General field application information is entered into the first section (e.g., date sprayed, field name, target application rate). The second section allows the user to input information about the input dataset types. For example, GPS data type, pressure or flow readings, and sprayer operation data files can be specified by the user. The third interactive section allows for the user to enter key sprayer set-up parameters. Spray nozzles are listed for selection by the user in the event pressure measurements are used to estimate boom flow rates. Nozzle spacing, as well as number of sections and nozzles per sections can be entered here (Figure 1).

Results

The four example fields analysed in this study showed substantial portions of the field receiving application rates deviating from the target application rate. Results indicated that 14.6%

to 36.8% of the total sprayed area likely received an application rates outside ±10% of the target rate. Off-rate turning and overlap application errors can be visibly observed in the generated coverage maps seen in Figures 2 and 3. Off-rate errors can be seen most commonly as the sprayer navigates the border of the fields and around any field inclusions. Overlap off-rate errors can be seen as the sprayer comes in and out of passes with the auto-section controls attempting to turn off to efficiently minimize over-application.

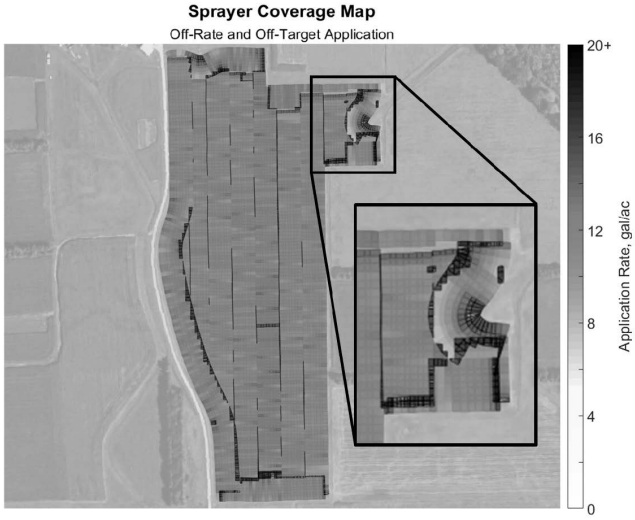

Fig. 2: High resolution as-applied coverage map of Field 1 with zoomed section showing off-rate and off-target errors present.

Fig. 3: High resolution as-applied coverage map of Field 3 generated by the PACT program.

A breakdown of errors present in the fields studied can be seen in Figure 4. Of the four fields, overlap off-target errors affected areas of the total sprayed areas ranging from 2.7% to 11.2%. Off-target errors varied across the four fields, but appeared to trend positively with increased field irregularities. Off-rate errors due to turning movements ranged from areas covering 6.7% to 14.7% of the total sprayed areas. These application rate errors covered substantial areas in each field examined, and are not commonly separated out explicitly in most FMIS programs. The remaining application error in the field is attributed to controller response error. The controller response errors would be the minimum possible due to the assumption that there are no areas receiving compounded off-rate and off-target errors. With the combined application reports and coverage maps, operators could identify the significance of the various error types as well as identify possible areas in field where improvements can be made.

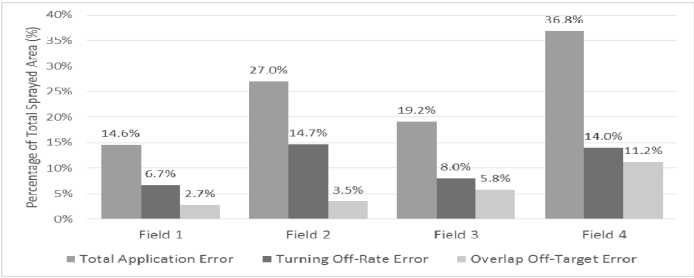

Fig. 4: Off-rate totals in the four fields studied as percentages of total sprayed areas.

A sample PACT generated report to be provided to the operator from one of the studied fields can be seen in Figure 5. The report will accompany series of maps similar to those seen previously in Figure 3. Breakdowns of the various error types and their percent presence among the field will be available in the report. Report interpretations could provide valuable information to producers looking to adopt new sprayer technologies. For instance, continuous high off-target error findings across multiple fields for a producer could lead to the justification of adding automatic boom section control.

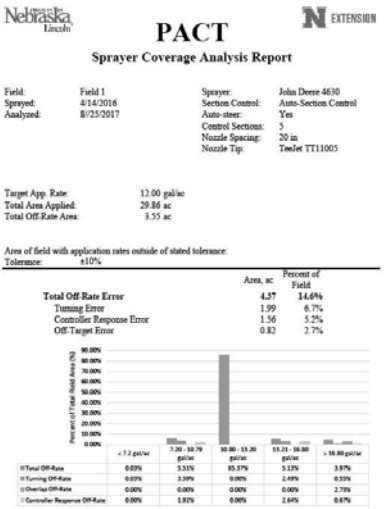

PACT

Sprayer Coverage Analysis Report

Field:	Field 1	Sprayer:	John Deere 4630
Sprayed:	4/14/2016	Section Control:	Auto-Section Control
Analyzed:	8/23/2017	Auto-steer:	Yes
		Control Sections:	5
		Nozzle Spacing:	20 in
		Nozzle Tip:	TeeJet TT11005

Target App. Rate:	12.00 gal/ac
Total Area Applied:	29.86 ac
Total Off-Rate Area:	3.55 ac

Area of field with application rates outside of stated tolerance:
Tolerance: ±10%

	Area, ac	Percent of Field
Total Off-Rate Error	**4.37**	**14.6%**
Turning Error	1.99	6.7%
Controller Response Error	1.56	5.2%
Off-Target Error	0.82	2.7%

Fig. 5: Sample operator feedback report generated from Field 1 of the study.

Conclusion

A program was successfully developed to aid in the planning of improved management practices for sprayer operators and report potential errors during post-application analyses. High resolution as-applied maps were successfully generated to illustrate locations where errors were expected to occur and help quantify off-target errors. Visual observation of the as-applied maps revealed locations where turning off-rate, off-target, and controller response errors occurred. Post-application reports were generated with quantifiable measurements of the various errors present. It is important to note that the developed program currently only examines an ideal performance of the system, once the fluid has left the nozzles the droplets are treated as if they were to fall ideally. Environmental factors (i.e. wind, topography, weather, etc.) that may affect the spray application are not taken into account. Further comparison of these program outputs to current FMIS feedback will allow for improved validation of the software. This combination of higher resolution coverage maps and calculated areas where off-target and off-rate errors occur should allow operators to make more informed decisions during spraying operations and while considering technology adoption.

References

[1] Atwood, D., Paisley-Jones, C.: Pesticides Industry Sales and Usage: 2008-2012 Market Estimates. United States Environmental Protection Agency, 2017, pp. 10.

[2] Luck, J. D., Sharda, A., Pitla, S. K., Fulton, J. P., and Shearer, S. A.: A Case Study Concerning the Effects of Controller Response and Turning Movements on Application Rate Uniformity with a Self-Propelled Sprayer. Transactions of the ASABE, Vol. 54(2), 2011, pp. 423-431.

[3] Luck, J. D., Zandonadi, R. S., Luck, B. D., and Shearer, S. A.: Reducing Pesticide Over-Application with Map-Based Automatic Boom Section Control on Agricultural Sprayers. Transactions of the ASABE, Vol. 53(3), 2010, pp. 685-690.

[4] Luck, J. D., Zandonadi, R. S., and Shearer, S. A.: A Case Study to Evaluate Field Shape Factors for Estimating Overlap Errors with Manual and Automatic Section Control. Transactions of the ASABE, Vol. 54(4), 2011, pp. 1237-1243.

[5] Giles, D. K., and Downey, D. Quality Control Verification and Mapping for Chemical Application. Precision Agriculture, Vol. 4, 2003, pp. 103-124.

Sensor study to identify process characteristics of crop and air flow in a combine harvester

Prof. Dr.-Ing. **T. Herlitzius**, Dr.-Ing. **R. Hübner**,
Dipl.-Ing. **A. Günther**, Dipl.-Ing. **Chr. Korn**,

Faculty of Mechanical Science and Engineering, TU Dresden;
S. Kirstein, Dipl.-Ing. **S. Müller**, Dipl.-Ing. **J. Miunske**,
Miunske GmbH, Großpostwitz

Abstract

Today`s demand for growing productivity of combine harvesters obliges a rise of automation. Market-available grain loss sensors cannot meet the accuracy requirements. Hence, a new approach to identify the working quality of combine harvester cleaning devices is tested at the chair of agricultural systems and technology. An optical sensor is used to detect grain flow in combination with a hot film sensor to detect air flow velocity. Multiple sensors are arranged in the sieve and chaffer area to capture the longitudinal and lateral distribution of grain separation and air velocity. This paper presents the results of preliminary studies of both measurement systems. The investigations carried out so far are very promising and suggest a much higher benefit compared to conventional measurement systems for grain loss. It also represents the new approach to measure process characteristics rather than process outputs in order to combine model based control algorithms with real process measurements.

Introduction and state of the art

Productivity enhancement and ease of operation are among the most important objectives of current research and development activities in the field of agricultural engineering. Due to the increasing complexity in the operation of combine harvesters, demands on the machine operator increase accordingly. The further development of today's complex machines and functional modules is only possible by system integration, e.g. linking the agricultural production chain and increasing the level of automation up to the fully automatic machine with and without operator. A step in this direction is the automation of subsystems, including the combine harvester cleaning device. Grain loss sensors of today's combine harvesters, which are primarily piezo-electric, account for about one percent of the total grain loss and can hardly distinguish between grain and non-grain components. This is not acceptable with regard to automatic

machine adjustment. While cleanliness and grain damage sensors slowly start to become mature, grain loss sensors are only marginally improved and rely heavily on manual calibration. Piezoelectric sensors are robust and low cost but have the following deficiencies:

- positioned within the mass flow and interfering with it,
- only a small portion of the mass flow is detected,
- impact energy varies not only due to disturbances and crop conditions but is also depending on sensor location in the material flow and machine settings,
- calibration is only valid for current conditions and machine settings

As a result, the capacity of the combine harvester is not fully utilized or too much grain is discharged back to the field. Furthermore, there is no measurement system for combine harvesters available at the market, which captures the distribution of the air flow velocity along the sieves of the cleaning device. According to e.g. [1] and [2], this distribution has an essential impact to the efficiency of the separation process. The air flow field depends among others on the fan speed, the throughput and the sieve opening. OEM`s are required to ensure an optimal machine setting even for continuously changing environmental conditions during the harvesting process (e.g. fluctuating mass throughput, different terrain, changing ambient and crop moisture) with the aid of suitable sensors. Today`s existing sensor technology in combine harvesters is not able to perform this sufficiently.

A comparison of contact free sensing technologies (capacitive, radar, optical, soft x-ray) with the assessment criteria: functional risk, cost, adaptability, moisture influence, ratio of grain to MOG, differentiation between grain and MOG or different crop types was made to explore the potential of sensing of separation characteristics of crop and air flow.

Light transmission in combination with hot film anemometry measurements turned out to be the preferred technology mix. A simplified test bed for baseline investigations was built and basic functionality was proven. Benefits of the new sensor technology are expected to be the following:

- no obstacle to the material flow,
- scanning of a larger portion of the material flow instead of taking a small sample as the current loss sensors do,
- measures for two physical separation characteristics (density of material flow and local air velocity),
- reflecting internal combine states instead of output parameters which improves dynamic control behaviour and accuracy.

The innovative core of the research, presented in this paper, is the development of a measuring system for combine harvesters which, for the first time, optically captures the grain separation and at the same time, realizes the measurement of the air velocity at the combine harvester

cleaning device elements. Sensors detecting the grain separation to ensure a low level of grain loss are among the basic requirements for the realization of robust and effective automatic combine setting algorithms. The characteristic separation curve of grain separation along the sieves of the cleaning device correlates with grain loss and cleanliness and provides together with the local air velocity the potential capability to be used as control variable for automatic settings of sieves and fan speed.

Sensing principle and prototypic sensor design

Sensing principles of optical detection of kernels are known from other application like seeders. Several patents [3] exist on air flow detection and optical sensors in agricultural machines. The patented uniqueness of the described sensor package lies in the combination of two physically independent measurement technologies, which both detect process relevant characteristics (see Fig. 1).

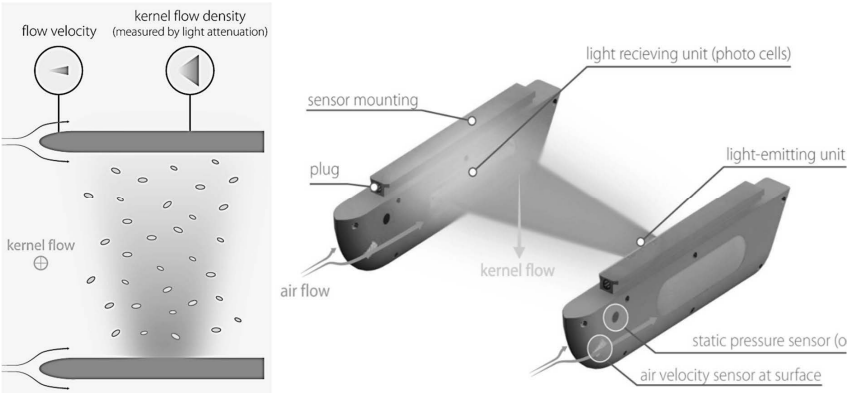

Fig. 1 Sensing principle and prototypic sensor system design

The optical part is based on light transmission through a determined section of the material flow. The sender emits a visible red light beam as triangular cone section, formed by a lens, which is focused enough to have high energy intensity with cone opening angles big enough to safely meet the receiver array of photodiodes without the need of its specific adjustments.

Air velocity in one certain direction, intentionally given by the position of the detector is measured with the sensing principle of hot film anemometry. Hot film sensors position and shape of the housing is CFD - optimized to avoid turbulence and to prevent dust deposits. The first prototype of a pair of sender and receiver is shown in Fig. 1 right hand side.

Electronics for detecting and signal processing is integrated in the sensor housing, which is common for all sensors. The sensor interface only consists of power supply and CAN-interface. Circuit boards occupy 270 mm^2 (30x90) and include power supply, photodiode array, LED with Lens, LED-driver, multiplexer, bus-controller and electronics for hot film anemometry. The second design iteration of the boards is shown in Fig. 2.

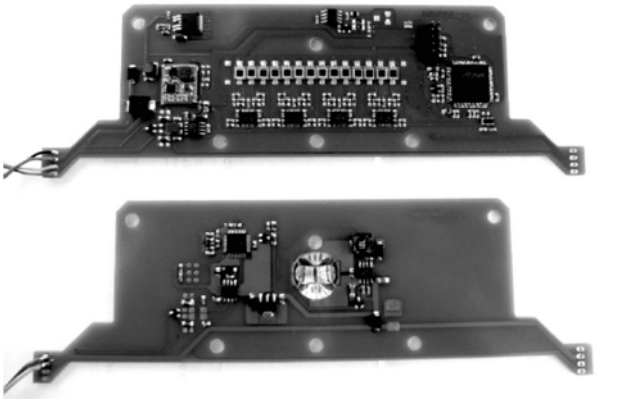

Fig. 2: Circuit boards (top: light receiving unit; bottom: light emitting unit)

Further approaches of even smaller boards in order to minimize undesired process interaction as much as possible are under review.

Preliminary tests of material flow detector

The development is split into three phases. The start with preliminary tests of each detecting principle separately has the objective to establish basic parameters of the design and understand potential limits. Integration of the technologies happens in the second step, where the prototypic sensor design is executed, build and tested in a real combine cleaning device under laboratory conditions. Eventually the last phase will be the field testing, which is supposed to get started after the lab results have proven enough maturity for the next design iteration.

The test rig used for preliminary test is shown in Fig. 3. Tests were carried out with Wheat, Canola and Barley, stored in material reservoir (n), the blower (a) was not used and grain flow is generated only by the just vertically oscillating sieve with an adjustable opening width (o), which is used to adjust feedrate. A scale (m) below channel (l) captures grain separation time dependently and enables calculation of average grain mass flow.

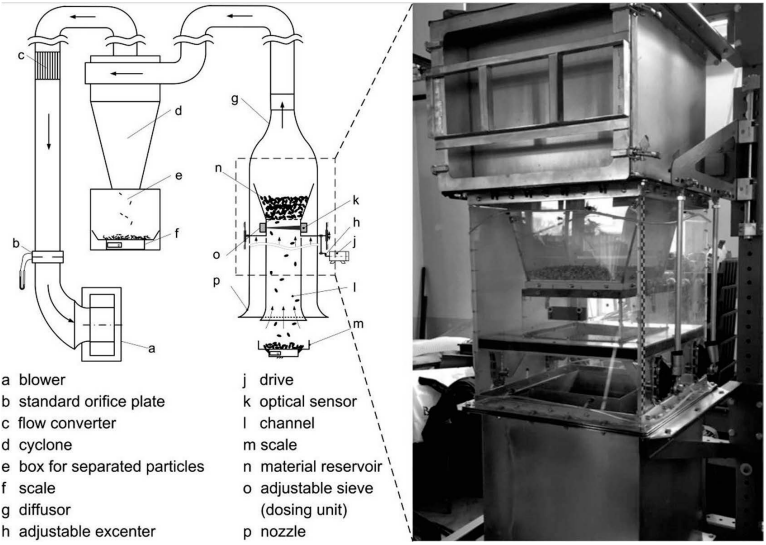

Fig. 3: Test rig for preliminary tests of material flow detector and air flow detector

A numerous amount of tests was done to prove feasibility and applicability of the optical detection method. Evaluation of raw data, as shown in Fig. 4 allowed to calibrate signal versus real mass flow at single diode level as well as for the complete pair of sender and receiver.

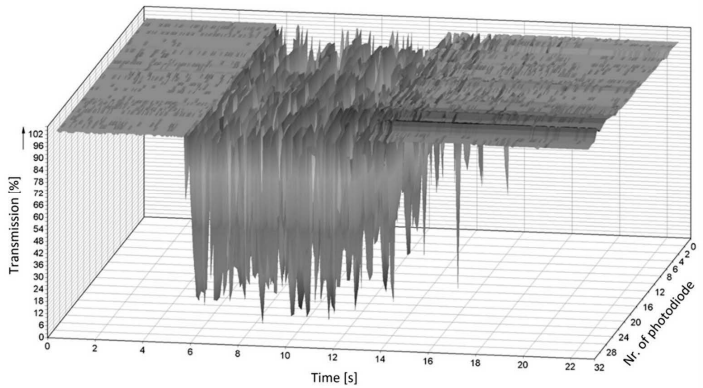

Fig. 4: Example of raw data of material flow detector

Transmission depicted in Fig. 4 ranges from 100 % transmission (no obstacles between photodiodes and LED) to 0 % transmission (LED switched off). Fig. 5 shows time-averaged values

of grain flow ($^{g}/_{s}$) and normalized sensor signal (% attenuation). The light attenuation is a combination of absorption and reflection when grain kernels are passing the beam. There is a clear correlation between sensor signal and grain flow as well as the expected non-linear behaviour. Saturation is to be expected beyond 2000 g/s, which is mainly dependent on flow density and distance of the travelled light. A potential source of error is ambient light, which can be addressed by calibration when required. Mass value calibration also depends on the type of crop.

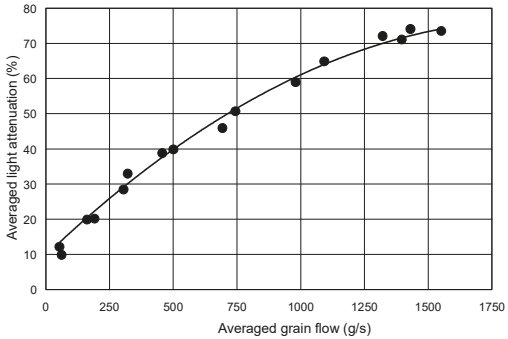

Fig. 5: Example for correlation between light attenuation and grain mass flow for Wheat

Preliminary tests of air flow detector

Similar to the optical part also the hot film detector was tested and calibrated with the test rig. Position and size of the detector fixed on a prototypic housing are shown in Fig. 6. Tests were performed with a test rig shown in Fig. 3 at different air speeds and angular position of the sensor package in the air flow.

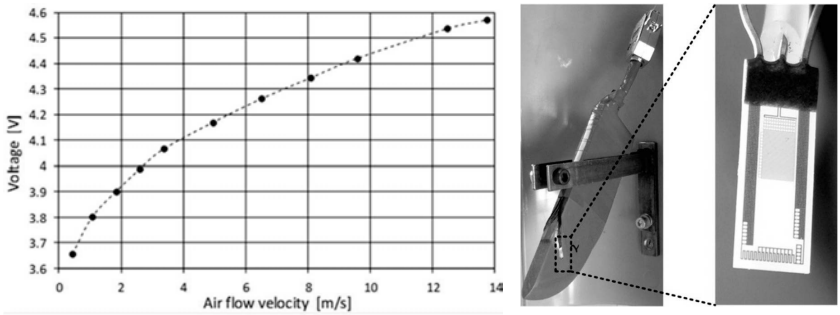

Fig. 6: Example for correlation between output voltage of sensor and mean air velocity in the test rig channel (measured by standard orifice plate)

Before the tests the shape of the housing was optimized using advanced CFD analysis. Goal of tests was to find and verify an optimal package position, which is independent from air flow direction as much as possible. Fig. 6 shows a typical behaviour of the measured voltage of the hot film sensor when it is exposed to different air velocities at the test stand.

Tests with combine cleaning device

Fig. 7 shows a sensor arrangement in a cleaning device lab test stand. Pairs of sensors are arranged below the sieve. The most rear pair is placed behind the sieve to capture tailings and separated material from chaffer extension.

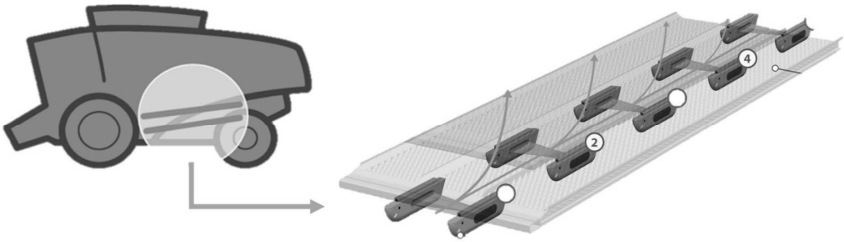

Fig. 7: Sensor arrangement (front captures grain; rear captures tailings)

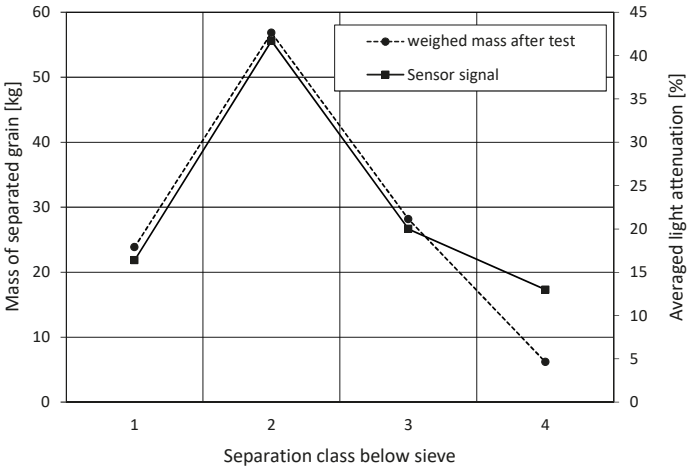

Fig. 8: Example for separation curve of grain (rear pair not shown).

Representative results can be seen in Fig. 8. The sensor system is capable to deliver information about the grain separation performance at different locations of the sieve element across a wide range of conditions

Conclusions and future work

Optical sensor and hot film anemometry are very promising detector technologies to measure combine internal process characteristics. The applicability could be proven for an arrangement below the sieve of a combine cleaning device. The signal interpretation to distinct between grain and MOG is at an early research state and may turn out to be a problematic challenge. Further tests will be planned with sensors at other places of process relevant material flow distribution. Meshes of sensors are tested to capture longitudinal and lateral distribution and analytical and empirical models have to be developed that describe the systematic separation behaviour in respect to process relevant quality outputs and performance indicators. Sensor fusion (superposition) of grain separation and air flow has the potential to deliver robust and real condition based process data for a closed loop control of productivity and quality.

References

[1] Freye, T. (1980): Untersuchungen zur Trennung von Korn-Spreu-Gemischen durch die Reinigungsanlage des Mähdreschers. Dissertation, Universität Hohenheim, MEG Forschungsbericht 47

[2] Dahany, A. (1994): Verbesserung der Leistungsfähigkeit luftdurchströmter Schwingsiebe bei der Korn-Spreu-Trennung im Mähdrescher durch Optimierung der Luftverteilung. Dissertation, Universität Hohenheim, MEG Forschungsbericht 245

[3] US6591145 B1 (2003), US4360998 A (1982), EP2401906 A1 (2012), US 2016/000008 A1 (2016)

Acknowledgement

Thanks to the companies Miunske GmbH and HKM Kunststoffverarbeitung GmbH for the outstanding collaboration in this project. Special thanks to Jörg Bernhardt who is not amongst us anymore for originally initiating and starting the work on the idea.

Material and Distribution Sensor (MADS) for Combine Material Flow

How to design and build a low-cost material sensor

Nick Butts (M.S.), **Bradley Schleusner** (B.S.), Dr. **Marshall Bremer**,
Appareo Systems, Fargo, ND, USA

Abstract

A modern combine is a highly complex factory on wheels. Understanding how grain flows through a combine is critical to improving productivity, reducing loss, and maximizing quality. In the past, engineers had to guess at the distribution of grain within a combine or utilize large test stands that provide a snapshot of combine performance. The Material and Distribution Sensors are a novel method to determine where grain is flowing throughout a combine. The sensors are designed to be low cost, robust, and placed within the combine at critical measurement locations. The sensors can be used to measure flow underneath the processor, chaffer, and tailings return as well as count individual grain impacts in order to accurately determine rotor and chaffer loss.

Understanding Material Flow

Understanding where material is flowing within the combine is critical to automating the combine performance [1]. If the distribution of material throughout the rotor can be measured, then the speed of the rotor can be adjusted automatically. Likewise, if the distribution of material on the cleaning shoe can be measured, the spacing of the sieve and chaffer can be adjusted to maximize grain cleanliness and minimize loss.

MADS Sensor Strip

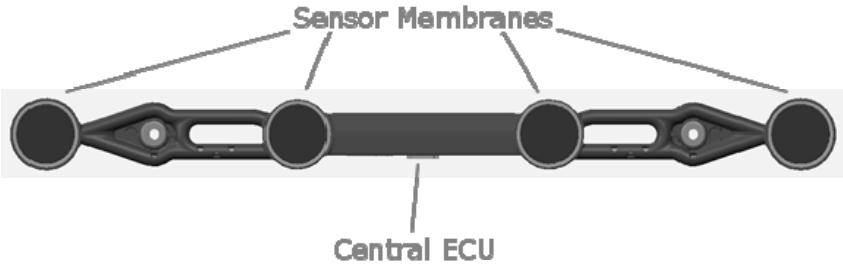

Fig. 1: MADS Sensor Strip

Appareo Systems, in conjunction with AGCO, designed and built the MADS Sensor Strips (figure 1). The MADS sensor strip is a low cost, rugged acoustic material sensor. It consists of four acoustic sensing membranes and a central Electronic Control Unit. Material impacts on the sensor's membrane surface generates an acoustic wave [2]. This wave travels into a horn designed to capture and focus the sound into a tube that conducts the sound into a MEMS microphone. The microphones convert the acoustic energy into electrical energy. A digital signal processor performs signal processing on the resulting digitized audio signal and determines two signal outputs. The first signal output is a mass flow metric based on the amount of material impacting the sensor membrane. The second metric is an impact count. The impact count is used for very low flow rates or sporadic impacts. The mass flow metric is used for higher flow rates.

The device communicates via the J1939 communication protocol with node address assigned via a unique tri-state input system. The MADS Sensor strip has three inputs that can each by in one of three states to allow up to 27 MADS Sensor strips to exist on a single CAN bus.

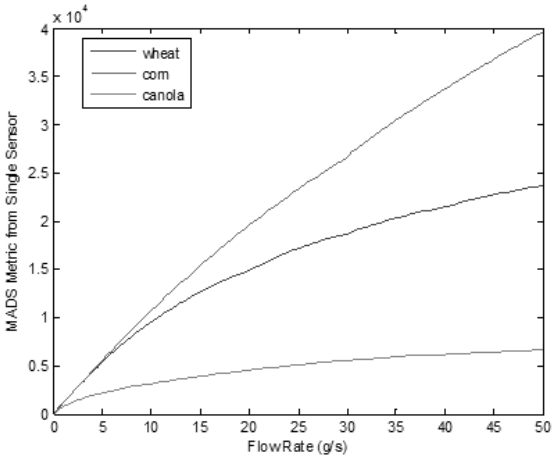

Fig. 2: MADS Metric vs flow rate

Figure 2 shows a graph of flow rates versus mass flow metric. Different mass material imparts more or less energy on the membrane. Hence the difference in metric versus flow rates. Material distribution can be visualized in real time throughout the combine. The resulting signals can be used for display purposes and combine automation.

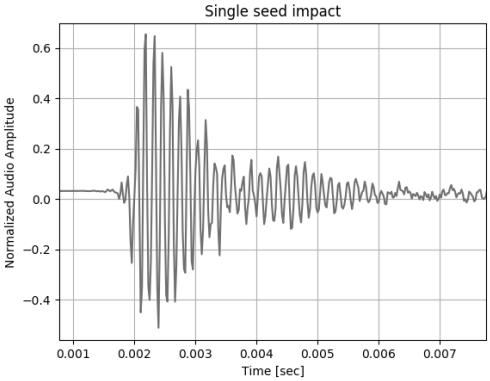

Fig. 3: Single Seed Impact

Figure 3 shows raw audio from an impact sound experiment. Seeds were dropped on the sensor with a rate between 4 and 360 seeds/test. Each test was 15 seconds in length resulting in a rate of 0.27 seeds/sec to a maximum of 24 seeds/second. There are some false positive in the test, so the seed count is slightly higher than the actual number of seeds dropped on the sensor. The seeds were dropped from a very short distance to simulate a low energy impact.

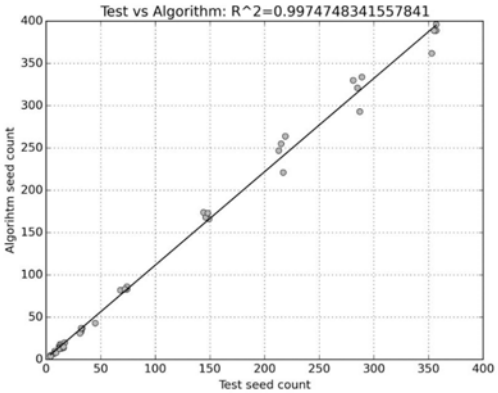

Fig. 4: Impact Counting Algorithm vs Total Seed Count

Figure 4 shows the resulting actual seed count versus algorithm seed count and the resulting linear fit accuracy. The sensor is particularly accurate at low flow rates.

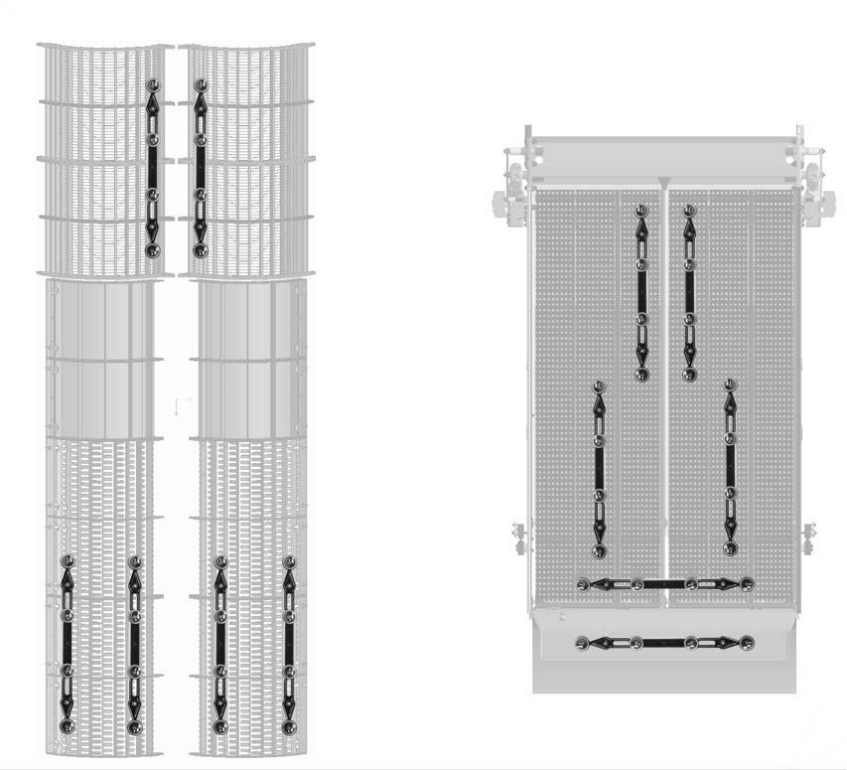

Fig. 5: Potential Sensor placement in a Combine

The first application for Appareo's acoustic technology is embedded in the Intelligent Ag Solutions Wireless Blockage Monitor (WBM). The WBM is a blockage monitor solution for air seeders. The second application for Appareo's acoustic technology is in combine material flow monitor. Figure 5 shows an example of the locations the MADS sensors could be placed in a combine. Four sensor strips are located underneath the processor area to measure distribution. Four sensor strips are located underneath the chaffer and above the sieve. These measure the distribution across the cleaning shoe. One sensor strip is in the tailings return area to measure the amount of material being recirculated in the combine. Two sensor strips are used as loss sensors, one after the cleaning shoe and one at the end of the processor area.

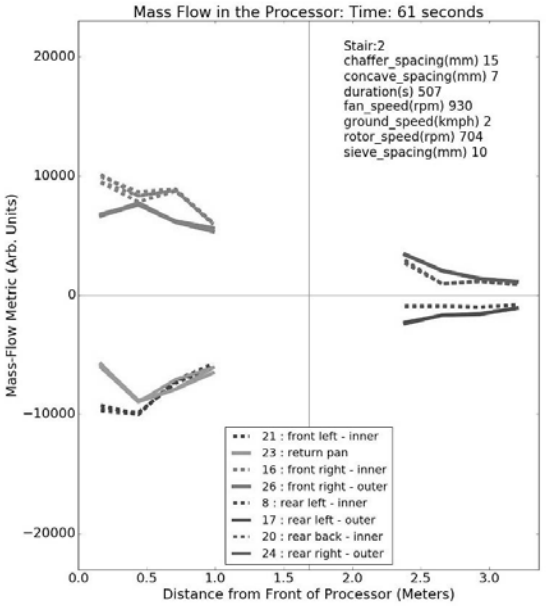

Fig. 6: Development Visualization of Sensor Data

Figure 6 shows a visualization of the processor area MADS sensor strip. The visualization shows the sensor mass flow metric 61 seconds after the start of the test. There is a total of 8 MADS sensor strips present in the processor area for this test. The area on the left shows all the MADS sensor strips under the processor area. The area on the right shows the mass flow metric and the impact metric for a MADS sensor strip located at the back end of the combine underneath the processor. This is called the blowing loss sensor and represents material that is being blown out the back of the combine.

Conclusion

The MADS sensor provides a unique insight into the internal material flow of a combine. Due to the acoustic nature of the sensors, numerous sensing points can be routed to a central Electronic Control Unit. Due to this advantage, the cost per sensing area is very low. The system is scalable by adding additional MADS sensor strips into a system. The software is field programmable and therefore the MADS sensor is adaptable to new applications and vehicles.

[1] Dr.-Ing Karl-Heinz Mertins and David W. Kmoch, „Subsystems for Automated Combines," *Land Technik AgEng,* 2001.

[2] D. T. Blackstock, Fundamentals of Physical Acoustics, Hoboken: John Wiley & Sons, Inc., 2000.

Computer based Control of the Separation Process in a Combine Harvester

M.Sc. **D. Hermann**, AGCO Research & Advanced Engineering Global Harvest, Randers, and Technical University of Denmark;
Ph.D. **F. Schøler**, B.Sc. **M. L. Bilde**, AGCO Research & Advanced Engineering Global Harvest, Randers;
Prof. **N. A. Andersen**, Prof. **O. Ravn**, Technical University of Denmark

Abstract

This paper addresses the design of a control system for a rotary threshing and separation system in a combine harvester. Utilising a distributed control architecture containing all observable crop flow parameters, the rotor speed is adjusted to maintain acceptable separation loss and grain damage using distributed impact sensors and a grain quality sensor (GQS). The GQS settling time for rotor speed changes is significantly reduced using a model based observer facilitating faster adjustment for grain losses in varying conditions.

1. Introduction

During a busy harvest it is desirable to utilise the full capacity of the combine harvester by operating at high throughput whilst maintaining an acceptable grain loss and grain quality. Hence the rotor speed in the threshing and separation system should be adjusted to separate grains from the chaff and straw particles with least possible loss and grain damage.
In modern combine harvesters the default machine settings are pre-set in the control computer for each crop type and in some cases adjusted by the operator during harvest after manual inspection of the residue, whereupon site specific conditions are often ignored.

Advances within sensor technologies and material flow models have procured a potential for automatic control of the machine settings, that is faster and more precise than a human operator. A sensor for grain quality was shown in [10], an acoustic impact type sensor strip for loss detection was presented in [1], an online separation loss monitoring algorithm in [7] and an online throughput prediction method in [6].

Section 2 presents a novel overall distributed control architecture and a novel rotor speed control scheme for the separation process. In Section 3 the design and implementation of the control system is described. Section 4 and 5 presents simulation and field test results.

2. Control Architecture

The threshing, separation and cleaning processes are assigned to numerous optimisation parameters for throughput, loss and quality, where many are even conflicting, see Fig. 1a.

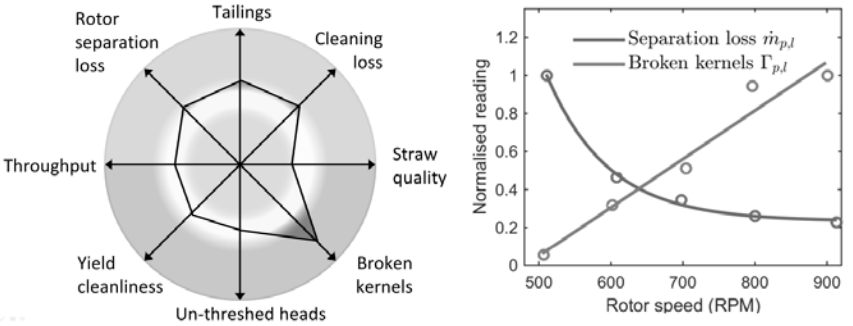

a) Overall optimisation problem for throughput, loss and quality parameters

b) Acquired field samples of rotor separation loss and broken kernels

Fig. 1: Combine harvester optimisation illustration and rotor speed impact in soybeans

In order to optimise the overall process it is vital to understand the underlying interdependencies [2, 4, 5, 9] in the multiple-input-multiple-output (MIMO) system as most actuator adjustments affect multiple parameters. The overall optimisation problem can be formulated as one common cost function for all process parameters. However, in order to simplify the controller complexity a hierarchical architecture is chosen with distributed control schemes for each actuator, where the control loop can be designed using standard methodologies for single-input-single-output (SISO) systems. This result in a shorter design and implementation phase as well as it reduces time for parameter tuning. For each actuator the dominant opposed process parameters are used to describe a cost function related to the overall optimisation goal. However some parameters are not directly available using state of the art process sensors, such as un-threshed heads or straw quality. The speed of the threshing and separation rotor is the dominating effect on the opposed parameters separation loss and grain damage; see field test samples in Fig. 1b.

An acoustic impact type sensor strip [1] with four membranes is used to measure the grain loss. Several sensor strips are placed strategically along the separation rotor to obtain the best possible measurement of the separation loss. The GQS is located in the top of the clean grain elevator measuring the relationship of broken kernels and materials other than grain (MOG) in the clean grain throughput. The windows size of the GQS captures approximately

100 grain kernels for each sample in small grain, i.e. a large number of images is required provide an accurate observation of grain damage significantly below 1%.

3. Rotor Speed Control Scheme

The objective for the rotor speed controller is to optimise the distributed cost function for separations loss and grain damage, i.e. balance the two opposed parameters. The closed-loop implementation is shown in Fig. 2a. Here the estimate of the broken kernels $\hat{\Gamma}_{p,b}$ is subtracted from the separation loss $\dot{m}_{p,l}$ normalised with the yield sensor reading $\dot{m}_y$. A model based observer is designed to estimate grain damage $\hat{\Gamma}_{p,b}$ using GQS reading $\Gamma_{p,b}$ and rotor speed ω_r, see Fig. 2b. A graphical user interface allows the operator to provide weights within a preselected range for grain loss $u_{\mathrm{p,l}}$ and grain damage $u_{\Gamma,\mathrm{b}}$.

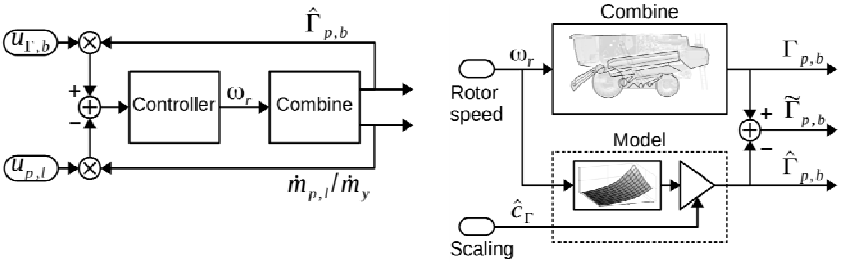

a) Closed-loop control scheme b) Grain damage observer

Fig. 2: Rotor speed control scheme and grain damage observer block diagram

3.1 Model generation

The static grain damage model is obtained from multiple rotor speed actuator curves, similar to Fig. 1b, obtained from material samples or averaged GQS readings over several minutes for each rotor speed set point, [5]. The obtained data points are then fitted to the model describing the static grain damage from rotor speed, given by $\Gamma_{p,b} = c_\Gamma \, exp^{(p_\Gamma \, \omega_p)}$.

3.2 Observer design

The Luenberger observers state-space vector $x = \left[c_\Gamma, \omega_p\right]^T$ is given by the model scaling parameter $\mathrm{c_r}$ and ω_p, the filtered state of the input vector $u = \omega_r$. The state ω_p is filtered with the time constant τ_p characterising the threshing and separation system dynamics. The continuous time state-space model is given by

$$\dot{x} = f(x) = \begin{bmatrix} \dot{c}_\Gamma \\ \dot{\omega}_p \end{bmatrix} = \begin{bmatrix} \sigma_c^2 \\ a_p \omega_p + b_p \omega_r \end{bmatrix} \qquad \text{and} \qquad \Gamma_{p,b} = \mathrm{y} = h(x) = c_\Gamma \, e^{(p_\Gamma \, \omega_p)},$$

for the zero-mean white noise variance σ_c^2, threshing and separation system dynamics a_p and b_p as well as the grain damage loss model parameter p_Γ. The GQS has a varying sample time T_{GQS} as it relies on a material flow in the clean grain elevator, correct paddle sample synchronisation and image processing time. For each GQS measurement update, the estimate is updated using $\hat{x}(k+1) = F\hat{x}(k) + Gu(k) + K(y - \hat{y})$, else the estimate is predicted according to $\hat{x}(k+1) = F\hat{x}(k) + Gu(k)$.

4. Simulation Results

The observer and closed-loop control system is tested by means of simulation, using a virtual combine [3, 5, 8]. The virtual combine facilitates simulation of all actuators inputs (u), states (x) and crop flow sensor readings (y). Figure 3 shows an open-loop (3a) and closed-loop (3b) simulation in soybeans for observer and controller verification respectively.

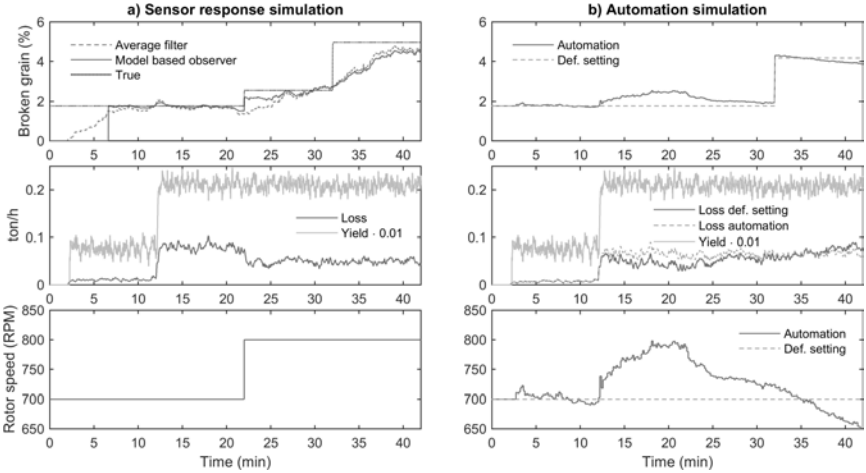

Fig. 3: Simulation of separation process with loss and grain damage sensors. Fig. 3a shows a simulation of the two observers for broken grain in open-loop. Fig. 3b shows a simulation with the closed-loop rotor speed controller.

In Figure 3a the first plot row shows the estimated and true percentage of broken kernels. Second plot the estimated separation loss $\dot{m}_{p,l}$ and yield sensor reading $\dot{m}_y$, and third plot the rotor speed ω_r. The combine enters crop after 2min and all estimates are initialised after 7min. After 12 min the throughput increases and causes a separation loss increase. Rotor speed is increased after 22min, reducing separation loss and increasing grain damage. No-

tice the rapid response from the model based observer compared to the average filter. After 32 min a change (disturbance) in the field conditions increases the grain damage significantly.

Figure 3b shows a similar sequence, except the operator optimisation focus ($u_{\Gamma,\mathrm{b}}$ and $u_{\mathrm{p,l}}$) is adjusted after 22 min. The controller increases the rotor speed as the separation loss increase with throughput after 12 min. After 22min the operator user input changes focus towards separation loss, causing the rotor speed to increase. When the disturbance in field conditions causes increased grain damage after 32min. the rotor speed is reduced to maintain the control balance.

5. Field Test Results

In Fig. 4 a field test sequence from barley is shown with same row division as in Fig. 3.

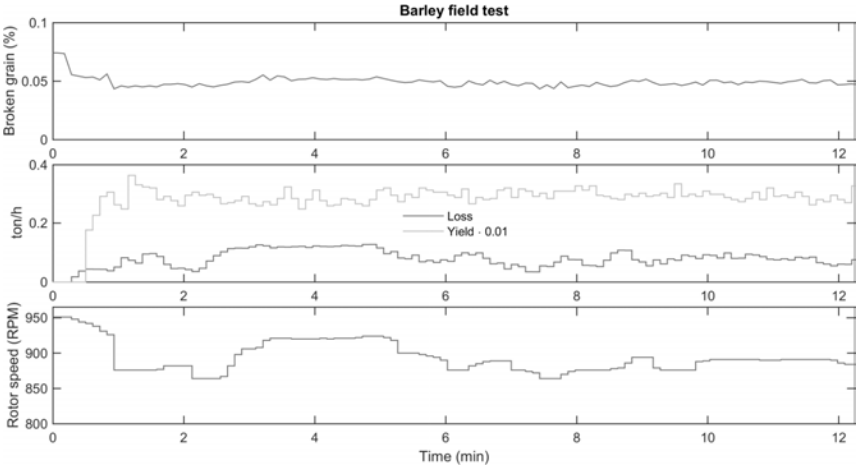

Fig. 4: Field test results for rotor speed controller for barley

In Fig. 4 the combine enters barley after 20 sec, with a high initial rotor speed which is rapidly decreased. The combine is operating in consistent yield density but varying separation loss. A increase in separation loss is observed between two and six minutes of operation, where the rotor speed is temporarily increased to reduce separation loss, causing a minor increase in broken kernels.

6. Conclusion

The paper described the distributed control architecture derived from the observable optimisation objectives. The rotor speed control scheme was presented explaining the interaction from separation loss and grain damage as well as operator interaction. Model generation and observer design was presented in order to reduce the settling for the GQS grain damage observation.

Simulation showed a reduction of the maximum separation loss and grain damage. Results from full scale field tests verified the actuator response to varying crop conditions. The automatic adjustment of the grain damage and separation loss balance indicates a significant improvement of the overall threshing and separation system performance.

Literature

[1] Butts, N.: Material and Distribution Sensor (MADS) for Combine Material Flow. Landtechnik AgEng, 2017

[2] Creassaerts, G., Saeys, W., Missotten, B. and De Baerdemaeker, J.: A generic input selection methodology for identification of the cleaning process on a combine harvester, Part I. Biosystems Engineering, volume 98, 2007, 10pp. 166-175

[3] Eggerl, A.: Model-based development of control algorithms for optimizing combine processes. Combine Harvester Symposium TU Dresden, 2010, 11p. 59-68

[4] Freye, T.: Untersuchungen zur Trennung von Korn-Spreu-Gemischen durch die Reinigungsanlage des Mähdreschers. Ph.D. Thesis. Universität Hohenheim, 1980

[5] Hermann, D., Bilde, M. L., Andersen, N. A. and Ravn, O.: A Framework for Semi-Automated Generation of a Virtual Combine Harvester. IFAC-papers online, volume 49-16, 2016, 6pp. 55-60

[6] Hermann, D., Bilde, M. L., Andersen, N. A. and Ravn, O.: On-the-go Throughput Prediction in a Combine Harvester using Sensor Fusion. CCTA conference proceedings, 2017, 6pp.

[7] Maertens, K., Ramon, H. and De Baerdemaeker, J.: An on-the-go monitoring algorithm for separation process in combine harvesters. Computer and Electronics in Agriculture volume 43, 2004, 11pp. 197-207

[8] Maertens, K. and De Baerdemaeker, J.: Design of a Virtual Combine Harvester. Mathematics and Computers in Simulation, 2004, 9pp. 49-57

[9] Miu, P.: Combine Harvesters Theory, Modeling, and Design. CRC Press, 2016

[10] Wallays, C., Saeys, W. and De Baerdemaeker, J.: Material other than grain and broken grain sensor for combine harvesters. Landtechnik AgEng, 2007, 6pp. 373-378